Title

Multiscale Modeling of Coupled Electro-Magneto-Thermo-Mechanical Media

ISBN

9798297601871

Author

Mettler, Linus Ken

Publication Date

2025-08-01

Peer reviewed|Thesis/dissertation

Multiscale Modeling of Coupled Electro-Magneto-Thermo-Mechanical Media

By

Linus Ken Mettler

A dissertation submitted in partial satisfaction of the
requirements for the degree of
Doctor of Philosophy

in

Engineering – Mechanical Engineering

in the

Graduate Division
of the
University of California, Berkeley

Committee in charge:
Professor Panayiotis Papadopoulos, Chair
Professor Sanjay Govindjee
Professor Kenneth N. Kamrin
Professor Robert L. Taylor

Summer 2025

Multiscale Modeling of Coupled
Electro-Magneto-Thermo-Mechanical Media

Abstract

Multiscale Modeling of Coupled
Electro-Magneto-Thermo-Mechanical Media

by

Linus Ken Mettler
Doctor of Philosophy in Engineering – Mechanical Engineering

University of California, Berkeley

Professor Panayiotis Papadopoulos, Chair

The theory of coupled electro-magneto-thermo-mechanical (EMTM) materials lies at the intersection between the theories of classical electromagnetism and continuum thermomechanics. In this dissertation, the balance laws and thermodynamics of EMTM materials are viewed from a pre-metric electrodynamics, that is, before introducing the aether relations. Upon a description of the transformation properties of the relevant fields under (non-relativistic) superposed rigid-body motions, it is shown that the balances of momenta are derivable from the balance of energy consistent with the Green-Naghdi-Rivlin theorem. Next, a multiscale homogenization theory is derived, whereby it is assumed that the characteristic length of the microscopic structure is sufficiently separated from the macroscopic dimensions for both scales to be viewed as a continuum. In accordance with the Irving-Kirkwood theory, homogenization is effected by postulating that the extensive quantities of mass, linear momentum, total energy, and electric charge are determined on the macroscopic scale by volumetric averages of their microscopic counterparts. Lastly, a 2-dimensional electrostatic finite element implementation of the multiscale EMTM model is presented to illustrate its applicability in practice.

Contents

1 Introduction **1**
1.1 Motivation and Context . . . 1
1.2 Prior Work . . . 2
1.3 Objectives and Scope . . . 5
1.4 Dissertation Roadmap . . . 6

2 Governing Equations of Thermomechanics **8**
2.1 Elements of Tensor Algebra and Calculus . . . 8
2.1.1 Vectors . . . 9
2.1.2 Second-Order Tensors . . . 10
2.1.3 Higher-Order Tensors . . . 13
2.1.4 Identites of Tensor Algebra . . . 15
2.1.5 Generalized Derivatives and Differential Operators . . . 16
2.1.6 Identites of Tensor Calculus . . . 17
2.1.7 Integral Theorems . . . 18
2.1.8 Potentials and the Helmholtz Theorem . . . 20
2.2 Kinematics of Large Deformations . . . 21
2.2.1 Motion . . . 21
2.2.2 Deformation . . . 22
2.2.3 Relations Between Spatial and Referential Derivatives . . . 25
2.2.4 Rate of Deformation . . . 27
2.2.5 Rate of Change of Integral Quantities . . . 29
2.3 Balance Equations . . . 30
2.3.1 Principle of Mass Conservation . . . 30
2.3.2 Principle of Linear Momentum Balance . . . 31
2.3.3 Principle of Angular Momentum Balance . . . 32
2.3.4 Principle of Energy Balance . . . 33
2.3.5 Second Law of Thermodynamics . . . 35
2.3.6 Method of Coleman and Noll . . . 35
2.3.7 Referential Form of the Balance Equations . . . 37
2.4 Superposed Rigid-Body Motions and Galilean Transformations . . . 39
2.4.1 Position, Velocity, and Acceleration . . . 40

2.4.2 Spatial Differential Operators . . . 41
2.4.3 Kinematic Quantities . . . 42
2.4.4 Thermomechanical Quantities . . . 43
2.4.5 Time Derivatives: Partial, Flux, and Path Derivatives . . . 44
2.4.6 Objectivity and Galilean Invariance . . . 46

3 Governing Equations of Electromagnetism 48
3.1 Maxwell's Equations . . . 49
3.1.1 Principle of Charge Conservation . . . 49
3.1.2 Faraday's Law of Induction . . . 51
3.1.3 Summary . . . 53
3.2 Polarization and Magnetization . . . 54
3.2.1 Polarization Charge . . . 55
3.2.2 Polarization Current . . . 55
3.2.3 Magnetization Current . . . 56
3.2.4 Maxwell's Equations for the Free Charges and Currents . . . 57
3.2.5 Summary . . . 58
3.3 Aether Relations . . . 59
3.4 Transformation Properties of Electromagnetic Fields . . . 61
3.4.1 Charge and Current Densities . . . 62
3.4.2 Charge and Current Potentials . . . 63
3.4.3 Electric and Magnetic Fields . . . 65
3.4.4 Electric and Magnetic Potentials . . . 66
3.4.5 Polarization and Magnetization . . . 68
3.4.6 Aether Relations under SRBM . . . 70
3.4.7 Summary . . . 72
3.5 Maxwell's Equations in Objective Terms . . . 73
3.5.1 Eulerian and Lagrangian Time Derivatives . . . 73
3.5.2 Faraday's Law of Induction Revisited . . . 75
3.5.3 Summary . . . 78
3.6 Maxwell's Equations in Referential Description . . . 79
3.6.1 Principle of Charge Conservation . . . 79
3.6.2 Faraday's Law of Induction . . . 80
3.6.3 Polarization and Magnetization . . . 82
3.6.4 Summary . . . 83
3.7 Magnetostatics and Electrostatics . . . 83
3.7.1 Total EM Fields . . . 84
3.7.2 With Polarization and Magnetization . . . 87

4 Coupled electro-magneto-thermo-mechanical Model **89**
4.1 Principles of Linear and Angular Momentum Balance 89
4.1.1 Lorentz Force Density 90
4.1.2 Linear Momentum 90
4.1.3 Angular Momentum 91
4.1.4 Maxwell Stress 92
4.2 Principle of Energy Balance 93
4.2.1 Power of the Electromagnetic Fields 93
4.2.2 Energy Balance 94
4.2.3 Poynting's Theorem 95
4.3 The Green-Naghdi-Rivlin Theorem 97
4.3.1 Standard GNR Procedure in Integral Form 98
4.3.2 Split into Objective and Non-Objective Terms 99
4.4 Second Law of Thermodynamics 101
4.4.1 Body Heating 101
4.4.2 Entropy Inequality 103
4.4.3 Method of Coleman and Noll 103
4.4.4 Balance Laws in Terms of the Helmholtz Free Energy 105
4.4.5 Invariance of the Constitutive Relations 106
4.4.6 Isotropy of the Helmholtz Free Energy 111

5 Multiscale Modeling **113**
5.1 Volume-Averaging Scheme 115
5.1.1 Overview 115
5.1.2 Properties of the Weighting Function 116
5.1.3 Useful Corollaries Involving the Weighting Function 119
5.2 Postulated Homogenization of Extensive Variables 121
5.3 Multiscale Balance Equations 123
5.3.1 Microscopic Scale 124
5.3.2 Macroscopic Scale 125
5.4 Homogenization of Governing Equations 127
5.4.1 Mass Density 128
5.4.2 Linear Momentum Density 129
5.4.3 Total Energy Density 132
5.4.4 Total Charge Density 135
5.4.5 Magnetic Monopole Density 137
5.4.6 Bound Charge Density 138
5.4.7 Aether Relations 140
5.4.8 Implications for Other (Non-Extensive) Quantities 141

6 Numerical Implementation of EMTM on Single Scale **144**
6.1 Initial/Boundary-Value Problem . . . 145
6.1.1 Governing Equations . . . 146
6.1.2 Constitutive Model . . . 150
6.1.3 Initial and Boundary Conditions . . . 162
6.1.4 Summary of Simplifying Assumptions . . . 164
6.2 Numerical Solution Strategy . . . 165
6.2.1 Weak Forms and Residuals . . . 166
6.2.2 Newton-Raphson Method . . . 169
6.2.3 Differentials of Residuals . . . 170
6.3 Implementation . . . 177
6.3.1 Voigt Notation . . . 178
6.3.2 Finite Element Discretization . . . 193
6.3.3 Global Residual and Stiffness Matrix . . . 198
6.3.4 Nodal Residual and Stiffness Matrix . . . 206
6.4 Verification of Implementation . . . 210
6.4.1 Material Properties . . . 211
6.4.2 Purely Thermomechanical Case . . . 212
6.4.3 Purely Electrostatic Case . . . 213
6.4.4 Convergence . . . 214
6.4.5 Numerical Tangent using Complex Arithmetic . . . 216

7 Numerical Implementation of EMTM on Two Scales **222**
7.1 RVE Boundary Conditions . . . 223
7.2 Homogenized RVE Response . . . 225
7.2.1 Homogenization of the Fluxes . . . 226
7.2.2 Linearization of Homogenization Formulae . . . 227
7.2.3 Finite Element Approximation . . . 229
7.2.4 Homogenized Material Moduli . . . 235
7.2.5 Summary . . . 247
7.3 Verification and Examples . . . 249
7.3.1 Outline of the Program Structure . . . 249
7.3.2 Homogeneous RVE . . . 255
7.3.3 Random Material Mixture . . . 260
7.3.4 Random Crystal Orientation . . . 265

8 Concluding Remarks **271**

Bibliography **274**

A Ancillary Derivations **288**
A.1 Corollaries of the Divergence Theorem . . . 288
A.2 Material Time Derivative of $\mathbf{T}^{-1}$ . . . 289
A.3 SRBM Transformation of Flux Derivative . . . 290
A.4 Invariance Properties of Electromagnetic Fields using Local Equations . . . 290
A.4.1 Current . . . 291
A.4.2 Charge and Current Potentials . . . 291
A.4.3 Electric and Magnetic Fields . . . 292
A.5 Electromagnetic Wave Equations . . . 292
A.6 Alternative Representations of the Balance Equations . . . 293
A.6.1 Linear Momentum Balance . . . 293
A.6.2 Angular Momentum Balance . . . 295
A.6.3 Energy Balance . . . 296

Acknowledgments

I would like to express my deepest gratitude to Prof. Papadopoulos for his unwavering patience, guidance, and generosity with his time. Our many discussions were instrumental in shaping this work and in helping me grow as a researcher.

Special thanks go to Prof. Taylor, who devoted countless hours to offering his invaluable expertise. Without his support, the numerical implementation of my project would not have been possible. He is a true inspiration and role model for myself and generations of researchers and engineers in the field.

I am also sincerely thankful to the remaining members of my dissertation committee, Prof. Govindjee and Prof. Kamrin, for their engagement with the subject matter and for their ability to ask challenging questions without being discouraging. I would also like to mention that a prior, formative experience as an exchange student under Prof. Govindjee has led me to pursue a PhD in continuum mechanics.

My heartfelt thanks go to my lab members and fellow students, in particular to Arjun, Guy, Ian, Magda, Miklos, and Sushrut. Their camaraderie, thoughtful conversations, and occasional comic relief helped make the journey enjoyable.

Finally, I owe my deepest personal gratitude to my wife, Sofia, for her constant love, patience, and encouragement. Her understanding and belief in me made all the difference during the most challenging moments. This achievement is as much hers as it is mine.

Chapter 1

Introduction

Coupled electro-magneto-thermo-mechanical (EMTM) behavior is observed in a wide variety of materials. In recent decades, such materials have attracted growing attention in the design of advanced engineered devices and systems. In many cases, a material's desired macroscopic characteristics arise not only from the EMTM properties of its constituents, but also from the inhomogeneous morphology of its microscopic structure. In this dissertation, the theoretical foundations of a thermodynamically consistent framework for EMTM behavior are discussed. Building on this foundation, a novel approach for the multiscale homogenization of the constitutive response of EMTM materials is proposed. Its applicability is subsequently demonstrated by way of a numerical implementation using the finite element method.

1.1 Motivation and Context

EMTM behavior encompasses a broad range of phenomena. For example, piezoelectricity and electrostriction describe the polarization of a material due to mechanical strain or, conversely, the deformation of a medium as a result of an applied electric field [4, 21, 73, 155]. Similarly, in piezomagnetism and magnetostriction, mechanical strain induces the magnetization of a material and *vice versa* [75, 80, 88]. On the other hand, magnetic shape memory alloys revert to a particular form when exposed to magnetic fields [100, 106, 134, 148, 150]. Meanwhile, the magnetocaloric effect refers to the temperature change experienced by certain materials when subjected to an external magnetic field [87, 116]. Of course, EMTM materials can simultaneously exhibit purely thermomechanical (TM) and electromagnetic (EM) behaviors. This includes the dielectric polarization and magnetization of the underlying medium in response to applied EM fields [23, 70, 139, 147], as well as transverse EM phenomena such as the Hall effect where a voltage develops perpendicular to the electric current and the magnetic field [34, 69, 119].

Coupled EMTM properties are exhibited by various inorganic, polymeric, and

even biological materials of engineering concern. For example, quartz, polyvinylidene fluoride, and bone all display piezoelectric behavior [76]. Such EMTM materials are of increasing interest in the context of multifunctional devices, from energy-harvesting piezoelectric composites [10, 25, 76], flexible actuators for soft robotics [9, 60, 128], solid-state thermoelectric refrigeration [87, 116, 121], to the design of EMTM metamaterials [98, 130, 161].

The aforementioned applications typically rely on the interplay between thermal, mechanical, electrical, and magnetic phenomena. Moreover, their functionality often originates not only from the EMTM properties of the materials themselves, but also from the morphology of their underlying microstructure. In cases where the material properties of the microscopic constituents are accessible to experimental testing, it is advantageous to infer the behavior of the bulk material from the arrangement of the microstructure. Provided that the microscopic and macroscopic scales are sufficiently separated, the continuum assumption holds on both scales and multiscale methods can be employed to deduce the macroscopic constitutive response by way of homogenization of the microscopic scale [31, 32, 50, 62, 63, 95, 162].

1.2 Prior Work

Despite decades of progress in the fields of electromagnetism and continuum mechanics, their intersection remains a topic of ongoing academic discourse. The classic monographs on electrodynamics typically do not consider the motion[1] of the underlying medium [26, 38, 69, 139], as the field is yet to fully embrace the concepts of modern continuum mechanics [103]. One point of debate in the coupled theory of EMTM materials stems from the conflict between the Newtonian description of the balance laws in continuum mechanics and the inherently relativistic nature of electromagnetism [56, 120, 133].

It is widely known that the governing equations of electromagnetism are invariant under Lorentz transformations [38, 69, 139], while conventional non-relativistic continuum mechanics is formulated under Euclidean objectivity [40, 146]. However, the pre-metric[2] Maxwell's equations are covariant under the general linear group $GL(4, \mathbb{R})$, which includes both Lorentzian and Galilean symmetry groups [30, 44, 46]. In their seminal work, Le Bellac and Lévy-Leblond [71] clarify that the incompatibility between the two theories originates in the choice of constitutive relations rather than the field equations themselves. It is the linearity

[1] For example, partial and material time derivatives are often conflated in the formulation of Faraday's law, leading to a lack of precision in the treatment of moving or deformable media.

[2] In pre-metric electrodynamics, Maxwell's equations are based on the conservation of electric charge and magnetic flux, but remain independent of a choice of coordinates or metric (*i.e.*, the speed of light c). The spacetime metric is introduced by the aether relations, which are viewed as the constitutive relations for spacetime itself [45].

of the aether relations which ultimately imposes Lorentz or Poincaré covariance onto the EM theory [33, 64, 103, 137].

The Lorentzian and Galilean transformations are asymptotically coincident, provided that the material body is bounded and its velocity (relative to a Galilean frame) is small compared to the speed of light, $v/c \ll 1$ [103, 147]. Moreover, two distinct (and mutually exclusive) quasi-static Galilean limits of Maxwell's equations are identified: The electric limit, where magnetic induction in Faraday's law is negligible, and the magnetic limit, where the displacement current in Ampère's law is disregarded [19, 47, 71, 123]. These limits furnish approximations of Maxwell's equations for the low-velocity regime, where continuum mechanics and electromagnetism can coexist under a unified framework consistent with Galilean invariance. However, this necessitates suitably modified (nonlinear or field-dependent) constitutive relations [33, 71, 133]. Some authors resolve the lack of form-invariance of the classical aether relations by replacing the electric field with the electromotive intensity, as well as the current potential with the magnetomotive intensity [56].

Another ongoing discourse in the literature concerns the formulation of the balance laws of linear and angular momenta, energy, and entropy for coupled EMTM continua. Truesdell and Toupin [147] laid the groundwork for the modern treatment of coupled EMTM in their authoritative handbook. However, as Hutter *et al.* [56] point out in their survey of electro-magneto-mechanical interaction models, there is no clear consensus regarding the definition of short-range effects (which give rise to surface tractions and hence the stress tensor) and long-range effects (such as body forces and body couples).[3] Likewise, the distinction between "heat" flux and energy supply is not unique, hence the flux can be both thermal and electromagnetic in nature [77, 102]. Moreover, conflicting definitions of "momentum" and "energy" among authors [23, 64] has led to considerable confusion [22], even though the resulting theories are ultimately found to align with each other [137].

The various approaches to obtaining the balance equations loosely fall into two main categories. In the first, the equations of conventional continuum mechanics are extended to account for any interactions with the EM fields [23, 29]. For example, the Lorentz force imposed by the EM fields onto the body[4] leads to the production of mechanical momentum. Similarly, the power exerted by the EM fields on the body, quantified by the inner product of electric current and the electric field, contributes to the internal or kinetic energy [102, 145]. The second approach, on the other hand, begins with an *a priori* assumption for the general form of the balance equations, which involve generalized quantities of linear and angular momenta, energy, stress tensor, and heat flux [41, 64]. The generalized quantities are later derived from thermodynamic principles.

[3] This can result in a non-zero EM stress tensor even outside of matter [22]. Nevertheless, ostensibly contradictory theories are often mutually compatible because a difference in the stress tensor can be absorbed as a divergence in the body force.

[4] This of course requires an equal and opposite force sustained by the EM fields [22, 114].

Most authors follow the Maxwell–Minkowski formulation, substituting the electromagnetic momentum and energy balances[5] into the EMTM balance equations [29, 56, 64, 102, 149]. However, this inadvertently imposes Lorentzian covariance onto the equations. Ericksen [22, 23] advocates instead deriving the constitutive equations prior to enforcing the aether relations. This is consistent with the pre-metric electrodynamics [46] mentioned earlier.

The electromagnetic properties of matter are accounted for by its polarization and magnetization. A variety of models exist, yielding different sets of Maxwell's equations [56]. The most prominent approach involves an additive decomposition of the charges and currents [23, 26, 38, 55, 102, 103]. Following the method of Coleman and Noll [17], constitutive relations for the stress, polarization, and magnetization are obtained from a Helmholtz potential, while thermodynamic restrictions are derived for the energy flux and the electric current [23, 64]. For this purpose, most authors adopt a modified form of the Clausius-Duhem inequality for EMTM media [23,55,64,77,101,102,137] involving a generalized heat flux [77,102], and transform the EM field quantities to the reference configuration [23,24,55,70,106,147].

Multiscale homogenization methods provide a framework to infer, analytically or computationally, the macroscopic behavior of a material from its underlying microstructure [32, 49, 50]. Provided that the two scales are sufficiently separated and each scale can be described by a continuum theory, the finite element method (FEM) may be employed at both scales to effect homogenization in what is known as the FE2 method or multilevel FEM [31,39,62,95,96,124]. The microstructure is typically resolved at the integration points of the macroscopic finite element mesh, where a representative volume element (RVE) emulates its constitutive response.[6]

Of particular interest is the first-order FE2 micro–macro modeling strategy developed by Kouznetsova *et al.* [63] for history-dependent, nonlinear behavior under large deformations. Each macroscopic Gauss point is associated with a local RVE boundary value problem whose deformation is prescribed using the macroscopic deformation gradient. Volume-averaging of the microscopic stress tensor furnishes the homogenized macroscopic stress and tangent stiffness. This method has been extended to thermal and thermo-mechanical problems in subsequent studies [127, 162, 163].

As in most FE2 schemes reported in the literature, the aforementioned method incorporates the Hill-Mandel criterion [49, 83] to ensure energetically consistent micro-macro coupling. However, this entails significant limitations with regard to (i) the allowable RVE boundary conditions, (ii) the study of microscale inertial effects, and (iii) the generalization of the criterion to the thermal domain. To address these shortcomings, Mandadapu *et al.* [82] introduce an alternative mechanism for

[5] The Lorentz force and the EM power can be expressed in terms of the EM field quantities using Maxwell's equations. In the aether frame, the ensuing expressions resemble EM balances of momentum and energy, respectively [38, 102]. However, these are not independent principles, but mere identities derived from Maxwell's equations [26, 64].

[6] In this scheme, the scales are sometimes referred to as weakly coupled [126].

upscaling of the relevant fields by prescribing a weighted volume-averaging scheme for the extensive quantities of mass, linear momentum, and total energy. This approach is rooted in the Irving-Kirkwood theory for the homogenization of atomistic and molecular quantities [57]. Successful implementations of this method have been reported for quasi-static [89] and dynamic [90] problems.

A host of analytical homogenization methods have been proposed to predict and optimize the properties of multiscale EMTM continua [7, 8, 42, 53, 58, 65, 104, 136]. Based on the work by Mori and Tanaka [99], these models are geared toward two-phase microstructures with idealized geometries such as elliptical inclusions or unidirectional fibers. In recent years, numerical strategies for the homogenization of coupled EMTM materials have been developed [11,86,112,151,157]. Such models typically rely on a generalized macro-homogeneity condition similar to the Hill-Mandel energy criterion. Most studies [73, 94, 125, 126] are limited to quasi-static conditions[7] and the EMTM coupling is implemented using heuristic constitutive relations rather than the thermodynamic framework discussed earlier.

1.3 Objectives and Scope

The preceding discussion underscores the need for a rigorous framework for the multiscale homogenization of EMTM media. Such a theory entails (i) governing equations conforming to the principles of objectivity and Galilean invariance, (ii) thermodynamically consistent constitutive relations, and (iii) a versatile and robust FE2 homogenization strategy.

The objectives of this dissertation are threefold. First, the governing equations of coupled EMTM media are discussed. Particular attention is directed towards the transformation properties of the EM fields under superposed rigid-body motions (SRBM), which are derived using the conventional methods of continuum mechanics rather than the four-dimensional Minkowski space-time formulation typically found in the literature. It is verified that, in a pre-metric setting, Maxwell's equations are indeed invariant under Galilean transformations. Moreover, it is shown that the EMTM balance equations provided by Ericksen [23] satisfy the Green-Naghdi-Rivlin theorem (GNR) [37, 156]. Hence, the postulated form-invariance of the energy balance under SRBM implies that the balances of mass, linear momentum, and angular momentum must hold.[8] This suggests that the choices of the energy and

[7] Any effects due to inertia, heat capacity, magnetic induction, or electric displacement current in the governing equations are neglected. Nevertheless, rate-dependent constitutive behavior may be included.

[8] Hutter *et al.* [56, Chapter 3.4] and Van de Ven [149, Chapter II] take a similar approach. However, the authors invoke a non-standard version of the aether relations, rendering the resulting Maxwell's equations incompatible with other EMTM theories. Even if the standard aether relations were employed, any Euclidean motion imposed by the GNR theorem would cause a departure from the aether frame, thus rendering the post-metric Maxwell's equations invalid.

momentum balances are mutually consistent.

Next, the Irving-Kirkwood-type homogenization method developed by Mandadapu *et al.* [82] is generalized to coupled EMTM continua. In addition to the prescribed volumetric averaging of mass, linear momentum, and total energy,[9] it is postulated that the electric charges homogenize like extensive quantities. This furnishes homogenization formulae for the polarization and magnetization.

Lastly, the EMTM homogenization scheme is implemented using the finite element method. This implementation is limited to quasi-static problems involving transversely isotropic, piezoelectric, thermoelastic solids. The FE2 method introduced by Kouznetsova *et al.* [63] is generalized to encompass the electric and magnetic potentials, which are imposed on the RVE boundary by the gradients of their macroscopic counterparts. The ensuing algorithm is tested on a range of simple, two-dimensional problems involving two types of RVE: (i) a mixture of two materials randomly assigned to the elements of the RVE mesh, and (ii) an RVE comprised of randomly oriented piezoelectric crystals.

1.4 Dissertation Roadmap

This dissertation is organized as follows: In Chapters 2 - 4 the relevant physical quantities and the governing equations are introduced. The discussion is organized in three parts. In Chapter 2, the theory of classical nonlinear continuum thermomechanics is presented. This includes the kinematics, the balance equations, and the concept of invariance and superposed rigid-body motion. While the theory is well-established in the literature, this chapter also serves to introduce the notational convention adopted throughout this document. Furthermore, some of the identities of tensor calculus introduced here will be employed in various derivations throughout the remainder of this text.

This is followed in Chapter 3 by a review of Maxwell's equations of electromagnetism along with the Galilean invariance properties of the corresponding field quantities. The subject is approached from the paradigm of classical continuum mechanics. For example, conservation laws are expressed in terms of integrals over material regions rather than fixed regions of space. To preserve a notation familiar to the continuum mechanist, the four-dimensional Minkowski space-time formulatio is avoided.

In Chapter 4, the governing laws of coupled electro-magneto-thermo-mechanical media are presented, including the balances of linear and angular momenta, the balance of energy, and the Clausius-Duhem inequality for entropy. The validity of

[9] Here, it is emphasized that "linear momentum" and "total energy" refer to the purely mechanical momentum and the sum of kinetic and internal energies, respectively. They do not include the electromagnetic momentum and energy, which are regarded as external to the body. In any case, the EM momentum and energy are not well-defined in the pre-metric form of Maxwell's equations.

the so-called Green-Naghdi-Rivlin theorem is verified and serves as additional reassurance for the choice of the aforementioned balance equations. Employing the method of Coleman and Noll, the entropy inequality informs the development of constitutive relations in agreement with the second law of thermodynamics. The balance laws, Maxwell's equations, and the constitutive relations collectively provide closure, *i.e.*, they provide a complete set of equations that form a well-defined boundary-value problem.

In Chapter 5, a multiscale homogenization theory is developed in accordance with the Irving-Kirkwood framework. First, the properties of the volumetric averaging scheme are discussed. This is followed by a list of extensive variables which are postulated to homogenize according to the averaging scheme. By enforcing certain balance equations on the microscopic and macroscopic scales, homogenization formulae can be inferred for the fluxes (*i.e.*, the stress, heat flux, polarization, and magnetization) as well as the volumetric sources (*i.e.*, the body force, body heating, and the charge density).

Chapter 6 is concerned with the single-scale finite element problem arising from the EMTM theory in Chapter 4. The simplifying assumptions, constitutive parameters, and the boundary conditions are described. Upon a brief review of the Newton-Raphson method, a detailed derivation of the residual and stiffness matrix is provided. The ensuing equations are implemented in a (2-dimensional, quasi-static) single-scale model, whose main purpose is to lay the foundation for the development of the multiscale finite element model.

Finally, the multiscale numerical model is examined in Chapter 7. The RVE boundary conditions, the volume-averaging Gaussian integration scheme, and the computation of the homogenized tangent stiffness are discussed. A finite element implementation of the multiscale homogenization scheme is devised using a rudimentary parallel processing strategy. To illustrate its applicability in practice, and a range of test problems is carried out using both homogeneous and inhomogeneous RVE models.

Lastly, brief concluding remarks are presented in Chapter 8, reflecting on the work conducted in this dissertation and outlining prospective steps to further enhance the proposed method's capabilities.

Chapter 2

Governing Equations of Thermomechanics

This chapter offers a summary of the theory of nonlinear continuum mechanics, starting with a review of tensors and the kinematics of large deformations. Upon presentation of the balance laws for momentum, energy, and entropy, the invariance properties of the thermomechanical quantities are examined. This theory is well-established and a wide variety of monographs may be consulted for further details and proofs, such as Chadwick [13], Curnier [18], Gurtin [40], Holzapfel [52], or Marsden and Hughes [84]. The concepts presented in this chapter will be relied upon throughout this text.

2.1 Elements of Tensor Algebra and Calculus

This section contains a superficial review some of the classical results of tensor algebra and calculus, which are frequently employed in this dissertation. A more rigorous discussion can be found, for example, in Sokolnikoff [132] or Synge and Schild [140]. Readers already familiar with the subject may consult this section for an overview of the adopted notation.

The discussion begins with a brief overview of the concept of vectors and tensors, along with the basic rules of their algebraic operations. This is followed by tensor calculus, *i.e.*, the generalization of differentiation to vector- or tensor-valued functions of vector- or tensor-valued arguments. The review concludes with a list of identities and integral theorems which play an important role in the manipulation of the mechanical, thermal, and electromagnetic balance equations.

It is mentioned beforehand that real-valued (*i.e.*, scalar) quantities α are denoted by latin or greek letters in light font, whereas boldface font is reserved for vectors $\mathbf{w}$ and second-order tensors $\mathbf{T}$. Vectors and tensors are discerned by the use of lower- and uppercase letters, respectively, unless historically established notation takes prece-

dence. Third- and fourth-order tensors $\mathbb{c}$ and $\mathbb{C}$, respectively, are represented by blackboard bold font. Round parentheses $(\cdot)$ indicate that the field contained therein is real- or vector-valued, while square brackets $[\cdot]$ signify second- or higher-order tensors. Braces $\{\cdot\}$ are used discretionarily to group larger expressions.

2.1.1 Vectors

A *vector* $\mathbf{w}$ is an element of the n-dimensional *linear* (or *vector*) *space* $\mathcal{V}^n$, which is subject to the usual basic properties pertaining to summation and multiplication between scalars and vectors. A set of vectors $\mathbf{w}_i \in \mathcal{V}^n$ is *linearly independent*, if the *null vector* $\mathbf{0} \in \mathcal{V}^n$ can be attained by a linear combination of $\mathbf{w}_i$ only when all factors $\alpha_i \in \mathbb{R}$ vanish,

$$\sum_i \alpha_i \mathbf{w}_i \;=\; \mathbf{0} \quad \leftrightarrow \quad \alpha_i \;=\; 0 \quad . \tag{2.1}$$

This further implies that any set $\{\mathbf{w}_1, \ldots, \mathbf{w}_n\} \in \mathcal{V}^n$ of n linearly independent vectors forms a *basis*, so that all elements in $\mathcal{V}^n$ can be represented by a unique linear combination thereof.

Within the scope of this dissertation, all vectors are considered to be elements of the 3-dimensional EUCLIDEAN *vector space* E^3 (also known as EUCLIDEAN *3-space*). The *dot product* (or *contraction*) of $\mathbf{w} \in E^3$ with another vector satisfies the property

$$\mathbf{w} \cdot \big(\alpha\,\mathbf{u} + \beta\,\mathbf{v}\big) \;=\; \alpha\big(\mathbf{w} \cdot \mathbf{u}\big) + \beta\big(\mathbf{v} \cdot \mathbf{w}\big) \quad \forall \quad \alpha, \beta \in \mathbb{R} \quad \text{and} \quad \mathbf{u}, \mathbf{v} \in E^3 \quad . \tag{2.2}$$

Two vectors $\mathbf{u}, \mathbf{v}$ are said to be *orthogonal* if $\mathbf{u} \cdot \mathbf{v} = 0$, while the *magnitude* (or EUCLIDEAN *distance*) of $\mathbf{w}$ is given by the *2-norm*[1] $|\mathbf{w}| = \|\mathbf{w}\|_2 = \sqrt{\mathbf{w} \cdot \mathbf{w}}$.

The preceding definitions give rise to the ability to orthogonalize and normalize vectors. Since mutually orthogonal vectors are linearly independent, an *orthonormal basis* $\mathbf{e}_i$ with $i = \{1, 2, 3\}$ may be constructed, *i.e.*,

$$\mathbf{e}_i \cdot \mathbf{e}_j \;=\; \delta_{ij} \quad , \quad \delta_{ij} \;=\; \begin{cases} 1 & \text{if} \quad i = j \\ 0 & \text{if} \quad i \neq j \end{cases} \quad , \tag{2.3}$$

where the so-called KRONECKER *delta* δ_{ij} allows for a more compact notation. Relative to this basis, any vector $\mathbf{w} \in E^3$ is uniquely resolved as a linear combination

$$\mathbf{w} \;=\; \sum_{i=1}^{3} w_i\,\mathbf{e}_i \;=\; w_i\,\mathbf{e}_i \quad , \quad w_i \;=\; \mathbf{w} \cdot \mathbf{e}_i \quad , \tag{2.4}$$

where $w_i \in \mathbb{R}$ represents the i-th CARTESIAN *component* of $\mathbf{w}$. In view of (2.3) and (2.4), the dot product is given in components by $\mathbf{u} \cdot \mathbf{v} = u_k v_k$.

[1] The notations $\|\mathbf{w}\|_2$ and $|\mathbf{w}|$ are used synonymously.

According to EINSTEIN's *summation convention*, the repeated occurrence of an index (or *dummy index*) signifies its summation, see Equation $(2.4)_1$. A single occurrence (or *free index*) can take any value $\{1,2,3\}$, see $(2.4)_2$. Unless stated otherwise, this convenient notation is tacitly adopted throughout this text.

The *cross* (or *vector*) *product* $\mathbf{u}\times\mathbf{v}$ of two vectors $\mathbf{u},\mathbf{v}\in E^3$ produces a vector given in components relative to the basis $\mathbf{e}_k$ by

$$\mathbf{u}\times\mathbf{v} \;=\; \epsilon_{ijk}\,u_i\,v_j\,\mathbf{e}_k \quad , \quad \epsilon_{ijk} \;=\; \begin{cases} 1 & \text{if} \quad \{i,j,k\}=\{1,2,3\},\{2,3,1\},\{3,1,2\} \\ -1 & \text{if} \quad \{i,j,k\}=\{3,2,1\},\{2,1,3\},\{1,3,2\} \\ 0 & \text{else} \end{cases} \quad , \tag{2.5}$$

where ϵ_{ijk} is the so-called *permutation* (or LEVI-CIVITA) *symbol*. This notation requires the basis to be *right-hand* orthonormal, *i.e.*, that the basis vectors $\mathbf{e}_k$ are numbered in an order that satisfies

$$\big(\mathbf{e}_i\times\mathbf{e}_j\big)\cdot\mathbf{e}_k \;=\; \epsilon_{ijk} \quad . \tag{2.6}$$

Moving forward it is assumed that all bases are arranged in accordance with the right-hand rule (2.6), which is of course more restrictive than the orthonormality condition of $(2.3)_1$. The *scalar triple product* of $\mathbf{u},\mathbf{v},\mathbf{w}\in E^3$ is given by

$$\big[\mathbf{u},\mathbf{v},\mathbf{w}\big] \;=\; \big(\mathbf{u}\times\mathbf{v}\big)\cdot\mathbf{w} \;=\; \mathbf{u}\cdot\big(\mathbf{v}\times\mathbf{w}\big) \quad , \tag{2.7}$$

where the permutation properties $[\mathbf{u},\mathbf{v},\mathbf{w}]=[\mathbf{v},\mathbf{w},\mathbf{u}]=-[\mathbf{w},\mathbf{v},\mathbf{u}]$ are inherited from Equation $(2.5)_2$. It is associated with the volume of a parallelepiped outlined by the vector triad $\mathbf{u},\mathbf{v},\mathbf{w}$. Following $(2.4)_1$ and (2.6), the scalar triple product is expressed in CARTESIAN components by $[\mathbf{u},\mathbf{v},\mathbf{w}]=\epsilon_{ijk}u_iv_jw_k$. Note that, unlike individual components of a vector, the dot and scalar triple products are independent of the choice of right-hand orthonormal basis.

2.1.2 Second-Order Tensors

The so-called *tensor product* $\mathbf{u}\otimes\mathbf{v}$ between two vectors $\mathbf{u},\mathbf{v}\in E^3$ is defined through its interaction with a third vector according to

$$\big[\mathbf{u}\otimes\mathbf{v}\big]\mathbf{w} \;=\; \big(\mathbf{v}\cdot\mathbf{w}\big)\mathbf{u} \quad \forall \quad \mathbf{w}\in E^3 \quad . \tag{2.8}$$

A *second-order* (or *second-rank*) *tensor* $\mathbf{T}$, or tensor for short, describes a *linear mapping* $\mathbf{t}:E^3\to E^3$ from one vector to another. A mapping $\mathbf{t}(\mathbf{w})=\mathbf{T}\mathbf{w}$ is linear, if it satisfies[2]

$$\mathbf{t}(\alpha\mathbf{u}+\beta\mathbf{v}) \;=\; \alpha\,\mathbf{t}(\mathbf{u}) + \beta\,\mathbf{t}(\mathbf{v}) \quad \forall \quad \alpha,\beta\in\mathbb{R} \quad \text{and} \quad \mathbf{u},\mathbf{v}\in E^3 \quad . \tag{2.9}$$

[2]Note the similarity with the dot product in (2.2), which may be regarded as a linear mapping $w:E^3\to\mathbb{R}$ from a vector to a scalar $w(\mathbf{u})=\mathbf{w}\cdot\mathbf{u}$.

Given the linearity of the dot product it is readily verified that $\mathbf{u}\otimes\mathbf{v}$ in (2.8) represents a tensor with six independent components. However, in view of $(2.4)_1$ and (2.9) it is concluded that a general tensor $\mathbf{T}$ comprises nine independent CARTESIAN components $T_{ij}\in\mathbb{R}$. It is uniquely resolved as a linear combination

$$\mathbf{T} \;=\; T_{ij}\,\mathbf{e}_i\otimes\mathbf{e}_j \quad , \quad T_{ij} \;=\; \mathbf{e}_i\cdot\mathbf{T}\,\mathbf{e}_j \quad , \tag{2.10}$$

where the nine tensor products $\mathbf{e}_i\otimes\mathbf{e}_j$ form a basis for the *linear space of second-order tensors* $\mathcal{L}(E^3,E^3)$ of which $\mathbf{T}$ is an element. The linear mapping $\mathbf{u}=\mathbf{T}\mathbf{v}$ is thus given in components relative to the basis $\mathbf{e}_i$ by $\mathbf{u}=T_{ij}v_j\mathbf{e}_i$.

The *tensor multiplication* $\mathbf{S}\mathbf{T}$ between two tensors $\mathbf{S},\mathbf{T}\in\mathcal{L}(E^3,E^3)$ is defined according to the rule

$$\big[\mathbf{S}\,\mathbf{T}\big]\,\mathbf{w} \;=\; \mathbf{S}\big(\mathbf{T}\,\mathbf{w}\big) \quad \forall \quad \mathbf{w}\in E^3 \quad , \tag{2.11}$$

from which it is deduced that its components are $\mathbf{S}\mathbf{T}=S_{ik}T_{kj}\,\mathbf{e}_i\otimes\mathbf{e}_j$.

The *trace* of a tensor is a scalar quantity defined through the relation

$$\mathrm{tr}\big[\mathbf{u}\otimes\mathbf{v}\big] \;=\; \mathbf{u}\cdot\mathbf{v} \quad \forall \quad \mathbf{u},\mathbf{v}\in E^3 \quad , \tag{2.12}$$

from which it is concluded that $\mathrm{tr}\,\mathbf{T}=T_{ij}\,\mathbf{e}_i\cdot\mathbf{e}_j=T_{kk}$ for all tensors $\mathbf{T}$. The trace is a so-called *principal invariant* of $\mathbf{T}$ because, whereas individual components T_{ij} typically depend on the choice of orthonormal basis, the trace T_{kk} does not.

Second-order tensors contain three independent principal invariants, defined by

$$\begin{aligned}
\mathrm{I}_{\mathbf{T}} \;&=\; \mathrm{tr}\,\mathbf{T} \quad , \\
\mathrm{II}_{\mathbf{T}} \;&=\; \frac{1}{2}\Big\{\big(\mathrm{tr}\,\mathbf{T}\big)^2-\mathrm{tr}\big[\mathbf{T}^2\big]\Big\} \quad , \\
\mathrm{III}_{\mathbf{T}} \;&=\; \frac{1}{6}\Big\{\big(\mathrm{tr}\,\mathbf{T}\big)^3-3\big(\mathrm{tr}\,\mathbf{T}\big)\mathrm{tr}\big[\mathbf{T}^2\big]+2\,\mathrm{tr}\big[\mathbf{T}^3\big]\Big\} \;=\; \det\mathbf{T} \quad ,
\end{aligned} \tag{2.13}$$

where $\mathbf{T}^2$ and $\mathbf{T}^3$ represent tensor multiplications of $\mathbf{T}$ with itself according to (2.11). The third invariant $\mathrm{III}_{\mathbf{T}}$ in $(2.13)_3$ corresponds to the *determinant* of $\mathbf{T}$, which is identical to its counterpart from linear algebra when expressed in CARTESIAN components T_{ij}.

The *eigenvalues* λ_i of a tensor are synonymous with the eigenvalues of the matrix components T_{ij} of $\mathbf{T}$ with respect to any orthonormal basis. They are obtained from the solution to the cubic polynomial

$$\det\big(\mathbf{T}-\lambda\mathbf{I}\big) \;=\; -\lambda^3+\mathrm{I}_{\mathbf{T}}\lambda^2-\mathrm{II}_{\mathbf{T}}\lambda+\mathrm{III}_{\mathbf{T}} \;=\; 0 \quad , \tag{2.14}$$

where the so-called *identity* (or *unit*) *tensor* $\mathbf{I}=\delta_{ij}\,\mathbf{e}_i\otimes\mathbf{e}_j$ (also denoted by $\mathbf{1}$ or $\mathbf{i}$ depending on context) maps vectors $\mathbf{w}$ and tensors $\mathbf{T}$ onto themselves, $\mathbf{w}=\mathbf{I}\mathbf{w}$ and

$\mathbf{T} = \mathbf{T}\mathbf{I} = \mathbf{I}\mathbf{T}$. Equation (2.14) is commonly referred to as the *characteristic equation*. The CAYLEY-HAMILTON *theorem* asserts that any tensor $\mathbf{T}$ satisfies its own characteristic equation

$$\mathbf{T}^3 - \mathrm{I}_{\mathbf{T}}\mathbf{T}^2 + \mathrm{II}_{\mathbf{T}}\mathbf{T} - \mathrm{III}_{\mathbf{T}}\mathbf{I} = \mathbf{0} \quad . \tag{2.15}$$

This implies that any[3] integer power $\mathbf{T}^n$ may be expressed by a linear combination of three successive integer powers of $\mathbf{T}$, with factors determined by the principal invariants.

The *transpose* $\mathbf{T}^{\mathrm{T}}$ of a second-order tensor $\mathbf{T} \in \mathcal{L}(E^3, E^3)$ is defined by the relation

$$\mathbf{u} \cdot \mathbf{T}\mathbf{v} = \mathbf{v} \cdot \mathbf{T}^{\mathrm{T}}\mathbf{u} \quad \forall \quad \mathbf{u}, \mathbf{v} \in E^3 \quad , \tag{2.16}$$

so that the transpose of $\mathbf{T} = T_{ij}\mathbf{e}_i \otimes \mathbf{e}_j$ is given by $\mathbf{T}^{\mathrm{T}} = T_{ij}\mathbf{e}_j \otimes \mathbf{e}_i$. A tensor $\mathbf{T}$ is *symmetric* if $\mathbf{T} = \mathbf{T}^{\mathrm{T}}$ (or $T_{ij} = T_{ji}$) and *skew-symmetric* if $\mathbf{T} = -\mathbf{T}^{\mathrm{T}}$ (or $T_{ij} = -T_{ji}$). Any tensor can be decomposed uniquely into its symmetric and skew-symmetric parts

$$\mathbf{T} = \frac{1}{2}\Big[\mathbf{T} + \mathbf{T}^{\mathrm{T}}\Big] + \frac{1}{2}\Big[\mathbf{T} - \mathbf{T}^{\mathrm{T}}\Big] = \mathrm{sym}\big[\mathbf{T}\big] + \mathrm{skw}\big[\mathbf{T}\big] \quad , \tag{2.17}$$

where $\mathrm{sym}[\mathbf{T}]$ (sometimes denoted by $\mathbf{T}^{\mathrm{s}}$) comprises six independent components and $\mathrm{skw}[\mathbf{T}]$ the remaining three. A tensor $\mathbf{T}$ is *positive-definite* if

$$\mathbf{w} \cdot \mathbf{T}\mathbf{w} > 0 \quad \forall \quad \mathbf{w} \neq \mathbf{0} \in E^3 \quad . \tag{2.18}$$

Note that positive-definiteness is a property of symmetric tensors only, since Equation (2.16) implies that $\mathbf{w} \cdot \mathbf{T}\mathbf{w} = 0$ for all skew-symmetric $\mathbf{T}$.

The *inverse* $\mathbf{T}^{-1}$ of a tensor $\mathbf{T} \in \mathcal{L}(E^3, E^3)$ is defined by the relation

$$\mathbf{T}\mathbf{u} = \mathbf{v} \quad \leftrightarrow \quad \mathbf{u} = \mathbf{T}^{-1}\mathbf{v} \quad \forall \quad \mathbf{u}, \mathbf{v} \in E^3 \quad . \tag{2.19}$$

A unique inverse exists if, and only if, $\det \mathbf{T} \neq 0$, in which case $\mathbf{T}$ is termed *invertible*. It follows immediately from $(2.19)_{1,2}$ that $\mathbf{T}^{-1}\mathbf{T} = \mathbf{I}$ and $\mathbf{T}\mathbf{T}^{-1} = \mathbf{I}$. It is mentioned that the inverse commutes with the transpose, therefore

$$\mathbf{T}^{-\mathrm{T}} = \big[\mathbf{T}^{\mathrm{T}}\big]^{-1} = \big[\mathbf{T}^{-1}\big]^{\mathrm{T}} \quad . \tag{2.20}$$

An invertible tensor $\mathbf{Q} \in \mathcal{L}(E^3, E^3)$ is called *orthogonal* if its inverse coincides with its transpose,

$$\mathbf{Q}^{\mathrm{T}} = \mathbf{Q}^{-1} \quad . \tag{2.21}$$

Its determinant is $\det \mathbf{Q} = \pm 1$, since $\det[\mathbf{Q}^{\mathrm{T}}\mathbf{Q}] = (\det \mathbf{Q})^2 = 1$. Orthogonal tensors are said to be elements of the *orthogonal group*, $\mathbf{Q} \in \mathrm{Orth}$. *Proper orthogonal* tensors are further restricted to $\det \mathbf{Q} = 1$, and are members of the *proper orthogonal group* Orth^+.

[3] This includes negative integers n if $\mathbf{T}$ is invertible, see (2.19).

The *contraction* (or *inner product*) $\mathbf{S}\cdot\mathbf{T}$ between two tensors $\mathbf{S},\mathbf{T}\in\mathcal{L}(E^3,E^3)$ is a scalar quantity defined as[4]

$$\mathbf{S}\cdot\mathbf{T} \;=\; \mathrm{tr}\big[\mathbf{S}\,\mathbf{T}^{\mathrm{T}}\big] \quad , \tag{2.22}$$

and therefore given in components by $\mathbf{S}\cdot\mathbf{T}=S_{ij}T_{ij}$. It follows that the trace may be written as a contraction $\mathrm{tr}\mathbf{T}=\mathbf{T}\cdot\mathbf{I}$. Two tensors are termed mutually *orthogonal* if $\mathbf{S}\cdot\mathbf{T}=0$, while the *2-norm* of a tensor is defined by $\|\mathbf{T}\|_2 \;=\; \sqrt{\mathbf{T}\cdot\mathbf{T}}$. It is readily verified that the tensor basis in $(2.10)_1$ is orthonormal,

$$\big[\mathbf{e}_i\otimes\mathbf{e}_j\big]\cdot\big[\mathbf{e}_k\otimes\mathbf{e}_l\big] \;=\; \delta_{ik}\,\delta_{jl} \;=\; \begin{cases} 1 & \text{if} \quad i=k \quad \text{and} \quad j=l \\ 0 & \text{else} \end{cases} \quad , \tag{2.23}$$

which is the tensor-valued counterpart to Equation (2.3). The components in $(2.10)_2$ are alternatively expressed by a contraction $T_{ij}=\mathbf{T}\cdot[\mathbf{e}_i\otimes\mathbf{e}_j]$ with the corresponding basis, akin to $(2.4)_2$ for vectors.

2.1.3 Higher-Order Tensors

As discussed in the preceding section, second-order tensors provide linear mappings from one vector to another. Higher-order tensors are needed to describe the mapping of second-order tensors. A *third-order tensor* $\mathfrak{c}\in\mathcal{L}(E^3,E^3,E^3)$ describes the linear mapping from a vector to a second-order tensor $\mathbf{C}:E^3\to\mathcal{L}(E^3,E^3)$, or from a second-order tensor to a vector $\mathbf{c}:\mathcal{L}(E^3,E^3)\to E^3$. Similarly, a *fourth-order tensor* $\mathbb{C}\in\mathcal{L}(E^3,E^3,E^3,E^3)$ represents a linear mapping between two second-order tensors $\mathbf{C}:\mathcal{L}(E^3,E^3)\to\mathcal{L}(E^3,E^3)$. In the context of this dissertation, the need for such mappings arises primarily from the constitutive relations. For example, piezoelectric behavior involves the coupling of electric polarization (a vector) with mechanical strain (a tensor), which is effectuated by a third-order tensor comprised of material parameters.

Repeated application of the tensor product, see (2.8), produces a chain $\mathbf{u}\otimes\ldots\otimes\mathbf{w}$ of n vectors $\mathbf{u},\ldots,\mathbf{w}\in E^3$. For $n=3$, its interaction with another vector or tensor are derived from

$$\begin{aligned} \big[\mathbf{u}\otimes\mathbf{v}\otimes\mathbf{w}\big]\,\mathbf{t} \;&=\; \big(\mathbf{w}\cdot\mathbf{t}\big)\big[\mathbf{u}\otimes\mathbf{v}\big] \quad \forall \quad \mathbf{t}\in E^3 \quad , \\ \big[\mathbf{u}\otimes\mathbf{v}\otimes\mathbf{w}\big]\,\mathbf{T} \;&=\; \big(\big[\mathbf{v}\otimes\mathbf{w}\big]\cdot\mathbf{T}\big)\,\mathbf{u} \quad \forall \quad \mathbf{T}\in\mathcal{L}(E^3,E^3) \quad , \end{aligned} \tag{2.24}$$

respectively, where the contraction $\big[\mathbf{v}\otimes\mathbf{w}\big]\cdot\mathbf{T}=v_i w_j T_{ij}$ is defined in (2.22). Similarly, a chain of $n=4$ vectors interacts with a tensor according to the rule

$$\big[\mathbf{t}\otimes\mathbf{u}\otimes\mathbf{v}\otimes\mathbf{w}\big]\,\mathbf{T} \;=\; \big(\big[\mathbf{v}\otimes\mathbf{w}\big]\cdot\mathbf{T}\big)\big[\mathbf{t}\otimes\mathbf{u}\big] \quad \forall \quad \mathbf{T}\in\mathcal{L}(E^3,E^3) \quad . \tag{2.25}$$

[4] In this dissertation it is assumed that contractions occur exclusively between tensors of *equal* order, both of which are thus consumed in their entirety, producing a scalar. It is left to the reader to infer the tensor order from context. Some authors instead employ a colon $(\mathbf{S}:\mathbf{T})$ to distinguish the contraction of second-order tensors from that of vectors $(\mathbf{u}\cdot\mathbf{v})$.

It is readily verified that (2.24) and (2.25) constitute linear mappings, and therefore represent n-th order[5] tensors.

In general, n-th order tensors comprise 3^n independent CARTESIAN components, which are uniquely resolved with respect to an orthonormal basis $\mathbf{e}_i \otimes ... \otimes \mathbf{e}_l$ for the linear space of n-th order tensors $\mathcal{L}(E^3, ..., E^3)$. The 3rd- and 4th-order tensors $\mathfrak{c} \in (E^3, E^3, E^3)$ and $\mathbb{C} \in (E^3, E^3, E^3, E^3)$ are expressed in components $\mathfrak{c}_{ijk}$ and $\mathbb{C}_{ijkl}$ by the linear combinations

$$\begin{aligned} \mathfrak{c} &= \mathfrak{c}_{ijk}\, \mathbf{e}_i \otimes \mathbf{e}_j \otimes \mathbf{e}_k \quad , \quad \mathfrak{c}_{ijk} = \big[\mathbf{e}_i \otimes \mathbf{e}_j\big] \cdot \big[\mathfrak{c}\, \mathbf{e}_k\big] = \mathbf{e}_i \cdot \big(\mathfrak{c}\, \big[\mathbf{e}_j \otimes \mathbf{e}_k\big]\big) \quad , \\ \mathbb{C} &= \mathbb{C}_{ijkl}\, \mathbf{e}_i \otimes \mathbf{e}_j \otimes \mathbf{e}_k \otimes \mathbf{e}_l \quad , \quad \mathbb{C}_{ijkl} = \big[\mathbf{e}_i \otimes \mathbf{e}_j\big] \cdot \big(\mathbb{C}\, \big[\mathbf{e}_k \otimes \mathbf{e}_l\big]\big) \quad . \end{aligned} \tag{2.26}$$

It follows from $(2.24)_{1,2}$ that linear mappings $\mathbf{T} = \mathfrak{c}\mathbf{w}$ and $\mathbf{w} = \mathfrak{c}\mathbf{T}$ are given in components by $\mathbf{T} = \mathfrak{c}_{ijk} w_k \mathbf{e}_i \otimes \mathbf{e}_j$ and $\mathbf{w} = \mathfrak{c}_{ijk} T_{jk} \mathbf{e}_i$, respectively, while (2.25) for $\mathbf{S} = \mathbb{C}\mathbf{T}$ furnishes $\mathbf{S} = \mathbb{C}_{ijkl} T_{kl} \mathbf{e}_i \otimes \mathbf{e}_j$. Note that these tensor multiplications often lack associativity. For example, it is observed that $(\mathfrak{c}\mathbf{S})\mathbf{T} \neq \mathfrak{c}[\mathbf{S}\mathbf{T}]$ and $[\mathbb{C}\mathbf{S}]\mathbf{T} \neq \mathbb{C}[\mathbf{S}\mathbf{T}]$, while the expressions $\mathfrak{c}(\mathbf{T}\mathbf{w})$ and $(\mathfrak{c}\mathbf{T})\cdot\mathbf{w}$ are not even of the same tensor order. However, such ambiguities are readily avoided by the judicious use of parentheses.

The contraction in (2.22) is generalized to higher orders according to

$$\begin{aligned} \mathfrak{c} \cdot \mathfrak{d} &= \mathfrak{c}_{ijk}\, \mathfrak{d}_{ijk} \quad , \\ \mathbb{C} \cdot \mathbb{D} &= \mathbb{C}_{ijkl}\, \mathbb{D}_{ijkl} \quad , \end{aligned} \tag{2.27}$$

from which orthogonality and the norm are derived. To align the notation in $(2.26)_{2,4}$ with Equation $(2.4)_2$ for vectors, the tensor components may alternatively be written in terms of contractions $\mathfrak{c}_{ijk} = \mathfrak{c} \cdot [\mathbf{e}_i \otimes \mathbf{e}_j \otimes \mathbf{e}_k]$ and $\mathbb{C}_{ijkl} = \mathbb{C} \cdot [\mathbf{e}_i \otimes \mathbf{e}_j \otimes \mathbf{e}_k \otimes \mathbf{e}_l]$, respectively.

Previously introduced vector and tensor operations may occasionally be substituted with higher-order tensor expressions. For example, the cross product (2.5) and scalar triple product (2.7) are given by

$$\begin{aligned} \mathbf{u} \times \mathbf{v} &= \epsilon_{ijk}\, u_i\, v_j\, \mathbf{e}_k = \mathfrak{e}\big[\mathbf{u} \otimes \mathbf{v}\big] \quad , \\ \big[\mathbf{u}, \mathbf{v}, \mathbf{w}\big] &= \epsilon_{ijk}\, u_i\, v_j\, w_k = \mathfrak{e} \cdot \big[\mathbf{u} \otimes \mathbf{v} \otimes \mathbf{w}\big] \quad , \end{aligned} \tag{2.28}$$

where $\mathfrak{e} = \epsilon_{ijk} \mathbf{e}_i \otimes \mathbf{e}_j \otimes \mathbf{e}_k$ represents the third-order *permutation tensor*. The symmetric and skew-symmetric parts of a tensor may be written as

$$\mathrm{sym}\big[\mathbf{T}\big] = \mathbb{I}^{\mathrm{sym}}\, \mathbf{T} \quad , \quad \mathrm{skw}\big[\mathbf{T}\big] = \mathbb{I}^{\mathrm{skw}}\, \mathbf{T} \quad , \tag{2.29}$$

by separating the *fourth-order identity tensor* $\mathbb{I} = \delta_{ik}\delta_{jl}\, \mathbf{e}_i \otimes \mathbf{e}_j \otimes \mathbf{e}_k \otimes \mathbf{e}_l = \mathbb{I}^{\mathrm{sym}} + \mathbb{I}^{\mathrm{skw}}$ into the components for the symmetric and skew-symmetric parts, $\frac{1}{2}(\delta_{ik}\delta_{jl} \pm \delta_{jk}\delta_{il})$. Lastly, the *trace identity tensor* is defined as $\mathbb{I}^{\mathrm{tr}} = \mathbf{I} \otimes \mathbf{I}$.

[5] Vectors may be regarded as first-order tensors and scalars are of order zero.

In conclusion, it is emphasized that tensors are *not* matrices. Only when expressed in CARTESIAN components relative to a right-hand orthonormal basis do analogies arise with the linear algebra of 3×3 matrices and 3×1 vectors. Note that the components T_{ij} in $(2.10)_2$ are defined by convention to preserve these similarities, despite the converse notation ($\mathbf{T}=T_{ji}\,\mathbf{e}_i\otimes\mathbf{e}_j$, $T_{ji}=\mathbf{e}_i\cdot\mathbf{T}\,\mathbf{e}_j$) being equally permissible. However, linear algebra struggles to describe higher-order tensor interactions, such as $\mathbf{S}=\mathbb{C}\mathbf{T}$. Alternative matrix representations have been devised to overcome this deficiency. For example, in the so-called VOIGT *notation* the components of symmetric tensors $\mathbf{S},\mathbf{T}$ are reduced to 6×1 vectors acted upon by 6×6 matrices instead of fourth-order tensors.

2.1.4 Identites of Tensor Algebra

The properties of the KRONECKER delta $(2.3)_2$ and permutation symbol $(2.5)_2$ lead to

$$\begin{aligned}\|\mathbf{I}\|_2^2 &= \mathbf{I}\cdot\mathbf{I} = \delta_{kk} &&= 3 \quad ,\\ \|\boldsymbol{\mathfrak{e}}\|_2^2 &= \boldsymbol{\mathfrak{e}}\cdot\boldsymbol{\mathfrak{e}} = \epsilon_{ijk}\,\epsilon_{ijk} &&= 6 \quad ,\\ \boldsymbol{\mathfrak{e}}\,\mathbf{I} &= \epsilon_{ijk}\,\delta_{jk}\,\mathbf{e}_i &&= \mathbf{0} \quad .\end{aligned} \tag{2.30}$$

Furthermore, it is readily verified that δ_{ij} and ϵ_{ijk} are related by

$$\begin{aligned}\epsilon_{ijk}\,\epsilon_{ijm} &= 2\,\delta_{km} \quad ,\\ \epsilon_{ijk}\,\epsilon_{ilm} &= \delta_{jl}\,\delta_{km} - \delta_{jm}\,\delta_{kl} \quad ,\\ \epsilon_{ijk}\,\epsilon_{lmn} &= \delta_{il}\big(\delta_{jm}\,\delta_{kn}-\delta_{jn}\,\delta_{km}\big)+\delta_{im}\big(\delta_{jn}\,\delta_{kl}-\delta_{jl}\,\delta_{kn}\big)+\delta_{in}\big(\delta_{jl}\,\delta_{km}-\delta_{jm}\,\delta_{kl}\big) \quad .\end{aligned} \tag{2.31}$$

Note that $(2.30)_3$ originates in the symmetry of $\mathbf{I}$ and skew-symmetry (with respect to any two of its indices) of $\boldsymbol{\mathfrak{e}}$. It fact, any symmetric and skew-symmetric tensors are mutually orthogonal,

$$\big[\mathrm{skw}\mathbf{S}\big]\cdot\big[\mathrm{sym}\mathbf{T}\big] = 0 \quad \forall \quad \mathbf{S},\mathbf{T}\in\mathcal{L}(E^3,E^3) \quad . \tag{2.32}$$

Using $(2.31)_2$, the so-called *vector triple product* is expressed by

$$\mathbf{u}\times\big(\mathbf{v}\times\mathbf{w}\big) = \big(\mathbf{u}\cdot\mathbf{w}\big)\mathbf{v}-\big(\mathbf{v}\cdot\mathbf{u}\big)\mathbf{w} \quad . \tag{2.33}$$

The principal invariants in (2.13) are derived from the requirement, that

$$\begin{aligned}\big[\mathbf{u},\mathbf{v},\mathbf{w}\big]\,\mathrm{I}_{\mathbf{T}} &= \big[\mathbf{T}\mathbf{u},\mathbf{v},\mathbf{w}\big]+\big[\mathbf{u},\mathbf{T}\mathbf{v},\mathbf{w}\big]+\big[\mathbf{u},\mathbf{v},\mathbf{T}\mathbf{w}\big] \quad ,\\ \big[\mathbf{u},\mathbf{v},\mathbf{w}\big]\,\mathrm{II}_{\mathbf{T}} &= \big[\mathbf{T}\mathbf{u},\mathbf{T}\mathbf{v},\mathbf{w}\big]+\big[\mathbf{u},\mathbf{T}\mathbf{v},\mathbf{T}\mathbf{w}\big]+\big[\mathbf{T}\mathbf{u},\mathbf{v},\mathbf{T}\mathbf{w}\big] \quad ,\\ \big[\mathbf{u},\mathbf{v},\mathbf{w}\big]\,\mathrm{III}_{\mathbf{T}} &= \big[\mathbf{T}\mathbf{u},\mathbf{T}\mathbf{v},\mathbf{T}\mathbf{w}\big] \quad ,\end{aligned} \tag{2.34}$$

for all vectors $\mathbf{u},\mathbf{v},\mathbf{w}\in E^3$. This highlights the close relationship between the invariants and the scalar triple product. Indeed, borrowing the terminology of linear

algebra, the determinant of $\mathbf{T}$ in $(2.34)_3$ can be stated as a scalar triple product of the 'column vectors' of its components, $\det \mathbf{T} = [\mathbf{T}\mathbf{e}_1, \mathbf{T}\mathbf{e}_2, \mathbf{T}\mathbf{e}_3]$. The determinant further exhibits the properties

$$\begin{aligned} \det\left[\mathbf{T}^{\mathrm{T}}\right] &= \det \mathbf{T} && , \\ \det\left[\alpha \mathbf{S}\mathbf{T}\right] &= \alpha^3 \det \mathbf{S} \det \mathbf{T} && , \\ \det\left[\mathbf{S}+\mathbf{T}\right] &\geq \det \mathbf{S} + \det \mathbf{T} && . \end{aligned} \tag{2.35}$$

It follows from $\det \mathbf{I} = 1$ and Equation $(2.35)_2$, that the determinant and the inverse are commutatitve, $\det[\mathbf{T}^{-1}] = (\det \mathbf{T})^{-1}$. The transpose (2.16) and inverse (2.19) of two (invertible) second-order tensors obey

$$\begin{aligned} \left[\mathbf{S}+\mathbf{T}\right]^{\mathrm{T}} &= \mathbf{S}^{\mathrm{T}} + \mathbf{T}^{\mathrm{T}} && , \\ \left[\mathbf{S}\mathbf{T}\right]^{\mathrm{T}} &= \mathbf{T}^{\mathrm{T}}\mathbf{S}^{\mathrm{T}} && , \\ \left[\mathbf{S}\mathbf{T}\right]^{-1} &= \mathbf{T}^{-1}\mathbf{S}^{-1} && . \end{aligned} \tag{2.36}$$

In view of the tensor product (2.8), multiplication (2.11), and transpose (2.16), it is seen that the the dot, vector, and tensor products can be rearranged according to

$$\begin{aligned} \mathbf{S}\mathbf{u} \cdot \mathbf{T}\mathbf{v} &= \mathbf{u} \cdot \mathbf{S}^{\mathrm{T}}\mathbf{T}\mathbf{v} = \mathbf{T}^{\mathrm{T}}\mathbf{S}\mathbf{u} \cdot \mathbf{v} && , \\ \mathbf{T}\mathbf{u} \times \mathbf{T}\mathbf{v} &= \big(\det \mathbf{T}\big)\, \mathbf{T}^{-\mathrm{T}}\big(\mathbf{u} \times \mathbf{v}\big) && , \\ \big(\mathbf{S}\mathbf{u}\big) \otimes \big(\mathbf{T}\mathbf{v}\big) &= \mathbf{S}\big[\mathbf{u} \otimes \mathbf{v}\big]\mathbf{T}^{\mathrm{T}} && , \end{aligned} \tag{2.37}$$

for all $\mathbf{u}, \mathbf{v} \in E^3$ and $\mathbf{S}, \mathbf{T} \in \mathcal{L}(E^3, E^3)$. For orthogonal tensors $\mathbf{Q} \in \mathrm{Orth}$, the identities in (2.37) simplify to

$$\begin{aligned} \mathbf{Q}\mathbf{u} \cdot \mathbf{Q}\mathbf{v} &= \mathbf{u} \cdot \mathbf{v} && , \\ \mathbf{Q}\mathbf{u} \times \mathbf{Q}\mathbf{v} &= \pm \mathbf{Q}\big(\mathbf{u} \times \mathbf{v}\big) && , \\ \big(\mathbf{Q}\mathbf{u}\big) \otimes \big(\mathbf{Q}\mathbf{v}\big) &= \mathbf{Q}\big[\mathbf{u} \otimes \mathbf{v}\big]\mathbf{Q}^{\mathrm{T}} && . \end{aligned} \tag{2.38}$$

According to $(2.38)_1$, orthogonal tensors $\mathbf{Q}$ preserve the length and relative angle between vectors they act upon. Equation $(2.38)_2$ implies the inversion of any vector triad if $\det \mathbf{Q} = -1$, whereas proper orthogonal tensors represent only rotations.

2.1.5 Generalized Derivatives and Differential Operators

Let $\mathcal{F}(\mathbf{x})$ be a real-, vector- or tensor-valued fields of a vector-valued argument $\mathbf{x}$. The *gradient* of $\mathcal{F}$ with respect to $\mathbf{x}$ is defined by the relation

$$\frac{\mathrm{d}}{\mathrm{d}\alpha}\Big[\mathcal{F}(\mathbf{x}+\alpha\mathbf{h})\Big]_{\alpha=0} = \frac{\partial \mathcal{F}}{\partial \mathbf{x}} \cdot \mathbf{h} = \big[\mathrm{grad}\, \mathcal{F}\big] \cdot \mathbf{h} = \mathrm{D}\mathcal{F}(\mathbf{x}, \mathbf{h}) \quad \forall \quad \mathbf{h} \in E^3 \quad , \tag{2.39}$$

where the dot $(\cdot)$ indicates either a dot product with the vector $\mathbf{h}$ if $\mathcal{F}$ is real-valued, or a tensor multiplication otherwise. Note that the application of the gradient to $\mathcal{F}$

increases its tensor order by one. Similarly, let $\mathcal{F}(\mathbf{T})$ instead depend on a tensor-valued argument $\mathbf{T}$. The *tensor derivative* of $\mathcal{F}$ with respect to $\mathbf{T}$ is defined such that it satisfies

$$\frac{\mathrm{d}}{\mathrm{d}\alpha}\Big[\mathcal{F}(\mathbf{T}+\alpha\mathbf{H})\Big]_{\alpha=0} \;=\; \frac{\partial\mathcal{F}}{\partial\mathbf{T}}\cdot\mathbf{H} \;=\; \mathrm{D}\mathcal{F}(\mathbf{T},\mathbf{H}) \quad \forall \quad \mathbf{H}\in\mathcal{L}(E^3,E^3) \quad , \tag{2.40}$$

where $(\,\cdot\,)$ represents a contraction if $\mathcal{F}$ is real-valued, or higher-order tensor multiplication otherwise, with the second-order tensor $\mathbf{H}$. The tensor derivative of $\mathcal{F}$ increases its tensor order by two. The right-hand side is called a Gâteaux *differential* or generalized directional derivative.

Let the vector $\mathbf{v}(\mathbf{x})$ and second-order tensor $\mathbf{T}(\mathbf{x})$ be continuously differentiable functions of $\mathbf{x}$, and let $\mathbf{h}$ be an arbitrary constant vector. Based on the gradient in (2.39), the *divergence* (of a vector and a tensor) and the *curl* (of a vector) are defined by

$$\begin{aligned} \operatorname{div}\mathbf{w} \;&=\; \operatorname{tr}\big[\operatorname{grad}\mathbf{w}\big] \quad , \\ \big(\operatorname{div}\mathbf{T}\big)\cdot\mathbf{h} \;&=\; \operatorname{div}\big(\mathbf{T}^{\mathrm{T}}\mathbf{h}\big) \quad , \\ \big(\operatorname{curl}\mathbf{w}\big)\cdot\mathbf{h} \;&=\; \operatorname{div}\big(\mathbf{w}\times\mathbf{h}\big) \quad . \end{aligned} \tag{2.41}$$

The gradient, divergence, and curl are more conveniently interpreted as differential operators, expressed using the Cartesian components x_i of $\mathbf{x}$ with respect to an orthonormal right-hand basis $\mathbf{e}_i$ by[6]

$$\operatorname{grad}[\,\cdot\,] \;=\; \frac{\partial[\,\cdot\,]}{\partial x_i}\otimes\mathbf{e}_i \quad , \quad \operatorname{div}[\,\cdot\,] \;=\; \frac{\partial[\,\cdot\,]}{\partial x_i}\cdot\mathbf{e}_i \quad , \quad \operatorname{curl}[\,\cdot\,] \;=\; \mathbf{e}_i\times\frac{\partial[\,\cdot\,]}{\partial x_i} \quad . \tag{2.42}$$

For example, the application of (2.42) to a vector $\mathbf{w}=w_i\mathbf{e}_i$ produces

$$\operatorname{grad}\mathbf{w} \;=\; w_{i,j}\mathbf{e}_i\otimes\mathbf{e}_j \quad , \quad \operatorname{div}\mathbf{w} \;=\; w_{i,i} \quad , \quad \operatorname{curl}\mathbf{w} \;=\; \epsilon_{ijk}w_{i,j}\mathbf{e}_k \quad . \tag{2.43}$$

For brevity, the spatial derivatives are identified in index notation by a preceding comma. For instance the components $w_{i,j}$ of the second-order tensor $[\operatorname{grad}\mathbf{w}]$ represent the partial derivative of component w_i with respect to coordinate basis $\mathbf{e}_j$.

2.1.6 Identites of Tensor Calculus

Some useful results of vector and tensor calculus are listed below without proof. To this end, let the real-valued $\alpha(\mathbf{x})$, vectors $\mathbf{u}(\mathbf{x})$, $\mathbf{v}(\mathbf{x})$, $\mathbf{w}(\mathbf{x})$, and second-order tensors $\mathbf{S}(\mathbf{x})$, $\mathbf{T}(\mathbf{x})$ be continuously differentiable fields of the vector $\mathbf{x}$. The gradient of a scalar is identically expressed as a divergence

$$\operatorname{grad}\big(\alpha\big) \;=\; \operatorname{div}\big[\alpha\mathbf{I}\big] \quad \text{where} \quad \mathbf{I} \;=\; \delta_{ij}\,\mathbf{e}_i\otimes\mathbf{e}_j \quad . \tag{2.44}$$

[6] The curl operator as expressed in $(2.42)_3$ applies only to vectors.

The product rule of differentiation is applied to the gradient to obtain the relations

$$\begin{aligned} \operatorname{grad}\big(\alpha\,\mathbf{w}\big) &= \alpha\,\operatorname{grad}\mathbf{w} + \mathbf{w}\otimes\operatorname{grad}\alpha \quad , \\ \operatorname{grad}\big(\mathbf{u}\cdot\mathbf{v}\big) &= \big[\operatorname{grad}^{\mathrm{T}}\mathbf{u}\big]\mathbf{v} + \big[\operatorname{grad}^{\mathrm{T}}\mathbf{v}\big]\mathbf{u} \quad , \end{aligned} \tag{2.45}$$

where the notation $\operatorname{grad}^{\mathrm{T}}\mathbf{w} = [\operatorname{grad}\mathbf{w}]^{\mathrm{T}} = w_{i,j}\,\mathbf{e}_j\otimes\mathbf{e}_i$ was used. Similarly, the product rule yields for the divergence

$$\begin{aligned} \operatorname{div}\big(\alpha\,\mathbf{w}\big) &= \alpha\,\operatorname{div}\mathbf{w} + \mathbf{w}\cdot\operatorname{grad}\alpha \quad , \\ \operatorname{div}\big[\alpha\,\mathbf{T}\big] &= \mathbf{T}\big(\operatorname{grad}\alpha\big) + \alpha\,\operatorname{div}\mathbf{T} \quad , \\ \operatorname{div}\big(\mathbf{T}\mathbf{w}\big) &= \mathbf{T}^{\mathrm{T}}\cdot\big[\operatorname{grad}\mathbf{w}\big] + \operatorname{div}\big[\mathbf{T}^{\mathrm{T}}\big]\cdot\mathbf{w} \quad , \\ \operatorname{div}\big[\mathbf{S}\mathbf{T}\big] &= \big[\operatorname{grad}\mathbf{S}\big]\,\mathbf{T} + \mathbf{S}\big(\operatorname{div}\mathbf{T}\big) \quad , \\ \operatorname{div}\big[\mathbf{u}\otimes\mathbf{v}\big] &= \big[\operatorname{grad}\mathbf{u}\big]\,\mathbf{v} + \big(\operatorname{div}\mathbf{v}\big)\,\mathbf{u} \quad , \\ \operatorname{div}\big(\mathbf{u}\times\mathbf{v}\big) &= \mathbf{v}\cdot\operatorname{curl}\mathbf{u} - \mathbf{u}\cdot\operatorname{curl}\mathbf{v} \quad . \end{aligned} \tag{2.46}$$

Note that $\operatorname{grad}\mathbf{S}$ in $(2.46)_4$ constitutes a third-order tensor, which according to $(2.24)_2$ produces a vector $[\operatorname{grad}\mathbf{S}]\mathbf{T}$. Meanwhile, the curl expands into

$$\begin{aligned} \operatorname{curl}\big(\alpha\,\mathbf{w}\big) &= \alpha\,\operatorname{curl}\mathbf{w} + \big(\operatorname{grad}\alpha\big)\times\mathbf{w} \quad , \\ \operatorname{curl}\big(\mathbf{u}\times\mathbf{v}\big) &= \operatorname{div}\big[\mathbf{u}\otimes\mathbf{v} - \mathbf{v}\otimes\mathbf{u}\big] \quad . \end{aligned} \tag{2.47}$$

It is further noted that in view of $(2.31)_2$ the vector product of a curl exhibits the property

$$\big(\operatorname{curl}\mathbf{u}\big)\times\mathbf{v} = \big[\operatorname{grad}\mathbf{u} - \operatorname{grad}^{\mathrm{T}}\mathbf{u}\big]\,\mathbf{v} \quad . \tag{2.48}$$

Lastly, the repeated application of differential operators leads to the identities

$$\begin{aligned} \operatorname{curl}\big(\operatorname{grad}\alpha\big) &= \mathbf{0} \quad , \\ \operatorname{div}\big(\operatorname{curl}\mathbf{w}\big) &= 0 \quad , \\ \operatorname{curl}\big(\operatorname{curl}\mathbf{w}\big) &= \operatorname{grad}\big(\operatorname{div}\mathbf{w}\big) - \Delta\mathbf{w} \quad , \\ \operatorname{grad}\big(\operatorname{div}\mathbf{w}\big) &= \operatorname{div}\big[\operatorname{grad}^{\mathrm{T}}\mathbf{w}\big] \quad , \end{aligned} \tag{2.49}$$

where $\Delta(\,\cdot\,) = \operatorname{div}\{\operatorname{grad}[\,\cdot\,]\}$ denotes the LAPLACE *operator*, which is given in components as $\Delta\alpha = \alpha_{,kk}$ for scalars and $\Delta\mathbf{w} = w_{i,kk}\,\mathbf{e}_i$ for vectors. The relations (2.45 - 49) are most conveniently verified in indicial notation.

2.1.7 Integral Theorems

Integral theorems are an essential tool for the manipulation of scalar- and vector-valued balance equations. Formal mathematical proofs of the upcoming theorems may be found in standard monographs on vector calculus, such as MARSDEN and TROMBA [85, Chapter 8] or STEWART [138, Chapter 16].

The *divergence* (or GAUSS') *theorem* states that for any open, bounded region[7] $\mathcal{P} \subset \mathcal{R}$ with piecewise smooth boundary $\partial\mathcal{P}$, the continuously differentiable vector-valued field $\mathbf{w}(\mathbf{x})$ satisfies

$$\int_{\mathcal{P}} \operatorname{div} \mathbf{w} \, \mathrm{d}v \;=\; \int_{\partial\mathcal{P}} \mathbf{w} \cdot \mathbf{n} \, \mathrm{d}a \quad . \tag{2.50}$$

The right-hand side represents the *flux of* $\mathbf{w}$ *through* $\partial\mathcal{P}$, where $\mathbf{n}(\mathbf{x})$ represents the outward normal unit vector to the boundary $\partial\mathcal{P}$. This classical form of the divergence theorem leads to a number of useful corollaries, two of which are frequently employed in this text. First, Equation (2.50) implies for the curl, that

$$\int_{\mathcal{P}} \operatorname{curl} \mathbf{w} \, \mathrm{d}v \;=\; \int_{\partial\mathcal{P}} \mathbf{n} \times \mathbf{w} \, \mathrm{d}a \quad . \tag{2.51}$$

Second, a continuously differentiable tensor-valued field $\mathbf{T}(\mathbf{x})$ satisfies

$$\int_{\mathcal{P}} \operatorname{div} \mathbf{T} \, \mathrm{d}v \;=\; \int_{\partial\mathcal{P}} \mathbf{T}\mathbf{n} \, \mathrm{d}a \quad . \tag{2.52}$$

A brief derivation of Equations (2.51) and (2.52) is provided in Appendix A.1.

The (KELVIN-) STOKES *theorem* asserts that for an open surface $\mathcal{A}$ bounded by a closed, non-intersecting curve $\mathcal{C}$,

$$\int_{\mathcal{A}} \operatorname{curl} \mathbf{w} \cdot \mathbf{n} \, \mathrm{d}a \;=\; \oint_{\mathcal{C}} \mathbf{w} \cdot \mathrm{d}\mathbf{x} \quad . \tag{2.53}$$

The flux of $\operatorname{curl}\mathbf{w}$ through $\mathcal{A}$ is thus equal to the *circulation of* $\mathbf{w}$ *around* $\mathcal{C}$, where $\mathrm{d}\mathbf{x}$ is the infinitesimal line element tracing the boundary $\mathcal{C}$ according to the right-hand rule around the surface normal $\mathbf{n}$. If the surface $\mathcal{A}$ is closed[8] then the right-hand side of (2.53) vanishes since $\mathcal{C} \in \emptyset$. In view of the divergence theorem (2.50) this confirms that $\operatorname{curl}\mathbf{w}$ is divergence-free, see Equation $(2.49)_2$. The STOKES theorem is a three dimensional generalization of the so-called GREEN*'s theorem* (not introduced here).

The *gradient theorem*, also called the *fundamental theorem of calculus for line integrals*, states that the *line* (or *path*) *integral* of the gradient of a differentiable scalar field $\alpha(\mathbf{x})$ is path independent,

$$\int_{\mathcal{S}} \operatorname{grad} \alpha \cdot \mathrm{d}\mathbf{x} \;=\; \left[\alpha\right]_{\mathbf{s}_1}^{\mathbf{s}_2} \quad . \tag{2.54}$$

Here, $\mathcal{S}$ symbolizes an arbitrary open path originating at a point $\mathbf{s}_1$ and ending at $\mathbf{s}_2$, with $[\alpha]_{\mathbf{s}_1}^{\mathbf{s}_2} = \alpha(\mathbf{s}_2) - \alpha(\mathbf{s}_1)$. The path is traced by infinitesimal line segments $\mathrm{d}\mathbf{x}$ in the

[7] The region is considered open if it does not contain its boundary, and bounded (*i.e.*, compact) if it may be enclosed by a finite sphere. A smooth boundary has a well-defined outward unit normal.

[8] The surface $\mathcal{A}$ is said to be closed if it is bounded (*i.e.*, compact) and has *no* boundary $\mathcal{C}$. Therefore, such a surface itself corresponds to the boundary $\partial\mathcal{P}$ of a bounded region $\mathcal{P}$.

appropriate direction along $\mathcal{S}$. According to (2.54), the integral depends only on the difference in value of α at the boundary. Vector fields which obey this property are termed *conservative*. Their circulation vanishes because $\mathbf{s}_1$ coincides with $\mathbf{s}_2$ when $\mathcal{S}$ is reduced to a closed curve $\mathcal{C}$. Using STOKES' theorem (2.53) and the localization theorem introduced below in (2.55) (applied to the open surface $\mathcal{A}$), this further implies that conservative vector fields are curl-free, *i.e.*, *irrotational*, which is in agreement with Equation $(2.49)_1$.

Finally, the *localization theorem* argues that a continuous (scalar, vectorial, or tensorial) quantity $\mathcal{F}(\mathbf{x})$, for which any arbitrary region $\mathcal{P} \subset \mathcal{R}$ yields

$$\int_{\mathcal{P}} \mathcal{F} \, \mathrm{d}v \;=\; 0 \quad \forall \quad \mathcal{P} \subset \mathcal{R} \quad \longleftrightarrow \quad \mathcal{F} \;=\; 0 \quad \forall \quad \mathbf{x} \in \mathcal{R} \tag{2.55}$$

must vanish everywhere in $\mathcal{R}$. This theorem allows for integral equations to be converted into a local, differential form. The same argument can be made for the localization of surface integrals over arbitrary open areas $\mathcal{A}$, as well as line integrals over arbitrary open paths $\mathcal{S}$. The theorem does *not* hold when the domain of the integral is closed. Indeed, *closed* surfaces $\partial\mathcal{P}$ or curves $\mathcal{C}$ can be converted into the *open* domains $\mathcal{P}$ or $\mathcal{A}$ using (2.50) or (2.53), respectively, upon which the localization theorem applies. However, the ensuing local equations confer information only about the divergence, gradient, or curl of the original quantity.

2.1.8 Potentials and the Helmholtz Theorem

Due to the structure of MAXWELL's equations of electromagnetism, it can be advantageous to view vector fields in terms of their irrotational and divergence-free parts. This is especially true in the context of electrostatics and magnetostatics, see Section 3.7. The following discussion is based on GRIFFITHS [38, Chapter 1.6].

Any irrotational vector field $\mathbf{w}(\mathbf{x})$ can be expressed by the gradient of a scalar potential $\alpha(\mathbf{x})$,

$$\operatorname{curl} \mathbf{w} \;=\; \mathbf{0} \quad \leftrightarrow \quad \mathbf{w} \;=\; -\operatorname{grad} \alpha \quad , \tag{2.56}$$

where the negative sign is placed by convention. Note that α is only unique to within an arbitrary constant. Note that $\mathbf{w}$ in (2.56) represents a conservative vector field and satisfies the gradient theorem (2.54).

Any divergence-free vector field $\mathbf{w}(\mathbf{x})$ can be written in terms of the curl of a vector potential $\mathbf{a}(\mathbf{x})$,

$$\operatorname{div} \mathbf{w} \;=\; \mathbf{0} \quad \leftrightarrow \quad \mathbf{w} \;=\; \operatorname{curl} \mathbf{a} \quad . \tag{2.57}$$

The potential $\mathbf{a}$ is determined to within an arbitrary irrotational field $\operatorname{grad} \alpha$ and thus not unique. Divergence-free vector fields are sometimes called *solenoidal* or *incompressible*.

Any arbitrary vector field $\mathbf{w}(\mathbf{x})$ can be decomposed into a linear combination of an irrotational part and a divergence-free part,

$$\mathbf{w} \;=\; -\operatorname{grad}\alpha + \operatorname{curl}\mathbf{a} \quad . \tag{2.58}$$

However, note that this decomposition is not unique because there are non-trivial vector fields (so-called *harmonic* vector fields) whose curl and divergence are both zero. Harmonic vector fields are thus attributable to either term on the right side of (2.58). Nevertheless, boundary conditions may be imposed on the potentials α and $\mathbf{a}$ in order to render the decomposition unique.[9]

Let $\mathbf{w}(\mathbf{x})$ represent an unknown differentiable vector field which satisfies the system of coupled differential equations,

$$\begin{aligned} \operatorname{div}\mathbf{w} \;&=\; d \quad , \\ \operatorname{curl}\mathbf{w} \;&=\; \mathbf{c} \quad , \end{aligned} \tag{2.59}$$

where $d(\mathbf{x})$ and $\mathbf{c}(\mathbf{x})$ are known scalar- and vector-valued functions, respectively.[10] Again, a unique solution is available only if provided with appropriate boundary conditions. For example, the Helmholtz *theorem* guarantees that $\mathbf{w}$ is uniquely defined by d and $\mathbf{c}$ if $\mathbf{w}(\mathbf{x})$ goes to zero at infinity, see Griffiths [38, Appendix B] for a proof.

2.2 Kinematics of Large Deformations

In preparation for the derivation of the global and local balance laws of thermomechanics, the mathematical framework for the description of the motion of solid continua is briefly discussed in the following.

2.2.1 Motion

Consider a so-called Lagrangian description of the motion of a continuous body, represented by an invertible mapping $\boldsymbol{\chi}\colon E^3 \times \mathbb{R} \mapsto E^3$, with

$$\mathbf{x} \;=\; \boldsymbol{\chi}(\mathbf{X}, t) \quad . \tag{2.60}$$

The *motion* $\boldsymbol{\chi}$ maps a *referential point* $\mathbf{X} \in \mathcal{R}_0$ of the body to its current *spatial position* $\mathbf{x} \in \mathcal{R}$ at *time* t, and is assumed to be continuously differentiable in both arguments. The inverse motion $\boldsymbol{\chi}^{-1}$, with

$$\mathbf{X} \;=\; \boldsymbol{\chi}^{-1}(\mathbf{x}, t) \quad , \tag{2.61}$$

[9] Boundary conditions ensure the uniqueness, for example, of the so-called Helmholtz-Hodge *decomposition*, see Abraham *et al.* [1], Bhatia *et al.* [6], and Tong *et al.* [143].

[10] For Equations $(2.59)_{1,2}$ to be well-posed, $\mathbf{c}$ must of course satisfy the condition $\operatorname{div}\mathbf{c} = 0$, see $(2.49)_2$.

identifies the material point $\mathbf{X}$ of the reference configuration, which at time t occupies a given spatial location $\mathbf{x}$. Note that the motion is inverted with respect to the first argument at *fixed* t. This is emphasized by some authors with the notation $\mathbf{x}=\boldsymbol{\chi}(\mathbf{X},t)=\boldsymbol{\chi}_t(\mathbf{X})$ and thus $\mathbf{X}=\boldsymbol{\chi}_t^{-1}(\mathbf{x})$. The vectors $\mathbf{x}$ and $\mathbf{X}$ are resolved in components with respect to fixed right-hand orthonormal bases $\mathbf{e}_i$ and $\mathbf{E}_A$ associated with the current and reference configurations, respectively, according to

$$\mathbf{x} \;=\; x_i\,\mathbf{e}_i \;=\; \chi_i(\mathbf{X},t)\,\mathbf{e}_i \quad \text{and} \quad \mathbf{X} \;=\; X_A\,\mathbf{E}_A \;=\; \chi_A^{-1}(\mathbf{x},t)\,\mathbf{E}_A \quad . \tag{2.62}$$

The lower- and upper-case indices refer to the spatial and referential bases, respectively.

The reference configuration $\mathcal{R}_0$ often, but not necessarily, corresponds to a previous state of the body such as an initially stress-free configuration. If so, a relative *displacement* $\mathbf{u}$ may be specified by

$$\mathbf{u} \;=\; \mathbf{x}-\mathbf{X} \;=\; u_A\,\mathbf{E}_A \;=\; u_i\,\mathbf{e}_i \quad , \tag{2.63}$$

whose components may be resolved in both the referential or current bases. With the aid of the motion (2.60) and its inverse, the functional form of $\mathbf{u}$ may be expressed either in terms of the referential coordinates $\hat{\mathbf{u}}(\mathbf{X},t)=\boldsymbol{\chi}(\mathbf{X},t)-\mathbf{X}$ (LAGRANGIAN description) or the spatial coordinates $\tilde{\mathbf{u}}(\mathbf{x},t)=\mathbf{x}-\boldsymbol{\chi}^{-1}(\mathbf{x},t)$ (EULERIAN description).

The distributions of physical quantities associated with a body (such as the temperature, electric current, or mechanical stress) are described by (real-, vector-, or tensor-valued) fields of the form $\mathcal{F}=\hat{\mathcal{F}}(\mathbf{X},t)=\tilde{\mathcal{F}}(\mathbf{x},t)$. Owing to the presumed invertibility of the motion (2.60), the referential and spatial descriptions of $\mathcal{F}$ are entirely interchangeable,

$$\mathcal{F} \;=\; \tilde{\mathcal{F}}(\mathbf{x},t) \;=\; \tilde{\mathcal{F}}(\boldsymbol{\chi}(\mathbf{X},t),t) \;=\; \hat{\mathcal{F}}(\mathbf{X},t) \;=\; \hat{\mathcal{F}}(\boldsymbol{\chi}^{-1}(\mathbf{x},t),t) \quad . \tag{2.64}$$

While representing the same physical quantity $\mathcal{F}$, the functional form of the two descriptions differs. However, the rules of differentiation and integration of $\mathcal{F}$ presented in Section 2.1 apply irrespectively.[11] Capitalized symbols $\mathrm{Grad}[\cdot]$, $\mathrm{Div}[\cdot]$, and $\mathrm{Curl}[\cdot]$ signify *referential* differential operators, as opposed to their *spatial* counterparts (2.42). For partial time derivatives, the *tilde* and *hat* accents help to clarify whether $\mathbf{x}$ or $\mathbf{X}$ is intended to be fixed, see later in Equation (2.95).

2.2.2 Deformation

Consider the linear mapping of an infinitesimal referential line element $\mathrm{d}\mathbf{X}$ at material point $\mathbf{X}$ to its deformed counterpart $\mathrm{d}\mathbf{x}$ at $(\mathbf{x},t)$, given by

$$\mathrm{d}\mathbf{x} \;=\; \mathbf{F}\,\mathrm{d}\mathbf{X} \quad . \tag{2.65}$$

[11] Note that the mapping $\boldsymbol{\chi}(\mathbf{X},t)$ is assumed to be continuously differentiable in $\mathbf{x}$ and t, see (2.60). Therefore if $\tilde{\mathcal{F}}(\mathbf{x},t)$ is differentiable, then so is $\hat{\mathcal{F}}(\mathbf{X},t)$. Furthermore, if the boundary $\partial\mathcal{P}$ of a bounded region $\mathcal{P}\subset\mathcal{R}$ is smooth, then so is $\partial\mathcal{P}_0$ of the reference configuration $\mathcal{P}_0\subset\mathcal{R}_0$.

The *deformation gradient* $\mathbf{F}$, which is thus a measure of both the stretch and rotation of $\mathrm{d}\mathbf{X}$, is defined as

$$\mathbf{F} \;=\; \frac{\partial \boldsymbol{\chi}(\mathbf{X},t)}{\partial \mathbf{X}} \;=\; \mathrm{Grad}\,\boldsymbol{\chi} \quad \text{or} \quad F_{iA} \;=\; \frac{\partial \chi_i}{\partial X_A} \;=\; \chi_{i,A} \quad , \tag{2.66}$$

where $\mathrm{Grad}[\cdot] = \frac{\partial [\cdot]}{\partial \mathbf{X}} = [\cdot]_{,A} \otimes \mathbf{E}_A$ is the referential version of Equation $(2.42)_1$. Note that $\mathbf{F} = F_{iA}\,\mathbf{e}_i \otimes \mathbf{E}_A$ is a so-called *two-point tensor*, because its components are rooted in both the spatial and the referential bases.[12] If the current configuration coincides with the reference, the deformation gradient evaluates to $\mathbf{F} = \mathbf{1}$, where $\mathbf{1} = \delta_{iA}\,\mathbf{e}_i \otimes \mathbf{E}_A$ denotes the *two-point unit tensor*.

The inverse deformation gradient $\mathbf{F}^{-1} = F^{-1}_{Ai}\,\mathbf{E}_A \otimes \mathbf{e}_i$ maps a spatial line element $\mathrm{d}\mathbf{x}$ at $(\mathbf{x},t)$ to its original $\mathrm{d}\mathbf{X} = \mathbf{F}^{-1}\mathrm{d}\mathbf{x}$ as in (2.65). It may be expressed by the spatial gradient of the inverse motion $(2.60)_2$,

$$\mathbf{F}^{-1} \;=\; \frac{\partial \boldsymbol{\chi}^{-1}(\mathbf{x},t)}{\partial \mathbf{x}} \;=\; \mathrm{grad}\,\boldsymbol{\chi}^{-1} \quad \text{or} \quad F^{-1}_{Ai} \;=\; \frac{\partial \chi^{-1}_A}{\partial x_i} \;=\; \chi^{-1}_{A,i} \quad . \tag{2.67}$$

The deformation gradient is invertible if the Jacobian *determinant*

$$J \;=\; \det \mathbf{F} \tag{2.68}$$

is non-zero. The *inverse function theorem* further states that the mapping $\boldsymbol{\chi}(\mathbf{X},t)$ is invertible at time t if J is non-zero everywhere, *i.e.*, $J \neq 0 \;\forall\; \mathbf{X} \in \mathcal{R}_0$. The smoothness of motion $\boldsymbol{\chi}$ in time thus implies that the sign of J cannot flip, so that $J > 0 \;\forall\; (\mathbf{x},t)$ remains positive[13] throughout.

A host of deformation measures may be constructed from $\mathbf{F}$. In the scope of this text, it is mentioned that according to the *polar decomposition theorem* invertible tensors may be uniquely decomposed into

$$\mathbf{F} \;=\; \mathbf{R}\mathbf{U} \;=\; \mathbf{V}\mathbf{R} \quad , \tag{2.69}$$

where the two-point tensor $\mathbf{R} = R_{iA}\,\mathbf{e}_i \otimes \mathbf{E}_A$ is orthogonal, and the (referential) *right* and (spatial) *left stretch tensors* $\mathbf{U} = U_{AB}\,\mathbf{E}_A \otimes \mathbf{E}_B$ and $\mathbf{V} = V_{ij}\,\mathbf{e}_i \otimes \mathbf{e}_j$, respectively, are symmetric positive-definite. The polar decomposition (2.69) separates the effects of rotation and stretch. The stretch tensors are related to the *right* and *left* Cauchy-Green *deformation tensors* $\mathbf{C}$ and $\mathbf{B}$ by

$$\mathbf{C} \;=\; \mathbf{F}^{\mathrm{T}}\mathbf{F} \;=\; \mathbf{U}^2 \quad , \quad \mathbf{B} \;=\; \mathbf{F}\mathbf{F}^{\mathrm{T}} \;=\; \mathbf{V}^2 \quad . \tag{2.70}$$

[12] This is due to the fact that $\mathbf{F}$ is the referential gradient of a spatial quantity. The two-pointed nature of $\mathbf{F}$ is of course consistent with Equation (2.65), which describes a linear mapping between vectors in the two configurations.

[13] Here it was assumed that the reference configuration (where $J = 1$) is physically attainable from the current state by a smooth, invertible path.

Lastly, the GREEN-LAGRANGE and EULER-ALMANSI[14] *strain tensors* $\mathbf{E}$ and $\mathbf{e}$ are convenient measures of strain for the formulation of constitutive relations in the referential and spatial bases, respectively,

$$\mathbf{E} \;=\; \frac{1}{2}\big[\mathbf{C}-\mathbf{I}\big] \quad , \quad \mathbf{e} \;=\; \frac{1}{2}\big[\mathbf{i}-\mathbf{B}^{-1}\big] \quad . \tag{2.71}$$

Here, $\mathbf{I}=\delta_{AB}\mathbf{E}_A\otimes\mathbf{E}_B$ and $\mathbf{i}=\delta_{ij}\mathbf{e}_i\otimes\mathbf{e}_j$ denote the *referential* and *spatial unit tensors*, respectively. A (local) absence of strain $\mathbf{E}=\mathbf{0}$ and $\mathbf{e}=\mathbf{0}$ implies that $\mathbf{U}=\mathbf{I}$ and $\mathbf{V}=\mathbf{i}$, which corresponds to a (locally) rigid rotation $\mathbf{F}=\mathbf{R}$ according to (2.69).

The displacement vector (2.63) offers an alternative description of the aforementioned deformation measures, which is more conducive to a numerical implementation using finite elements. For convenience, the *referential displacement gradient* $\mathbf{H}$ is defined by

$$\mathbf{H} \;=\; \mathrm{Grad}\,\mathbf{u} \quad \text{or} \quad H_{AB} \;=\; u_{A,B} \quad , \tag{2.72}$$

and the *spatial displacement gradient* $\mathbf{h}$ by

$$\mathbf{h} \;=\; \mathrm{grad}\,\mathbf{u} \quad \text{or} \quad h_{ij} \;=\; u_{i,j} \quad . \tag{2.73}$$

The deformation gradient may then be written as

$$\mathbf{F} \;=\; \mathbf{1}\big[\mathbf{I}+\mathbf{H}\big] \quad \text{or} \quad F_{iA} \;=\; \delta_{iA}+\delta_{iB}\,u_{B,A} \quad , \tag{2.74}$$

and its inverse

$$\mathbf{F}^{-1} \;=\; \mathbf{1}^{\mathrm{T}}\big[\mathbf{i}-\mathbf{h}\big] \quad \text{or} \quad F^{-1}_{Ai} \;=\; \delta_{Ai}-\delta_{Aj}\,u_{j,i} \quad . \tag{2.75}$$

The displacement gradients $\mathbf{H}$ and $\mathbf{h}$ thus quantify the departure of $\mathbf{F}$ and $\mathbf{F}^{-1}$ from identity, respectively. The referential deformation and strain tensors become

$$\begin{aligned} \mathbf{C} \;&=\; \mathbf{I}+2\,\mathrm{sym}\big[\mathbf{H}\big]+\mathbf{H}^{\mathrm{T}}\mathbf{H} \quad \text{or} \quad C_{AB} \;=\; \delta_{AB}+u_{A,B}+u_{B,A}+u_{C,A}\,u_{C,B} \quad , \\ \mathbf{E} \;&=\; \mathrm{sym}\big[\mathbf{H}\big]+\tfrac{1}{2}\mathbf{H}^{\mathrm{T}}\mathbf{H} \quad \text{or} \quad E_{AB} \;=\; \tfrac{1}{2}\big[u_{A,B}+u_{B,A}+u_{C,A}\,u_{C,B}\big] \quad . \end{aligned} \tag{2.76}$$

Likewise, their spatial counterparts $\mathbf{B}^{-1}=\mathbf{F}^{-\mathrm{T}}\mathbf{F}^{-1}$ and $\mathbf{e}$ read

$$\begin{aligned} \mathbf{B}^{-1} \;&=\; \mathbf{i}-2\,\mathrm{sym}\big[\mathbf{h}\big]+\mathbf{h}^{\mathrm{T}}\mathbf{h} \quad \text{or} \quad B^{-1}_{ij} \;=\; \delta_{ij}-u_{i,j}-u_{j,i}+u_{k,i}\,u_{k,j} \quad , \\ \mathbf{e} \;&=\; \mathrm{sym}\big[\mathbf{h}\big]-\tfrac{1}{2}\mathbf{h}^{\mathrm{T}}\mathbf{h} \quad \text{or} \quad E_{AB} \;=\; \tfrac{1}{2}\big[u_{i,j}+u_{j,i}-u_{k,i}\,u_{k,j}\big] \quad . \end{aligned} \tag{2.77}$$

Meanwhile, the inverse of the right CAUCHY-GREEN tensor $\mathbf{C}^{-1}=\mathbf{F}^{-1}\mathbf{F}^{-\mathrm{T}}$ is expressed as

$$\mathbf{C}^{-1} \;=\; \mathbf{1}^{\mathrm{T}}\big\{\mathbf{i}-2\,\mathrm{sym}\big[\mathbf{h}\big]+\mathbf{h}\,\mathbf{h}^{\mathrm{T}}\big\}\mathbf{1} \quad \text{or} \quad C^{-1}_{AB} \;=\; \delta_{iA}\,\delta_{jB}\big\{\delta_{ij}-u_{i,j}-u_{j,i}+u_{k,i}\,u_{k,j}\big\} \quad . \tag{2.78}$$

[14] In Chapter 3 the lower-case bold symbol $\mathbf{e}$ will be repurposed to denote the electric field vector. However, the EULER-ALMANSI strain makes a reappearance in the discussion of constitutive equations in Section 6.1.2.

According to Equation (2.65), an infinitesimal referential *volume element* defined by the parallelepiped $\mathrm{d}V = \mathrm{d}\mathbf{X}^1 \cdot (\mathrm{d}\mathbf{X}^2 \times \mathrm{d}\mathbf{X}^3)$ is mapped to the volume $\mathrm{d}v$ in the current configuration via

$$\mathrm{d}v \;=\; \mathrm{d}\mathbf{x}^1 \cdot (\mathrm{d}\mathbf{x}^2 \times \mathrm{d}\mathbf{x}^3) \;=\; \mathbf{F}\mathrm{d}\mathbf{X}^1 \cdot (\mathbf{F}\mathrm{d}\mathbf{X}^2 \times \mathbf{F}\mathrm{d}\mathbf{X}^3) \;=\; J\mathrm{d}V \quad , \tag{2.79}$$

which follows immediately from the property of the scalar triple product in $(2.34)_3$. An infinitesimal referential *area element* $\mathbf{N}\mathrm{d}A = \mathrm{d}\mathbf{X}^1 \times \mathrm{d}\mathbf{X}^2$ with area $\mathrm{d}A$ and unit normal $\mathbf{N}$ is mapped to $\mathbf{n}\mathrm{d}a = \mathrm{d}\mathbf{x}^1 \times \mathrm{d}\mathbf{x}^2$ in the current configuration by

$$\mathbf{n}\mathrm{d}a \;=\; J\mathbf{F}^{-\mathrm{T}}\mathbf{N}\mathrm{d}A \;=\; \mathbf{F}^*\mathbf{N}\mathrm{d}A \quad . \tag{2.80}$$

Nanson*'s formula* (2.80) is obtained directly from the identity $(2.37)_2$, or by taking the inner product of $\mathbf{N}\mathrm{d}A$ with an arbitrary $\mathrm{d}\mathbf{X}^3$ and applying Equation (2.79). The tensor

$$\mathbf{F}^* \;=\; J\mathbf{F}^{-\mathrm{T}} \tag{2.81}$$

is the so-called *adjugate* of $\mathbf{F}$, which also coincides with tensor derivative $\mathbf{F}^* = \frac{\partial J}{\partial \mathbf{F}}$ of the Jacobian determinant J with respect to $\mathbf{F}$, see (2.40). The notation $\mathbf{F}^*$ is not to be confused with the flux derivative $\overset{\star}{\mathbf{w}}$ introduced later in (2.106), which is a type of time derivative for vector-valued fields.

2.2.3 Relations Between Spatial and Referential Derivatives

Recall the interchangeability (2.64) between the Eulerian and Lagrangian descriptions of a field $\mathcal{F}$. Due to chain rule, the spatial and referential derivatives of $\mathcal{F}$ are related to each other by the deformation gradient (2.66) or its inverse (2.67). For example, the gradient of a scalar field $\alpha = \tilde{\alpha}(\mathbf{x}, t) = \hat{\alpha}(\mathbf{X}, t)$ furnishes

$$\operatorname{grad}\alpha \;=\; \frac{\partial \alpha}{\partial x_i} \;=\; \frac{\partial \alpha}{\partial X_A}\frac{\partial X_A}{\partial x_i}\mathbf{e}_i \;=\; \mathbf{F}^{-\mathrm{T}}\big(\operatorname{Grad}\alpha\big) \quad , \tag{2.82}$$

and thus, given a second scalar field β,

$$\operatorname{grad}\alpha \cdot \operatorname{grad}\beta \;=\; \big(\operatorname{Grad}\alpha\big) \cdot \mathbf{C}^{-1}\big(\operatorname{Grad}\beta\big) \quad . \tag{2.83}$$

Analogously, the gradient of a spatial vector field $\mathbf{w} = \tilde{\mathbf{w}}(\mathbf{x}, t) = \hat{\mathbf{w}}(\mathbf{X}, t)$ is given by

$$\operatorname{grad}\mathbf{w} \;=\; \frac{\partial w_i}{\partial x_j} \;=\; \frac{\partial w_i}{\partial X_A}\frac{\partial X_A}{\partial x_j}\mathbf{e}_i \otimes \mathbf{e}_j \;=\; \big[\operatorname{Grad}\mathbf{w}\big]\mathbf{F}^{-1} \quad , \tag{2.84}$$

and its divergence by

$$\operatorname{div}\mathbf{w} \;=\; \frac{\partial w_i}{\partial x_i} \;=\; \frac{\partial w_i}{\partial X_A}\frac{\partial X_A}{\partial x_i} \;=\; \big[\operatorname{Grad}\mathbf{w}\big] \cdot \mathbf{F}^{-\mathrm{T}} \quad . \tag{2.85}$$

Finally, the divergence of a spatial tensor field $\mathbf{T}=\tilde{\mathbf{T}}(\mathbf{x},t)=\hat{\mathbf{T}}(\mathbf{X},t)$ is expressed by

$$\operatorname{div}\mathbf{T} \;=\; \frac{\partial T_{ij}}{\partial x_j} \;=\; \frac{\partial T_{ij}}{\partial X_A}\frac{\partial X_A}{\partial x_j} \;=\; \big[\operatorname{Grad}\mathbf{T}\big]\mathbf{F}^{-\mathrm{T}} \quad , \tag{2.86}$$

where $\operatorname{Grad}\mathbf{T}$ constitutes a third-order two-point tensor, see $(2.24)_2$.

NANSON's formula (2.80) and the divergence theorem (2.52) for $\mathbf{T}\equiv\mathbf{i}$ imply that

$$\mathbf{0} \;=\; \int_{\mathcal{P}} \operatorname{div}\mathbf{i}\,\mathrm{d}v \;=\; \int_{\partial\mathcal{P}} \mathbf{n}\,\mathrm{d}a \;=\; \int_{\partial\mathcal{P}_0} J\mathbf{F}^{-\mathrm{T}}\mathbf{N}\,\mathrm{d}A \;=\; \int_{\mathcal{P}_0} \operatorname{Div}\big[J\mathbf{F}^{-\mathrm{T}}\big]\,\mathrm{d}V \quad , \tag{2.87}$$

where $\mathcal{P}\subset\mathcal{R}$ and $\mathcal{P}_0\subset\mathcal{R}_0$ are regions of the body in the current and referential configurations, respectively. The localization theorem (2.55) thus furnishes for the adjugate $\mathbf{F}^*$ in (2.81) the property

$$\operatorname{Div}\big[J\mathbf{F}^{-\mathrm{T}}\big] \;=\; \mathbf{0} \quad . \tag{2.88}$$

Conversely, by applying the above argument to the referential form of the divergence theorem using $\operatorname{Div}\mathbf{I}=\mathbf{0}$, it is found that the inverse of $\mathbf{F}^*$ satisfies

$$\operatorname{div}\big[J^{-1}\mathbf{F}^{\mathrm{T}}\big] \;=\; \mathbf{0} \quad . \tag{2.89}$$

The so-called PIOLA *identity* (2.88) (sometimes called the EULER-PIOLA-JACOBI *identity*) affords a simple relation between the divergence of a spatial vector $\mathbf{w}$ or tensor $\mathbf{T}$ and their referential counterparts,

$$\begin{aligned} J\operatorname{div}\mathbf{w} \;&=\; \operatorname{Div}\mathbf{w}_0 \quad \text{with} \quad \mathbf{w}_0 \;=\; J\mathbf{F}^{-1}\mathbf{w} \quad , \\ J\operatorname{div}\mathbf{T} \;&=\; \operatorname{Div}\mathbf{T}_0 \quad \text{with} \quad \mathbf{T}_0 \;=\; J\mathbf{T}\mathbf{F}^{-\mathrm{T}} \quad , \end{aligned} \tag{2.90}$$

where the identities in $(2.46)_{3,4}$, (2.85), and (2.86) were used. The referential[15] quantities $\mathbf{w}_0$ and $\mathbf{T}_0$ are called PIOLA *transforms* of the spatial fields $\mathbf{w}$ and $\mathbf{T}$. For a physical interpretation it is noted that NANSON's formula (2.80) furnishes the relations

$$\int_{\mathcal{A}} \mathbf{w}\cdot\mathbf{n}\,\mathrm{d}a \;=\; \int_{\mathcal{A}_0} \mathbf{w}_0\cdot\mathbf{N}\,\mathrm{d}A \quad \text{and} \quad \int_{\mathcal{A}} \mathbf{T}\,\mathbf{n}\,\mathrm{d}a \;=\; \int_{\mathcal{A}_0} \mathbf{T}_0\,\mathbf{N}\,\mathrm{d}A \quad , \tag{2.91}$$

where $\mathcal{A}$ and $\mathcal{A}_0$ are the current and referential configurations of an arbitrary, open material surface, respectively. Equation $(2.91)_1$ represents the flux of $\mathbf{w}$ through $\mathcal{A}$, so that $\mathbf{w}_0$ may be interpreted as a flux density measured per unit (and relative to the orientation of) referential area. Equation $(2.91)_2$ describes the flux of a tensor, which in the context of continuum mechanics corresponds to the traction exerted on $\mathcal{A}$ by

[15] More precisely, only the last index of a PIOLA transform is referential, such that it may operate on a referential vector or divergence. For example, $\mathbf{T}_0$ is a two-point tensor with components $[T_0]_{iA}=JT_{ij}F^{-1}_{Aj}$.

the so-called stress tensor $\mathbf{T}$. Therefore, $\mathbf{T}_0$ symbolizes the stress tensor per unit (and orientation of) referential area.[16]

The list of transformations (2.82 - 86) between the spatial and referential descriptions of differential operators remains incomplete without the curl. Rather than a straightforward application of chain rule, its derivation is based on the definition $(2.41)_3$ of the curl by which it is transformed into a divergence. It is first noted that

$$\mathrm{Curl}\big(\mathbf{F}^{\mathrm{T}}\mathbf{h}\big) \;=\; \epsilon_{ABC}\,\chi_{i,CB}\,h_i\,\mathbf{E}_A \;=\; \mathbf{0} \quad , \tag{2.92}$$

due to the symmetry of $\chi_{i,CB}$ and the skew-symmetry of ϵ_{ABC} with respect to the latter two indices, see $(2.30)_3$. Hence, with the aid of (2.85), (2.81), $(2.46)_3$, (2.88), $(2.37)_2$, $(2.46)_6$, and (2.92) (in order of their application), it is observed that

$$\begin{aligned}
\big(\mathrm{curl}\,\mathbf{w}\big)\cdot\mathbf{h} \;&=\; \mathrm{div}\big(\mathbf{w}\times\mathbf{h}\big)\\
&=\; \big[\mathrm{Grad}\big(\mathbf{w}\times\mathbf{h}\big)\big]\cdot\mathbf{F}^{-\mathrm{T}}\\
&=\; J^{-1}\mathbf{F}^{*}\cdot\big[\mathrm{Grad}\big(\mathbf{w}\times\mathbf{h}\big)\big]\\
&=\; J^{-1}\big\{\mathrm{Div}\big(\mathbf{F}^{*\mathrm{T}}\big(\mathbf{w}\times\mathbf{h}\big)\big) \;-\; \mathrm{Div}\big[\mathbf{F}^{*}\big]\cdot\big(\mathbf{w}\times\mathbf{h}\big)\big\}\\
&=\; J^{-1}\mathrm{Div}\big(\mathbf{F}^{\mathrm{T}}\mathbf{w}\times\mathbf{F}^{\mathrm{T}}\mathbf{h}\big)\\
&=\; J^{-1}\big\{\mathbf{F}^{\mathrm{T}}\mathbf{h}\cdot\mathrm{Curl}\big(\mathbf{F}^{\mathrm{T}}\mathbf{w}\big) \;-\; \mathbf{F}^{\mathrm{T}}\mathbf{w}\cdot\mathrm{Curl}\big(\mathbf{F}^{\mathrm{T}}\mathbf{h}\big)\big\}\\
&=\; J^{-1}\mathbf{F}\,\mathrm{Curl}\big(\mathbf{F}^{\mathrm{T}}\mathbf{w}\big)\cdot\mathbf{h} \qquad\qquad \forall \text{ constant } \mathbf{h} \quad .
\end{aligned} \tag{2.93}$$

Finally, in view of the arbitrariness of the constant vector $\mathbf{h}$ it is concluded that

$$\mathrm{curl}\,\mathbf{w} \;=\; J^{-1}\mathbf{F}\,\mathrm{Curl}\big(\mathbf{F}^{\mathrm{T}}\mathbf{w}\big) \quad . \tag{2.94}$$

2.2.4 Rate of Deformation

The *material* (or *total*) *time derivative* $\dot{\mathcal{F}} = \frac{\mathrm{d}}{\mathrm{d}t}\mathcal{F}$ describes the rate of change of a quantity as experienced by a material point, thus taking into account the motion of the body. On the other hand, the partial time derivative $\frac{\partial}{\partial t}\tilde{\mathcal{F}}(\mathbf{x},t)$ determines the rate of change of $\mathcal{F}$ at a fixed spatial location $\mathbf{x}$. The two time derivatives are related by chain rule,

$$\dot{\mathcal{F}} \;=\; \frac{\mathrm{d}\mathcal{F}}{\mathrm{d}t} \;=\; \frac{\partial\hat{\mathcal{F}}(\mathbf{X},t)}{\partial t} \;=\; \frac{\partial\tilde{\mathcal{F}}(\mathbf{x},t)}{\partial t} + \frac{\partial\tilde{\mathcal{F}}(\mathbf{x},t)}{\partial x_i}\frac{\partial\chi_i(\mathbf{X},t)}{\partial t} \quad . \tag{2.95}$$

Let the scalar-, vector-, and (second-order) tensor-valued spatial fields $\tilde{\alpha}(\mathbf{x},t)$, $\tilde{\mathbf{w}}(\mathbf{x},t)$, and $\tilde{\mathbf{T}}(\mathbf{x},t)$ be continuously differentiable in both arguments. Equation (2.95) be-

[16] In the context of this work, the flux density $\mathbf{w}$ is typically associated with heat flux or electric current density, see later in Equations (2.123) and (3.3). The stress tensor $\mathbf{T}$ is introduced in Equation (2.114).

comes

$$\begin{aligned}
\dot{\alpha} &= \frac{\partial\tilde{\alpha}}{\partial t} + \big(\operatorname{grad}\tilde{\alpha}\big)\cdot\mathbf{v} \quad \text{or} \quad \dot{\alpha} = \frac{\partial\tilde{\alpha}}{\partial t} + \tilde{\alpha}_{,i}\cdot v_i \quad , \\
\dot{\mathbf{w}} &= \frac{\partial\tilde{\mathbf{w}}}{\partial t} + \big[\operatorname{grad}\tilde{\mathbf{w}}\big]\mathbf{v} \quad \text{or} \quad \dot{w}_i = \frac{\partial\tilde{w}_i}{\partial t} + \tilde{w}_{i,j}\,v_j \quad , \\
\dot{\mathbf{T}} &= \frac{\partial\tilde{\mathbf{T}}}{\partial t} + \big[\operatorname{grad}\tilde{\mathbf{T}}\big]\mathbf{v} \quad \text{or} \quad \dot{T}_{ij} = \frac{\partial\tilde{T}_{ij}}{\partial t} + \tilde{T}_{ij,k}v_k \quad ,
\end{aligned} \tag{2.96}$$

where $\mathbf{v}=\dot{\mathbf{x}}\,(=\dot{\mathbf{u}})$ is the *material velocity*. Its LAGRANGIAN form is readily obtained from $\hat{\mathbf{v}}(\mathbf{X},t)=\frac{\partial}{\partial t}\boldsymbol{\chi}(\mathbf{X},t)$ and converted to EULERIAN form $\tilde{\mathbf{v}}(\mathbf{x},t)=\hat{\mathbf{v}}(\boldsymbol{\chi}^{-1}(\mathbf{x},t),t)$ using (2.64).

Similar to the deformation gradient (2.66), the *spatial velocity gradient* $\mathbf{L}$ relates an infinitesimal spatial material line element $\mathrm{d}\mathbf{x}$ to the corresponding velocity increment $\mathrm{d}\mathbf{v}$,

$$\mathrm{d}\mathbf{v} = \mathbf{L}\,\mathrm{d}\mathbf{x} \quad \text{where} \quad \mathbf{L} = \operatorname{grad}\tilde{\mathbf{v}} = \tilde{v}_{i,j}\,\mathbf{e}_i\otimes\mathbf{e}_j \quad . \tag{2.97}$$

The increment $\mathrm{d}\mathbf{v}$ quantifies how much the material velocity $\mathbf{v}$ varies at a point separated from $\mathbf{x}$ by $\mathrm{d}\mathbf{x}$. Unlike the two-point tensor $\mathbf{F}$, the velocity gradient $\mathbf{L}$ is entirely spatial. It may also be computed from the LAGRANGIAN description $\hat{\mathbf{v}}(\mathbf{X},t)$ by Equation (2.84), $\mathbf{L}=[\operatorname{Grad}\hat{\mathbf{v}}]\mathbf{F}^{-1}$.

The rate of change $\dot{\mathrm{d}v}$ of an infinitesimal volume element is obtained by taking the material time derivative of Equation $(2.79)_2$,

$$\dot{\mathrm{d}v} = (\operatorname{tr}\mathbf{L})\mathrm{d}v = (\operatorname{div}\mathbf{v})\mathrm{d}v \quad , \tag{2.98}$$

where the identity $\operatorname{tr}\mathbf{L}=\operatorname{tr}(\operatorname{grad}\mathbf{v})=\operatorname{div}\mathbf{v}$ was used. A comparison between $(2.79)_3$ and $(2.98)_2$ implies that

$$\dot{J} = J\operatorname{div}\mathbf{v} \quad . \tag{2.99}$$

The material time derivative of $\mathbf{F}$ may be written in terms of the velocity gradient as

$$\dot{\mathbf{F}} = \frac{\mathrm{d}}{\mathrm{d}t}\left[\frac{\partial\boldsymbol{\chi}(\mathbf{X},t)}{\partial\mathbf{X}}\right] = \frac{\partial}{\partial\mathbf{X}}\left(\frac{\partial\boldsymbol{\chi}(\mathbf{X},t)}{\partial t}\right) = \frac{\partial\hat{\mathbf{v}}(\mathbf{X},t)}{\partial\mathbf{X}} = \frac{\partial\tilde{\mathbf{v}}(\mathbf{x},t)}{\partial\mathbf{x}}\frac{\partial\boldsymbol{\chi}(\mathbf{X},t)}{\partial\mathbf{X}} = \mathbf{L}\mathbf{F} \quad . \tag{2.100}$$

In order to commute the derivatives of $\boldsymbol{\chi}(\mathbf{X},t)$ with respect to $\mathbf{X}$ and t in (2.100), it was assumed that the mixed derivative is continuous. Note that Equation $(2.97)_1$ may also be interpreted as the material time derivative $\dot{\mathrm{d}\mathbf{x}}$ of an infinitesimal line element, since

$$\dot{\mathrm{d}\mathbf{x}} = \dot{\mathbf{F}\,\mathrm{d}\mathbf{X}} = \dot{\mathbf{F}}\,\mathrm{d}\mathbf{X} = \mathbf{L}\mathbf{F}\,\mathrm{d}\mathbf{X} = \mathbf{L}\,\mathrm{d}\mathbf{x} \quad . \tag{2.101}$$

Finally, the tensor derivative (2.40) may be employed to express the material time derivative of the inverse of an invertible tensor $\dot{\mathbf{T}^{-1}}$ in terms of $\dot{\mathbf{T}}$,

$$\dot{\mathbf{T}^{-1}} = \left[\frac{\partial\mathbf{T}^{-1}}{\partial\mathbf{T}}\right]\cdot\dot{\mathbf{T}} = -\mathbf{T}^{-1}\dot{\mathbf{T}}\mathbf{T}^{-1} \quad , \tag{2.102}$$

see Appendix A.2 for a derivation. Unsurprisingly, the material time derivative does *not* commute with the inverse. Given Equations (2.99 - 102), which imply that $\dot{\overline{\mathbf{F}^{-1}}} = -\mathbf{F}^{-1}\mathbf{L}$, the material time derivative $\dot{\overline{\mathbf{n}\mathrm{d}a}}$ of Nanson's formula (2.80) can be expressed as

$$\begin{aligned} \dot{\overline{\mathbf{n}\mathrm{d}a}} &= \big[\dot{J}\mathbf{F}^{-\mathrm{T}} + J\dot{\overline{\mathbf{F}^{-\mathrm{T}}}}\big]\mathbf{N}\mathrm{d}A \\ &= \Big[\big(\mathrm{tr}\,\mathbf{L}\big)\mathbf{i} - \mathbf{L}^{\mathrm{T}}\Big]\mathbf{n}\mathrm{d}a \;=\; \Big[\big(\mathrm{div}\,\mathbf{v}\big)\mathbf{i} - \big[\mathrm{grad}\,\mathbf{v}\big]^{\mathrm{T}}\Big]\mathbf{n}\mathrm{d}a \quad . \end{aligned} \tag{2.103}$$

2.2.5 Rate of Change of Integral Quantities

Balance equations often involve the total time derivative of quantities, which are integrated over a material region, surface, or path. Consider a continuously differentiable real, vector, or tensor-valued field $\mathcal{F}(\mathbf{x}, t)$ integrated over an open, bounded material region $\mathcal{P}$ with smooth boundary $\partial\mathcal{P}$. In light of Equation (2.98), its material time derivative is given by

$$\begin{aligned} \frac{\mathrm{d}}{\mathrm{d}t}\int_{\mathcal{P}} \mathcal{F}\,\mathrm{d}v &= \int_{\mathcal{P}} \big\{\dot{\mathcal{F}} + \mathcal{F}\,\mathrm{div}\,\mathbf{v}\big\}\,\mathrm{d}v \\ &= \int_{\mathcal{P}} \frac{\partial \mathcal{F}}{\partial t}\,\mathrm{d}v + \int_{\partial\mathcal{P}} \mathcal{F}(\mathbf{v}\cdot\mathbf{n})\,\mathrm{d}a \quad , \end{aligned} \tag{2.104}$$

where Equations $(2.46)_1$, $(2.96)_1$, and (2.50) were used to obtain $(2.104)_2$. This result is known as the Reynolds' *transport theorem* and will be employed frequently in the manipulation of balance equations. Equation $(2.104)_2$ identifies two contributions to the rate of change of the total amount of $\mathcal{F}$ contained in a *material* region $\mathcal{P}$. The first quantity describes the change of $\mathcal{F}$ contained in the *fixed* region currently occupied by $\mathcal{P}$, and the second term is due to the motion of the boundary $\partial\mathcal{P}$ at the velocity $\mathbf{v}$.

A similar expression may be derived for surface integrals. Let $\mathbf{w}(\mathbf{x}, t)$ be a continuously differentiable vector field and $\mathcal{A}$ a smooth (open or closed) material surface with corresponding unit normal $\mathbf{n}(\mathbf{x}, t)$. The material time derivative of the flux of $\mathbf{w}$ through $\mathcal{A}$ is written with the aid of (2.103) as

$$\frac{\mathrm{d}}{\mathrm{d}t}\int_{\mathcal{A}} \mathbf{w}\cdot\mathbf{n}\,\mathrm{d}a \;=\; \int_{\mathcal{A}} \overset{\star}{\mathbf{w}}\cdot\mathbf{n}\,\mathrm{d}a \quad , \tag{2.105}$$

where the so-called *flux derivative*[17] $\overset{\star}{\mathbf{w}}$ of $\mathbf{w}$ is given by

$$\begin{aligned} \overset{\star}{\mathbf{w}} &= \dot{\mathbf{w}} + \big(\mathrm{div}\,\mathbf{v}\big)\mathbf{w} - \big(\mathrm{grad}\,\mathbf{v}\big)\mathbf{w} \\ &= \frac{\partial \mathbf{w}}{\partial t} + \mathrm{div}\big(\mathbf{w}\otimes\mathbf{v}\big) - \big(\mathrm{grad}\,\mathbf{v}\big)\mathbf{w} \\ &= \frac{\partial \mathbf{w}}{\partial t} + \big(\mathrm{div}\,\mathbf{w}\big)\mathbf{v} + \mathrm{curl}\big(\mathbf{w}\times\mathbf{v}\big) \quad . \end{aligned} \tag{2.106}$$

[17] Some older works, such as Toupin [145] or Hutter [55], refer to $\overset{\star}{\mathbf{w}}$ as the *convected time derivative*.

Equations $(2.106)_{2,3}$ are derived with the aid of $(2.46)_5$, $(2.47)_2$, and $(2.96)_2$. If needed, STOKES' theorem (2.53) may be employed to further convert the curl in $(2.106)_3$ into the circulation of $\mathbf{w}\times\mathbf{v}$ around the boundary $\mathcal{C}$.

Finally, consider a continuously differentiable vector field $\mathbf{w}(\mathbf{x},t)$ integrated in direction $\mathrm{d}\mathbf{x}$ along the material path $\mathcal{S}$ at time t. Its total time derivative is conveniently expressed using the notation

$$\frac{\mathrm{d}}{\mathrm{d}t}\int_{\mathcal{S}}\mathbf{w}\cdot\mathrm{d}\mathbf{x} \;=\; \int_{\mathcal{S}}\mathring{\mathbf{w}}\cdot\mathrm{d}\mathbf{x} \quad , \tag{2.107}$$

where the *path derivative* $\mathring{\mathbf{w}}$ of $\mathbf{w}$ is obtained with (2.101) as

$$\begin{aligned}\mathring{\mathbf{w}} \;&=\; \dot{\mathbf{w}} + \big[\operatorname{grad}\mathbf{v}\big]^{\mathrm{T}}\mathbf{w}\\ &=\; \overset{\star}{\mathbf{w}} - \big(\operatorname{div}\mathbf{v}\big)\mathbf{w} + 2\operatorname{sym}\big[\operatorname{grad}\mathbf{v}\big]\mathbf{w}\\ &=\; \frac{\partial\mathbf{w}}{\partial t} + \big(\operatorname{curl}\mathbf{w}\big)\times\mathbf{v} + \operatorname{grad}\big(\mathbf{w}\cdot\mathbf{v}\big) \quad .\end{aligned} \tag{2.108}$$

The comparison in (2.108) between $\mathring{\mathbf{w}}$ and the total, partial, and flux derivatives is readily verified with $(2.45)_2$, (2.48), $(2.96)_2$, and $(2.106)_1$. The last term in $(2.108)_3$ may be further simplified using the gradient theorem (2.54).

2.3 Balance Equations

The mathematical building blocks are now in place to discuss the balance equations of classical nonlinear continuum mechanics. These well-established laws will serve as a starting point for the coupled electro-magneto-thermo-mechanical equations.

2.3.1 Principle of Mass Conservation

The *mass* $m(\mathcal{P})>0$ is an *extensive* property of a material region $\mathcal{P}\subset\mathcal{R}$ of the body, *i.e.*, the combined mass of multiple non-intersecting regions is additive. The *mass density* $\rho(\mathbf{x},t)>0$ is obtained from the ratio of mass $m(\mathcal{P})$ per volume $\operatorname{vol}(\mathcal{P})$ of a region around $\mathbf{x}$ at time t, in the limit where the volume becomes infinitesimal,

$$m(\mathcal{P}) \;=\; \int_{\mathcal{P}}\rho\,\mathrm{d}v \quad \text{where} \quad \rho \;=\; \lim\frac{m(\mathcal{P})}{\operatorname{vol}(\mathcal{P})} \quad . \tag{2.109}$$

In reality discontinuities arise when the limit approaches a granular or molecular length scale of the material. It may nevertheless be approximated by a continuum with continuously differentiable $\rho(\mathbf{x},t)$, if sufficient scale separation can be ensured between the characteristic macroscopic dimension of the body and its microscopic structure. This notion, discussed in more detail in the introduction to Chapter 5, is referred to as the *continuum assumption*. A more rigorous discussion of the concept of mass

in continuum mechanics is provided, for example, by TRUESDELL and TOUPIN [147, Section 155].

Conservation of mass requires that the total mass contained in any *material* region $\mathcal{P} \subset \mathcal{R}$ be constant in time. The principle of mass conservation is formally expressed in integral form by

$$\dot{m}(\mathcal{P}) \;=\; \frac{\mathrm{d}}{\mathrm{d}t}\int_{\mathcal{P}} \rho \,\mathrm{d}v \;=\; \int_{\mathcal{P}} \left\{\dot{\rho} + \rho \,\mathrm{div}\,\mathbf{v}\right\} \mathrm{d}v \;=\; 0 \quad , \tag{2.110}$$

where the transport theorem $(2.104)_1$ was invoked. Due to the arbitrariness of $\mathcal{P}$ and the continuity of the integrand in parentheses, the localization theorem (2.55) may be applied to deduce

$$\dot{\rho} + \rho \,\mathrm{div}\,\mathbf{v} \;=\; 0 \quad . \tag{2.111}$$

Equation (2.111) constitutes the local form of conservation of mass.

A convenient corollary of the REYNOLDS' transport theorem $(2.104)_1$ and conservation of mass (2.111) is obtained for material time derivatives of the form

$$\begin{aligned} \frac{\mathrm{d}}{\mathrm{d}t}\int_{\mathcal{P}} \rho\mathcal{F} \,\mathrm{d}v \;&=\; \int_{\mathcal{P}} \left\{\dot{\overline{\rho\mathcal{F}}} + \rho\mathcal{F} \,\mathrm{div}\,\mathbf{v}\right\} \mathrm{d}v \\ &=\; \int_{\mathcal{P}} \left\{\big(\dot{\rho} + \rho \,\mathrm{div}\,\mathbf{v}\big)\mathcal{F} + \rho\dot{\mathcal{F}}\right\} \mathrm{d}v \\ &=\; \int_{\mathcal{P}} \rho\dot{\mathcal{F}} \,\mathrm{d}v \quad , \end{aligned} \tag{2.112}$$

where $\mathcal{F}(\mathbf{x}, t)$ is a continuously differentiable real, vector, or scalar field. Expressions of this kind often arise for *specific* quantities, that is, for fields $\mathcal{F}$ that are defined per unit mass (and thus $\rho\mathcal{F}$ per unit volume). Equation (2.112) furnishes a straightforward rule to convert the material time derivative of an integral into the integral of a material time derivative.

2.3.2 Principle of Linear Momentum Balance

The *linear momentum* $\mathrm{d}\mathbf{p}$ of an infinitesimal volume element $\mathrm{d}v$ of mass $\mathrm{d}m = \rho \mathrm{d}v$ traveling at velocity $\mathbf{v}$ is defined by $\mathrm{d}\mathbf{p} = \mathrm{d}m\mathbf{v}$. Like mass, linear momentum is an extensive quantity due to its additive nature. Akin to NEWTON's second law, the *principle of linear momentum balance* states that the rate of change of linear momentum for any material region $\mathcal{P}$ is equal to the sum of external forces acting on it.

Two types of external forces are identified. *Surface tractions* $\mathbf{t}_{(\mathbf{n})}(\mathbf{x}, t)$ per unit area are exerted on the region's boundary $\partial\mathcal{P}$, typically by the material adjacent to the region. A differential area $\mathrm{d}a$ of the boundary is thus subjected to a traction force $\mathrm{d}\mathbf{f} = \mathbf{t}_{(\mathbf{n})}\mathrm{d}a$. The subscript $[\cdot]_{(\mathbf{n})}$ indicates the dependence of $\mathbf{t}_{(\mathbf{n})}$ on the outward normal unit vector $\mathbf{n}$. Secondly, a distribution of *body forces* $\mathbf{f}_{\mathrm{B}}(\mathbf{x}, t)$ per unit mass may

act throughout the region, for example due to gravitational forces.[18] A differential volume $\mathrm{d}v$ experiences a body force $\mathrm{d}\mathbf{f} = \rho \mathbf{f}_{\mathrm{B}} \mathrm{d}v$.

The corresponding integral statement of momentum balance thus reads

$$\frac{\mathrm{d}}{\mathrm{d}t} \int_{\mathcal{P}} \rho \mathbf{v} \, \mathrm{d}v \;=\; \int_{\partial \mathcal{P}} \mathbf{t}_{(\mathbf{n})} \, \mathrm{d}a + \int_{\mathcal{P}} \rho \mathbf{f}_{\mathrm{B}} \, \mathrm{d}v \quad . \tag{2.113}$$

Noll*'s theorem* [108, Theorem 4] states that the surface traction $\mathbf{t}_{(\mathbf{n})}$ depends on the local tangent plane to the boundary (*i.e.*, its normal vector $\mathbf{n}$), provided that the volume integrals in (2.113) are bounded and $\partial \mathcal{P}$ smooth. Moreover, according to Cauchy*'s stress theorem*, the dependence of $\mathbf{t}_{(\mathbf{n})}$ on the orientation $\mathbf{n}$ is linear. The local state of stress is thus fully described by the so-called Cauchy *stress tensor*[19] $\mathbf{T}(\mathbf{x}, t)$, where

$$\mathbf{t}_{(\mathbf{n})} \;=\; \mathbf{T}\mathbf{n} \quad \text{with} \quad \mathbf{T}(\mathbf{x}, t) \;=\; \sum_i \mathbf{t}_{(\mathbf{e}_i)} \otimes \mathbf{e}_i \quad . \tag{2.114}$$

This well-known result follows from the momentum balance (2.113) applied to an infinitesimal tetrahedral region, see Gurtin [40, Section 14], for example.

The divergence theorem (2.52) is employed to convert the boundary integral in (2.113) into a volume integral. The time derivative (2.112) and localization theorem (2.55) furnish the local form of the principle of linear momentum balance,

$$\rho \mathbf{a} \;=\; \operatorname{div} \mathbf{T} + \rho \mathbf{f}_{\mathrm{B}} \quad , \tag{2.115}$$

where $\mathbf{a}(\mathbf{x}, t) = \dot{\mathbf{v}}(\mathbf{x}, t)$ is the *acceleration* vector.[20]

2.3.3 Principle of Angular Momentum Balance

Similar to the preceding discussion of linear momentum, the *angular momentum* $\mathrm{d}\mathbf{l}$ of an infinitesimal volume element $\mathrm{d}v$ located at $\mathbf{x}$ is defined by[21] $\mathrm{d}\mathbf{l} = \mathbf{x} \times (\mathrm{d}m \mathbf{v})$, again an extensive quantity. The *principle of angular momentum balance* asserts that the rate of change of angular momentum of a region is equal to the sum of all external moments acting upon it. This is expressed in integral form by

$$\frac{\mathrm{d}}{\mathrm{d}t} \int_{\mathcal{P}} \mathbf{x} \times \rho \mathbf{v} \, \mathrm{d}v \;=\; \int_{\partial \mathcal{P}} \mathbf{x} \times \mathbf{t}_{(\mathbf{n})} \, \mathrm{d}a + \int_{\mathcal{P}} \mathbf{x} \times \rho \mathbf{f}_{\mathrm{B}} \, \mathrm{d}v \quad . \tag{2.116}$$

[18] In classical continuum mechanics, including this dissertation, Newton's view of gravity as a force (per unit mass) is adopted, rather than the relativistic interpretation through space-time curvature.

[19] To prevent potential confusion, the reader is reminded that the same symbol $\mathbf{T}$ occasionally represents arbitrary tensor fields in the discussion of general mathematical identities. Its appropriate interpretation is evident from the surrounding context.

[20] The same symbol $\mathbf{a}$ is introduced in Equation (3.12) for the magnetic potential. The acceleration is represented by $\dot{\mathbf{v}}$ when necessary to preempt any confusion.

[21] Here, angular momentum is defined from the perspective of the origin of the spatial coordinate system.

Note that this postulate differs from the linear momentum balance in (2.113). It can be shown that the statement is independent of the point with respect to which the moments are defined. Indeed, for any alternative $\mathbf{x}' = \mathbf{x} + \mathbf{c}$ with constant $\mathbf{c}$, Equation (2.116) is recovered using (2.115).

In order to derive the local form, the material time derivative is moved to the integrand using Equation (2.112) and $[\mathbf{x} \times \mathbf{v}]^{\bullet} = \mathbf{x} \times \mathbf{a}$. The second term in (2.116) is more conveniently expressed in components by $\mathbf{t}_{(\mathbf{n})} = \mathbf{T}\mathbf{n} = T_{ij} n_j \mathbf{e}_i = \mathbf{t}_j n_j$, so that the integrand

$$\mathbf{x} \times \mathbf{t}_{(\mathbf{n})} \;=\; \mathbf{x} \times \big(T_{ij} n_j \mathbf{e}_i\big) \;=\; \big[(\mathbf{x} \times T_{ij}\mathbf{e}_i) \otimes \mathbf{e}_j\big]\big(n_k \mathbf{e}_k\big) \tag{2.117}$$

takes a form conducive to the application of the divergence theorem (2.52). Therefore,

$$\begin{aligned} \int_{\partial\mathcal{P}} \mathbf{x} \times \mathbf{t}_{(\mathbf{n})} \, \mathrm{d}a \;&=\; \int_{\mathcal{P}} \operatorname{div}\big[(\mathbf{x} \times T_{ij}\mathbf{e}_i) \otimes \mathbf{e}_j\big] \, \mathrm{d}v \\ &= \int_{\mathcal{P}} (\mathbf{x} \times T_{ij}\mathbf{e}_i)_{,j} \, \mathrm{d}v \\ &= \int_{\mathcal{P}} \big\{\mathbf{x}_{,j} \times T_{ij}\mathbf{e}_i \,+\, \mathbf{x} \times T_{ij,j}\mathbf{e}_i\big\} \, \mathrm{d}v \\ &= \int_{\mathcal{P}} \big\{T_{ij}\mathbf{e}_j \times \mathbf{e}_i \,+\, \mathbf{x} \times \operatorname{div}\mathbf{T}\big\} \, \mathrm{d}v \quad , \end{aligned} \tag{2.118}$$

where the subscript $(\cdot)_{,j}$ indicates a spatial derivative with respect to the j-th coordinate direction. Equation (2.116) simplifies to

$$\int_{\mathcal{P}} T_{ij}\mathbf{e}_j \times \mathbf{e}_i \, \mathrm{d}v \;=\; \int_{\mathcal{P}} \mathbf{x} \times \big(\rho\mathbf{a} - \operatorname{div}\mathbf{T} - \rho\mathbf{f}_{\mathrm{B}}\big) \, \mathrm{d}v \;=\; \mathbf{0} \quad , \tag{2.119}$$

where the linear momentum balance (2.115) was used. Invoking the localization theorem and the fact that $\mathbf{e}_j \times \mathbf{e}_i$ is skew-symmetric in (i, j), it is concluded that the stress tensor must be symmetric, *i.e.*,

$$\mathbf{T} \;=\; \mathbf{T}^{\mathrm{T}} \quad . \tag{2.120}$$

Equation (2.120) constitutes the local form of the principle of angular momentum balance.

2.3.4 Principle of Energy Balance

The *principle of energy balance* is a version of the first law of thermodynamics suited for continuum thermomechanical systems. It postulates that the rate of change of total internal energy contained in a region is balanced by the power of external forces as well as the heat transferred to and from it. The energy balance models the convertibility between thermal and mechanical energy.

The principle of energy balance is stated in integral form as

$$\frac{\mathrm{d}}{\mathrm{d}t}\int_{\mathcal{P}} \rho\left(\frac{1}{2}\mathbf{v}\cdot\mathbf{v}+\varepsilon\right)\mathrm{d}v \;=\; \int_{\mathcal{P}} \rho\mathbf{f}_{\mathrm{B}}\cdot\mathbf{v}\,\mathrm{d}v + \int_{\partial\mathcal{P}} \mathbf{t}_{(\mathbf{n})}\cdot\mathbf{v}\,\mathrm{d}a \\ + \int_{\mathcal{P}} \rho r\,\mathrm{d}v - \int_{\partial\mathcal{P}} q_{(\mathbf{n})}\,\mathrm{d}a \quad . \tag{2.121}$$

The *specific internal energy* $\varepsilon(\mathbf{x},t)$ per unit mass accounts for mechanical strain energy, thermal energy, and any other potential sources (*e.g.*, chemical), except for kinetic energy. The *specific total energy* $e(\mathbf{x},t)$ per unit mass is thus defined as

$$e \;=\; \frac{1}{2}\mathbf{v}\cdot\mathbf{v}+\varepsilon \quad . \tag{2.122}$$

Note that $\rho\varepsilon\mathrm{d}v$ and $\rho e\mathrm{d}v$ are extensive quantities. The second and third integrals in (2.121) represent the power exerted on region $\mathcal{P}$ by body forces and surface tractions, respectively. The fourth term contains the *external supply of heat* per unit mass $r(\mathbf{x},t)$, typically absorbed (or emitted when $r<0$) through radiation. Lastly, $q_{(\mathbf{n})}(\mathbf{x},t)$ is the *heat flux* per unit area across boundary $\partial\mathcal{P}$, which takes account of conduction and convection. Heat is transferred *out* of the system when $q_{(\mathbf{n})}>0$ by convention, therefore the corresponding term in (2.121) carries a negative sign.

In a procedure identical to the derivation of CAUCHY's stress theorem (2.114), it can be shown from the energy balance (2.121) that

$$q_{(\mathbf{n})} \;=\; \mathbf{q}\cdot\mathbf{n} \quad \text{with} \quad \mathbf{q}(\mathbf{x},t) \;=\; \sum_i q_{(\mathbf{e}_i)}\mathbf{e}_i \quad . \tag{2.123}$$

where $\mathbf{q}(\mathbf{x},t)$ is the *heat flux vector*. Heat exits the region when $\mathbf{q}$ points toward the outward normal $\mathbf{n}$, consistent with the sign convention for $q_{(\mathbf{n})}$.

In view of the preceding result, the integral statement (2.121) can be localized using the time derivative (2.112), the divergence theorem (2.50), and the localization theorem (2.55), giving rise to the local form of the principle of energy balance,

$$\rho\left[\tfrac{1}{2}\mathbf{v}\cdot\mathbf{v}+\varepsilon\right]^{\bullet} \;=\; \rho\mathbf{f}_{\mathrm{B}}\cdot\mathbf{v} + \operatorname{div}\left(\mathbf{T}^{\mathrm{T}}\mathbf{v}\right) + \rho r - \operatorname{div}\mathbf{q} \quad . \tag{2.124}$$

The traction term in (2.124) can be expanded according to the product rule in $(2.46)_3$ and the definition of the velocity gradient in (2.97),

$$\rho\mathbf{a}\cdot\mathbf{v} + \rho\dot{\varepsilon} \;=\; \rho\mathbf{f}_{\mathrm{B}}\cdot\mathbf{v} + (\operatorname{div}\mathbf{T})\cdot\mathbf{v} + \mathbf{T}\cdot\mathbf{L} + \rho r - \operatorname{div}\mathbf{q} \quad . \tag{2.125}$$

The first, third, and fourth term of (2.125) constitute the so-called *balance of mechanical power*, which corresponds to the linear momentum balance (2.115) dotted with velocity $\mathbf{v}$. It is eliminated from (2.125) and the remaining terms

$$\rho\dot{\varepsilon} \;=\; \mathbf{T}\cdot\mathbf{L} + \rho r - \operatorname{div}\mathbf{q} \quad , \tag{2.126}$$

comprise the local statement of the *balance of thermal energy*. It is mentioned that the integral $\int_{\mathcal{P}} \mathbf{T}\cdot\mathbf{L}\,\mathrm{d}v$ is called the *stress power*, since it quantifies the rate at which the stresses perform work in $\mathcal{P}$. Note that only the symmetric part $\mathbf{D}=\mathrm{sym}[\mathbf{L}]$ of the velocity gradient contributes to the stress power, because $\mathbf{T}$ is symmetric on account of (2.120).

2.3.5 Second Law of Thermodynamics

In the context of continuum mechanics, there exists some ambiguity as to the exact formulation of the second law of thermodynamics. It is often enforced by means of the Clausius-Duhem *inequality*,

$$\frac{\mathrm{d}}{\mathrm{d}t}\int_{\mathcal{P}} \rho\eta\,\mathrm{d}v \;\geq\; \int_{\mathcal{P}} \frac{\rho r}{\theta}\,\mathrm{d}v - \int_{\partial\mathcal{P}} \frac{q_{(\mathbf{n})}}{\theta}\,\mathrm{d}a \quad , \tag{2.127}$$

where the existence of a *specific entropy* $\eta(\mathbf{x},t)$ and *absolute temperature* $\theta(\mathbf{x},t)>0$ is assumed. The entropy $\rho\eta\mathrm{d}v$ contained in a unit volume is extensive. Inequality (2.127) states that the rate of increase of entropy contained in a material region must be greater than the external supply of entropy through the volume $\mathcal{P}$ minus the entropy flux $q_{(\mathbf{n})}/\theta$ across its boundary $\partial\mathcal{P}$.[22] The negative sign arises from the convention in the definition of the outward heat flux.

The local form of the Clausius-Duhem inequality is obtained from its integral statement (2.127) by application of time derivative (2.112), divergence theorem (2.50) for the heat flux (2.123), and the localization theorem (2.55),

$$\rho\dot{\eta} \;\geq\; \frac{\rho r}{\theta} - \mathrm{div}\left(\frac{\mathbf{q}}{\theta}\right) \quad . \tag{2.128}$$

An equivalent representation of (2.128) is obtained by using product rule $(2.46)_1$ and substituting the energy balance (2.126) for $\mathrm{div}\,\mathbf{q}$,

$$\rho\big(\dot{\varepsilon}-\theta\dot{\eta}\big) - \mathbf{T}\cdot\mathbf{L} + \mathbf{q}\cdot\big(\mathrm{grad}\,\theta\big)/\theta \;\leq\; 0 \quad . \tag{2.129}$$

2.3.6 Method of Coleman and Noll

In a procedure known as the *method of* Coleman *and* Noll [17], thermodynamic restrictions on the constitutive equations can be deduced from (2.129). To this end, the *specific* Helmholtz *free energy*

$$\Psi \;=\; \varepsilon - \eta\theta \tag{2.130}$$

[22] Müller [101] points out that the entropy flux (*i.e.*, $\mathbf{q}/\theta$) in this context is assumed to be proportional to the heat flux: "*The motivation for this relation rests upon the definition of entropy in thermostatics and on an approximate calculation of the entropy flux based on the kinetic theory of gases*".

is defined, so that (2.129) becomes

$$\rho\dot{\Psi} + \rho\eta\dot{\theta} - \mathbf{T}\cdot\mathbf{L} + \mathbf{q}\cdot\big(\operatorname{grad}\theta\big)/\theta \;\leq\; 0 \quad . \tag{2.131}$$

Suppose, for example, a class of so-called *thermoelastic* materials whose HELMHOLTZ free energy takes a functional dependence

$$\Psi \;=\; \check{\Psi}(\mathbf{F},\theta,\operatorname{grad}\theta) \quad . \tag{2.132}$$

Its material time derivative is

$$\dot{\Psi} \;=\; \frac{\partial\check{\Psi}}{\partial\mathbf{F}}\cdot\dot{\mathbf{F}} + \frac{\partial\check{\Psi}}{\partial\theta}\dot{\theta} + \frac{\partial\check{\Psi}}{\partial\operatorname{grad}\theta}\cdot\overset{\cdot}{\overline{\operatorname{grad}\theta}} \quad , \tag{2.133}$$

where the tensor derivative is defined in (2.40) and $\dot{\mathbf{F}}$ given by (2.100). Substituting $\dot{\Psi}$ into Equation (2.131) furnishes

$$\left(\rho\frac{\partial\check{\Psi}}{\partial\mathbf{F}}\mathbf{F}^{\mathrm{T}} - \mathbf{T}\right)\cdot\mathbf{L} + \rho\left(\frac{\partial\check{\Psi}}{\partial\theta} + \eta\right)\dot{\theta} + \rho\left(\frac{\partial\check{\Psi}}{\partial\operatorname{grad}\theta}\right)\cdot\overset{\cdot}{\overline{\operatorname{grad}\theta}} + \frac{\mathbf{q}\cdot\operatorname{grad}\theta}{\theta} \;\leq\; 0 \quad . \tag{2.134}$$

This inequality must hold for all $\mathbf{x}\in\mathcal{R}$ and t, including the initial conditions. Since the initial distributions of $\mathbf{x}$, $\mathbf{v}$, and θ can be chosen at will, so can the individual components of their gradients $\mathbf{F}$, $\mathbf{L}$, and $\operatorname{grad}\theta$. In addition, $\dot{\theta}$ and $\overset{\cdot}{\overline{\operatorname{grad}\theta}}$ may be determined arbitrarily by means of an appropriate distribution of body heating r. Hence, the only way to uphold inequality (2.134) is to require

$$\begin{aligned} \mathbf{T} \;&=\; \rho\frac{\partial\check{\Psi}}{\partial\mathbf{F}}\mathbf{F}^{\mathrm{T}} \quad , & \frac{\partial\check{\Psi}}{\partial\operatorname{grad}\theta} \;&=\; \mathbf{0} \quad , \\ \eta \;&=\; -\frac{\partial\check{\Psi}}{\partial\theta} \quad , & \mathbf{q}\cdot\operatorname{grad}\theta \;&\leq\; 0 \quad , \end{aligned} \tag{2.135}$$

where $\theta>0$ was used in $(2.135)_4$. Since any time t may be viewed as initial, Equations (2.135) must hold at all times.

According to $(2.135)_2$ the free energy of thermoelastic materials (2.132) must be independent of $\operatorname{grad}\theta$, that is, $\Psi=\check{\Psi}(\mathbf{F},\theta)$. Meanwhile $(2.135)_4$ indicates that $\mathbf{q}$ opposes the direction of $\operatorname{grad}\theta$. Heat thus flows in direction of decreasing temperature, a well known consequence of the second law of thermodynamics. The symmetry of the CAUCHY stress (2.120) ostensibly places an additional restriction on $\check{\Psi}(\mathbf{F},\theta)$ so as not to clash with $(2.135)_1$. However, it will be shown in Section 4.4.5 that, in the case of thermoelastic materials $\Psi=\check{\Psi}(\mathbf{F},\theta)$, this is automatically satisfied when Ψ is required to be invariant under superposed rigid-body transformations.

2.3.7 Referential Form of the Balance Equations

In view of the distinction between the EULERIAN and LAGRANGIAN descriptions introduced in Section 2.2.1, it may be desirable to evaluate the integrals of the preceding balance equations with respect to a referential region $\mathcal{P}_0$ rather than its current configuration $\mathcal{P}$. Furthermore, a LAGRANGIAN formulation is often advantageous in the discussion of the constitutive equations, see Section 6.1.2.

A referential statement for the conservation of mass is obtained as follows: Let the *mass density* of the *reference* configuration be denoted by $\rho_0(\mathbf{X},t)>0$. It is determined from the limit

$$m(\mathcal{P}_0) \;=\; \int_{\mathcal{P}_0} \rho_0 \,\mathrm{d}V \quad \text{where} \quad \rho_0 \;=\; \lim \frac{m(\mathcal{P}_0)}{\mathrm{vol}(\mathcal{P}_0)} \quad . \tag{2.136}$$

The mass $m(\mathcal{P}_0)$ contained within the volume $\mathrm{vol}(\mathcal{P}_0)$ of a referential region $\mathcal{P}_0$ around $\mathbf{X}$ at time t_0 is conserved. Therefore, at any time t of the motion the deformed region $\mathcal{P}$ must contain the same mass $m(\mathcal{P})=m(\mathcal{P}_0)$. A comparison between the spatial and referential integrals in $(2.109)_1$ and $(2.136)_1$ immediately yields

$$\rho_0 \;=\; \rho J \quad , \tag{2.137}$$

where use was made of the relation in (2.79) and the localization theorem. This corresponds to a referential description of conservation of mass, see SERRIN [129, Section B.I.5].

The balance of linear momentum (2.113) is expressed referentially as

$$\frac{\mathrm{d}}{\mathrm{d}t}\int_{\mathcal{P}_0} \rho_0 \mathbf{v} \,\mathrm{d}V \;=\; \int_{\partial\mathcal{P}_0} \mathbf{p}_{(\mathbf{N})} \,\mathrm{d}A + \int_{\mathcal{P}_0} \rho_0 \mathbf{f}_{\mathrm{B}} \,\mathrm{d}V \quad , \tag{2.138}$$

where the volume integrals follow from $\rho \mathrm{d}v = \rho_0 \mathrm{d}V$, see $(2.109)_1$ and $(2.136)_1$. Meanwhile, the *surface traction* $\mathbf{p}_{(\mathbf{N})}(\mathbf{X},t)$ per unit *referential* area[23] is defined through the requirement that $\mathrm{d}\mathbf{f} = \mathbf{t}_{(\mathbf{n})}\mathrm{d}a = \mathbf{p}_{(\mathbf{N})}\mathrm{d}A$. By applying CAUCHY's stress theorem (2.114) to $\mathbf{p}_{(\mathbf{N})} = \mathbf{P}\mathbf{N}$ the local form becomes

$$\rho_0 \mathbf{a} \;=\; \mathrm{Div}\,\mathbf{P} + \rho_0 \mathbf{f}_{\mathrm{B}} \quad , \tag{2.139}$$

which is the referential version of (2.115). It follows from NANSON's formula (2.80) that the so-called *first* PIOLA-KIRCHHOFF *stress tensor* $\mathbf{P}(\mathbf{X},t)$ is related to the CAUCHY stress tensor $\mathbf{T}$ via

$$\mathbf{P} \;=\; J\mathbf{T}\mathbf{F}^{-\mathrm{T}} \quad \text{or} \quad \mathbf{T} \;=\; J^{-1}\mathbf{P}\mathbf{F}^{\mathrm{T}} \quad . \tag{2.140}$$

[23] Note that, despite quantifying the traction relative to the referential area, $\mathbf{p}_{(\mathbf{N})}$ is a *spatial* vector, *i.e.*, resolved in the spatial bases $\mathbf{e}_i$. It differs from $\mathbf{t}_{(\mathbf{n})}$ only in magnitude, not direction.

Note that $\mathbf{P}$ corresponds to the PIOLA transform of $\mathbf{T}$ derived in $(2.90)_2$. Lastly, it is mentioned that $\mathbf{P} = P_{iA}\,\mathbf{e}_i \otimes \mathbf{E}_A$ is a two-point tensor whose components are rooted in both the spatial and referential bases similar to $\mathbf{F}$.

The referential forms of the balance of angular momentum (2.116) and its local counterpart (2.120) are given by

$$\frac{\mathrm{d}}{\mathrm{d}t}\int_{\mathcal{P}_0} \mathbf{x} \times \rho_0 \mathbf{v}\,\mathrm{d}V \;=\; \int_{\partial\mathcal{P}_0} \mathbf{x} \times \mathbf{p}_{(\mathbf{N})}\,\mathrm{d}A + \int_{\mathcal{P}_0} \mathbf{x} \times \rho_0 \mathbf{f}_{\mathrm{B}}\,\mathrm{d}V \quad , \tag{2.141}$$

and

$$\mathbf{P}\mathbf{F}^{\mathrm{T}} \;=\; \mathbf{F}\mathbf{P}^{\mathrm{T}} \quad , \tag{2.142}$$

where the local form is obtained using the same procedure employed in Section 2.3.3. Of course the spatial and referential angular momentum balances (2.120) and (2.142) are in agreement with the PIOLA transform in (2.140).

The principle of energy balance (2.121) and its local version (2.124) are stated in referential form as

$$\frac{\mathrm{d}}{\mathrm{d}t}\int_{\mathcal{P}_0} \rho_0 \left(\frac{1}{2}\mathbf{v}\cdot\mathbf{v} + \varepsilon\right)\mathrm{d}V \;=\; \int_{\mathcal{P}_0} \rho_0 \mathbf{f}_{\mathrm{B}}\cdot\mathbf{v}\,\mathrm{d}V + \int_{\partial\mathcal{P}_0} \mathbf{p}_{(\mathbf{N})}\cdot\mathbf{v}\,\mathrm{d}A + \int_{\mathcal{P}_0} \rho_0 r\,\mathrm{d}V - \int_{\partial\mathcal{P}_0} q_{0(\mathbf{N})}\,\mathrm{d}A \quad , \tag{2.143}$$

and

$$\rho_0 \left[\tfrac{1}{2}\mathbf{v}\cdot\mathbf{v} + \varepsilon\right]^{\bullet} \;=\; \rho_0 \mathbf{f}_{\mathrm{B}}\cdot\mathbf{v} + \mathrm{Div}\big(\mathbf{P}^{\mathrm{T}}\mathbf{v}\big) + \rho_0 r - \mathrm{Div}\,\mathbf{q}_0 \quad . \tag{2.144}$$

The *heat flux* per unit *referential* area $q_{0(\mathbf{N})}(\mathbf{X}, t)$ is defined via $q_{(\mathbf{n})}\mathrm{d}a = q_{0(\mathbf{N})}\mathrm{d}A$. It follows from NANSON's formula (2.80) and CAUCHY's theorem for the heat flux in (2.123) that

$$\mathbf{q}_0 \;=\; J\mathbf{F}^{-1}\mathbf{q} \quad \text{or} \quad \mathbf{q} \;=\; J^{-1}\mathbf{F}\,\mathbf{q}_0 \quad . \tag{2.145}$$

As expected, the *referential heat flux vector* $\mathbf{q}_0$ corresponds to the PIOLA transform of $\mathbf{q}$, see $(2.90)_1$. It quantifies the heat flux relative to the area and orientation of a *referential* boundary segment.

Recall from (2.126) that the balance of mechanical power (*i.e.*, the momentum balance contracted with the velocity $\mathbf{v}$) may be subtracted from the energy balance to yield the balance of thermal energy. Following the same procedure, the referential statements (2.139) and (2.144) furnish

$$\rho_0 \dot{\varepsilon} \;=\; \mathbf{P}\cdot\dot{\mathbf{F}} + \rho_0 r - \mathrm{Div}\,\mathbf{q}_0 \quad . \tag{2.146}$$

It is readily verified with Equations (2.100) and $(2.140)_1$ that the preceding result is consistent with the spatial version in (2.126), and that the stress power expended in $\mathcal{P}$ is expressed referentially as

$$\int_{\mathcal{P}} \mathbf{T}\cdot\mathbf{L}\,\mathrm{d}v \;=\; \int_{\mathcal{P}_0} \mathbf{P}\cdot\dot{\mathbf{F}}\,\mathrm{d}V \quad . \tag{2.147}$$

The first PIOLA-KIRCHHOFF stress tensor $\mathbf{P}$ is thus called *energy* (or *work*) *conjugate* to the deformation gradient $\mathbf{F}$. The stress power may alternatively be expressed with respect to the GREEN-LAGRANGE strain tensor $\mathbf{E}$ according to

$$\int_{\mathcal{P}} \mathbf{T}\cdot\mathbf{L}\,\mathrm{d}v \;=\; \int_{\mathcal{P}_0} \mathbf{S}\cdot\dot{\mathbf{E}}\,\mathrm{d}V \quad , \tag{2.148}$$

where the so-called *second* PIOLA-KIRCHHOFF *stress tensor* $\mathbf{S}(\mathbf{X},t)$ is defined by

$$\mathbf{S} \;=\; \mathbf{F}^{-1}\mathbf{P} \;=\; J\mathbf{F}^{-1}\mathbf{T}\mathbf{F}^{-\mathrm{T}} \quad \text{or} \quad \mathbf{P} \;=\; \mathbf{F}\mathbf{S} \quad \text{or} \quad \mathbf{T} \;=\; J^{-1}\mathbf{F}\mathbf{S}\mathbf{F}^{\mathrm{T}} \quad . \tag{2.149}$$

Note that $\mathbf{S}=S_{AB}\mathbf{E}_A\otimes\mathbf{E}_B$ is entirely referential, as opposed to the two-point tensor $\mathbf{P}$ and spatial tensor $\mathbf{T}$. The symmetry of $\mathbf{T}$ in (2.120) implies that $\mathbf{S}$ is likewise symmetric. The relation in (2.148) is readily obtained from the material time derivative of $(2.71)_1$ by invoking the symmetry of $\mathbf{S}$.

Lastly, the integral form of the CLAUSIUS-DUHEM inequality in (2.127) is written in terms of the referential configuration according to

$$\frac{\mathrm{d}}{\mathrm{d}t}\int_{\mathcal{P}_0}\rho_0\eta\,\mathrm{d}V \;\geq\; \int_{\mathcal{P}_0}\frac{\rho_0 r}{\theta}\,\mathrm{d}V \;-\; \int_{\partial\mathcal{P}_0}\frac{q_{0(\mathbf{N})}}{\theta}\,\mathrm{d}A \quad , \tag{2.150}$$

or in local form

$$\rho_0\dot{\eta} \;\geq\; \frac{\rho_0 r}{\theta} \;-\; \mathrm{Div}\left(\frac{\mathbf{q}_0}{\theta}\right) \quad . \tag{2.151}$$

Similarly, the inequality in (2.129) is stated referentially as

$$\rho_0\left(\dot{\varepsilon}-\theta\dot{\eta}\right) \;-\; \mathbf{P}\cdot\dot{\mathbf{F}} \;+\; \mathbf{q}_0\cdot\left(\mathrm{Grad}\,\theta\right)/\theta \;\leq\; 0 \quad , \tag{2.152}$$

where use was made of the preceding result for the referential stress power. Note that the thermodynamic restrictions (2.135) on the constitutive equations, attained in Section 2.3.6 using the method of COLEMAN and NOLL, can be identically reproduced using the referential description.

2.4 Superposed Rigid-Body Motions and Galilean Transformations

In order to examine the transformation properties of physical quantities, the concept of *superposed rigid-body motions* (SRBM) is presented. Following common practice in classical continuum mechanics, SRBMs are viewed as rotations and translations of the body rather than of the coordinate system.

2.4.1 Position, Velocity, and Acceleration

Rigid body motion is prescribed by subjecting all material points $\mathbf{x}$ to a *uniform proper orthogonal rotation* $\mathbf{Q}(t) \in \mathrm{Orth}^+$, see (2.21), followed by a *uniform translation* $\mathbf{c}(t)$ according to

$$\mathbf{x}^+ = \mathbf{Q}\mathbf{x} + \mathbf{c} \quad \text{and} \quad t^+ = t \quad . \tag{2.153}$$

It is readily verified that EUCLIDEAN distances $|\mathbf{x}_2 - \mathbf{x}_1|$ are preserved, which is why Equation (2.153) is also known as a EUCLIDEAN *transformation*. On the other hand, a GALILEAN *transformation* is a special case of (2.153), where the motion consists of a translation at constant velocity $\mathbf{v}_0$ and fixed rotation $\mathbf{Q}_0$, such that

$$\mathbf{x}^+ \overset{\text{Gal.}}{=} \mathbf{Q}_0\big(\mathbf{x} + \mathbf{v}_0 t\big) \quad \text{and} \quad t^+ = t \quad . \tag{2.154}$$

The equation superscript $\overset{\text{Gal.}}{=}$ is intended to avoid confusion between general (EUCLIDEAN) SRBM (2.153) and GALILEAN transformations (2.154).

The velocity of the transformed system is obtained by taking the material time derivative of $\mathbf{x}^+$. For general SRBMs (2.153),

$$\begin{aligned} \dot{\mathbf{x}}^+ = \mathbf{v}^+ &= \mathbf{Q}\mathbf{v} + \dot{\mathbf{Q}}\mathbf{x} + \dot{\mathbf{c}} \\ &= \mathbf{Q}\big(\mathbf{v} + \boldsymbol{\Omega}\mathbf{x} + \mathbf{Q}^{\mathrm{T}}\dot{\mathbf{c}}\big) \\ &= \mathbf{Q}\big(\mathbf{v} + \boldsymbol{\beta}\big) \quad , \end{aligned} \tag{2.155}$$

where a tensor $\boldsymbol{\Omega}(t)$ and vector $\boldsymbol{\beta}(\mathbf{x}, t)$ are defined for notational convenience,

$$\begin{aligned} \boldsymbol{\Omega}(t) &= \mathbf{Q}^{\mathrm{T}}\dot{\mathbf{Q}} \quad , \\ \boldsymbol{\beta}(\mathbf{x}, t) &= \mathbf{Q}^{\mathrm{T}}\big(\dot{\mathbf{Q}}\mathbf{x} + \dot{\mathbf{c}}\big) \quad \big(= \boldsymbol{\Omega}\mathbf{x} + \mathbf{Q}^{\mathrm{T}}\dot{\mathbf{c}}\big) \quad . \end{aligned} \tag{2.156}$$

It follows from the orthogonality of $\mathbf{Q}$ that $\boldsymbol{\Omega}$ is skew-symmetric,

$$\boldsymbol{\Omega} = -\boldsymbol{\Omega}^{\mathrm{T}} \quad . \tag{2.157}$$

Therefore its operation $\boldsymbol{\Omega}\mathbf{w}$ on an arbitrary vector $\mathbf{w}$ can alternatively be described by a vector product with the *axial vector* $\boldsymbol{\omega}$,

$$\boldsymbol{\Omega}\mathbf{w} = \boldsymbol{\omega} \times \mathbf{w} \quad \text{where} \quad \boldsymbol{\omega}(t) = \tfrac{1}{2}\Omega_{ji}\epsilon_{ijk}\mathbf{e}_k \quad . \tag{2.158}$$

Furthermore, it is observed that material time derivatives $\dot{\boldsymbol{\Omega}}$, $\ddot{\boldsymbol{\Omega}}$, *etc.*, remain skew-symmetric. Powers $\boldsymbol{\Omega}^n$ are symmetric when n is even, and skew when n is odd. The linearity of $\boldsymbol{\beta}$ with respect to $\mathbf{x}$ and skew-symmetry of $\boldsymbol{\Omega}$ further imply that

$$\begin{aligned} \mathrm{grad}\,\boldsymbol{\beta} &= \mathbf{Q}^{\mathrm{T}}\dot{\mathbf{Q}} = \boldsymbol{\Omega} \quad , \\ \mathrm{div}\,\boldsymbol{\beta} &= \mathrm{tr}\big[\mathrm{grad}\,\boldsymbol{\beta}\big] = \mathrm{tr}(\boldsymbol{\Omega}) = 0 \quad . \end{aligned} \tag{2.159}$$

For GALILEAN transformations (2.154) the parameters of the SRBM simplify to

$$\begin{aligned} \mathbf{Q}(t) &\overset{\text{Gal.}}{=} \mathbf{Q}_0 \quad , \quad \mathbf{c}(t) \overset{\text{Gal.}}{=} \mathbf{Q}_0\mathbf{v}_0 t \quad , \quad \boldsymbol{\beta}(\mathbf{x},t) \overset{\text{Gal.}}{=} \mathbf{v}_0 \quad , \\ \boldsymbol{\Omega}(t) &\overset{\text{Gal.}}{=} \mathbf{0} \quad , \quad \dot{\mathbf{c}}(t) \overset{\text{Gal.}}{=} \mathbf{Q}_0\mathbf{v}_0 \quad , \quad \dot{\boldsymbol{\beta}}(\mathbf{x},t) \overset{\text{Gal.}}{=} \mathbf{0} \quad . \end{aligned} \tag{2.160}$$

Transformation formulae for general SRBMs, like Equation (2.155) for the velocity, are readily specialized to GALILEAN transformations using the relations (2.160).

Another material time derivative on $(2.155)_{1,3}$ yields the acceleration of the body under general SRBMs,

$$\begin{aligned} \ddot{\mathbf{x}}^+ = \dot{\mathbf{v}}^+ = \mathbf{a}^+ &= \mathbf{Q}\big(\mathbf{a} + 2\boldsymbol{\Omega}\mathbf{v} + \boldsymbol{\Omega}^2\mathbf{x} + \dot{\boldsymbol{\Omega}}\mathbf{x} + \mathbf{Q}^{\mathrm{T}}\ddot{\mathbf{c}}\big) \\ &= \mathbf{Q}\Big\{\big(\mathbf{a}+\dot{\boldsymbol{\beta}}\big) + \boldsymbol{\Omega}\big(\mathbf{v}+\boldsymbol{\beta}\big)\Big\} \quad , \end{aligned} \tag{2.161}$$

where use was made of $\dot{\mathbf{Q}} = \mathbf{Q}\boldsymbol{\Omega}$ and $\ddot{\mathbf{Q}} = \mathbf{Q}\big[\boldsymbol{\Omega}^2 + \dot{\boldsymbol{\Omega}}\big]$.

2.4.2 Spatial Differential Operators

The transformation of the differential operators (2.42) under SRBMs is examined next. These properties will be applied frequently in the transformation of the balance equations. Appealing to Equation (2.153), the mixed gradients of the position vectors $\mathbf{x}^+$ and $\mathbf{x}$ are, respectively,

$$\operatorname{grad}\mathbf{x}^+ = \frac{\partial \mathbf{x}^+}{\partial \mathbf{x}} = \mathbf{Q} \quad \text{and} \quad \operatorname{grad}^+\mathbf{x} = \frac{\partial \mathbf{x}}{\partial \mathbf{x}^+} = \mathbf{Q}^{-1} = \mathbf{Q}^{\mathrm{T}} \quad , \tag{2.162}$$

where grad^+ signifies the gradient with respect to the transformed position $\mathbf{x}^+$. The gradient of a scalar field $\alpha^+ = \bar{\alpha}^+(\mathbf{x}^+,t) = \bar{\alpha}^+(\mathbf{Q}(t)\mathbf{x}+\mathbf{c}(t),t) = \tilde{\alpha}^+(\mathbf{x},t)$ transforms by chain rule according to

$$\operatorname{grad}^+\alpha^+ = \frac{\partial \bar{\alpha}^+}{\partial \mathbf{x}^+} = \frac{\partial \tilde{\alpha}^+}{\partial \mathbf{x}}\frac{\partial \mathbf{x}}{\partial \mathbf{x}^+} = \mathbf{Q}\operatorname{grad}\alpha^+ \quad . \tag{2.163}$$

The gradient of a vector field $\mathbf{w}^+ = \bar{\mathbf{w}}^+(\mathbf{x}^+,t) = \tilde{\mathbf{w}}^+(\mathbf{x},t)$ obeys

$$\operatorname{grad}^+\mathbf{w}^+ = \frac{\partial \bar{\mathbf{w}}^+}{\partial \mathbf{x}^+} = \frac{\partial \tilde{\mathbf{w}}^+}{\partial \mathbf{x}}\frac{\partial \mathbf{x}}{\partial \mathbf{x}^+} = \big[\operatorname{grad}\mathbf{w}^+\big]\mathbf{Q}^{\mathrm{T}} = \mathbf{Q}\big[\operatorname{grad}\big(\mathbf{Q}^{\mathrm{T}}\mathbf{w}^+\big)\big]\mathbf{Q}^{\mathrm{T}} \quad , \tag{2.164}$$

where the uniformity of $\mathbf{Q}(t)$ was exploited.

Similarly, chain rule furnishes transformation relations for the divergence of vector fields $\mathbf{w}^+$ and tensor fields $\mathbf{T}^+ = \bar{\mathbf{T}}^+(\mathbf{x}^+,t) = \tilde{\mathbf{T}}^+(\mathbf{x},t)$,

$$\operatorname{div}^+\mathbf{w}^+ = \frac{\partial \bar{w}_i^+}{\partial x_i^+} = \frac{\partial \tilde{w}_i^+}{\partial x_j}\frac{\partial x_j}{\partial x_i^+} = \operatorname{grad}\mathbf{w}^+ \cdot \mathbf{Q} = \operatorname{div}\big(\mathbf{Q}^{\mathrm{T}}\mathbf{w}^+\big) \quad , \tag{2.165}$$

and

$$\operatorname{div}^+\mathbf{T}^+ = \frac{\partial \bar{T}^+_{ij}}{\partial x^+_j}\mathbf{e}_i = \frac{\partial \tilde{T}^+_{ij}}{\partial x_k}\frac{\partial x_k}{\partial x^+_j}\mathbf{e}_i = \frac{\partial \tilde{T}^+_{ij}}{\partial x_k}Q_{jk}\mathbf{e}_i = \operatorname{div}\big[\mathbf{T}^+\mathbf{Q}\big] = \mathbf{Q}\operatorname{div}\big[\mathbf{Q}^{\mathrm{T}}\mathbf{T}^+\mathbf{Q}\big] \quad , \tag{2.166}$$

respectively.

The transformation of the curl is conveniently obtained by first converting it to a divergence using its definition $(2.41)_3$, upon which transformation (2.165) is applied. With the aid of $(2.37)_2$,

$$\begin{aligned} \big(\operatorname{curl}^+\mathbf{w}^+\big)\cdot\mathbf{h} &= \operatorname{div}^+\big(\mathbf{w}^+\times\mathbf{h}\big) \\ &= \operatorname{div}\big(\mathbf{Q}^{\mathrm{T}}(\mathbf{w}^+\times\mathbf{h})\big) \\ &= \operatorname{div}\big(\mathbf{Q}^{\mathrm{T}}\mathbf{w}^+\times\mathbf{Q}^{\mathrm{T}}\mathbf{h}\big) \\ &= \operatorname{curl}\big(\mathbf{Q}^{\mathrm{T}}\mathbf{w}^+\big)\cdot\mathbf{Q}^{\mathrm{T}}\mathbf{h} \\ &= \mathbf{Q}\operatorname{curl}\big(\mathbf{Q}^{\mathrm{T}}\mathbf{w}^+\big)\cdot\mathbf{h} \quad \forall \text{ constant } \mathbf{h} \quad , \end{aligned} \tag{2.167}$$

and hence

$$\operatorname{curl}^+\mathbf{w}^+ = \mathbf{Q}\operatorname{curl}\big(\mathbf{Q}^{\mathrm{T}}\mathbf{w}^+\big) \quad . \tag{2.168}$$

It is mentioned that the preceding result is readily verified in integral form by applying the STOKES theorem (2.53) to $\int_{\mathcal{A}^+}\operatorname{curl}^+\mathbf{w}^+\cdot\mathbf{n}^+\mathrm{d}a^+$ and employing the transformations for $\mathrm{d}\mathbf{x}^+$, $\mathbf{n}^+$, and $\mathrm{d}a^+$ discussed later in $(2.170)_{2-4}$.

Note the similarity of the transformations in (2.163 - 166) and (2.168) with the relations between the spatial and referential derivatives in Equations (2.82), (2.84 - 86), and (2.94). This is of course to be expected, given that the SRBM in $(2.153)_1$ represents a motion from $\mathbf{x}$ to $\mathbf{x}^+$, with 'deformation gradient' $\mathbf{Q}$ and $\mathbf{Q}^{\mathrm{T}}$ in $(2.162)_{1,2}$ assuming the role $\mathbf{F}$ and $\mathbf{F}^{-1}$ in (2.66) and (2.67).

With the definition and properties of superposed rigid-body motions in place, the transformation rules for individual physical quantities are examined next. First the kinematic quantities are derived, followed by the thermomechanical fields.

2.4.3 Kinematic Quantities

The transformation of the deformation gradient (2.66) and its polar decomposition (2.69) follows immediately from the superposed motion (2.153),

$$\mathbf{F}^+ = \frac{\partial \mathbf{x}^+}{\partial \mathbf{x}}\frac{\partial \chi}{\partial \mathbf{X}} = \mathbf{Q}\mathbf{F} \quad , \quad \mathbf{R}^+ = \mathbf{Q}\mathbf{R} \quad , \quad \mathbf{U}^+ = \mathbf{U} \quad , \quad \mathbf{V}^+ = \mathbf{Q}\mathbf{V}\mathbf{Q}^{\mathrm{T}} \quad . \tag{2.169}$$

The transformation of the JACOBIAN J (2.68) is obtained from (2.165) and $(2.169)_1$. Furthermore, it follows that the infinitesimal material line elements $\mathrm{d}\mathbf{x}$ (2.65), area elements $\mathbf{n}\mathrm{d}a$ (2.80), and volume elements $\mathrm{d}v$ (2.79) transform according to

$$J^+ = J \quad , \quad \mathrm{d}\mathbf{x}^+ = \mathbf{Q}\mathrm{d}\mathbf{x} \quad , \quad \mathbf{n}^+ = \mathbf{Q}\mathbf{n} \quad , \quad \mathrm{d}a^+ = \mathrm{d}a \quad , \quad \mathrm{d}v^+ = \mathrm{d}v \quad . \tag{2.170}$$

The transformation of the spatial velocity gradient $\mathbf{L}$ (2.97) is obtained with the aid of $(2.155)_3$, $(2.159)_1$, and (2.164),

$$\mathbf{L}^+ = \operatorname{grad}^+\mathbf{v}^+ = \mathbf{Q}\operatorname{grad}\big(\mathbf{v}+\boldsymbol{\beta}\big)\mathbf{Q}^{\mathrm{T}} = \mathbf{Q}\big[\mathbf{L}+\boldsymbol{\Omega}\big]\mathbf{Q}^{\mathrm{T}} \quad . \tag{2.171}$$

This result is consistent with Equation (2.100) for $\dot{\mathbf{F}}$ and $(2.169)_1$ in the sense that

$$\overline{\dot{\mathbf{F}}^+} = \dot{\mathbf{Q}}\mathbf{F}+\mathbf{Q}\dot{\mathbf{F}} = \mathbf{Q}\boldsymbol{\Omega}\mathbf{F}+\mathbf{Q}\mathbf{L}\mathbf{F} = \mathbf{Q}\big[\mathbf{L}+\boldsymbol{\Omega}\big]\mathbf{Q}^{\mathrm{T}}\mathbf{Q}\mathbf{F} = \mathbf{L}^+\mathbf{F}^+ = (\dot{\mathbf{F}})^+ \quad . \tag{2.172}$$

Finally it is seen from (2.171) that, despite $\mathbf{v}^+$ transforming according to (2.155), its divergence

$$\operatorname{div}^+\mathbf{v}^+ = \operatorname{tr}\big[\mathbf{L}^+\big] = \big[\mathbf{L}+\boldsymbol{\Omega}\big]\cdot\mathbf{i} = \operatorname{tr}\mathbf{L} = \operatorname{div}\mathbf{v} \quad . \tag{2.173}$$

remains unchanged under SRBM because $\boldsymbol{\Omega}$ is skew. This is in agreement with Equations (2.98) for $\overline{\mathrm{d}v}^{\cdot}$ and $(2.170)_5$ for $\mathrm{d}v^+$. The result in (2.173) may alternatively be derived from Equations $(2.155)_3$, $(2.159)_2$, and (2.165).

2.4.4 Thermomechanical Quantities

To derive transformation rules for thermomechanical fields it is postulated that

$$\mathbf{t}^+_{(\mathbf{n}^+)} = \mathbf{Q}\mathbf{t}_{(\mathbf{n})} \quad , \quad \varepsilon^+ = \varepsilon \quad , \quad r^+ = r \quad , \quad q^+_{(\mathbf{n}^+)} = q_{(\mathbf{n})} \quad . \tag{2.174}$$

Applying the transformation $(2.170)_3$ for $\mathbf{n}^+$ to CAUCHY's stress theorem (2.114) and its heat flux counterpart (2.123) leads to

$$\mathbf{T}^+ = \mathbf{Q}\mathbf{T}\mathbf{Q}^{\mathrm{T}} \quad , \quad \mathbf{q}^+ = \mathbf{Q}\mathbf{q} \quad . \tag{2.175}$$

The divergence of the stress and heat flux (2.175) with respect to $\mathbf{x}^+$ simplifies to

$$\begin{aligned} \operatorname{div}^+\mathbf{T}^+ &= \operatorname{div}(\mathbf{T}^+\mathbf{Q}) = \operatorname{div}(\mathbf{Q}\mathbf{T}) = Q_{ij}T_{jk,k}\mathbf{e}_i = \mathbf{Q}\operatorname{div}\mathbf{T} \quad , \\ \operatorname{div}^+\mathbf{q}^+ &= \operatorname{div}(\mathbf{Q}^{\mathrm{T}}\mathbf{q}^+) = \operatorname{div}\mathbf{q} \quad , \end{aligned} \tag{2.176}$$

where Equations (2.165) and (2.166) were used.

It is further postulated that the balance equations derived in Section 2.3 are *form-invariant* under SRBM. This means that different observers experience the same laws of motion despite their disagreement on the measured value of individual quantities like acceleration (2.161). The balances of mass (2.111) and linear momentum (2.115), respectively, furnish the transformations

$$\rho^+ = \rho \quad , \quad \mathbf{f}^+_{\mathrm{B}} = \mathbf{Q}\big(\mathbf{f}_{\mathrm{B}}-\mathbf{a}\big)+\mathbf{a}^+ \quad , \tag{2.177}$$

where Equations (2.155), $(2.171)_3$, and $(2.176)_1$ were employed. The balances of angular momentum (2.120) and thermal energy (2.126) are automatically satisfied by the

transformed quantities (2.171), $(2.174)_{2,3}$, and $(2.175)_{1,2}$. Finally, the temperature θ of a material point is postulated to be unaffected by SRBM, so that the invariance of the entropy inequality (2.128) implies

$$\theta^+ = \theta \quad , \quad \eta^+ = \eta \quad , \quad \Psi^+ = \Psi \quad . \tag{2.178}$$

The expression for $\mathbf{f}_{\mathrm{B}}^+$ in Equation $(2.177)_2$ is relatively complicated in view of transformation (2.161) for $\mathbf{a}^+$. However, a simple relation may be found for the power of the body force,

$$\begin{aligned} \mathbf{f}_{\mathrm{B}}^+ \cdot \mathbf{v}^+ &= \Big(\mathbf{Q}\big(\mathbf{f}_{\mathrm{B}} - \mathbf{a}\big) + \mathbf{a}^+\Big) \cdot \mathbf{Q}\big(\mathbf{v} + \boldsymbol{\beta}\big) \\ &= \big(\mathbf{f}_{\mathrm{B}} - \mathbf{a}\big) \cdot \big(\mathbf{v} + \boldsymbol{\beta}\big) + \big(\mathbf{a} + \dot{\boldsymbol{\beta}}\big) \cdot \big(\mathbf{v} + \boldsymbol{\beta}\big) + \boldsymbol{\Omega}\big(\mathbf{v} + \boldsymbol{\beta}\big) \cdot \big(\mathbf{v} + \boldsymbol{\beta}\big) \\ &= \big(\mathbf{f}_{\mathrm{B}} + \dot{\boldsymbol{\beta}}\big) \cdot \big(\mathbf{v} + \boldsymbol{\beta}\big) \quad , \end{aligned} \tag{2.179}$$

where the skew-symmetry of $\boldsymbol{\Omega}$ (2.157) was used.

2.4.5 Time Derivatives: Partial, Flux, and Path Derivatives

In the discussion of transformation properties of partial time derivatives, it must be explicitly specified whether $\mathbf{x}^+$ or $\mathbf{x}$ shall be fixed, because the SRBM in (2.153) generally evolves with time.[24] Notwithstanding, the chain rule (2.95) for the total time derivative applies to both functional representations $\mathcal{F}^+ = \bar{\mathcal{F}}^+(\mathbf{x}^+, t) = \tilde{\mathcal{F}}^+(\mathbf{x}, t)$, hence using $(2.96)_{1,2}$

$$\begin{aligned} \dot{\alpha}^+ &= \left.\frac{\partial \bar{\alpha}^+}{\partial t}\right|_{\mathbf{x}^+ \text{ fix}} + \big(\mathrm{grad}^+ \bar{\alpha}^+\big) \cdot \mathbf{v}^+ = \left.\frac{\partial \tilde{\alpha}^+}{\partial t}\right|_{\mathbf{x} \text{ fix}} + \big(\mathrm{grad}\, \tilde{\alpha}^+\big) \cdot \mathbf{v} \quad , \\ \dot{\mathbf{w}}^+ &= \left.\frac{\partial \bar{\mathbf{w}}^+}{\partial t}\right|_{\mathbf{x}^+ \text{ fix}} + \big(\mathrm{grad}^+ \bar{\mathbf{w}}^+\big)\mathbf{v}^+ = \left.\frac{\partial \tilde{\mathbf{w}}^+}{\partial t}\right|_{\mathbf{x} \text{ fix}} + \big(\mathrm{grad}\, \tilde{\mathbf{w}}^+\big)\mathbf{v} \quad . \end{aligned} \tag{2.180}$$

Equations (2.180) do *not* assert that the material time derivative of a field $\mathcal{F}^+$ is invariant under SRBM. They merely observe that $\dot{\mathcal{F}}^+$ is independent of its functional representation in terms of $(\mathbf{x}^+, t)$ *vs.* $(\mathbf{x}, t)$ by virtue of being *material*. Equations (2.180) furnish a relation between the partial time derivatives of $\bar{\mathcal{F}}^+$ and $\tilde{\mathcal{F}}^+$, more succinctly expressed using $(2.155)_3$, (2.163) and (2.164) by

$$\begin{aligned} \frac{\partial \bar{\alpha}^+}{\partial t} &= \frac{\partial \tilde{\alpha}^+}{\partial t} - \big(\mathrm{grad}\, \alpha^+\big) \cdot \boldsymbol{\beta} \quad , \\ \frac{\partial \bar{\mathbf{w}}^+}{\partial t} &= \frac{\partial \tilde{\mathbf{w}}^+}{\partial t} - \big[\mathrm{grad}\, \mathbf{w}^+\big]\boldsymbol{\beta} \quad , \end{aligned} \tag{2.181}$$

[24] This is unlike the spatial differential operators of Section 2.4.2, which are unambiguous in the sense that time t is considered fixed irrespective of whether the partial derivatives are with respect to $\mathbf{x}^+$ or $\mathbf{x}$.

where $\boldsymbol{\beta}$ is defined by $(2.156)_2$. The subscripts of Equation (2.180) are dropped for brevity, leaving only the *bar* and *tilde* accents to indicate whether $\mathbf{x}^+$ or $\mathbf{x}$ shall be fixed in partial time derivatives. However, most quantities throughout this dissertation are *not* explicitely equipped with an accent even when partial time derivatives are involved, such as in $(2.104)_2$. Instead, it is tacitly assumed that their representation is EULERIAN. Hence, $\mathcal{F}^+ = \bar{\mathcal{F}}^+(\mathbf{x}^+, t)$ and $\mathcal{F} = \tilde{\mathcal{F}}(\mathbf{x}, t)$ are understood to be functions of their corresponding spatial positions $\mathbf{x}^+$ and $\mathbf{x}$, respectively.[25]

The preceding discussion illustrates that partial time derivatives, much like the differential operators in Section 2.4.2, are subject to transformation rules under SRBM. This raises the question of how the the flux derivative $\overset{\star}{\mathbf{w}}$ transforms under the general SRBM of (2.153). Applied to $\bar{\mathbf{w}}^+(\mathbf{x}^+, t)$, the definition of the flux derivative $(2.106)_3$ reads

$$\big(\bar{\mathbf{w}}^+\big)^\star = \frac{\partial \bar{\mathbf{w}}^+}{\partial t} + \big(\mathrm{div}^+ \mathbf{w}^+\big)\mathbf{v}^+ - \mathrm{curl}^+\big(\mathbf{v}^+ \times \mathbf{w}^+\big) \quad , \tag{2.182}$$

whose transformations are given by Equations $(2.155)_3$, (2.165), (2.168), and $(2.181)_2$. Upon some rearrangements it can be shown that

$$\begin{aligned} \big(\bar{\mathbf{w}}^+\big)^\star &= \mathbf{Q}\Big\{\frac{\partial}{\partial t}\Big(\mathbf{Q}^{\mathrm{T}}\tilde{\mathbf{w}}^+\Big) + \mathrm{div}\big(\mathbf{Q}^{\mathrm{T}}\mathbf{w}^+\big)\mathbf{v} - \mathrm{curl}\big\{\mathbf{v} \times \big(\mathbf{Q}^{\mathrm{T}}\mathbf{w}^+\big)\big\}\Big\} \\ &= \mathbf{Q}\big(\mathbf{Q}^{\mathrm{T}}\tilde{\mathbf{w}}^+\big)^\star \quad . \end{aligned} \tag{2.183}$$

A detailed derivation of (2.183) is provided in Appendix A.3.

Similarly, it follows from (2.171), (2.173), and (2.183) that the path derivative in $(2.108)_3$ transforms according to

$$\begin{aligned} \big(\bar{\mathbf{w}}^+\big)^\circ &= \big(\bar{\mathbf{w}}^+\big)^\star - \big(\mathrm{div}^+ \mathbf{v}^+\big)\mathbf{w}^+ + 2\big[\mathrm{sym}\,\mathbf{L}^+\big]\mathbf{w}^+ \\ &= \mathbf{Q}\Big\{\big(\mathbf{Q}^{\mathrm{T}}\tilde{\mathbf{w}}^+\big)^\star - \big(\mathrm{div}\,\mathbf{v}\big)\big(\mathbf{Q}^{\mathrm{T}}\mathbf{w}^+\big) + 2\big[\mathrm{sym}\,\mathbf{L}\big]\mathbf{Q}^{\mathrm{T}}\mathbf{w}^+\Big\} \\ &= \mathbf{Q}\big(\mathbf{Q}^{\mathrm{T}}\tilde{\mathbf{w}}^+\big)^\circ \quad . \end{aligned} \tag{2.184}$$

As in the preceding discussion for partial time derivatives, it is again emphasized that the accents $\bar{\mathbf{w}}^+$ *vs.* $\tilde{\mathbf{w}}^+$ stipulate whether the flux and path derivatives are to be taken with respect to the transformed or the untransformed representation of $\mathbf{w}^+$, respectively. This affects not only differential operators and partial time derivatives of $\bar{\mathbf{w}}^+(\mathbf{x}^+, t)$ *vs.* $\tilde{\mathbf{w}}^+(\mathbf{x}, t)$, but also the velocity $\mathbf{v}^+$ *vs.* $\mathbf{v}$ in the definitions of the flux and path derivatives (2.106) and (2.108). As per the aforementioned convention for partial time derivatives, in the absence of accents the derivatives refer to the natural EULERIAN representation of $\mathbf{w}^+ = \bar{\mathbf{w}}^+(\mathbf{x}^+, t)$ and $\mathbf{w} = \tilde{\mathbf{w}}(\mathbf{x}, t)$.

[25] For example, let a vector field $\mathbf{w}$ transform according to $\mathbf{w}^+ = \mathbf{Q}\mathbf{w}$. Equation $(2.181)_2$ is expressed without accents by $\frac{\partial}{\partial t}(\mathbf{w}^+) = \frac{\partial}{\partial t}(\mathbf{Q}\mathbf{w}) - [\mathrm{grad}(\mathbf{Q}\mathbf{w})]\boldsymbol{\beta}$, where $\mathbf{x}^+$ is fixed in $\frac{\partial}{\partial t}(\mathbf{w}^+)$ and $\mathbf{x}$ is fixed for $\frac{\partial}{\partial t}(\mathbf{Q}\mathbf{w})$, because its natural EULERIAN functional representation is $\mathbf{Q}(t)\tilde{\mathbf{w}}(\mathbf{x}, t)$.

2.4.6 Objectivity and Galilean Invariance

A field is termed *objective* if it transforms under SRBM in the same way its coordinate basis does.[26] Real-, vector-, and tensor-valued spatial fields are thus objective if $\alpha^+ = \alpha$, $\mathbf{w}^+ = \mathbf{Q}\mathbf{w}$, and $\mathbf{T}^+ = \mathbf{Q}\mathbf{T}\mathbf{Q}^{\mathrm{T}}$. Given a set of objective fields α, β, $\mathbf{u}$, $\mathbf{v}$, $\mathbf{S}$, and $\mathbf{T}$, any multiplication (such as $\alpha\mathbf{w}$, $\mathbf{T}\mathbf{w}$, $\mathbf{S}\mathbf{T}$) or contraction (such as $\alpha\beta$, $\mathbf{u}\cdot\mathbf{w}$, $\mathbf{S}\cdot\mathbf{T}$) thereof results in an objective quantity as well.

A superposed rigid-body motion where the body forces $\mathbf{f}_{\mathrm{B}}^+ = \mathbf{Q}\mathbf{f}_{\mathrm{B}}$ transform objectively is called *inertial*. Inertial motions do not introduce artificial body forces and exhibit an objective acceleration $\mathbf{a}^+$ as evident from $(2.177)_2$. Galilean transformations (2.154) are inertial (and *vice versa*), see (2.160 - 161), so that the two terms are used synonymously. Fields that transform objectively under Galilean transformations are termed Galilean *invariant*.

Of course, all objective fields are Galilean invariant but not all Galilean invariant fields are objective. This is to say that general objectivity is more restrictive than invariance under the limited subset of Galilean transformations. For example, the acceleration $\mathbf{a}^+$ is (by definition) invariant under inertial motions, but not for general SRBM's. The velocity gradient $\mathbf{L}^+$, although Galilean invariant, is not objective according to (2.171). Note that the stress power $\mathbf{T}^+\cdot\mathbf{L}^+$ is nevertheless objective on account of the symmetry of $\mathbf{T}$ and skew-symmetry of $\mathbf{\Omega}$.

The transformation rules in (2.163 - 166) and (2.168) for the differential operators are found to preserve the objectivity of the fields they act upon. This means, for example, that $\mathrm{grad}^+\mathbf{w}^+ = \mathbf{Q}[\mathrm{grad}\mathbf{w}]\mathbf{Q}^{\mathrm{T}}$, $\mathrm{div}^+\mathbf{T}^+ = \mathbf{Q}\,\mathrm{div}\mathbf{T}$, and $\mathrm{curl}^+\mathbf{w}^+ = \mathbf{Q}\,\mathrm{curl}\mathbf{w}$ are themselves objective, provided that $\mathbf{w}^+$ and $\mathbf{T}^+$ are objective.

Among the total time derivatives $(2.96)_{1-3}$ only the scalar-valued fields preserve objectivity. Nevertheless, the material time derivatives of vectors and tensors are Galilean invariant since, for example, $(\mathbf{w}^+)^{\bullet} = \mathbf{Q}\dot{\mathbf{w}} + \dot{\mathbf{Q}}\mathbf{w} = \mathbf{Q}\dot{\mathbf{w}}$ *etc*. Partial time derivatives $(2.181)_{1,2}$ are neither objective nor Galilean invariant due to the convective contribution of $\boldsymbol{\beta}$ as defined in $(2.156)_2$.

The flux derivative (2.106) and the path derivative (2.108) of objective vectors transform according to $(\bar{\mathbf{w}}^+)^{\star} = \mathbf{Q}(\tilde{\mathbf{w}})^{\star}$ and $(\bar{\mathbf{w}}^+)^{\circ} = \mathbf{Q}(\tilde{\mathbf{w}})^{\circ}$, respectively, see (2.183 - 184). Hence it is concluded that (unlike the total and partial time derivatives) the flux and path derivatives of objective vector fields are again objective. This result is not surprising: Due to the materiality of the integral domains $\mathcal{A}$ and $\mathcal{S}$, the flux $\int_{\mathcal{A}} \mathbf{w}\cdot\mathbf{n}\,da$ in (2.105) and the path integral $\int_{\mathcal{S}} \mathbf{w}\cdot\mathrm{d}\mathbf{x}$ in (2.107) are invariant scalar quantities provided that $\mathbf{w}^+ = \mathbf{Q}\mathbf{w}$ is objective. Therefore, its material time derivative must be objective, too.

[26] Objective transformations are akin to a *push-forward* operation of the spatial fields α, $\mathbf{w}$, $\mathbf{T}$ to the transformed spatial fields α^+, $\mathbf{w}^+$, $\mathbf{T}^+$. The corresponding *pull-back* is $\alpha = \alpha^+$, $\mathbf{w} = \mathbf{Q}^{\mathrm{T}}\mathbf{w}^+$, $\mathbf{T} = \mathbf{Q}^{\mathrm{T}}\mathbf{T}^+\mathbf{Q}$. According to this narrative, $\mathbf{Q}$ may be regarded as a deformation gradient between the two spatial configurations, with a multiplicative decomposition $(2.169)_1$ for the total deformation $\mathbf{F}^+$.

Lastly, it is mentioned that the PIOLA transform of a vector, see $(2.90)_1$, transforms according to $\mathbf{w}_0^+ = J\mathbf{F}^{-1}(\mathbf{Q}^{\mathrm{T}}\mathbf{w}^+)$. It is thus concluded from Equation $(2.175)_2$ that the referential form of the heat flux $\mathbf{q}_0$ in $(2.145)_1$ is invariant under SRBM, or $\mathbf{q}_0^+ = \mathbf{q}_0$. Similarly, the second PIOLA-KIRCHHOFF stress tensor in (2.149) transforms via $\mathbf{S}^+ = J\mathbf{F}^{-1}[\mathbf{Q}^{\mathrm{T}}\mathbf{T}^+\mathbf{Q}]\mathbf{F}^{-\mathrm{T}} = \mathbf{S}$, which is invariant under SRBM due to the objectivity of $\mathbf{T}$ according to $(2.175)_1$.

Chapter 3

Governing Equations of Electromagnetism

In this chapter the governing equations of electromagnetism (EM) are summarized, in particular Maxwell's equations. This serves as background for the formulation of amended balance equations in Chapter 4 for coupled electro-magneto-thermo-mechanical (EMTM) continua that reflect the contribution of the EM fields to the balance equations of momentum and energy.

As Müller *et al.* [103, Section 1] point out in their recent review article, the field of electrodynamics is yet to fully embrace the concepts and methods of modern continuum mechanics. Indeed, the classic monographs on the subject, for example Feynman [26], Griffiths [38], Landau and Lifshitz [69], or Stratton [139], present the governing equations without considering any deformation (or even rigid motion, for that matter) of the underlying medium. Integral statements are often evaluated over regions, surfaces, or curves that are assumed to be *fixed* in space, which inadvertently blurs the line between partial and material time derivatives. While working well in vacuum, this can lead to a lack of precision in formulating the EM laws for moving or deformable media.[1]

For this reason, the upcoming discussion is based primarily on the monographs by Hutter *et al.* [56], Kovetz [64], and Müller [102], whose approaches are more closely aligned with the notation and paradigms of classical continuum mechanics. Furthermore, it is mentioned that Truesdell and Toupin [147] laid the groundwork for the modern treatment of the subject, and references to their encyclopedic article are ubiquitous in literature.

Many of the aforementioned monographs at least occasionally resort to the four-dimensional Minkowski space-time formulation. This is particularly true in the con-

[1] This issue is exemplified by the treatment of Faraday's law by Feynman [26, Equations 17.2 and 17.3] and Griffiths [38, Equations 7.14 and 7.15]. Despite dealing with the motion of a physical wire through a magnetic field, both authors use partial and total time derivatives interchangeably, which impedes a proper discussion of the flux derivative and its physical interpretation.

text of LORENTZ transformations and relativity theory,[2] such as in FEYNMAN [26, Chapter 25], but also for the derivation of transformation properties under EUCLIDEAN SRBM, for example, by ERICKSEN [23]. However, in an effort to preserve the three-dimensional notation introduced in Chapter 2, the four-vector formalism and MINKOWSKI space-time is avoided here.

This chapter is organized as follows: MAXWELL's equations are first presented in their most general form, *i.e.*, written in terms of the total EM fields irrespective of any interactions with the underlying medium. This is followed by the introduction of polarization and magnetization, as well as the aether relations. Together, they form the basis for the modeling of EM behavior within an underlying continuum. After a discussion of the transformation properties of the EM fields under SRBM, MAXWELL's equations are reformulated in terms of objective (GALILEAN invariant) fields. Finally, a brief review of electrostatics and magnetostatics is offered.

In the scope of this dissertation the electromagnetic fields are considered continuously differentiable, thus permitting the application of the divergence theorem (2.50) and STOKES' theorem (2.53). This assumption greatly simplifies the manipulation of equations but precludes, for example, jumps in the EM fields across surfaces that are often present due to local accumulations of electric charges.

3.1 Maxwell's Equations

MAXWELL's well-known equations of electromagnetism originate from the conservation of electric charge as well as from FARADAY's law of induction. As with the balance laws of Section 2.3, the physical principles are first discussed on the basis of their integral forms, which are thereafter localized to yield their differential form.

3.1.1 Principle of Charge Conservation

The first pair of MAXWELL's equations derives from the *principle of charge conservation*. It states that the rate of change of *electric charge* $Q(\mathcal{P})$ contained in material region $\mathcal{P}$ is balanced by the flow of electric current conducted across its boundary $\partial\mathcal{P}$. The integral form of this statement reads

$$\dot{Q}(\mathcal{P}) \;=\; \frac{\mathrm{d}}{\mathrm{d}t}\int_{\mathcal{P}} q \,\mathrm{d}v \;=\; -\int_{\partial\mathcal{P}} j_{(\mathbf{n})}\,\mathrm{d}a \quad , \tag{3.1}$$

where $q(\mathbf{x},t)$ is the *electric charge density* (per unit volume) and $j_{(\mathbf{n})}(\mathbf{x},t)$ represents the outward conduction of charges across $\partial\mathcal{P}$ (per unit area). The charge $Q(\mathcal{P})$ is an extensive quantity. In order to depict a collection of elementary charges as a

[2] Continuum mechanists are unlikely to encounter conditions which depart from the non-relativistic NEWTONIAN theory. The special theory of relativity is briefly mentioned in Section 3.4.6 but not pursued any further.

continuous distribution, a continuum assumption similar to that in (2.109) is made. A slightly different, albeit equally valid, statement of charge conservation may be more familiar to physicists, according to which

$$\int_{\mathcal{P}} \frac{\partial q}{\partial t} \, \mathrm{d}v \;=\; -\int_{\partial\mathcal{P}} J_{(\mathbf{n})} \, \mathrm{d}a \quad . \tag{3.2}$$

Here, the rate of change of the electric charge is computed for a *fixed* spatial region $\mathcal{P}$ and the outward flow $J_{(\mathbf{n})}(\mathbf{x}, t)$ is quantified relative to the coordinate system rather than the material boundary in motion. The EULERIAN description (3.2) is best suited for the discussion of EM in vacuum or in fluid media, as opposed to the LAGRANGIAN viewpoint (3.1) adopted for rigid or solid continua.[3] A more nuanced interpretation of this distinction arises from the transformation of the EM fields under SRBM, see Sections 3.4 and 3.5.

Analogous to CAUCHY's theorem for the heat flux (2.123), it can be shown using Equation (3.1) that

$$j_{(\mathbf{n})} \;=\; \mathbf{j} \cdot \mathbf{n} \quad , \tag{3.3}$$

where $\mathbf{j}(\mathbf{x}, t)$ is the *electric conduction current density* (per unit area).[4] In view of the REYNOLDS transport theorem in $(2.104)_2$, Equations (3.1) and (3.2) yield the relation

$$J_{(\mathbf{n})} \;=\; \mathbf{J} \cdot \mathbf{n} \quad \text{where} \quad \mathbf{J} \;=\; \mathbf{j} + q\mathbf{v} \quad . \tag{3.4}$$

As expected, the *total current density* $\mathbf{J}(\mathbf{x}, t)$ consists of the conduction current $\mathbf{j}$ plus a convective term $q\mathbf{v}$ which accounts for the material motion of the electrically charged body. Granted sufficient differentiability of q and $\mathbf{j}$, the divergence theorem (2.50) and localization theorem (2.55) furnish the local form of Equation (3.2) as

$$\frac{\partial q}{\partial t} + \operatorname{div} \mathbf{J} \;=\; 0 \quad . \tag{3.5}$$

Note that some monographs, for example GRIFFITHS [38, Equation 8.4], refer to (3.5) as the *continuity equation*. However, this ambiguous terminology is avoided here because depending on context it may refer to the conservation of mass in (2.111) (or, for that matter, the transport equation of any other conserved extensive quantity).

[3] Note that this terminology is somewhat different from its original usage in Sections 2.2.1 and 2.3.7, where the distinction between the EULERIAN (current) and LAGRANGIAN (referential) originates in the functional form $\tilde{\mathcal{F}}(\mathbf{x}, t)$ or $\hat{\mathcal{F}}(\mathbf{X}, t)$ chosen to express the relevant quantities. Here, the nomenclature focuses on whether an integral domain is considered fixed or material when taking a time derivative.

[4] It is once more emphasized that (3.1) balances the charge inside a *material* region, so that the current density $\mathbf{j}$ is measured *relative* to the body and is therefore associated with electrical *conduction* through the body.

Equation (3.2) is identically satisfied by the so-called *charge potential* $\mathbf{d}(\mathbf{x},t)$ and *current potential* $\mathbf{h}(\mathbf{x},t)$,[5] which are related to q and $\mathbf{J}$ according to

$$\begin{aligned} \int_{\mathcal{P}} q\,\mathrm{d}v &= \int_{\partial\mathcal{P}} \mathbf{d}\cdot\mathbf{n}\,\mathrm{d}a \quad , \\ \int_{\mathcal{A}} \mathbf{J}\cdot\mathbf{n}\,\mathrm{d}a &= \oint_{\mathcal{C}} \mathbf{h}\cdot\mathrm{d}\mathbf{x} - \int_{\mathcal{A}} \frac{\partial\mathbf{d}}{\partial t}\cdot\mathbf{n}\,\mathrm{d}a \quad . \end{aligned} \tag{3.6}$$

Gauss' *law* $(3.6)_1$ and Ampère*'s circuital law* $(3.6)_2$ constitute the first pair of Maxwell's equations. Note that the circulation of $\mathbf{h}$ in $(3.6)_2$ vanishes when substituted into (3.2), because $\partial\mathcal{P}$ is a closed surface without a boundary edge $\mathcal{C}=\emptyset$.

Assuming the necessary differentiability of $\mathbf{d}$ and $\mathbf{h}$, Equations (3.6) are localized using the divergence theorem (2.50), Stokes' theorem (2.53), and localization theorem (2.55),

$$\begin{aligned} q &= \operatorname{div}\mathbf{d} \quad , \\ \mathbf{J} &= \operatorname{curl}\mathbf{h} - \frac{\partial\mathbf{d}}{\partial t} \quad . \end{aligned} \tag{3.7}$$

It is readily verified that these local statements of Gauss' and Ampère's laws satisfy the local form of charge conservation (3.5), since the contribution of $\mathbf{h}$ vanishes on account of identity $(2.49)_2$. However, it is mentioned that Equations (3.7) do not produce unique solutions for the charge-current potentials $\{\mathbf{d},\mathbf{h}\}$. Indeed, (3.5) is satisfied by any

$$\begin{aligned} \mathbf{d}' &= \mathbf{d} + \operatorname{curl}\mathbf{y} \quad , \\ \mathbf{h}' &= \mathbf{h} + \frac{\partial\mathbf{y}}{\partial t} + \operatorname{grad}\Psi \quad , \end{aligned} \tag{3.8}$$

where $\Psi(\mathbf{x},t)$ and $\mathbf{y}(\mathbf{x},t)$ are arbitrary real- and vector-valued fields,[6] respectively. This result follows immediately from the identities for $\operatorname{curl}(\operatorname{grad}\Psi)$ and $\operatorname{div}(\operatorname{curl}\mathbf{y})$ in Equations $(2.49)_{1,2}$.

3.1.2 Faraday's Law of Induction

The second pair of Maxwell's equations derives from Faraday*'s law of induction*, which describes the induction of an electromotive force on an electrical circuit due to a change in the magnetic field. In an Eulerian description (sometimes referred to as the Maxwell-Faraday *equation*), it is argued that the rate of change of magnetic

[5] In (older) literature, $\mathbf{d}$ is also referred to as the *electric displacement*, and $\mathbf{h}$ as the *magnetic force* or *magnetic intensity*. This nomenclature is due to the aether relations, see Section 3.3, according to which the charge and current potentials are closely related to the electric and magnetic fields, respectively.

[6] The arbitrary scalar field Ψ of $(3.8)_2$ is not to be confused with the Helmholtz potential in (2.130).

flux through any *fixed* area $\mathcal{A}$ equals the negative circulation[7] of the electric field around its boundary $\mathcal{C}$,

$$\int_{\mathcal{A}} \frac{\partial \mathbf{b}}{\partial t} \cdot \mathbf{n} \, \mathrm{d}a \;=\; -\oint_{\mathcal{C}} \mathbf{e} \cdot \mathrm{d}\mathbf{x} \quad , \tag{3.9}$$

where $\mathbf{e}(\mathbf{x}, t)$ denotes the *electric field* and $\mathbf{b}(\mathbf{x}, t)$ the *magnetic field*.[8] Both $\mathbf{b}$ and $\mathbf{e}$ are considered *intensive* (as opposed to extensive) quantities.

In the special case of (3.9) where $\mathcal{A}$ consists of a closed surface $\partial\mathcal{P}$, the right-hand side vanishes since $\mathcal{C} = \emptyset$. If it is further assumed that at some time in the past $\mathbf{b} = \mathbf{0}$ on $\partial\mathcal{P}$, then Equation (3.9) furnishes Gauss' *law for magnetism*,

$$\int_{\partial\mathcal{P}} \mathbf{b} \cdot \mathbf{n} \, \mathrm{d}a \;=\; 0 \quad . \tag{3.10}$$

Since the net magnetic flux across the boundary of any region $\mathcal{P}$ is zero, Equation (3.10) implies the absence of magnetic sources (*i.e.*, magnetic monopoles), which is in agreement with experimental observation. This is in contrast with Gauss' law $(3.6)_1$, where electric charges assume the role of sources (*i.e.*, electric monopoles) for the charge potential $\mathbf{d}$. It is nevertheless mentioned that, much like the total charge $Q(\mathcal{P})$, the total amount of magnetic monopoles contained in $\mathcal{P}$ would be considered an extensive quantity, were it not zero.

Equations (3.9) and (3.10) are localized by means of the divergence theorem (2.50), Stokes' theorem (2.53), and the localization theorem (2.55). Gauss' law for magnetism and Faraday's law become

$$\begin{aligned} \operatorname{div} \mathbf{b} \;&=\; 0 \quad , \\ \frac{\partial \mathbf{b}}{\partial t} + \operatorname{curl} \mathbf{e} \;&=\; \mathbf{0} \quad , \end{aligned} \tag{3.11}$$

which constitute the local form of Maxwell's second pair of equations.

An alternative description of Equations (3.9) and (3.10) can be devised using a real-valued *electric potential* $\phi(\mathbf{x}, t)$ and vector-valued *magnetic potential*[9] $\mathbf{a}(\mathbf{x}, t)$. In integral form they are related to the electromagnetic fields $\{\mathbf{e}, \mathbf{b}\}$ via

$$\begin{aligned} \int_{\mathcal{S}} \mathbf{e} \cdot \mathrm{d}\mathbf{x} \;&=\; -\int_{\mathcal{S}} \frac{\partial \mathbf{a}}{\partial t} \cdot \mathrm{d}\mathbf{x} - \big[\phi\big]_{\mathbf{s}_1}^{\mathbf{s}_2} \quad , \\ \int_{\mathcal{A}} \mathbf{b} \cdot \mathbf{n} \, \mathrm{d}a \;&=\; \oint_{\mathcal{C}} \mathbf{a} \cdot \mathrm{d}\mathbf{x} \qquad\qquad\qquad . \end{aligned} \tag{3.12}$$

[7] The circulation of $\mathbf{e}$ may be interpreted as the work (per unit charge) done on a small test charge as it completes one revolution around the (fixed) boundary $\mathcal{C}$ according to the right-hand rule, see Section 3.5.2 for a more detailed discussion.

[8] Some authors refer to the magnetic field $\mathbf{b}$ as the *magnetic flux density* or *magnetic induction*.

[9] The magnetic potential $\mathbf{a}$ is not to be confused with the acceleration vector represented by the same symbol, see Equation (2.115).

Unlike the closed boundary $\mathcal{C}$ around $\mathcal{A}$, the arbitrary open curve $\mathcal{S}$ forms a path from point $\mathbf{s}_1$ to $\mathbf{s}_2$, see the notation in (2.54). FARADAY's law (3.9) is recovered by reducing the open path $\mathcal{S}$ in $(3.12)_1$ to a closed curve $\mathcal{C}$, which eliminates the contribution of ϕ. Similarly, GAUSS' law for magnetism (3.10) is immediately satisfied by Equation $(3.12)_2$ when $\partial\mathcal{P}$ is substituted for $\mathcal{A}$.

Equations (3.12) are localized using STOKES' theorem (2.53), the gradient theorem (2.54), and the localization theorem (2.55) applied to $\mathcal{A}$ and $\mathcal{S}$,

$$\begin{aligned} \mathbf{e} &= -\frac{\partial \mathbf{a}}{\partial t} - \operatorname{grad}\phi \quad , \\ \mathbf{b} &= \operatorname{curl}\mathbf{a} \qquad\qquad . \end{aligned} \tag{3.13}$$

Like the charge-current potentials $\{\mathbf{d}, \mathbf{h}\}$ in (3.8), the electromagnetic potentials $\{\phi, \mathbf{a}\}$ are not unique. In view of identity $(2.49)_1$ for $\operatorname{curl}(\operatorname{grad}\Psi)$, Equations (3.13) are satisfied by any pair $\{\phi', \mathbf{a}'\}$ with

$$\begin{aligned} \phi' &= \phi - \frac{\partial \Psi}{\partial t} \quad , \\ \mathbf{a}' &= \mathbf{a} + \operatorname{grad}\Psi \quad , \end{aligned} \tag{3.14}$$

where $\Psi(\mathbf{x}, t)$ is an arbitrary real-valued field.[10] The relations (3.14) are referred to as *gauge transformations*. Equations $(3.13)_{1,2}$ offer an alternative description for GAUSS' law for magnetism and FARADAY's law $(3.11)_{1,2}$ in terms of electromagnetic potentials, which is exploited in the context of electrostatics and magnetostatics in Section 3.7.

3.1.3 Summary

MAXWELL's equations of electromagnetism are expressed in local form according to Equations $(3.7)_{1,2}$ and $(3.11)_{1,2}$,

$$\begin{aligned} \operatorname{div}\mathbf{d} &= q \qquad\qquad , \\ \operatorname{curl}\mathbf{h} &= \mathbf{J} + \frac{\partial \mathbf{d}}{\partial t} \quad , \\ \operatorname{div}\mathbf{b} &= 0 \qquad\qquad , \\ \operatorname{curl}\mathbf{e} &= -\frac{\partial \mathbf{b}}{\partial t} \qquad . \end{aligned} \tag{3.15}$$

The four equations consist of two pairs[11] of disjoint systems of equations for the fields $\{\mathbf{d}, \mathbf{h}\}$ and $\{\mathbf{e}, \mathbf{b}\}$. A tally of the number of unknowns indicates that the equations on their own are under-determined. However, the charge-current potentials

[10] As before, the arbitrary scalar field Ψ in (3.14) is not to be confused with the HELMHOLTZ potential (2.130).

[11] More precisely the 'four' expressions (3.15) comprise *eight* equations, on account of the two scalar and two vector-valued statements. Each disjoint 'pair' thus contains four equations.

are intimately related to the electromagnetic fields via the aether relations discussed in Section 3.3. Alternative forms of MAXWELL's equations will be derived later in Sections 3.5 and 3.6.

3.2 Polarization and Magnetization

The laws of electromagnetism in Section 3.1 make no mention of the physical origin of the electric charge and current densities q and $\mathbf{J}$. Equations (3.15) model the cumulative effect of all charge-currents and are thus equally valid in vacuum and in matter. However, when dealing with EM fields in matter, it is often desirable to separate the equations governing the freely moving charges and currents from the effects of the bound charge-currents associated with polarization and magnetization of the medium. Since MAXWELL's equations are linear in the electromagnetic fields[12] a simple additive decomposition for the free and bound EM fields suffices.

The upcoming discussion of polarizable and magnetizable matter is based on the monographs of GRIFFITHS [38, Chapters 4 and 6], KOVETZ [64, Chapters 7, 9, and 11], and MÜLLER [102, Chapters 9.4-9.6]. The former, in particular, offers a convenient overview of the constitutive behavior of EM continua as well as the (sub-)atomic or molecular mechanisms from which they originate.

Conductors are materials which contain free electrons that are not associated with any particular atom. In contrast, *dielectric materials* are insulators whose electrons are bound to its nuclei or molecules. Although the movement of such charges is greatly inhibited, an *electric dipole moment*[13] nevertheless arises in the presence of an external electric field. Furthermore, polar molecules are themselves tiny dipoles which may slightly reorient from their previously random equilibrium positions. They collectively result in *dielectric polarization* of the material when acted upon by an electric field, which is manifested by a change in the electric charge distribution and an apparent electric current.

Magnetic materials exhibit a similar behavior, whereby they respond to an externally applied magnetic field with a *magnetic dipole moment*, which in turn results in an apparent electric current. This *magnetization* originates from looping currents generated by the electron cloud surrounding the nucleus, as well as a collective alignment of the spin of elementary particles. In some cases this magnetization remains even in the absence of an external magnetic field.[14] Materials which respond to the

[12] Note that Equations (3.15) are linear only because the charge-currents $\{q, \mathbf{j}\}$ are featured in the form of source terms. In practice, the oftentimes complicated dependence of the charge-currents on the EM fields usually renders the equations nonlinear, as remarked by KOVETZ [64, Chapter 13].

[13] The dipole moment is caused by a small eccentricity between the positively charged nucleus and its electron cloud. Under the action of a sufficiently strong electric field, atoms may even become ionized, rendering the material a conductor.

[14] Ferromagnetic materials below the CURIE temperature may be magnetized permanently by an external magnetic field. This history-dependent process is not completely reversible - a hysteresis

external magnetic field by a net attractive force are classified as *paramagnets*, whereas a net repulsive force is experienced by *diamagnets*.

3.2.1 Polarization Charge

To account for the effect of polarization on charge distribution, a distinction is introduced between free and bound charges. The *free charge density* $q_{\mathrm{F}}(\mathbf{x},t)$ is associated with free electrons or ions, whereas the *bound charge density* $q_{\mathrm{R}}(\mathbf{x},t)$ models the charge distribution caused by the aforementioned electric dipole moments. Together they form the overall charge density distribution $q = q_{\mathrm{F}} + q_{\mathrm{R}}$.

The bound charge contained in a material region $\mathcal{P}$ is called *polarization charge*, such that in any region $\mathcal{P}$ with boundary $\partial\mathcal{P}$,

$$\int_{\mathcal{P}} q_{\mathrm{R}}\,\mathrm{d}v \;=\; -\int_{\partial\mathcal{P}} \mathbf{p}\cdot\mathbf{n}\,\mathrm{d}a \quad , \tag{3.16}$$

where $\mathbf{p}(\mathbf{x},t)$ represents the *dielectric polarization density*, which may be thought of as the average electric dipole moment (in units of charge times distance) per unit volume. The surface integral in (3.16) represents the excess of electric charge inside $\mathcal{P}$ due to dipoles 'cut' across the boundary $\partial\mathcal{P}$.[15] By sign convention, the vector $\mathbf{p}$ points from the negative to the positive side of the local average electric dipole, thus placing negative charges inside of $\mathcal{P}$ when $\mathbf{p}$ points in direction of the outward normal $\mathbf{n}$.

Only if $\mathbf{p}$ varies along the boundary $\partial\mathcal{P}$ does the surface integral make a net contribution to the overall charge. This is also reflected in the local form of (3.16),

$$q_{\mathrm{R}} \;=\; -\mathrm{div}\,\mathbf{p} \quad , \tag{3.17}$$

which follows from the divergence theorem (2.50) and the localization theorem (2.55).

3.2.2 Polarization Current

Let the *free conduction current density* $\mathbf{j}_{\mathrm{F}}(\mathbf{x},t)$ be associated with the conduction of free charges. Since the polarization of bound charges can effect changes in the overall charge distribution, temporal variations in $\mathbf{p}$ will simultaneously amount to a *polarization current density* $\mathbf{j}_{\mathrm{P}}(\mathbf{x},t)$ per unit area, given by

$$\int_{\mathcal{A}} \mathbf{j}_{\mathrm{P}}\cdot\mathbf{n}\,\mathrm{d}a \;=\; \frac{\mathrm{d}}{\mathrm{d}t}\int_{\mathcal{A}} \mathbf{p}\cdot\mathbf{n}\,\mathrm{d}a \quad . \tag{3.18}$$

loop is observed when plotting the magnetization against the external field, much like the stress-strain curves of elasto-plastic materials.

[15] To draw this analogy a continuum assumption is made, whereby the size of a dipole (*i.e.*, the distance by which opposite elementary charges are separated) is much smaller than the characteristic length of $\mathcal{P}$. Individual dipoles are so numerous and infinitesimal in strength that a continuous distribution $\mathbf{p}$ arises. Similar assumptions were previously made for the mass and charge densities ρ and q, respectively.

The right-hand side of (3.18) represents the net transfer of charges across the material surface $\mathcal{A}$ due to changes in orientation of the electric dipoles. Following the sign convention for $\mathbf{p}$, net positive charge is moving in direction $\mathbf{n}$ when $\mathbf{p}\cdot\mathbf{n}$ increases, causing a net positive outward current $\mathbf{j}_\mathrm{P}\cdot\mathbf{n}$. This is in agreement with the sign convention for $\mathbf{j}$ employed in the discussion of charge conservation. Note that independent of the free charges, Equations (3.16) and (3.18) satisfy the integral form (3.1) of conservation of electric charge.

Locally, Equation (3.18) is expressed using the flux derivative (2.105) and localization theorem (2.55) for arbitrary surface integrals by

$$\mathbf{j}_\mathrm{P} \;=\; \overset{\star}{\mathbf{p}} \quad . \tag{3.19}$$

Of course the fields q_R and $\mathbf{j}_\mathrm{P}$, too, satisfy the local form of the principle of charge conservation (3.5), since

$$\begin{aligned} \frac{\partial q_\mathrm{R}}{\partial t} + \operatorname{div}\big(\mathbf{j}_\mathrm{P} + q_\mathrm{R}\mathbf{v}\big) \;&=\; \operatorname{div}\bigg(-\frac{\partial \mathbf{p}}{\partial t} + \overset{\star}{\mathbf{p}} - \big(\operatorname{div}\mathbf{p}\big)\mathbf{v}\bigg) \\ &=\; \operatorname{div}\bigg(\overset{\star}{\mathbf{p}} - \frac{\partial \mathbf{p}}{\partial t} - \big(\operatorname{div}\mathbf{p}\big)\mathbf{v} + \operatorname{curl}\big(\mathbf{v}\times\mathbf{p}\big)\bigg) \;=\; 0 \quad , \end{aligned} \tag{3.20}$$

where Equations $(2.49)_2$ and $(2.106)_3$ were used.

3.2.3 Magnetization Current

In addition to $\mathbf{j}_\mathrm{F}$ and $\mathbf{j}_\mathrm{P}$, magnetization contributes to the overall conduction current $\mathbf{j}$ a *magnetization current density* $\mathbf{j}_\mathrm{M}(\mathbf{x},t)$ per unit area. This is due to the equivalence between magnetic dipole moments and infinitesimal loops of electric current. The magnetization current obeys

$$\int_{\mathcal{A}} \mathbf{j}_\mathrm{M}\cdot\mathbf{n}\,\mathrm{d}a \;=\; \oint_{\mathcal{C}} \boldsymbol{\mathcal{M}}\cdot\mathrm{d}\mathbf{x} \quad , \tag{3.21}$$

where the *magnetization density* $\boldsymbol{\mathcal{M}}(\mathbf{x},t)$ represents the magnetic dipole moment (in units of electric current times area) per unit volume. The line element $\mathrm{d}\mathbf{x}$ traces the boundary $\mathcal{C}$ according to the right-hand rule around the normal $\mathbf{n}$ of surface $\mathcal{A}$. The boundary line integral adds up the infinitesimal current loops 'pierced through' by $\mathrm{d}\mathbf{x}$.[16] If a magnetic dipole points in direction $\mathrm{d}\mathbf{x}$, its corresponding current loop carries a positive contribution to the current through $\mathcal{A}$ in direction $\mathbf{n}$ following the right-hand rule around $\boldsymbol{\mathcal{M}}$.

The line integral (3.21) causes a net current through $\mathcal{A}$ only when $\boldsymbol{\mathcal{M}}$ varies along the edge $\mathcal{C}$, such that the resulting circulation of $\boldsymbol{\mathcal{M}}$ is non-zero. This is reflected in

[16] A continuum assumption analogous to that made for $\mathbf{p}$ applies to the size and magnitude of elementary magnetic dipoles, so as to arrive at a continuous density $\boldsymbol{\mathcal{M}}$.

local form by a magnetization current of

$$\mathbf{j}_{\mathrm{M}} \;=\; \operatorname{curl}\boldsymbol{\mathcal{M}} \quad , \tag{3.22}$$

where STOKES' theorem (2.53) and the localization theorem (2.55) were used. Note that $\mathbf{j}_{\mathrm{M}}$ automatically satisfies charge conservation (3.5) (with $q_{\mathrm{M}} = 0$) because, in view of $(2.49)_2$, it is divergence-free.

3.2.4 Maxwell's Equations for the Free Charges and Currents

The preceding discussion leads to the conclusion that the net electric charge $Q(\mathcal{P})$ contained in a material region $\mathcal{P}$ is given by

$$\int_{\mathcal{P}} q \,\mathrm{d}v \;=\; \int_{\mathcal{P}} q_{\mathrm{F}} \,\mathrm{d}v - \int_{\partial\mathcal{P}} \mathbf{p}\cdot\mathbf{n}\,\mathrm{d}a \quad , \tag{3.23}$$

and the overall conduction current through a material surface $\mathcal{A}$ is

$$\int_{\mathcal{A}} \mathbf{j}\cdot\mathbf{n}\,\mathrm{d}a \;=\; \int_{\mathcal{A}} \mathbf{j}_{\mathrm{F}}\cdot\mathbf{n}\,\mathrm{d}a + \frac{\mathrm{d}}{\mathrm{d}t}\int_{\mathcal{A}} \mathbf{p}\cdot\mathbf{n}\,\mathrm{d}a + \oint_{\mathcal{C}} \boldsymbol{\mathcal{M}}\cdot\mathrm{d}\mathbf{x} \quad , \tag{3.24}$$

see Equations (3.16), (3.18), and (3.21).

The free charge-currents $\{q_{\mathrm{F}}, \mathbf{j}_{\mathrm{F}}\}$ are given in local form as

$$\begin{aligned} q_{\mathrm{F}} \;&=\; q - q_{\mathrm{R}} \quad , \\ \mathbf{j}_{\mathrm{F}} \;&=\; \mathbf{j} - \mathbf{j}_{\mathrm{R}} \quad , \end{aligned} \tag{3.25}$$

where the *bound conduction current density* $\mathbf{j}_{\mathrm{R}}(\mathbf{x}, t)$ accounts for both polarization and magnetization. The bound charge-currents $\{q_{\mathrm{R}}, \mathbf{j}_{\mathrm{R}}\}$ are thus given with the aid of (3.17), (3.19), and (3.22) by

$$\begin{aligned} q_{\mathrm{R}} \;&=\; -\operatorname{div}\mathbf{p} \quad , \\ \mathbf{j}_{\mathrm{R}} \;&=\; \mathbf{j}_{\mathrm{P}} + \mathbf{j}_{\mathrm{M}} \;=\; \overset{\star}{\mathbf{p}} + \operatorname{curl}\boldsymbol{\mathcal{M}} \quad . \end{aligned} \tag{3.26}$$

These are determined by constitutive relations for $\mathbf{p}$ an $\boldsymbol{\mathcal{M}}$, see Section 6.1.2, which depend primarily on the electromagnetic fields $\{\mathbf{e}, \mathbf{b}\}$ but may be coupled with deformation or temperature. The total (conductive plus convective) current density (3.4) may likewise be decomposed into its bound and free parts. Appealing to the flux derivative $(2.106)_3$, the *free* and *bound total current densities* $\mathbf{J}_{\mathrm{F}}(\mathbf{x}, t)$ and $\mathbf{J}_{\mathrm{R}}(\mathbf{x}, t)$ are expressed as

$$\begin{aligned} \mathbf{J}_{\mathrm{F}} \;&=\; \mathbf{j}_{\mathrm{F}} + q_{\mathrm{F}}\mathbf{v} \;=\; \mathbf{J} - \mathbf{J}_{\mathrm{R}} \quad , \\ \mathbf{J}_{\mathrm{R}} \;&=\; \mathbf{j}_{\mathrm{R}} + q_{\mathrm{R}}\mathbf{v} \;=\; \operatorname{curl}\boldsymbol{\mathcal{M}} + \overset{\star}{\mathbf{p}} - \big(\operatorname{div}\mathbf{p}\big)\mathbf{v} \;=\; \operatorname{curl}\mathbf{m} + \frac{\partial \mathbf{p}}{\partial t} \quad , \end{aligned} \tag{3.27}$$

where the MINKOWSKI *magnetization* $\mathbf{m}(\mathbf{x},t)$ is defined by

$$\mathbf{m} \;=\; \boldsymbol{\mathcal{M}} - \mathbf{v}\times\mathbf{p} \quad . \tag{3.28}$$

Recall that the local statement of charge conservation (3.5) is linear in q and $\mathbf{j}$. It is satisfied independently by each pair $\{q,\mathbf{j}\}$, $\{q_{\mathrm{R}},\mathbf{j}_{\mathrm{P}}\}$, $\{0,\mathbf{j}_{\mathrm{M}}\}$, and thus any linear combination thereof, including $\{q_{\mathrm{F}},\mathbf{j}_{\mathrm{F}}\}$. The ensuing MAXWELL equations $(3.15)_{1,2}$ preserve this linearity, suggesting an additive decomposition of the potentials $\{\mathbf{d},\mathbf{h}\}$ as well. Since the *bound charge-current potentials* $\{\mathbf{d}_{\mathrm{R}},\mathbf{h}_{\mathrm{R}}\}$ are determined constitutively, only the part of MAXWELL's equations associated with the *free charge-current potentials* $\{\mathbf{d}_{\mathrm{F}},\mathbf{h}_{\mathrm{F}}\}$ is of interest. The free part of GAUSS' law $(3.15)_1$ is expressed as

$$q_{\mathrm{F}} \;=\; q - q_{\mathrm{R}} \;=\; \operatorname{div}\big(\mathbf{d}+\mathbf{p}\big) \;=\; \operatorname{div}\mathbf{d}_{\mathrm{F}} \quad , \tag{3.29}$$

whereas AMPÈRE's circuital law $(3.15)_2$ reduces to

$$\mathbf{J}_{\mathrm{F}} \;=\; \mathbf{J} - \mathbf{J}_{\mathrm{R}} \;=\; \operatorname{curl}\big(\mathbf{h}-\mathbf{m}\big) - \frac{\partial}{\partial t}\Big(\mathbf{d}+\mathbf{p}\Big) \;=\; \operatorname{curl}\mathbf{h}_{\mathrm{F}} - \frac{\partial \mathbf{d}_{\mathrm{F}}}{\partial t} \quad . \tag{3.30}$$

The free charge-current potentials $\{\mathbf{d}_{\mathrm{F}},\mathbf{h}_{\mathrm{F}}\}$ are thus given by

$$\begin{aligned} \mathbf{d}_{\mathrm{F}} \;&=\; \mathbf{d} + \mathbf{p} \quad , \\ \mathbf{h}_{\mathrm{F}} \;&=\; \mathbf{h} - \mathbf{m} \quad , \end{aligned} \tag{3.31}$$

and the bound potentials $\{\mathbf{d}_{\mathrm{R}},\mathbf{h}_{\mathrm{R}}\}$ are obtained constitutively from

$$\begin{aligned} \mathbf{d}_{\mathrm{R}} \;&=\; \mathbf{d} - \mathbf{d}_{\mathrm{F}} \;=\; -\mathbf{p} \quad , \\ \mathbf{h}_{\mathrm{R}} \;&=\; \mathbf{h} - \mathbf{h}_{\mathrm{F}} \;=\; \mathbf{m} \quad . \end{aligned} \tag{3.32}$$

It is mentioned that in literature MAXWELL's first pair of equations is often stated in terms of the free parts (3.29) and (3.30), whilst tacitly dropping the subscript $[\cdot]_{\mathrm{F}}$ for brevity, such as in GRIFFITHS [38, Chapters 4.3.1 and 6.3.1]. The reader is thus cautioned to take note of whether the charge-currents and their potentials refer to the total fields or only free part thereof.

3.2.5 Summary

In the presence of magnetization or polarization, the charge-currents $\{q,\mathbf{J}\}$ and their potentials $\{\mathbf{d},\mathbf{h}\}$ are additively decomposed into the contributions of the free and bound parts. MAXWELL's first set of equations in $(3.15)_{1,2}$ is replaced with (3.29) and (3.30) for the free parts,

$$\begin{aligned} \operatorname{div}\mathbf{d}_{\mathrm{F}} \;&=\; q_{\mathrm{F}} \quad , \\ \operatorname{curl}\mathbf{h}_{\mathrm{F}} \;&=\; \mathbf{J}_{\mathrm{F}} + \frac{\partial \mathbf{d}_{\mathrm{F}}}{\partial t} \quad , \end{aligned} \tag{3.33}$$

while the second set $(3.15)_{3,4}$ remains unchanged. The bound charge-current potentials $\{\mathbf{d}_{\mathrm{R}}, \mathbf{h}_{\mathrm{R}}\} = \{-\mathbf{p}, \mathbf{m}\}$ are determined primarily by the electromagnetic fields $\{\mathbf{e}, \mathbf{b}\}$ through constitutive equations. They cause bound charge-currents amounting to

$$\begin{aligned} q_{\mathrm{R}} &= -\operatorname{div}\mathbf{p} \quad , \\ \mathbf{J}_{\mathrm{R}} &= \operatorname{curl}\mathbf{m} + \frac{\partial \mathbf{p}}{\partial t} \quad , \end{aligned} \tag{3.34}$$

according to $(3.26)_1$, $(3.27)_2$.

3.3 Aether Relations

Recall that Maxwell's Equations $(3.15)_{1-4}$ are comprised of two sets of disjoint equations. The first set of equations describes the charge-current potentials $\{\mathbf{d}, \mathbf{h}\}$ and arises from the principle of charge conservation, see Section 3.1.1. The second set comprises Faraday's law of induction for the electromagnetic fields $\{\mathbf{b}, \mathbf{e}\}$, see Section 3.1.2.

However, experimental evidence suggests a universal relation between the two sets, called the Maxwell-Lorentz *aether relations*. In the classical, non-relativistic theory these relations depend on the Galilean frame in which they are formulated.[17] There exists an inertial frame called the *aether frame* in which

$$\begin{aligned} \mathbf{d} &\overset{\text{Aet.}}{=} \varepsilon_0 \mathbf{e} \quad , \\ \mathbf{h} &\overset{\text{Aet.}}{=} \mathbf{b}/\mu_0 \quad , \end{aligned} \tag{3.35}$$

where the (positive) scalars ε_0 and μ_0 are fundamental constants of nature termed the *electric permittivity* and *magnetic permeability* of vacuum, respectively. According to the *National Institute of Standards and Technology* [117], their values are given by $\varepsilon_0 = 8.854\,187\,818\,8(14) \times 10^{-12}\,\mathrm{F/m}$ and $\mu_0 = 1.256\,637\,061\,27(20) \times 10^{-6}\,\mathrm{H/m}$. Note that the superscript $\overset{\text{Aet.}}{=}$ in (3.35) signifies that an equation holds only in the aether frame.

Curiously, the aether relations provide closure to Maxwell's equations *not* by connecting the 'physical' fields $\{q, \mathbf{J}\}$ with $\{\mathbf{b}, \mathbf{e}\}$, or perhaps the potentials $\{\mathbf{d}, \mathbf{h}\}$ with $\{\phi, \mathbf{a}\}$. Instead, by setting the charge-current potentials directly proportional to the electromagnetic fields, the indeterminacy previously granted to the potentials in (3.8) no longer holds, as pointed out by Kovetz [64, Chapter 5].

Note that the aether relations may be regarded as constitutive equations[18] for the electromagnetic behavior of empty space, where the universal constants ε_0 and μ_0 take

[17] Frame-dependency implies that the aether relations (3.35) are *not* form-invariant under SRBM. This raises serious issues with the classical treatment of frame invariance in EM, as discussed in Section 3.4.6.

[18] See, for example, Hehl and Obukhov [45]: "*We may consider* [...] *as constitutive relations for spacetime itself.*"

the place of material properties. They determine, for example, the *speed of light* c in vacuum

$$c \;=\; \sqrt{\frac{1}{\varepsilon_0 \mu_0}} \quad , \tag{3.36}$$

which evaluates to exactly[19] $c = 299\,792\,458\,\mathrm{m/s}$ [117]. A brief derivation of the corresponding wave equations is provided in Appendix A.5.

It is emphasized that the aether relations (3.35) hold both in vacuum and in matter. They refer to the total (free and bound) charge-current potentials irrespective of the underlying medium. Moreover, the additive decomposition of $\{q, \mathbf{j}\}$ and $\{\mathbf{d}, \mathbf{h}\}$ discussed in the preceding section for polarizable and magnetizable media applies to the aether relations as well. Equations (3.31) are substituted into (3.35) to furnish

$$\begin{aligned} \mathbf{d}_\mathrm{F} &\overset{\text{Aet.}}{=} \varepsilon_0 \mathbf{e} + \mathbf{p} \quad , \\ \mathbf{h}_\mathrm{F} &\overset{\text{Aet.}}{=} \mathbf{b}/\mu_0 - \mathbf{m} \quad . \end{aligned} \tag{3.37}$$

Recall that $\{\mathbf{p}, \mathbf{m}\}$ are determined constitutively from the electromagnetic fields $\{\mathbf{e}, \mathbf{b}\}$ (and potentially from coupling with the thermomechanical quantities). The aether relations of the form (3.37) thus represent constitutive equations which explicitly account for the electromagnetic properties of the continuum body.

It is common for physics textbooks to state the aether relations (3.37) in the alternative form

$$\begin{aligned} \mathbf{d}_\mathrm{F} &\overset{\text{Aet.}}{=} \varepsilon \mathbf{e} \quad , \\ \mathbf{b} &\overset{\text{Aet.}}{=} \mu \mathbf{h}_\mathrm{F} \quad , \end{aligned} \tag{3.38}$$

where the subscript $[\cdot]_\mathrm{F}$ for the free charge-current potentials is often ommitted, such as in Feynman [27, Chapter 10-4] or Griffiths [38, Chapter 4.4.1]. The constitutive properties of the medium are encapsulated in the permittivity[20] ε and permeability μ. Various alternative measures of permittivity and permeability are used across different disciplines and applications, such as the dimensionless *relative permittivity* ε_r and *relative permeability* μ_r, or the *electric susceptibility* χ_e and *magnetic susceptibility* χ_m. They are related to ε and μ via

$$\begin{aligned} \varepsilon_r &= \varepsilon/\varepsilon_0 \quad , \quad \chi_e = \varepsilon_r - 1 \quad , \\ \mu_r &= \mu/\mu_0 \quad , \quad \chi_m = \mu_r - 1 \quad . \end{aligned} \tag{3.39}$$

The two descriptions (3.37) and (3.38) can be reconciled only if $\mathbf{p}$ and $\mathbf{m}$ are collinear to $\mathbf{e}$ and $\mathbf{b}$, respectively, with the corresponding proportionality factors determined by scalar constitutive functions. However, this precludes any anisotropic electromagnetic behavior and severely limits the possibilities for coupling between EM and deformation.

[19] According to the modern definition of the *Système International* (or *SI*), a meter corresponds to the distance travelled by light through vacuum in exactly $1/c$ seconds.

[20] Note that the same symbol is used to denote the specific internal energy, see Equation (2.121).

Recall from Section 3.2 that dielectric materials polarize under an external electric field due to the development or reorientation of electric dipoles. Given the physical origins of this effect, it is expected that $\mathbf{p}$ cannot oppose $\mathbf{e}$, so that $\mathbf{e}\cdot\mathbf{p}>0$. It may thus be concluded from a comparison between $(3.37)_1$ and $(3.38)_1$ that the permittivity of polarizable matter exceeds the vacuum permittivity, $\varepsilon>\varepsilon_0$ or $\varepsilon_r>1$. On the other hand, the magnetic permeability μ of matter does not suffer the same limitation. In paramagnetic materials the permeability exceeds the vacuum value $\mu>\mu_0$, whereas diamagnets exhibit[21] $\mu<\mu_0$. In most materials the paramagnetic (attractive) effect dominates over the diamagnetic (repulsive) effect, which in turn implies that the phase velocity of EM waves in such media does not exceed the vacuum speed c, see the wave equation in (A.21).

In an aether frame, the relations in (3.35) may be employed to replace the charge-current potentials $\{\mathbf{d},\mathbf{h}\}$ in the first pair of MAXWELL's equations with the electromagnetic fields $\{\mathbf{e},\mathbf{b}\}$. The local form in (3.15) thus becomes

$$\begin{aligned} \varepsilon_0 \operatorname{div}\mathbf{e} &\overset{\text{Aet.}}{=} q && , \quad \operatorname{div}\mathbf{b} = 0 && , \\ \operatorname{curl}\mathbf{b}/\mu_0 &\overset{\text{Aet.}}{=} \mathbf{J} + \varepsilon_0\frac{\partial\mathbf{e}}{\partial t} && , \quad \operatorname{curl}\mathbf{e} = -\frac{\partial\mathbf{b}}{\partial t} && . \end{aligned} \tag{3.40}$$

The integral forms of GAUSS' law $(3.6)_1$ and AMPÈRE's circuital law $(3.6)_2$ are stated in an aether frame as

$$\begin{aligned} \int_{\mathcal{P}} q\,\mathrm{d}v &\overset{\text{Aet.}}{=} \varepsilon_0\int_{\partial\mathcal{P}}\mathbf{e}\cdot\mathbf{n}\,\mathrm{d}a && , \\ \mu_0\int_{\mathcal{A}}\mathbf{J}\cdot\mathbf{n}\,\mathrm{d}a &\overset{\text{Aet.}}{=} \oint_{\mathcal{C}}\mathbf{b}\cdot\mathrm{d}\mathbf{x} - \frac{1}{c^2}\int_{\mathcal{A}}\frac{\partial\mathbf{e}}{\partial t}\cdot\mathbf{n}\,\mathrm{d}a && , \end{aligned} \tag{3.41}$$

where (3.36) for the vacuum speed of light c was used. In some cases the $1/c^2$-term may be negligible. FARADAY's law of induction (3.9) and GAUSS' law for magnetism (3.10) remain unchanged since they are already expressed in $\{\mathbf{e},\mathbf{b}\}$.

3.4 Transformation Properties of Electromagnetic Fields

In this section, the transformation properties under classical SRBMs are derived for all relevant EM fields. These results are used to examine the aforementioned lack of form-invariance of the aether relations. The transformation rules derived here motivate the formulation of MAXWELL's equations comprised of only objective terms

[21] Due to its quantum origins, the diamagnetic effect is relatively weak so that the measured permeability in most cases remains very close to μ_0. A notable exception are superconductors, whose magnetic permeability vanishes, or $\chi_m=-1$, in what is called the MEISSNER effect, see FEYNMAN [27, Chapter 21-6] or LANDAU and LIFSHITZ [75, Chapter 6].

in Section 3.5. They are furthermore used to verify the validity of the Green-Naghdi-Rivlin theorem for the fully coupled electro-magneto-thermo-mechanical balance equations in Section 4.3.

The analysis rests on the following two assumptions: First, it is postulated that the charge $Q(\mathcal{P})$ contained in a material region $\mathcal{P}$ is unaffected by SRBM and is, therefore, objective, so that $Q^+(\mathcal{P}^+) = Q(\mathcal{P})$. The same premise holds separately for the free and bound charges $Q_{\mathrm{F}}(\mathcal{P})$ and $Q_{\mathrm{R}}(\mathcal{P})$, as well as the (non-existent) magnetic monopoles. Second, the governing equations of EM presented in Sections 3.1 and 3.2 (but not the aether relations) are postulated to be form-invariant,[22] which is the same attribute ascribed to the thermomechanical balance equations in Section 2.4.4. The upcoming analysis is based on the integral form of the governing equations. An alternative derivation using their local forms is presented in Appendix A.4, which also serves to corroborate the results from this section.

3.4.1 Charge and Current Densities

The first assumption is expressed in integral form as

$$Q^+(\mathcal{P}^+) \;=\; \int_{\mathcal{P}^+} q^+ \mathrm{d}v^+ \;=\; \int_{\mathcal{P}} q \,\mathrm{d}v \;=\; Q(\mathcal{P}) \quad . \tag{3.42}$$

The statement is localized with the aid of $(2.170)_5$ and the localization theorem (2.55) to

$$q^+ \;=\; q \quad . \tag{3.43}$$

Unsurprisingly, the charge density q transforms objectively.

From the material time derivative of (3.42) and the postulated form-invariance of the integral form of charge conservation (3.1) it is concluded that

$$\dot{Q}^+(\mathcal{P}^+) \;=\; -\int_{\partial\mathcal{P}^+} j^+_{(\mathbf{n})} \,\mathrm{d}a^+ \;=\; -\int_{\partial\mathcal{P}} j_{(\mathbf{n})} \,\mathrm{d}a \;=\; \dot{Q}(\mathcal{P}) \quad . \tag{3.44}$$

In view of the transformation rules $(2.170)_{3,4}$ and Cauchy's theorem (3.3) for $j_{(\mathbf{n})}$, the condition is restated as

$$\int_{\partial\mathcal{P}} \left(\mathbf{j}^+ - \mathbf{Q}\,\mathbf{j}\right) \cdot \mathbf{Q}\,\mathbf{n} \,\mathrm{d}a \;=\; 0 \quad . \tag{3.45}$$

[22] This derivation makes explicit use of the form-invariance of the integral forms of charge conservation (3.1), Gauss' law $(3.6)_1$, Ampère's circuital law $(3.6)_2$, Faraday's law of induction (3.9), Gauss' law for magnetism (3.10), the electromagnetic potentials $(3.12)_{1,2}$, as well as the definitions for the polarization charge (3.16), polarization current (3.18), and magnetization current (3.21). Postulating the form-invariance of all governing equations is internally consistent, albeit not always mutually independent. For example, the form-invariance of the Lagrangian and Eulerian descriptions of charge conservation (3.1) and (3.2) implies the form-invariance of the definition of total current $(3.4)_2$.

The divergence and localization theorems (2.50) and (2.55) thus furnish the transformation rule

$$\operatorname{div}\big(\mathbf{Q}^{\mathrm{T}}\mathbf{j}^{+}-\mathbf{j}\big) \;=\; 0 \quad , \tag{3.46}$$

or equivalently

$$\mathbf{j}^{+} \;=\; \mathbf{Q}\big(\mathbf{j}+\operatorname{curl}\mathbf{y}\big) \quad , \tag{3.47}$$

where $\mathbf{y}(\mathbf{x},t)$ is an unknown vector-valued field. Therefore $\operatorname{curl}\mathbf{y}$ is understood to be an unspecified divergence-free 'integration constant'. From a physical standpoint there is no room for arbitrariness in $\mathbf{j}^{+}$ and the only reasonable resolution is for $\operatorname{curl}\mathbf{y}$ to vanish,

$$\mathbf{j}^{+} \;=\; \mathbf{Q}\mathbf{j} \quad , \tag{3.48}$$

so that the conduction current density $\mathbf{j}$ transforms objectively. Note that balance equations are concerned only with the *net* flow of a quantity across the boundary, and are thus unsuitable for a conclusive derivation of the transformation properties of the flux.[23] From a mathematical perspective the issue traces back to the closed domain $\partial\mathcal{P}$ of the boundary integral in (3.1) which, as discussed at the end of Section 2.1.7, necessitates the use of the divergence theorem prior to localization. Of course, a similar loss of information is incurred when the Stokes and gradient theorems are applied, see Equations (2.50 - 54).

The form-invariance of the definition for the total (conductive plus convective) current density $(3.4)_2$ furnishes the transformation

$$\mathbf{J}^{+} \;=\; \mathbf{j}^{+}+q^{+}\mathbf{v}^{+} \;=\; \mathbf{Q}\big(\mathbf{J}+q\boldsymbol{\beta}\big) \quad , \tag{3.49}$$

where $(2.155)_3$, (3.43), and (3.48) were used. Unlike $\mathbf{j}^{+}$, the total current $\mathbf{J}^{+}$ is *not* objective due to the dependence of the convective term $q^{+}\mathbf{v}^{+}$ on the material velocity. The same result may be obtained from the invariance of the Eulerian form of charge conservation (3.2) with the aid of Equations $(2.46)_1$, (2.50), $(2.159)_2$, $(2.181)_1$, $(2.170)_{3-5}$, and (3.43).

3.4.2 Charge and Current Potentials

The imposition of form-invariance on the integral statement of Gauss' law $(3.6)_1$ leads to

$$\int_{\partial\mathcal{P}^{+}}\mathbf{d}^{+}\cdot\mathbf{n}^{+}\,\mathrm{d}a^{+} \;=\; \int_{\mathcal{P}^{+}}q^{+}\mathrm{d}v^{+} \;=\; \int_{\mathcal{P}}q\,\mathrm{d}v \;=\; \int_{\partial\mathcal{P}}\mathbf{d}\cdot\mathbf{n}\,\mathrm{d}a \quad , \tag{3.50}$$

or upon the use of Equations $(2.170)_{3-5}$ and (3.43)

$$\int_{\partial\mathcal{P}}\big\{\mathbf{Q}\,\mathbf{d}-\mathbf{d}^{+}\big\}\cdot\mathbf{Q}\,\mathbf{n}\,\mathrm{d}a \;=\; 0 \quad . \tag{3.51}$$

[23] For example, the boundary traction $\mathbf{t}_{(\mathbf{n})}$ and heat flux $q_{(\mathbf{n})}$ in Section 2.4.4, whose transformation properties cannot be unambiguously determined from the form-invariance of the momentum and energy balances, are simply *postulated* to be objective according to $(2.174)_{1,4}$. In the context of charge conservation, this is akin to postulating that $j^{+}_{(\mathbf{n}^{+})}=j_{(\mathbf{n})}$.

The divergence and localization theorems (2.50) and (2.55) thus furnish an objective transformation of the charge potential

$$\mathbf{d}^{+} \,=\, \mathbf{Q}\,\mathbf{d}' \quad \text{where} \quad \mathbf{d}' \,=\, \mathbf{d} + \operatorname{curl}\mathbf{y} \quad , \tag{3.52}$$

to within an unspecified divergence-free term.[24] Unlike before, this term may not necessarily be dismissed on physical grounds, since the charge potential is not an observable quantity itself. However, its divergence-free part does not affect the physical fields q and $\mathbf{j}$ as long as it falls within the indeterminate part of the charge-current potentials $\{\mathbf{d},\mathbf{h}\}$ according to $(3.8)_1$.

Form-invariance of AMPÈRE's circuital law $(3.6)_2$ is expressed by

$$\int_{\mathcal{A}^+} \mathbf{J}^{+}\cdot\mathbf{n}^{+}\mathrm{d}a^{+} \,=\, \oint_{\mathcal{C}^+} \mathbf{h}^{+}\cdot\mathrm{d}\mathbf{x}^{+} - \int_{\mathcal{A}^+} \frac{\partial\mathbf{d}^{+}}{\partial t}\cdot\mathbf{n}^{+}\mathrm{d}a^{+} \quad , \tag{3.53}$$

where the partial time derivative assumes a functional form $\mathbf{d}^{+}\!=\bar{\mathbf{d}}^{+}(\mathbf{x}^{+},t)$ according to the notational convention outlined in $(2.181)_2$. The transformation rules in $(2.170)_{2-4}$, (3.49), and $(3.52)_1$, as well as the uniformity of $\mathbf{Q}$ lead to

$$\int_{\mathcal{A}} \big(\mathbf{J} + q\boldsymbol{\beta}\big)\cdot\mathbf{n}\,\mathrm{d}a \,=\, \oint_{\mathcal{C}} \mathbf{Q}^{\mathrm{T}}\mathbf{h}^{+}\cdot\mathrm{d}\mathbf{x} - \int_{\mathcal{A}} \Big\{\mathbf{Q}^{\mathrm{T}}\dot{\mathbf{Q}}\,\mathbf{d}' + \frac{\partial\mathbf{d}'}{\partial t} - \big[\operatorname{grad}\mathbf{d}'\big]\boldsymbol{\beta}\Big\}\cdot\mathbf{n}\,\mathrm{d}a \quad , \tag{3.54}$$

where $(3.8)_1$ is employed for the sake of brevity. The left-hand side of (3.54) is substituted with the untransformed version of AMPÈRE's circuital law and rearranged to read

$$\oint_{\mathcal{C}} \big\{\mathbf{Q}^{\mathrm{T}}\mathbf{h}^{+} - \mathbf{h}\big\}\cdot\mathrm{d}\mathbf{x} - \int_{\mathcal{A}} \Big\{q\boldsymbol{\beta} + \boldsymbol{\Omega}\,\mathbf{d}' + \frac{\partial}{\partial t}\big(\operatorname{curl}\mathbf{y}\big) - \big[\operatorname{grad}\mathbf{d}'\big]\boldsymbol{\beta}\Big\}\cdot\mathbf{n}\,\mathrm{d}a \,=\, 0 \quad . \tag{3.55}$$

It is seen with the aid of $(2.46)_5$, $(2.47)_2$, $(2.159)_{1,2}$, and $(3.15)_1$ that parts of the argument in the surface integral can be restated as

$$\begin{aligned} \operatorname{curl}\big(\boldsymbol{\beta}\times\mathbf{d}'\big) \,&=\, \operatorname{div}\big[\boldsymbol{\beta}\otimes\mathbf{d}' - \mathbf{d}'\otimes\boldsymbol{\beta}\big] \\ &=\, \big[\operatorname{grad}\boldsymbol{\beta}\big]\mathbf{d}' + \big(\operatorname{div}\mathbf{d}'\big)\boldsymbol{\beta} - \big[\operatorname{grad}\mathbf{d}'\big]\boldsymbol{\beta} - \big(\operatorname{div}\boldsymbol{\beta}\big)\mathbf{d}' \\ &=\, \boldsymbol{\Omega}\,\mathbf{d}' + q\boldsymbol{\beta} - \big[\operatorname{grad}\mathbf{d}'\big]\boldsymbol{\beta} \quad . \end{aligned} \tag{3.56}$$

In view of STOKES theorem (2.53), and the commutativity between the curl and the partial time derivative, Equation (3.55) thus simplifies to

$$\int_{\mathcal{A}} \operatorname{curl}\Big\{\mathbf{Q}^{\mathrm{T}}\mathbf{h}^{+} - \mathbf{h} - \frac{\partial\mathbf{y}}{\partial t} - \boldsymbol{\beta}\times\mathbf{d}'\Big\}\cdot\mathbf{n}\,\mathrm{d}a \,=\, 0 \quad . \tag{3.57}$$

[24] Although represented by the same symbol $\mathbf{y}(\mathbf{x},t)$, the 'integration constant' $\operatorname{curl}\mathbf{y}$ is different from the one featured in Equation (3.47).

Due to the arbitrariness of the open surface $\mathcal{A}$ this statement can be localized to obtain the transformation of the current potential to within an unspecified irrotational (curl-free) term $\operatorname{grad}\Psi$ according to

$$\mathbf{h}^+ = \mathbf{Q}\big(\mathbf{h}' + \boldsymbol{\beta}\times\mathbf{d}'\big) \quad \text{where} \quad \mathbf{h}' = \mathbf{h} + \frac{\partial \mathbf{y}}{\partial t} + \operatorname{grad}\Psi \quad . \tag{3.58}$$

As anticipated, the 'integration constants' $\Psi(\mathbf{x},t)$ and $\mathbf{y}(\mathbf{x},t)$ in $(3.52)_2$ and $(3.58)_2$ fall precisely within the non-uniqueness in $(3.8)_{1,2}$ of the charge-current potentials $\{\mathbf{d},\mathbf{h}\}$. The conservation of charge in (3.5) is satisfied by MAXWELL's Equations $(3.15)_{1,2}$ for any choice of Ψ and $\mathbf{y}$. It is thus concluded that the transformations $(3.52)_1$ and $(3.58)_1$ of the charge-current potentials simplify to

$$\begin{aligned} \mathbf{d}^+ &= \mathbf{Q}\mathbf{d} \quad , \\ \mathbf{h}^+ &= \mathbf{Q}\big(\mathbf{h} + \boldsymbol{\beta}\times\mathbf{d}\big) \quad , \end{aligned} \tag{3.59}$$

where Ψ and $\mathbf{y}$ are neglected without loss of generality since they carry no physical significance.

While $\mathbf{h}^+$ is clearly not objective (nor GALILEAN invariant), an objective counterpart may be constructed from $\mathbf{d}$ and $\mathbf{h}$. Indeed, it is readily verified from $(2.155)_3$ and $(3.59)_{1,2}$ that the so-called *magnetomotive intensity* $\boldsymbol{\mathcal{H}}(\mathbf{x},t)$, defined as

$$\boldsymbol{\mathcal{H}} = \mathbf{h} - \mathbf{v}\times\mathbf{d} \quad , \tag{3.60}$$

transforms objectively, since

$$\boldsymbol{\mathcal{H}}^+ = \mathbf{h}^+ - \mathbf{v}^+\times\mathbf{d}^+ = \mathbf{Q}\big(\mathbf{h} - \mathbf{v}\times\mathbf{d}\big) = \mathbf{Q}\boldsymbol{\mathcal{H}} \quad . \tag{3.61}$$

3.4.3 Electric and Magnetic Fields

The objectivity of magnetic monopoles and the form-invariance of GAUSS' law for magnetism (3.10) suggest that

$$\int_{\partial\mathcal{P}^+} \mathbf{b}^+\cdot\mathbf{n}^+ \mathrm{d}a^+ = \int_{\partial\mathcal{P}} \mathbf{b}\cdot\mathbf{n}\,\mathrm{d}a = 0 \quad . \tag{3.62}$$

It follows immediately using $(2.170)_{3,4}$ that

$$\mathbf{b}^+ = \mathbf{Q}\mathbf{b} \quad . \tag{3.63}$$

Note that, again, an arbitrary divergence-free term $\operatorname{curl}\mathbf{y}$ arises from the use of the divergence and localization theorems, but is dismissed on physical grounds similar to (3.48).

The transformation of the electric field is obtained by appealing to the form-invariance of FARADAY's law of induction (3.9),

$$\int_{\mathcal{A}^+} \frac{\partial \mathbf{b}^+}{\partial t} \cdot \mathbf{n}^+ \mathrm{d}a^+ \;=\; -\oint_{\mathcal{C}^+} \mathbf{e}^+ \cdot \mathrm{d}\mathbf{x}^+ \quad . \tag{3.64}$$

The transformations $(2.181)_2$, $(2.170)_{2-4}$, and (3.63) are inserted to obtain

$$\int_{\mathcal{A}} \Big\{ \boldsymbol{\Omega}\,\mathbf{b} + \frac{\partial \mathbf{b}}{\partial t} - \big[\mathrm{grad}\,\mathbf{b}\big]\boldsymbol{\beta} \Big\} \cdot \mathbf{n}\,\mathrm{d}a \;=\; -\oint_{\mathcal{C}} \mathbf{Q}^{\mathrm{T}}\mathbf{e}^+ \cdot \mathrm{d}\mathbf{x} \quad , \tag{3.65}$$

after which the partial time derivative is substituted with the untransformed statement of FARADAY's law. As in Equation (3.56), the remaining terms in the surface integral are simplified using $(2.46)_5$, $(2.47)_2$, $(2.159)_{1,2}$, and $(3.15)_3$, furnishing

$$\int_{\mathcal{A}} \mathrm{curl} \Big\{ \mathbf{Q}^{\mathrm{T}}\mathbf{e}^+ - \mathbf{e} + \boldsymbol{\beta} \times \mathbf{b} \Big\} \cdot \mathbf{n}\,\mathrm{d}a \;=\; 0 \quad . \tag{3.66}$$

Upon the use of the localization theorem, it is concluded that the electric field transforms according to

$$\mathbf{e}^+ \;=\; \mathbf{Q}\big(\mathbf{e} - \boldsymbol{\beta} \times \mathbf{b}\big) \quad , \tag{3.67}$$

where, again, an arbitrary irrotational term $\mathrm{grad}\,\Psi$ is dismissed on physical grounds.

The so-called *electromotive intensity* $\boldsymbol{\mathcal{E}}(\mathbf{x}, t)$, defined as

$$\boldsymbol{\mathcal{E}} \;=\; \mathbf{e} + \mathbf{v} \times \mathbf{b} \quad , \tag{3.68}$$

forms an objective counterpart to the electric field. Indeed, Equations $(2.155)_3$, (3.63), and (3.67) immediately yield

$$\boldsymbol{\mathcal{E}}^+ \;=\; \mathbf{e}^+ + \mathbf{v}^+ \times \mathbf{b}^+ \;=\; \mathbf{Q}\big(\mathbf{e} + \mathbf{v} \times \mathbf{b}\big) \;=\; \mathbf{Q}\boldsymbol{\mathcal{E}} \quad . \tag{3.69}$$

The electromotive intensity is important for the LAGRANGIAN viewpoint of FARADAY's law of induction, see Equation $(3.100)_3$. A detailed discussion of its implications is provided in Section 3.5.2.

3.4.4 Electric and Magnetic Potentials

Recall from Section 3.1.2 that the electromagnetic fields $\{\mathbf{e}, \mathbf{b}\}$ can be alternatively represented by electromagnetic potentials $\{\phi, \mathbf{a}\}$. FARADAY's law of induction (3.9) and GAUSS' law for magnetism (3.10) are subsumed by Equations $(3.12)_{1,2}$, whose form-invariance is exploited to derive the transformation under SRBM of the EM potentials.

Starting with the derivation of the magnetic potential $\mathbf{a}^+$, it is seen from the transformations in $(2.170)_{3,4}$ and (3.63) that the form-invariance of $(3.12)_2$ implies

$$\oint_{\mathcal{C}} \mathbf{a} \cdot \mathrm{d}\mathbf{x} \;=\; \int_{\mathcal{A}} \mathbf{b} \cdot \mathbf{n}\,\mathrm{d}a \;=\; \int_{\mathcal{A}^+} \mathbf{b}^+ \cdot \mathbf{n}^+ \mathrm{d}a^+ \;=\; \oint_{\mathcal{C}^+} \mathbf{a}^+ \cdot \mathrm{d}\mathbf{x}^+ \quad . \tag{3.70}$$

Hence it follows from the STOKES theorem (2.53) and the transformation of the curl (2.168) that

$$\int_{\mathcal{A}} \operatorname{curl}\big(\mathbf{Q}^{\mathrm{T}}\mathbf{a}^{+} - \mathbf{a}\big) \cdot \mathbf{n}\, \mathrm{d}a \;=\; 0 \quad . \tag{3.71}$$

Given the arbitrariness of the open surface $\mathcal{A}$, this statement is readily localized to obtain

$$\mathbf{a}^{+} \;=\; \mathbf{Q}\,\mathbf{a}' \quad \text{where} \quad \mathbf{a}' \;=\; \mathbf{a} + \operatorname{grad}\Psi \quad . \tag{3.72}$$

Here, $\Psi(\mathbf{x}, t)$ represents an arbitrary real-valued 'integration constant'. As with the charge-current potentials in Section 3.4.2, this term is not disregarded on physical grounds since it falls within the range of indeterminacy of the gauge transformation $(3.14)_2$, although it is yet to be verified that the term carries over to ϕ^{+} in line with $(3.14)_1$.

The transformation of the electric potential ϕ^{+} is deduced from the form-invariance of Equation $(3.12)_1$, that is,

$$\int_{\mathcal{S}^{+}} \mathbf{e}^{+} \cdot \mathrm{d}\mathbf{x}^{+} \;=\; -\int_{\mathcal{S}^{+}} \frac{\partial \mathbf{a}^{+}}{\partial t} \cdot \mathrm{d}\mathbf{x}^{+} - \big[\phi^{+}\big]_{\mathbf{s}_1^{+}}^{\mathbf{s}_2^{+}} \quad . \tag{3.73}$$

Similar to partial time derivatives, the potential difference (or voltage) must take into account the functional representation of $\phi^{+} = \bar{\phi}^{+}(\mathbf{x}^{+}, t) = \tilde{\phi}^{+}(\mathbf{x}, t)$,

$$\big[\bar{\phi}^{+}\big]_{\mathbf{s}_1^{+}}^{\mathbf{s}_2^{+}} \;=\; \bar{\phi}^{+}(\mathbf{s}_2^{+}, t) - \bar{\phi}^{+}(\mathbf{s}_1^{+}, t) \;=\; \tilde{\phi}^{+}(\mathbf{s}_2, t) - \tilde{\phi}^{+}(\mathbf{s}_1, t) \;=\; \big[\tilde{\phi}^{+}\big]_{\mathbf{s}_1}^{\mathbf{s}_2} \quad , \tag{3.74}$$

where the boundary points $\mathbf{s}_1^{+}$ and $\mathbf{s}_2^{+}$ of the open path $\mathcal{S}^{+}$ symbolize the transformed counterparts for $\mathbf{s}_1$ and $\mathbf{s}_2$ of $\mathcal{S}$. This observation is of course in agreement with the gradient theorem (2.54) and the transformations in (2.163) and $(2.170)_2$. Using $(3.14)_2$ for brevity, Equation (3.73) becomes

$$\int_{\mathcal{S}} \big(\mathbf{e} - \boldsymbol{\beta} \times \mathbf{b}\big) \cdot \mathrm{d}\mathbf{x} \;=\; -\int_{\mathcal{S}} \Big\{\mathbf{Q}^{\mathrm{T}}\dot{\mathbf{Q}}\,\mathbf{a}' + \frac{\partial \mathbf{a}'}{\partial t} - \big[\operatorname{grad}\mathbf{a}'\big]\boldsymbol{\beta}\Big\} \cdot \mathrm{d}\mathbf{x} - \big[\tilde{\phi}^{+}\big]_{\mathbf{s}_1}^{\mathbf{s}_2} \quad , \tag{3.75}$$

where $(2.181)_2$, $(2.170)_2$, (3.67), and $(3.72)_1$ were employed. The untransformed version of $(3.12)_1$ is substituted for $\mathbf{e}$ to yield

$$\big[\tilde{\phi}^{+} - \tilde{\phi}\big]_{\mathbf{s}_1}^{\mathbf{s}_2} + \int_{\mathcal{S}} \Big\{-\boldsymbol{\beta} \times \big(\operatorname{curl}\mathbf{a}'\big) + \boldsymbol{\Omega}\,\mathbf{a}' + \frac{\partial}{\partial t}\big(\operatorname{grad}\Psi\big) - \big[\operatorname{grad}\mathbf{a}'\big]\boldsymbol{\beta}\Big\} \cdot \mathrm{d}\mathbf{x} \;=\; 0 \quad , \tag{3.76}$$

where $\mathbf{b} = \operatorname{curl}\mathbf{a}'$ following $(2.49)_1$ and $(3.13)_2$. In order to simplify the argument of the path integral, it is noted that

$$\begin{aligned} \operatorname{grad}\big(\boldsymbol{\beta} \cdot \mathbf{a}'\big) \;&=\; \big[\operatorname{grad}\boldsymbol{\beta}\big]^{\mathrm{T}}\mathbf{a}' + \big[\operatorname{grad}\mathbf{a}'\big]^{\mathrm{T}}\boldsymbol{\beta} \\ &=\; -\big[\operatorname{grad}\boldsymbol{\beta}\big]\,\mathbf{a}' - \big(\big[\operatorname{grad}\mathbf{a}'\big]\boldsymbol{\beta} - \big[\operatorname{grad}\mathbf{a}'\big]^{\mathrm{T}}\boldsymbol{\beta}\big) + \big[\operatorname{grad}\mathbf{a}'\big]\boldsymbol{\beta} \\ &=\; -\boldsymbol{\Omega}\,\mathbf{a}' - \big(\operatorname{curl}\mathbf{a}'\big) \times \boldsymbol{\beta} + \big[\operatorname{grad}\mathbf{a}'\big]\boldsymbol{\beta} \quad , \end{aligned} \tag{3.77}$$

where use was made of $(2.45)_2$, (2.48), and the skew-symmetry of $\boldsymbol{\Omega} = -[\mathrm{grad}\,\boldsymbol{\beta}]^{\mathrm{T}}$ in $(2.159)_1$. Furthermore, the electric potentials in Equation (3.76) are moved inside the path integral using the gradient theorem (2.54), furnishing

$$\int_{\mathcal{S}} \mathrm{grad}\Big\{\phi^+ - \phi + \frac{\partial \Psi}{\partial t} - \boldsymbol{\beta}\cdot\mathbf{a}'\Big\}\cdot \mathrm{d}\mathbf{x} \;=\; 0 \quad . \tag{3.78}$$

Given the arbitrariness of the open path $\mathcal{S}$ this statement is readily localized to

$$\phi^+ \;=\; \phi' + \boldsymbol{\beta}\cdot\mathbf{a}' \quad \text{where} \quad \phi' \;=\; \phi - \frac{\partial \Psi}{\partial t} + \psi \quad , \tag{3.79}$$

where $\psi(t)$ is an arbitrary uniform real-valued field arising from the integration of the gradient. Recall from $(3.72)_{1,2}$ that $\Psi(\mathbf{x},t)$ enters the transformation of $\mathbf{a}^+$ only in terms of its gradient, so that in $(3.79)_2$ ψ is simply absorbed into Ψ (in the sense that $\Psi' = \Psi + \psi t$). Hence, the unspecified 'integration constant' Ψ enters both charge-current potentials $\{\phi^+, \mathbf{a}^+\}$ as prescribed by the gauge transformations $(3.14)_{1,2}$ and can thus be disregarded without consequence. It is concluded that the transformation of the EM potentials are given by

$$\begin{aligned} \phi^+ \;&=\; \phi + \boldsymbol{\beta}\cdot\mathbf{a} \quad , \\ \mathbf{a}^+ \;&=\; \mathbf{Q}\,\mathbf{a} \quad . \end{aligned} \tag{3.80}$$

Evidently, $\mathbf{a}^+$ transforms objectively whereas ϕ^+ does not. An objective counterpart for the electric potential is readily obtained as[25]

$$\varphi(\mathbf{x},t) \;=\; \phi - \mathbf{v}\cdot\mathbf{a} \quad , \tag{3.81}$$

whose objectivity

$$\varphi^+ \;=\; \phi^+ - \mathbf{v}^+\cdot\mathbf{a}^+ \;=\; \phi - \mathbf{v}\cdot\mathbf{a} \;=\; \varphi \quad , \tag{3.82}$$

is readily verified with $(2.155)_3$ and $(3.80)_{1,2}$. The reader is reminded that, while $\mathbf{v}$ denotes the material velocity, $\mathbf{a}$ denotes the magnetic potential rather than the acceleration. The latter will be denoted $\dot{\mathbf{v}}$ where necessary to avoid confusion.

3.4.5 Polarization and Magnetization

Recall that the postulated invariance of $Q(\mathcal{P})$ (*i.e.*, the total amount of electric charge contained in a material region $\mathcal{P}$) is assumed to hold separately for the free and bound charges, $Q_{\mathrm{F}}(\mathcal{P}) = Q^+_{\mathrm{F}}(\mathcal{P}^+)$ and $Q_{\mathrm{R}}(\mathcal{P}) = Q^+_{\mathrm{R}}(\mathcal{P}^+)$. Due to the additive nature of this decomposition, see (3.25) and (3.26), and the linearity of Maxwell's Equations $(3.15)_{1,2}$, the ensuing transformation formulae for the free and bound parts of

[25] Note that the symbol φ for the objective version of the electric potential will be repurposed in the context of electrostatics, starting in Section 3.7, where it will replace $\mathbf{a}$ as a magnetic potential.

the EM fields are largely identical to those of the total fields. Given the similarity with the preceding discussion of the total EM fields, their derivation is not presented in full detail here.

It follows from the above postulate that the free and bound charge densities $q_{\rm F}$ and $q_{\rm R}$ transform objectively,

$$q_{\rm F}^{+} \;=\; q_{\rm F} \quad , \quad q_{\rm R}^{+} \;=\; q_{\rm R} \quad . \tag{3.83}$$

Recall that the conservation of charge is satisfied independently by the charge-currents $\{q_{\rm F}, \mathbf{j}_{\rm F}\}$, $\{q_{\rm R}, \mathbf{j}_{\rm P}\}$, and $\{0, \mathbf{j}_{\rm M}\}$ associated with conduction, polarization, and magnetization. Hence the form-invariance of (3.1) and $(3.6)_{1,2}$ for the free parts furnishes

$$\begin{aligned} \mathbf{j}_{\rm F}^{+} \;&=\; \mathbf{Q}\,\mathbf{j}_{\rm F} \qquad\qquad\quad , \\ \mathbf{d}_{\rm F}^{+} \;&=\; \mathbf{Q}\,\mathbf{d}_{\rm F} \qquad\qquad\quad , \\ \mathbf{h}_{\rm F}^{+} \;&=\; \mathbf{Q}\big(\mathbf{h}_{\rm F} + \boldsymbol{\beta}\times\mathbf{d}_{\rm F}\big) \quad . \end{aligned} \tag{3.84}$$

The derivation of this result is entirely analogous to that of the total fields $\mathbf{j}$, $\mathbf{d}$, and $\mathbf{h}$, see (3.48) and $(3.59)_{1,2}$, including the dismissal of 'integration constants'. A comparison between the free and the total fields leads to the transformation of the bound parts

$$\begin{aligned} \mathbf{j}_{\rm R}^{+} \;&=\; \mathbf{Q}\,\mathbf{j}_{\rm R} \qquad\qquad\quad , \\ \big(-\mathbf{d}_{\rm R}^{+} \;=\big)\;\; \mathbf{p}^{+} \;&=\; \mathbf{Q}\,\mathbf{p} \qquad\qquad\quad , \\ \big(\,\mathbf{h}_{\rm R}^{+} \;=\big)\; \mathbf{m}^{+} \;&=\; \mathbf{Q}\big(\mathbf{m} - \boldsymbol{\beta}\times\mathbf{p}\big) \quad . \end{aligned} \tag{3.85}$$

This result is consistent with the form-invariance of (3.16), (3.18), and (3.21) (to within a divergence-free term in $\mathbf{j}_{\rm R}^{+}$, $\mathbf{p}^{+}$, and an irrotational term in $\mathbf{m}^{+}$, all of which are discounted for physical reasons). Note that the sign of the vector product in $(3.85)_3$ differs from $(3.59)_2$ and $(3.84)_3$ due to the sign convention introduced in the definition of $\mathbf{p}$.

In view of the preceding results, the transformations of the total (conductive plus convective) free and bound currents $(3.27)_{1,2}$ are given by

$$\begin{aligned} \mathbf{J}_{\rm F}^{+} \;&=\; \mathbf{Q}\big(\mathbf{J}_{\rm F} + q_{\rm F}\,\boldsymbol{\beta}\big) \quad , \\ \mathbf{J}_{\rm R}^{+} \;&=\; \mathbf{Q}\big(\mathbf{J}_{\rm R} + q_{\rm R}\,\boldsymbol{\beta}\big) \quad . \end{aligned} \tag{3.86}$$

The *free magnetomotive intensity* $\boldsymbol{\mathcal{H}}_{\rm F}(\mathbf{x},t)$ represents an objective replacement for the free current potential $\mathbf{h}_{\rm F}$, where

$$\boldsymbol{\mathcal{H}}_{\rm F} \;=\; \mathbf{h}_{\rm F} \,-\, \mathbf{v}\times\mathbf{d}_{\rm F} \quad . \tag{3.87}$$

In view of (3.28), $(3.32)_{1,2}$, and (3.60), the magnetomotive intensity $\boldsymbol{\mathcal{H}}$ is additively decomposed into the free and bound parts $\boldsymbol{\mathcal{H}}_{\rm F} = \boldsymbol{\mathcal{H}} - \boldsymbol{\mathcal{M}}$ and $\boldsymbol{\mathcal{H}}_{\rm R} = \boldsymbol{\mathcal{M}}$. Their transformation is given by

$$\begin{aligned} \boldsymbol{\mathcal{H}}_{\rm F}^{+} \;&=\; \mathbf{Q}\,\boldsymbol{\mathcal{H}}_{\rm F} \quad , \\ \big(\,\boldsymbol{\mathcal{H}}_{\rm R}^{+} \;=\big)\; \boldsymbol{\mathcal{M}}^{+} \;&=\; \mathbf{Q}\,\boldsymbol{\mathcal{M}} \quad , \end{aligned} \tag{3.88}$$

as opposed to their non-objective alternative in $(3.84)_3$ and $(3.85)_3$.

3.4.6 Aether Relations under SRBM

The aether relations raise a fundamental issue with the non-relativistic treatment of frame invariance. The objective fields $\mathbf{d}$ and $\mathbf{b}$ in (3.35) are directly proportional to the non-objective fields $\mathbf{e}$ and $\mathbf{h}$. The aether relations are therefore *not* form-invariant under general SRBMs as defined by (2.153), or even under GALILEAN transformations (2.154). Although the aether frame is always inertial, not every inertial frame is an aether frame. For example, it is readily seen from Equations $(3.59)_{1,2}$, (3.63), and (3.67) that the relations (3.35) cannot hold in a frame moving at constant velocity relative to the aether frame.

Before the advent of the theory of special relativity, the prevailing scientific understanding was that the propagation of light, like acoustic waves, requires a medium, see WHITTAKER [154] for a historical recount. The existence of such a *luminiferous aether*, and the corresponding aether frame in which it is at rest, would imply that the speed of light depends on the frame of the observer. However, the concept was largely abandoned when the celebrated MICHELSON-MORLEY experiments [91–93] provided experimental evidence to the contrary. This led to the development of the LORENTZ *transformations*,

$$\begin{aligned} \mathbf{x}^+ &= \mathbf{Q}_0\left\{\mathbf{x}+\frac{\gamma^2}{\gamma+1}\frac{\mathbf{v}_0\cdot\mathbf{x}}{c^2}\mathbf{v}_0-\gamma\,\mathbf{v}_0\,t\right\} \\ t^+ &= \pm\gamma\left(t-\frac{\mathbf{v}_0\cdot\mathbf{x}}{c^2}\right) \end{aligned} \qquad \text{where} \qquad \begin{aligned} v_0 &= |\mathbf{v}_0| \\ \gamma &= \frac{1}{\sqrt{1-v_0^2/c^2}} \end{aligned} \tag{3.89}$$

under which frame invariance is achieved for both the MAXWELL equations (3.15) and the aether relations (3.35) simultaneously. Any frame reached from the aether frame by means of a LORENTZ transformation is called a LORENTZ *frame*, which is itself another aether frame.

In order to avoid a complex solution for (3.89) the parameter v_0 is assumed not to exceed the vacuum speed of light, $0<v_0<c$, see (3.36). Indeed, in the limit where v_0 approaches c the parameter γ tends toward infinity. Conversely, for $v_0\ll c$ (and thus $\mathbf{v}_0\cdot\mathbf{x}\ll c^2$ and $\gamma\doteq 1$) Equations (3.89) approach the classical limit given by the GALILEAN transformation in (2.154).[26] Note that outside of the classical limit, the LORENTZ transformations preserve neither time intervals t_2-t_1 nor EUCLIDEAN distances $|\mathbf{x}_2-\mathbf{x}_1|$, rendering these parameters dependent on the observer. The concession that the notions of time and space are not absolute, of course, led to the revision of classical theories such as mechanics, thermodynamics, and gravitation under the framework of relativity theory.

The above remarks highlight the fact that electromagnetism is a fundamentally relativistic phenomenon. The development of a consistent framework for the cou-

[26] See, for example, STEIGMANN [137]: "[...] *these transformations are asymptotically coincident if the material velocity relative to a Galilean frame is much smaller than c and if the diameter of the material body is bounded.*"

pled electro-magneto-thermo-mechanical model necessitates a relativistic treatment of thermomechanics. Under the relativistic framework, LORENTZ frames take up the role of GALILEAN frames and the thermomechanical balance equations must be revised to ensure their frame-invariance under LORENTZ transformations. While a fully formed theory of relativistic continuum mechanics exists,[27] this is unpractical for engineering applications and beyond the scope of this dissertation.

The lack of form-invariance of the aether relations is discussed extensively in the literature, see GOLDIN and SHTELEN [33], KOVETZ [64, Section 12], LE BELLAC and LÉVY-LEBLOND [71], or MÜLLER *et al.* [103, Section 5.3]. Some authors[28] propose an alternative (non-relativistic) form of the aether relations (3.35) according to which

$$\mathbf{d} \overset{\text{Aet.}}{=} \varepsilon_0 \boldsymbol{\mathcal{E}} \quad \text{and} \quad \boldsymbol{\mathcal{H}} \overset{\text{Aet.}}{=} \mathbf{b}/\mu_0 \quad . \tag{3.90}$$

Likewise, if the free and bound parts are explicitly accounted for, form-invariance of the aether relations (3.37) is restored by setting

$$\mathbf{d}_{\mathrm{F}} \overset{\text{Aet.}}{=} \varepsilon_0 \boldsymbol{\mathcal{E}} + \mathbf{p} \quad \text{and} \quad \boldsymbol{\mathcal{H}}_{\mathrm{F}} \overset{\text{Aet.}}{=} \mathbf{b}/\mu_0 - \boldsymbol{\mathcal{M}} \quad . \tag{3.91}$$

The lack of objectivity of $\mathbf{e}$ and $\mathbf{h} = \mathbf{h}_{\mathrm{F}} + \mathbf{m}$ is thus reconciled by substitution with their objective counterparts. However, note that Equations (3.90) and (3.91) are in direct conflict with (3.35) and (3.37) even at modest velocities unless the convective terms are negligible, that is, $\mathbf{v} \times \mathbf{b} \ll \mathbf{e}$ and $\mathbf{v} \times \mathbf{d} \ll \mathbf{h}$.

In the course of this dissertation, however, the question of the aether frame is avoided altogether by presenting the theory *before* application of the aether equations and thus independent of the frame of reference. The aether relations are regarded as constitutive relations whose role is to provide closure for an otherwise underdetermined set of balance equations. They need not be specified for the upcoming discussion of the balance equations for the coupled EMTM continuum. As with the mechanical and thermal constitutive relations, no assumptions will be made at the outset regarding the form of the aether relations.

[27] Relativistic continuum mechanical theories are typically formulated in the four-dimensional MINKOWSKI space-time notation, employing a *four-velocity* v^μ and *energy-momentum tensor* $T^{\mu\nu}$. Areas of application are in astrophysics (*e.g.*, the modeling of neutron stars and accretion disks) and in high-energy physics (*e.g.*, quark-gluon plasma dynamics in heavy-ion collisions), see for example BEIG and SCHMIDT [5], CARTER and QUINTANA [12], and LANDAU and LIFSHITZ [68, Chapter XV].

[28] See, for example, HUTTER *et al.* [56, Chapter 3.4], where the conventional aether relations in Equations 3.4.3 are replaced with 3.4.13.

3.4.7 Summary

The charge-current densities $\{q, \mathbf{J}\}$ and the corresponding potentials $\{\mathbf{d}, \mathbf{h}\}$ transform according to (3.43), (3.49), $(3.59)_{1,2}$, $(3.83)_{1,2}$, $(3.84)_{2,3}$, $(3.85)_{2,3}$, and $(3.86)_{1,2}$ via

$$\begin{aligned}
q^+ &= q \quad , \quad \mathbf{J}^+ = \mathbf{Q}\big(\mathbf{J} + q\boldsymbol{\beta}\big) \quad , \quad \mathbf{d}^+ = \mathbf{Q}\mathbf{d} \quad , \quad \mathbf{h}^+ = \mathbf{Q}\big(\mathbf{h} + \boldsymbol{\beta}\times\mathbf{d}\big) \quad , \\
q_{\mathrm{F}}^+ &= q_{\mathrm{F}} \quad , \quad \mathbf{J}_{\mathrm{F}}^+ = \mathbf{Q}\big(\mathbf{J}_{\mathrm{F}} + q_{\mathrm{F}}\boldsymbol{\beta}\big) \quad , \quad \mathbf{d}_{\mathrm{F}}^+ = \mathbf{Q}\mathbf{d}_{\mathrm{F}} \quad , \quad \mathbf{h}_{\mathrm{F}}^+ = \mathbf{Q}\big(\mathbf{h}_{\mathrm{F}} + \boldsymbol{\beta}\times\mathbf{d}_{\mathrm{F}}\big) \quad , \\
q_{\mathrm{R}}^+ &= q_{\mathrm{R}} \quad , \quad \mathbf{J}_{\mathrm{R}}^+ = \mathbf{Q}\big(\mathbf{J}_{\mathrm{R}} + q_{\mathrm{R}}\boldsymbol{\beta}\big) \quad , \quad \mathbf{p}^+ = \mathbf{Q}\mathbf{p} \quad , \quad \mathbf{m}^+ = \mathbf{Q}\big(\mathbf{m} - \boldsymbol{\beta}\times\mathbf{p}\big) \quad .
\end{aligned} \tag{3.92}$$

The free and bound parts of each field undergo the same transformations as their combined counterparts. The current densities $\mathbf{J}_{[\cdot]}$ and the current potentials $\mathbf{h}_{[\cdot]}$ (or MINKOWSKI magnetization $\mathbf{m}$) are not objective.[29] They are alternatively represented by the conduction currents $\mathbf{j}_{[\cdot]} = \mathbf{J}_{[\cdot]} - q_{[\cdot]}\mathbf{v}$ and the magnetomotive intensities $\boldsymbol{\mathcal{H}}_{[\cdot]} = \mathbf{h}_{[\cdot]} - \mathbf{v}\times\mathbf{d}_{[\cdot]}$ (or magnetization density $\boldsymbol{\mathcal{M}} = \mathbf{m} + \mathbf{v}\times\mathbf{p}$), which transform objectively as

$$\begin{aligned}
\mathbf{j}^+ &= \mathbf{Q}\mathbf{j} \quad , \quad \boldsymbol{\mathcal{H}}^+ = \mathbf{Q}\boldsymbol{\mathcal{H}} \quad , \\
\mathbf{j}_{\mathrm{F}}^+ &= \mathbf{Q}\mathbf{j}_{\mathrm{F}} \quad , \quad \boldsymbol{\mathcal{H}}_{\mathrm{F}}^+ = \mathbf{Q}\boldsymbol{\mathcal{H}}_{\mathrm{F}} \quad , \\
\mathbf{j}_{\mathrm{R}}^+ &= \mathbf{Q}\mathbf{j}_{\mathrm{R}} \quad , \quad \boldsymbol{\mathcal{M}}^+ = \mathbf{Q}\boldsymbol{\mathcal{M}} \quad ,
\end{aligned} \tag{3.93}$$

following the results in (3.48), (3.61), $(3.84)_1$, $(3.85)_1$, and $(3.88)_{1,2}$.

The EM fields $\{\mathbf{e}, \mathbf{b}\}$ and the corresponding potentials $\{\phi, \mathbf{a}\}$ transform via

$$\mathbf{e}^+ = \mathbf{Q}\big(\mathbf{e} - \boldsymbol{\beta}\times\mathbf{b}\big) \quad , \quad \mathbf{b}^+ = \mathbf{Q}\mathbf{b} \quad , \quad \phi^+ = \phi + \boldsymbol{\beta}\cdot\mathbf{a} \quad , \quad \mathbf{a}^+ = \mathbf{Q}\mathbf{a} \quad , \tag{3.94}$$

see (3.63), (3.67), and $(3.80)_{1,2}$. The electric field $\mathbf{e}$ and electric potential ϕ are not objective, but the electromotive intensity $\boldsymbol{\mathcal{E}} = \mathbf{e} + \mathbf{v}\times\mathbf{b}$ and its potential $\varphi = \phi - \mathbf{v}\cdot\mathbf{a}$ are,

$$\boldsymbol{\mathcal{E}}^+ = \mathbf{Q}\boldsymbol{\mathcal{E}} \quad , \quad \varphi^+ = \varphi \quad , \tag{3.95}$$

see Equations (3.69) and (3.82).

Recall that the above transformation properties were derived from the form-invariance of the governing equations and the postulated invariance of the (free and bound) charges contained in a material region. This gave rise to undetermined 'integration constants' in the transformation formulae of the current, electromagnetic fields, polarization, and magnetization, all of which were disallowed on the basis that any arbitrariness in these fields would be unphysical. However, any such ambiguities can be eliminated if it is instead postulated that $\mathbf{j}$ and $\boldsymbol{\mathcal{E}}$ as well as $\mathbf{p}$ and $\boldsymbol{\mathcal{M}}$ are objective, or

$$\begin{aligned}
\int_{\mathcal{A}} \mathbf{j}\cdot\mathbf{n}\,\mathrm{d}a &= \int_{\mathcal{A}^+} \mathbf{j}^+\cdot\mathbf{n}^+\mathrm{d}a^+ \quad , \quad \int_{\mathcal{S}} \boldsymbol{\mathcal{E}}\cdot\mathrm{d}\mathbf{x} = \int_{\mathcal{S}^+} \boldsymbol{\mathcal{E}}^+\cdot\mathrm{d}\mathbf{x}^+ \quad , \\
\int_{\mathcal{A}} \mathbf{p}\cdot\mathbf{n}\,\mathrm{d}a &= \int_{\mathcal{A}^+} \mathbf{p}^+\cdot\mathbf{n}^+\mathrm{d}a^+ \quad , \quad \int_{\mathcal{S}} \boldsymbol{\mathcal{M}}\cdot\mathrm{d}\mathbf{x} = \int_{\mathcal{S}^+} \boldsymbol{\mathcal{M}}^+\cdot\mathrm{d}\mathbf{x}^+ \quad .
\end{aligned} \tag{3.96}$$

[29] The subscript indicates that a statement is valid for the free, bound, and the total fields. For example, $\mathbf{J}_{[\cdot]}$ represents $\mathbf{J}$, $\mathbf{J}_{\mathrm{F}}$, and $\mathbf{J}_{\mathrm{R}}$ simultaneously.

This assumption is akin to the postulates in $(2.174)_{1,4}$ for the traction vector and heat flux. Any arbitrariness remaining in the transformations of the charge-current potentials and the electromagnetic potentials is absorbed into the non-uniqueness of the potentials in $(3.8)_{1,2}$ and $(3.14)_{1,2}$.

3.5 Maxwell's Equations in Objective Terms

It was discussed in Section 2.2.1 that the distinction between the EULERIAN and LAGRANGIAN descriptions in continuum mechanics hinges on the configuration with respect to which a physical quantity is functionally expressed. This distinction also affects the balance laws, where integrals are either evaluated with respect to the current or the referential domains, $\mathcal{R}$ or $\mathcal{R}_0$, and where time derivatives are either partial or material, respectively.

The resulting LAGRANGIAN statements and PIOLA transforms in Section 2.3.7 are predicated on the existence of a reference configuration. However, the discussion of the laws of electromagnetism does not usually involve deformable media. As a result, the governing EM equations are typically presented in EULERIAN form.

Nevertheless, it was argued in Section 3.1.1 that the governing equations can adopt an EULERIAN (*i.e.*, spatial) or LAGRANGIAN (*i.e.*, material) viewpoint in the following sense: In the former, the rate of change of a conserved quantity is computed for a *fixed* spatial region, resulting in a partial time derivative inside the integral such as in (3.2). In the latter, the rate of change is measured for a spatial region whose boundary *convects* with the motion $\boldsymbol{\chi}(\mathbf{X}, t)$, which leads to a total time derivative as seen in (3.1).

3.5.1 Eulerian and Lagrangian Time Derivatives

The aforementioned classification is used in this section to examine the relationship between time derivatives and objectivity under SRBM. It is observed that the LAGRANGIAN perspective on time derivatives naturally leads to the objective fields $\mathbf{j}$, $\boldsymbol{\mathcal{H}}$, $\boldsymbol{\mathcal{M}}$, $\boldsymbol{\mathcal{E}}$, and φ, whereas the EULERIAN perspective produces their non-objective counterparts $\mathbf{J}$, $\mathbf{h}$, $\mathbf{m}$, $\mathbf{e}$, and ϕ. This is due to the lack of objectivity of partial time derivatives, see (2.181), which must be compensated by the remaining terms in the balance equation to maintain overall form-invariance of the EM laws. Meanwhile, governing equations that do not involve time derivatives cannot be categorized as either EULERIAN or LAGRANGIAN. They feature the objective fields q, $\mathbf{d}$, $\mathbf{p}$, $\mathbf{b}$, and $\mathbf{a}$, see Equations $(3.6)_1$, $(3.7)_1$, (3.10), $(3.11)_1$, $(3.12)_2$, and $(3.13)_2$.

The conservation of electric charge is reproduced from Equations (3.1), (3.2),

and (3.5) as

$$\begin{aligned} \int_{\mathcal{P}} \frac{\partial q}{\partial t}\,\mathrm{d}v + \int_{\partial\mathcal{P}} \mathbf{J}\cdot\mathbf{n}\,\mathrm{d}a \;&=\; 0 \quad , \qquad \frac{\partial q}{\partial t} + \operatorname{div}\mathbf{J} \;=\; 0 \quad , \\ \frac{\mathrm{d}}{\mathrm{d}t}\int_{\mathcal{P}} q\,\mathrm{d}v + \int_{\partial\mathcal{P}} \mathbf{j}\cdot\mathbf{n}\,\mathrm{d}a \;&=\; 0 \quad , \quad \dot{q} + q\operatorname{div}\mathbf{v} + \operatorname{div}\mathbf{j} \;=\; 0 \quad , \end{aligned} \tag{3.97}$$

where the Reynolds transport theorem (2.104) was used to localize the integral form $(3.97)_3$ of the Lagrangian representation to obtain Equation $(3.97)_4$. It is entirely comprised of objective terms according to (2.165), (2.173), (3.43), and (3.48). Note that, even though the region $\mathcal{P}$ and its boundary $\partial\mathcal{P}$ in $(3.97)_{1,3}$ are always considered material (and thus time dependent), the distinction between the Eulerian and Lagrangian viewpoints arises from the placement of the time derivatives. The Eulerian form $(3.97)_1$ is characterized by a partial time derivative of the integrand, whereas the Lagrangian statement $(3.97)_3$ features a material time derivative of the entire integral.

Similarly, Ampère's circuital law $(3.6)_2$ and $(3.7)_2$ is rearranged according to

$$\begin{aligned} \oint_{\mathcal{C}} \mathbf{h}\cdot\mathrm{d}\mathbf{x} \;&=\; \int_{\mathcal{A}} \mathbf{J}\cdot\mathbf{n}\,\mathrm{d}a + \int_{\mathcal{A}} \frac{\partial\mathbf{d}}{\partial t}\cdot\mathbf{n}\,\mathrm{d}a \quad , \quad \operatorname{curl}\mathbf{h} \;=\; \mathbf{J} + \frac{\partial\mathbf{d}}{\partial t} \quad , \\ \oint_{\mathcal{C}} \boldsymbol{\mathcal{H}}\cdot\mathrm{d}\mathbf{x} \;&=\; \int_{\mathcal{A}} \mathbf{j}\cdot\mathbf{n}\,\mathrm{d}a + \frac{\mathrm{d}}{\mathrm{d}t}\int_{\mathcal{A}} \mathbf{d}\cdot\mathbf{n}\,\mathrm{d}a \quad , \quad \operatorname{curl}\boldsymbol{\mathcal{H}} \;=\; \mathbf{j} + \overset{\star}{\mathbf{d}} \quad , \end{aligned} \tag{3.98}$$

where the flux derivative (2.105) was employed to deduce the local statement $(3.98)_4$ featuring only objective terms. As before, while $\mathcal{A}$ denotes an arbitrary material surface, the Eulerian statement $(3.98)_1$ involves a partial time derivative inside the integral, as opposed to the material time derivative in front of the integral in the Lagrangian statement $(3.98)_3$. Equation $(3.98)_1$ represents the rate of change of the flux of $\mathbf{d}$ through the fixed spatial surface $\mathcal{A}|_{t=\tau}$ occupied by $\mathcal{A}$ at any given time $t=\tau$, whereas the material time derivative in $(3.98)_3$ quantifies the rate of change while accounting for the motion of $\mathcal{A}$.

Naturally, the laws governing polarization and magnetization in (3.24) and $(3.26)_2$ are already expressed in Lagrangian form, since they quantify the constitutive response of the underlying medium. Hence, the bound part of Ampère's circuital law reads

$$\begin{aligned} \oint_{\mathcal{C}} \mathbf{m}\cdot\mathrm{d}\mathbf{x} \;&=\; \int_{\mathcal{A}} \mathbf{J}_{\mathrm{R}}\cdot\mathbf{n}\,\mathrm{d}a - \int_{\mathcal{A}} \frac{\partial\mathbf{p}}{\partial t}\cdot\mathbf{n}\,\mathrm{d}a \quad , \quad \operatorname{curl}\mathbf{m} \;=\; \mathbf{J}_{\mathrm{R}} - \frac{\partial\mathbf{p}}{\partial t} \quad , \\ \oint_{\mathcal{C}} \boldsymbol{\mathcal{M}}\cdot\mathrm{d}\mathbf{x} \;&=\; \int_{\mathcal{A}} \mathbf{j}_{\mathrm{R}}\cdot\mathbf{n}\,\mathrm{d}a - \frac{\mathrm{d}}{\mathrm{d}t}\int_{\mathcal{A}} \mathbf{p}\cdot\mathbf{n}\,\mathrm{d}a \quad , \quad \operatorname{curl}\boldsymbol{\mathcal{M}} \;=\; \mathbf{j}_{\mathrm{R}} - \overset{\star}{\mathbf{p}} \quad , \end{aligned} \tag{3.99}$$

where $(3.99)_1$ is the integral form of the Eulerian statement in $(3.27)_2$.

The integral and local forms of FARADAY's law of induction (3.9) and $(3.11)_2$, respectively, are rewritten as

$$\begin{aligned} \int_{\mathcal{A}} \frac{\partial \mathbf{b}}{\partial t} \cdot \mathbf{n}\, \mathrm{d}a + \oint_{\mathcal{C}} \mathbf{e} \cdot \mathrm{d}\mathbf{x} \;=\; 0 \quad &, \quad \frac{\partial \mathbf{b}}{\partial t} + \operatorname{curl} \mathbf{e} \;=\; \mathbf{0} \quad , \\ \frac{\mathrm{d}}{\mathrm{d}t} \int_{\mathcal{A}} \mathbf{b} \cdot \mathbf{n}\, \mathrm{d}a + \oint_{\mathcal{C}} \boldsymbol{\mathcal{E}} \cdot \mathrm{d}\mathbf{x} \;=\; 0 \quad &, \quad \overset{\star}{\mathbf{b}} + \operatorname{curl} \boldsymbol{\mathcal{E}} \;=\; \mathbf{0} \quad , \end{aligned} \tag{3.100}$$

where the flux derivative (2.105) was once more employed to localize the material time derivative in $(3.100)_3$.

Lastly, the integral and local statements for the EM potentials in Equations $(3.12)_1$ and $(3.13)_1$, respectively, are reformulated in objective terms as

$$\begin{aligned} \int_{\mathcal{S}} \mathbf{e} \cdot \mathrm{d}\mathbf{x} \;=\; -\int_{\mathcal{S}} \frac{\partial \mathbf{a}}{\partial t} \cdot \mathrm{d}\mathbf{x} - \big[\phi\big]_{\mathbf{s}_1}^{\mathbf{s}_2} \quad &, \quad \mathbf{e} \;=\; -\frac{\partial \mathbf{a}}{\partial t} - \operatorname{grad} \phi \quad , \\ \int_{\mathcal{S}} \boldsymbol{\mathcal{E}} \cdot \mathrm{d}\mathbf{x} \;=\; -\frac{\mathrm{d}}{\mathrm{d}t} \int_{\mathcal{S}} \mathbf{a} \cdot \mathrm{d}\mathbf{x} - \big[\varphi\big]_{\mathbf{s}_1}^{\mathbf{s}_2} \quad &, \quad \boldsymbol{\mathcal{E}} \;=\; -\mathring{\mathbf{a}} - \operatorname{grad} \varphi \quad , \end{aligned} \tag{3.101}$$

where the path derivative (2.107) was employed to localize the material time derivative and obtain the objective form $(3.101)_4$. Here, the reader is cautioned not to confuse the electric potential ϕ and its objective counterpart φ, see (3.81).

3.5.2 Faraday's Law of Induction Revisited

Induction was originally discovered by HENRY and FARADAY in experiments with electric circuits and magnets, before MAXWELL included the differential statement of $(3.100)_2$ in his equations. Thus the preceding discussion on the interplay between time derivatives and objectivity warrants a closer look at the integral forms $(3.100)_{1,3}$ of FARADAY's law. This section also highlights the usefulness of the basic concepts of continuum mechanics for the study of electromagnetism.

EMF and Lorentz Force

Let the closed path $\mathcal{C}$ represent a circuit comprised of a thin wire immersed in a magnetic field $\mathbf{b}$, and let $\mathcal{A}$ denote the area enclosed by $\mathcal{C}$. The so-called *electromotive force*[30] (or *EMF* for short) $\mathcal{E}$ is defined as the circulation of the electromotive intensity $\boldsymbol{\mathcal{E}}$ around $\mathcal{C}$,

$$\mathcal{E} \;=\; \oint_{\mathcal{C}} \boldsymbol{\mathcal{E}} \cdot \mathrm{d}\mathbf{x} \quad . \tag{3.102}$$

Despite its name, the EMF does not represent an actual force, but carries the units of energy per charge. A physical interpretation for $\mathcal{E}$ is developed in the following.

[30] The EMF $\mathcal{E}$ and the electromotive intensity $\boldsymbol{\mathcal{E}}$ are distinguishable by their font weight - the former being a scalar, and the latter a vectorial quantity.

The LORENTZ *force*[31] $\mathbf{F}_{\mathrm{Li}}$ quantifies the force due to interactions with the EM fields experienced by a free point charge Q_{i} moving at a particle velocity $\mathbf{v}_{\mathrm{i}}$. It is given by

$$\mathbf{F}_{\mathrm{Li}} \;=\; Q_{\mathrm{i}}\big(\mathbf{e} + \mathbf{v}_{\mathrm{i}} \times \mathbf{b}\big) \quad , \tag{3.103}$$

where the EM fields $\{\mathbf{e}, \mathbf{b}\}$ are measured in the same inertial frame relative to which Q_{i} is found to move at velocity $\mathbf{v}_{\mathrm{i}}$. Note that $\mathbf{F}_{\mathrm{Li}}$ comprises an *electric* contribution parallel to $\mathbf{e}$ and a *magnetic* part perpendicular to $\mathbf{b}$ and $\mathbf{v}_{\mathrm{i}}$.

Recall from Section 3.1.2 that the circulation of the electric field $\mathbf{e}$, featured in Equation $(3.100)_1$, may be interpreted as the work (per unit charge) done by the EM fields on a test charge in one revolution around the *fixed* path $\mathcal{C}$. To see this, consider a hypothetical test charge Q_{i} which is allowed to move freely along the circuit $\mathcal{C}$. The test charge is assumed to be infinitesimally small so as not to alter the EM fields. It is readily seen that the work (per unit charge) done by the LORENTZ force in one cycle is

$$\frac{1}{Q_{\mathrm{i}}} \oint_{\mathcal{C}} \mathbf{F}_{\mathrm{Li}} \cdot \mathrm{d}\mathbf{x} \;=\; \oint_{\mathcal{C}} \mathbf{e} \cdot \mathrm{d}\mathbf{x} \quad . \tag{3.104}$$

Note that the magnetic contribution to $\mathbf{F}_{\mathrm{Li}}$ does not perform any work, since the particle velocity $\mathbf{v}_{\mathrm{i}}$ around $\mathcal{C}$ is tangential to $\mathrm{d}\mathbf{x}$ and therefore $\mathbf{v}_{\mathrm{i}} \times \mathbf{b}$ is perpendicular to $\mathrm{d}\mathbf{x}$.

On the other hand, the definitions for $\boldsymbol{\mathcal{E}}$ in (3.68) and $\mathcal{E}$ in (3.102) furnish

$$\mathcal{E} \;=\; \oint_{\mathcal{C}} \mathbf{e} \cdot \mathrm{d}\mathbf{x} + \oint_{\mathcal{C}} \big(\mathbf{v}_{\perp} \times \mathbf{b}\big) \cdot \mathrm{d}\mathbf{x} \quad , \tag{3.105}$$

where $\mathbf{v}_{\perp} = \mathbf{v} - \mathbf{v}_{\parallel}$ denotes the component of the material velocity $\mathbf{v}$ perpendicular to $\mathrm{d}\mathbf{x}$. The EMF thus accounts for two kinds of work on Q_{i}: the work due to a curl in the electric field, see (3.104), plus the work done by the magnetic field due to changes in the shape of the circuit, $\mathbf{v}_{\perp} \times \mathbf{b}$.[32] The EMF may be regarded as an electric potential, or a 'driving force' for charges to travel around the circuit. It is once again stressed that the convective motion of $\mathcal{C}$ must be accounted for, since it is considered to be material.

Experimental Setups and the Flux Rule

As already mentioned in the introduction to Chapter 3, monographs on electromagnetism often conflate the partial and material time derivatives without fully exploiting

[31] In Section 4.1.1, the LORENTZ force will be generalized into a distributed body force experienced by the charge-current densities $\{q, \mathbf{J}\}$. This will play an important role for the formulation of the balances of linear and angular momenta.

[32] For any time t, this hypothetical work is measured instantaneously all around the circuit. The picture of a single point charge traveling around $\mathcal{C}$ is thus somewhat inadequate.

the tools developed in continuum mechanics. This includes, for example, FEYNMAN [26, Chapter 17] and GRIFFITHS [38, Chapter 7.2], upon which the upcoming discussion is based.

Experiments on induction identify two physical mechanisms by which an EMF is induced around $\mathcal{C}$:

1. The circuit moves, while the magnetic field remains steady. This includes
   (a) a rigid translation of $\mathcal{C}$ (in which case $\mathbf{b}$ must be non-uniform), or
   (b) a change in the size $\mathcal{A}$ of the circuit.
2. The magnetic field is varied, while the circuit remains stationary. This is effected by
   (a) a permanent magnet being moved relative to the circuit,[33] or by
   (b) a stationary electromagnet whose strength is modulated.

Irrespective of physical origin, the experiments show that the EMF is always equal to the negative rate of change of magnetic flux through $\mathcal{A}$,

$$\mathcal{E} \;=\; -\frac{\mathrm{d}\Phi}{\mathrm{d}t} \quad \text{where} \quad \Phi \;=\; \int_{\mathcal{A}} \mathbf{b}\cdot\mathbf{n}\,\mathrm{d}a \quad . \tag{3.106}$$

This so-called *flux rule* is of course none other than the integral statement of the LAGRANGIAN viewpoint in $(3.100)_3$. This is not surprising, given that the experimental setup adopts an inherently LAGRANGIAN viewpoint since the measurements of flux and EMF are performed relative to the wire.

The motional EMF generated in experiments of Category (1) is represented by the term $\mathbf{v}_\perp\times\mathbf{b}$ in (3.105), and it is readily verified that it matches the change in flux due to the corresponding change in $\mathcal{A}$. Indeed, when viewed through the lens of continuum mechanics, the rate of change of magnetic flux is expressed as

$$\frac{\mathrm{d}\Phi}{\mathrm{d}t} \;=\; \int_{\mathcal{A}} \frac{\partial\mathbf{b}}{\partial t}\cdot\mathbf{n}\,\mathrm{d}a \;-\; \oint_{\mathcal{C}} \left(\mathbf{v}_\perp\times\mathbf{b}\right)\cdot\mathrm{d}\mathbf{x} \quad , \tag{3.107}$$

where the STOKES' theorem (2.53), flux derivative $(2.106)_3$, and GAUSS' law for magnetism $(3.11)_1$ were used. To explain the EMF in experiments of type (2), however, an electric field is needed. This, of course, led FARADAY to conclude that the divergence-free part of $\mathbf{e}$ is *induced* by the change in $\mathbf{b}$ according to $(3.100)_1$.[34] The same result is obtained from a comparison of (3.105 - 107).

[33] Note that Experiments 1.(a) and 2.(a) are mere GALILEAN transformations of one another, see (2.154), viewed either from the frame of the magnet or the frame of the circuit.

[34] In contrast, the irrotational part of $\mathbf{e}$ is due to *static charges*, see GAUSS' flux theorem later in (3.147).

From a continuum mechanics perspective the LAGRANGIAN form of FARADAY's law $(3.100)_3$, and thus the flux rule in (3.106), may be viewed as a balance equations for the magnetic flux Φ. This is in contrast to FEYNMAN [26], who states:

> "*Our examples involve situations to which the 'flux rule' cannot be applied - either because there is no wire at all or because the path taken by induced currents moves about within an extended volume of a conductor.* [...] *The part of the EMF that comes from the E-field does not depend on the existence of a physical wire (as does the* $\mathbf{v} \times \mathbf{b}$ *part).*"

But the continuum interpretation of the flux rule, of course, does *not* require a physical wire nor the existence of a reference configuration. The only requisite is knowledge of the velocity field of the underlying medium. In vacuum (*i.e.*, where $\mathbf{v}$ is unavailable) the EULERIAN viewpoint suffices and $\mathcal{A}$ may be assumed to be fixed.

3.5.3 Summary

The LAGRANGIAN viewpoint on time derivatives in Equations $(3.98)_4$ and $(3.100)_4$ furnishes an alternative set of MAXWELL's equations,

$$\begin{aligned} \operatorname{div} \mathbf{d} &= q &&, \\ \operatorname{curl} \boldsymbol{\mathcal{H}} &= \mathbf{j} + \overset{\star}{\mathbf{d}} &&, \\ \operatorname{div} \mathbf{b} &= 0 &&, \\ \operatorname{curl} \boldsymbol{\mathcal{E}} &= -\overset{\star}{\mathbf{b}} &&, \end{aligned} \tag{3.108}$$

which is entirely equivalent to the original version in $(3.15)_{1-4}$, yet formulated solely using objective terms.[35] Note that $(3.108)_{1,3}$ remain unaltered due to their lack of time derivatives.

In the presence of polarization or magnetization, GAUSS' law and AMPÈRE's circuital law are further decomposed into

$$\begin{aligned} \operatorname{div} \mathbf{d}_{\mathrm{F}} &= q_{\mathrm{F}} &&, \quad q_{\mathrm{R}} = -\operatorname{div} \mathbf{p} &&, \\ \operatorname{curl} \boldsymbol{\mathcal{H}}_{\mathrm{F}} &= \mathbf{j}_{\mathrm{F}} + \overset{\star}{\mathbf{d}}_{\mathrm{F}} &&, \quad \mathbf{j}_{\mathrm{R}} = \operatorname{curl} \boldsymbol{\mathcal{M}} + \overset{\star}{\mathbf{p}} &&, \end{aligned} \tag{3.109}$$

for the free and bound parts of $\{q, \mathbf{J}\}$ and $\{\mathbf{d}, \mathbf{h}\}$. As before, Equations $(3.33)_1$ and $(3.34)_1$ remain unchanged, whereas $(3.33)_2$ and $(3.34)_2$ are replaced by $(3.98)_4$ and $(3.99)_4$ using the objective measures.

[35] For example, recall from (2.183) and the discussion in Section 2.4.6 that the flux derivative of an objective vector is also objective. Note that, although Equations $(3.108)_{1-4}$ are sometimes referred to as the 'objective form' of MAXWELL's equations, it should be understood that the equations as a whole are always objective (by postulate).

It is of course readily verified that the EULERIAN statements in $(3.97)_{1,2}$-$(3.101)_{1,2}$ are equivalent to their LAGRANGIAN counterparts in $(3.97)_{3,4}$-$(3.101)_{3,4}$. For example, the flux derivative (2.106) and GAUSS' law for magnetism $(3.11)_1$ may be used to show that $(3.100)_{2,4}$ are interchangeable.

3.6 Maxwell's Equations in Referential Description

In Section 2.3.7, the integrals of the thermomechanical balance equations are rewritten with respect to the referential configuration. This furnishes referential versions for the global and the local forms of each balance law. In the process of converting the boundary integrals (*i.e.*, the flux terms) into referential form, PIOLA transforms (2.90) emerge for the first PIOLA-KIRCHHOFF stress tensor (2.140) and the referential heat flux (2.145).

If a reference configuration is available, as is often the case in electro-magneto-thermo-mechanics, it is possible to apply the same technique to express MAXWELL's equations in referential form, whereby the EM fields are pulled back to the reference configuration. The referential equations are often used to examine the constitutive relations and material symmetries of EMTM continua. Indeed, referential versions of MAXWELL's equations can be found in ERICKSEN [23, Appendix], HUTTER [55, Section 2] or LAX and NELSON [70].

The referential form of MAXWELL's equations is derived as follows: First, the objective version of MAXWELL's equations is written in integral form, see Section 3.5.1, where all time derivatives are already material. Next, the integration variables are transformed to the referential frame using (2.65) for line elements, (2.79) for volume elements, and NANSON's formula (2.80) for area elements. Lastly, the referential EM fields are defined and the corresponding referential equations are converted to local form.

3.6.1 Principle of Charge Conservation

The conservation of charge in $(3.97)_3$ is expressed referentially as

$$\frac{\mathrm{d}}{\mathrm{d}t}\int_{\mathcal{P}_0} q_0 \,\mathrm{d}V + \int_{\partial\mathcal{P}_0} \mathbf{j}_0 \cdot \mathbf{N}\,\mathrm{d}A \;=\; 0 \quad . \tag{3.110}$$

The referential charge density and the referential conduction current density

$$q_0 \;=\; Jq \quad \text{and} \quad \mathbf{j}_0 \;=\; J\mathbf{F}^{-1}\mathbf{j} \;=\; J\mathbf{F}^{-1}\big(\mathbf{J} - q\mathbf{v}\big) \tag{3.111}$$

are determined from the requirements, that $q_0\mathrm{d}V = q\mathrm{d}v$ and $\mathbf{j}_0\cdot\mathbf{N}\mathrm{d}A = \mathbf{j}\cdot\mathbf{n}\mathrm{d}a$. The total current in $(3.4)_2$ was used for the last step in $(3.111)_2$. Equation (3.110) is

localized to

$$\dot{q}_0 + \mathrm{Div}\,\mathbf{j}_0 \;=\; 0 \quad . \tag{3.112}$$

It is readily verified with the aid of $(2.46)_3$, (2.88), and (2.99) that this result is in agreement with the local equation in $(3.97)_4$ (multiplied by J).

Gauss' law $(3.6)_1$, which does not contain any time derivatives, is converted to the material frame according to

$$\int_{\mathcal{P}_0} q_0 \,\mathrm{d}V \;=\; \int_{\partial\mathcal{P}_0} \mathbf{d}_0 \cdot \mathbf{N}\,\mathrm{d}A \quad , \tag{3.113}$$

where q_0 was already defined in $(3.111)_1$. The referential charge potential is given by the Piola transform

$$\mathbf{d}_0 \;=\; J\mathbf{F}^{-1}\mathbf{d} \quad , \tag{3.114}$$

so as to satisfy the condition $\mathbf{d}_0 \cdot \mathbf{N}\,\mathrm{d}A = \mathbf{d}\cdot\mathbf{n}\,\mathrm{d}a$. The local form of (3.113) is

$$q_0 \;=\; \mathrm{Div}\,\mathbf{d}_0 \quad . \tag{3.115}$$

It follows immediately from the property in $(2.90)_1$ that the preceding statement is consistent with the spatial form of Gauss' law $(3.108)_1$ (multiplied by J).

Next, Ampère's circuital law $(3.98)_3$ is written in terms of referential integration variables as

$$\oint_{\mathcal{C}_0} \boldsymbol{\mathcal{H}}_0 \cdot \mathrm{d}\mathbf{X} \;=\; \int_{\mathcal{A}_0} \mathbf{j}_0 \cdot \mathbf{N}\,\mathrm{d}A + \frac{\mathrm{d}}{\mathrm{d}t}\int_{\mathcal{A}_0} \mathbf{d}_0 \cdot \mathbf{N}\,\mathrm{d}A \quad , \tag{3.116}$$

where $(3.111)_2$ and (3.114) were used for $\mathbf{j}_0$ and $\mathbf{d}_0$, respectively. A referential counterpart of the current potential is obtained from the requirement that $\boldsymbol{\mathcal{H}}_0 \cdot \mathrm{d}\mathbf{X} = \boldsymbol{\mathcal{H}} \cdot \mathrm{d}\mathbf{x}$, hence

$$\boldsymbol{\mathcal{H}}_0 \;=\; \mathbf{F}^{\mathrm{T}}\boldsymbol{\mathcal{H}} \;=\; \mathbf{F}^{\mathrm{T}}\big(\mathbf{h} - \mathbf{v}\times\mathbf{d}\big) \quad , \tag{3.117}$$

where the definition of the magnetomotive intensity in (3.60) was employed. The local form of (3.116) is given by

$$\mathrm{Curl}\,\boldsymbol{\mathcal{H}}_0 \;=\; \mathbf{j}_0 + \dot{\mathbf{d}}_0 \quad . \tag{3.118}$$

It is seen from (2.94), $(2.97)_2$, (2.99), (2.100), (2.102), and $(2.106)_1$ that Equation (3.118) is consistent with $(3.108)_2$ (premultiplied by $J\mathbf{F}^{-1}$).

3.6.2 Faraday's Law of Induction

Similarly to (3.113), Gauss' law for magnetism (3.10) is restated in the referential configuration as

$$\int_{\partial\mathcal{P}_0} \mathbf{b}_0 \cdot \mathbf{N}\,\mathrm{d}A \;=\; 0 \quad , \tag{3.119}$$

where the magnetic field is given by the PIOLA transform

$$\mathbf{b}_0 \;=\; J\mathbf{F}^{-1}\mathbf{b} \quad . \tag{3.120}$$

Localization of (3.119) furnishes

$$\mathrm{Div}\,\mathbf{b}_0 \;=\; 0 \quad . \tag{3.121}$$

Again, in view of the property for PIOLA transforms in $(2.90)_1$, it is readily verified that this represents the referential version of $(3.108)_3$ (times J).

Next, FARADAY's law of induction in $(3.100)_3$ is transformed to the material configuration according to

$$\frac{\mathrm{d}}{\mathrm{d}t}\int_{\mathcal{A}_0} \mathbf{b}_0\cdot\mathbf{N}\,\mathrm{d}A + \oint_{\mathcal{C}_0} \boldsymbol{\mathcal{E}}_0\cdot\mathrm{d}\mathbf{X} \;=\; 0 \quad . \tag{3.122}$$

Similar to (3.117), the referential version of the electric field is determined from the condition $\boldsymbol{\mathcal{E}}_0\cdot\mathrm{d}\mathbf{X} = \boldsymbol{\mathcal{E}}\cdot\mathrm{d}\mathbf{x}$, or

$$\boldsymbol{\mathcal{E}}_0 \;=\; \mathbf{F}^{\mathrm{T}}\boldsymbol{\mathcal{E}} \;=\; \mathbf{F}^{\mathrm{T}}\big(\mathbf{e}+\mathbf{v}\times\mathbf{b}\big) \quad , \tag{3.123}$$

where (3.68) was used. Localization of Equation (3.122) furnishes

$$\dot{\mathbf{b}}_0 + \mathrm{Curl}\,\boldsymbol{\mathcal{E}}_0 \;=\; \mathbf{0} \quad , \tag{3.124}$$

which is, of course, in agreement with ($J\mathbf{F}^{-1}$ times) Equation $(3.108)_4$.

Lastly, Equations $(3.101)_3$ and $(3.12)_2$ for the electromagnetic potentials[36] are expressed in material coordinates as

$$\begin{aligned} \int_{\mathcal{S}_0} \boldsymbol{\mathcal{E}}_0\cdot\mathrm{d}\mathbf{X} \;&=\; -\frac{\mathrm{d}}{\mathrm{d}t}\int_{\mathcal{S}_0}\mathbf{a}_0\cdot\mathrm{d}\mathbf{X} - \big[\varphi_0\big]_{\mathbf{S}_1}^{\mathbf{S}_2} \quad , \\ \int_{\mathcal{A}_0} \mathbf{b}_0\cdot\mathbf{N}\,\mathrm{d}A \;&=\; \oint_{\mathcal{C}_0}\mathbf{a}_0\cdot\mathrm{d}\mathbf{X} \qquad\qquad\qquad , \end{aligned} \tag{3.125}$$

where $\mathbf{b}_0$ and $\boldsymbol{\mathcal{E}}_0$ are given by (3.120) and (3.123), respectively. Since $\mathbf{a}_0\cdot\mathrm{d}\mathbf{X} = \mathbf{a}\cdot\mathrm{d}\mathbf{x}$, it is concluded that the referential counterparts for the EM potentials are given by

$$\begin{aligned} \varphi_0 \;&=\; \varphi \;=\; \phi - \mathbf{v}\cdot\mathbf{a} \quad , \\ \mathbf{a}_0 \;&=\; \mathbf{F}^{\mathrm{T}}\mathbf{a} \qquad\qquad , \end{aligned} \tag{3.126}$$

where the relation in (3.81) was used. Note that, although no transformation is needed to obtain φ_0 from φ, the referential quantity is considered to be a LAGRANGIAN function and it is evaluated in $(3.125)_1$ in terms of the referential location of the

[36] The reader is reminded that $\mathbf{a}$ in this context represents the magnetic potential, not the acceleration.

start- and endpoints $\mathbf{S}_1$ and $\mathbf{S}_2$ of the path $\mathcal{S}_0$. In contrast, φ is an EULERIAN function evaluated at $\mathbf{s}_1$ and $\mathbf{s}_2$ in Equation $(3.101)_3$. The integral forms in (3.125) furnish the local statements

$$\boldsymbol{\mathcal{E}}_0 \;=\; -\dot{\mathbf{a}}_0 - \operatorname{Grad}\varphi_0 \quad \text{and} \quad \mathbf{b}_0 \;=\; \operatorname{Curl}\mathbf{a}_0 \quad , \tag{3.127}$$

which correspond to ($\mathbf{F}^{\mathrm{T}}$ times) Equation $(3.101)_4$ and ($J\mathbf{F}^{-1}$ times) $(3.13)_2$, respectively, as is verified using (2.82), (2.94), (2.100), $(2.108)_1$, (3.120), and $(3.126)_{1,2}$.

3.6.3 Polarization and Magnetization

Recall that the first pair of MAXWELL's equations may be decomposed into the free and bound parts for polarizable or magnetizable materials, see Equations $(3.33)_{1,2}$ and $(3.34)_{1,2}$, or in objective terms in Equations $(3.109)_{1-4}$. Their conversion to referential form is carried out using the same procedure as in Section 3.6.1 for the total fields. The integral form of GAUSS' law and AMPÈRE's circuital law are written in referential coordinates as

$$\begin{aligned} \int_{\mathcal{P}_0} q_{\mathrm{F}0}\,\mathrm{d}V \;&=\; \int_{\partial\mathcal{P}_0} \mathbf{d}_{\mathrm{F}0}\cdot\mathbf{N}\,\mathrm{d}A \quad , \\ \oint_{\mathcal{C}_0} \boldsymbol{\mathcal{H}}_{\mathrm{F}0}\cdot\mathrm{d}\mathbf{X} \;&=\; \int_{\mathcal{A}_0} \mathbf{j}_{\mathrm{F}0}\cdot\mathbf{N}\,\mathrm{d}A + \frac{\mathrm{d}}{\mathrm{d}t}\int_{\mathcal{A}_0} \mathbf{d}_{\mathrm{F}0}\cdot\mathbf{N}\,\mathrm{d}A \quad , \end{aligned} \tag{3.128}$$

for the free parts, and

$$\begin{aligned} \int_{\mathcal{P}_0} q_{\mathrm{R}0}\,\mathrm{d}V \;&=\; -\int_{\partial\mathcal{P}_0} \mathbf{p}_0\cdot\mathbf{N}\,\mathrm{d}A \quad , \\ \oint_{\mathcal{C}_0} \boldsymbol{\mathcal{M}}_0\cdot\mathrm{d}\mathbf{X} \;&=\; \int_{\mathcal{A}_0} \mathbf{j}_{\mathrm{R}0}\cdot\mathbf{N}\,\mathrm{d}A - \frac{\mathrm{d}}{\mathrm{d}t}\int_{\mathcal{A}_0} \mathbf{p}_0\cdot\mathbf{N}\,\mathrm{d}A \quad , \end{aligned} \tag{3.129}$$

for bound parts. Here, the referential (free and bound) charge-currents transform the same way as the total quantities $(3.111)_{1,2}$,

$$\begin{aligned} q_{\mathrm{F}0} \;&=\; J q_{\mathrm{F}} \quad , \quad \mathbf{j}_{\mathrm{F}0} \;=\; J\mathbf{F}^{-1}\mathbf{j}_{\mathrm{F}} \;= J\mathbf{F}^{-1}\big(\mathbf{J}_{\mathrm{F}} - q_{\mathrm{F}}\mathbf{v}\big) \quad , \\ q_{\mathrm{R}0} \;&=\; J q_{\mathrm{R}} \quad , \quad \mathbf{j}_{\mathrm{R}0} \;=\; J\mathbf{F}^{-1}\mathbf{j}_{\mathrm{R}} \;= J\mathbf{F}^{-1}\big(\mathbf{J}_{\mathrm{R}} - q_{\mathrm{R}}\mathbf{v}\big) \quad . \end{aligned} \tag{3.130}$$

Meanwhile, the referential (free and bound) charge-current potentials are defined as

$$\begin{aligned} \mathbf{d}_{\mathrm{F}0} \;&=\; J\mathbf{F}^{-1}\mathbf{d}_{\mathrm{F}} \quad , \quad \boldsymbol{\mathcal{H}}_{\mathrm{F}0} \;=\; \mathbf{F}^{\mathrm{T}}\boldsymbol{\mathcal{H}}_{\mathrm{F}} \;= \mathbf{F}^{\mathrm{T}}\big(\mathbf{h}_{\mathrm{F}} - \mathbf{v}\times\mathbf{d}_{\mathrm{F}}\big) \quad , \\ \mathbf{p}_0 \;&=\; J\mathbf{F}^{-1}\mathbf{p} \quad , \quad \boldsymbol{\mathcal{M}}_0 \;=\; \mathbf{F}^{\mathrm{T}}\boldsymbol{\mathcal{M}} \;= \mathbf{F}^{\mathrm{T}}\big(\mathbf{m} + \mathbf{v}\times\mathbf{p}\big) \quad . \end{aligned} \tag{3.131}$$

The integral statements in $(3.128)_{1,2}$ and $(3.129)_{1,2}$ are localized to furnish

$$\begin{aligned} \operatorname{Div}\mathbf{d}_{\mathrm{F}0} \;&=\; q_{\mathrm{F}0} \quad , \quad q_{\mathrm{R}0} \;=\; -\operatorname{Div}\mathbf{p}_0 \quad , \\ \operatorname{Curl}\boldsymbol{\mathcal{H}}_{\mathrm{F}0} \;&=\; \mathbf{j}_{\mathrm{F}0} + \dot{\mathbf{d}}_{\mathrm{F}0} \quad , \quad \mathbf{j}_{\mathrm{R}0} \;=\; \operatorname{Curl}\boldsymbol{\mathcal{M}}_0 + \dot{\mathbf{p}}_0 \quad , \end{aligned} \tag{3.132}$$

which constitute the referential counterparts of Equations $(3.109)_{1-4}$.

3.6.4 Summary

If a reference configuration is available, MAXWELL's equations are expressed in material form according to

$$\begin{aligned} \operatorname{Div}\mathbf{d}_0 &= q_0 \quad , \\ \operatorname{Curl}\boldsymbol{\mathcal{H}}_0 &= \mathbf{j}_0 + \dot{\mathbf{d}}_0 \quad , \\ \operatorname{Div}\mathbf{b}_0 &= 0 \quad , \\ \operatorname{Curl}\boldsymbol{\mathcal{E}}_0 &= -\dot{\mathbf{b}}_0 \quad . \end{aligned} \tag{3.133}$$

This set of equations is consistent with the original EULERIAN version $(3.15)_{1-4}$ as well as the objective form in $(3.108)_{1-4}$. The EM fields are pulled back to the reference configuration via the transforms

$$\begin{aligned} q_0 &= Jq \quad , \quad \mathbf{j}_0 = J\mathbf{F}^{-1}\mathbf{j} = J\mathbf{F}^{-1}\big(\mathbf{J} - q\mathbf{v}\big) \quad , \\ \mathbf{d}_0 &= J\mathbf{F}^{-1}\mathbf{d} \quad , \quad \boldsymbol{\mathcal{H}}_0 = \mathbf{F}^{\mathrm{T}}\boldsymbol{\mathcal{H}} = \mathbf{F}^{\mathrm{T}}\big(\mathbf{h} - \mathbf{v}\times\mathbf{d}\big) \quad , \\ \mathbf{b}_0 &= J\mathbf{F}^{-1}\mathbf{b} \quad , \quad \boldsymbol{\mathcal{E}}_0 = \mathbf{F}^{\mathrm{T}}\boldsymbol{\mathcal{E}} = \mathbf{F}^{\mathrm{T}}\big(\mathbf{e} + \mathbf{v}\times\mathbf{b}\big) \quad . \end{aligned} \tag{3.134}$$

Note that the referential counterparts for the *non-objective* fields $\mathbf{J}$, $\mathbf{h}$, and $\mathbf{e}$ are considered to be $\mathbf{j}_0$, $\boldsymbol{\mathcal{H}}_0$, and $\boldsymbol{\mathcal{E}}_0$, respectively (*i.e.*, they are identical to the pull-back of $\mathbf{j}$, $\boldsymbol{\mathcal{H}}$, and $\boldsymbol{\mathcal{E}}$).

For polarizable and magnetizable materials, the first pair of MAXWELL's equations is decomposed into $(3.132)_{1-4}$ for the free and bound parts. The referential quantities involved are defined according to the transformations in $(3.130)_{1,2}$ and $(3.131)_{1,2}$.

3.7 Magnetostatics and Electrostatics

The speed with which changes in the EM fields propagate through vacuum or matter is on the order of the speed of light. Thermomechanical continua respond much slower to external stimuli, on the order of the speed of sound.[37] Coupled EMTM continua are subject to the same limitations and therefore, for size and time scales of engineering significance, it may often be assumed that changes in the EM fields are (*quasi-*)*static*. This means that fluctuations in the externally applied EM fields are orders of magnitude slower than the time it takes for light to propagate across the characteristic length of the problem domain.[38] It may be equivalently argued that the wavelengths of the electromagnetic problem far exceed the dimensions of the body.

[37] Thermal equilibrium is arguably reached even slower than mechanical equilibrium. Although thermal vibrations do propagate at the speed of sound, the randomness of their motion results in a comparatively slow thermal diffusion process.

[38] A similar argument is made in classical thermomechanics, whereby a dynamic system may be considered quasi-static if the external stimuli are applied slow enough for the internal forces to achieve equilibrium at all times, so that the contribution of the acceleration vector to the momentum balance may be neglected, see (2.115).

Under such conditions, the governing EM equations simplify significantly by uncoupling[39] into an electric and a magnetic part, each of which is governed by a scalar or vectorial POISSON's equation. These simplified equations are introduced in this section, first for the total EM fields, followed by a formulation accounting for the free and bound parts in polarizable and magnetizable materials.

3.7.1 Total EM Fields

The EM fields are considered (quasi-)static, if they do not change over time (or if they do so very slowly relative to the speed of light). As a consequence, there is ample time for the EM problem to equilibrate, which implies that the contributions of time derivatives to the charge balance and to MAXWELL's Equations are negligible.

In the context of EMTM, the EM fields may be seen as 'static' either from a spatial or from a referential perspective. In the spatial interpretation, the charge-currents $\{q, \mathbf{J}\}$, their potentials $\{\mathbf{d}, \mathbf{h}\}$, and the EM fields $\{\mathbf{e}, \mathbf{b}\}$ are assumed to be *steady*, which means that they depend only on the spatial location $\mathbf{x}$ but not on time t. This implies that the *partial* time derivatives in $(3.15)_{2,4}$ are negligible. On the other hand, the referential view requires that $\{q, \mathbf{j}\}$, $\{\mathbf{d}, \boldsymbol{\mathcal{H}}\}$, and $\{\boldsymbol{\mathcal{E}}, \mathbf{b}\}$ depend on $\mathbf{X}$ but not on t, and thus the *flux* derivatives in $(3.108)_{2,4}$ are set to zero. Both interpretations cannot be true simultaneously unless the TM problem is also (quasi-)static, $\mathbf{v} \doteq \mathbf{0}$, which eliminates any convective terms.

Time-Independent Maxwell's Equations

In adopting the spatial viewpoint, MAXWELL's equations $(3.15)_{1-4}$ simplify to

$$\begin{aligned} \operatorname{div}\mathbf{d} &= q \quad , \\ \operatorname{curl}\mathbf{h} &= \mathbf{J} \quad , \\ \operatorname{div}\mathbf{b} &= 0 \quad , \\ \operatorname{curl}\mathbf{e} &= \mathbf{0} \quad . \end{aligned} \tag{3.135}$$

In conjunction with the aether relations in (3.35), they furnish for the electric field

$$\operatorname{div}\mathbf{e} \overset{\text{Aet.}}{=} q/\varepsilon_0 \quad , \quad \operatorname{curl}\mathbf{e} = \mathbf{0} \quad , \tag{3.136}$$

and for the magnetic flux density

$$\operatorname{div}\mathbf{b} = 0 \quad , \quad \operatorname{curl}\mathbf{b} \overset{\text{Aet.}}{=} \mu_0\mathbf{J} \quad . \tag{3.137}$$

[39] In order for the equations to be fully decoupled, the constitutive function must also separate the electric (*i.e.*, polarization) and magnetic (*i.e.*, magnetization) responses. If so, the two parts independently describe the electrostatic and the magnetostatic conditions, respectively.

It is concluded that the electric field $\mathbf{e}$ is irrotational whereas the magnetic field $\mathbf{b}$ is divergence-free (as always). The total current $\mathbf{J}$ is divergence-free following $(3.137)_2$, which is in agreement with a steady distribution of charge q according to the charge balance (3.5).

Static Solution using Potentials

Let $\mathbf{e}$ and $\mathbf{b}$ be given by

$$\mathbf{e}(\mathbf{x}) \;=\; -\operatorname{grad}\phi(\mathbf{x},t) \quad , \quad \mathbf{b}(\mathbf{x}) \;=\; \operatorname{curl}\mathbf{a}(\mathbf{x},t) \tag{3.138}$$

where the real-valued *electrostatic potential*[40] $\phi(\mathbf{x},t)$ and vector-valued *magnetostatic potential* $\mathbf{a}(\mathbf{x},t)$ can depend on time t only insofar as they produce steady electromagnetic fields. Note that Equations $(3.138)_{1,2}$ coincide with the time-independent form of the governing equations of the electromagnetic potentials in $(3.13)_{1,2}$ which were devised to replace FARADAY's law of induction. Equations $(3.136)_2$ and $(3.137)_1$ are automatically satisfied by the potentials in (3.138) due to the identities $(2.49)_{1,2}$. Meanwhile $(3.136)_1$ furnishes a scalar POISSON*'s equation* for ϕ,

$$\Delta\phi \overset{\text{Aet.}}{=} -q/\varepsilon_0 \quad , \tag{3.139}$$

with LAPLACE operator $\Delta[\cdot]=\operatorname{div}(\operatorname{grad}[\cdot])$. Equation $(3.137)_2$ leads to a coupled set of partial differential equations for $\mathbf{a}$,

$$\operatorname{curl}\big(\operatorname{curl}\mathbf{a}\big) \;=\; \operatorname{grad}(\operatorname{div}\mathbf{a}) - \Delta\mathbf{a} \overset{\text{Aet.}}{=} \mu_0\mathbf{J} \quad , \tag{3.140}$$

where the identity in $(2.49)_3$ was used. Recall that the potentials $\{\phi,\mathbf{a}\}$ do not uniquely solve MAXWELL's equations $(3.15)_{3,4}$.[41] They are subject to the gauge transformations (3.14) whose arbitrary parameter Ψ may be selected so as to simplify the above differential equations for $\mathbf{a}$. The so-called COULOMB *gauge* uniquely determines $\{\phi,\mathbf{a}\}$ by setting

$$\lim_{|\mathbf{x}|\to\infty}\phi \;=\; 0 \quad \text{and} \quad \operatorname{div}\mathbf{a} \;=\; 0 \quad . \tag{3.141}$$

The electromagnetic equations are thus reduced to a pair of POISSON's equations

$$\Delta\phi(\mathbf{x}) \overset{\text{Aet.}}{=} -q(\mathbf{x})/\varepsilon_0 \quad \text{and} \quad \Delta\mathbf{a}(\mathbf{x}) \overset{\text{Aet.}}{=} -\mu_0\mathbf{J}(\mathbf{x}) \quad , \tag{3.142}$$

where $\mathbf{a}$ is subject to the constraint in $(3.141)_2$.

---

[40] The negative sign in $(3.138)_1$, indicating that the electric field points towards decreasing electric potential, is placed by convention. This is consistent with the fact that electric fields point from positive charges to negative ones.

[41] This is unlike the charge-current potentials, whose arbitrariness (3.8) is forfeited due to the use of the aether relations in the derivation of (3.136) and (3.137).

Equation $(3.142)_2$ describes a *magnetostatic* system, which may sustain steady currents and their ensuing magnetic fields so long as the distribution of charge is not altered. In an *electrostatic* system, however, the charges q are assumed to be *stationary*[42] (*i.e.*, remain fixed in place) so that the presence of any current $\mathbf{J}$ is precluded. AMPÈRE's law $(3.137)_2$ thus renders $\mathbf{b}$ irrotational (*i.e.*, $\operatorname{curl}\mathbf{b}=\mathbf{0}$). In the absence of any magnetization, the current potential

$$\mathbf{h}(\mathbf{x}) \overset{\text{Aet.}}{=} \mathbf{b}(\mathbf{x})/\mu_0 \;=\; -\operatorname{grad}\varphi(\mathbf{x}) \tag{3.143}$$

may therefore be expressed in terms of a real-valued magnetic potential $\varphi(\mathbf{x})$. Therefore in electrostatics the magnetic flux derives from a scalar LAPLACE's equation

$$\Delta\varphi(\mathbf{x}) \overset{\text{Aet.}}{=} 0 \quad , \tag{3.144}$$

according to GAUSS' law $(3.137)_1$. This greatly simplifies the solution of the EM equations by circumventing numerical challenges posed by differential equations involving the curl operator.

Alternative Derivation of Static Equations

It is mentioned that, rather than by eliminating time derivatives from MAXWELL's equations, the preceding results can also be derived[43] from two well-known experimental principles in electrostatics and magnetostatics.

The first principle is COULOMB*'s law*, which is an inverse-square law quantifying the EM interaction force between two stationary point charges. Since the electric field represents the force per unit test charge, COULOMB's law states that a collection of i point charges Q_i situated at $\mathbf{x}_i$ contribute to the electric field at location $\mathbf{x}$ an amount

$$\mathbf{e}(\mathbf{x}) \;=\; \frac{1}{4\pi\varepsilon_0}\sum_i Q_i\frac{\mathbf{x}-\mathbf{x}_i}{|\mathbf{x}-\mathbf{x}_i|^3} \quad . \tag{3.145}$$

The electrostatic Equations $(3.136)_{1,2}$ and $(3.138)_1$ are obtained from (3.145) in the limit, where a distribution of infinitesimal charges $\mathrm{d}Q_i = q\mathrm{d}v$ is integrated over all $\mathbf{x}_i$.

[42] Note the difference between steady and stationary: A steady charge distribution implies that the amount of charge enclosed in any fixed spatial region remains constant. Individual charges may still move, so long as the net exchange across the boundary of any such region is zero, or $\operatorname{div}\mathbf{J}=0$ according to (3.5). Stationary charges, on the other hand, do not move at all. This implies not only that q is steady, but also that there is no current $\mathbf{J}$.

[43] A detailed derivation is provided, for example, by DORFMANN and OGDEN [21, Chapters 2.1 and 2.2].

The derivation makes use of the identities[44]

$$\begin{aligned} \operatorname{grad}\left(\frac{1}{|\mathbf{x}-\mathbf{x}_i|}\right) &= -\frac{\mathbf{x}-\mathbf{x}_i}{|\mathbf{x}-\mathbf{x}_i|^3} \quad , \\ \operatorname{div}\left(\frac{\mathbf{x}-\mathbf{x}_i}{|\mathbf{x}-\mathbf{x}_i|^3}\right) &= 0 \qquad\qquad\quad . \end{aligned} \tag{3.146}$$

In particular, it can be shown that (3.145) furnishes Gauss' *law* (or Gauss' *flux theorem*),

$$\int_{\partial\mathcal{P}} \mathbf{e}\cdot\mathbf{n}\,\mathrm{d}a \;=\; Q(\mathcal{P})/\varepsilon_0 \quad , \tag{3.147}$$

which states that the resultant flux of the electric field $\mathbf{e}$ across any closed surface $\partial\mathcal{P}$ is proportional to the total charge $Q(\mathcal{P})$ contained therein. This is the integral form of $(3.136)_1$.

The second principle is the Biot-Savart *law*, which represents the magnetostatic equivalent of Coulomb's law. It quantifies the magnetic field produced by i finite electric currents I_i carried by thin wires along the paths $\mathcal{S}_i$ in direction $\mathrm{d}\mathbf{x}_i$,

$$\mathbf{b}(\mathbf{x}) \;=\; \frac{\mu_0}{4\pi}\sum_i I_i \int_{\mathcal{S}_i} \frac{\mathrm{d}\mathbf{x}_i\times\big(\mathbf{x}-\mathbf{x}_i\big)}{|\mathbf{x}-\mathbf{x}_i|^3} \quad . \tag{3.148}$$

Equation $(3.137)_2$ is obtained in the limit, where the wire is replaced by infinitesimal distributed currents $\mathrm{d}I_i = |\mathbf{J}|\mathrm{d}a$, and thus $\mathrm{d}I_i\mathrm{d}\mathbf{x}_i = \mathbf{J}\mathrm{d}v$, integrated over all $\mathbf{x}_i$. The magnetostatic Equations $(3.137)_{1,2}$ and $(3.138)_2$ are deduced with the aid of the identities in $(2.47)_1$ and $(3.146)_{1,2}$.

3.7.2 With Polarization and Magnetization

The preceding discussion is readily extended to polarizable and magnetizable materials. It is first noted that the prescription (3.138) for the steady $\mathbf{e}$ and $\mathbf{b}$ in terms of potentials, as well as the ensuing Poisson's equations (3.142), remain valid as long as $\{q,\mathbf{J}\}$ pertain to the *total* charge-currents. Furthermore, recall that the charge-currents may be additively decomposed into their free and bound parts, which are, in turn, described by Maxwell's equations of the form (3.33) and (3.34). Therefore, to obtain the magnetostatic equations of a polarizable or magnetizable material, it suffices to expand the right-hand side of (3.142) into its free and bound parts,

$$\Delta\phi \overset{\text{Aet.}}{=} -\big(q_{\mathrm{F}} - \operatorname{div}\mathbf{p}\big)/\varepsilon_0 \quad \text{and} \quad \Delta\mathbf{a} \overset{\text{Aet.}}{=} -\mu_0\big(\mathbf{J}_{\mathrm{F}} + \operatorname{curl}\mathbf{m}\big) \quad . \tag{3.149}$$

As before, it is required that $\mathbf{a}$ satisfy the constraint in $(3.141)_2$. The electromagnetic fields $\{\mathbf{e},\mathbf{b}\}$ are deduced from $\{\phi,\mathbf{a}\}$ through (3.138), after which the (free) charge-current potentials $\{\mathbf{d}_{\mathrm{F}},\mathbf{h}_{\mathrm{F}}\}$ are obtained with the extended aether relations (3.37).

[44] Note that Equations $(3.146)_{1,2}$ imply that $1/|\mathbf{x}-\mathbf{x}_i|$ is a fundamental solution of Laplace's equation.

Note that $\mathbf{p}$ and $\mathbf{m}$ are assumed to be steady, so that Equation $(3.34)_2$ reduces to $\mathbf{J}_\mathrm{R} = \operatorname{curl}\mathbf{m}$.

Consider the electrostatic case, where the free and bound charges are assumed to be stationary and thus the corresponding currents are negligible. Since $\operatorname{curl}\mathbf{h}_\mathrm{F} = \mathbf{0}$ due to $(3.33)_2$, the current potential may be expressed by

$$\mathbf{h}_\mathrm{F}(\mathbf{x}) \;=\; -\operatorname{grad}\varphi_\mathrm{F}(\mathbf{x}) \quad . \tag{3.150}$$

Given $\mathbf{b} \overset{\text{Aet.}}{=} \mu_0(\mathbf{h}_\mathrm{F} + \mathbf{m})$ from $(3.37)_2$, Gauss' law for magnetism $(3.15)_3$ furnishes a Poisson equation for φ_F,

$$\Delta\varphi_\mathrm{F}(\mathbf{x}) \overset{\text{Aet.}}{=} \operatorname{div}\mathbf{m}(\mathbf{x}) \quad , \tag{3.151}$$

which represents the generalized counterpart of Equation (3.144).

Chapter 4

Coupled electro-magneto-thermo-mechanical Model

This chapter examines the coupled electro-magneto-thermo-mechanical model, or EMTM for short, merging the concepts of classical thermomechanics from Chapter 2 and electromagnetism from Chapter 3. This discussion is based on the account by Ericksen [23] as well as the so-called Maxwell–Minkowski *formulation*, see Hutter *et al.* [56]. The analysis is structured similarly to Section 2.3, whose balance laws are amended to reflect the contributions of the EM fields to the linear and angular momenta as well as energy. In view of the wide dissimilitude found in literature for formulating the coupled balance equations, alternative (but in essence equivalent) representations thereof are presented in Appendix A.6. A discussion of the extended Green-Naghdi-Rivlin theorem follows, from which it is concluded that the energy and momentum equations are mutually consistent. Finally, the entropy inequality and its implications and restrictions imposed on the constitutive equations is discussed.

4.1 Principles of Linear and Angular Momentum Balance

To derive the balances of linear and angular momenta for the coupled EMTM material, the forces exerted on the material body by the electromagnetic fields need to be quantified. Although the EM fields are regarded as external to the material body, they interact with the body through its (free or bound) electric charges and currents. Forces imparted on those charges are considered to be acting on the continuum of the material body, akin to the body forces $\rho\mathbf{f}_{\mathrm{B}}$ in Equation (2.113).

4.1.1 Lorentz Force Density

Recall that the interaction between moving charges and the EM fields is characterized by the LORENTZ force. As already stated in Equation (3.103), a single point charge Q_i moving at a velocity $\mathbf{v}_\mathrm{i}$ (as measured relative to an inertial frame) is subjected to a corresponding LORENTZ force of

$$\mathbf{F}_{\mathrm{L}\mathrm{i}} \;=\; Q_\mathrm{i}\mathbf{e} + Q_\mathrm{i}\mathbf{v}_\mathrm{i} \times \mathbf{b} \quad . \tag{4.1}$$

It is important to distinguish the particle velocity $\mathbf{v}_\mathrm{i}$ from the material velocity $\mathbf{v}$. If Q_i is a free point charge within a material body, then $\mathbf{v}_\mathrm{i}$ accounts for both conduction of Q_i relative to the material, as well as convection due to motion $\mathbf{v}$.

The distribution of infinitesimal point charges Q_i is related to the charge density q in the same way point masses M_i are related to the mass density ρ of the continuum. The charge density q is thus obtained from the charge $Q(\mathcal{P})$ contained in region $\mathcal{P}$ using the same limiting process outlined in Equation $(2.109)_1$ for ρ. Furthermore, the total current density $\mathbf{J}$ is obtained when this limit is applied to the movement of infinitesimal point charges $Q_\mathrm{i}\mathbf{v}_\mathrm{i}$. Thus $\mathbf{J}$ can be thought of as a charge-weighted volume average of the velocity of infinitesimal point charges.

This hypothetical approach for Q_i and $Q_\mathrm{i}\mathbf{v}_\mathrm{i}$ in Equation (4.1) furnishes, in the limit of infinitesimal point charges, the LORENTZ *force density* $\mathbf{f}_\mathrm{L}(\mathbf{x}, t)$ (per unit volume)

$$\mathbf{f}_\mathrm{L} \;=\; q\mathbf{e} + \mathbf{J} \times \mathbf{b} \;=\; q\boldsymbol{\mathcal{E}} + \mathbf{j} \times \mathbf{b} \quad . \tag{4.2}$$

The alternative expression $(4.2)_2$ is readily obtained from the definitions of the total current $\mathbf{J}$ in $(3.4)_2$ and the electromotive intensity $\boldsymbol{\mathcal{E}}$ in (3.68).

The LORENTZ force density transforms objectively under SRBM because q, $\mathbf{j}$, $\mathbf{b}$, and $\boldsymbol{\mathcal{E}}$ are objective. Indeed, using the transformations (3.43), (3.48), (3.63), (3.69) and the identity $(2.37)_2$,

$$\mathbf{f}_\mathrm{L}^{+} \;=\; \mathbf{Q}\mathbf{f}_\mathrm{L} \quad . \tag{4.3}$$

This result may seem surprising, given that the LORENTZ force of point charge Q_i depends on its (non-objective) velocity $\mathbf{v}_\mathrm{i}$ relative to $\mathbf{b}$. However, this effect is cancelled by the (non-objective) transformation of the contribution due to $\mathbf{e}$.

The LORENTZ force density may be further decomposed into the contributions of the free and bound charges. With $\mathbf{e}$ and $\mathbf{b}$ unaffected by this distinction, the linearity of the expression $(4.2)_1$ with respect to q and $\mathbf{J}$ implies that the free and bound LORENTZ force densities are additive as well,

$$\mathbf{f}_\mathrm{L} \;=\; (\mathbf{f}_\mathrm{L})_\mathrm{F} + (\mathbf{f}_\mathrm{L})_\mathrm{R} \;=\; \big(q_\mathrm{F} + q_\mathrm{R}\big)\mathbf{e} + \big(\mathbf{J}_\mathrm{F} + \mathbf{J}_\mathrm{R}\big) \times \mathbf{b} \quad . \tag{4.4}$$

4.1.2 Linear Momentum

The net LORENTZ force experienced by a material region $\mathcal{P}$ is given by the volume integral of $\mathbf{f}_\mathrm{L}$, hence MÜLLER [102, Chapter 9.5] refers to $\mathbf{f}_\mathrm{L}$ as the "*production density*

of mechanical momentum".[1] This EM force is exerted in addition to the boundary tractions on $\partial\mathcal{P}$ and the body forces in $\mathcal{P}$, suggesting that the integral statement of linear momentum balance takes the form

$$\frac{\mathrm{d}}{\mathrm{d}t}\int_{\mathcal{P}} \rho\mathbf{v}\,\mathrm{d}v \;=\; \int_{\partial\mathcal{P}} \mathbf{T}\mathbf{n}\,\mathrm{d}a + \int_{\mathcal{P}} \rho\mathbf{f}_{\mathrm{B}}\,\mathrm{d}v + \int_{\mathcal{P}} \mathbf{f}_{\mathrm{L}}\,\mathrm{d}v \quad . \tag{4.5}$$

This is the EMTM counterpart of (2.113). Application of the divergence theorem (2.52), the material time derivative rule (2.112), and the localization theorem furnishes the local form of linear momentum balance,

$$\rho\mathbf{a} \;=\; \mathrm{div}\,\mathbf{T} + \rho\mathbf{f}_{\mathrm{B}} + \mathbf{f}_{\mathrm{L}} \quad , \tag{4.6}$$

which is the corresponding extension of (2.115). Note that the LORENTZ force is is assumed to impart on the continuum as a whole, rather than on individual charged particles. This may be justified by EM interactions between the free and bound charges, whereby the linear momentum associated with the motion of electrons or ions relative to the overall medium is neglected.

4.1.3 Angular Momentum

In analogy to Equation (2.116), the integral statement of the principle of angular momentum balance takes the form

$$\frac{\mathrm{d}}{\mathrm{d}t}\int_{\mathcal{P}} \mathbf{x}\times\rho\mathbf{v}\,\mathrm{d}v \;=\; \int_{\partial\mathcal{P}} \mathbf{x}\times\mathbf{t}_{(\mathbf{n})}\,\mathrm{d}a + \int_{\mathcal{P}} \mathbf{x}\times\rho\mathbf{f}_{\mathrm{B}}\,\mathrm{d}v + \int_{\mathcal{P}} \mathbf{x}\times\mathbf{f}_{\mathrm{L}}\,\mathrm{d}v \quad . \tag{4.7}$$

The EM fields are assumed not to exert any distributed moments on the material. Instead, they only enter (4.7) through the LORENTZ force. As in the thermomechanical case, $\mathbf{f}_{\mathrm{L}}$ along with most other terms cancel out due to the linear balance (4.6). Therefore, the angular momentum balance is not affected by EM effects.[2] Following the procedure in Section 2.3.3, see Equation (2.118), the local form of angular momentum balance reads

$$\mathbf{T} \;=\; \mathbf{T}^{\mathrm{T}} \quad . \tag{4.8}$$

Equation (4.8) for the EMTM model is identical to its TM counterpart (2.120).

[1] This of course implies that an equal and opposite force is exerted by the medium on the electromagnetic fields. Indeed, as ERICKSEN [22] points out in reference to the earlier work by PAGE [114] on radiation pressure, the EM fields *can* sustain forces.

[2] Note that the stress tensor $\mathbf{T}$ itself *does* in general depend on the EM fields through the constitutive equations. However, it must remain symmetric according to (4.8).

4.1.4 Maxwell Stress

The Lorentz force may be expressed solely in terms of the EM fields $\mathbf{d}$, $\mathbf{h}$, $\mathbf{e}$, and $\mathbf{b}$ by eliminating q and $\mathbf{J}$ using Maxwell's first pair of equations. This equation can be made to resemble a balance of electromagnetic momentum similar in form to (2.115), albeit only in the aether frame. This method is used by some authors[3] to reformulate the balances of linear and angular momenta to include an EM momentum, see Appendices A.6.1 and A.6.2, respectively. However, such alternative forms of the balance equations apply only to the aether frame and will not be used in the context of this disseration. Furthermore, the increased number of terms are found to unnecessarily complicate some of the derivations, in particular for the Green-Naghdi-Rivlin Theorem in Section 4.3 and the multiscale homogenization scheme discussed in Sections 5.3 and 5.4.

Employing all of Maxwell's Equations $(3.15)_{1-4}$ and the identities of tensor calculus in $(2.46)_5$ and (2.48), the Lorentz force $(4.2)_1$ becomes

$$\begin{aligned}
\mathbf{f}_{\mathrm{L}} &= \big(\operatorname{div}\mathbf{d}\big)\mathbf{e} + \left(\operatorname{curl}\mathbf{h} - \frac{\partial \mathbf{d}}{\partial t}\right) \times \mathbf{b} \\
&= -\frac{\partial}{\partial t}\big(\mathbf{d}\times\mathbf{b}\big) + \big(\operatorname{div}\mathbf{d}\big)\mathbf{e} + \big(\operatorname{curl}\mathbf{e}\big)\times\mathbf{d} + \big(\operatorname{curl}\mathbf{h}\big)\times\mathbf{b} \\
&= -\frac{\partial}{\partial t}\big(\mathbf{d}\times\mathbf{b}\big) + \big(\operatorname{div}\mathbf{d}\big)\mathbf{e} + \Big(\big[\operatorname{grad}\mathbf{e}\big]\mathbf{d} - \big[\operatorname{grad}\mathbf{e}\big]^{\mathrm{T}}\mathbf{d}\Big) \\
&\qquad\qquad + \big(\operatorname{div}\mathbf{b}\big)\mathbf{h} + \Big(\big[\operatorname{grad}\mathbf{h}\big]\mathbf{b} - \big[\operatorname{grad}\mathbf{h}\big]^{\mathrm{T}}\mathbf{b}\Big) \\
&= -\frac{\partial}{\partial t}\big(\mathbf{d}\times\mathbf{b}\big) + \mathbf{t}_{\mathrm{M}} \quad ,
\end{aligned} \tag{4.9}$$

where the force density $\mathbf{t}_{\mathrm{M}}$ is defined by

$$\mathbf{t}_{\mathrm{M}} = \operatorname{div}\big[\mathbf{e}\otimes\mathbf{d} + \mathbf{h}\otimes\mathbf{b}\big] - \Big(\big[\operatorname{grad}\mathbf{e}\big]^{\mathrm{T}}\mathbf{d} + \big[\operatorname{grad}\mathbf{h}\big]^{\mathrm{T}}\mathbf{b}\Big) \quad . \tag{4.10}$$

The term $\mathbf{d}\times\mathbf{b}$ in (4.9) may be interpreted as a momentum density of the electromagnetic field. Its rate of change is measured with a partial, not material, time derivative at a fixed location $\mathbf{x}$. Only in the aether frame (3.35) can the vector $\mathbf{t}_{\mathrm{M}}$ be written in terms of the divergence of a tensor, in which case using identities (2.44) and $(2.45)_2$,

$$\mathbf{t}_{\mathrm{M}} \overset{\text{Aet.}}{=} \operatorname{div}\mathbf{T}_{\mathrm{M}} \quad \text{where} \quad \mathbf{T}_{\mathrm{M}} = \big[\mathbf{e}\otimes\mathbf{d} + \mathbf{h}\otimes\mathbf{b}\big] - \tfrac{1}{2}\big(\mathbf{e}\cdot\mathbf{d} + \mathbf{h}\cdot\mathbf{b}\big)\mathbf{i} \quad . \tag{4.11}$$

Note that the definitions of $\mathbf{t}_{\mathrm{M}}$ and $\mathbf{T}_{\mathrm{M}}$ are independent of the aether frame, see (4.10) and $(4.11)_2$, respectively. Only the identity in $(4.11)_1$ relies on the aether relations. Following the premise that (4.9) constitutes a momentum balance, $\mathbf{T}_{\mathrm{M}}$ may be interpreted as a stress tensor. In the aether frame this so-called Maxwell *stress* $\mathbf{T}_{\mathrm{M}}$ is

[3] See, for example, Hutter *et al.* [56, Chapter 3.4], Kovetz [64, Section 54], Müller [102, Chapter 9.5], and Van de Ven [149, Chapter II].

symmetric.[4] Note that unlike the mechanical momentum balance (2.115), the balance equation (4.9) is not an independent principle, but instead follows directly from the definition of the LORENTZ force and the MAXWELL equations.

An analogous derivation can be devised in terms of the objective fields $\mathbf{d}$, $\boldsymbol{\mathcal{H}}$, $\boldsymbol{\mathcal{E}}$, and $\mathbf{b}$. Starting with the objective LORENTZ force $(4.2)_2$ and applying the objective form of MAXWELL equations $(3.108)_{1,2}$ for the elimination of q and $\mathbf{j}$, the procedure in (4.9) leads to

$$\mathbf{f}_{\mathrm{L}} = -\big(\overset{\star}{\mathbf{d}}\times\mathbf{b}+\mathbf{d}\times\overset{\star}{\mathbf{b}}\big)+\operatorname{div}\big[\boldsymbol{\mathcal{E}}\otimes\mathbf{d}+\boldsymbol{\mathcal{H}}\otimes\mathbf{b}\big]-\Big(\big[\operatorname{grad}\boldsymbol{\mathcal{E}}\big]^{\mathrm{T}}\mathbf{d}+\big[\operatorname{grad}\boldsymbol{\mathcal{H}}\big]^{\mathrm{T}}\mathbf{b}\Big) \quad . \tag{4.12}$$

This relation is written entirely in terms of objective fields. This is possible because the LORENTZ force, too, is objective. It should be noted however that $\mathbf{t}_{\mathrm{M}}$ and $\mathbf{T}_{\mathrm{M}}$ are *not* objective, since the partial time derivative in (4.9) is not objective (even though the momentum term $\mathbf{d}\times\mathbf{b}$ is objective).

4.2 Principle of Energy Balance

Energy is transferred to and from the coupled EMTM continuum not only through the power of the external forces and external supply of heat, but also on account of the power of the electromagnetic fields. This energy transfer originates from the interaction between the external EM field and the electric charges contained in the material region. Similarly to the preceding discussion of the LORENTZ force, the EM power is considered to act on the continuum material as a whole. The continuum body, not the charges themselves, is considered to carry the resulting (kinetic, strain, thermal, *etc.*) energy.

4.2.1 Power of the Electromagnetic Fields

In view of the LORENTZ force density $\mathbf{f}_{\mathrm{L}}$ derived in Section 4.1.1, it may be tempting to conclude that the corresponding power imparted on the body is simply $\mathbf{f}_{\mathrm{L}}\cdot\mathbf{v}$. However, the LORENTZ force is mediated by the electric charges $Q(\mathcal{P})$ contained in region $\mathcal{P}$, not the medium itself. In the presence of a conduction current $\mathbf{j}$ these charges move (on average) relative to the material body.

To identify the power density of the EM field, its effect is first examined for a hypothetical point charge Q_{i}. According to Equation (4.1), the LORENTZ force $\mathbf{F}_{\mathrm{Li}}$ is exerted on Q_{i} traveling at velocity $\mathbf{v}_{\mathrm{i}}$. The corresponding power P_{Li} amounts to

$$P_{\mathrm{Li}} \;=\; \mathbf{F}_{\mathrm{Li}}\cdot\mathbf{v}_{\mathrm{i}} \;=\; Q_{\mathrm{i}}\mathbf{v}_{\mathrm{i}}\cdot\mathbf{e} \quad . \tag{4.13}$$

[4] It is emphasized that $\{\mathbf{d},\mathbf{h}\}$ in $(4.11)_2$ refer to the *total* charge-current potentials, for which the aether relations $(3.35)_{1,2}$ apply irrespective of the underlying medium. Therefore, the MAXWELL stress $\mathbf{T}_{\mathrm{M}}$ is always symmetric (in the aether frame). For polarizable or magnetizable continua $\mathbf{T}_{\mathrm{M}}$ may be further decomposed into its free and bound parts. However, to guarantee the symmetry of these individual parts the medium must be electromagnetically isotropic, see Equations $(3.38)_{1,2}$.

The energy of the point charge increases when $\mathbf{F}_{\mathrm{L}i}\cdot\mathbf{v}_i>0$. The portion $Q_i\mathbf{v}_i\times\mathbf{b}$ of $\mathbf{F}_{\mathrm{L}i}$ is orthogonal to the direction $\mathbf{v}_i$ of travel and does not contribute to the power. As argued in (4.2), the volume average of $Q_i\mathbf{v}_i$ converges in the continuum limit to the total current density $\mathbf{J}$. The EM power density imparted on the continuum is therefore given by

$$p_{\mathrm{L}} \;=\; \mathbf{J}\cdot\mathbf{e} \;=\; \mathbf{j}\cdot\mathbf{e} + q\big(\mathbf{e}+\mathbf{v}\times\mathbf{b}\big)\cdot\mathbf{v} \quad , \tag{4.14}$$

where (3.4) was used to further expand $\mathbf{J}\cdot\mathbf{e}$ into a form reminiscent of the Lorentz force in (4.1). The result in $(4.14)_2$ thus offers an alternative interpretation of the EM power $\mathbf{J}\cdot\mathbf{e}$ by separating it into two physical origins: The first term is caused by conduction of $\mathbf{j}$ relative to the field $\mathbf{e}$. The second part describes convection, *i.e.*, the power due to the Lorentz force as if charge density q were material, *i.e.* moving with the material body at $\mathbf{v}$.

Unlike the Lorentz force in (4.2), the EM power density is *not* objective. Indeed, it is readily shown with Equations $(2.155)_3$, (3.48), (3.69), and (4.3) that

$$\mathbf{J}^+\cdot\mathbf{e}^+ \;=\; \mathbf{J}\cdot\mathbf{e} + \mathbf{f}_{\mathrm{L}}\cdot\boldsymbol{\beta} \;=\; \mathbf{j}\cdot\boldsymbol{\mathcal{E}} + \mathbf{f}_{\mathrm{L}}\cdot\big[\mathbf{v}+\boldsymbol{\beta}\big] \quad . \tag{4.15}$$

It is thus impossible to write (4.14) purely in objective terms. Nevertheless, consider an alternative expression in terms of the objective quantities $\mathbf{j}$, $\boldsymbol{\mathcal{E}}$, $\mathbf{f}_{\mathrm{L}}$, and the (non-objective) material velocity $\mathbf{v}$,

$$\mathbf{J}\cdot\mathbf{e} \;=\; \mathbf{j}\cdot\boldsymbol{\mathcal{E}} + \mathbf{f}_{\mathrm{L}}\cdot\mathbf{v} \quad . \tag{4.16}$$

Equation (4.16) follows a pattern that will recur in the context of the Green-Naghdi-Rivlin theorem in Section 4.3, whereby a non-objective scalar field can be uniquely[5] decomposed into an objective part (here $\mathbf{j}\cdot\boldsymbol{\mathcal{E}}$) plus the scalar product of an objective vector ($\mathbf{f}_{\mathrm{L}}$) with the velocity $\mathbf{v}$.

As with the Lorentz force density $\mathbf{f}_{\mathrm{L}}$, the power density in (4.14) or (4.16) can be further split into the contributions of free and bound fields. The linearity of $\mathbf{J}\cdot\mathbf{e}$ with respect to $\mathbf{J}$ (or $\mathbf{j}$ and $\mathbf{f}_{\mathrm{L}}$) again suggests an additive decomposition into the two parts. The distinction between free and bound parts of $\mathbf{j}\cdot\boldsymbol{\mathcal{E}}$ will become significant in the discussion of the entropy inequality and constitutive relations in Section 4.4.

4.2.2 Energy Balance

The principle of energy balance for the coupled EMTM material is postulated as

$$\begin{aligned}\frac{\mathrm{d}}{\mathrm{d}t}\int_{\mathcal{P}}\rho\left(\frac{1}{2}\mathbf{v}\cdot\mathbf{v}+\varepsilon\right)\mathrm{d}v \;=\; &\int_{\mathcal{P}}\rho\mathbf{f}_{\mathrm{B}}\cdot\mathbf{v}\,\mathrm{d}v + \int_{\partial\mathcal{P}}\mathbf{t}_{(\mathbf{n})}\cdot\mathbf{v}\,\mathrm{d}a \\ &+\int_{\mathcal{P}}\rho r\,\mathrm{d}v - \int_{\partial\mathcal{P}}q_{(\mathbf{n})}\,\mathrm{d}a + \int_{\mathcal{P}}\mathbf{J}\cdot\mathbf{e}\,\mathrm{d}v \quad .\end{aligned} \tag{4.17}$$

[5]The decomposition is unique in the sense that its (objective and non-objective) scalar parts are unique. The components of $\mathbf{f}_{\mathrm{L}}$ orthogonal to $\mathbf{v}$ are arbitrary.

Here, the original statement (2.121) is amended only by an additional term accounting for the power $\mathbf{J}\cdot\mathbf{e}$ due to the interaction between the electric charges of the body and the electromagnetic field. The term represents an external supply of energy by the EM field. The energy associated with the EM field itself is not considered part of the internal energy of the material body. The total (kinetic plus internal) energy density per unit volume is given by $\rho e = \rho(\frac{1}{2}\mathbf{v}\cdot\mathbf{v}+\varepsilon)$, see (2.122).

The local form of (4.17) is obtained using CAUCHY's theorems (2.114) and (2.123), the divergence theorem (2.50), the material time derivative rule (2.112), and the localization theorem, leading to

$$\rho\big[\tfrac{1}{2}\mathbf{v}\cdot\mathbf{v}+\varepsilon\big]^{\bullet} \;=\; \rho\mathbf{f}_{\mathrm{B}}\cdot\mathbf{v} \,+\, \operatorname{div}\big(\mathbf{T}^{\mathrm{T}}\mathbf{v}\big) \,+\, \rho r \,-\, \operatorname{div}\mathbf{q} \,+\, \mathbf{J}\cdot\mathbf{e} \quad . \tag{4.18}$$

This is the generalization of Equation (2.124) to EMTM materials. The balance of thermal energy may be derived following the procedure in (2.125), as

$$\rho\dot{\varepsilon} \;=\; \mathbf{T}\cdot\mathbf{L} \,+\, \rho r \,-\, \operatorname{div}\mathbf{q} \,+\, \mathbf{j}\cdot\boldsymbol{\mathcal{E}} \quad . \tag{4.19}$$

This constitutes the electromagnetic generalization of Equation (2.126). The term $\mathbf{j}\cdot\boldsymbol{\mathcal{E}}$ is sometimes interpreted as JOULE *heating*.[6]

Recall that the conservation of mass (2.111) was used to derive identity (2.112) and thus also (4.18). Whereas the energy balance in (4.17) is a standalone postulate, its local form (4.18) is not. Furthermore, the thermal energy balance (4.19) requires knowledge of the balances of linear and angular momenta. However, the GREEN-NAGHDI-RIVLIN theorem deduces the conservation of mass and momentum directly from the postulated energy equation, see Section 4.3.

4.2.3 Poynting's Theorem

Recall the expressions (4.9) of the LORENTZ force in terms of the EM fields, which in the aether frame resembles a momentum balance equation. Conversely, when the power density $\mathbf{J}\cdot\mathbf{e}$ is written in terms of these fields, the resulting equation takes the form of an energy balance equation as long as the aether relations hold. This fact can be exploited to include electromagnetic energy as part of the energy balance of the coupled EMTM material, see Appendix A.6.3. However, this form is not employed in this dissertation because it entails an unnecessary increase in the number of terms, while being (arguably) beneficial only in the aether frame.

[6] Recall from $(3.25)_2$ and $(3.26)_2$ that the conduction current $\mathbf{j}$ can be split into the free and bound parts. Joule heating is primarily attributed to the free current $\mathbf{j}_{\mathrm{F}}\cdot\boldsymbol{\mathcal{E}}$, see the discussion around (4.53). Nevertheless, the bound currents due to polarization $\overset{\star}{\mathbf{p}}$ and magnetization $\operatorname{curl}\boldsymbol{\mathcal{M}}$ in principle, too, contribute to heating in (4.19). The distinction between free and bound parts of $\mathbf{j}\cdot\boldsymbol{\mathcal{E}}$ is important for the constitutive description of the EM properties of the continuum.

Using Equations $(2.46)_6$ and $(3.15)_{2,4}$, POYNTING*'s theorem* expresses the EM power as

$$\begin{aligned}\mathbf{J}\cdot\mathbf{e} &= \left(\operatorname{curl}\mathbf{h} - \frac{\partial\mathbf{d}}{\partial t}\right)\cdot\mathbf{e} \\ &= -\operatorname{div}\big(\mathbf{e}\times\mathbf{h}\big) - \mathbf{e}\cdot\frac{\partial\mathbf{d}}{\partial t} + \mathbf{h}\cdot\operatorname{curl}\mathbf{e} \\ &= -\operatorname{div}\big(\mathbf{e}\times\mathbf{h}\big) - \left(\mathbf{e}\cdot\frac{\partial\mathbf{d}}{\partial t} + \mathbf{h}\cdot\frac{\partial\mathbf{b}}{\partial t}\right) \quad .\end{aligned} \tag{4.20}$$

In the aether frame, the relations (3.35) allow further simplification of the partial time derivatives of (4.20) into the form

$$-\frac{\partial u}{\partial t} \overset{\text{Aet.}}{=} \operatorname{div}\mathbf{s} + \mathbf{J}\cdot\mathbf{e} \quad \text{where} \quad \mathbf{s} = \mathbf{e}\times\mathbf{h} \quad \text{and} \quad u = \frac{1}{2}\big(\mathbf{e}\cdot\mathbf{d} + \mathbf{h}\cdot\mathbf{b}\big) \quad , \tag{4.21}$$

or as some authors put it purely in terms of $\mathbf{e}$ and $\mathbf{b}$,

$$-\frac{1}{2}\frac{\partial}{\partial t}\left(\varepsilon_0\mathbf{e}\cdot\mathbf{e} + \frac{1}{\mu_0}\mathbf{b}\cdot\mathbf{b}\right) \overset{\text{Aet.}}{=} \frac{1}{\mu_0}\operatorname{div}\big(\mathbf{e}\times\mathbf{b}\big) + \mathbf{J}\cdot\mathbf{e} \quad . \tag{4.22}$$

Equations $(4.21)_1$ or (4.22) resemble an energy balance, whereby the rate of change of energy u stored in the EM field per unit volume is balanced by the outward flux $\mathbf{s}$ (called the POYNTING *vector*) of energy across the boundary and the work imparted onto charges through the LORENTZ force.

It is emphasized here that (4.21) is not an independent principle, but merely the result of a rearrangement of MAXWELL's equations and thus an identity which must be satisfied by all of its solutions. The interpretation of (4.22) as a balance law of EM energy appears to be somewhat controversial, with a wide range of proponents[7] and detractors.[8] As FEYNMAN [26, Chapter 27] points out, there are infinite possible ways to use MAXWELL's equations to devise a flux $\mathbf{s}$ and energy u such that they satisfy an energy balance of the form $(4.21)_1$. However, such alternative expressions typically involve higher-order derivatives. The definitions $(4.21)_{2,3}$ for energy flux and energy density are indeed remarkably simple, with u comprising the electrostatic energy plus the magnetic energy.

Note that the objective part $\mathbf{j}\cdot\boldsymbol{\mathcal{E}}$ of the power density, see Equation (4.16), may be expressed similarly to POYNTING's theorem (4.20) in terms of the objective EM fields. Independently of the aether frame, Equations $(2.46)_6$ and $(3.108)_{2,3}$ furnish

$$\mathbf{j}\cdot\boldsymbol{\mathcal{E}} = -\operatorname{div}\big(\boldsymbol{\mathcal{E}}\times\boldsymbol{\mathcal{H}}\big) - \big[\boldsymbol{\mathcal{E}}\cdot\overset{\star}{\mathbf{d}} + \boldsymbol{\mathcal{H}}\cdot\overset{\star}{\mathbf{b}}\big] \quad . \tag{4.23}$$

[7] For example GRIFFITHS [38, Chapter 8.1.2]: "[...] *the work done on the charges by the electromagnetic force is equal to the decrease in energy stored in the field, less the energy that flowed out through the surface.*" MÜLLER [102, after Equation 9.59] draws similar conclusions.

[8] For example KOVETZ [64, after Equation 55.4]: "[...] *is often, and erroneously, regarded as a balance law for 'electromagnetic energy'.*"

Using the vector triple product in (2.33), it can be shown that the objective field $\boldsymbol{\mathcal{E}} \times \boldsymbol{\mathcal{H}}$ is related to the POYNTING vector $\mathbf{s} = \mathbf{e} \times \mathbf{h}$ by

$$\begin{aligned}
\boldsymbol{\mathcal{E}} \times \boldsymbol{\mathcal{H}} &= \big(\mathbf{e} + \mathbf{v} \times \mathbf{b}\big) \times \big(\mathbf{h} - \mathbf{v} \times \mathbf{d}\big) \\
&= \mathbf{e} \times \mathbf{h} - \big[(\mathbf{e} \cdot \mathbf{d})\mathbf{v} - (\mathbf{v} \cdot \mathbf{e})\mathbf{d}\big] + \big[(\mathbf{v} \cdot \mathbf{h})\mathbf{b} - (\mathbf{h} \cdot \mathbf{b})\mathbf{v}\big] - \big(\big[\mathbf{v} \times \mathbf{b}\big] \cdot \mathbf{d}\big)\mathbf{v} \\
&= \mathbf{e} \times \mathbf{h} + \big[\mathbf{e} \otimes \mathbf{d} + \mathbf{h} \otimes \mathbf{b}\big]^{\mathrm{T}} \mathbf{v} - \big(\mathbf{e} \cdot \mathbf{d} + \mathbf{h} \cdot \mathbf{b}\big)\mathbf{v} - \big(\big[\mathbf{b} \times \mathbf{d}\big] \cdot \mathbf{v}\big)\mathbf{v} \\
&= \mathbf{s} + \big[\mathbf{T}_{\mathrm{M}} - u\mathbf{i} + \big(\mathbf{d} \times \mathbf{b}\big) \otimes \mathbf{v}\big]^{\mathrm{T}} \mathbf{v} \quad , \qquad (4.24)
\end{aligned}$$

where $\mathbf{T}_{\mathrm{M}}$ is the MAXWELL stress $(4.11)_2$, u is the EM energy density $(4.21)_3$, and $\mathbf{d} \times \mathbf{b}$ the EM momentum density in Equation (4.9).[9]

Neither the POYNTING vector $\mathbf{s}$ nor the energy density u are objective. The transformation of u under superposed rigid-body motion is obtained from (3.59), (3.63) and (3.67),

$$u^{+} \;=\; u + \big(\mathbf{d} \times \mathbf{b}\big) \cdot \boldsymbol{\beta} \quad . \qquad (4.25)$$

4.3 The Green-Naghdi-Rivlin Theorem

The GREEN-NAGHDI-RIVLIN *theorem* (GNR) [37] is a profound result in continuum mechanics, according to which the balance equations of mass, linear momentum and angular momentum can be *derived* from the principle of energy balance. This is achieved by postulating form-invariance of the energy balance under superposed rigid-body motion in covariant theories. This is similar to NOETHER*'s first theorem* [107] of mathematical physics, where certain frame indifferences in LAGRANGIAN or HAMILTONIAN systems imply corresponding balance laws.[10]

It is mentioned that HUTTER *et al.* [56, Chapter 3.4] advocate for a similar approach based on the work by VAN DE VEN [149, Chapter II]. However, they start with a vastly more complex energy equation (see [56, Equation 3.4.19]), which incorporates the MAXWELL stress (4.10) and POYNTING's theorem (4.20) similar to the balance equations presented in Section A.6. Furthermore, they seem to employ the alternative aether relations in (3.90), which is in conflict with the more widely adopted relations (3.35). The upcoming derivation refrains from using the aether relations altogether, thus avoiding this point of contention.

[9] The interpretation of $\mathbf{s}$, $\mathbf{T}_{\mathrm{M}}$, u, and $\mathbf{d} \times \mathbf{b}$ as EM 'energy flux', 'stress', 'energy' and 'momentum' is reasonable only in the aether frame. Nevertheless, their definition does not rely on the aether relations so the quantities may be used outside of the aether frame, for example in (4.24).

[10] See MARSDEN and HUGHES [84, Chapter 5.5] for an introduction to NOETHER's theorem in the context of elasticity. Furthermore, YAVARI and MARSDEN [156] discuss the connection between covariance and NOETHER's theorem for continua with microstructure.

4.3.1 Standard GNR Procedure in Integral Form

The GNR theorem is typically derived as follows: It is postulated that the energy balance (4.17) is form-invariant under arbitrary SRBMs, which requires the balance equation to be equally satisfied by the transformed quantities

$$\frac{\mathrm{d}}{\mathrm{d}t}\int_{\mathcal{P}^+}\rho^+\Big(\frac{1}{2}\mathbf{v}^+\cdot\mathbf{v}^+ + \varepsilon^+\Big)\,\mathrm{d}v^+ = \int_{\mathcal{P}^+}\rho^+\mathbf{f}_{\mathrm{B}}^+\cdot\mathbf{v}^+\,\mathrm{d}v^+ + \int_{\partial\mathcal{P}^+}\mathbf{t}^+_{(\mathbf{n}^+)}\cdot\mathbf{v}^+\,\mathrm{d}a^+ + \int_{\mathcal{P}^+}\rho^+ r^+\,\mathrm{d}v^+ - \int_{\partial\mathcal{P}^+} q^+_{(\mathbf{n}^+)}\,\mathrm{d}a^+ + \int_{\mathcal{P}^+}\mathbf{J}^+\cdot\mathbf{e}^+\,\mathrm{d}v^+ \quad . \quad (4.26)$$

The original energy balance (4.17) is then subtracted from (4.26) using the relevant transformation formulae for SRBM. By their very nature, the non-objective fields cannot be entirely eliminated, whereas the objective terms (such as $\rho\varepsilon$, ρr, and $q_{(\mathbf{n})}$) cancel right away. The transformation rules in $(2.155)_3$, $(2.174)_{1-4}$, (2.179), and (4.15) furnish

$$\frac{\mathrm{d}}{\mathrm{d}t}\int_{\mathcal{P}}\rho\big(\tfrac{1}{2}\boldsymbol{\beta}\cdot\boldsymbol{\beta}+\mathbf{v}\cdot\boldsymbol{\beta}\big)\,\mathrm{d}v - \int_{\partial\mathcal{P}}\mathbf{t}_{(\mathbf{n})}\cdot\boldsymbol{\beta}\,\mathrm{d}a - \int_{\mathcal{P}}\big(\rho\mathbf{f}_{\mathrm{B}}+\mathbf{f}_{\mathrm{L}}\big)\cdot\boldsymbol{\beta}\,\mathrm{d}v - \int_{\mathcal{P}}\rho\dot{\boldsymbol{\beta}}\cdot\big(\mathbf{v}+\boldsymbol{\beta}\big)\,\mathrm{d}v = 0 \quad . \quad (4.27)$$

This equation enforces the form-invariance of the energy equation and must be satisfied by all SRBMs. In the following, two particular SRBMs are deliberately chosen to extract the conditions necessary for (4.27) to hold. This gives rise to the conservation of mass and the balances of linear and angular momenta.

To this end consider the Galilean transformation (2.154), for which $\boldsymbol{\beta}=\mathbf{v}_0$, $\dot{\boldsymbol{\beta}}=\mathbf{0}$, and $\boldsymbol{\Omega}=\mathbf{0}$, see Equations (2.160). Since $\mathbf{v}_0$ is uniform in $(\mathbf{x},t)$ it may be removed from the integrals and material time derivatives, so that

$$\mathbf{v}_0\cdot\left\{\frac{\mathrm{d}}{\mathrm{d}t}\int_{\mathcal{P}}\rho\mathbf{v}\,\mathrm{d}v - \int_{\partial\mathcal{P}}\mathbf{t}_{(\mathbf{n})}\mathrm{d}a - \int_{\mathcal{P}}\rho\mathbf{f}_{\mathrm{B}}\,\mathrm{d}v - \int_{\mathcal{P}}\mathbf{f}_{\mathrm{L}}\,\mathrm{d}v\right\} + \big(\tfrac{1}{2}\mathbf{v}_0\cdot\mathbf{v}_0\big)\left\{\frac{\mathrm{d}}{\mathrm{d}t}\int_{\mathcal{P}}\rho\,\mathrm{d}v\right\} = 0 \quad . \quad (4.28)$$

Equation (4.28) represents a scalar requirement for form-invariance of the energy to hold under all Galilean transformations. The arbitrariness of the constant vector $\mathbf{v}_0$ immediately furnishes[11] the balances of mass (2.110) and linear momentum (4.5). It is concluded that the electromagnetic generalization of the energy balance (4.17) is

[11] This is readily verified, for example, by requiring (4.28) to hold for both signs of $\pm\mathbf{v}_0$ and taking the sum (or the difference) between the two resulting conditions. The linear independence of $|\mathbf{v}_0|^2$ and the three components of $\mathbf{v}_0$ allows the scalar condition (4.28) to give rise to four independent balance equations.

indeed consistent with the generalized linear momentum balance (4.5). This result hinges on the transformation rule for the EM power (4.15), whose lack of objectivity is quantified by the LORENTZ force.

Next, consider a superposed motion (2.153) with an arbitrary constant angular velocity $\dot{\mathbf{Q}} = \boldsymbol{\Omega}_0$, and without translation $\dot{\mathbf{c}} = \mathbf{0}$. For convenience, pick a time t_0 at which the momentary rotation $\mathbf{Q} = \mathbf{I}$ and translation $\mathbf{c} = \mathbf{0}$ are trivial. It follows from $(2.156)_{1,2}$ that $\boldsymbol{\Omega} = \boldsymbol{\Omega}_0$, $\boldsymbol{\beta} = \boldsymbol{\Omega}_0 \mathbf{x}$, and $\dot{\boldsymbol{\beta}} = \boldsymbol{\Omega}_0 \mathbf{v}$. The skew-symmetry of $\boldsymbol{\Omega}_0$ may be invoked to write $\boldsymbol{\beta} = \boldsymbol{\omega}_0 \times \mathbf{x}$ in terms of the axial vector $\boldsymbol{\omega}_0$ according to (2.158). Equation (4.27) furnishes

$$\boldsymbol{\omega}_0 \cdot \left\{ \frac{\mathrm{d}}{\mathrm{d}t} \int_{\mathcal{P}} \mathbf{x} \times \rho \mathbf{v} \, \mathrm{d}v - \int_{\partial \mathcal{P}} \mathbf{x} \times \mathbf{t}_{(\mathbf{n})} \, \mathrm{d}a - \int_{\mathcal{P}} \mathbf{x} \times \rho \mathbf{f}_{\mathrm{B}} \, \mathrm{d}v - \int_{\mathcal{P}} \mathbf{x} \times \mathbf{f}_{\mathrm{L}} \, \mathrm{d}v \right\}$$
$$+ \tfrac{1}{2} \boldsymbol{\Omega}_0^2 \cdot \left\{ \int_{\mathcal{P}} \rho \big[\mathbf{v} \otimes \mathbf{x} - \mathbf{x} \otimes \mathbf{v} \big] \, \mathrm{d}v - \int_{\mathcal{P}} \big\{ \dot{\rho} + \rho \operatorname{div} \mathbf{v} \big\} \big[\mathbf{x} \otimes \mathbf{x} \big] \, \mathrm{d}v \right\} = 0 \quad , \quad (4.29)$$

where the permutation property of the triple scalar product (2.7) and the uniformity of $\boldsymbol{\Omega}_0$ (and thus $\boldsymbol{\omega}_0$) were exploited. Similar to the previous argument for $\mathbf{v}_0$, the arbitrariness of $\boldsymbol{\omega}_0$ implies that the balance of angular momentum (4.7) must hold. Meanwhile, the second term is quadratic in $\boldsymbol{\omega}_0$ and is independently satisfied by the balance of mass.[12]

If the energy equation was comprised only of objective terms, then form-invariance would hold trivially and no additional information could be attained. Only when quantities depart from objectivity, will the GNR procedure yield any requirements for maintaining form-invariance. This motivates the derivation of an alternative form of the energy balance in Section 4.3.2, which distinguishes between objective and non-objective parts.

Lastly, it is mentioned that knowledge of the transformation properties is necessary to derive the GNR theorem. However, the transformations (2.177) are themselves motivated by the form-invariance of mass conservation and linear momentum balance, making the argument somewhat circular. Nevertheless, the GNR theorem provides a useful indication that the choice of balance equations is consistent.

4.3.2 Split into Objective and Non-Objective Terms

There is an entirely equivalent but more suggestive way to express the energy balance (4.17), provided that the relevant fields are sufficiently smooth to apply the divergence theorem. The upcoming derivation aims to separate the objective from the non-objective quantities. In line with the premise of the GREEN-NAGHDI-RIVLIN

[12] Note that $\boldsymbol{\Omega}_0^2$ is symmetric on account of the skew-symmetry of $\boldsymbol{\Omega}_0$. Indeed there are up to 6 linearly independent quadratic combinations of the components of the axial vector $\boldsymbol{\omega}_0$. Meanwhile, the first integral on the second line of (4.29) is skew-symmetric, therefore its contraction with $\boldsymbol{\Omega}_0^2$ vanishes.

theorem, no knowledge of mass conservation or the linear and angular momentum balances shall be assumed. The divergence theorem (2.50) and REYNOLDS' transport theorem $(2.104)_1$ are used, but these involve only tensor calculus and kinematics, not the balance equations. Note that Equation (2.112), although more practical, is expressly avoided because of its reliance on conservation of mass.

The two surface integrals in (4.17) are converted to volume integrals using the divergence theorem in (2.50) along with CAUCHY's theorems (2.114) and (2.123). Any non-objective terms are decomposed into their objective and non-objective constituents. For example, the EM power $\mathbf{J}\cdot\mathbf{e}$ is split into $\mathbf{j}\cdot\boldsymbol{\mathcal{E}}$ and $\mathbf{f}_{\mathrm{L}}\cdot\mathbf{v}$ following (4.16). Meanwhile, the traction term $\operatorname{div}(\mathbf{T}^{\mathrm{T}}\mathbf{v})$ is separated with identity $(2.46)_3$ into

$$\operatorname{div}\big(\mathbf{T}^{\mathrm{T}}\mathbf{v}\big) \;=\; \operatorname{sym}\big[\mathbf{T}\big]\cdot\mathbf{L} + \operatorname{skw}\big[\mathbf{T}\big]\cdot\mathbf{L} + \big(\operatorname{div}\mathbf{T}\big)\cdot\mathbf{v} \quad , \tag{4.30}$$

of which only the first term is objective,[13] see (2.171) and $(2.175)_1$. The energy balance (4.17) becomes

$$\begin{aligned}\Big\{\frac{\mathrm{d}}{\mathrm{d}t}\int_{\mathcal{P}}\rho\frac{1}{2}\mathbf{v}\cdot\mathbf{v}\,\mathrm{d}v - \int_{\mathcal{P}}\big\{\rho\mathbf{f}_{\mathrm{B}}+\operatorname{div}\mathbf{T}+\mathbf{f}_{\mathrm{L}}\big\}\cdot\mathbf{v}\,\mathrm{d}v - \int_{\mathcal{P}}\operatorname{skw}\big[\mathbf{T}\big]\cdot\mathbf{L}\,\mathrm{d}v\Big\}\\ + \Big\{\frac{\mathrm{d}}{\mathrm{d}t}\int_{\mathcal{P}}\rho\varepsilon\,\mathrm{d}v - \int_{\mathcal{P}}\big\{\operatorname{sym}\big[\mathbf{T}\big]\cdot\mathbf{L}+\rho r-\operatorname{div}\mathbf{q}+\mathbf{j}\cdot\boldsymbol{\mathcal{E}}\big\}\mathrm{d}v\Big\} \;=\; 0 \quad ,\end{aligned} \tag{4.31}$$

where the first line comprises the non-objective terms and the second line is entirely objective. Note that the objective terms together constitute the integral form of the balance of thermal energy (4.19),

$$\frac{\mathrm{d}}{\mathrm{d}t}\int_{\mathcal{P}}\rho\varepsilon\,\mathrm{d}v \;=\; \int_{\mathcal{P}}\operatorname{sym}\big[\mathbf{T}\big]\cdot\mathbf{L}\,\mathrm{d}v + \int_{\mathcal{P}}\rho r\,\mathrm{d}v - \int_{\partial\mathcal{P}}q_{(\mathbf{n})}\,\mathrm{d}a + \int_{\mathcal{P}}\mathbf{j}\cdot\boldsymbol{\mathcal{E}}\,\mathrm{d}v \quad . \tag{4.32}$$

In order to localize Equation (4.31), REYNOLDS' transport theorem $(2.104)_1$ is applied to the material time derivatives, furnishing

$$\begin{aligned}\big\{\dot\rho+\rho\operatorname{div}\mathbf{v}\big\}\tfrac{1}{2}|\mathbf{v}|^2 + \big\{\rho\mathbf{a}-\rho\mathbf{f}_{\mathrm{B}}-\operatorname{div}\mathbf{T}-\mathbf{f}_{\mathrm{L}}\big\}\cdot\mathbf{v} - \big\{\operatorname{skw}\big[\mathbf{T}\big]\big\}\cdot\mathbf{L}\\ + \big\{\dot\rho+\rho\operatorname{div}\mathbf{v}\big\}\varepsilon + \big\{\rho\dot\varepsilon-\operatorname{sym}\big[\mathbf{T}\big]\cdot\mathbf{L}-\rho r+\operatorname{div}\mathbf{q}-\mathbf{j}\cdot\boldsymbol{\mathcal{E}}\big\} \;=\; 0 \quad .\end{aligned} \tag{4.33}$$

This is a version of the local form of energy balance (4.18) whose derivation does *not* rely on prior knowledge of any other balance equations. The first three terms represent the non-objective quantities. Each contains in braces $\{\cdot\}$ an *objective*[14]

[13] It was argued in Section 2.4.6 that the stress power $\mathbf{T}\cdot\mathbf{L}$ is entirely objective. However, this statement relies on the symmetry of $\mathbf{T}$ and thus angular momentum balance. Without such knowledge, $\mathbf{T}$ must be separated into its symmetric part $\operatorname{sym}[\mathbf{T}]=\frac{1}{2}[\mathbf{T}+\mathbf{T}^{\mathrm{T}}]$, and skew-symmetric part $\operatorname{skw}[\mathbf{T}]=\frac{1}{2}[\mathbf{T}-\mathbf{T}^{\mathrm{T}}]$.

[14] Strictly speaking, $\mathbf{a}$ and $\mathbf{f}_{\mathrm{B}}$ are objective only under inertial motions. Still, under general SRBM the term $(\mathbf{f}_{\mathrm{B}}-\mathbf{a})$ is objective, see $(2.177)_2$.

scalar-, vector-, or tensor-valued expression which is contracted with the *non-objective* quantities $(\mathbf{v}\cdot\mathbf{v})$, $\mathbf{v}$, or $\operatorname{grad}\mathbf{v}$, respectively. The lack of objectivity is thus confined entirely to the contraction with a velocity term. The expressions in braces correspond to the local forms of conservation of mass (2.111) and the balances of linear (4.6) and angular (4.8) momentum. The remainder of (4.33) consists only of objective quantities and furnishes the local form of the balance of thermal energy (4.19).

Of course, the aforementioned balance equations are readily extracted from Equation (4.33) using the procedure outlined in Section 4.3.1. Subtracting (4.33) from its transformed counterpart leads to

$$\big\{\dot\rho+\rho\operatorname{div}\mathbf{v}\big\}\big(\tfrac{1}{2}\boldsymbol{\beta}\cdot\boldsymbol{\beta}+\mathbf{v}\cdot\boldsymbol{\beta}\big)+\big\{\rho\mathbf{a}-\rho\mathbf{f}_{\mathrm{B}}-\operatorname{div}\mathbf{T}-\mathbf{f}_{\mathrm{L}}\big\}\cdot\boldsymbol{\beta}-\big\{\operatorname{skw}\big[\mathbf{T}\big]\big\}\cdot\boldsymbol{\Omega}\;=\;0\quad,\tag{4.34}$$

where use was made of $(2.155)_3$ and (2.171), with all other fields transforming objectively. Equation (4.34) must hold for all SRBMs (2.153), where $\mathbf{c}(t)$ and $\mathbf{Q}(t)$ are arbitrary differentiable functions so long as $\mathbf{Q}\in\operatorname{Orth}^{+}$ (proper orthogonal). At some fixed time t_0, not only can $\mathbf{Q}_0$ and $\mathbf{c}_0$ be specified freely but also their time derivatives, provided that $\boldsymbol{\Omega}_0$ is skew-symmetric. Thus, $\boldsymbol{\Omega}_0=\mathbf{Q}_0^{\mathrm{T}}\dot{\mathbf{Q}}_0$ and $\boldsymbol{\beta}_0=\boldsymbol{\Omega}_0\mathbf{x}+\mathbf{Q}_0^{\mathrm{T}}\dot{\mathbf{c}}_0$ are mutually independent. Condition (4.34) therefore necessitates that all three expressions in braces vanish, furnishing the expected balance equations in (2.111), (4.6), and (4.8).

Lastly, it is emphasized that Equation (4.33) cannot be derived if a lack of continuous differentiability in $\mathbf{T}$ or $\mathbf{q}$ prevents the use of the divergence theorem. Under such circumstances only the integral form (4.17) may be used for the purpose of the GNR theorem, see Section 4.3.1. In any case, the divergence theorem for $\mathbf{T}$ is necessary to obtain the balance of thermal energy, even in its integral form (4.32).

4.4 Second Law of Thermodynamics

In this section the Clausius-Duhem inequality is applied to the EMTM model. The energy equation is first reorganized and substituted into a modified entropy inequality. Following the method of Coleman and Noll, thermodynamic restrictions for the constitutive equations are deduced. Lastly, the requirement of invariance of the constitutive equations is examined, as well as its implications for the balance equations.

4.4.1 Body Heating

Before discussing the entropy inequality, the balance of thermal energy (4.19) is first rewritten in terms of the free and bound fields. To this end, the EM power density $\mathbf{j}\cdot\boldsymbol{\mathcal{E}}$ is separated into the contributions of the free and bound parts. For the bound part

in particular, Equations $(2.46)_6$, $(3.108)_3$ and $(3.109)_4$ furnish

$$\begin{aligned} \mathbf{j}\cdot\boldsymbol{\mathcal{E}} - \mathbf{j}_{\mathrm{F}}\cdot\boldsymbol{\mathcal{E}} \;=\; \mathbf{j}_{\mathrm{R}}\cdot\boldsymbol{\mathcal{E}} \;&=\; \big(\operatorname{curl}\boldsymbol{\mathcal{M}} + \overset{\star}{\mathbf{p}}\big)\cdot\boldsymbol{\mathcal{E}} \\ &=\; -\operatorname{div}\big(\boldsymbol{\mathcal{E}}\times\boldsymbol{\mathcal{M}}\big) + \boldsymbol{\mathcal{E}}\cdot\overset{\star}{\mathbf{p}} + \boldsymbol{\mathcal{M}}\cdot\operatorname{curl}\boldsymbol{\mathcal{E}} \\ &=\; -\operatorname{div}\big(\boldsymbol{\mathcal{E}}\times\boldsymbol{\mathcal{M}}\big) - \big[-\boldsymbol{\mathcal{E}}\cdot\overset{\star}{\mathbf{p}} + \boldsymbol{\mathcal{M}}\cdot\overset{\star}{\mathbf{b}}\big] \quad . \end{aligned} \tag{4.35}$$

The structure of relation (4.35) is analogous to the objective version of POYNTING's theorem (4.23), but applied only to the bound quantities. Likewise, POYNTING's original statement (4.20) may be rederived for the bound parts,

$$\mathbf{j}_{\mathrm{R}}\cdot\mathbf{e} \;=\; -\operatorname{div}\big(\mathbf{e}\times\mathbf{m}\big) - \left[-\mathbf{e}\cdot\frac{\partial\mathbf{p}}{\partial t} + \mathbf{m}\cdot\frac{\partial\mathbf{b}}{\partial t}\right] \quad . \tag{4.36}$$

The flux derivatives in (4.35) are expressed in terms of material time derivatives using definition $(2.106)_1$, where $\operatorname{grad}\mathbf{v} = \mathbf{L}$ and $\operatorname{div}\mathbf{v} = \operatorname{tr}\mathbf{L} = \mathbf{i}\cdot\mathbf{L}$,

$$\begin{aligned} \boldsymbol{\mathcal{E}}\cdot\overset{\star}{\mathbf{p}} - \boldsymbol{\mathcal{M}}\cdot\overset{\star}{\mathbf{b}} \;&=\; \big[\boldsymbol{\mathcal{E}}\cdot\mathbf{p}\big]^{\bullet} - \dot{\boldsymbol{\mathcal{E}}}\cdot\mathbf{p} + \boldsymbol{\mathcal{E}}\cdot\big(\overset{\star}{\mathbf{p}} - \dot{\mathbf{p}}\big) - \boldsymbol{\mathcal{M}}\cdot\dot{\mathbf{b}} - \boldsymbol{\mathcal{M}}\cdot\big(\overset{\star}{\mathbf{b}} - \dot{\mathbf{b}}\big) \\ &=\; \big[\boldsymbol{\mathcal{E}}\cdot\mathbf{p}\big]^{\bullet} - \dot{\boldsymbol{\mathcal{E}}}\cdot\mathbf{p} - \boldsymbol{\mathcal{M}}\cdot\dot{\mathbf{b}} + \Big[\big(\boldsymbol{\mathcal{E}}\cdot\mathbf{p} - \boldsymbol{\mathcal{M}}\cdot\mathbf{b}\big)\mathbf{i} - \big(\boldsymbol{\mathcal{E}}\otimes\mathbf{p} - \boldsymbol{\mathcal{M}}\otimes\mathbf{b}\big)\Big]\cdot\mathbf{L} \quad . \end{aligned} \tag{4.37}$$

With Equations (4.35) and (4.37), the body heating per unit volume ρr in the balance of thermal energy (4.19) may thus be expressed by

$$\begin{aligned} \rho r \;&=\; \rho\dot{\varepsilon} - \mathbf{T}\cdot\mathbf{L} + \operatorname{div}\mathbf{q} - \mathbf{j}\cdot\boldsymbol{\mathcal{E}} \\ &=\; \rho\dot{\varepsilon} - \big[\boldsymbol{\mathcal{E}}\cdot\mathbf{p}\big]^{\bullet} - \Big[\mathbf{T} + \big(\boldsymbol{\mathcal{E}}\cdot\mathbf{p} - \boldsymbol{\mathcal{M}}\cdot\mathbf{b}\big)\mathbf{i} - \big(\boldsymbol{\mathcal{E}}\otimes\mathbf{p} - \boldsymbol{\mathcal{M}}\otimes\mathbf{b}\big)\Big]\cdot\mathbf{L} \\ &\qquad + \mathbf{p}\cdot\dot{\boldsymbol{\mathcal{E}}} + \boldsymbol{\mathcal{M}}\cdot\dot{\mathbf{b}} + \operatorname{div}\big(\mathbf{q} + \boldsymbol{\mathcal{E}}\times\boldsymbol{\mathcal{M}}\big) - \mathbf{j}_{\mathrm{F}}\cdot\boldsymbol{\mathcal{E}} \\ &=\; \rho\dot{\varepsilon} - \big[\boldsymbol{\mathcal{E}}\cdot\mathbf{p}\big]^{\bullet} - \big(\boldsymbol{\mathcal{E}}\cdot\mathbf{p}\big)\operatorname{tr}\mathbf{L} - \boldsymbol{\tau}\cdot\mathbf{L} + \mathbf{p}\cdot\dot{\boldsymbol{\mathcal{E}}} + \boldsymbol{\mathcal{M}}\cdot\dot{\mathbf{b}} + \operatorname{div}\hat{\mathbf{q}} - \mathbf{j}_{\mathrm{F}}\cdot\boldsymbol{\mathcal{E}} \quad , \end{aligned} \tag{4.38}$$

where a stress $\boldsymbol{\tau}$ and a generalized heat flux $\hat{\mathbf{q}}$ are defined for convenience according to

$$\boldsymbol{\tau} \;=\; \mathbf{T} - \big(\boldsymbol{\mathcal{M}}\cdot\mathbf{b}\big)\mathbf{i} - \big(\boldsymbol{\mathcal{E}}\otimes\mathbf{p} - \boldsymbol{\mathcal{M}}\otimes\mathbf{b}\big) \quad , \quad \hat{\mathbf{q}} \;=\; \mathbf{q} + \boldsymbol{\mathcal{E}}\times\boldsymbol{\mathcal{M}} \quad . \tag{4.39}$$

A qualitative physical interpretation of $\boldsymbol{\mathcal{E}}\times\boldsymbol{\mathcal{M}}$ as an energy flux is provided by LIU and MÜLLER [77, Section 6] and MÜLLER [102, Figure 9.5] using a simple example in thermal equilibrium. Magnetization currents caused by a uniform magnetic field, in the presence of an electromotive force, lead to a transfer of energy perpendicular to $\boldsymbol{\mathcal{E}}$ and $\boldsymbol{\mathcal{M}}$.

4.4.2 Entropy Inequality

For the purpose of this dissertation, the CLAUSIUS-DUHEM inequality for EMTM materials is taken to be (in local form)

$$\rho\dot{\eta} \;\geq\; \frac{\rho r}{\theta} - \operatorname{div}\!\left(\frac{\hat{\mathbf{q}}}{\theta}\right) \quad . \tag{4.40}$$

This may be restated using the product rule in $(2.46)_1$ as

$$\rho r \;-\; \rho\theta\dot{\eta} \;-\; \operatorname{div}\hat{\mathbf{q}} + \hat{\mathbf{q}}\cdot\frac{\operatorname{grad}\theta}{\theta} \;\leq\; 0 \quad . \tag{4.41}$$

Note that the inequality in (4.40) departs from the purely thermomechanical version (2.128) invoked by COLEMAN and NOLL [17] insofar as the entropy flux (*i.e.*, the term $\hat{\mathbf{q}}/\theta$ inside the divergence) is in general *not* anymore proportional to the heat flux $\mathbf{q}$, see $(4.39)_2$. The additional electromagnetic energy flux $\boldsymbol{\mathcal{E}}\times\boldsymbol{\mathcal{M}}$ in (4.40) compensates for the same term in (4.38), which would otherwise complicate the derivation of thermodynamic restrictions on the constitutive equations, see Section 4.4.3.

A wide range of authors adopt the inequality in (4.40). The justification for (4.40) is based on MÜLLER [101], who dispenses with the prescribed proportionality between the entropy flux and the heat flux and proposes that the entropy flux is determined constitutively instead. ERICKSEN [23, Equation 3.17], HUTTER [55, Equation $4.21_{(2)}$], LIU and MÜLLER [77, Equation $3.23_{(2)}$], as well as MÜLLER [102, Equation 9.124] use this method to conclude that $(4.39)_2$ and (4.40) hold. Although KOVETZ [64, Equation 54.12] appears to postulate (2.128), it is seen upon further inspection of his definition for $\mathbf{q}$ that he is, too, in agreement with the extended inequality in (4.40), as pointed out by STEIGMANN [137, Equations 60 and 67]. Meanwhile, TOUPIN [145] does not treat magnetization ($\boldsymbol{\mathcal{M}}=\mathbf{0}$), rendering the issue moot since the two energy fluxes $\hat{\mathbf{q}}$ and $\mathbf{q}$ coincide.

4.4.3 Method of Coleman and Noll

The specific HELMHOLTZ free energy, introduced for thermomechanics in (2.130), is augmented by a term $\boldsymbol{\mathcal{E}}\cdot\mathbf{p}$ to account for dielectric polarization,

$$\Psi \;=\; \varepsilon \;-\; \eta\theta \;-\; \boldsymbol{\mathcal{E}}\cdot\mathbf{p}/\rho \quad . \tag{4.42}$$

Recall that the free energy Ψ, internal energy ε, and entropy η are *specific* quantities (per unit mass), whereas $\mathbf{p}$ is a density (per unit volume) and thus divided by ρ. Equation (4.42) is consistent with HUTTER *et al.* [56, Equation 3.4.29], KOVETZ [64, Equation 55.7], and STEIGMANN [137, Equation 70]. However, note that ERICKSEN [23, Equation 3.19] takes a different route, as he states, "*to indicate how one can make another choice*".[15]

[15] ERICKSEN's choice for the HELMHOLTZ free energy results in constitutive relations where the roles of two conjugate EM quantities are reversed: $\mathbf{e}=\rho\check{\Psi}_{\mathbf{p}}$ and $\mathbf{b}=\rho\check{\Psi}_{\boldsymbol{\mathcal{M}}}$ are determined from a

The material time derivative of the free energy (4.42) is expressed as

$$\rho\dot{\Psi} \;=\; \rho\dot{\varepsilon} - \rho\theta\dot{\eta} - \rho\eta\dot{\theta} - \overline{\boldsymbol{\mathcal{E}}\cdot\mathbf{p}} - \big(\boldsymbol{\mathcal{E}}\cdot\mathbf{p}\big)\,\mathrm{tr}\,\mathbf{L} \quad , \tag{4.43}$$

where the conservation of mass (2.111) was employed. Following the method of Coleman and Noll in Section 2.3.6, the body heating per unit volume ρr in the entropy inequality (4.41) is substituted with (4.38). It is thus concluded with (4.43), that

$$\rho\dot{\Psi} + \rho\eta\dot{\theta} - \boldsymbol{\tau}\cdot\mathbf{L} + \mathbf{p}\cdot\dot{\boldsymbol{\mathcal{E}}} + \boldsymbol{\mathcal{M}}\cdot\dot{\mathbf{b}} - \mathbf{j}_{\mathrm{F}}\cdot\boldsymbol{\mathcal{E}} + \hat{\mathbf{q}}\cdot\mathrm{grad}\,\theta/\theta \;\leq\; 0 \quad . \tag{4.44}$$

This is the electromagnetic generalization of the entropy inequality in (2.131).

Consider a class of materials whose Helmholtz free energy is given by a constitutive function of the form[16]

$$\Psi \;=\; \check{\Psi}(\mathbf{F},\boldsymbol{\mathcal{E}},\mathbf{b},\theta) \quad . \tag{4.45}$$

In view of relation (2.100), its material time derivative is given by

$$\begin{aligned}\dot{\Psi} \;&=\; \frac{\partial\check{\Psi}}{\partial\mathbf{F}}\mathbf{F}^{\mathrm{T}}\cdot\mathbf{L} + \frac{\partial\check{\Psi}}{\partial\boldsymbol{\mathcal{E}}}\cdot\dot{\boldsymbol{\mathcal{E}}} + \frac{\partial\check{\Psi}}{\partial\mathbf{b}}\cdot\dot{\mathbf{b}} + \frac{\partial\check{\Psi}}{\partial\theta}\dot{\theta} \\ &=\; \check{\Psi}_{\mathbf{F}}\,\mathbf{F}^{\mathrm{T}}\cdot\mathbf{L} + \check{\Psi}_{\boldsymbol{\mathcal{E}}}\cdot\dot{\boldsymbol{\mathcal{E}}} + \check{\Psi}_{\mathbf{b}}\cdot\dot{\mathbf{b}} + \check{\Psi}_{\theta}\,\dot{\theta} \quad ,\end{aligned} \tag{4.46}$$

where the subscripts denote partial derivatives of $\check{\Psi}$ with respect to the corresponding argument.[17] Recall that the derivatives $\check{\Psi}_{\boldsymbol{\mathcal{E}}}$ and $\check{\Psi}_{\mathbf{b}}$ with respect to the vector-valued arguments $\boldsymbol{\mathcal{E}}$ and $\mathbf{b}$ are defined by the generalized directional derivative for vectors (2.39), and $\check{\Psi}_{\mathbf{F}}$ according to Equation (2.40) for tensor derivatives. Inequality (4.44) now reads

$$\begin{aligned}&\big[\rho\check{\Psi}_{\mathbf{F}}\mathbf{F}^{\mathrm{T}} - \boldsymbol{\tau}\big]\cdot\mathbf{L} + \big(\rho\check{\Psi}_{\boldsymbol{\mathcal{E}}} + \mathbf{p}\big)\cdot\dot{\boldsymbol{\mathcal{E}}} + \big(\rho\check{\Psi}_{\mathbf{b}} + \boldsymbol{\mathcal{M}}\big)\cdot\dot{\mathbf{b}} \\ &\qquad + \rho\big(\check{\Psi}_{\theta} + \eta\big)\dot{\theta} - \mathbf{j}_{\mathrm{F}}\cdot\boldsymbol{\mathcal{E}} + \hat{\mathbf{q}}\cdot\mathrm{grad}\,\theta/\theta \;\leq\; 0 \quad \forall(\mathbf{x},t) \quad .\end{aligned} \tag{4.47}$$

As discussed in the lead-up to conclusion (2.135) for the thermomechanical case, due to the arbitrariness of the initial distributions of $(\mathbf{F},\boldsymbol{\mathcal{E}},\mathbf{b},\theta)$ and their material time derivatives, inequality (4.47) furnishes the conditions

$$\begin{aligned}\boldsymbol{\tau} \;&=\; \rho\check{\Psi}_{\mathbf{F}}\mathbf{F}^{\mathrm{T}} \quad , \quad \mathbf{p} \;=\; -\rho\check{\Psi}_{\boldsymbol{\mathcal{E}}} \quad , \quad \boldsymbol{\mathcal{M}} \;=\; -\rho\check{\Psi}_{\mathbf{b}} \quad , \\ \eta \;&=\; -\check{\Psi}_{\theta} \quad , \qquad 0 \;\leq\; \mathbf{j}_{\mathrm{F}}\cdot\boldsymbol{\mathcal{E}} - \hat{\mathbf{q}}\cdot\mathrm{grad}\,\theta/\theta \quad .\end{aligned} \tag{4.48}$$

---

derivative of Ψ with respect to $\mathbf{p}$ and $\boldsymbol{\mathcal{M}}$, respectively, as opposed to the result in $(4.48)_{2,3}$. The two approaches are related via Legendre transforms.

[16] It was already argued in $(2.135)_2$ that Ψ does not depend on $\mathrm{grad}\,\theta$. Other functional dependencies may be ruled out in a similar fashion. For example, Ψ is independent of $\dot{\boldsymbol{\mathcal{E}}}$ because (4.44) does not contain any terms for $\ddot{\boldsymbol{\mathcal{E}}}$.

[17] The derivative with respect to $\mathbf{F}$, as in $\check{\Psi}_{\mathbf{F}}$, should not be confused with the subscript used to indicate the free part of the charge-currents $\{q_{\mathrm{F}},\mathbf{J}_{\mathrm{F}}\}$ and their potentials $\{\mathbf{d}_{\mathrm{F}},\mathbf{h}_{\mathrm{F}}\}$. The difference is discernible from the font weight of the subscript, as well as from the surrounding context.

Equations $(4.48)_{1-4}$ provide constitutive relations for the stress $\boldsymbol{\tau}$, polarization $\mathbf{p}$, magnetization $\boldsymbol{\mathcal{M}}$, and entropy η. For the CAUCHY stress in particular, it follows from definition $(4.39)_1$ and $(4.48)_{1-3}$ that

$$\begin{aligned}\mathbf{T} &= \boldsymbol{\tau} + \big(\boldsymbol{\mathcal{M}}\cdot\mathbf{b}\big)\,\mathbf{i} + \boldsymbol{\mathcal{E}}\otimes\mathbf{p} - \boldsymbol{\mathcal{M}}\otimes\mathbf{b} \\ &= \rho\Big[\check{\Psi}_{\mathbf{F}}\mathbf{F}^{\mathrm{T}} - \big(\check{\Psi}_{\mathbf{b}}\cdot\mathbf{b}\big)\,\mathbf{i} - \boldsymbol{\mathcal{E}}\otimes\check{\Psi}_{\boldsymbol{\mathcal{E}}} + \check{\Psi}_{\mathbf{b}}\otimes\mathbf{b}\Big] \quad .\end{aligned} \tag{4.49}$$

Meanwhile, the last remnant of the entropy inequality in $(4.48)_5$ imposes limitations on the constitutive relations governing $\mathbf{j}_{\mathrm{F}}$ and $\hat{\mathbf{q}}$. Unlike Ψ (and thus its derivatives $\mathbf{T}$, $\mathbf{p}$, $\boldsymbol{\mathcal{M}}$, and η), whose functional dependencies are restricted by the terms available in (4.44), it is entirely possible for $\mathbf{j}_{\mathrm{F}}$ and $\hat{\mathbf{q}}$ to depend, for example, on $\operatorname{grad}\theta$.[18] The implications of $(4.48)_5$ are discussed by KOVETZ [64, Chapter 57] for the subclass of linearly conducting perfect fluids. Any process for which $\boldsymbol{\mathcal{E}}=\mathbf{0}$ and $\operatorname{grad}\theta=\mathbf{0}$ is *reversible* since the entropy inequality reduces to an equality. Such states are typically associated with thermodynamic *equilibrium* or *quasi-static* processes.

4.4.4 Balance Laws in Terms of the Helmholtz Free Energy

The preceding results may be employed to express the balance equations in terms of the HELMHOLTZ potential. Recall that the LORENTZ force $(4.2)_2$ may be additively decomposed into its free and bound parts, $(\mathbf{f}_{\mathrm{L}})_{\mathrm{F}}$ and $(\mathbf{f}_{\mathrm{L}})_{\mathrm{R}}$, so that using $(3.109)_{3,4}$ and $(4.48)_{2,3}$

$$\begin{aligned}\mathbf{f}_{\mathrm{L}} &= \big(q_{\mathrm{F}}+q_{\mathrm{R}}\big)\boldsymbol{\mathcal{E}} + \big(\mathbf{j}_{\mathrm{F}}+\mathbf{j}_{\mathrm{R}}\big)\times\mathbf{b} \\ &= (\mathbf{f}_{\mathrm{L}})_{\mathrm{F}} - \big(\operatorname{div}\mathbf{p}\big)\boldsymbol{\mathcal{E}} + \big(\operatorname{curl}\boldsymbol{\mathcal{M}}+\dot{\mathbf{p}}\big)\times\mathbf{b} \\ &= (\mathbf{f}_{\mathrm{L}})_{\mathrm{F}} + \operatorname{div}\big(\rho\check{\Psi}_{\boldsymbol{\mathcal{E}}}\big)\boldsymbol{\mathcal{E}} - \Big(\operatorname{curl}\big(\rho\check{\Psi}_{\mathbf{b}}\big)+\big[\rho\check{\Psi}_{\boldsymbol{\mathcal{E}}}\big]^{\star}\Big)\times\mathbf{b} \quad .\end{aligned} \tag{4.50}$$

This is used to write the balance of linear momentum (4.6) as

$$\begin{aligned}\rho\mathbf{a} &= \operatorname{div}\big[\boldsymbol{\tau}+(\boldsymbol{\mathcal{M}}\cdot\mathbf{b})\mathbf{i}+\boldsymbol{\mathcal{E}}\otimes\mathbf{p}-\boldsymbol{\mathcal{M}}\otimes\mathbf{b}\big]+\rho\mathbf{f}_{\mathrm{B}}+(\mathbf{f}_{\mathrm{L}})_{\mathrm{F}}-(\operatorname{div}\mathbf{p})\boldsymbol{\mathcal{E}}+(\operatorname{curl}\boldsymbol{\mathcal{M}}+\dot{\mathbf{p}})\times\mathbf{b} \\ &= \operatorname{div}\boldsymbol{\tau} + \rho\mathbf{f}_{\mathrm{B}} + (\mathbf{f}_{\mathrm{L}})_{\mathrm{F}} + \dot{\mathbf{p}}\times\mathbf{b} + \big[\operatorname{grad}\boldsymbol{\mathcal{E}}\big]\mathbf{p} + \big[\operatorname{grad}\mathbf{b}\big]^{\mathrm{T}}\boldsymbol{\mathcal{M}} \\ &= \operatorname{div}\big(\rho\check{\Psi}_{\mathbf{F}}\mathbf{F}^{\mathrm{T}}\big) + \rho\mathbf{f}_{\mathrm{B}} + (\mathbf{f}_{\mathrm{L}})_{\mathrm{F}} - \big[\rho\check{\Psi}_{\boldsymbol{\mathcal{E}}}\big]^{\star}\times\mathbf{b} - \rho\big[\operatorname{grad}\boldsymbol{\mathcal{E}}\big]\check{\Psi}_{\boldsymbol{\mathcal{E}}} - \rho\big[\operatorname{grad}\mathbf{b}\big]^{\mathrm{T}}\check{\Psi}_{\mathbf{b}} \quad ,\end{aligned} \tag{4.51}$$

where use was made of identities (2.44), $(2.45)_2$, $(2.46)_5$, (2.48), and GAUSS' law for magnetism $(3.15)_3$.

[18] Note that the functional dependencies of constitutive relations are additionally subject to invariance considerations. For instance, the objectivity of Ψ, $\mathbf{j}_{\mathrm{F}}$, and $\hat{\mathbf{q}}$ under SRBM implies that they cannot explicitly depend on the location $\mathbf{x}$ or material velocity $\mathbf{v}$. The form-invariance of the HELMHOLTZ potential is discussed in more detail in Section 4.4.5.

The balance of angular momentum (4.8) requires symmetry of the CAUCHY stress, which is already expressed in terms of Ψ in (4.49). It will be shown in Section 4.4.5 that this is satisfied automatically by the invariance of the constitutive function for Ψ under SRBM, see (4.55), (4.67), and (4.70).

Lastly, the thermal energy balance (4.19) is reformulated as follows: First, Equations (4.43) and (4.46) are combined to obtain an expression for the rate of change of internal energy $\rho\dot{\varepsilon}$,

$$\begin{aligned}\rho\dot{\varepsilon} &= \rho\big(\check{\Psi}_{\mathbf{F}}\mathbf{F}^{\mathrm{T}}\cdot\mathbf{L}+\check{\Psi}_{\boldsymbol{\mathcal{E}}}\cdot\dot{\boldsymbol{\mathcal{E}}}+\check{\Psi}_{\mathbf{b}}\cdot\dot{\mathbf{b}}+\check{\Psi}_{\theta}\dot{\theta}\big)+\rho\theta\dot{\eta}+\rho\eta\dot{\theta}+\big(\boldsymbol{\mathcal{E}}\cdot\mathbf{p}\big)^{\cdot}+\big(\boldsymbol{\mathcal{E}}\cdot\mathbf{p}\big)\operatorname{tr}\mathbf{L}\\ &= \boldsymbol{\tau}\cdot\mathbf{L}-\mathbf{p}\cdot\dot{\boldsymbol{\mathcal{E}}}-\boldsymbol{\mathcal{M}}\cdot\dot{\mathbf{b}}+\rho\theta\dot{\eta}+\big(\boldsymbol{\mathcal{E}}\cdot\mathbf{p}\big)^{\cdot}+\big(\boldsymbol{\mathcal{E}}\cdot\mathbf{p}\big)\operatorname{tr}\mathbf{L}\quad,\end{aligned}\tag{4.52}$$

where the constitutive relations $(4.48)_{1-4}$ were used. This may be conveniently inserted into the balance of thermal energy in the form of (4.38), where $\mathbf{j}\cdot\boldsymbol{\mathcal{E}}$ was split into the free and bound contributions, furnishing

$$\rho\theta\dot{\eta} = \rho r-\operatorname{div}\hat{\mathbf{q}}+\mathbf{j}_{\mathrm{F}}\cdot\boldsymbol{\mathcal{E}}\quad.\tag{4.53}$$

Here, the free conduction current $\mathbf{j}_{\mathrm{F}}$ and the generalized heat flux $\hat{\mathbf{q}}$ are determined by constitutive equations subject to $(4.48)_5$. Similar to the balance of thermal energy in (4.19), the form (4.53) of the energy balance suggests the interpretation of $\mathbf{j}_{\mathrm{F}}\cdot\boldsymbol{\mathcal{E}}$ as JOULE heating. However, KOVETZ [64, after Equation 56.18] takes issue with this terminology, calling Equation (4.53) an "*excuse, rather than the justification*" for the use of the name. Note again that $\hat{\mathbf{q}}$ may comprise not only the heat flux, but an additional EM contribution provided that the material is magnetizable, see $(4.39)_2$.

4.4.5 Invariance of the Constitutive Relations

Under superposed rigid-body motions, both the external stimuli (say, the deformation gradient $\mathbf{F}$) and the corresponding response of the material (say, the stress $\mathbf{T}$) transform according to the established rules. It is reasonable to expect the material behavior to be independent of the observer, which implies that the constitutive relation between $\mathbf{F}$ and $\mathbf{T}$ is form-invariant under SRBM. It is thus postulated that the response function $\mathbf{T}=\check{\mathbf{T}}(\mathbf{F})$ satisfies $\mathbf{T}^{+}=\check{\mathbf{T}}(\mathbf{F}^{+})$ for all SRBMs, where the functional form of $\check{\mathbf{T}}(\,\cdot\,)$ remains unchanged. The form-invariance of the constitutive relations is discussed, for example, by PIPKIN and RIVLIN [118, Section 2].

Invariance of the Helmholtz Free Energy

The constitutive relation for the HELMHOLTZ free energy is postulated to be invariant under SRBM,

$$\Psi^{+} = \check{\Psi}(\mathbf{F}^{+},\boldsymbol{\mathcal{E}}^{+},\mathbf{b}^{+},\theta^{+})\quad,\tag{4.54}$$

where the functional form of $\check{\Psi}(\,\cdot\,)$ is identical in (4.45) and (4.54). It is readily verified that $\Psi^{+}=\Psi$ is objective according to its definition (4.42) using the transformation

formulae in $(2.174)_2$, $(2.177)_1$, $(2.178)_{1,2}$, (3.69), and $(3.85)_2$. It is therefore concluded with $(2.169)_1$ and (3.63) that

$$\Psi^+ \,=\, \check{\Psi}(\mathbf{Q}\mathbf{F},\mathbf{Q}\boldsymbol{\mathcal{E}},\mathbf{Q}\mathbf{b},\theta) \,=\, \check{\Psi}(\mathbf{F},\boldsymbol{\mathcal{E}},\mathbf{b},\theta) \,=\, \Psi \quad \forall\, \mathbf{Q}(t)\in \mathrm{Orth}^+ \quad . \tag{4.55}$$

This represents the requirement of form-invariance of the HELMHOLTZ free energy.

Equation (4.55) must be satisfied by any proper orthogonal $\mathbf{Q}$. In particular, pick the case where $\mathbf{Q}\equiv\mathbf{R}^{\mathrm{T}}$ exactly cancels the rotation $\mathbf{R}$ contained in $\mathbf{F}=\mathbf{R}\mathbf{U}$ of the polar decomposition (2.69). For this choice of $\mathbf{Q}$, Equation (4.55) becomes

$$\Psi \,=\, \check{\Psi}(\mathbf{U},\mathbf{R}^{\mathrm{T}}\boldsymbol{\mathcal{E}},\mathbf{R}^{\mathrm{T}}\mathbf{b},\theta) \quad , \tag{4.56}$$

where $\mathbf{U}$ is the left stretch tensor. This expression is advantageous in that its arguments are unaffected by SRBMs,[19] see $(2.169)_{2,3}$. When written in terms of these arguments, the constitutive function $\check{\Psi}(\,\cdot\,)$ is automatically form-invariant.

Referential Description

Let the HELMHOLTZ free energy be described by a different constitutive function $\bar{\Psi}(\,\cdot\,)$ which is related to $\check{\Psi}(\,\cdot\,)$ via

$$\Psi \,=\, \check{\Psi}(\mathbf{U},\mathbf{R}^{\mathrm{T}}\boldsymbol{\mathcal{E}},\mathbf{R}^{\mathrm{T}}\mathbf{b},\theta) = \bar{\Psi}(\mathbf{U}^2,\mathbf{U}\,\mathbf{R}^{\mathrm{T}}\boldsymbol{\mathcal{E}},\mathbf{U}\,\mathbf{R}^{\mathrm{T}}\mathbf{b},\theta) = \bar{\Psi}(\mathbf{C},\mathbf{F}^{\mathrm{T}}\boldsymbol{\mathcal{E}},\mathbf{F}^{\mathrm{T}}\mathbf{b},\theta) \quad . \tag{4.57}$$

This expression makes use of the left CAUCHY-GREEN tensor $\mathbf{C}$ in $(2.70)_1$ and the symmetry of $\mathbf{U}$. The arguments in $\bar{\Psi}(\,\cdot\,)$ are entirely pulled back to the reference configuration and are unaffected by SRBMs. It is once again emphasized that the functional form of $\bar{\Psi}(\,\cdot\,)$ differs from that of $\check{\Psi}(\,\cdot\,)$.

Recall the constitutive relations in $(4.48)_{1-3}$ according to which the stress, polarization, and magnetization are obtained from derivatives of the HELMHOLTZ potential with respect to $\mathbf{F}$, $\boldsymbol{\mathcal{E}}$, and $\mathbf{b}$, respectively. The preceding discussion on alternative functional representations for Ψ raises the question of how $\check{\Psi}_{\mathbf{F}}$, $\check{\Psi}_{\boldsymbol{\mathcal{E}}}$, and $\check{\Psi}_{\mathbf{b}}$ are related to the derivatives with respect to the referential arguments $\bar{\Psi}_{\mathbf{C}}$, $\bar{\Psi}_{\mathbf{F}^{\mathrm{T}}\boldsymbol{\mathcal{E}}}$, and $\bar{\Psi}_{\mathbf{F}^{\mathrm{T}}\mathbf{b}}$. To this end, consider the tensor derivative of $\mathbf{C}=\mathbf{F}^{\mathrm{T}}\mathbf{F}$ with respect to $\mathbf{F}$, which furnishes a fourth-order tensor whose components are given by

$$\big[\mathbf{C}_{\mathbf{F}}\big]_{ABiC} \,=\, \frac{\partial C_{AB}}{\partial F_{iC}} \,=\, \frac{\partial}{\partial F_{iC}}\big(F_{jA}F_{jB}\big) \,=\, \delta_{AC}F_{iB}+F_{iA}\delta_{BC} \quad . \tag{4.58}$$

Note that, like $\mathbf{F}$, the components of $\mathbf{C}_{\mathbf{F}}$ are resolved partly in the referential and in the current bases. Similarly, the tensor derivative of $\mathbf{F}^{\mathrm{T}}\boldsymbol{\mathcal{E}}$ with respect to $\mathbf{F}$ furnishes the third-order tensor

$$\big[\big(\mathbf{F}^{\mathrm{T}}\boldsymbol{\mathcal{E}}\big)_{\mathbf{F}}\big]_{AiB} \,=\, \frac{\partial}{\partial F_{iB}}\big(F_{jA}\mathcal{E}_j\big) \,=\, \delta_{AB}\mathcal{E}_i \quad , \tag{4.59}$$

[19] In effect, the arguments have been pulled back to an intermediate configuration which is stretched, but not rotated relative to the reference configuration. These intermediate quantities, for example $\mathbf{U}=U_{AB}\mathbf{E}_A\otimes\mathbf{E}_B$ and $\mathbf{R}^{\mathrm{T}}\boldsymbol{\mathcal{E}}=[R_{iA}\mathbf{e}_i\otimes\mathbf{E}_A]^{\mathrm{T}}[\mathcal{E}_j\mathbf{e}_j]=R_{iA}\mathcal{E}_i\mathbf{E}_A$, are thus resolved in the referential bases $\mathbf{E}_A$, which makes them indifferent to superposed rotations in the spatial configuration.

and the vector derivative of $\mathbf{F}^{\mathrm{T}}\boldsymbol{\mathcal{E}}$ with respect to $\boldsymbol{\mathcal{E}}$ is

$$\big[(\mathbf{F}^{\mathrm{T}}\boldsymbol{\mathcal{E}})_{\boldsymbol{\mathcal{E}}}\big]_{Ai} \;=\; \frac{\partial}{\partial \mathcal{E}_i}\big(F_{jA}\mathcal{E}_j\big) \;=\; F_{iA} \quad . \tag{4.60}$$

For the functional form $\Psi = \bar{\Psi}(\mathbf{C}, \mathbf{F}^{\mathrm{T}}\boldsymbol{\mathcal{E}}, \mathbf{F}^{\mathrm{T}}\mathbf{b}, \theta)$ it is thus concluded by chain rule that

$$\begin{aligned}
\big[\Psi_{\mathbf{F}}\big]_{iC} \;=\; \frac{\partial \Psi}{\partial F_{iC}} \;&=\; \frac{\partial \bar{\Psi}}{\partial C_{AB}}\frac{\partial C_{AB}}{\partial F_{iC}} + \frac{\partial \bar{\Psi}}{\partial F_{kA}\mathcal{E}_k}\frac{\partial F_{jA}\mathcal{E}_j}{\partial F_{iC}} + \frac{\partial \bar{\Psi}}{\partial F_{kA}b_k}\frac{\partial F_{jA}b_j}{\partial F_{iC}} \\
&=\; F_{iA}\frac{\partial \bar{\Psi}}{\partial C_{CA}} + F_{iA}\frac{\partial \bar{\Psi}}{\partial C_{AC}} + \frac{\partial \bar{\Psi}}{\partial F_{kC}\mathcal{E}_k}\mathcal{E}_i + \frac{\partial \bar{\Psi}}{\partial F_{kC}b_k}b_i \\
&=\; \big[2\mathbf{F}\bar{\Psi}_{\mathbf{C}} + \boldsymbol{\mathcal{E}}\otimes\bar{\Psi}_{\mathbf{F}^{\mathrm{T}}\boldsymbol{\mathcal{E}}} + \mathbf{b}\otimes\bar{\Psi}_{\mathbf{F}^{\mathrm{T}}\mathbf{b}}\big]_{iC} \quad ,
\end{aligned} \tag{4.61}$$

and

$$\begin{aligned}
\big(\Psi_{\boldsymbol{\mathcal{E}}}\big)_i \;=\; \frac{\partial \Psi}{\partial \mathcal{E}_i} \;&=\; \frac{\partial \bar{\Psi}}{\partial F_{kA}\mathcal{E}_k}\frac{\partial F_{jA}\mathcal{E}_j}{\partial \mathcal{E}_i} \\
&=\; F_{iA}\frac{\partial \bar{\Psi}}{\partial F_{kA}\mathcal{E}_k} \\
&=\; \big(\mathbf{F}\bar{\Psi}_{\mathbf{F}^{\mathrm{T}}\boldsymbol{\mathcal{E}}}\big)_i \quad ,
\end{aligned} \tag{4.62}$$

where Equations (4.58 - 60) and the symmetry of $\mathbf{C}$ (and therefore $\bar{\Psi}_{\mathbf{C}}$) were used.

Alternatively, suppose the HELMHOLTZ free energy is described by a function $\breve{\Psi}(\cdot)$ which is related to $\bar{\Psi}(\cdot)$ by

$$\Psi \;=\; \bar{\Psi}(\mathbf{C}, \mathbf{F}^{\mathrm{T}}\boldsymbol{\mathcal{E}}, \mathbf{F}^{\mathrm{T}}\mathbf{b}, \theta) \;=\; \breve{\Psi}(\mathbf{E}, \mathbf{F}^{\mathrm{T}}\boldsymbol{\mathcal{E}}, \mathbf{F}^{\mathrm{T}}\mathbf{b}, \theta) \quad . \tag{4.63}$$

Here, $\mathbf{E}$ denotes the GREEN-LAGRANGE strain tensor from $(2.71)_1$. Note the trivial identity

$$\big[\mathbf{E}_{\mathbf{C}}\big]_{ABCD} \;=\; \frac{\partial E_{AB}}{\partial C_{CD}} \;=\; \frac{\partial}{\partial C_{CD}}\big(\tfrac{1}{2}C_{AB} - I_{AB}\big) \;=\; \tfrac{1}{2}\big(\delta_{AC}\delta_{BD}\big) \;=\; \tfrac{1}{2}\big[\,\mathbb{I}\,\big]_{ABCD} \quad , \tag{4.64}$$

where $\mathbb{I}$ is the (referential) fourth-order identity tensor, see (2.29). Equation (4.61) is thus alternatively expressed as

$$\Psi_{\mathbf{F}} \;=\; \mathbf{F}\breve{\Psi}_{\mathbf{E}} + \boldsymbol{\mathcal{E}}\otimes\breve{\Psi}_{\mathbf{F}^{\mathrm{T}}\boldsymbol{\mathcal{E}}} + \mathbf{b}\otimes\breve{\Psi}_{\mathbf{F}^{\mathrm{T}}\mathbf{b}} \quad , \tag{4.65}$$

where chain rule and (4.64) were used to write $\bar{\Psi}_{\mathbf{C}} = \frac{1}{2}\breve{\Psi}_{\mathbf{E}}$.

It is mentioned that similar inferences can be drawn from the chain rule for derivatives of $\Psi = \check{\Psi}(\mathbf{U}, \mathbf{R}^{\mathrm{T}}\boldsymbol{\mathcal{E}}, \mathbf{R}^{\mathrm{T}}\mathbf{b}, \theta)$. However, the tensor derivatives $\mathbf{R}_{\mathbf{F}}$ and $\mathbf{U}_{\mathbf{F}}$ of the polar decomposition are less straightforward, see CHEN and WHEELER [14] and WHEELER [153], and are thus avoided here.

Implications for the Angular Momentum Balance

Unlike in the purely thermomechanical case $(2.135)_1$, the result in (4.61) implies that $\boldsymbol{\tau}$ is in general *not* symmetric, since

$$\boldsymbol{\tau} \;=\; \rho\Psi_{\mathbf{F}}\mathbf{F}^{\mathrm{T}} \;=\; \rho\Big[2\mathbf{F}\bar{\Psi}_{\mathbf{C}}\mathbf{F}^{\mathrm{T}} + \boldsymbol{\mathcal{E}}\otimes\big(\mathbf{F}\bar{\Psi}_{\mathbf{F}^{\mathrm{T}}\boldsymbol{\mathcal{E}}}\big) + \mathbf{b}\otimes\big(\mathbf{F}\bar{\Psi}_{\mathbf{F}^{\mathrm{T}}\mathbf{b}}\big)\Big] \quad . \tag{4.66}$$

This is a direct consequence of the invariance requirement (4.55) imposed on Ψ, which prevents the electromagnetic fields in the arguments of $\bar{\Psi}(\,\cdot\,)$ from being uncoupled from the deformation (in general).[20] Nevertheless, it is readily verified with (4.49), (4.62), and (4.66) that the CAUCHY stress

$$\mathbf{T} \;=\; \rho\Big[2\mathbf{F}\bar{\Psi}_{\mathbf{C}}\mathbf{F}^{\mathrm{T}} + \mathbf{b}\otimes\check{\Psi}_{\mathbf{b}} + \check{\Psi}_{\mathbf{b}}\otimes\mathbf{b} - \big(\check{\Psi}_{\mathbf{b}}\cdot\mathbf{b}\big)\,\mathbf{i}\Big] \quad , \tag{4.67}$$

is indeed symmetric as required by the balance of angular momentum.[21]

The preceding derivation shows that the balance of angular momentum (4.8) follows naturally from the requirement of form-invariance of the HELMHOLTZ potential, because it implies that Ψ can be functionally represented by $\Psi = \bar{\Psi}(\mathbf{C}, \mathbf{F}^{\mathrm{T}}\boldsymbol{\mathcal{E}}, \mathbf{F}^{\mathrm{T}}\mathbf{b}, \theta)$. This result can be replicated directly from (4.55) without resorting to the representation (4.57) as follows: Invocation of form-invariance of the total time derivative $\dot{\Psi}^{+} = \dot{\Psi}$ furnishes

$$\begin{aligned}
&\frac{\partial}{\partial(\mathbf{QF})}\big[\check{\Psi}(\mathbf{QF},\mathbf{Q}\boldsymbol{\mathcal{E}},\mathbf{Qb},\theta)\big]\cdot\big[\mathbf{QF}\big]^{\bullet} + \frac{\partial}{\partial(\mathbf{Q}\boldsymbol{\mathcal{E}})}\big[\check{\Psi}(\mathbf{QF},\mathbf{Q}\boldsymbol{\mathcal{E}},\mathbf{Qb},\theta)\big]\cdot\big[\mathbf{Q}\boldsymbol{\mathcal{E}}\big]^{\bullet} \\
&\qquad + \frac{\partial}{\partial(\mathbf{Qb})}\big[\check{\Psi}(\mathbf{QF},\mathbf{Q}\boldsymbol{\mathcal{E}},\mathbf{Qb},\theta)\big]\cdot\big[\mathbf{Qb}\big]^{\bullet} + \frac{\partial}{\partial\theta}\big[\check{\Psi}(\mathbf{QF},\mathbf{Q}\boldsymbol{\mathcal{E}},\mathbf{Qb},\theta)\big]\,\dot{\theta} \\
&\qquad\qquad = \frac{\partial}{\partial\mathbf{F}}\big[\check{\Psi}(\mathbf{F},\boldsymbol{\mathcal{E}},\mathbf{b},\theta)\big]\cdot\dot{\mathbf{F}} + \frac{\partial}{\partial\boldsymbol{\mathcal{E}}}\big[\check{\Psi}(\mathbf{F},\boldsymbol{\mathcal{E}},\mathbf{b},\theta)\big]\cdot\dot{\boldsymbol{\mathcal{E}}} \\
&\qquad\qquad\qquad + \frac{\partial}{\partial\mathbf{b}}\big[\check{\Psi}(\mathbf{F},\boldsymbol{\mathcal{E}},\mathbf{b},\theta)\big]\cdot\dot{\mathbf{b}} + \frac{\partial}{\partial\theta}\big[\check{\Psi}(\mathbf{F},\boldsymbol{\mathcal{E}},\mathbf{b},\theta)\big]\,\dot{\theta} \quad .
\end{aligned} \tag{4.68}$$

This condition must be satisfied for all SRBMs of the form (2.153) with proper orthogonal tensor $\mathbf{Q}(t)\in\mathrm{Orth}^{+}$, including the special case where $\mathbf{Q}=\mathbf{i}$ and $\dot{\mathbf{Q}}=\mathbf{Q}\boldsymbol{\Omega}=\boldsymbol{\Omega}_0$ at some instant in time.[22] In that case Equation (4.68) reduces to

$$\frac{\partial[\check{\Psi}(\mathbf{F},\boldsymbol{\mathcal{E}},\mathbf{b},\theta)]}{\partial\mathbf{F}}\cdot\boldsymbol{\Omega}_0\mathbf{F} + \frac{\partial[\check{\Psi}(\mathbf{F},\boldsymbol{\mathcal{E}},\mathbf{b},\theta)]}{\partial\boldsymbol{\mathcal{E}}}\cdot\boldsymbol{\Omega}_0\boldsymbol{\mathcal{E}} + \frac{\partial[\check{\Psi}(\mathbf{F},\boldsymbol{\mathcal{E}},\mathbf{b},\theta)]}{\partial\mathbf{b}}\cdot\boldsymbol{\Omega}_0\mathbf{b} \;=\; 0 \quad , \tag{4.69}$$

[20] It is observed that (4.66) is symmetric only if $\mathbf{p}$ and $\boldsymbol{\mathcal{M}}$ are collinear to $\boldsymbol{\mathcal{E}}$ and $\mathbf{b}$, respectively, see $(4.48)_{2,3}$ and (4.62). This is achieved if Ψ depends on the EM fields only through their norms $|\boldsymbol{\mathcal{E}}|$ and $|\mathbf{b}|$, thereby avoiding any coupling terms.

[21] Equation (4.67) is intended only to demonstrate the symmetry of $\mathbf{T}$ and should be used with caution, because it employs a combination of both functional representations $\check{\Psi}(\,\cdot\,)$ and $\bar{\Psi}(\,\cdot\,)$. For example, it does *not* imply that $\mathbf{T}$ is independent of the derivative $\Psi_{\boldsymbol{\mathcal{E}}}$ with respect to the electromotive intensity $\boldsymbol{\mathcal{E}}$.

[22] This is the same superposed motion prescribed by the GREEN-NAGHDI-RIVLIN theorem to deduce the momentum balance from (4.29).

where $[\mathbf{QF}]^{\cdot} = \dot{\mathbf{Q}}\mathbf{F} + \mathbf{Q}\dot{\mathbf{F}} = \boldsymbol{\Omega}_0\mathbf{F} + \dot{\mathbf{F}}$ was used. The above requirement is more succinctly expressed as

$$\big[\check{\Psi}_{\mathbf{F}}\mathbf{F}^{\mathrm{T}} + \check{\Psi}_{\boldsymbol{\mathcal{E}}} \otimes \boldsymbol{\mathcal{E}} + \check{\Psi}_{\mathbf{b}} \otimes \mathbf{b}\big] \cdot \boldsymbol{\Omega}_0 = 0 \quad . \tag{4.70}$$

It is concluded from the arbitrariness of the three independent components in $\boldsymbol{\Omega}_0$ that the bracketed term in (4.70) is symmetric. A comparison with Equation (4.49) immediately yields the symmetry of the CAUCHY stress $\mathbf{T}$, because the skew-symmetry of $\boldsymbol{\Omega}_0$ implies that $(\check{\Psi}_{\boldsymbol{\mathcal{E}}} \otimes \boldsymbol{\mathcal{E}}) \cdot \boldsymbol{\Omega}_0 = -(\boldsymbol{\mathcal{E}} \otimes \check{\Psi}_{\boldsymbol{\mathcal{E}}}) \cdot \boldsymbol{\Omega}_0$ as well as $\mathbf{i} \cdot \boldsymbol{\Omega}_0 = \operatorname{tr} \boldsymbol{\Omega}_0 = 0$.

Invariance of the Dissipative Fluxes

Recall that, unlike $\mathbf{T}$, $\mathbf{p}$, $\boldsymbol{\mathcal{M}}$, and η, the generalized heat flux $\hat{\mathbf{q}}$ and the free electric current $\mathbf{j}_{\mathrm{F}}$ are *not* derived from a thermodynamic potential. Their constitutive functions, restricted only by the entropy inequality in $(4.48)_5$, are nevertheless subject to the same requirement of form-invariance as Ψ. In view of Equation (2.163), which states that gradients of objective scalar fields transform as objective vectors, it is concluded that the functional representation

$$\begin{aligned} \mathbf{j}_{\mathrm{F}} &= \mathbf{R}\,\bar{\mathbf{j}}_{\mathrm{F}}(\mathbf{C}, \mathbf{F}^{\mathrm{T}}\boldsymbol{\mathcal{E}}, \mathbf{F}^{\mathrm{T}}\mathbf{b}, \mathbf{F}^{\mathrm{T}}\operatorname{grad}\theta, \theta) \quad , \\ \hat{\mathbf{q}} &= \mathbf{R}\,\bar{\hat{\mathbf{q}}}(\mathbf{C}, \mathbf{F}^{\mathrm{T}}\boldsymbol{\mathcal{E}}, \mathbf{F}^{\mathrm{T}}\mathbf{b}, \mathbf{F}^{\mathrm{T}}\operatorname{grad}\theta, \theta) \quad , \end{aligned} \tag{4.71}$$

automatically satisfies form-invariance. All function arguments are pulled back to the reference configuration and thus invariant under SRBM. The resulting flux vector is subsequently rotated by $\mathbf{R}$, which is determined from the polar decomposition of $\mathbf{F}$ in (2.69). In view of the transformation of $\mathbf{R}^{+}$ in $(2.169)_2$, this ensures that the resulting $\mathbf{j}_{\mathrm{F}}$ and $\hat{\mathbf{q}}$ transform objectively.

Rather than relying on the polar decomposition to express the generalized heat flux and the free conduction current in $(4.71)_{1,2}$, it may be more convenient to formulate the constitutive functions for their referential counterparts $\mathbf{j}_{\mathrm{F}0}$ and $\hat{\mathbf{q}}_0$ instead. Form-invariance is satisfied because, as remarked at the end of Section 2.4.6, the PIOLA transform of any objective vector is invariant under SRBM.

Recall from $(3.130)_2$ that the referential free conduction current $\mathbf{j}_{\mathrm{F}0}$ is given by the PIOLA transform of $\mathbf{j}_{\mathrm{F}}$. This raises the question of how the generalized heat flux $\hat{\mathbf{q}}$ is pulled back to the reference configuration. In view of the results for $\mathbf{q}_0$, $\boldsymbol{\mathcal{E}}_0$, and $\boldsymbol{\mathcal{M}}_0$ in Equations (2.145), (3.123), and $(3.131)_4$, respectively, the definition of the generalized heat flux $\hat{\mathbf{q}}$ in $(4.39)_2$ furnishes

$$\hat{\mathbf{q}} = \mathbf{q} + \boldsymbol{\mathcal{E}} \times \boldsymbol{\mathcal{M}} = J^{-1}\mathbf{F}\mathbf{q}_0 + \big(\mathbf{F}^{-\mathrm{T}}\boldsymbol{\mathcal{E}}_0\big) \times \big(\mathbf{F}^{-\mathrm{T}}\boldsymbol{\mathcal{M}}_0\big) = J^{-1}\mathbf{F}\big\{\mathbf{q}_0 + \boldsymbol{\mathcal{E}}_0 \times \boldsymbol{\mathcal{M}}_0\big\} \quad , \tag{4.72}$$

where the identity in $(2.37)_2$ was employed. It is thus concluded that the referential form of the generalized heat flux, that is,

$$\hat{\mathbf{q}}_0 = \mathbf{q}_0 + \boldsymbol{\mathcal{E}}_0 \times \boldsymbol{\mathcal{M}}_0 = J\mathbf{F}^{-1}\hat{\mathbf{q}} \quad , \tag{4.73}$$

is given by the PIOLA transform of $\hat{\mathbf{q}}$.

The constitutive functions in (4.71) are thus alternatively expressed by invariant referential functions for $\mathbf{j}_{\mathrm{F}0}$ and $\hat{\mathbf{q}}_0$ of the form

$$\begin{aligned} J\mathbf{F}^{-1}\mathbf{j}_{\mathrm{F}} &= \bar{\mathbf{j}}_{\mathrm{F}0}(\mathbf{C},\mathbf{F}^{\mathrm{T}}\boldsymbol{\mathcal{E}},\mathbf{F}^{\mathrm{T}}\mathbf{b},\mathbf{F}^{\mathrm{T}}\mathrm{grad}\,\theta,\theta) = \breve{\mathbf{j}}_{\mathrm{F}0}(\mathbf{E},\mathbf{F}^{\mathrm{T}}\boldsymbol{\mathcal{E}},\mathbf{F}^{\mathrm{T}}\mathbf{b},\mathbf{F}^{\mathrm{T}}\mathrm{grad}\,\theta,\theta) \quad , \\ J\mathbf{F}^{-1}\hat{\mathbf{q}} &= \bar{\hat{\mathbf{q}}}_0(\mathbf{C},\mathbf{F}^{\mathrm{T}}\boldsymbol{\mathcal{E}},\mathbf{F}^{\mathrm{T}}\mathbf{b},\mathbf{F}^{\mathrm{T}}\mathrm{grad}\,\theta,\theta) = \breve{\hat{\mathbf{q}}}_0(\mathbf{E},\mathbf{F}^{\mathrm{T}}\boldsymbol{\mathcal{E}},\mathbf{F}^{\mathrm{T}}\mathbf{b},\mathbf{F}^{\mathrm{T}}\mathrm{grad}\,\theta,\theta) \quad . \end{aligned} \tag{4.74}$$

Note that the gradients in (4.71) and (4.74) may be simplified to $\mathbf{F}^{\mathrm{T}}\mathrm{grad}\,\theta = \mathrm{Grad}\,\theta$ using the chain rule in (2.82).

4.4.6 Isotropy of the Helmholtz Free Energy

The condition of invariance in (4.55) does *not* imply isotropy of the material response. Rather, it states that the material response function (here $\breve{\Psi}$) 'commutes' with the SRBM: The response of the transformed system may be obtained either from the transformed stimuli acting on the rotated body, or by transforming the response of the untransformed system. It is expected that all reasonable constitutive models preserve invariance under SRBM.

Isotropy, on the other hand, imposes much more far-reaching restrictions on the constitutive equations. It asserts that the material response does not change when the reference configuration (but *not* the orientation of the external stimuli) is rotated. This corresponds to a transformation $\mathbf{F}^{-} = \mathbf{F}\mathbf{Q}$,[23] whereby a referential line element $\mathrm{d}\mathbf{X}$ is rotated by $\mathbf{Q}$ before it is mapped into $\mathrm{d}\mathbf{x}$ by the deformation gradient $\mathbf{F}$. Therefore, $\mathbf{Q}$ represents a set of transformations which map the reference configuration onto constitutively equivalent configurations. In the case of isotropy, the set of $\mathbf{Q}$ coincides with the orthogonal group.

Appealing to the polar decomposition theorem (2.69),

$$\begin{aligned} \mathbf{F}^{-} = \mathbf{F}\mathbf{Q} &= \mathbf{V}\mathbf{R}\mathbf{Q} = \mathbf{V}^{-}\mathbf{R}^{-} \\ &= \mathbf{R}\mathbf{U}\mathbf{Q} = \mathbf{R}^{-}\mathbf{U}^{-} \quad , \end{aligned} \tag{4.75}$$

it follows that the polar factors transform according to

$$\mathbf{R}^{-} = \mathbf{R}\mathbf{Q} \quad , \quad \mathbf{U}^{-} = \mathbf{Q}^{\mathrm{T}}\mathbf{U}\mathbf{Q} \quad , \quad \mathbf{V}^{-} = \mathbf{V} \quad , \quad \mathbf{C}^{-} = \mathbf{Q}^{\mathrm{T}}\mathbf{C}\mathbf{Q} \quad . \tag{4.76}$$

It is readily verified that Equations $(4.76)_{1-4}$ preserve the orthogonality of $\mathbf{R}^{-}$ and the symmetry of $\mathbf{U}^{-}$, $\mathbf{V}^{-}$, and $\mathbf{C}^{-}$. Since $\boldsymbol{\mathcal{E}}^{-} = \boldsymbol{\mathcal{E}}$ and $\mathbf{b}^{-} = \mathbf{b}$ are not rotated, the condition

[23] The notation $\mathbf{F}^{-} = \mathbf{F}\mathbf{Q}$ is used to separate transformations of material symmetries from transformations under SRBM, $\mathbf{F}^{+} = \mathbf{Q}\mathbf{F}$, see $(2.169)_1$. Note that the rotation tensors in the two formulae are different: the former $\mathbf{Q}$ is orthogonal and resolved in the referential bases, whereas the latter $\mathbf{Q}$ is proper orthogonal and resolved spatially.

of isotropy of the HELMHOLTZ potential for the functional representations (4.56) and (4.57) is encapsulated by

$$\begin{aligned} \Psi &= \check{\Psi}(\mathbf{U}, \mathbf{R}^{\mathrm{T}}\boldsymbol{\mathcal{E}}, \mathbf{R}^{\mathrm{T}}\mathbf{b}, \theta) = \check{\Psi}(\mathbf{Q}^{\mathrm{T}}\mathbf{U}\mathbf{Q}, \mathbf{Q}^{\mathrm{T}}\mathbf{R}^{\mathrm{T}}\boldsymbol{\mathcal{E}}, \mathbf{Q}^{\mathrm{T}}\mathbf{R}^{\mathrm{T}}\mathbf{b}, \theta) \\ &= \bar{\Psi}(\mathbf{C}, \mathbf{F}^{\mathrm{T}}\boldsymbol{\mathcal{E}}, \mathbf{F}^{\mathrm{T}}\mathbf{b}, \theta) = \bar{\Psi}(\mathbf{Q}^{\mathrm{T}}\mathbf{C}\mathbf{Q}, \mathbf{Q}^{\mathrm{T}}\mathbf{F}^{\mathrm{T}}\boldsymbol{\mathcal{E}}, \mathbf{Q}^{\mathrm{T}}\mathbf{F}^{\mathrm{T}}\mathbf{b}, \theta) \quad \forall\, \mathbf{Q} \in \mathrm{Orth} \quad . \end{aligned} \tag{4.77}$$

Equations (4.77) describe an *isotropic scalar-valued function* of a tensor, two vectors, and a scalar variable.

Representation theorems delineate the most general form a function can take whilst subject to a given symmetry group. TRUESDELL and NOLL [146, Chapter B.II] provide a summary[24] of representation theorems for scalar- and tensor-valued functions of vector-, and (symmetric) tensor-valued arguments, which are invariant under the full orthogonal group (*i.e.*, isotropic). It is concluded that an isotropic function of the form $\Psi = \bar{\Psi}(\mathbf{C}, \mathbf{F}^{\mathrm{T}}\boldsymbol{\mathcal{E}}, \mathbf{F}^{\mathrm{T}}\mathbf{b}, \theta)$ can depend at most on the scalar arguments

$$\begin{aligned} &\mathrm{I}_{\mathbf{C}} \quad , \quad (\mathbf{F}^{\mathrm{T}}\boldsymbol{\mathcal{E}})\cdot(\mathbf{F}^{\mathrm{T}}\boldsymbol{\mathcal{E}}) \quad , \quad (\mathbf{F}^{\mathrm{T}}\boldsymbol{\mathcal{E}})\cdot(\mathbf{F}^{\mathrm{T}}\mathbf{b}) \quad , \quad (\mathbf{F}^{\mathrm{T}}\mathbf{b})\cdot(\mathbf{F}^{\mathrm{T}}\mathbf{b}) \quad , \\ &\mathrm{II}_{\mathbf{C}} \quad , \quad (\mathbf{F}^{\mathrm{T}}\boldsymbol{\mathcal{E}})\cdot\mathbf{C}(\mathbf{F}^{\mathrm{T}}\boldsymbol{\mathcal{E}}) \quad , \quad (\mathbf{F}^{\mathrm{T}}\boldsymbol{\mathcal{E}})\cdot\mathbf{C}(\mathbf{F}^{\mathrm{T}}\mathbf{b}) \quad , \quad (\mathbf{F}^{\mathrm{T}}\mathbf{b})\cdot\mathbf{C}(\mathbf{F}^{\mathrm{T}}\mathbf{b}) \quad , \\ &\mathrm{III}_{\mathbf{C}} \quad , \quad (\mathbf{F}^{\mathrm{T}}\boldsymbol{\mathcal{E}})\cdot\mathbf{C}^2(\mathbf{F}^{\mathrm{T}}\boldsymbol{\mathcal{E}}) \quad , \quad (\mathbf{F}^{\mathrm{T}}\boldsymbol{\mathcal{E}})\cdot\mathbf{C}^2(\mathbf{F}^{\mathrm{T}}\mathbf{b}) \quad , \quad (\mathbf{F}^{\mathrm{T}}\mathbf{b})\cdot\mathbf{C}^2(\mathbf{F}^{\mathrm{T}}\mathbf{b}) \quad , \quad \theta \quad . \end{aligned} \tag{4.78}$$

Here, $\mathrm{I}_{\mathbf{C}}$, $\mathrm{II}_{\mathbf{C}}$, and $\mathrm{III}_{\mathbf{C}}$ represent the principal invariants of $\mathbf{C}$ as defined in $(2.13)_{1-3}$. The arguments may alternatively be written in terms of the left CAUCHY-GREEN tensor $(2.70)_2$ as

$$\begin{aligned} &\mathrm{I}_{\mathbf{B}} \quad , \quad \boldsymbol{\mathcal{E}}\cdot\boldsymbol{\mathcal{E}} \quad , \quad \boldsymbol{\mathcal{E}}\cdot\mathbf{b} \quad , \quad \mathbf{b}\cdot\mathbf{b} \quad , \\ &\mathrm{II}_{\mathbf{B}} \quad , \quad \boldsymbol{\mathcal{E}}\cdot\mathbf{B}\boldsymbol{\mathcal{E}} \quad , \quad \boldsymbol{\mathcal{E}}\cdot\mathbf{B}\mathbf{b} \quad , \quad \mathbf{b}\cdot\mathbf{B}\mathbf{b} \quad , \\ &\mathrm{III}_{\mathbf{B}} \quad , \quad \boldsymbol{\mathcal{E}}\cdot\mathbf{B}^2\boldsymbol{\mathcal{E}} \quad , \quad \boldsymbol{\mathcal{E}}\cdot\mathbf{B}^2\mathbf{b} \quad , \quad \mathbf{b}\cdot\mathbf{B}^2\mathbf{b} \quad , \quad \theta \quad . \end{aligned} \tag{4.79}$$

Here, use was made of the CAYLEY-HAMILTON theorem (2.15) to express $\mathbf{B} = \mathbf{F}\mathbf{F}^{\mathrm{T}}$, $\mathbf{B}^2 = \mathbf{F}\mathbf{C}\mathbf{F}^{\mathrm{T}}$, and $\mathbf{B}^3 = \mathbf{F}\mathbf{C}^2\mathbf{F}^{\mathrm{T}}$ in (4.78) in terms of $\mathbf{i}$, $\mathbf{B}$, and $\mathbf{B}^2$ in Equations (4.79). The so-called *integrity bases* in (4.78) and (4.79) may be employed in the construction of form-invariant, isotropic constitutive relations. Less restrictive material symmetries, such as *transverse isotropy* or *orthotropy*, may be enforced by introducing so-called *structural* tensors, see ZHENG [158].

[24] Their summary is based on the work by PIPKIN and RIVLIN [118], SMITH [131], SPENCER and RIVLIN [135], WEYL [152] and others.

Chapter 5

Multiscale Modeling

In Chapters 2 - 4, integral forms of the balance equations of thermomechanics (TM), MAXWELL's equations of electromagnetism (EM), and the balance equations of coupled electro-magneto-thermo-mechanical (EMTM) materials were postulated. Thereafter, the local counterparts of the governing equations were deduced. In the presence of discontinuities, the local equations must be augmented with appropriate jump conditions arising from the localization of piece-wise smooth regions. However, in the context of this dissertations, it is assumed that the fields are sufficiently smooth for the integral theorems in Section 2.1.7 to hold everywhere in the body. This, in turn, implies that the continuum assumption, first introduced after Equation (2.109), must hold throughout.

In the continuum-on-continuum multiscale setting presented here, it is assumed that the microstructure is sufficiently separated in scale (both length and time) to allow for both the microscopic and the macroscopic scales to be treated as continua. It is thus required that the dimensions of the macroscopic problem far exceed the characteristic length of the microstructure, and that the macroscopic load duration allows perturbations to propagate well beyond the microscopic scale. Under such assumptions the continuum variables (such as density, polarization, or stress) sufficiently approximate the behavior of the body.

The constitutive relations of the continuum model are often quantified by experimental tests on macroscopic material samples. The makeup and arrangement of the microstructure, which gives rise to the macroscopic behavior measured, is thereby disregarded. However, in some cases the material properties of the microscale constituents are accessible to experimental testing (such as micro-indentation). It may thus be desirable to infer the bulk material response from the constitutive properties and morphology of the underlying microscale structure. When sufficient scale separation can be established between the micro- and macroscales, and if the continuum assumption holds on both scales, multiscale methods may be employed to obtain the macroscopic fields (such as stress, heat flux, or polarization) through homogenization of the microscopic variables, for example, see HILL [49,50], KOUZNETSOVA *et al.* [62,

63], Miehe *et al.* [95], and Özdemir *et al.* [162].

In this chapter, a multiscale homogenization method proposed in recent years by Mandadapu *et al.* [82] for thermomechanical behavior is extended to coupled electro-magneto-thermo-mechanical (EMTM) materials. Their approach is rooted in the seminal work by Irving and Kirkwood [57], who develop a method to derive continuum thermomechanical balance equations from the behavior at the molecular scale. Thereby, atomistic variables (such as the position and momentum used in the kinetic theory of gases, as well as intermolecular forces) are upscaled to obtain expressions for the stress and the heat flux of the continuum.

The work by Mandadapu *et al.* [82] extends the Irving-Kirkwood method to upscaling between two continuum scales. Homogenization is effected by prescribing a weighted volume-averaging scheme for the densities of the extensive quantities of mass, linear momentum, and total energy.[1] Due to the extensivity of these quantities, their macroscale densities per unit volume (*i.e.*, the mass density ρ, the linear momentum density $\rho\mathbf{v}$, and the total energy density ρe) are naturally expected to be volume averages of their microscale counterparts. Thus, they lend themselves to the prescription of a volume averaging homogenization scheme to relate the quantities between the two scales. The balance equations of the microscopic and macroscopic continua, along with the prescribed volume-averaging scheme, furnish homogenization formulae for the macroscopic stress, heat flux, body force, and body heating. A numerical implementation of this homogenization theory is presented by Mercer *et al.* [89] for the purely mechanical, quasistatic case and by Mercer *et al.* [90] for purely mechanical high-frequency wave propagation.

For the EMTM material described in this dissertation, the macroscopic densities of the extensive quantities of mass, linear momentum, total energy, total and bound electric charge, and magnetic 'monopole'[2] are attributed to the volume-averaging homogenization rule. Since both scales satisfy the continuum assumption, the behavior at each scale can be described by balance equations of the form derived in Chapter 4 as well as by Maxwell's equations. Therefore, the homogenization schemes for the stress tensor $\mathbf{T}$, the total external force density $\rho\mathbf{f}_{\mathrm{B}}+\mathbf{f}_{\mathrm{L}}$, the heat flux $\mathbf{q}$, and the total body heating $\rho r+\mathbf{j}\cdot\boldsymbol{\mathcal{E}}$ are inferred from a comparison between the linear momentum and energy balance equations at the two scales. The EM fields $\mathbf{d}$, $\mathbf{h}$, $\mathbf{e}$, $\mathbf{b}$, and the total current $\mathbf{J}$ are homogenized using the Maxwell equations in conjunction with the prescribed volume-averaging scheme for the total electric charge density q and the

[1] As first introduced in Section 2.3.1, an extensive property (*e.g.*, the linear momentum) is additive when non-intersecting material regions are combined. Note, however, that the density thereof (*e.g.*, the momentum density) is *not* extensive since the division of an extensive quantity by another extensive quantity (*e.g.*, the volume) yields an intensive variable.

[2] Magnetic monopoles are the magnetic counterpart of the electric charge. Experimental evidence suggests that magnetic dipoles physically always originate from looping currents or electron spin, hence magnetic monopoles are not known to exist. They are nevertheless considered an extensive quantity in the context of this theory, albeit always amounting to zero.

magnetic 'monopole' density. Likewise, homogenizations of the polarization $\mathbf{p}$ and MINKOWSKI magnetization $\mathbf{m}$ are obtained from the bound parts of MAXWELL's equations in conjunction with the volume-averaging scheme for the bound charge density q_{R}.

This chapter is organized as follows: First, the underlying assumptions and properties of the volume-averaging scheme are introduced. The homogenization scheme is then prescribed to the densities of the aforementioned extensive quantities. Thereafter, homogenization rules for the remaining variables are systematically obtained from the balance equations and MAXWELL's equations at the two scales.

5.1 Volume-Averaging Scheme

The scheme, according to which the aforementioned densities of extensive quantities shall be homogenized, is based on the method by MANDADAPU *et al.* [82]. In this section, the volume-averaging homogenization rule is introduced along with its postulated properties.

5.1.1 Overview

Consider a body which in the spatial configuration occupies the open, bounded material region $\mathcal{R}$. Let $\mathbf{y} \in \mathcal{R}$ denote the *position of a material point of the macroscopic scale*. Each point $\mathbf{y}$ is associated with a surrounding region on the microscopic scale, where a material point is denoted by the position $\mathbf{x} \in \mathcal{R}$. For a schematic representation of the two scales see Figure 5.1. The corresponding material velocities in the macro- and microscales are thus given by

$$\mathbf{v}^{\mathrm{M}}(\mathbf{y}, t) \;=\; \dot{\mathbf{y}} \quad \text{and} \quad \mathbf{v}^{\mathrm{m}}(\mathbf{x}, t) \;=\; \dot{\mathbf{x}} \quad , \tag{5.1}$$

respectively, where the superscripts $(\,\cdot\,)^{\mathrm{M}}$ and $(\,\cdot\,)^{\mathrm{m}}$ signify quantities in the macroscale and in the microscale, respectively.

Furthermore, let $\mathcal{G}^{\mathrm{m}}(\mathbf{x}, t)$ be the (real- or vector-valued) continuously differentiable density (per unit volume) of an extensive quantity defined at the microscopic scale in $\mathcal{R}$, say, for example, the linear momentum density $\rho^{\mathrm{m}}\mathbf{v}^{\mathrm{m}}$. Its macroscopic counterpart $\mathcal{G}^{\mathrm{M}}(\mathbf{y}, t)$ is defined by the *weighted volume-averaging homogenization scheme*

$$\mathcal{G}^{\mathrm{M}}(\mathbf{y}, t) \;=\; \int_{\mathcal{R}} \mathcal{G}^{\mathrm{m}}(\mathbf{x}, t)\, g(\mathbf{y}, \mathbf{x})\, \mathrm{d}v^{\mathrm{m}} \quad . \tag{5.2}$$

The preceding integral is evaluated for the independent variable $\mathbf{x}$ of the microscale, thus producing a macroscale function of $\mathbf{y}$. For any given macroscale point $\mathbf{y}$, the continuously differentiable function $g(\mathbf{y}, \mathbf{x})$ quantifies the weight of the contribution of $\mathcal{G}^{\mathrm{m}}(\mathbf{x}, t)$ at position $\mathbf{x}$ in the vicinity $\mathbf{y}$ to the macroscopic value $\mathcal{G}^{\mathrm{M}}(\mathbf{y}, t)$. It will

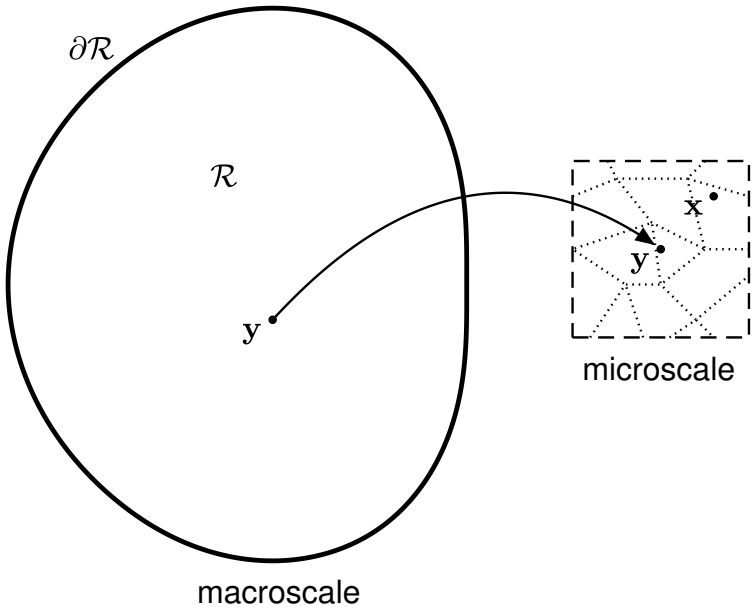

Figure 5.1: Schematic representation of the microscopic and macroscopic scales in the current configuration. At any given macroscopic point $\mathbf{y}$ the microscopic scale is represented by an RVE with points $\mathbf{x}$. Reproduced from MANDADAPU *et al.* [82].

be postulated later that $g(\mathbf{y},\mathbf{x})$ is non-zero only within a small subregion of $\mathcal{R}$. This subregion constitutes the *representative volume element* (RVE).

The volume-weighted average of the form (5.2) (rather than, say, a mass-weighted one) is a natural choice given that $\mathcal{G}^{\mathrm{m}}(\mathbf{x},t)$ represents an extensive quantity per unit volume. The density $\mathcal{G}^{\mathrm{M}}$ in the macroscopic scale, by the very definition of extensivity, constitutes the volumetric average of the corresponding microscopic density $\mathcal{G}^{\mathrm{m}}$. Alternatively, let an extensive quantity be expressed per unit mass $\mathcal{F}^{\mathrm{m}}(\mathbf{x},t)$ using the relation $\mathcal{G}^{\mathrm{m}}=\rho^{\mathrm{m}}\mathcal{F}^{\mathrm{m}}$, see also in (2.112). In this case, of course, the homogenization scheme in (5.2) may be viewed as a mass-weighted average of the *specific* quantity $\mathcal{F}^{\mathrm{m}}$,

$$\mathcal{F}^{\mathrm{M}}(\mathbf{y},t) \;=\; \int_{\mathcal{R}} \mathcal{F}^{\mathrm{m}}(\mathbf{x},t)\, f(\mathbf{y},\mathbf{x})\, \mathrm{d}v^{\mathrm{m}} \quad , \tag{5.3}$$

where the weighting function is replaced with $f(\mathbf{y},\mathbf{x})=\rho^{\mathrm{m}}(\mathbf{x},t)g(\mathbf{y},\mathbf{x})$.

5.1.2 Properties of the Weighting Function

The postulated properties of $g(\mathbf{y},\mathbf{x})$ are discussed in the following. Note that the conditions introduced in (i)-(v) are adopted identically from [82].

(i) Since the homogenization (5.2) represents a weighted volume average of $\mathcal{G}^{\mathrm{m}}(\mathbf{x},t)$, the weight density function $g(\mathbf{y},\mathbf{x})$ is normalized, that is,

$$\int_{\mathcal{R}} g(\mathbf{y},\mathbf{x})\, \mathrm{d}v^{\mathrm{m}} \;=\; 1 \quad . \tag{5.4}$$

This ensures, for example, that a uniform microscale distribution $\mathcal{G}^{\mathrm{m}}$ results in the same constant value for $\mathcal{G}^{\mathrm{M}}$, as to be expected from a consistent averaging scheme.

(ii) As part of the scale separation and continuum assumptions, it is required that

$$l^{\mathrm{m}} \ll \mathrm{supp}\big\{g(\mathbf{y},\mathbf{x})\big\} \ll \mathcal{R} \quad , \tag{5.5}$$

where l^{m} represents the characteristic length of the microstructure and the support[3] of $g(\mathbf{y},\mathbf{x})$ is denoted by $\mathrm{supp}\{g(\mathbf{y},\mathbf{x})\}$. Therefore, the weighted average for $\mathcal{G}^{\mathrm{M}}$ encompasses a sufficiently large region of the microstructure to be considered continuous, yet small enough compared to the overall size of the macroscale body $\mathcal{R}$ for a good spatial resolution of the macroscopic problem.

(iii) This property of $g(\mathbf{y},\mathbf{x})$ concerns the locality of $\mathcal{G}^{\mathrm{M}}$. It is assumed that the value of $\mathcal{G}^{\mathrm{M}}(\mathbf{y},t)$ is more sensitive to contributions $\mathcal{G}^{\mathrm{m}}(\mathbf{x},t)$ of points $\mathbf{x}$ close to $\mathbf{y}$. In particular, it is required that

$$g(\mathbf{y},\mathbf{x}) \quad \text{attains a maximum when} \quad \mathbf{x} \equiv \mathbf{y} \quad . \tag{5.6}$$

(iv) It is assumed for practical purposes that the averaging scheme in (5.2) encompasses only interior locations $\mathbf{x}$, so that

$$g(\mathbf{y},\mathbf{x}) \,=\, 0 \quad \text{on} \quad \partial\mathcal{R} \quad \text{when} \quad \mathbf{y} \in \mathcal{R} \quad . \tag{5.7}$$

The value of $\mathcal{G}^{\mathrm{M}}$ at $\mathbf{y}$ is thus unaffected by $\mathcal{G}^{\mathrm{m}}$ on the boundary.

(v) Lastly, it is postulated that the function $g(\mathbf{y},\mathbf{x})$ is invariant under superposed rigid-body motions, that is,

$$g(\mathbf{y},\mathbf{x}) \,=\, g^{+}(\mathbf{y}^{+},\mathbf{x}^{+}) \,=\, g(\mathbf{y}^{+},\mathbf{x}^{+}) \quad . \tag{5.8}$$

Equation (5.8) implies that

$$g(\mathbf{y},\mathbf{x}) \,=\, g(\mathbf{Q}\mathbf{y}+\mathbf{c},\mathbf{Q}\mathbf{x}+\mathbf{c}) \quad \forall\, \mathbf{Q}(t) \in \mathrm{Orth}^{+} \quad , \quad \forall\, \mathbf{c}(t) \in E^{3} \quad , \tag{5.9}$$

where the transformation in (2.153) was used for SRBM of the locations $\mathbf{x}^{+}$ and $\mathbf{y}^{+}$ at both scales. For relation (5.9) to hold under all translations $\mathbf{c}(t)$, the function

[3]The support is defined as follows: First define $\mathrm{supp}\{g(\mathbf{y}_0,\mathbf{x})\}$ for a fixed macroscale point $\mathbf{y}_0 \in \mathcal{R}$. The support of $g(\mathbf{y}_0,\mathbf{x})$ is understood to be the characteristic length of the smallest possible subregion $\mathcal{P}^{\mathrm{m}} \subset \mathcal{R}$ of the body $\mathcal{R}$, for which the points $\mathbf{x} \in \mathcal{P}^{\mathrm{m}}$ map to a non-zero value of $g(\mathbf{y}_0,\mathbf{x})$. Therefore, the support of $g(\mathbf{y},\mathbf{x})$ denotes the characteristic length obtained in this way for all macroscale points $\mathbf{y} \in \mathcal{R}$.

may depend only on the relative position $\mathbf{x}-\mathbf{y}$. The condition for form-invariance simplifies to

$$\check{g}(\mathbf{x}-\mathbf{y}) \;=\; \check{g}(\mathbf{x}^{+}-\mathbf{y}^{+}) \;=\; \check{g}(\mathbf{Q}(\mathbf{x}-\mathbf{y})) \quad \forall\, \mathbf{Q}(t)\in \mathrm{Orth}^{+} \quad . \tag{5.10}$$

Note that this is a special case of the representation theorem in (4.78) where the function depends only on a single, vector-valued argument. Equation (5.10) is satisfied for all proper orthogonal $\mathbf{Q}(t)$ only when g depends solely on the norm $|\mathbf{x}-\mathbf{y}|$ but not its direction, see Truesdell and Noll [146, Chapter B.II]. It is therefore concluded that $g(\mathbf{y},\mathbf{x})$ is a spherically symmetric function of $\mathbf{x}$ centered around a given $\mathbf{y}$.[4] This is functionally represented by the real-valued argument $\bar{g}(|\mathbf{x}-\mathbf{y}|)$, from which it follows that gradients with respect to $\mathbf{x}$ and $\mathbf{y}$ are related by

$$\mathrm{grad}_{\mathbf{x}}\, g(\mathbf{y},\mathbf{x}) \;=\; -\mathrm{grad}_{\mathbf{y}}\, g(\mathbf{y},\mathbf{x}) \quad . \tag{5.11}$$

The material time derivative $\dot{g}(\mathbf{y},\mathbf{x}) = \mathrm{grad}_{\mathbf{y}}\, g(\mathbf{y},\mathbf{x})\cdot\dot{\mathbf{y}} + \mathrm{grad}_{\mathbf{x}}\, g(\mathbf{y},\mathbf{x})\cdot\dot{\mathbf{x}}$ is thus related to the velocities (5.1) via

$$\dot{g}(\mathbf{y},\mathbf{x}) \;=\; -\mathrm{grad}_{\mathbf{y}}\, g(\mathbf{y},\mathbf{x})\cdot\big(\mathbf{v}^{\mathrm{m}}-\mathbf{v}^{\mathrm{M}}\big) \;=\; \mathrm{grad}_{\mathbf{x}}\, g(\mathbf{y},\mathbf{x})\cdot\big(\mathbf{v}^{\mathrm{m}}-\mathbf{v}^{\mathrm{M}}\big) \quad , \tag{5.12}$$

where $(\mathbf{v}^{\mathrm{m}}-\mathbf{v}^{\mathrm{M}})$ may be interpreted as a deviation of the microscale velocity $\mathbf{v}^{\mathrm{m}}$ from the local 'average' $\mathbf{v}^{\mathrm{M}}$.

In the multiscale context a subscript is attached to differential operators to clarify whether the operation is to be performed with respect to the micro- or macroscale position, such as in Equation (5.11 - 12). For example, $\mathrm{Div}_{\mathbf{Y}}(\,\cdot\,)$ represents a divergence with respect to the referential macroscopic location $\mathbf{Y}$. Despite the preceding results, the weighting function will simply be denoted $g(\mathbf{y},\mathbf{x})$ with the tacit understanding that the function can be written in terms of the real-valued argument $\bar{g}(|\mathbf{x}-\mathbf{y}|)$.

Note that the assumptions in (5.4 - 8) are at odds with each other when $\mathbf{y}$ is close to the boundary. Condition (5.7) implies that the support of $g(\mathbf{y},\mathbf{x})$ must narrow so as not to include any boundary contribution from $\mathbf{x}\in\partial\mathcal{R}$. In the limit as $\mathbf{y}$ approaches $\partial\mathcal{R}$, the weight density $g(\mathbf{y},\mathbf{x})$ becomes a Dirac *delta function* (also known as *δ-distribution*) and no averaging takes place. This is in violation of the continuum assumption in (5.5), according to which the support of $g(\mathbf{y},\mathbf{x})$ is much larger than the underlying microstructure. Moreover, it was concluded from the form-invariance property in (5.8) that the weight density can be functionally dependent only of the distance $|\mathbf{x}-\mathbf{y}|$ but not its absolute position. This implies that $g(\mathbf{y},\mathbf{x})$ cannot vary across the body so that the *same* homogenization weights apply everywhere in $\mathcal{R}$.

[4] This picture is based on the premise that any given point $\mathbf{y}$ of the macroscale is surrounded by a region of microstructure, where $g(\mathbf{y},\mathbf{x})$ weighs the contribution $\mathcal{G}^{\mathrm{m}}(\mathbf{x},t)$ to the average $\mathcal{G}^{\mathrm{M}}(\mathbf{y},t)$. It is of course mathematically equally valid to interpret $g(\mathbf{y},\mathbf{x})$ as a spherically symmetric function of $\mathbf{y}$ around a fixed $\mathbf{x}$.

The aforementioned shortcomings of the homogenization scheme near the boundary can be rectified, for example, by additionally allowing $g(\mathbf{y},\mathbf{x})$ to depend on the position of the nearest point on the boundary $\partial\mathcal{R}$ relative to any given macroscale point $\mathbf{y}$. Since such a vector is objective, the form-invariance in (5.8) would not be compromised. Thus by relaxing the restrictions on $g(\mathbf{y},\mathbf{x})$ with regard to its spherical symmetry and uniformity across $\mathcal{R}$, the assumptions in (5.4 - 8) become mutually compatible. However, in the interest of simplicity, the inconsistency at the boundary is disregarded in the context of this dissertation with the understanding that the homogenization scheme is valid only in interior regions.

5.1.3 Useful Corollaries Involving the Weighting Function

The properties of the weighting function postulated in Section 5.1.2 give rise to a number of useful corollaries for the homogenization of quantities involving differential operators. In particular, the property in (5.7) is exploited to eliminate boundary integrals, while (5.11) is used to transform microscopic derivatives to macroscopic ones. The relations derived here afford a seamless conversion between differential operators in the two scales. They will be employed repeatedly in Section 5.4, where the balance equations as well as the MAXWELL equations are homogenized.

Let $\mathbf{w}^{\mathrm{m}}(\mathbf{x})$ represent a continuously differentiable vector-valued spatial quantity on the microscopic scale, and let $\mathbf{w}^{\mathrm{M}}(\mathbf{y})$ denote its macroscopic counterpart. It is irrelevant for the upcoming argument whether or not the fields are also time-dependent. It is seen that the homogenization of the microscale divergence $\mathrm{div}_{\mathbf{x}}\,\mathbf{w}^{\mathrm{m}}$ can be expressed as

$$\begin{aligned}
\int_{\mathcal{R}} \big(\mathrm{div}_{\mathbf{x}}\,\mathbf{w}^{\mathrm{m}}\big)\, g(\mathbf{y},\mathbf{x})\,\mathrm{d}v^{\mathrm{m}} &= \int_{\mathcal{R}} \Big\{\mathrm{div}_{\mathbf{x}}\big(\mathbf{w}^{\mathrm{m}} g(\mathbf{y},\mathbf{x})\big) - \mathbf{w}^{\mathrm{m}}\cdot\mathrm{grad}_{\mathbf{x}}\, g(\mathbf{y},\mathbf{x})\Big\}\,\mathrm{d}v^{\mathrm{m}} \\
&= \int_{\partial\mathcal{R}} \mathbf{w}^{\mathrm{m}}\, \underbrace{g(\mathbf{y},\mathbf{x})}_{=0}\cdot\mathbf{n}^{\mathrm{m}}\,\mathrm{d}a^{\mathrm{m}} + \int_{\mathcal{R}} \mathbf{w}^{\mathrm{m}}\cdot\mathrm{grad}_{\mathbf{y}}\, g(\mathbf{y},\mathbf{x})\,\mathrm{d}v^{\mathrm{m}} \\
&= \int_{\mathcal{R}} \Big\{\mathrm{div}_{\mathbf{y}}\big(\mathbf{w}^{\mathrm{m}} g(\mathbf{y},\mathbf{x})\big) - \underbrace{\big(\mathrm{div}_{\mathbf{y}}\,\mathbf{w}^{\mathrm{m}}\big)}_{=0}\, g(\mathbf{y},\mathbf{x})\Big\}\,\mathrm{d}v^{\mathrm{m}} \\
&= \mathrm{div}_{\mathbf{y}}\Big\{\int_{\mathcal{R}} \mathbf{w}^{\mathrm{m}} g(\mathbf{y},\mathbf{x})\,\mathrm{d}v^{\mathrm{m}}\Big\} \quad , \qquad (5.13)
\end{aligned}$$

i.e., the weighted volume-average of the divergence of $\mathbf{w}^{\mathrm{m}}$ is equal to the divergence of the weighted volume-average of $\mathbf{w}^{\mathrm{m}}$. This result is achieved as follows: First, the integrand $(\mathrm{div}_{\mathbf{x}}\,\mathbf{w}^{\mathrm{m}})g(\mathbf{y},\mathbf{x})$ is expanded into a boundary integral plus a term involving $\mathrm{grad}_{\mathbf{x}}\, g(\mathbf{y},\mathbf{x})$ by appealing to the identity in $(2.46)_1$ and the standard form of the divergence theorem (2.50). The former vanishes on account of the boundary property in (5.7), whereas the latter is converted into a macroscopic gradient $\mathrm{grad}_{\mathbf{y}}\, g(\mathbf{y},\mathbf{x})$ by application of the property in (5.11). The product rule in $(2.46)_1$ is reapplied, this

time with respect to the macroscopic position $\mathbf{y}$, to convert the gradient back into a divergence. However, the term $\operatorname{div}_{\mathbf{y}} \mathbf{w}^{\mathrm{m}}$ vanishes because the microscopic quantity $\mathbf{w}^{\mathrm{m}}$ is functionally independent of $\mathbf{y}$. Likewise, the divergence operator can be removed from the integral since the integral domain $\int_{\mathcal{R}} (\,\cdot\,)\,\mathrm{d}v^{\mathrm{m}}$ is microscopic and thus independent of $\mathbf{y}$, thus furnishing the result in (5.13).

Next, consider the homogenization of the microscale quantity $\operatorname{curl}_{\mathbf{x}} \mathbf{w}^{\mathrm{m}}$. An identical line of argument furnishes the property

$$\begin{aligned}
\int_{\mathcal{R}} \big(\operatorname{curl}_{\mathbf{x}} \mathbf{w}^{\mathrm{m}}\big)\, g(\mathbf{y},\mathbf{x})\,\mathrm{d}v^{\mathrm{m}} &= \int_{\mathcal{R}} \Big\{\operatorname{curl}_{\mathbf{x}}\big(\mathbf{w}^{\mathrm{m}} g(\mathbf{y},\mathbf{x})\big) - \operatorname{grad}_{\mathbf{x}} g(\mathbf{y},\mathbf{x}) \times \mathbf{w}^{\mathrm{m}}\Big\}\,\mathrm{d}v^{\mathrm{m}} \\
&= \int_{\partial\mathcal{R}} \mathbf{n}^{\mathrm{m}} \times \mathbf{w}^{\mathrm{m}} \underbrace{g(\mathbf{y},\mathbf{x})}_{=0}\,\mathrm{d}a^{\mathrm{m}} + \int_{\mathcal{R}} \operatorname{grad}_{\mathbf{y}} g(\mathbf{y},\mathbf{x}) \times \mathbf{w}^{\mathrm{m}}\,\mathrm{d}v^{\mathrm{m}} \\
&= \int_{\mathcal{R}} \Big\{\operatorname{curl}_{\mathbf{y}}\big(\mathbf{w}^{\mathrm{m}} g(\mathbf{y},\mathbf{x})\big) - \underbrace{\big(\operatorname{curl}_{\mathbf{y}} \mathbf{w}^{\mathrm{m}}\big)}_{=0}\, g(\mathbf{y},\mathbf{x})\Big\}\,\mathrm{d}v^{\mathrm{m}} \\
&= \operatorname{curl}_{\mathbf{y}}\Big\{\int_{\mathcal{R}} \mathbf{w}^{\mathrm{m}} g(\mathbf{y},\mathbf{x})\,\mathrm{d}v^{\mathrm{m}}\Big\} \quad . \qquad (5.14)
\end{aligned}$$

It is thus concluded that the weighted volume-average of the curl of $\mathbf{w}^{\mathrm{m}}$ corresponds to the curl of the weighted volume-average of $\mathbf{w}^{\mathrm{m}}$. Here, the product rule for the curl in $(2.47)_1$ and the corollary of the divergence theorem in (2.51) were used to expand the integrand into a boundary integral plus a term involving $\operatorname{grad}_{\mathbf{x}} g(\mathbf{y},\mathbf{x})$. As before, the boundary term vanishes on account of (5.7). The gradient is written in terms of $\mathbf{y}$ using (5.11) and converted to the curl by reapplication of (2.51). Lastly, the independence of the microscopic quantities $\mathbf{w}^{\mathrm{m}}$ and $\mathrm{d}v^{\mathrm{m}}$ from the macroscopic position $\mathbf{y}$ is exploited to obtain the result in Equation (5.14).

The last property concerns the homogenization of the divergence of a continuously differentiable tensor field $\mathbf{T}^{\mathrm{m}}(\mathbf{x})$,[5] which may or may not be time-dependent. It is readily seen using the product rule in $(2.46)_2$ along with the tensorial statement of

[5]Note that in the context of this derivation $\mathbf{T}^{\mathrm{m}}$ denotes an arbitrary tensor-valued quantity not limited to the CAUCHY stress. Nevertheless, no effort is made here to generalize the notation because this property will indeed be applied only to the CAUCHY stress.

the divergence theorem in (2.52), that

$$\begin{aligned}\int_{\mathcal{R}} \big(\operatorname{div}_{\mathbf{x}} \mathbf{T}^{\mathrm{m}}\big) g(\mathbf{y},\mathbf{x})\,\mathrm{d}v^{\mathrm{m}} &= \int_{\mathcal{R}} \Big\{\operatorname{div}_{\mathbf{x}}\big[\mathbf{T}^{\mathrm{m}} g(\mathbf{y},\mathbf{x})\big] - \mathbf{T}^{\mathrm{m}} \operatorname{grad}_{\mathbf{x}} g(\mathbf{y},\mathbf{x})\Big\}\,\mathrm{d}v^{\mathrm{m}} \\ &= \int_{\partial\mathcal{R}} \mathbf{T}^{\mathrm{m}} \underbrace{g(\mathbf{y},\mathbf{x})}_{=0} \mathbf{n}^{\mathrm{m}}\,\mathrm{d}a^{\mathrm{m}} + \int_{\mathcal{R}} \mathbf{T}^{\mathrm{m}} \operatorname{grad}_{\mathbf{y}} g(\mathbf{y},\mathbf{x})\,\mathrm{d}v^{\mathrm{m}} \\ &= \int_{\mathcal{R}} \Big\{\operatorname{div}_{\mathbf{y}}\big[\mathbf{T}^{\mathrm{m}} g(\mathbf{y},\mathbf{x})\big] - \underbrace{\big(\operatorname{div}_{\mathbf{y}} \mathbf{T}^{\mathrm{m}}\big)}_{=0} g(\mathbf{y},\mathbf{x})\Big\}\,\mathrm{d}v^{\mathrm{m}} \\ &= \operatorname{div}_{\mathbf{y}}\Big\{\int_{\mathcal{R}} \mathbf{T}^{\mathrm{m}} g(\mathbf{y},\mathbf{x})\,\mathrm{d}v^{\mathrm{m}}\Big\} \quad . \end{aligned} \tag{5.15}$$

This result states that the weighted volume-average of the divergence of a tensor is equal to the divergence of the weighted volume-average thereof. The derivation in (5.15) is not narrated here since it employs the same strategy used in (5.13 - 14).

5.2 Postulated Homogenization of Extensive Variables

As previously argued, extensive variables naturally lend themselves to a volume-averaging homogenization method because their macroscopic densities constitute volumetric averages of their microscopic counterparts. However, not *all* ostensibly extensive quantities can simultaneously be associated with this averaging method, for this would inevitably lead to inconsistencies that would contradict the balance equations or other relations of the homogenized continuum. One such example of a conflicting choice is between total and internal energy, see later in Equation (5.90). This is to say that the variables which are prescribed with the volume-averaging homogenization scheme in (5.2) should be chosen judiciously.

In the prior work by Mandadapu *et al.* [82] it is postulated that the densities of the extensive variables of mass, linear momentum, and total (kinetic plus internal) energy homogenize according to (5.2). To incorporate the electromagnetic aspect of the materials studied in this dissertation, the densities of the total and bound electric charges and of the 'magnetic monopoles' are further added to this list. The homogenized macroscopic fields are thus given by

(a) the mass density ρ,

$$\rho^{\mathrm{M}}(\mathbf{y},t) = \int_{\mathcal{R}} \rho^{\mathrm{m}}(\mathbf{x},t)\, g(\mathbf{y},\mathbf{x})\,\mathrm{d}v^{\mathrm{m}} \quad , \tag{5.16}$$

(b) the linear momentum density $\rho\mathbf{v}$,

$$\rho^{\mathrm{M}}(\mathbf{y},t)\,\mathbf{v}^{\mathrm{M}}(\mathbf{y},t) = \int_{\mathcal{R}} \rho^{\mathrm{m}}(\mathbf{x},t)\,\mathbf{v}^{\mathrm{m}}(\mathbf{x},t)\, g(\mathbf{y},\mathbf{x})\,\mathrm{d}v^{\mathrm{m}} \quad , \tag{5.17}$$

(c) the total energy density,

$$\rho^{\mathrm{M}}(\mathbf{y},t)\,e^{\mathrm{M}}(\mathbf{y},t) \;=\; \int_{\mathcal{R}} \rho^{\mathrm{m}}(\mathbf{x},t)\,e^{\mathrm{m}}(\mathbf{x},t)\,g(\mathbf{y},\mathbf{x})\,\mathrm{d}v^{\mathrm{m}} \quad , \tag{5.18}$$

(d) the total electric charge density q,

$$q^{\mathrm{M}}(\mathbf{y},t) \;=\; \int_{\mathcal{R}} q^{\mathrm{m}}(\mathbf{x},t)\,g(\mathbf{y},\mathbf{x})\,\mathrm{d}v^{\mathrm{m}} \quad , \tag{5.19}$$

(e) and the bound electric charge density q_{R},

$$q_{\mathrm{R}}^{\mathrm{M}}(\mathbf{y},t) \;=\; \int_{\mathcal{R}} q_{\mathrm{R}}^{\mathrm{m}}(\mathbf{x},t)\,g(\mathbf{y},\mathbf{x})\,\mathrm{d}v^{\mathrm{m}} \quad . \tag{5.20}$$

It is mentioned that, in view of the postulated homogenization of the mass density in (5.16), Equations (5.17) and (5.18) may equivalently be regarded as definitions for the homogenization of $\mathbf{v}^{\mathrm{M}}(\mathbf{y},t)$ and $e^{\mathrm{M}}(\mathbf{y},t)$, respectively. This is explored in more detail in Section 5.4.8. The critical point, however, is that homogenization is volume averaged only for the densities of *extensive* quantities (of which velocity is not one, but linear momentum is). Homogenization formulae for such (non-extensive) quantities may be derived if desired, but are not needed for the solution of the boundary-value problem of the homogenized macroscopic scale.

Recall that, unlike Gauss' law $(3.6)_1$ for the charge potential, the magnetic counterpart in (3.10) does not feature any source terms. Such 'magnetic monopoles', if they indeed existed, would be considered extensive akin to (5.20). Hence, it is assumed *a priori* that 'magnetic monopoles' vanish on both scales. An analogy is drawn between electric charge *versus* 'magnetic monopoles', as well as their respective potentials $\mathbf{d}$ and $\mathbf{b}$. This approach will be used in Section 5.4.5 to obtain a homogenization rule for the magnetic flux density $\mathbf{b}^{\mathrm{M}}(\mathbf{y},t)$, as well as in Section 5.4.6 for the magnetization density $\mathbf{m}^{\mathrm{M}}(\mathbf{y},t)$.

It is emphasized that the homogenization of total energy in (5.18) refers to the kinetic plus the internal energy, see the definition in (2.122). According to the integral form of the principle of energy balance in (4.17) for coupled EMTM materials, the electromagnetic energy is *not* considered part of the total energy. Instead, the energy balance accounts for the power $\mathbf{J}\cdot\mathbf{e}$ of the EM fields imparted on the body due to the effect of the surrounding electromagnetic field on electric charges contained in the body, which affects the balance of total (kinetic and thermal) energy. Therefore, according to this viewpoint, the EM fields are *not* considered part of the body and the EM energy itself is *not* included in the energy balance. Instead, electromagnetism only affects the balances of momenta and energy through the interactions of the EM fields with the charges contained in the body.[6] The postulated homogenizations in

[6]This point of view is opposed to the alternative representation, employed by Kovetz [64] and others, of the balance laws discussed in Appendix A.6. In particluar, Equation (A.43) states the energy balance for the combined kinetic, internal, and electromagnetic parts, that is, $\frac{1}{2}\mathbf{v}\cdot\mathbf{v}+\varepsilon+u/\rho$.

Equations (5.18) and (5.19) represent a natural extension of this viewpoint, whereby the total (kinetic and thermal) energy and the electric charges are assumed to be extensive quantities, whereas the EM part of the energy is viewed as external to the body and thus not extensive.

5.3 Multiscale Balance Equations

Both the microscopic and macroscopic scales are assumed to independently satisfy the continuum assumption. As previously discussed, this requires sufficient scale separation (both in space and time) along with the property in (5.5) concerning the characteristic length of the support of the weight density $g(\mathbf{y}, \mathbf{x})$. If the continuum requirements are met, it is expected that MAXWELL's equations presented in Chapter 3 and the balance equations of Section 4 are valid at both scales. These governing equations form the basis for the derivation of homogenization rules for the remaining electromagnetic and thermomechanical variables using the postulated volumetric averages of the extensive quantities in Section 5.2.

In particular, the integral form of the statement of conservation of mass (2.110), linear momentum (4.5), angular momentum (4.7), and energy (4.17) are adopted identically for the microscopic and macroscopic scales of the multiscale model. Likewise, the integral forms of MAXWELL's Equations $(3.6)_{1,2}$, (3.9), and (3.10) are assumed to apply on both scales, which implies that the principle of charge conservation in (3.2) is valid, too. Lastly, it is assumed that the polarization and magnetization satisfy the first pair of MAXWELL's Equations on both scales, see the integral statements in (3.16) and $(3.99)_1$.

In the interest of brevity, the aforementioned integral statements are not repeated here. Of course, all previous quantities $(\,\cdot\,)$ are now given by functions $(\,\cdot\,)^{\mathrm{m}}(\mathbf{x}, t)$ and $(\,\cdot\,)^{\mathrm{M}}(\mathbf{y}, t)$ depending on their scale. Volumetric balance statements are expressed in terms of integrals over arbitrary (open, bounded) material subregions $\mathcal{P}^{\mathrm{m}} \subset \mathcal{R}$ or $\mathcal{P}^{\mathrm{M}} \subset \mathcal{R}$ and their (smooth) boundaries $\partial\mathcal{P}^{\mathrm{m}}$ or $\partial\mathcal{P}^{\mathrm{M}}$, respectively. Meanwhile, balances of flux integrals are stated with respect to arbitrary (open, bounded) material surfaces $\mathcal{A}^{\mathrm{m}}$ or $\mathcal{A}^{\mathrm{M}}$ and their (smooth) boundaries $\mathcal{C}^{\mathrm{m}}$ or $\mathcal{C}^{\mathrm{M}}$. Differential operators are understood to act with respect to either the micro- or macroscale position, $\mathbf{x}$ or $\mathbf{y}$, and are equipped with a corresponding subscript to avoid confusion, such as $\mathrm{div}_{\mathbf{x}}(\,\cdot\,)$ or $\mathrm{Curl}_{\mathbf{Y}}(\,\cdot\,)$.

Lastly, it is noted that the conclusions drawn in Section 2.1 for the identities and integral theorems of tensor calculus as well as in Section 2.2 for the kinematics are valid for the continuum at both scales. Since the divergence, localization, and REYNOLDS' transport theorems are applicable on both scales, the integral forms of the governing equations are readily converted into their local expressions. The relevant microscopic and macroscopic equations are briefly summarized here in preparation for the homogenization in Section 5.4.

5.3.1 Microscopic Scale

In the multiscale setting, the microscopic scale represents the most fundamental level for which the continuum approximation holds. It is thus assumed *a priori* that all governing equations and definitions introduced in Chapters 3 and 4 must hold, of which the most important results are listed in the following. In particular, the local forms of the balances of mass (2.111), linear momentum (4.6), and energy (4.18) are given by

$$\begin{aligned}
\dot{\rho}^{\mathrm{m}}(\mathbf{x},t) &= -\rho^{\mathrm{m}}(\mathbf{x},t)\,\mathrm{div}_{\mathbf{x}}\big\{\mathbf{v}^{\mathrm{m}}(\mathbf{x},t)\big\} \quad , \\
\rho^{\mathrm{m}}(\mathbf{x},t)\,\dot{\mathbf{v}}^{\mathrm{m}}(\mathbf{x},t) &= \mathrm{div}_{\mathbf{x}}\big\{\mathbf{T}^{\mathrm{m}}(\mathbf{x},t)\big\} + \rho^{\mathrm{m}}(\mathbf{x},t)\,\mathbf{f}_{\mathrm{B}}^{\mathrm{m}}(\mathbf{x},t) + \mathbf{f}_{\mathrm{L}}^{\mathrm{m}}(\mathbf{x},t) \quad , \\
\rho^{\mathrm{m}}(\mathbf{x},t)\,\dot{e}^{\mathrm{m}}(\mathbf{x},t) &= \mathrm{div}_{\mathbf{x}}\big\{\big[\mathbf{T}^{\mathrm{m}}(\mathbf{x},t)\big]^{\mathrm{T}}\mathbf{v}^{\mathrm{m}}(\mathbf{x},t)\big\} + \big\{\rho^{\mathrm{m}}(\mathbf{x},t)\,\mathbf{f}_{\mathrm{B}}^{\mathrm{m}}(\mathbf{x},t)+\mathbf{f}_{\mathrm{L}}^{\mathrm{m}}(\mathbf{x},t)\big\}\cdot\mathbf{v}^{\mathrm{m}}(\mathbf{x},t) \\
&\quad - \mathrm{div}_{\mathbf{x}}\big\{\mathbf{q}^{\mathrm{m}}(\mathbf{x},t)\big\} + \rho^{\mathrm{m}}(\mathbf{x},t)\,r^{\mathrm{m}}(\mathbf{x},t) + \mathbf{j}^{\mathrm{m}}(\mathbf{x},t)\cdot\boldsymbol{\mathcal{E}}^{\mathrm{m}}(\mathbf{x},t) \quad ,
\end{aligned} \tag{5.21}$$

respectively, where the definition in (2.122) was used for the total energy density $\rho^{\mathrm{m}}e^{\mathrm{m}}$. Note that Equation $(5.21)_3$ differs from (4.18) in that the power of the EM fields is split into its objective and non-objective parts. This is achieved using the microscopic version of (4.16) for the EM power density,

$$\mathbf{J}^{\mathrm{m}}(\mathbf{x},t)\cdot\mathbf{e}^{\mathrm{m}}(\mathbf{x},t) = \mathbf{j}^{\mathrm{m}}(\mathbf{x},t)\cdot\boldsymbol{\mathcal{E}}^{\mathrm{m}}(\mathbf{x},t) + \mathbf{f}_{\mathrm{L}}^{\mathrm{m}}(\mathbf{x},t)\cdot\mathbf{v}^{\mathrm{m}}(\mathbf{x},t) \quad . \tag{5.22}$$

Recall that this relation was derived in (4.16) solely using the definitions of the total current density $(3.4)_2$, the electromotive intensity (3.68), and the Lorentz force (4.2), which are given in the microscopic scale by

$$\begin{aligned}
\mathbf{J}^{\mathrm{m}}(\mathbf{x},t) &= \mathbf{j}^{\mathrm{m}}(\mathbf{x},t) + q^{\mathrm{m}}(\mathbf{x},t)\,\mathbf{v}^{\mathrm{m}}(\mathbf{x},t) \quad , \\
\boldsymbol{\mathcal{E}}^{\mathrm{m}}(\mathbf{x},t) &= \mathbf{e}^{\mathrm{m}}(\mathbf{x},t) + \mathbf{v}^{\mathrm{m}}(\mathbf{x},t)\times\mathbf{b}^{\mathrm{m}}(\mathbf{x},t) \quad , \\
\mathbf{f}_{\mathrm{L}}^{\mathrm{m}}(\mathbf{x},t) &= q^{\mathrm{m}}(\mathbf{x},t)\,\mathbf{e}^{\mathrm{m}}(\mathbf{x},t) + \mathbf{J}^{\mathrm{m}}(\mathbf{x},t)\times\mathbf{b}^{\mathrm{m}}(\mathbf{x},t) \quad .
\end{aligned} \tag{5.23}$$

Of course, Equations (5.22) and $(5.23)_{1,3}$ are satisfied separately by the free and bound parts of q^{M} and $\mathbf{j}^{\mathrm{M}}$ as well.

The local forms of Maxwell's Equations $(3.15)_{1-4}$ are reproduced on the microscopic scale according to

$$\begin{aligned}
q^{\mathrm{m}}(\mathbf{x},t) &= \mathrm{div}_{\mathbf{x}}\big\{\mathbf{d}^{\mathrm{m}}(\mathbf{x},t)\big\} \quad , \\
\mathbf{J}^{\mathrm{m}}(\mathbf{x},t) + \frac{\partial}{\partial t}\big\{\mathbf{d}^{\mathrm{m}}(\mathbf{x},t)\big\} &= \mathrm{curl}_{\mathbf{x}}\big\{\mathbf{h}^{\mathrm{m}}(\mathbf{x},t)\big\} \quad , \\
\frac{\partial}{\partial t}\big\{\mathbf{b}^{\mathrm{m}}(\mathbf{x},t)\big\} &= -\mathrm{curl}_{\mathbf{x}}\big\{\mathbf{e}^{\mathrm{m}}(\mathbf{x},t)\big\} \quad , \\
0 &= \mathrm{div}_{\mathbf{x}}\big\{\mathbf{b}^{\mathrm{m}}(\mathbf{x},t)\big\} \quad .
\end{aligned} \tag{5.24}$$

They comprise Gauss' law, Ampère's circuital law, Faraday's law of induction, and Gauss' law for magnetism. Equations $(5.24)_{1,2}$ pertain to the *total* fields, which

decompose additively into the free and bound parts. For polarizable ($\mathbf{d}_{\mathrm{R}} = -\mathbf{p}$) or magnetizable ($\mathbf{h}_{\mathrm{R}} = \mathbf{m}$) materials, the first pair of MAXWELL's equations is given separately according to Equations $(3.33)_{1,2}$ and $(3.34)_{1,2}$ by

$$\begin{aligned} q^{\mathrm{m}}_{\mathrm{F}}(\mathbf{x},t) &= \mathrm{div}_{\mathbf{x}}\big\{\mathbf{d}^{\mathrm{m}}_{\mathrm{F}}(\mathbf{x},t)\big\} \quad , \quad \mathbf{J}^{\mathrm{m}}_{\mathrm{F}}(\mathbf{x},t) + \frac{\partial}{\partial t}\big\{\mathbf{d}^{\mathrm{m}}_{\mathrm{F}}(\mathbf{x},t)\big\} = \mathrm{curl}_{\mathbf{x}}\big\{\mathbf{h}^{\mathrm{m}}_{\mathrm{F}}(\mathbf{x},t)\big\} \quad , \\ q^{\mathrm{m}}_{\mathrm{R}}(\mathbf{x},t) &= -\mathrm{div}_{\mathbf{x}}\big\{\mathbf{p}^{\mathrm{m}}(\mathbf{x},t)\big\} \quad , \quad \mathbf{J}^{\mathrm{m}}_{\mathrm{R}}(\mathbf{x},t) - \frac{\partial}{\partial t}\big\{\mathbf{p}^{\mathrm{m}}(\mathbf{x},t)\big\} = \mathrm{curl}_{\mathbf{x}}\big\{\mathbf{m}^{\mathrm{m}}(\mathbf{x},t)\big\} \quad . \end{aligned} \tag{5.25}$$

The local form of electric charge conservation (3.5), which gave rise to the first pair $(3.15)_{1,2}$ of MAXWELL's equations, is stated as

$$\frac{\partial}{\partial t}\big\{q^{\mathrm{m}}(\mathbf{x},t)\big\} = -\mathrm{div}_{\mathbf{x}}\big\{\mathbf{J}^{\mathrm{m}}(\mathbf{x},t)\big\} \quad . \tag{5.26}$$

As previously discussed in Section 3.2, the free and bound parts $\{q^{\mathrm{m}}_{\mathrm{F}}, \mathbf{J}^{\mathrm{m}}_{\mathrm{F}}\}$ and $\{q^{\mathrm{m}}_{\mathrm{R}}, \mathbf{J}^{\mathrm{m}}_{\mathrm{R}}\}$ of the charge-currents separately satisfy the conservation of charge,

$$\begin{aligned} \frac{\partial}{\partial t}\big\{q^{\mathrm{m}}_{\mathrm{F}}(\mathbf{x},t)\big\} &= -\mathrm{div}_{\mathbf{x}}\big\{\mathbf{J}^{\mathrm{m}}_{\mathrm{F}}(\mathbf{x},t)\big\} \quad , \\ \frac{\partial}{\partial t}\big\{q^{\mathrm{m}}_{\mathrm{R}}(\mathbf{x},t)\big\} &= -\mathrm{div}_{\mathbf{x}}\big\{\mathbf{J}^{\mathrm{m}}_{\mathrm{R}}(\mathbf{x},t)\big\} \quad . \end{aligned} \tag{5.27}$$

Finally, the aether relations (3.35) are given in the microscale by

$$\begin{aligned} \mathbf{d}^{\mathrm{m}}(\mathbf{x},t) &\overset{\text{Aet.}}{=} \varepsilon_0 \mathbf{e}^{\mathrm{m}}(\mathbf{x},t) \quad , \\ \mathbf{h}^{\mathrm{m}}(\mathbf{x},t) &\overset{\text{Aet.}}{=} \mathbf{b}^{\mathrm{m}}(\mathbf{x},t)/\mu_0 \quad , \end{aligned} \tag{5.28}$$

or alternatively

$$\begin{aligned} \mathbf{d}^{\mathrm{m}}_{\mathrm{F}}(\mathbf{x},t) &\overset{\text{Aet.}}{=} \varepsilon_0 \mathbf{e}^{\mathrm{m}}(\mathbf{x},t) + \mathbf{p}^{\mathrm{m}}(\mathbf{x},t) \quad , \\ \mathbf{h}^{\mathrm{m}}_{\mathrm{F}}(\mathbf{x},t) &\overset{\text{Aet.}}{=} \mathbf{b}^{\mathrm{m}}(\mathbf{x},t)/\mu_0 - \mathbf{m}^{\mathrm{m}}(\mathbf{x},t) \quad , \end{aligned} \tag{5.29}$$

where the polarization and magnetization are explicitly accounted for, see $(3.37)_{1,2}$. Note that the upcoming derivation does *not* rely on the aether relations unless explicitly indicated by the superscript $\overset{\text{Aet.}}{=}$, see Section 5.4.7.

5.3.2 Macroscopic Scale

It was previously argued that the macroscopic scale satisfies the continuum assumption, too, hence the governing equations derived in Chapters 3 and 4 are valid on both scales. However, unlike in the microscopic scale, the macroscopic quantities are determined from the microscopic fields by way of homogenization. Appropriate homogenization rules for these fields (say, for example, the stress $\mathbf{T}^{\mathrm{M}}(\mathbf{y},t)$ or the polarization $\mathbf{p}^{\mathrm{M}}(\mathbf{y},t)$) are derived by enforcing the desired governing equations on the

macroscopic scale while applying the prescribed volumetric averages of the extensive quantities from Section 5.2.

Therefore, rather than an *a priori* assumption of the validity of all macroscopic governing equations, the homogenization formulae are defined such that the resulting fields indeed satisfy the desired macroscopic balance equation. Nevertheless, it is tacitly understood that all equations derived in the context of the continuum theory are valid in the macroscopic scale, provided that homogenization formulae are defined consistently for all relevant fields.

In this section, only those equations are listed which will be enforced in Section 5.4 to derive homogenization formulae for macroscopic fields of interest. Recall that the macroscopic fields are functions of the position $\mathbf{y}$ rather than $\mathbf{x}$. The macroscale balance equations read

$$\begin{aligned}
\dot{\rho}^{\mathrm{M}}(\mathbf{y},t) &= -\rho^{\mathrm{M}}(\mathbf{y},t)\,\mathrm{div}_{\mathbf{y}}\big\{\mathbf{v}^{\mathrm{M}}(\mathbf{y},t)\big\} \quad , \\
\rho^{\mathrm{M}}(\mathbf{y},t)\,\dot{\mathbf{v}}^{\mathrm{M}}(\mathbf{y},t) &= \mathrm{div}_{\mathbf{y}}\big\{\mathbf{T}^{\mathrm{M}}(\mathbf{y},t)\big\} + \rho^{\mathrm{M}}(\mathbf{y},t)\,\mathbf{f}_{\mathrm{B}}^{\mathrm{M}}(\mathbf{y},t) + \mathbf{f}_{\mathrm{L}}^{\mathrm{M}}(\mathbf{y},t) \quad , \\
\rho^{\mathrm{M}}(\mathbf{y},t)\,\dot{e}^{\mathrm{M}}(\mathbf{y},t) &= \mathrm{div}_{\mathbf{y}}\big\{\big[\mathbf{T}^{\mathrm{M}}(\mathbf{y},t)\big]^{\mathrm{T}}\mathbf{v}^{\mathrm{M}}(\mathbf{y},t)\big\} + \big\{\rho^{\mathrm{M}}(\mathbf{y},t)\,\mathbf{f}_{\mathrm{B}}^{\mathrm{M}}(\mathbf{y},t) + \mathbf{f}_{\mathrm{L}}^{\mathrm{M}}(\mathbf{y},t)\big\}\cdot\mathbf{v}^{\mathrm{M}}(\mathbf{y},t) \\
&\quad - \mathrm{div}_{\mathbf{y}}\big\{\mathbf{q}^{\mathrm{M}}(\mathbf{y},t)\big\} + \rho^{\mathrm{M}}(\mathbf{y},t)\,r^{\mathrm{M}}(\mathbf{y},t) + \mathbf{j}^{\mathrm{M}}(\mathbf{y},t)\cdot\boldsymbol{\mathcal{E}}^{\mathrm{M}}(\mathbf{y},t) \quad ,
\end{aligned} \tag{5.30}$$

which are entirely analogous to their microscopic counterparts in Equations $(5.21)_{1-3}$. Note that the angular momentum balance $\mathbf{T}^{\mathrm{M}} = \mathbf{T}^{\mathrm{M}^{\mathrm{T}}}$ is not explicitly enforced here. However, it will be shown in Equation (5.45) that the symmetry of $\mathbf{T}^{\mathrm{M}}$ follows from the linear momentum balance $(5.30)_2$ provided that $\mathbf{T}^{\mathrm{m}} = \mathbf{T}^{\mathrm{m}^{\mathrm{T}}}$. The Maxwell Equations $(5.24)_{1-4}$ for the macroscopic scale read

$$\begin{aligned}
q^{\mathrm{M}}(\mathbf{y},t) &= \mathrm{div}_{\mathbf{y}}\big\{\mathbf{d}^{\mathrm{M}}(\mathbf{y},t)\big\} \quad , \\
\mathbf{J}^{\mathrm{M}}(\mathbf{y},t) + \frac{\partial}{\partial t}\big\{\mathbf{d}^{\mathrm{M}}(\mathbf{y},t)\big\} &= \mathrm{curl}_{\mathbf{y}}\big\{\mathbf{h}^{\mathrm{M}}(\mathbf{y},t)\big\} \quad , \\
\frac{\partial}{\partial t}\big\{\mathbf{b}^{\mathrm{M}}(\mathbf{y},t)\big\} &= -\mathrm{curl}_{\mathbf{y}}\big\{\mathbf{e}^{\mathrm{M}}(\mathbf{y},t)\big\} \quad , \\
0 &= \mathrm{div}_{\mathbf{y}}\big\{\mathbf{b}^{\mathrm{M}}(\mathbf{y},t)\big\} \quad .
\end{aligned} \tag{5.31}$$

The first pair $(5.31)_{1,2}$ may be further separated into the free and bound contributions. For the purposes of homogenization in Section 5.4 only the bound part is used, that is,

$$\begin{aligned}
q_{\mathrm{R}}^{\mathrm{M}}(\mathbf{y},t) &= -\mathrm{div}_{\mathbf{y}}\big\{\mathbf{p}^{\mathrm{M}}(\mathbf{y},t)\big\} \quad , \\
\mathbf{J}_{\mathrm{R}}^{\mathrm{M}}(\mathbf{y},t) - \frac{\partial}{\partial t}\big\{\mathbf{p}^{\mathrm{M}}(\mathbf{y},t)\big\} &= \mathrm{curl}_{\mathbf{y}}\big\{\mathbf{m}^{\mathrm{M}}(\mathbf{y},t)\big\} \quad .
\end{aligned} \tag{5.32}$$

Equations $(5.32)_{1,2}$ constitute the macroscopic counterparts of $(5.25)_{3,4}$. The local form of conservation of electric charge is given in the macroscale by

$$\frac{\partial}{\partial t}\big\{q^{\mathrm{M}}(\mathbf{y},t)\big\} = -\mathrm{div}_{\mathbf{y}}\big\{\mathbf{J}^{\mathrm{M}}(\mathbf{y},t)\big\} \quad , \tag{5.33}$$

or separately for the bound charge-currents according to

$$\frac{\partial}{\partial t}\big\{q_{\mathrm{R}}^{\mathrm{M}}(\mathbf{y},t)\big\} \;=\; -\mathrm{div}_{\mathbf{y}}\big\{\mathbf{J}_{\mathrm{R}}^{\mathrm{M}}(\mathbf{y},t)\big\} \quad . \tag{5.34}$$

These are the macroscopic counterparts of Equations (5.26) and $(5.27)_2$. It is pointed out that the charge balances (5.33) and (5.34) follow immediately from $(5.31)_{1,2}$ and $(5.32)_{1,2}$, respectively. They may thus be regarded as a consequence of the MAXWELL equations rather than separately enforced governing equations.

It is mentioned that there is no particular reason to expect the aether relations, given in the microscale by (5.28 - 29), to be automatically satisfied in the macroscopic scale. They are not derived from any balance equation, but instead represent constitutive equations of the homogenized material. As such, they may well differ from their microscopic counterparts. Nevertheless, it will be shown in Section 5.4.7 that the aether relations are indeed satisfied on the macroscopic scale.

Lastly, it is pointed out that each extensive thermomechanical variable whose homogenization was postulated in (5.16 - 18) is associated with a corresponding balance law $(5.30)_{1-3}$ enforced on the macroscopic scale. Similarly, the total and the bound electric charges postulated in (5.19 - 20) are associated with the charge balances in (5.33 - 34). However, there is no clear one-to-one correspondence between the homogenized extensive quantities and the MAXWELL equations. For example, the homogenization of charge q^{M} is simultaneously associated with the charge balance (5.33) and the first pair of MAXWELL's Equations $(5.31)_{1,2}$.

5.4 Homogenization of Governing Equations

In this section, the as of yet unspecified homogenization formulae for the macroscopic fields featured in the governing equations of Section 5.3.2 (such as $\mathbf{T}^{\mathrm{M}}$, $\mathbf{J}^{\mathrm{M}}$, *etc.*) are obtained as follows: First, the microscopic balance equations of Section 5.3.1 are substituted into the volume-weighted averaging integrals postulated in Section 5.2. Appealing to the properties of the weighting function $g(\mathbf{y},\mathbf{x})$ outlined in Section 5.1, the homogenized balance equations are manipulated into a form comparable to the macroscopic equations listed in Section 5.3.2. The missing homogenization formulae may then be inferred from a comparison of the ensuing expression with the corresponding macroscopic balance equation. Therefore, in effect, the homogenization formulae are deliberately chosen to ensure that the balance equations of the macroscopic continuum are indeed satisfied. For the sake of brevity, the arguments of the fields $(\cdot)^{\mathrm{M}}(\mathbf{y},t)$ and $(\cdot)^{\mathrm{m}}(\mathbf{x},t)$ are omitted from now on, leaving only the superscript letter to distinguish between micro- and macroscale functions.

5.4.1 Mass Density

Recall the postulated homogenization rules for the macroscopic mass density $\rho^{\mathrm{M}}(\mathbf{y},t)$ and for the linear momentum density $\rho^{\mathrm{M}}(\mathbf{y},t)\,\mathbf{v}^{\mathrm{M}}(\mathbf{y},t)$ in Equations (5.16) and (5.17), respectively. Given that the local statement of conservation of mass $(5.21)_1$ is valid at the microscopic level, it is yet to be verified whether the aforementioned homogenization formulae are consistent with the conservation of mass $(5.30)_1$ at the macroscopic scale. To this end, the material time derivative of (5.16) is taken, furnishing

$$\begin{aligned}\dot{\rho}^{\mathrm{M}} &= \frac{\mathrm{d}}{\mathrm{d}t}\int_{\mathcal{R}} \rho^{\mathrm{m}} g(\mathbf{y},\mathbf{x})\,\mathrm{d}v^{\mathrm{m}} \\ &= \int_{\mathcal{R}} \rho^{\mathrm{m}} \dot{g}(\mathbf{y},\mathbf{x})\,\mathrm{d}v^{\mathrm{m}} \\ &= \int_{\mathcal{R}} \rho^{\mathrm{m}}\,\mathrm{grad}_{\mathbf{y}}\, g(\mathbf{y},\mathbf{x})\cdot\mathbf{v}^{\mathrm{M}}\,\mathrm{d}v^{\mathrm{m}} - \int_{\mathcal{R}} \rho^{\mathrm{m}}\,\mathrm{grad}_{\mathbf{y}}\, g(\mathbf{y},\mathbf{x})\cdot\mathbf{v}^{\mathrm{m}}\,\mathrm{d}v^{\mathrm{m}} \quad . \end{aligned} \tag{5.35}$$

Here, the Reynolds' transport theorem of the form (2.112) was employed,[7] upon which Equation $(5.12)_1$ was substituted for $\dot{g}(\mathbf{y},\mathbf{x})$. Since the integral $\int_{\mathcal{R}}(\,\cdot\,)\,\mathrm{d}v^{\mathrm{m}}$ pertains to the microscopic argument $\mathbf{x}$ it is concluded that the macroscopic gradient operator $\mathrm{grad}_{\mathbf{y}}(\,\cdot\,)$ and the macroscopic velocity $\mathbf{v}^{\mathrm{M}}$ may be removed from the integral of the first term in (5.35). Furthermore, given that $\rho^{\mathrm{m}}\mathbf{v}^{\mathrm{m}}$ is functionally independent of the macroscopic position $\mathbf{y}$, the gradient for the second term in (5.35) is readily converted to a divergence by means of the identity in $(2.46)_1$, that is, $\mathrm{grad}_{\mathbf{y}}\, g\cdot(\rho^{\mathrm{m}}\mathbf{v}^{\mathrm{m}}) = \mathrm{div}_{\mathbf{y}}(g\rho^{\mathrm{m}}\mathbf{v}^{\mathrm{m}})$. Equation (5.35) therefore simplifies to

$$\begin{aligned}\dot{\rho}^{\mathrm{M}} &= \int_{\mathcal{R}} \mathrm{grad}_{\mathbf{y}}\big(\rho^{\mathrm{m}} g(\mathbf{y},\mathbf{x})\big)\,\mathrm{d}v^{\mathrm{m}}\cdot\mathbf{v}^{\mathrm{M}} - \int_{\mathcal{R}} \mathrm{div}_{\mathbf{y}}\big(\rho^{\mathrm{m}} g(\mathbf{y},\mathbf{x})\mathbf{v}^{\mathrm{m}}\big)\,\mathrm{d}v^{\mathrm{m}} \\ &= \mathrm{grad}_{\mathbf{y}}\Big\{\int_{\mathcal{R}} \rho^{\mathrm{m}} g(\mathbf{y},\mathbf{x})\,\mathrm{d}v^{\mathrm{m}}\Big\}\cdot\mathbf{v}^{\mathrm{M}} - \mathrm{div}_{\mathbf{y}}\Big\{\int_{\mathcal{R}} \rho^{\mathrm{m}}\mathbf{v}^{\mathrm{m}} g(\mathbf{y},\mathbf{x})\,\mathrm{d}v^{\mathrm{m}}\Big\} \\ &= \mathrm{grad}_{\mathbf{y}}\big(\rho^{\mathrm{M}}\big)\cdot\mathbf{v}^{\mathrm{M}} - \mathrm{div}_{\mathbf{y}}\big(\rho^{\mathrm{M}}\mathbf{v}^{\mathrm{M}}\big) \\ &= -\rho^{\mathrm{M}}\,\mathrm{div}_{\mathbf{y}}\,\mathbf{v}^{\mathrm{M}} \quad , \end{aligned} \tag{5.36}$$

where use was made of definitions (5.16) and (5.17), as well as identity $(2.46)_1$ once again. This result of course corresponds to the macroscopic statement for the conservation of mass, see $(5.30)_1$. Equation (5.36) confirms that the choice of homogenization for (5.16) and (5.17) it is indeed consistent. In other words, if the mass density homogenizes by volume-averaging rule (5.16), then the momentum density must homogenize according to (5.17) in order for the macroscopic continuum variables to satisfy the conservation of mass.

[7] Recall that the conservation of mass (2.111) was used to derive this identity. When applied in (5.35), this relies on the *micro*scopic mass balance $(5.30)_1$. Since the derivation aims to show that the *macro*scopic balance is identically satisfied, the use of (2.112) does not compromise the validity of the result.

5.4.2 Linear Momentum Density

The balance of linear momentum is given on the microscopic and macroscopic scales by Equations $(5.21)_2$ and $(5.30)_2$. The homogenizations of some quantities involved in these equations are already known. Specifically, the macroscopic densities of mass ρ^{M} and linear momentum $\rho^{\mathrm{M}}\mathbf{v}^{\mathrm{M}}$ are determined by (5.16) and (5.17), respectively. Yet to be determined are the homogenization formulae for the CAUCHY stress tensor $\mathbf{T}^{\mathrm{M}}(\mathbf{y},t)$ and for the density of total external forces $\rho^{\mathrm{M}}(\mathbf{y},t)\,\mathbf{f}_{\mathrm{B}}^{\mathrm{M}}(\mathbf{y},t)+\mathbf{f}_{\mathrm{L}}^{\mathrm{M}}(\mathbf{y},t)$.

In this section, aforementioned quantities are deduced from the postulated macroscopic balance $(5.30)_2$ as follows: First, it is noted that by product rule and Equation $(5.30)_1$ the rate of change of macroscopic linear momentum is given by

$$\rho^{\mathrm{M}}\dot{\mathbf{v}}^{\mathrm{M}} \;=\; \big(\rho^{\mathrm{M}}\mathbf{v}^{\mathrm{M}}\big)^{\bullet} - \dot{\rho}^{\mathrm{M}}\mathbf{v}^{\mathrm{M}} \;=\; \big(\rho^{\mathrm{M}}\mathbf{v}^{\mathrm{M}}\big)^{\bullet} + \big(\mathrm{div}_{\mathbf{y}}\,\mathbf{v}^{\mathrm{M}}\big)\rho^{\mathrm{M}}\mathbf{v}^{\mathrm{M}} \quad . \tag{5.37}$$

In order to write the macroscopic statement of linear momentum balance in terms of the microscopic variables, the quantities on the right-hand side of (5.37) are expressed using their homogenization rules. Next, upon minor manipulations, the microscopic momentum balance $(5.21)_2$ is substituted into the right-hand side. Lastly, the ensuing expression is made to look like the macroscale momentum equation $(5.30)_2$, from which $\mathbf{T}^{\mathrm{M}}$ and $\mathbf{f}_{\mathrm{B}}^{\mathrm{M}}$ are deduced.

The material time derivative of the homogenization of linear momentum $\rho^{\mathrm{M}}\mathbf{v}^{\mathrm{M}}$ in (5.17) is given by

$$\begin{aligned}
\big(\rho^{\mathrm{M}}\mathbf{v}^{\mathrm{M}}\big)^{\bullet} \;&=\; \frac{\mathrm{d}}{\mathrm{d}t}\int_{\mathcal{R}} \rho^{\mathrm{m}}\mathbf{v}^{\mathrm{m}} g(\mathbf{y},\mathbf{x})\,\mathrm{d}v^{\mathrm{m}} \\
&=\; \int_{\mathcal{R}} \rho^{\mathrm{m}}\big(\mathbf{v}^{\mathrm{m}} g(\mathbf{y},\mathbf{x})\big)^{\bullet}\,\mathrm{d}v^{\mathrm{m}} \\
&=\; \int_{\mathcal{R}} \rho^{\mathrm{m}}\dot{\mathbf{v}}^{\mathrm{m}} g(\mathbf{y},\mathbf{x})\,\mathrm{d}v^{\mathrm{m}} + \underbrace{\int_{\mathcal{R}} \rho^{\mathrm{m}}\mathbf{v}^{\mathrm{m}}\Big\{\mathrm{grad}_{\mathbf{y}}\, g(\mathbf{y},\mathbf{x})\cdot\big(\mathbf{v}^{\mathrm{M}}-\mathbf{v}^{\mathrm{m}}\big)\Big\}\,\mathrm{d}v^{\mathrm{m}}}_{\text{(i)}} \quad ,
\end{aligned} \tag{5.38}$$

where use was made of the REYNOLDS transport theorem of the form (2.112) for the microscale and Equation $(5.12)_1$ for $\dot{g}(\mathbf{y},\mathbf{x})$. The last integral in (5.38) is further expanded and rearranged as

$$\begin{aligned}
\text{(i)} \;&=\; \int_{\mathcal{R}} \rho^{\mathrm{m}}\big[\mathbf{v}^{\mathrm{m}}\otimes\mathrm{grad}_{\mathbf{y}}\, g(\mathbf{y},\mathbf{x})\big]\,\mathbf{v}^{\mathrm{M}}\,\mathrm{d}v^{\mathrm{m}} - \int_{\mathcal{R}} \rho^{\mathrm{m}}\big[\mathbf{v}^{\mathrm{m}}\otimes\mathbf{v}^{\mathrm{m}}\big]\,\mathrm{grad}_{\mathbf{y}}\, g(\mathbf{y},\mathbf{x})\,\mathrm{d}v^{\mathrm{m}} \\
&=\; \underbrace{\mathrm{grad}_{\mathbf{y}}\Big\{\int_{\mathcal{R}} \rho^{\mathrm{m}}\mathbf{v}^{\mathrm{m}} g(\mathbf{y},\mathbf{x})\,\mathrm{d}v^{\mathrm{m}}\Big\}\mathbf{v}^{\mathrm{M}}}_{\text{(ii)}} - \mathrm{div}_{\mathbf{y}}\underbrace{\Big\{\int_{\mathcal{R}} \rho^{\mathrm{m}}\big[\mathbf{v}^{\mathrm{m}}\otimes\mathbf{v}^{\mathrm{m}}\big] g(\mathbf{y},\mathbf{x})\,\mathrm{d}v^{\mathrm{m}}\Big\}}_{\text{(iii)}} \quad ,
\end{aligned} \tag{5.39}$$

where the independence of the microscopic variables on $\mathbf{y}$ was exploited to remove $\mathbf{v}^{\mathrm{M}}$ and the gradients from the integrals, in part with the aid of $(2.46)_2$. The first term of (5.39) is expanded using identity in $(2.46)_5$ to write

$$\text{(ii)} \;=\; \Big[\mathrm{grad}_{\mathbf{y}}\big(\rho^{\mathrm{M}}\mathbf{v}^{\mathrm{M}}\big)\Big]\,\mathbf{v}^{\mathrm{M}} \;=\; \mathrm{div}_{\mathbf{y}}\Big[\rho^{\mathrm{M}}\mathbf{v}^{\mathrm{M}}\otimes\mathbf{v}^{\mathrm{M}}\Big] - \big(\mathrm{div}_{\mathbf{y}}\,\mathbf{v}^{\mathrm{M}}\big)\rho^{\mathrm{M}}\mathbf{v}^{\mathrm{M}} \quad . \tag{5.40}$$

Note that the last term in (5.40) partially cancels with (5.37), hence the the time derivative on the left-hand side of (5.38) can be simplified. Meanwhile, the second part of (5.39) is alternatively expressed as

$$\begin{aligned}
\text{(iii)} \;&=\; \int_{\mathcal{R}} \rho^{\mathrm{m}}\Big[\big(\mathbf{v}^{\mathrm{m}}-\mathbf{v}^{\mathrm{M}}\big)\otimes\big(\mathbf{v}^{\mathrm{m}}-\mathbf{v}^{\mathrm{M}}\big) + \mathbf{v}^{\mathrm{m}}\otimes\mathbf{v}^{\mathrm{M}} + \mathbf{v}^{\mathrm{M}}\otimes\mathbf{v}^{\mathrm{m}} - \mathbf{v}^{\mathrm{M}}\otimes\mathbf{v}^{\mathrm{M}}\Big]\, g(\mathbf{y},\mathbf{x})\,\mathrm{d}v^{\mathrm{m}} \\
&=\; \int_{\mathcal{R}} \rho^{\mathrm{m}}\big(\mathbf{v}^{\mathrm{m}}-\mathbf{v}^{\mathrm{M}}\big)\otimes\big(\mathbf{v}^{\mathrm{m}}-\mathbf{v}^{\mathrm{M}}\big)\, g(\mathbf{y},\mathbf{x})\,\mathrm{d}v^{\mathrm{m}} + \int_{\mathcal{R}} \rho^{\mathrm{m}}\mathbf{v}^{\mathrm{m}}\, g(\mathbf{y},\mathbf{x})\,\mathrm{d}v^{\mathrm{m}}\otimes\mathbf{v}^{\mathrm{M}} \\
&\qquad + \mathbf{v}^{\mathrm{M}}\otimes\int_{\mathcal{R}} \rho^{\mathrm{m}}\mathbf{v}^{\mathrm{m}}\, g(\mathbf{y},\mathbf{x})\,\mathrm{d}v^{\mathrm{m}} - \int_{\mathcal{R}} \rho^{\mathrm{m}}\, g(\mathbf{y},\mathbf{x})\,\mathrm{d}v^{\mathrm{m}}\,\mathbf{v}^{\mathrm{M}}\otimes\mathbf{v}^{\mathrm{M}} \\
&=\; \int_{\mathcal{R}} \rho^{\mathrm{m}}\big(\mathbf{v}^{\mathrm{m}}-\mathbf{v}^{\mathrm{M}}\big)\otimes\big(\mathbf{v}^{\mathrm{m}}-\mathbf{v}^{\mathrm{M}}\big)\, g(\mathbf{y},\mathbf{x})\,\mathrm{d}v^{\mathrm{m}} + \rho^{\mathrm{M}}\mathbf{v}^{\mathrm{M}}\otimes\mathbf{v}^{\mathrm{M}} \quad ,
\end{aligned} \tag{5.41}$$

where (5.16) and (5.17) were employed. Note that the last term in (5.41) cancels with the first term in (5.40). It is thus concluded from (5.37 - 41) that the rate of change of macroscopic linear momentum may be expressed by

$$\rho^{\mathrm{M}}\dot{\mathbf{v}}^{\mathrm{M}} \;=\; \underbrace{\int_{\mathcal{R}} \rho^{\mathrm{m}}\dot{\mathbf{v}}^{\mathrm{m}}\, g(\mathbf{y},\mathbf{x})\,\mathrm{d}v^{\mathrm{m}}}_{\text{(iv)}} - \mathrm{div}_{\mathbf{y}}\Big\{\int_{\mathcal{R}} \rho^{\mathrm{m}}\big(\mathbf{v}^{\mathrm{m}}-\mathbf{v}^{\mathrm{M}}\big)\otimes\big(\mathbf{v}^{\mathrm{m}}-\mathbf{v}^{\mathrm{M}}\big)\, g(\mathbf{y},\mathbf{x})\,\mathrm{d}v^{\mathrm{m}}\Big\} \quad . \tag{5.42}$$

According to Equation (5.42) the homogenization rule for $\rho^{\mathrm{M}}\dot{\mathbf{v}}^{\mathrm{M}}$ deviates from the volume-averaging scheme (5.2) by an amount determined by the fluctuation of the microscopic velocity $\mathbf{v}^{\mathrm{m}}$ away from the macroscopic 'average' $\mathbf{v}^{\mathrm{M}}$.[8]

Lastly, the microscopic balance of linear momentum $(5.21)_2$ is substituted into the first integral of Equation (5.42),

$$\begin{aligned}
\text{(iv)} \;&=\; \int_{\mathcal{R}} \Big\{\mathrm{div}_{\mathbf{x}}\,\mathbf{T}^{\mathrm{m}} + \rho^{\mathrm{m}}\mathbf{f}_{\mathrm{B}}^{\mathrm{m}} + \mathbf{f}_{\mathrm{L}}^{\mathrm{m}}\Big\}\, g(\mathbf{y},\mathbf{x})\,\mathrm{d}v^{\mathrm{m}} \\
&=\; \mathrm{div}_{\mathbf{y}}\Big\{\int_{\mathcal{R}} \mathbf{T}^{\mathrm{m}}\, g(\mathbf{y},\mathbf{x})\,\mathrm{d}v^{\mathrm{m}}\Big\} + \int_{\mathcal{R}} \big(\rho^{\mathrm{m}}\mathbf{f}_{\mathrm{B}}^{\mathrm{m}} + \mathbf{f}_{\mathrm{L}}^{\mathrm{m}}\big)\, g(\mathbf{y},\mathbf{x})\,\mathrm{d}v^{\mathrm{m}} \quad ,
\end{aligned} \tag{5.43}$$

where the corollary in (5.15) was used to remove the divergence operator from the

[8] The reader is reminded that the micro- and macroscopic velocities are given by the material time derivatives of the respective position vectors $\mathbf{x}$ and $\mathbf{y}$, respectively, see (5.1).

integral. Equation (5.42) thus becomes

$$\begin{aligned}\rho^{\mathrm{M}}\dot{\mathbf{v}}^{\mathrm{M}} \;=\; \mathrm{div}_{\mathbf{y}}\Big\{\int_{\mathcal{R}}\Big[\mathbf{T}^{\mathrm{m}}-\rho^{\mathrm{m}}\big(\mathbf{v}^{\mathrm{m}}-\mathbf{v}^{\mathrm{M}}\big)\otimes\big(\mathbf{v}^{\mathrm{m}}-\mathbf{v}^{\mathrm{M}}\big)\Big]g(\mathbf{y},\mathbf{x})\,\mathrm{d}v^{\mathrm{m}}\Big\}\\ +\int_{\mathcal{R}}\big(\rho^{\mathrm{m}}\mathbf{f}_{\mathrm{B}}^{\mathrm{m}}+\mathbf{f}_{\mathrm{L}}^{\mathrm{m}}\big)g(\mathbf{y},\mathbf{x})\,\mathrm{d}v^{\mathrm{m}}\quad,\end{aligned}\tag{5.44}$$

where the terms are grouped into boundary tractions (as indicated by the divergence) and volumetric forces.

Note the similarity between the result in (5.44) and the macroscopic balance of linear momentum $(5.30)_2$. To ensure that the macroscopic balance takes the desired form it is concluded that the macroscopic stress tensor is given, to within a divergence-free tensor-valued function of $(\mathbf{y},t)$,[9] by

$$\begin{aligned}\mathbf{T}^{\mathrm{M}}(\mathbf{y},t) \;=\; &\int_{\mathcal{R}}\mathbf{T}^{\mathrm{m}}(\mathbf{x},t)\,g(\mathbf{y},\mathbf{x})\,\mathrm{d}v^{\mathrm{m}}\\ &-\int_{\mathcal{R}}\rho^{\mathrm{m}}(\mathbf{x},t)\big(\mathbf{v}^{\mathrm{m}}(\mathbf{x},t)-\mathbf{v}^{\mathrm{M}}(\mathbf{y},t)\big)\otimes\big(\mathbf{v}^{\mathrm{m}}(\mathbf{x},t)-\mathbf{v}^{\mathrm{M}}(\mathbf{y},t)\big)\,g(\mathbf{y},\mathbf{x})\,\mathrm{d}v^{\mathrm{m}}\quad.\end{aligned}\tag{5.45}$$

The deviation of (5.42) from a pure volume average is thus carried over to the stress tensor. The macroscopic stress (5.45) comprises the volume average of microscopic stress $\mathbf{T}^{\mathrm{m}}$ plus a momentum-like term due to the difference $\mathbf{v}^{\mathrm{m}}-\mathbf{v}^{\mathrm{M}}$ between the material velocities at the two scales. It accounts for the effects of micro-inertia due to microscopic fluctuations in the velocity, similar to the effects of particle inertia in the Irving-Kirkwood theory [57]. It is seen from (5.45) that $\mathbf{T}^{\mathrm{M}}$ is symmetric as long as $\mathbf{T}^{\mathrm{m}}$ is, thereby satisfying the angular momentum balance on the macroscale automatically.

The comparison between (5.44) and $(5.30)_2$ further implies that the sum of the body- and Lorentz force densities homogenizes as

$$\rho^{\mathrm{M}}(\mathbf{y},t)\,\mathbf{f}_{\mathrm{B}}^{\mathrm{M}}(\mathbf{y},t)+\mathbf{f}_{\mathrm{L}}^{\mathrm{M}}(\mathbf{y},t) \;=\; \int_{\mathcal{R}}\Big(\rho^{\mathrm{m}}(\mathbf{x},t)\mathbf{f}_{\mathrm{B}}^{\mathrm{m}}(\mathbf{x},t)+\mathbf{f}_{\mathrm{L}}^{\mathrm{m}}(\mathbf{x},t)\Big)\,g(\mathbf{y},\mathbf{x})\,\mathrm{d}v^{\mathrm{m}}\quad.\tag{5.46}$$

This is in accordance with the weighted volume-averaging scheme in (5.2) albeit *not* for each force individually, as will be discussed in Section 5.4.8. Indeed, from the viewpoint of the macroscale initial/boundary-value problem (IBVP) the distinction between the Lorentz force and other body forces is irrelevant.

[9] It is argued by Mandadapu *et al.* [82] that "*at any given point* $\mathbf{y}$ *and time* t*, this function may be set to zero, provided that the balance laws and assorted boundary conditions are satisfied simultaneously in both scales.*"

5.4.3 Total Energy Density

The macroscopic *total* energy density per unit volume is given by the postulated volumetric averaging scheme in (5.18). Yet to be determined are the homogenizations for the volumetric heat sources $\rho^{\mathrm{M}}(\mathbf{y},t)r^{\mathrm{M}}(\mathbf{y},t)+\mathbf{j}^{\mathrm{M}}(\mathbf{y},t)\cdot\boldsymbol{\mathcal{E}}^{\mathrm{M}}(\mathbf{y},t)$ and for the macroscopic heat flux $\mathbf{q}^{\mathrm{M}}(\mathbf{y},t)$. They are derived in this section using the microscopic and macroscopic statements for the balance of energy, see Equations $(5.21)_3$ and $(5.30)_3$, following the same approach adopted in Section 5.4.2 for the linear momentum.

The rate of change of macroscopic total energy density is expressed in terms of the microscopic fields using Equations (2.112), $(5.12)_1$, (5.18), and $(5.30)_1$,

$$\begin{aligned}\rho^{\mathrm{M}}\dot{e}^{\mathrm{M}} &= \big[\rho^{\mathrm{M}}e^{\mathrm{M}}\big]^{\bullet} - \dot{\rho}^{\mathrm{M}}e^{\mathrm{M}}\\ &= \frac{\mathrm{d}}{\mathrm{d}t}\int_{\mathcal{R}}\rho^{\mathrm{m}}e^{\mathrm{m}}g(\mathbf{y},\mathbf{x})\,\mathrm{d}v^{\mathrm{m}} + \rho^{\mathrm{M}}e^{\mathrm{M}}\,\mathrm{div}_{\mathbf{y}}\,\mathbf{v}^{\mathrm{M}}\\ &= \int_{\mathcal{R}}\rho^{\mathrm{m}}\dot{e}^{\mathrm{m}}g(\mathbf{y},\mathbf{x})\,\mathrm{d}v^{\mathrm{m}} + \rho^{\mathrm{M}}e^{\mathrm{M}}\,\mathrm{div}_{\mathbf{y}}\,\mathbf{v}^{\mathrm{M}}\\ &\qquad + \underbrace{\int_{\mathcal{R}}\rho^{\mathrm{m}}e^{\mathrm{m}}\Big[\mathrm{grad}_{\mathbf{y}}\,g(\mathbf{y},\mathbf{x})\cdot\big(\mathbf{v}^{\mathrm{M}}-\mathbf{v}^{\mathrm{m}}\big)\Big]\,\mathrm{d}v^{\mathrm{m}}}_{\text{(i)}}\quad .\end{aligned}\tag{5.47}$$

The term involving $\mathrm{grad}_{\mathbf{y}}\,g(\mathbf{y},\mathbf{x})$ is expanded according to

$$\text{(i)} \;=\; \underbrace{\mathrm{grad}_{\mathbf{y}}\Big\{\int_{\mathcal{R}}\rho^{\mathrm{m}}e^{\mathrm{m}}g(\mathbf{y},\mathbf{x})\,\mathrm{d}v^{\mathrm{m}}\Big\}\cdot\mathbf{v}^{\mathrm{M}}}_{\text{(ii)}} - \mathrm{div}_{\mathbf{y}}\underbrace{\Big\{\int_{\mathcal{R}}\rho^{\mathrm{m}}e^{\mathrm{m}}g(\mathbf{y},\mathbf{x})\mathbf{v}^{\mathrm{m}}\,\mathrm{d}v^{\mathrm{m}}\Big\}}_{\text{(iii)}}\quad ,\tag{5.48}$$

where $(2.46)_1$ was used, as well as the independence from $\mathbf{y}$ of the microscopic fields. The above two terms are more conveniently rewritten as

$$\begin{aligned}\text{(ii)} &= \mathrm{grad}_{\mathbf{y}}\big(\rho^{\mathrm{M}}e^{\mathrm{M}}\big)\cdot\mathbf{v}^{\mathrm{M}} = \mathrm{div}_{\mathbf{y}}\big(\rho^{\mathrm{M}}e^{\mathrm{M}}\mathbf{v}^{\mathrm{M}}\big) - \rho^{\mathrm{M}}e^{\mathrm{M}}\,\mathrm{div}_{\mathbf{y}}\,\mathbf{v}^{\mathrm{M}}\\ \text{(iii)} &= \int_{\mathcal{R}}\rho^{\mathrm{m}}e^{\mathrm{m}}g(\mathbf{y},\mathbf{x})\big(\mathbf{v}^{\mathrm{m}}-\mathbf{v}^{\mathrm{M}}\big)\,\mathrm{d}v^{\mathrm{m}} + \rho^{\mathrm{M}}e^{\mathrm{M}}\mathbf{v}^{\mathrm{M}}\quad ,\end{aligned}\tag{5.49}$$

where (5.18) was employed. It is thus concluded from (5.47 - 49) that the rate of change of macroscopic total energy density may be expressed as

$$\rho^{\mathrm{M}}\dot{e}^{\mathrm{M}} = \int_{\mathcal{R}}\rho^{\mathrm{m}}\dot{e}^{\mathrm{m}}g(\mathbf{y},\mathbf{x})\,\mathrm{d}v^{\mathrm{m}} - \mathrm{div}_{\mathbf{y}}\underbrace{\Big\{\int_{\mathcal{R}}\rho^{\mathrm{m}}e^{\mathrm{m}}g(\mathbf{y},\mathbf{x})\big(\mathbf{v}^{\mathrm{m}}-\mathbf{v}^{\mathrm{M}}\big)\,\mathrm{d}v^{\mathrm{m}}\Big\}}_{\text{(iv)}}\quad .\tag{5.50}$$

The preceding homogenization does not observe a volumetric average due to the deviation of the microscale velocity from its macroscopic 'average'. Note the similarity between the homogenization formulae for the rates of change of the (scalar)

energy $\rho^{\mathrm{M}}\dot{e}^{\mathrm{M}}$ in (5.50) and of the (vector-valued) momentum $\rho^{\mathrm{M}}\dot{\mathbf{v}}^{\mathrm{M}}$ in (5.42). The microscale velocity fluctuations enter linearly in the former and quadratically in the latter.

An instructive alternative formulation of (5.50) can be derived using the identity

$$\int_{\mathcal{R}} \rho^{\mathrm{m}} g(\mathbf{y},\mathbf{x})\big(\mathbf{v}^{\mathrm{m}}-\mathbf{v}^{\mathrm{M}}\big)\,\mathrm{d}v^{\mathrm{m}} \;=\; \mathbf{0} \quad , \tag{5.51}$$

which is readily derived from (5.16) and (5.17). The term in the divergence of (5.50) may thus be rewritten as

$$\begin{aligned}
\text{(iv)} \;&=\; \int_{\mathcal{R}} \rho^{\mathrm{m}}\Big[\varepsilon^{\mathrm{m}}+\tfrac{1}{2}\mathbf{v}^{\mathrm{m}}\cdot\mathbf{v}^{\mathrm{m}}\Big] g(\mathbf{y},\mathbf{x})\big(\mathbf{v}^{\mathrm{m}}-\mathbf{v}^{\mathrm{M}}\big)\,\mathrm{d}v^{\mathrm{m}} \\
&=\; \int_{\mathcal{R}} \rho^{\mathrm{m}}\Big[\varepsilon^{\mathrm{m}}+\tfrac{1}{2}\big(\mathbf{v}^{\mathrm{m}}-\mathbf{v}^{\mathrm{M}}\big)\cdot\big(\mathbf{v}^{\mathrm{m}}-\mathbf{v}^{\mathrm{M}}\big)\Big] g(\mathbf{y},\mathbf{x})\big(\mathbf{v}^{\mathrm{m}}-\mathbf{v}^{\mathrm{M}}\big)\,\mathrm{d}v^{\mathrm{m}} \\
&\qquad + \int_{\mathcal{R}} \rho^{\mathrm{m}}\Big[\big(\mathbf{v}^{\mathrm{m}}-\mathbf{v}^{\mathrm{M}}\big)\cdot\mathbf{v}^{\mathrm{M}}\Big] g(\mathbf{y},\mathbf{x})\big(\mathbf{v}^{\mathrm{m}}-\mathbf{v}^{\mathrm{M}}\big)\,\mathrm{d}v^{\mathrm{m}} \\
&=\; \int_{\mathcal{R}} \rho^{\mathrm{m}}\tilde{e}^{\mathrm{m}} g(\mathbf{y},\mathbf{x})\big(\mathbf{v}^{\mathrm{m}}-\mathbf{v}^{\mathrm{M}}\big)\,\mathrm{d}v^{\mathrm{m}} \\
&\qquad + \left[\int_{\mathcal{R}} \rho^{\mathrm{m}}\big(\mathbf{v}^{\mathrm{m}}-\mathbf{v}^{\mathrm{M}}\big)\otimes\big(\mathbf{v}^{\mathrm{m}}-\mathbf{v}^{\mathrm{M}}\big) g(\mathbf{y},\mathbf{x})\,\mathrm{d}v^{\mathrm{m}}\right]\mathbf{v}^{\mathrm{M}} \quad ,
\end{aligned} \tag{5.52}$$

where $\tilde{e}^{\mathrm{m}}$ is an alternative measure of microscale total energy density per unit mass, introduced by Mandadapu *et al.* [82, Equation 2.40] according to

$$\tilde{e}^{\mathrm{m}} \;=\; \varepsilon^{\mathrm{m}}+\tfrac{1}{2}\big(\mathbf{v}^{\mathrm{m}}-\mathbf{v}^{\mathrm{M}}\big)\cdot\big(\mathbf{v}^{\mathrm{m}}-\mathbf{v}^{\mathrm{M}}\big) \quad . \tag{5.53}$$

It represents the sum of internal and kinetic energies, where the kinetic energy is measured not from the reference frame but instead relative to a convected frame moving at the 'average' local velocity $\mathbf{v}^{\mathrm{M}}$ of the macroscopic material. Of course, this frame is neither inertial nor does it correspond to a rigid-body motion relative to the reference frame. Nevertheless, a convenient consequence of this formulation is that the last term in Equation (5.52) mirrors the amount to which the macroscopic stress $\mathbf{T}^{\mathrm{M}}$ deviates from the volumetric average of $\mathbf{T}^{\mathrm{m}}$ in Equation (5.45). With (5.52) the homogenization of the rate of change of total energy density in (5.50) can be restated as

$$\begin{aligned}
\rho^{\mathrm{M}}\dot{e}^{\mathrm{M}} \;=\; &\underbrace{\int_{\mathcal{R}} \rho^{\mathrm{m}}\dot{e}^{\mathrm{m}} g(\mathbf{y},\mathbf{x})\,\mathrm{d}v^{\mathrm{m}}}_{\text{(v)}} - \mathrm{div}_{\mathbf{y}}\left\{\int_{\mathcal{R}} \rho^{\mathrm{m}}\tilde{e}^{\mathrm{m}} g(\mathbf{y},\mathbf{x})\big(\mathbf{v}^{\mathrm{m}}-\mathbf{v}^{\mathrm{M}}\big)\,\mathrm{d}v^{\mathrm{m}}\right\} \\
&- \mathrm{div}_{\mathbf{y}}\left\{\left[\int_{\mathcal{R}} \rho^{\mathrm{m}}\big(\mathbf{v}^{\mathrm{m}}-\mathbf{v}^{\mathrm{M}}\big)\otimes\big(\mathbf{v}^{\mathrm{m}}-\mathbf{v}^{\mathrm{M}}\big) g(\mathbf{y},\mathbf{x})\,\mathrm{d}v^{\mathrm{m}}\right]\mathbf{v}^{\mathrm{M}}\right\} \quad .
\end{aligned} \tag{5.54}$$

Lastly the microscopic balance of energy $(5.21)_3$ is substituted into the first term on the right-hand side of Equation (5.54),

$$\begin{aligned}
\text{(v)} \;&=\; \int_{\mathcal{R}} \operatorname{div}_{\mathbf{x}}\big(\mathbf{T}^{\mathrm{mT}}\mathbf{v}^{\mathrm{m}}\big)\, g(\mathbf{y},\mathbf{x})\,\mathrm{d}v^{\mathrm{m}} + \int_{\mathcal{R}} \big(\rho^{\mathrm{m}}\,\mathbf{f}_{\mathrm{B}}^{\mathrm{m}} + \mathbf{f}_{\mathrm{L}}^{\mathrm{m}}\big)\cdot\mathbf{v}^{\mathrm{m}}\, g(\mathbf{y},\mathbf{x})\,\mathrm{d}v^{\mathrm{m}} \\
&\qquad - \int_{\mathcal{R}} \operatorname{div}_{\mathbf{x}}\big(\mathbf{q}^{\mathrm{m}}\big)\, g(\mathbf{y},\mathbf{x})\,\mathrm{d}v^{\mathrm{m}} + \int_{\mathcal{R}} \big(\rho^{\mathrm{m}}\, r^{\mathrm{m}} + \mathbf{j}^{\mathrm{m}}\cdot\boldsymbol{\mathcal{E}}^{\mathrm{m}}\big)\, g(\mathbf{y},\mathbf{x})\,\mathrm{d}v^{\mathrm{m}} \\
&=\; \operatorname{div}_{\mathbf{y}}\Big\{\underbrace{\int_{\mathcal{R}} \mathbf{T}^{\mathrm{mT}}\mathbf{v}^{\mathrm{m}}\, g(\mathbf{y},\mathbf{x})\,\mathrm{d}v^{\mathrm{m}}}_{\text{(vi)}}\Big\} + \underbrace{\int_{\mathcal{R}} \big(\rho^{\mathrm{m}}\,\mathbf{f}_{\mathrm{B}}^{\mathrm{m}} + \mathbf{f}_{\mathrm{L}}^{\mathrm{m}}\big)\cdot\mathbf{v}^{\mathrm{m}}\, g(\mathbf{y},\mathbf{x})\,\mathrm{d}v^{\mathrm{m}}}_{\text{(vii)}} \\
&\qquad - \operatorname{div}_{\mathbf{y}}\Big\{\int_{\mathcal{R}} \mathbf{q}^{\mathrm{m}}\, g(\mathbf{y},\mathbf{x})\,\mathrm{d}v^{\mathrm{m}}\Big\} + \int_{\mathcal{R}} \big(\rho^{\mathrm{m}}\, r^{\mathrm{m}} + \mathbf{j}^{\mathrm{m}}\cdot\boldsymbol{\mathcal{E}}^{\mathrm{m}}\big)\, g(\mathbf{y},\mathbf{x})\,\mathrm{d}v^{\mathrm{m}} \quad , \qquad (5.55)
\end{aligned}$$

where the property in (5.13) was used to convert the divergences. Recall that the stress $\mathbf{T}^{\mathrm{M}}$ and the external forces $\rho^{\mathrm{M}}\mathbf{f}_{\mathrm{B}}^{\mathrm{M}} + \mathbf{f}_{\mathrm{L}}^{\mathrm{M}}$ in the macroscopic scale were derived in the preceding section, see (5.45) and (5.46), respectively. It is thus more convenient to express (5.55) in terms of the velocity fluctuations

$$\begin{aligned}
\text{(vi)} \;&=\; \Big[\int_{\mathcal{R}} \mathbf{T}^{\mathrm{m}}\, g(\mathbf{y},\mathbf{x})\,\mathrm{d}v^{\mathrm{m}}\Big]^{\mathrm{T}}\mathbf{v}^{\mathrm{M}} + \int_{\mathcal{R}} \mathbf{T}^{\mathrm{mT}}\big(\mathbf{v}^{\mathrm{m}} - \mathbf{v}^{\mathrm{M}}\big)\, g(\mathbf{y},\mathbf{x})\,\mathrm{d}v^{\mathrm{m}} \\
&=\; \mathbf{T}^{\mathrm{M}^{\mathrm{T}}}\mathbf{v}^{\mathrm{M}} + \int_{\mathcal{R}} \mathbf{T}^{\mathrm{mT}}\big(\mathbf{v}^{\mathrm{m}} - \mathbf{v}^{\mathrm{M}}\big)\, g(\mathbf{y},\mathbf{x})\,\mathrm{d}v^{\mathrm{m}} \\
&\qquad + \Big[\int_{\mathcal{R}} \rho^{\mathrm{m}}\big(\mathbf{v}^{\mathrm{m}} - \mathbf{v}^{\mathrm{M}}\big)\otimes\big(\mathbf{v}^{\mathrm{m}} - \mathbf{v}^{\mathrm{M}}\big)\, g(\mathbf{y},\mathbf{x})\,\mathrm{d}v^{\mathrm{m}}\Big]\mathbf{v}^{\mathrm{M}} \quad , \qquad (5.56)
\end{aligned}$$

and

$$\text{(vii)} \;=\; \big(\rho^{\mathrm{M}}\,\mathbf{f}_{\mathrm{B}}^{\mathrm{M}} + \mathbf{f}_{\mathrm{L}}^{\mathrm{M}}\big)\cdot\mathbf{v}^{\mathrm{M}} + \int_{\mathcal{R}} \big(\rho^{\mathrm{m}}\,\mathbf{f}_{\mathrm{B}}^{\mathrm{m}} + \mathbf{f}_{\mathrm{L}}^{\mathrm{m}}\big)\cdot\big(\mathbf{v}^{\mathrm{m}} - \mathbf{v}^{\mathrm{M}}\big)\, g(\mathbf{y},\mathbf{x})\,\mathrm{d}v^{\mathrm{m}} \quad . \qquad (5.57)$$

The last term in Equation (5.56) ultimately cancels with the last term in (5.54), so that Equations (5.54 - 57) furnish

$$\begin{aligned}
\rho^{\mathrm{M}}\dot{e}^{\mathrm{M}} \;&=\; \operatorname{div}_{\mathbf{y}}\big(\mathbf{T}^{\mathrm{M}^{\mathrm{T}}}\mathbf{v}^{\mathrm{M}}\big) + \big(\rho^{\mathrm{M}}\,\mathbf{f}_{\mathrm{B}}^{\mathrm{M}} + \mathbf{f}_{\mathrm{L}}^{\mathrm{M}}\big)\cdot\mathbf{v}^{\mathrm{M}} \\
&\qquad - \operatorname{div}_{\mathbf{y}}\Big\{\int_{\mathcal{R}} \Big[\mathbf{q}^{\mathrm{m}} + \rho^{\mathrm{m}}\tilde{e}^{\mathrm{m}}\big(\mathbf{v}^{\mathrm{m}} - \mathbf{v}^{\mathrm{M}}\big) - \mathbf{T}^{\mathrm{mT}}\big(\mathbf{v}^{\mathrm{m}} - \mathbf{v}^{\mathrm{M}}\big)\Big]\, g(\mathbf{y},\mathbf{x})\,\mathrm{d}v^{\mathrm{m}}\Big\} \\
&\qquad + \int_{\mathcal{R}} \Big[\rho^{\mathrm{m}}\, r^{\mathrm{m}} + \mathbf{j}^{\mathrm{m}}\cdot\boldsymbol{\mathcal{E}}^{\mathrm{m}} + \big(\rho^{\mathrm{m}}\,\mathbf{f}_{\mathrm{B}}^{\mathrm{m}} + \mathbf{f}_{\mathrm{L}}^{\mathrm{m}}\big)\cdot\big(\mathbf{v}^{\mathrm{m}} - \mathbf{v}^{\mathrm{M}}\big)\Big]\, g(\mathbf{y},\mathbf{x})\,\mathrm{d}v^{\mathrm{m}} \quad . \qquad (5.58)
\end{aligned}$$

Here, all remaining terms are identified either as boundary heat fluxes (as indicated by the divergence) or volumetric sources of heat, similar to the expression in (5.44) for linear momentum.

A comparison with the macroscopic energy balance $(5.30)_3$ yields a homogenization rule for the heat flux which is given to within a divergence-free vector function of $(\mathbf{y}, t)$ by

$$\mathbf{q}^{\mathrm{M}} = \int_{\mathcal{R}} \Big[\mathbf{q}^{\mathrm{m}} + \rho^{\mathrm{m}} \tilde{e}^{\mathrm{m}} \big(\mathbf{v}^{\mathrm{m}} - \mathbf{v}^{\mathrm{M}} \big) - \mathbf{T}^{\mathrm{mT}} \big(\mathbf{v}^{\mathrm{m}} - \mathbf{v}^{\mathrm{M}} \big) \Big] g(\mathbf{y}, \mathbf{x}) \, \mathrm{d}v^{\mathrm{m}} \quad . \tag{5.59}$$

The heat flux at the macroscopic scale thus accounts for the weighted volumetric average of the microscopic heat flux plus two additional contributions. Recall that $\tilde{e}^{\mathrm{m}}$ represents an alternative measure of total microscopic energy which accounts for the internal energy plus the kinetic energy due to microscopic velocity fluctuations $\mathbf{v}^{\mathrm{m}} - \mathbf{v}^{\mathrm{M}}$ relative to the 'average' velocity, see (5.53). The second term in (5.59) is thus interpreted as a convective transport of internal energy across the boundary of a macroscopic region due to microscopic velocity fluctuations. The third term represents the flux of energy across the boundary of a macroscopic region due to work performed by the stresses in the presence of microscopic velocity fluctuations.

Meanwhile, the total body heating is found to homogenize according to

$$\rho^{\mathrm{M}} r^{\mathrm{M}} + \mathbf{j}^{\mathrm{M}} \cdot \boldsymbol{\mathcal{E}}^{\mathrm{M}} = \int_{\mathcal{R}} \Big[\rho^{\mathrm{m}} r^{\mathrm{m}} + \mathbf{j}^{\mathrm{m}} \cdot \boldsymbol{\mathcal{E}}^{\mathrm{m}} + \big(\rho^{\mathrm{m}} \mathbf{f}_{\mathrm{B}}^{\mathrm{m}} + \mathbf{f}_{\mathrm{L}}^{\mathrm{m}} \big) \cdot \big(\mathbf{v}^{\mathrm{m}} - \mathbf{v}^{\mathrm{M}} \big) \Big] g(\mathbf{y}, \mathbf{x}) \, \mathrm{d}v^{\mathrm{m}} \quad . \tag{5.60}$$

The macroscopic rate of volumetric heating consists not only of the weighted volumetric average of the microscopic counterpart, but also the rate of work performed by the external forces $\rho^{\mathrm{m}} \mathbf{f}_{\mathrm{B}}^{\mathrm{m}} + \mathbf{f}_{\mathrm{L}}^{\mathrm{m}}$ as a result of microscopic velocity fluctuations $\mathbf{v}^{\mathrm{m}} - \mathbf{v}^{\mathrm{M}}$ relative to the 'average'. Note that the external heating $\rho^{\mathrm{M}} r^{\mathrm{M}} + \mathbf{j}^{\mathrm{M}} \cdot \boldsymbol{\mathcal{E}}^{\mathrm{M}}$ is homogenized as a whole, irrespective of its physical origin. Indeed, the distinction between JOULE heating and any other external sources of volumetric heating is irrelevant for the macroscopic problem. The same argument was made in (5.46) for the external body forces. Additional macroscopic relations can be invoked to obtain individual homogenization formulae for $\rho^{\mathrm{M}} r^{\mathrm{M}}$ and $\mathbf{j}^{\mathrm{M}} \cdot \boldsymbol{\mathcal{E}}^{\mathrm{M}}$ if necessary, see Section 5.4.8.

5.4.4 Total Charge Density

Recall that the microscopic charge density $q^{\mathrm{m}}(\mathbf{x}, t)$ is related to the current $\mathbf{J}^{\mathrm{m}}(\mathbf{x}, t)$ through the conservation of electric charge in Equation (5.26). Furthermore, the first pair of MAXWELL's Equations $(5.24)_{1,2}$ connects the charge-currents $\{q^{\mathrm{m}}, \mathbf{J}^{\mathrm{m}}\}$ to the charge-current potentials $\mathbf{d}^{\mathrm{m}}(\mathbf{x}, t)$ and $\mathbf{h}^{\mathrm{m}}(\mathbf{x}, t)$. The same continuum equations shall be enforced on the macroscopic variables, see Equations $(5.31)_{1,2}$ and (5.33). The three aforementioned governing equations in the two scales are related via the postulated volume-averaging scheme in (5.19) for $q^{\mathrm{M}}(\mathbf{y}, t)$. Therefore, they can be employed to derive consistent homogenization rules for $\mathbf{J}^{\mathrm{M}}(\mathbf{y}, t)$, $\mathbf{d}^{\mathrm{M}}(\mathbf{y}, t)$, and $\mathbf{h}^{\mathrm{M}}(\mathbf{y}, t)$.

Total Current

The derivation of the homogenization of $\mathbf{J}^{\mathrm{M}}(\mathbf{y},t)$ begins with the partial time derivative of the volume-weighted average in (5.19), into which microscopic charge balance (5.26) is inserted, furnishing

$$\begin{aligned}\frac{\partial q^{\mathrm{M}}}{\partial t} &= \frac{\partial}{\partial t}\int_{\mathcal{R}} q^{\mathrm{m}} g(\mathbf{y},\mathbf{x})\,\mathrm{d}v^{\mathrm{m}} \\ &= \int_{\mathcal{R}} \frac{\partial q^{\mathrm{m}}}{\partial t} g(\mathbf{y},\mathbf{x})\,\mathrm{d}v^{\mathrm{m}} \\ &= -\int_{\mathcal{R}} \left(\mathrm{div}_{\mathbf{x}}\,\mathbf{J}^{\mathrm{m}}\right) g(\mathbf{y},\mathbf{x})\,\mathrm{d}v^{\mathrm{m}} \quad . \end{aligned} \tag{5.61}$$

In order to obtain an expression comparable to (5.33) the weighted volumetric average of the divergence $\int \mathrm{div}_{\mathbf{x}}(\,\cdot\,)g$ in (5.61) must be converted into the divergence $\mathrm{div}_{\mathbf{y}}\int(\,\cdot\,)g$ of the weighted volume-average. This of course corresponds exactly with the corollary in (5.13) derived from the properties of $g(\mathbf{y},\mathbf{x})$ postulated in Section 5.1.2, so that

$$\frac{\partial q^{\mathrm{M}}}{\partial t} = -\mathrm{div}_{\mathbf{y}}\left\{\int_{\mathcal{R}} \mathbf{J}^{\mathrm{m}} g(\mathbf{y},\mathbf{x})\,\mathrm{d}v^{\mathrm{m}}\right\} \quad . \tag{5.62}$$

It is therefore concluded by comparison with (5.33) that the macroscale current, to within a divergence-free vector function of $(\mathbf{y},t)$, homogenizes according to

$$\mathbf{J}^{\mathrm{M}}(\mathbf{y},t) = \int_{\mathcal{R}} \mathbf{J}^{\mathrm{m}}(\mathbf{x},t)\, g(\mathbf{y},\mathbf{x})\,\mathrm{d}v^{\mathrm{m}} \quad . \tag{5.63}$$

Charge Potential

Recall that the microscopic charge density $q^{\mathrm{m}}(\mathbf{x},t)$ is related to the charge potential $\mathbf{d}^{\mathrm{m}}(\mathbf{x},t)$ via Gauss' law in Equation $(5.24)_1$. Its macroscopic counterpart $q^{\mathrm{M}}(\mathbf{y},t)$ is postulated to homogenize according to (5.19). Hence, by enforcing Gauss' law on the macroscopic scale the homogenization of $\mathbf{d}^{\mathrm{M}}(\mathbf{y},t)$ may be inferred. This leads to

$$\begin{aligned} q^{\mathrm{M}} &= \int_{\mathcal{R}} q^{\mathrm{m}} g(\mathbf{y},\mathbf{x})\,\mathrm{d}v^{\mathrm{m}} \\ &= \int_{\mathcal{R}} \left(\mathrm{div}_{\mathbf{x}}\,\mathbf{d}^{\mathrm{m}}\right) g(\mathbf{y},\mathbf{x})\,\mathrm{d}v^{\mathrm{m}} \\ &= \mathrm{div}_{\mathbf{y}}\left\{\int_{\mathcal{R}} \mathbf{d}^{\mathrm{m}} g(\mathbf{y},\mathbf{x})\,\mathrm{d}v^{\mathrm{m}}\right\} \quad , \end{aligned} \tag{5.64}$$

where, again, the microscale term $\int \mathrm{div}_{\mathbf{x}}(\,\cdot\,)g$ is converted to a macroscopic $\mathrm{div}_{\mathbf{y}}\int(\,\cdot\,)g$ using the property in (5.13). A comparison with $(5.31)_1$ thus yields the homogenization of $\mathbf{d}^{\mathrm{M}}$ to within a divergence-free vector function of $(\mathbf{y},t)$,

$$\mathbf{d}^{\mathrm{M}}(\mathbf{y},t) = \int_{\mathcal{R}} \mathbf{d}^{\mathrm{m}}(\mathbf{x},t)\, g(\mathbf{y},\mathbf{x})\,\mathrm{d}v^{\mathrm{m}} \quad . \tag{5.65}$$

Current Potential

AMPÈRE's circuital law $(5.24)_2$ relates the total current $\mathbf{J}^{\mathrm{m}}(\mathbf{x},t)$ and the charge potential $\mathbf{d}^{\mathrm{m}}(\mathbf{x},t)$ to the current potential $\mathbf{h}^{\mathrm{m}}(\mathbf{x},t)$. Since the macroscopic $\mathbf{J}^{\mathrm{M}}(\mathbf{y},t)$ and $\mathbf{d}^{\mathrm{M}}(\mathbf{y},t)$ are already given by Equations (5.63) and (5.65), respectively, the macroscopic counterpart $(5.31)_2$ can be invoked to deduce the homogenization of $\mathbf{h}^{\mathrm{M}}(\mathbf{y},t)$. To this end, the left-hand side of $(5.31)_2$ is expressed as

$$\begin{aligned}\mathbf{J}^{\mathrm{M}}+\frac{\partial\mathbf{d}^{\mathrm{M}}}{\partial t} &= \int_{\mathcal{R}}\mathbf{J}^{\mathrm{m}}g(\mathbf{y},\mathbf{x})\,\mathrm{d}v^{\mathrm{m}}+\frac{\partial}{\partial t}\int_{\mathcal{R}}\mathbf{d}^{\mathrm{m}}g(\mathbf{y},\mathbf{x})\,\mathrm{d}v^{\mathrm{m}}\\ &= \int_{\mathcal{R}}\left(\mathbf{J}^{\mathrm{m}}+\frac{\partial\mathbf{d}^{\mathrm{m}}}{\partial t}\right)g(\mathbf{y},\mathbf{x})\,\mathrm{d}v^{\mathrm{m}}\\ &= \int_{\mathcal{R}}\left(\mathrm{curl}_{\mathbf{x}}\,\mathbf{h}^{\mathrm{m}}\right)g(\mathbf{y},\mathbf{x})\,\mathrm{d}v^{\mathrm{m}}\quad . \end{aligned}\tag{5.66}$$

Next, the curl operator in $\int\mathrm{curl}_{\mathbf{x}}(\cdot)\,g$ is removed from the integral to $\mathrm{curl}_{\mathbf{y}}\int(\cdot)\,g$ using the property in (5.14), so that

$$\mathbf{J}^{\mathrm{M}}+\frac{\partial\mathbf{d}^{\mathrm{M}}}{\partial t} = \mathrm{curl}_{\mathbf{y}}\left\{\int_{\mathcal{R}}\mathbf{h}^{\mathrm{m}}g(\mathbf{y},\mathbf{x})\,\mathrm{d}v^{\mathrm{m}}\right\}\quad .\tag{5.67}$$

Therefore, by comparison with $(5.31)_2$, the macroscopic current potential is given to within a curl-free vector function of $(\mathbf{y},t)$ by

$$\mathbf{h}^{\mathrm{M}}(\mathbf{y},t) = \int_{\mathcal{R}}\mathbf{h}^{\mathrm{m}}(\mathbf{x},t)g(\mathbf{y},\mathbf{x})\,\mathrm{d}v^{\mathrm{m}}\quad .\tag{5.68}$$

5.4.5 Magnetic Monopole Density

GAUSS' law for magnetism on the microscale $(5.24)_4$ states that the magnetic flux density $\mathbf{b}^{\mathrm{m}}(\mathbf{x},t)$ is divergence-free. This is analogous to GAUSS' law $(5.24)_1$ for the charge potential $\mathbf{d}^{\mathrm{m}}(\mathbf{x},t)$ in the case where the charge distribution $q^{\mathrm{m}}(\mathbf{x},t)$ vanishes. As previously discussed in (3.10) this implies the absence of any lone 'magnetic charges', which is in line with experimental evidence that magnetism manifests only in the form of magnetic dipoles arising from circular electric currents.

The (vanishing) magnetic monopoles, like electric charges, are considered an extensive quantity. Their density distribution is thus postulated to follow the homogenization scheme (5.2), which of course reduces trivially in this case. Nevertheless, this premise yields homogenization formulae for $\mathbf{b}^{\mathrm{M}}(\mathbf{y},t)$ and $\mathbf{e}^{\mathrm{M}}(\mathbf{y},t)$.

Magnetic Flux Density

The volume-weighted average defined in (5.2) is applied to the entirety of the microscopic form of GAUSS' law for magnetism $(5.24)_4$. The property in (5.13) for the

homogenization of divergences leads to

$$\begin{aligned} 0 &= \int_{\mathcal{R}} \big(\mathrm{div}_{\mathbf{x}}\, \mathbf{b}^{\mathrm{m}}\big) g(\mathbf{y},\mathbf{x})\, \mathrm{d}v^{\mathrm{m}} \\ &= \mathrm{div}_{\mathbf{y}} \Big\{ \int_{\mathcal{R}} \mathbf{b}^{\mathrm{m}} g(\mathbf{y},\mathbf{x})\, \mathrm{d}v^{\mathrm{m}} \Big\} \quad . \end{aligned} \tag{5.69}$$

A comparison with the macroscopic counterpart $(5.31)_4$ yields the homogenization of $\mathbf{b}^{\mathrm{M}}$ to within a divergence-free vector function of $(\mathbf{y}, t)$,

$$\mathbf{b}^{\mathrm{M}}(\mathbf{y},t) = \int_{\mathcal{R}} \mathbf{b}^{\mathrm{m}}(\mathbf{x},t) g(\mathbf{y},\mathbf{x})\, \mathrm{d}v^{\mathrm{m}} \quad . \tag{5.70}$$

Electric Field

Given the preceding result for $\mathbf{b}^{\mathrm{M}}(\mathbf{y},t)$, Faraday's law of induction is invoked on both scales, $(5.24)_3$ and $(5.31)_3$, respectively, to deduce a homogenization rule for the macroscopic electric field $\mathbf{e}^{\mathrm{M}}(\mathbf{y},t)$. Due to the similarity with Ampère's law $(5.24)_2$ in the case $\mathbf{J}^{\mathrm{m}}=\mathbf{0}$, the derivation closely follows Equations (5.66 - 68). In particular,

$$\begin{aligned} \frac{\partial \mathbf{b}^{\mathrm{M}}}{\partial t} &= \int_{\mathcal{R}} \frac{\partial \mathbf{b}^{\mathrm{m}}}{\partial t} g(\mathbf{y},\mathbf{x})\, \mathrm{d}v^{\mathrm{m}} \\ &= -\int_{\mathcal{R}} \big(\mathrm{curl}_{\mathbf{x}}\, \mathbf{e}^{\mathrm{m}}\big) g(\mathbf{y},\mathbf{x})\, \mathrm{d}v^{\mathrm{m}} \\ &= -\mathrm{curl}_{\mathbf{y}} \Big\{ \int_{\mathcal{R}} \mathbf{e}^{\mathrm{m}} g(\mathbf{y},\mathbf{x})\, \mathrm{d}v^{\mathrm{m}} \Big\} \quad . \end{aligned} \tag{5.71}$$

It is thus concluded by comparison with $(5.31)_3$ that $\mathbf{e}^{\mathrm{M}}$ is given to within a curl-free vector function of $(\mathbf{y}, t)$ by

$$\mathbf{e}^{\mathrm{M}}(\mathbf{y},t) = \int_{\mathcal{R}} \mathbf{e}^{\mathrm{m}}(\mathbf{x},t) g(\mathbf{y},\mathbf{x})\, \mathrm{d}v^{\mathrm{m}} \quad . \tag{5.72}$$

5.4.6 Bound Charge Density

The homogenization formulae for $\mathbf{J}^{\mathrm{M}}$, $\mathbf{d}^{\mathrm{M}}$, and $\mathbf{h}^{\mathrm{M}}$ were derived in Section 5.4.4 using the volume-weighted average postulated for q^{M} in conjunction with the premise that the first pair of Maxwell's equations are valid on the macroscopic scale. Likewise, the postulated volumetric average of $q_{\mathrm{R}}^{\mathrm{M}}$ in (5.20) furnishes homogenization formulae for $\mathbf{J}_{\mathrm{R}}^{\mathrm{M}}$, $\mathbf{p}^{\mathrm{M}}$, and $\mathbf{m}^{\mathrm{M}}$. This is achieved by enforcing the bound parts of charge conservation in (5.34) and of Maxwell's first pair of Equations $(5.32)_{1,2}$, respectively, on the macroscale. Note that this process is entirely analogous to the one in Section 5.4.4.

Total Bound Current

The partial time derivative of the prescribed homogenization in (5.20) for the bound charges $q_{\mathrm{R}}^{\mathrm{M}}(\mathbf{y},t)$ yields

$$\begin{aligned}\frac{\partial q_{\mathrm{R}}^{\mathrm{M}}}{\partial t} &= \int_{\mathcal{R}} \frac{\partial q_{\mathrm{R}}^{\mathrm{m}}}{\partial t} g(\mathbf{y},\mathbf{x})\,\mathrm{d}v^{\mathrm{m}} \\ &= -\int_{\mathcal{R}} \left(\mathrm{div}_{\mathbf{x}}\,\mathbf{J}_{\mathrm{R}}^{\mathrm{m}}\right) g(\mathbf{y},\mathbf{x})\,\mathrm{d}v^{\mathrm{m}} \\ &= -\mathrm{div}_{\mathbf{y}}\left\{\int_{\mathcal{R}} \mathbf{J}_{\mathrm{R}}^{\mathrm{m}} g(\mathbf{y},\mathbf{x})\,\mathrm{d}v^{\mathrm{m}}\right\} \quad , \end{aligned} \tag{5.73}$$

where the microscopic charge conservation in $(5.27)_2$ and the divergence property in (5.13) were used. It is thus inferred from the macroscopic statement of charge conservation in (5.34) that, up to a divergence-free term, the total bound current $\mathbf{J}_{\mathrm{R}}^{\mathrm{M}}(\mathbf{y},t)$ reads

$$\mathbf{J}_{\mathrm{R}}^{\mathrm{M}}(\mathbf{y},t) = \int_{\mathcal{R}} \mathbf{J}_{\mathrm{R}}^{\mathrm{m}}(\mathbf{x},t)\, g(\mathbf{y},\mathbf{x})\,\mathrm{d}v^{\mathrm{m}} \quad . \tag{5.74}$$

Polarization

The bound part of Gauss' law $(5.25)_3$ is inserted into (5.20) to write

$$\begin{aligned} q_{\mathrm{R}}^{\mathrm{M}} &= \int_{\mathcal{R}} q_{\mathrm{R}}^{\mathrm{m}} g(\mathbf{y},\mathbf{x})\,\mathrm{d}v^{\mathrm{m}} \\ &= -\int_{\mathcal{R}} \left(\mathrm{div}_{\mathbf{x}}\,\mathbf{p}^{\mathrm{m}}\right) g(\mathbf{y},\mathbf{x})\,\mathrm{d}v^{\mathrm{m}} \\ &= -\mathrm{div}_{\mathbf{y}}\left\{\int_{\mathcal{R}} \mathbf{p}^{\mathrm{m}} g(\mathbf{y},\mathbf{x})\,\mathrm{d}v^{\mathrm{m}}\right\} \quad , \end{aligned} \tag{5.75}$$

where (5.13) was used. By enforcing the macroscopic counterpart $(5.32)_1$ it is concluded that the polarization $\mathbf{p}^{\mathrm{M}}(\mathbf{y},t)$ homogenizes to within a divergence-free term according to

$$\mathbf{p}^{\mathrm{M}}(\mathbf{y},t) = \int_{\mathcal{R}} \mathbf{p}^{\mathrm{m}}(\mathbf{x},t)\, g(\mathbf{y},\mathbf{x})\,\mathrm{d}v^{\mathrm{m}} \quad . \tag{5.76}$$

Magnetization

Equations (5.14), (5.74) and (5.76) are employed to homogenize AMPÈRE's circuital law $(5.25)_4$ for the bound fields, furnishing

$$\begin{aligned}\mathbf{J}_{\mathrm{R}}^{\mathrm{M}} - \frac{\partial \mathbf{p}^{\mathrm{M}}}{\partial t} &= \int_{\mathcal{R}} \mathbf{J}_{\mathrm{R}}^{\mathrm{m}} g(\mathbf{y},\mathbf{x})\,\mathrm{d}v^{\mathrm{m}} - \frac{\partial}{\partial t}\int_{\mathcal{R}} \mathbf{p}^{\mathrm{m}} g(\mathbf{y},\mathbf{x})\,\mathrm{d}v^{\mathrm{m}} \\ &= \int_{\mathcal{R}} \left(\mathbf{J}_{\mathrm{R}}^{\mathrm{m}} - \frac{\partial \mathbf{p}^{\mathrm{m}}}{\partial t}\right) g(\mathbf{y},\mathbf{x})\,\mathrm{d}v^{\mathrm{m}} \\ &= \int_{\mathcal{R}} \left(\mathrm{curl}_{\mathbf{x}}\,\mathbf{m}^{\mathrm{m}}\right) g(\mathbf{y},\mathbf{x})\,\mathrm{d}v^{\mathrm{m}} \\ &= \mathrm{curl}_{\mathbf{y}}\left\{\int_{\mathcal{R}} \mathbf{m}^{\mathrm{m}} g(\mathbf{y},\mathbf{x})\,\mathrm{d}v^{\mathrm{m}}\right\} \quad . \end{aligned} \tag{5.77}$$

A comparison with the macroscopic AMPÈRE's law $(5.32)_2$ yields the homogenization of the MINKOWSKI magnetization $\mathbf{m}^{\mathrm{M}}(\mathbf{y},t)$,

$$\mathbf{m}^{\mathrm{M}}(\mathbf{y},t) = \int_{\mathcal{R}} \mathbf{m}^{\mathrm{m}}(\mathbf{x},t)\, g(\mathbf{y},\mathbf{x})\,\mathrm{d}v^{\mathrm{m}} \quad , \tag{5.78}$$

to within a curl-free term.

5.4.7 Aether Relations

According to Equations (5.19), (5.63), (5.65), (5.68), (5.70), and (5.72), the homogenization formulae of q^{M}, $\mathbf{J}^{\mathrm{M}}$, $\mathbf{d}^{\mathrm{M}}$, $\mathbf{h}^{\mathrm{M}}$, $\mathbf{b}^{\mathrm{M}}$, and $\mathbf{e}^{\mathrm{M}}$ obey the weighted volumetric averaging scheme outlined in (5.2). This is not entirely surprising given that MAXWELL's partial differential equations are linear, thereby avoiding any products between two homogenization integrals.

The microscopic aether relations in $(5.28)_{1,2}$ describe a proportional relationship between the pairs of fields $\{\mathbf{d}^{\mathrm{m}},\mathbf{e}^{\mathrm{m}}\}$ and $\{\mathbf{h}^{\mathrm{m}},\mathbf{b}^{\mathrm{m}}\}$. Since their macroscopic counterparts follow the same homogenization rule, the aether relations are automatically preserved on the macroscopic scale,

$$\begin{aligned}\mathbf{d}^{\mathrm{M}}(\mathbf{y},t) &= \int_{\mathcal{R}} \mathbf{d}^{\mathrm{m}} g(\mathbf{y},\mathbf{x})\,\mathrm{d}v^{\mathrm{m}} \\ &\overset{\text{Aet.}}{=} \int_{\mathcal{R}} \varepsilon_0 \mathbf{e}^{\mathrm{m}} g(\mathbf{y},\mathbf{x})\,\mathrm{d}v^{\mathrm{m}} = \varepsilon_0 \mathbf{e}^{\mathrm{M}}(\mathbf{y},t) \quad , \end{aligned} \tag{5.79}$$

and

$$\begin{aligned}\mathbf{h}^{\mathrm{M}}(\mathbf{y},t) &= \int_{\mathcal{R}} \mathbf{h}^{\mathrm{m}} g(\mathbf{y},\mathbf{x})\,\mathrm{d}v^{\mathrm{m}} \\ &\overset{\text{Aet.}}{=} \int_{\mathcal{R}} \left(\mathbf{b}^{\mathrm{m}}/\mu_0\right) g(\mathbf{y},\mathbf{x})\,\mathrm{d}v^{\mathrm{m}} = \mathbf{b}^{\mathrm{M}}(\mathbf{y},t)/\mu_0 \quad . \end{aligned} \tag{5.80}$$

Likewise, recall from (5.20), (5.74), (5.76), and (5.78) that the bound quantities $q_{\mathrm{R}}^{\mathrm{M}}$, $\mathbf{J}_{\mathrm{R}}^{\mathrm{M}}$, $\mathbf{p}^{\mathrm{M}}$, and $\mathbf{m}^{\mathrm{M}}$ homogenize as weighted volumetric averages. It is therefore concluded that the free parts $q_{\mathrm{F}}^{\mathrm{M}}$, $\mathbf{J}_{\mathrm{F}}^{\mathrm{M}}$, $\mathbf{d}_{\mathrm{F}}^{\mathrm{M}}$, and $\mathbf{h}_{\mathrm{F}}^{\mathrm{M}}$ are volume averages, too. This implies that the additive decomposition of the electric charges-currents $\{q, \mathbf{J}\}$ into their free and bound parts, as well as the additive decompositions of the charge-current potentials $\{\mathbf{d}, \mathbf{h}\}$, are preserved on the macroscopic scale. Hence the extended aether relations $(5.29)_{1,2}$, too, are preserved on the macroscopic scale,

$$\begin{aligned} \mathbf{d}_{\mathrm{F}}^{\mathrm{M}}(\mathbf{y},t) &\overset{\text{Aet.}}{=} \varepsilon_0 \mathbf{e}^{\mathrm{M}}(\mathbf{y},t) + \mathbf{p}^{\mathrm{M}}(\mathbf{y},t) \quad , \\ \mathbf{h}_{\mathrm{F}}^{\mathrm{M}}(\mathbf{y},t) &\overset{\text{Aet.}}{=} \mathbf{b}^{\mathrm{M}}(\mathbf{y},t)/\mu_0 - \mathbf{m}^{\mathrm{M}}(\mathbf{y},t) \quad . \end{aligned} \tag{5.81}$$

The preceding discussion highlights that the notion of extensivity applies separately to the free and the bound charges. The clear delineation between free and bound quantities on the microscopic scale is retained at the macroscopic level, because the linearity of MAXWELL's equations allows the free and bound fields to coexist independently of each other. This is in stark contrast to the distinction (or the lack thereof) between the kinetic and internal energies, for example, where microscopic terms associated with the kinetic energy of velocity fluctuations are upscaled into macroscopic contributions to the internal energy.[10] As a result, only the *total* energy is postulated to homogenize according to the weighted volumetric average for extensive quantities, see (5.18), but not the internal or kinetic energies.

5.4.8 Implications for Other (Non-Extensive) Quantities

It may be inferred from Equations (5.16) and (5.17) that the macroscale velocity $\mathbf{v}^{\mathrm{M}}$ is related to $\mathbf{v}^{\mathrm{m}}$ by a homogenization of the form

$$\mathbf{v}^{\mathrm{M}}(\mathbf{y},t) \;=\; \frac{\rho^{\mathrm{M}}(\mathbf{y},t)\,\mathbf{v}^{\mathrm{M}}(\mathbf{y},t)}{\rho^{\mathrm{M}}(\mathbf{y},t)} \;=\; \frac{\int_{\mathcal{R}} \rho^{\mathrm{m}}(\mathbf{x},t)\,\mathbf{v}^{\mathrm{m}}(\mathbf{x},t)\,g(\mathbf{y},\mathbf{x})\,\mathrm{d}v^{\mathrm{m}}}{\int_{\mathcal{R}} \rho^{\mathrm{m}}(\mathbf{x},t)\,g(\mathbf{y},\mathbf{x})\,\mathrm{d}v^{\mathrm{m}}} \quad , \tag{5.82}$$

which connects the motion of material points $\mathbf{x}$ at the microscale to the motion of $\mathbf{y}$ at the macroscale, see Equation (5.1). This interdependence of $\dot{\mathbf{y}}$ on $\dot{\mathbf{x}}$ is a direct consequence of the definition of mass ρ^{M} and momentum densities $\rho^{\mathrm{M}}\mathbf{v}^{\mathrm{M}}$ by volume averages.

The results in Equations (5.46) and (5.60), which provide the homogenizations for the external volumetric forces (*i.e.*, the sum of the body force and the LORENTZ force densities $\rho^{\mathrm{M}}\mathbf{f}_{\mathrm{B}}^{\mathrm{M}} + \mathbf{f}_{\mathrm{L}}^{\mathrm{M}}$) and for the volumetric heating (*i.e.*, the sum of the external heat source and JOULE heating $\rho^{\mathrm{M}} r^{\mathrm{M}} + \mathbf{j}^{\mathrm{M}} \cdot \boldsymbol{\mathcal{E}}^{\mathrm{M}}$), respectively. Although it was previously pointed out that only the combined quantities are relevant for the IBVP posed by

[10] The entangled nature of the microscopic velocity fluctuations and the macroscopic heat flux and body heating are discussed in the context of Equations (5.59 - 60).

the balance equations and MAXWELL's equations, these results nevertheless raise the question of what $\rho^{\mathrm{M}}\mathbf{f}_{\mathrm{B}}^{\mathrm{M}}$ and $\rho^{\mathrm{M}} r^{\mathrm{M}}$ are given as individually.

To this end, recall Equations (5.22) and $(5.23)_{1-3}$ for the microscopic scale. For the sake of argument, let the same relations be enforced on the macroscopic scale, that is,

$$\mathbf{J}^{\mathrm{M}}(\mathbf{y},t)\cdot\mathbf{e}^{\mathrm{M}}(\mathbf{y},t) \;=\; \mathbf{j}^{\mathrm{M}}(\mathbf{y},t)\cdot\boldsymbol{\mathcal{E}}^{\mathrm{M}}(\mathbf{y},t) + \mathbf{f}_{\mathrm{L}}^{\mathrm{M}}(\mathbf{y},t)\cdot\mathbf{v}^{\mathrm{M}}(\mathbf{y},t) \quad , \tag{5.83}$$

and

$$\begin{aligned}
\mathbf{J}^{\mathrm{M}}(\mathbf{y},t) &= \mathbf{j}^{\mathrm{M}}(\mathbf{y},t) + q^{\mathrm{M}}(\mathbf{y},t)\,\mathbf{v}^{\mathrm{M}}(\mathbf{y},t) &&, \\
\boldsymbol{\mathcal{E}}^{\mathrm{M}}(\mathbf{y},t) &= \mathbf{e}^{\mathrm{M}}(\mathbf{y},t) + \mathbf{v}^{\mathrm{M}}(\mathbf{y},t)\times\mathbf{b}^{\mathrm{M}}(\mathbf{y},t) &&, \\
\mathbf{f}_{\mathrm{L}}^{\mathrm{M}}(\mathbf{y},t) &= q^{\mathrm{M}}(\mathbf{y},t)\,\mathbf{e}^{\mathrm{M}}(\mathbf{y},t) + \mathbf{J}^{\mathrm{M}}(\mathbf{y},t)\times\mathbf{b}^{\mathrm{M}}(\mathbf{y},t) &&.
\end{aligned} \tag{5.84}$$

Note that Equation (5.83) is derived from (5.84) and may thus be viewed as a consequence of enforcing the latter relations. Equations $(5.84)_{1-3}$ impose new conditions used to derive the homogenization of $\mathbf{j}^{\mathrm{M}}$, $\boldsymbol{\mathcal{E}}^{\mathrm{M}}$, and $\mathbf{f}_{\mathrm{L}}^{\mathrm{M}}$, respectively, which are in addition to the minimal set of assumptions listed in Section 5.3.2. The new requirements do not cause any contradictions with previous results since $\mathbf{j}^{\mathrm{M}}$, $\boldsymbol{\mathcal{E}}^{\mathrm{M}}$, and $\mathbf{f}_{\mathrm{L}}^{\mathrm{M}}$ are yet unspecified.

The homogenization of the *conduction* current $\mathbf{j}^{\mathrm{M}}(\mathbf{y},t)$ is less straightforward than the *total* current $\mathbf{J}^{\mathrm{M}}(\mathbf{y},t)$. According to Equation $(5.84)_1$ the conduction current is obtained by subtracting the convective contribution,

$$\mathbf{j}^{\mathrm{M}}(\mathbf{y},t) \;=\; \int_{\mathcal{R}} \mathbf{J}^{\mathrm{m}}\, g(\mathbf{y},\mathbf{x})\,\mathrm{d}v^{\mathrm{m}} - \frac{\int_{\mathcal{R}} q^{\mathrm{m}}\, g(\mathbf{y},\mathbf{x})\,\mathrm{d}v^{\mathrm{m}} \int_{\mathcal{R}} \rho^{\mathrm{m}}\,\mathbf{v}^{\mathrm{m}}\, g(\mathbf{y},\mathbf{x})\,\mathrm{d}v^{\mathrm{m}}}{\int_{\mathcal{R}} \rho^{\mathrm{m}}\, g(\mathbf{y},\mathbf{x})\,\mathrm{d}v^{\mathrm{m}}} \quad , \tag{5.85}$$

where the homogenizations (5.19), (5.82), and (5.63) were used. Likewise, the bound part of the conduction current $\mathbf{j}_{\mathrm{R}}^{\mathrm{M}}(\mathbf{y},t)$ is obtained by enforcing Equation $(5.84)_1$ for the bound parts, $\mathbf{j}_{\mathrm{R}}^{\mathrm{M}} = \mathbf{J}_{\mathrm{R}}^{\mathrm{M}} - q_{\mathrm{R}}^{\mathrm{M}}\mathbf{v}^{\mathrm{M}}$, and employing Equations (5.20), (5.74), and (5.82).

The macroscopic definition of the electromotive intensity $\boldsymbol{\mathcal{E}}^{\mathrm{M}}$ in $(5.84)_2$ implies that its homogenization is expressed as

$$\boldsymbol{\mathcal{E}}^{\mathrm{M}}(\mathbf{y},t) \;=\; \int_{\mathcal{R}} \mathbf{e}^{\mathrm{m}} g(\mathbf{y},\mathbf{x})\,\mathrm{d}v^{\mathrm{m}} + \frac{\int_{\mathcal{R}} \rho^{\mathrm{m}}\mathbf{v}^{\mathrm{m}} g(\mathbf{y},\mathbf{x})\,\mathrm{d}v^{\mathrm{m}} \times \int_{\mathcal{R}} \mathbf{b}^{\mathrm{m}} g(\mathbf{y},\mathbf{x})\,\mathrm{d}v^{\mathrm{m}}}{\int_{\mathcal{R}} \rho^{\mathrm{m}} g(\mathbf{y},\mathbf{x})\,\mathrm{d}v^{\mathrm{m}}} \quad , \tag{5.86}$$

where use is made of the homogenizations in (5.70), (5.72), and (5.82).

Lastly, the LORENTZ force density is obtained from the definition in $(5.84)_3$, the postulated extensivity of the electric charge (5.19), and the derived homogenizations of the electromagnetic quantities in Equations (5.63), (5.70), and (5.72),

$$\mathbf{f}_{\mathrm{L}}^{\mathrm{M}}(\mathbf{y},t) = \int_{\mathcal{R}} q^{\mathrm{m}}\, g(\mathbf{y},\mathbf{x})\,\mathrm{d}v^{\mathrm{m}} \int_{\mathcal{R}} \mathbf{e}^{\mathrm{m}} g(\mathbf{y},\mathbf{x})\,\mathrm{d}v^{\mathrm{m}} + \int_{\mathcal{R}} \mathbf{J}^{\mathrm{m}}\, g(\mathbf{y},\mathbf{x})\,\mathrm{d}v^{\mathrm{m}} \times \int_{\mathcal{R}} \mathbf{b}^{\mathrm{m}} g(\mathbf{y},\mathbf{x})\,\mathrm{d}v^{\mathrm{m}} \quad . \tag{5.87}$$

It is readily verified that this result agrees with Equation (5.83) for the EM power density. This is no surprise, because just enough (but not too many) homogenization

rules and macroscale equations have been stipulated to derive all quantities without contradiction.

Expressions for $\rho^{\mathrm{M}}\mathbf{f}_{\mathrm{B}}^{\mathrm{M}}$ and $\rho^{\mathrm{M}}r^{\mathrm{M}}$ are readily obtained from (5.46) and (5.60) in conjunction with (5.16) and the preceding results in (5.85 - 87). For example, even though the total external force density $\rho^{\mathrm{M}}\mathbf{f}_{\mathrm{B}}^{\mathrm{M}}+\mathbf{f}_{\mathrm{L}}^{\mathrm{M}}$ is found to homogenize in accordance with the volumetric averaging scheme (5.2), its two constituents do *not*, since Equation (5.87) already establishes that the LORENTZ force density on its own fails to obey a simple volume average. The resulting homogenization formula for $\mathbf{f}_{\mathrm{B}}^{\mathrm{M}}$ is not printed here in its entirety.

Recall that the total energy density per unit mass (2.122) is defined by the sum of the kinetic and internal energies. This relation certainly applies in the microscopic scale, but can be additionally enforced in the macroscopic scale as

$$e^{\mathrm{M}}(\mathbf{y},t) \;=\; \tfrac{1}{2}\mathbf{v}^{\mathrm{M}}(\mathbf{y},t)\cdot\mathbf{v}^{\mathrm{M}}(\mathbf{y},t) + \varepsilon^{\mathrm{M}}(\mathbf{y},t) \quad . \tag{5.88}$$

The homogenization for the *total* energy density per unit volume $\rho^{\mathrm{M}}e^{\mathrm{M}}$ is postulated by the volume-averaging scheme in (5.18). The homogenization of the *kinetic* part is readily available, here stated per unit volume using Equations (5.16) and (5.17),

$$\tfrac{1}{2}\rho^{\mathrm{M}}\mathbf{v}^{\mathrm{M}}\cdot\mathbf{v}^{\mathrm{M}} \;=\; \frac{1}{2}\frac{\int_{\mathcal{R}}\rho^{\mathrm{m}}\mathbf{v}^{\mathrm{m}}g(\mathbf{y},\mathbf{x})\,\mathrm{d}v^{\mathrm{m}}\cdot\int_{\mathcal{R}}\rho^{\mathrm{m}}\mathbf{v}^{\mathrm{m}}g(\mathbf{y},\mathbf{x})\,\mathrm{d}v^{\mathrm{m}}}{\int_{\mathcal{R}}\rho^{\mathrm{m}}g(\mathbf{y},\mathbf{x})\,\mathrm{d}v^{\mathrm{m}}} \quad . \tag{5.89}$$

Unlike (5.18), this expression does not represent a simple volumetric average. In view of the additive decomposition (5.88) the internal energy density $\rho^{\mathrm{M}}\varepsilon^{\mathrm{M}}$, too, cannot obey the volume-averaging scheme (5.2) on its own. It is instead given by

$$\rho^{\mathrm{M}}\varepsilon^{\mathrm{M}} \;=\; \int_{\mathcal{R}}\rho^{\mathrm{m}}\,e^{\mathrm{m}}g(\mathbf{y},\mathbf{x})\,\mathrm{d}v^{\mathrm{m}} - \frac{1}{2}\frac{\left|\int_{\mathcal{R}}\rho^{\mathrm{m}}\mathbf{v}^{\mathrm{m}}g(\mathbf{y},\mathbf{x})\,\mathrm{d}v^{\mathrm{m}}\right|^2}{\int_{\mathcal{R}}\rho^{\mathrm{m}}g(\mathbf{y},\mathbf{x})\,\mathrm{d}v^{\mathrm{m}}} \quad . \tag{5.90}$$

This example highlights the fact that, despite the total and internal energies being ostensibly extensive quantities, only either $\rho^{\mathrm{M}}e^{\mathrm{M}}$ or $\rho^{\mathrm{M}}\varepsilon^{\mathrm{M}}$ may be defined by a volumetric average of the microscopic counterpart, but not both. Indeed it can even be argued, within the context of multiscale homogenization, that the kinetic and internal energies are *not* in fact extensive quantities. This is because quantities associated with the kinetic energy in the microscale become entangled with the internal energy on the macroscale during the process of upscaling from continuum to continuum. The notion of extensivity of the kinetic and internal energies, *i.e.*, that their total value corresponds to the sum of the individual parts, disintegrates when applied to the homogenization across two scales.

In closing, it is reiterated that the imposition of additional macroscopic relations for the sake of deriving homogenization formulae for more quantities is not advocated for, especially since they are unnecessary for the solution of the IBVP posed by the EMTM balance equations. It is instead preferred to enforce only the minimum number of necessary relations on the macroscopic scale.

Chapter 6

Numerical Implementation of EMTM on Single Scale

In Chapter 4, the balance equations and constitutive restrictions for coupled electro-magneto-thermo-mechanical materials were introduced. In the present chapter, a numerical implementation thereof is presented using the *finite element method* (FEM). Although this implementation operates on a single scale continuum, it serves as background for the multiscale algorithm of Chapter 7. Indeed, the single-scale model forms the basis for the *micro*scopic scale in the multiscale algorithm, for the microscale employs the constitutive equations to compute average stresses, fluxes, and tangents to be sent to the macroscale. Ultimately, the goal of Chapters 6 and 7 is to provide a practical demonstration of the multiscale homogenization scheme introduced in Chapter 5.

A number of simplifying assumptions are introduced to the governing equations and the problem setup, so as not to unnecessarily complicate the numerical implementation of the EMTM model and detract from the aforementioned main objective. Most notably, it is assumed that the problem is entirely static. In particular, the problem is assumed to be electrostatic, which leads to a substantial simplification of the governing EM equations.[1] Furthermore, the implementation is limited to 2-dimensional problems in an effort to keep the computational cost of the ensuing multiscale algorithm of Chapter 7 relatively low. Hence the domain of the finite element model consists of a 2-dimensional shape, whereby the physical continuum is assumed to extend infinitely toward the out-of-plane directions. The boundary conditions, external loads, constitutive parameters, and solution fields (*i.e.*, the displacements, temperature, *etc.*) are allowed to vary only within the in-plane dimensions of the

[1] Even the magnetostatic case poses numerical challenges related to the null-space of the curl operator, which are typically addressed using so-called edge elements. The numerical implementation of electrodynamics is beyond the scope of this dissertation and the reader is referred to Ciarlet *et al.* [15], Demkowicz [20], Hiptmair *et al.* [51], Lee [72], Monk [97], Nicaise [105], and Nedelec [109, 110].

finite element domain. This also implies that any deformations occur in *plane strain*.

This chapter is organized as follows: First, the so-called *initial/boundary-value problem* (IBVP) is formulated for the single scale, which later forms the basis for the microscopic scale of the multiscale (or FE2 for short) model. This includes the governing laws, constitutive relations, and the initial and boundary conditions. Second, to make the problem amenable to solution by finite elements (FE), the so-called *weak form* and the corresponding residuals are derived. Third, upon a brief review of the NEWTON-RAPHSON method, the differentials of the residuals are deduced in preparation for the application of the method to solve the nonlinear system of equations. Next, a standard finite element discretization is introduced to convert the continuous fields and differential equations into finite-dimensional approximations. This furnishes a set of algebraic equations for the nodal values of the relevant fields $\mathbf{u}$, θ, ϕ, and φ. Lastly, a 2-dimensional version of the ensuing residuals and tangents is implemented in FEAP [142], and validated for accuracy and convergence. Note that the discussion and implementation of the FEM relies in part on the books by HUGHES [54], OTTOSEN and PETERSSON [113], and the first two volumes of ZIENKIEWICZ and TAYLOR [159, 160].

6.1 Initial/Boundary-Value Problem

In this section a well-posed[2] IBVP is formulated for the single-scale model. The IBVP encompasses the balance equations, the constitutive model, the initial conditions, and the boundary conditions. This discussion concludes with a summary of all simplifying assumptions invoked throughout this section.

Note that the dependent variables (*i.e.*, the unknown scalar-, vector-, and tensor-valued fields of the IBVP) can be grouped into three main categories. These groups are referred to henceforth using the following nomenclature:

(i) The displacement vector $\mathbf{u}$, the temperature θ, and the EM potentials $\{\phi, \mathbf{a}\}$ (or the electrostatic potentials $\{\phi, \varphi\}$) are called the *primary variables*. Their primacy stems from the fact that the gradients (see (ii) below) and the constitutive response (see (iii) below) are derived from them. One balance equation is available per each primary variable, which in a discrete setting are associated with *degrees of freedom* (DoF).

Note that, due to their trivial relation to the primary variables, material time derivatives thereof are not afforded their own category or nomenclature. For example, the velocity $\dot{\mathbf{u}}$ and the acceleration $\ddot{\mathbf{u}}$ represent the same primary variable $\mathbf{u}$, which is associated with the vector-valued balance equation of linear

[2] An IBVP is considered well posed if it has a unique solution which depends continuously on the initial and boundary conditions.

momentum.[3]

(ii) Quantities which are defined in terms of the (spatial or referential) gradients of the primary variables, are collectively referred to as the *gradient quantities*. The expressions by which they are derived from the primary variables are called the *gradient relations*.

For example, the EM fields $\{\mathbf{e}, \mathbf{b}\}$ are gradient quantities because they are given by the spatial gradient and the spatial curl of the EM potentials $\{\phi, \mathbf{a}\}$, respectively, see Equations $(3.138)_{1,2}$. This category also comprises the kinematic quantities introduced in Section 2.2. For example, the GREEN-LAGRANGE strain tensor $\mathbf{E}$ is expressed in terms of the referential displacement gradient (2.72) according to $(2.76)_2$. Note that rates of deformation, such as the spatial velocity gradient $\mathbf{L}$, are also considered to be gradient quantities.

(iii) The so-called *fluxes* quantify the response of the continuum to the external stimuli. The fluxes are obtained from the *constitutive relations*, which are given by explicit functions of the primary variables and their gradient quantities, see for example the functional dependence of the constitutive functions in (4.57) and $(4.74)_{1,2}$. Since the fluxes prominently feature in the balance equations, knowledge of the constitutive relations is indispensable for a solution.

Examples of fluxes are the CAUCHY stress tensor $\mathbf{T}$, the generalized heat flux $\hat{\mathbf{q}}$, the polarization $\mathbf{p}$, the magnetization $\boldsymbol{\mathcal{M}}$, and the free conduction current $\mathbf{j}_{\mathrm{F}}$. Their referential counterparts (such as the second PIOLA-KIRCHHOFF stress tensor $\mathbf{S}$, or the referential polarization vector $\mathbf{p}_0$) are also considered to be fluxes. Since, arguably, the aether relations may be viewed as constitutive relations, the charge-current potentials $\{\mathbf{d}, \mathbf{h}\}$ may be considered fluxes, too.[4]

6.1.1 Governing Equations

MAXWELL's equations of electromagnetism and the thermomechanical balance equations for coupled electro-magneto-thermo-mechanical media have been discussed in ample detail in Chapters 3 and 4, respectively. Here, the relevant equations are briefly reviewed and simplifications are introduced where appropriate.

[3] In a two-dimensional setting, of course, there are only two non-zero components of displacement $\mathbf{u}$ and thus only two non-trivial components of the linear momentum balance.

[4] In electromagnetism the distinction between gradient quantities and fluxes is not always clear cut. For example, for electrostatics the free current potential $\mathbf{h}_{\mathrm{F}}$ is obtained from the gradient in (3.150). Hence $\mathbf{h}_{\mathrm{F}}$ is seen as a gradient quantity, whereas $\boldsymbol{\mathcal{M}}$ (and thus $\mathbf{b}$ via the aether relations) represent fluxes.

Thermomechanical Part

The displacement and temperature fields are governed by the balances of linear momentum and thermal energy. Their differential statements are given for EMTM materials by Equations (4.6) and (4.19), respectively, or[5]

$$\begin{aligned} \rho\ddot{\mathbf{u}} &= \operatorname{div}\mathbf{T} + \rho\mathbf{f}_{\mathrm{B}} + \mathbf{f}_{\mathrm{L}} \quad , \\ \rho\dot{\varepsilon} &= \mathbf{T}\cdot\mathbf{L} + \rho r - \operatorname{div}\mathbf{q} + \mathbf{j}\cdot\boldsymbol{\mathcal{E}} \quad . \end{aligned} \tag{6.1}$$

Note that the balance of angular momentum in (4.8) can be satisfied automatically by an appropriate constitutive equation for the stress which enforces symmetry of $\mathbf{T}$. Furthermore, the conservation of mass (2.111) does not need to be enforced separately for solid materials: If the density in the reference configuration at time t_0 is given by a field $\rho_0(\mathbf{X}) > 0$, then the density of the current configuration follows trivially from

$$\rho = \frac{\rho_0}{J} \quad \text{with} \quad J = \det\mathbf{F} = \det\left[\mathbf{I} + \frac{\partial\mathbf{u}}{\partial\mathbf{X}}\right] > 0 \quad , \tag{6.2}$$

where J is the JACOBIAN determinant defined in (2.68). Here, use was made of the referential form of the mass balance, see (2.137). The referential configuration is assumed to be free of internal stresses while in thermal equilibrium at temperature θ_0 and devoid of any EM fields. In the interest of simplicity the reference configuration is assumed to coincide with initial configuration at time $t_0 = 0$. The motion (2.60) at t_0 thus returns $\mathbf{x}_0 = \boldsymbol{\chi}(\mathbf{X}, 0) = \mathbf{X}$. This of course implies zero displacements $\mathbf{u}_0 = \mathbf{u}(\mathbf{x}, 0) = \mathbf{0}$, a trivial deformation gradient $\mathbf{F}_0 = \mathbf{F}(\mathbf{x}, 0) = \mathbf{1}$ with corresponding JACOBIAN $J(\mathbf{x}, 0) = J_0 = 1$, and a referential density of $\rho(\mathbf{x}, 0) = \rho_0$.

It is assumed that the mechanical problem is (quasi-)static, and thus the internal stresses and external forces are (approximately) in equilibrium. This means not only that the acceleration is negligible, but also that the velocity (and any convective terms arising from it) are insignificant. The thermal problem, too, is assumed to have reached steady state so that the internal energy is approximately constant. In summary, it is assumed that

$$\dot{\mathbf{u}} \doteq \mathbf{0} \quad , \quad \ddot{\mathbf{u}} \doteq \mathbf{0} \quad , \quad \dot{\varepsilon} \doteq \mathbf{0} \quad . \tag{6.3}$$

The preceding assumptions may be regarded as limitations imposed on the range of physical problems that this numerical model encompasses for a single scale continuum. However, in the context of multiscale modeling a physical justification for the approximations in $(6.3)_{1-3}$ is available for the microscopic scale: Recall from the introduction to Chapter 5 that the characteristic length and time of the microscopic

[5] Since the displacement (2.63) is considered to be the primary variable of the mechanical finite element problem, the velocity and acceleration are expressed in terms of material time derivatives of $\mathbf{u}$. Moreover, this precludes any potential confusion with the notation for the magnetic potential $\mathbf{a}$.

scale are much smaller than on the macroscopic scale. Therefore, even though dynamic effects may be significant on the macroscopic scale, over microscopic distances such disturbances will propagate quickly and equilibrium is reached almost instantly.[6] Hence, for the microscopic problem the rates of change of momentum $\rho\ddot{\mathbf{u}}$ and internal energy $\rho\dot{\varepsilon}$ may be neglected since they are far outweighed by the other terms in Equations $(6.1)_{1,2}$.

Next, it is assumed that the external volumetric loads in the linear momentum and thermal energy balances $(6.1)_{1,2}$ are negligible. In particular, the contributions of the external body force $\mathbf{f}_\mathrm{B}$ and body heating r, as well as the LORENTZ force $\mathbf{f}_\mathrm{L}$ and JOULE heating $\mathbf{j}\cdot\boldsymbol{\mathcal{E}}$ are set to vanish,

$$\mathbf{f}_\mathrm{B} \doteq \mathbf{0} \quad , \quad r \doteq 0 \quad , \quad \mathbf{f}_\mathrm{L} \doteq \mathbf{0} \quad , \quad \mathbf{j}\cdot\boldsymbol{\mathcal{E}} \doteq 0 \quad . \tag{6.4}$$

All volumetric source terms are thus eliminated from the balance equations. Only the stress-divergence and flux-divergence terms remain in the (microscopic) balance Equations $(6.1)_{1,2}$. In the context of multiscale modeling, again, a physical argument is made in favor of the simplifications in (6.4) on the basis of the scale separation between the microscopic model and the macroscopic problem: On the macroscopic scale the aforementioned volume source terms are assumed to be bounded. It follows that at microscopic length scales their contribution (per volume) is far outweighed by the boundary terms (per surface) due to traction and heat flux, hence Equations $(6.4)_{1-4}$ are justified.

The approximations in $(6.3)_{2,3}$ and $(6.4)_{1,2}$ are attributed to the microscopic scale by many authors in the context of multiscale modeling, see, for example, FISH and FAN [28], KOUZNETSOVA [62], SENGUPTA *et al.* [127], and ÖZDEMIR *et al.* [162]. Meanwhile, the conditions in $(6.4)_{3,4}$ for the EM terms appear to be used inadvertently by some authors, see LABUSCH [67] and SCHRÖDER *et al.* [126], where the EM effects are not *a priori* included in the TM balance equations.

Electromagnetic Part

Recall that the EM problem is described by MAXWELL's Equations (3.15). The charge-current potentials additively decompose into their free and bound parts, which separately obey (3.33) and (3.34), respectively.

However, it was argued in Section 3.7 that the typical timescale for the propagation of EM phenomena is much shorter than the duration of thermomechanical effects. Since the TM problem is already assumed to be in equilibrium, see $(6.3)_{1-3}$, the EM problem is likewise considered to be (quasi-)static. This, of course, implies that

[6] The microscale may be considered to be quasi-static only when its *microscopic length* scale is put vis-à-vis the *macroscopic time* scale of external loading. This limitation does not allow shock waves, for example, whose time and length scales are both microscopic. However, such examples violate the continuum assumption made at the outset of Chapter 5, upon which the present multiscale model is based.

the EM fields are steady and that the EM problem simplifies to a set of uncoupled POISSON equations, reproduced from $(3.138)_{1,2}$ and $(3.149)_{1,2}$ as

$$\begin{aligned} \Delta\phi &\overset{\text{Aet.}}{=} -\big(q_{\mathrm{F}} - \operatorname{div}\mathbf{p}\big)/\varepsilon_0 \quad \text{where} \quad \mathbf{e} \,=\, -\operatorname{grad}\phi \quad , \\ \Delta\mathbf{a} &\overset{\text{Aet.}}{=} -\mu_0\big(\mathbf{J}_{\mathrm{F}} + \operatorname{curl}\mathbf{m}\big) \quad \text{where} \quad \mathbf{b} \,=\, \operatorname{curl}\mathbf{a} \quad . \end{aligned} \tag{6.5}$$

The EM potentials $\{\phi, \mathbf{a}\}$ are additionally subject to the COULOMB gauge in (3.141). Recall that Equations (6.5) emerge under the assumption that the *partial* time derivatives in $(3.15)_{2,4}$ are negligible, as opposed to the *flux* derivatives in $(3.108)_{2,4}$. However, since the underlying material is assumed to be at rest according to $(6.3)_1$, the aforementioned time derivatives coincide. Indeed it is seen from Equations (2.96), (2.106), and (2.108) that the total, partial, flux, and path derivatives are identical when $\mathbf{v}$ (*i.e.*, $\dot{\mathbf{u}}$) vanishes. Moreover, the convective contributions to the EM quantities is negligible, so that

$$\mathbf{J}_{\mathrm{F}} \doteq \mathbf{j}_{\mathrm{F}} \quad , \quad \mathbf{m} \doteq \boldsymbol{\mathcal{M}} \quad , \quad \mathbf{h} \doteq \boldsymbol{\mathcal{H}} \quad , \quad \mathbf{e} \doteq \boldsymbol{\mathcal{E}} \quad , \tag{6.6}$$

where the relations in (3.4), (3.28), (3.60), and (3.68) were used.

For the purposes of this numerical implementation, it is additionally assumed that the free charge-current distributions are negligible,

$$q_{\mathrm{F}} \doteq 0 \quad , \quad \mathbf{j}_{\mathrm{F}} \doteq \mathbf{0} \quad . \tag{6.7}$$

Note that the former may be regarded as an initial condition, see later in $(6.63)_4$, whereas the latter results from a constitutive assumption, see later in (6.54). The governing Equations (6.5) thus further simplify to

$$\begin{aligned} \Delta\phi &\overset{\text{Aet.}}{=} \operatorname{div}\mathbf{p}/\varepsilon_0 \quad \text{where} \quad \mathbf{e} \,=\, -\operatorname{grad}\phi \quad , \\ \Delta\varphi_{\mathrm{F}} &\overset{\text{Aet.}}{=} \operatorname{div}\mathbf{m} \quad \text{where} \quad \mathbf{b} \overset{\text{Aet.}}{=} \mu_0\big(\mathbf{h}_{\mathrm{F}} + \mathbf{m}\big) \quad , \quad \mathbf{h}_{\mathrm{F}} \,=\, -\operatorname{grad}\varphi_{\mathrm{F}} \quad , \end{aligned} \tag{6.8}$$

see (3.150) and (3.151), where the vector-valued magnetostatic equation in $(6.5)_3$ reduces to a scalar POISSON equation. Note that the electric and magnetic parts of the governing Equations (6.8) are mutually uncoupled and identical in form. Due to the assumptions made in $(6.4)_{3,4}$, the EM equations interact with the TM balances (and *vice versa*) only through the constitutive functions. It is thus concluded that, under the simplified conditions outlined here, there is an analogy between magneto-mechanical effects (such as *piezomagnetism*) and electro-mechanical ones (such as *piezoelectricity*). The magnetic equation is regarded as a dummy equation, hence for simplicity

$$\mathbf{m} \doteq \mathbf{0} \quad , \quad \hat{\mathbf{q}} \doteq \mathbf{q} \quad , \tag{6.9}$$

where the latter expression follows from $(4.39)_2$, $(6.6)_{2,4}$, and $(6.9)_1$. The constitutive model in Section 6.1.2 will instead focus only on electro-mechanical behavior. The magnetic equation devolves into a LAPLACE equation which is entirely uncoupled from the mechanical, thermal, and electrostatic problems. It will nevertheless be implemented here as a dummy equation.

Summary

The governing equations for a dynamic thermomechanical problem coupled with a (quasi-) electrostatic problem are given by

$$\begin{aligned} \rho\,\ddot{\mathbf{u}} &= \operatorname{div}\mathbf{T} + \rho\,\mathbf{f}_{\mathrm{B}} + \mathbf{f}_{\mathrm{L}} && , \\ \rho\dot{\varepsilon} &= \mathbf{T}\cdot\mathbf{L} + \rho r - \operatorname{div}\mathbf{q} + \mathbf{j}\cdot\boldsymbol{\mathcal{E}} && , \\ \Delta\phi &= \big(\operatorname{div}\mathbf{p} - q_{\mathrm{F}}\big)/\varepsilon_0 && , \\ \Delta\varphi_{\mathrm{F}} &= \operatorname{div}\mathbf{m} && . \end{aligned} \tag{6.10}$$

In the context of this demonstration it is assumed that the single-scale TM problem is static, see (6.3), and that volumetric source terms are negligible, see (6.4). As a result, all but the stress-divergence and flux-divergence terms vanish from the (microscopic) balance Equations $(6.1)_{1,2}$. It is furthermore assumed that the EM problem is electrostatic, see (6.8), and that the magnetization is neglected. Therefore, the governing equations of the simplified single-scale EMTM model are given by

$$\begin{aligned} \operatorname{div}\mathbf{T} &= \mathbf{0} && , \\ \operatorname{div}\mathbf{q} &= 0 && , \\ \Delta\phi &= \operatorname{div}\mathbf{p}/\varepsilon_0 && , \\ \Delta\varphi &= 0 && . \end{aligned} \tag{6.11}$$

If desired, the electric field and the current potential are recovered from the gradient relations

$$\mathbf{e} = -\operatorname{grad}\phi \quad \text{and} \quad \mathbf{h}_{\mathrm{F}} = -\operatorname{grad}\varphi \quad . \tag{6.12}$$

It is tacitly understood that the material frame, which is inertial due to $(6.3)_2$, is an aether frame and the corresponding superscript $\overset{\text{Aet.}}{=}$ is dropped. In the absence of magnetization $\mathbf{m}$ the bound current potential $\mathbf{h}_{\mathrm{R}}$ vanishes so that $\mathbf{h} = \mathbf{h}_{\mathrm{F}}$ and $\varphi = \varphi_{\mathrm{F}}$, see $(3.32)_2$, hence the subscript in φ_{F} is dropped. The magnetic field is obtained trivially from $\mathbf{b} = \mu_0\mathbf{h}$, see Equation $(3.35)_2$.

6.1.2 Constitutive Model

Recall from Section 4.4.3 that constitutive functions are needed for the Helmholtz free energy Ψ, defined in (4.42), as well as for the dissipative fluxes $\mathbf{j}_{\mathrm{F}}$ and $\hat{\mathbf{q}}$, all of which are expressed as functions of the relevant gradient quantities. The constitutive model is subject to thermodynamic restrictions deduced from the Clausius-Duhem inequality using the method of Coleman and Noll. In particular, the polarization $\mathbf{p}$, magnetization $\boldsymbol{\mathcal{M}}$, entropy η, and the Cauchy stress $\mathbf{T}$ are obtained from derivatives of Ψ according to $(4.48)_{2-4}$ and (4.49), respectively. Moreover, the entropy inequality reduces to the condition in $(4.48)_5$, which imposes a thermodynamic

restriction on the constitutive functions for the dissipative fluxes $\mathbf{j}_{\mathrm{F}}$ and $\hat{\mathbf{q}}$. It is additionally assumed that the constitutive functions depend solely on the *current* values of the primary variables and gradient quantities. Consequently, this model is limited to history-independent material behavior.

The constitutive equations provide *closure* to the governing equations of the IBVP, *i.e.*, they supply the necessary number of additional equations for what would otherwise be an underdetermined system of equations (6.11 - 12). The combined number of balance equations, gradient relations, and the constitutive relations is commensurate with the number of unknown quantities of the IBVP. Therefore, a unique solution is available if adequate initial and boundary conditions are prescribed.

Helmholtz free energy

It was discussed in Section 4.4.5 that the HELMHOLTZ free energy, when expressed using any of the functional forms

$$\Psi \;=\; \check{\Psi}(\mathbf{U},\mathbf{R}^{\mathrm{T}}\boldsymbol{\mathcal{E}},\mathbf{R}^{\mathrm{T}}\mathbf{b},\theta) \;=\; \bar{\Psi}(\mathbf{C},\mathbf{F}^{\mathrm{T}}\boldsymbol{\mathcal{E}},\mathbf{F}^{\mathrm{T}}\mathbf{b},\theta) \;=\; \breve{\Psi}(\mathbf{E},\mathbf{F}^{\mathrm{T}}\boldsymbol{\mathcal{E}},\mathbf{F}^{\mathrm{T}}\mathbf{b},\theta) \quad , \tag{6.13}$$

automatically complies with the invariance requirement in Equation (4.55). The dielectric polarization, the magnetization, and the CAUCHY stress are given by $(4.48)_{2,3}$ and (4.49), respectively, or

$$\begin{aligned} \mathbf{p} \;&=\; -\rho\check{\Psi}_{\boldsymbol{\mathcal{E}}} \quad , \\ \boldsymbol{\mathcal{M}} \;&=\; -\rho\check{\Psi}_{\mathbf{b}} \quad , \\ \mathbf{T} \;&=\; \rho\Big[\check{\Psi}_{\mathbf{F}}\mathbf{F}^{\mathrm{T}} - \big(\check{\Psi}_{\mathbf{b}}\cdot\mathbf{b}\big)\,\mathbf{i} - \boldsymbol{\mathcal{E}}\otimes\check{\Psi}_{\boldsymbol{\mathcal{E}}} + \check{\Psi}_{\mathbf{b}}\otimes\mathbf{b}\Big] \quad . \end{aligned} \tag{6.14}$$

For the functional form $\Psi=\bar{\Psi}(\mathbf{C},\mathbf{F}^{\mathrm{T}}\boldsymbol{\mathcal{E}},\mathbf{F}^{\mathrm{T}}\mathbf{b},\theta)$ it was shown in (4.61) and (4.62) that the chain rule furnishes

$$\Psi_{\mathbf{F}} \;=\; 2\mathbf{F}\bar{\Psi}_{\mathbf{C}} + \boldsymbol{\mathcal{E}}\otimes\bar{\Psi}_{\mathbf{F}^{\mathrm{T}}\boldsymbol{\mathcal{E}}} + \mathbf{b}\otimes\bar{\Psi}_{\mathbf{F}^{\mathrm{T}}\mathbf{b}} \quad \text{and} \quad \Psi_{\boldsymbol{\mathcal{E}}} \;=\; \mathbf{F}\bar{\Psi}_{\mathbf{F}^{\mathrm{T}}\boldsymbol{\mathcal{E}}} \quad . \tag{6.15}$$

Similarly, the alternative form $\Psi \;=\; \breve{\Psi}(\mathbf{E},\mathbf{F}^{\mathrm{T}}\boldsymbol{\mathcal{E}},\mathbf{F}^{\mathrm{T}}\mathbf{b},\theta)$ leads to the relation in (4.65), or

$$\Psi_{\mathbf{F}} \;=\; \mathbf{F}\bar{\Psi}_{\mathbf{E}} + \boldsymbol{\mathcal{E}}\otimes\bar{\Psi}_{\mathbf{F}^{\mathrm{T}}\boldsymbol{\mathcal{E}}} + \mathbf{b}\otimes\bar{\Psi}_{\mathbf{F}^{\mathrm{T}}\mathbf{b}} \quad , \tag{6.16}$$

whereas $\Psi_{\boldsymbol{\mathcal{E}}}$ remains unchanged from $(6.15)_2$.

According to the assumption in $(6.9)_1$, the magnetization (and thus the dependence of Ψ on the magnetic field $\mathbf{b}$) is neglected.[7] Therefore, the HELMHOLTZ potential $\Psi=\breve{\Psi}(\mathbf{E},\mathbf{F}^{\mathrm{T}}\boldsymbol{\mathcal{E}},\mathbf{F}^{\mathrm{T}}\mathbf{b},\theta)$ is formulated for dielectric materials with linear electromechanical coupling according to

$$\begin{aligned} \Psi \;=\; &\tfrac{1}{2}\mathbb{C}\cdot\big[\mathbf{E}\otimes\mathbf{E}\big] - \mathbb{C}\mathbf{A}\cdot\mathbf{E}\big(\theta-\theta_0\big) + c\big\{\theta-\theta_0-\theta\log\big(\theta/\theta_0\big)\big\} \\ &+ \mathbf{c}_1\cdot\mathbf{F}^{\mathrm{T}}\boldsymbol{\mathcal{E}} + \mathbf{c}_2\cdot\big[\mathbf{E}\otimes\mathbf{F}^{\mathrm{T}}\boldsymbol{\mathcal{E}}\big] - \tfrac{1}{2}\varepsilon_0\mathbf{c}_3\cdot\big[\mathbf{F}^{\mathrm{T}}\boldsymbol{\mathcal{E}}\otimes\mathbf{F}^{\mathrm{T}}\boldsymbol{\mathcal{E}}\big] \quad , \end{aligned} \tag{6.17}$$

[7] It was argued that, because the equations describing electro-mechanical and magneto-mechanical behavior are formally similar, the magnetic part may be regarded as a dummy equation for the purposes of this demonstration.

where the notation in (2.24 - 27) for the multiplication and contraction of higher-order tensors is employed. In CARTESIAN components using EINSTEIN's summation convention, the preceding expression reads

$$\begin{aligned}\Psi \;=\; & \tfrac{1}{2} E_{AB}\mathbb{C}_{ABCD}E_{CD} \;-\; E_{AB}\mathbb{C}_{ABCD}A_{CD}\big(\theta-\theta_0\big) \;+\; c\big\{\theta-\theta_0-\theta\log\big(\theta/\theta_0\big)\big\} \\ & +\; c_{1A}F_{iA}\boldsymbol{\mathcal{E}}_i \;+\; \mathfrak{c}_{2ABC}E_{AB}F_{jC}\boldsymbol{\mathcal{E}}_j \;-\; \tfrac{1}{2}\varepsilon_0 c_{3AB}F_{iA}\boldsymbol{\mathcal{E}}_i F_{jB}\boldsymbol{\mathcal{E}}_j \quad .\end{aligned} \tag{6.18}$$

The material parameters $\mathbb{C}$, $\mathbf{A}$, $\mathbf{c}_1$, $\mathfrak{c}_2$, $\mathbf{c}_3$ are resolved in the referential bases, since they represent linear transformations of the referential gradient quantities $\mathbf{E}$ and $\mathbf{F}^{\mathrm{T}}\boldsymbol{\mathcal{E}}$. This guarantees the aforementioned form-invariance of Ψ under superposed rigid-body motion. Recall that the GREEN-LAGRANGE strain tensor $\mathbf{E}$ was defined in $(2.71)_1$. Moreover, recall from Equation (3.123) that $\mathbf{F}^{\mathrm{T}}\boldsymbol{\mathcal{E}}$ represents the referential counterpart to the electric field. In light of the approximations introduced in Equations $(6.6)_4$ and $(6.12)_1$, it is readily seen that

$$\boldsymbol{\mathcal{E}}_0 \;=\; \mathbf{F}^{\mathrm{T}}\boldsymbol{\mathcal{E}} \;\doteq\; \mathbf{F}^{\mathrm{T}}\mathbf{e} \;=\; -\mathbf{F}^{\mathrm{T}}\mathrm{grad}\,\phi \;=\; -\mathrm{Grad}\,\phi \quad , \tag{6.19}$$

where the final equality follows from the chain rule in (2.82). It is thus concluded that the term $\mathbf{F}^{\mathrm{T}}\boldsymbol{\mathcal{E}}$ represents the referential gradient of the electric potential ϕ. Note that, although the material parameters may themselves be functions of the temperature θ, it is assumed for simplicity that they are constant.

The first line of Equation (6.17) models the thermo-elastic part of the constitutive behavior similar to SENGUPTA *et al.* [127, Equation 63]. The first term represents the elastically stored *strain energy* per unit mass of the SAINT VENANT-KIRCHHOFF *hyperelastic material model* (SVK), where the fourth-order tensor $\mathbb{C}$ contains the *elastic moduli*. This constitutes an extension to large deformations of the linearly elastic model also known as the *generalized* HOOKE*'s law*. However, the reader is cautioned that the SVK finite elasticity model is flawed under extreme strains. For example, in the limit where a volume element is compressed to a point, *i.e.*, $J=\mathrm{d}v/\mathrm{d}V\to 0$, the elastically stored energy in Ψ does *not* tend to infinity. Furthermore, the SVK model is non-polyconvex, which has implications for the existence of an equilibrium state, see BALL [3], CIARLET [16], and RAOULT [122].

The second-order tensor $\mathbf{A}$ comprises the anisotropic *thermal expansion coefficients*, so that $\mathbf{A}(\theta-\theta_0)$ quantifies the unconstrained thermal strain relative to a reference temperature θ_0. The thermal expansion coefficients simplify to $\mathbf{A}=\alpha\mathbf{I}$ in the isotropic case. Lastly, c represents the *volumetric heat capacity*.[8]

The second line of Equation (6.17) describes the properties of the dielectric and includes terms of up to quadratic order in $\mathbf{F}^{\mathrm{T}}\boldsymbol{\mathcal{E}}$. The first term is governed by the

[8] This parameter relates to the entropy via the result in $(4.48)_4$, see SENGUPTA *et al.* [127, Section 8.1] for an interpretation of this term. It may be more convenient to relate internal energy and temperature via $\varepsilon=c_{\mathrm{P}}(\theta-\theta_0)$, where c_{P} represents the *specific heat capacity*. However, the internal energy is not needed in the absence of any transient thermal effects, as assumed in $(6.3)_3$.

vector-valued material parameter $\mathbf{c}_1$. The term is linear in the electromotive intensity $\boldsymbol{\mathcal{E}}$ so that, in view of $(6.14)_1$, its contribution to the polarization is independent of $\boldsymbol{\mathcal{E}}$. This phenomenon is known as *pyroelectricity* because the polarization $\mathbf{p}$ arises spontaneously, *i.e.*, in the absence of any electromotive intensity $\boldsymbol{\mathcal{E}}$. Note that this model accounts only for irreversible pyroelectric polarization because any history dependence of Ψ was ruled out. Therefore, this model precludes behavior such as *ferroelectricity*.[9]

The second term on the second line of (6.17) couples the GREEN-LAGRANGE strain tensor $\mathbf{E}$ with the referential form of the electromotive intensity $\mathbf{F}^{\mathrm{T}}\boldsymbol{\mathcal{E}}$ via the third-order material tensor $\mathfrak{c}_2$. This electro-mechanical interaction is referred to as *piezoelectricity*, where polarization is caused by mechanical deformation and *vice versa*.[10] Like pyroelectricity, piezoelectricity can induce polarization even in the absence of $\boldsymbol{\mathcal{E}}$.

The last term on the right-hand side of (6.17) is quadratic in $\boldsymbol{\mathcal{E}}$ and thus yields a polarization which is proportional to $\boldsymbol{\mathcal{E}}$. Note that a comparison between the general aether relations $(3.37)_1$ and the isotropic version $(3.38)_1$ yields the relation $\mathbf{p}/\varepsilon_0 = \chi_e \mathbf{e}$, where χ_e represents the isotropic electric susceptibility, see $(3.39)_2$. Therefore, in view of the approximation in $(6.6)_4$ it is readily seen that the second-order tensor $\boldsymbol{\chi}$, defined as

$$\boldsymbol{\chi} \;=\; \rho \mathbf{F}\,\mathbf{c}_3\mathbf{F}^{\mathrm{T}} \quad , \tag{6.20}$$

may be interpreted as the (spatial) *electric susceptibility tensor*, which is a generalization of χ_e for anisotropic, deformable materials. Note that the constitutive model (6.17) does not, for example, accommodate the *magnetocaloric effect*, whereby an external magnetic field causes a change in temperature experienced by some materials, see PECHARSKY and GSCHNEIDNER, JR [116].

Due to the symmetry of $\mathbf{E}$ in (6.17) (as well as the major symmetry in the fourth-order tensor $\mathbf{E}\otimes\mathbf{E}$) it may be assumed without loss of generality that $\mathbb{C}$ is both majorly and minorly symmetric, *i.e.*, $\mathbb{C}_{ABCD} = \mathbb{C}_{CDAB}$ and $\mathbb{C}_{ABCD} = \mathbb{C}_{BACD} = \mathbb{C}_{ABDC}$, respectively. Likewise, the thermal expansion tensor $\mathbf{A}$ is symmetric, $A_{AB} = A_{BA}$, and the piezoelectric tensor $\mathfrak{c}_2$ is symmetric in the first two indices, $\mathfrak{c}_{2ABC} = \mathfrak{c}_{2BAC}$. Finally, the symmetry of $\mathbf{F}^{\mathrm{T}}\boldsymbol{\mathcal{E}}\otimes\mathbf{F}^{\mathrm{T}}\boldsymbol{\mathcal{E}}$ implies that $\mathbf{c}_3$ (and thus the electric susceptibility tensor $\boldsymbol{\chi}$) may be assumed symmetric, $c_{3AB} = c_{3BA}$.

---

[9] Ferroelectrets are a subgroup of the pyroelectrets, where the polarization can be reversed by application of an external electric field, see KÄNZIG [66]. Ferroelectricity is the electric counterpart of ferromagnetism, although (unlike the latter) the former behavior is unrelated to iron, see KOVETZ [64, Sections 69 and 71].

[10] A wide range of materials exhibit piezoelectric properties, including inorganic (crystalline or ceramic) materials such as *quartz*, polymeric materials such as *polyvinylidene fluoride* (PVDF), and even biological materials such as bone; see LIU *et al.* [76].

Stress and Polarization

Application of the result from the method of COLEMAN and NOLL in $(6.14)_1$ yields for the polarization

$$\mathbf{p} \;=\; -\rho\mathbf{F}\big\{\mathbf{c}_1 + \mathbf{E}\cdot\mathfrak{c}_2 - \varepsilon_0\mathbf{c}_3\mathbf{F}^{\mathrm{T}}\boldsymbol{\mathcal{E}}\big\} \quad , \tag{6.21}$$

where the symmetry of $\mathbf{c}_3$ was used. In indicial notation Equation (6.21) reads

$$p_i \;=\; -\rho F_{iA}\big\{c_{1A} + E_{BC}c_{2BCA} - \varepsilon_0 c_{3AB}F_{jB}\mathbf{E}_j\big\} \quad . \tag{6.22}$$

Similarly, the relation for the CAUCHY stress tensor in $(6.14)_3$ furnishes

$$\begin{aligned} \mathbf{T} \;&=\; \rho\check{\Psi}_{\mathbf{F}}\mathbf{F}^{\mathrm{T}} - \rho\boldsymbol{\mathcal{E}}\otimes\check{\Psi}_{\boldsymbol{\mathcal{E}}} \\ &=\; \rho\mathbf{F}\big\{\mathbb{C}\mathbf{E} - \mathbb{C}\mathbf{A}\big(\theta-\theta_0\big) + \mathfrak{c}_2\big(\mathbf{F}^{\mathrm{T}}\boldsymbol{\mathcal{E}}\big)\big\}\mathbf{F}^{\mathrm{T}} \quad , \end{aligned} \tag{6.23}$$

where the major symmetry of $\mathbb{C}$ was employed. The preceding result is written in components as

$$T_{ij} \;=\; \rho F_{iA}\big\{\mathbb{C}_{ABCD}E_{CD} - \mathbb{C}_{ABCD}A_{CD}\big(\theta-\theta_0\big) + \mathfrak{c}_{2ABC}F_{kC}E_k\big\}F_{jB} \quad . \tag{6.24}$$

The magnetization in $(6.14)_2$ vanishes by design, $\boldsymbol{\mathcal{M}}=\mathbf{0}$, given that Ψ is assumed to be independent of $\mathbf{b}$.

In view of the PIOLA transform in $(3.131)_3$, the referential counterpart $\mathbf{p}_0$ of the polarization $\mathbf{p}$ in (6.21) is given by

$$\mathbf{p}_0 \;=\; J\mathbf{F}^{-1}\mathbf{p} \;=\; -\rho_0\big\{\mathbf{c}_1 + \mathbf{E}\cdot\mathfrak{c}_2 - \varepsilon_0\mathbf{c}_3\boldsymbol{\mathcal{E}}_0\big\} \quad , \tag{6.25}$$

where (2.137) was used for the density and (6.19) replaces the term $\mathbf{F}^{\mathrm{T}}\boldsymbol{\mathcal{E}}$. Similarly, the second PIOLA-KIRCHHOFF stress tensor $\mathbf{S}$, defined in (2.149), is obtained from (6.23) as

$$\mathbf{S} \;=\; J\mathbf{F}^{-1}\mathbf{T}\mathbf{F}^{-\mathrm{T}} \;=\; \rho_0\big\{\mathbb{C}\mathbf{E} - \mathbb{C}\mathbf{A}\big(\theta-\theta_0\big) + \mathfrak{c}_2\boldsymbol{\mathcal{E}}_0\big\} \quad . \tag{6.26}$$

Alternatively, the expressions for the spatial fluxes $\mathbf{p}$ and $\mathbf{T}$ in (6.21) and (6.23) are simplified by absorbing the deformation gradients $\mathbf{F}$ into the material parameters. To this end, it is first noted that the GREEN-LAGRANGE and the EULER-ALMANSI strain tensors $\mathbf{E}$ and $[\mathbf{e}]$ are related via[11]

$$\mathbf{F}^{\mathrm{T}}[\mathbf{e}]\mathbf{F} \;=\; \frac{1}{2}\mathbf{F}^{\mathrm{T}}\big[\mathbf{i} - \mathbf{B}^{-1}\big]\mathbf{F} \;=\; \frac{1}{2}\big[\mathbf{C} - \mathbf{I}\big] \;=\; \mathbf{E} \quad , \tag{6.27}$$

see (2.70 - 71). It follows from (6.27) that Equations (6.21) and (6.23) simplify to

$$\mathbf{p} \;=\; -\rho\big\{\overline{\mathbf{c}}_1 + [\mathbf{e}]\cdot\overline{\mathfrak{c}}_2 - \varepsilon_0\overline{\mathbf{c}}_3\boldsymbol{\mathcal{E}}\big\} \quad , \tag{6.28}$$

[11] In this context, brackets are used to distinguish the EULER-ALMANSI tensor $[\mathbf{e}]$ from the vector-valued electric field $\mathbf{e}$.

and

$$\mathbf{T} \;=\; \rho\big\{\overline{\mathbb{C}}[\mathbf{e}] - \overline{\mathbb{C}\mathbf{A}}\big(\theta-\theta_0\big) + \overline{\mathfrak{c}}_2\boldsymbol{\mathcal{E}}\big\} \quad . \tag{6.29}$$

Here, the spatial counterparts of the material tensors are defined according to

$$\begin{aligned}
\overline{\mathbf{c}}_1 \;&=\; \mathbf{F}\mathbf{c}_1 && \text{or} && \overline{c}_{1i} \;&=\; F_{iA}c_{1A} && ,\\
\overline{\mathfrak{c}}_2 \;&=\; \ldots && \text{or} && \overline{\mathbb{c}}_{2ijk} \;&=\; F_{iA}F_{jB}\mathbb{c}_{2ABC}F_{kC} && ,\\
\overline{\mathbf{c}}_3 \;&=\; \mathbf{F}\mathbf{c}_3\mathbf{F}^{\mathrm{T}} && \text{or} && \overline{c}_{3ij} \;&=\; F_{iA}c_{3AB}F_{jB} && ,\\
\overline{\mathbb{C}} \;&=\; \ldots && \text{or} && \overline{\mathbb{C}}_{ijkl} \;&=\; F_{iA}F_{jB}\mathbb{C}_{ABCD}F_{kC}F_{lD} && ,\\
\overline{\mathbb{C}\mathbf{A}} \;&=\; \mathbf{F}\big[\mathbb{C}\mathbf{A}\big]\mathbf{F}^{\mathrm{T}} && \text{or} && \overline{\mathbb{C}A}_{ij} \;&=\; F_{iA}\mathbb{C}_{ABCD}A_{CD}F_{jB} && .
\end{aligned} \tag{6.30}$$

The transformations in $(6.30)_{1-5}$ represent *contravariant push-forward* operations, where each referential 'leg' $\mathbf{E}_A$ is pushed to the current configuration $\mathbf{e}_i$ by the application of $\mathbf{F} = F_{iA}\mathbf{e}_i\otimes\mathbf{E}_A$. In view of the relations in $(6.30)_{4,5}$, the spatial form $\overline{\mathbf{A}}$ of the thermal expansion coefficient tensor is given by

$$\overline{\mathbf{A}} \;=\; \mathbf{F}^{-\mathrm{T}}\mathbf{A}\mathbf{F}^{-1} \quad \text{or} \quad \overline{A}_{ij} \;=\; F^{-1}_{Ai}A_{AB}F^{-1}_{Bj} \quad , \tag{6.31}$$

which is a *covariant push-forward*.

If the referential material parameters $\mathbf{c}_1$, $\mathfrak{c}_2$, $\mathbf{c}_3$, $\mathbb{C}$, and $\mathbb{C}\mathbf{A}$ are assumed to be functions only of the temperature (*i.e.*, independent of the deformation), then the corresponding spatial parameters $\overline{\mathbf{c}}_1$, $\overline{\mathfrak{c}}_2$, $\overline{\mathbf{c}}_3$, $\overline{\mathbb{C}}$, and $\overline{\mathbb{C}\mathbf{A}}$ in (6.30) must evolve with $\mathbf{F}$. This leads to a material nonlinearity under large deformations.

The symmetries observed in the referential tensors $\mathfrak{c}_2$, $\mathbf{c}_3$, $\mathbb{C}$, and $\mathbf{A}$ (hence also in $\mathbb{C}\mathbf{A}$) are preserved by the conversions to spatial form in (6.30 - 31). This is because every referential index (say, A) is pushed to the current configuration index (say, i) by application of the same F_{iA} (or in the case of $\mathbf{A}$ by the same F^{-1}_{Ai}), so that the interchangeability of two referential indices implies the interchangeability of their spatial counterparts. In particular, it is readily seen that $\overline{\mathbb{c}}_{2ijk} = \overline{\mathbb{c}}_{2jik}$, $\overline{c}_{3ij} = \overline{c}_{3ji}$, $\overline{\mathbb{C}}_{ijkl} = \overline{\mathbb{C}}_{klij}$, $\overline{\mathbb{C}}_{ijkl} = \overline{\mathbb{C}}_{jikl} = \overline{\mathbb{C}}_{ijlk}$, and $\overline{A}_{ij} = \overline{A}_{ji}$.

Comparison with Kovetz

For dielectrics with linear electro-mechanical behavior, Kovetz [64, Equation 68.5] proposes a potential of the form

$$\begin{aligned}
\Psi \;&=\; \mathbf{a}\cdot\mathbf{F}^{\mathrm{T}}\boldsymbol{\mathcal{E}} + \mathbb{b}\cdot\big[\mathbf{F}^{\mathrm{T}}\mathbf{F}\otimes\mathbf{F}^{\mathrm{T}}\boldsymbol{\mathcal{E}}\big] - \tfrac{1}{2}\varepsilon_0\mathbf{c}\cdot\big[\mathbf{F}^{\mathrm{T}}\boldsymbol{\mathcal{E}}\otimes\mathbf{F}^{\mathrm{T}}\boldsymbol{\mathcal{E}}\big]\\
&=\; F_{iA}a_A\boldsymbol{\mathcal{E}}_i + F_{iA}F_{iB}\mathbb{b}_{ABC}F_{jC}\boldsymbol{\mathcal{E}}_j - \tfrac{1}{2}\varepsilon_0 F_{iA}c_{AB}F_{jB}\boldsymbol{\mathcal{E}}_i\boldsymbol{\mathcal{E}}_j \quad .
\end{aligned} \tag{6.32}$$

The vector $\mathbf{a}$, third-order tensor $\mathbb{b}$, and the second-order tensor $\mathbf{c}$ represent the (referential) material parameters, which are again assumed to be functions only of the temperature. Equation (6.32) bears a resemblance to the second line of (6.17), whose material parameters $\mathbf{c}_1$, $\mathfrak{c}_2$ and $\mathbf{c}_3$ associated with pyroelectricity, piezoelectricity, and

electric susceptibility, respectively, appear to coincide with KOVETZ' material parameters $\mathbf{a}$, $\mathbb{b}$, and $\mathbf{c}$. Nevertheless, one crucial difference persists: The second term $\mathbb{b}$ in (6.32) couples the right CAUCHY-GREEN deformation tensor $\mathbf{C}=\mathbf{F}^{\mathrm{T}}\mathbf{F}$ with $\boldsymbol{\mathcal{E}}$, whereas in Equation (6.17) the parameter $\mathbb{c}_2$ instead contracts with the GREEN-LAGRANGE strain tensor $\mathbf{E}=\frac{1}{2}[\mathbf{C}-\mathbf{I}]$. Although KOVETZ attributes the term $\mathbb{b}$ to piezoelectricity, it should be pointed out that this term contains both piezoelectric and pyroelectric contributions. Indeed, even in the absence of any deformation (*i.e.*, when $\mathbf{F}\doteq\mathbf{I}$ and thus $\mathbf{C}\doteq\mathbf{I}$), a non-zero polarization originates from this term. By instead coupling $\boldsymbol{\mathcal{E}}$ to $\mathbf{E}$, Equation (6.17) ensures that the piezoelectric term vanishes in the absence of deformation, $\mathbf{E}\doteq\mathbf{0}$. In order to reconcile the two versions for Ψ, a part of $\mathbb{b}$ must be absorbed into the pyroelectric vector, or

$$\begin{aligned} \mathbf{c}_1 &= \mathbf{a}+\mathbf{I}\cdot\mathbb{b} \quad \text{or} \quad c_{1C} = a_C+\delta_{AB}\,\mathbb{b}_{ABC} \quad , \\ \mathbb{c}_2 &= 2\mathbb{b} \quad \text{or} \quad \mathbb{c}_{2ABC} = 2\,\mathbb{b}_{ABC} \quad . \end{aligned} \tag{6.33}$$

Comparison with Schröder

SCHRÖDER *et al.* [126, Equations 56-61] adopt a linear piezoelectric model expressed using a generalized matrix notation as[12]

$$\begin{pmatrix} \boldsymbol{\sigma} \\ -\mathbf{d} \end{pmatrix} = \begin{bmatrix} \mathbb{C} & -\mathbb{e}^{\mathrm{T}} \\ -\mathbb{e} & -\boldsymbol{\epsilon} \end{bmatrix} \begin{pmatrix} \boldsymbol{\varepsilon} \\ \mathbf{e} \end{pmatrix} \quad , \tag{6.34}$$

where $\boldsymbol{\sigma}$ and $\boldsymbol{\varepsilon}$ denote the stress and strain tensors, respectively, under the assumption of small deformations.[13] The fluxes are represented by the 'vector' on the left of (6.34) whereas the gradient quantities are on the right. The material parameters are contained in the square 'matrix'. Note that SCHRÖDER *et al.* view the charge potential $\mathbf{d}$, rather than the polarization $\mathbf{p}$, as a flux. This is in agreement with the interpretation that the aether relations in (3.37) represent constitutive relations, as previously discussed under (iii) of the introduction to Section 6.1.

To compare the material parameters in (6.34) with the HELMHOLTZ potential of the form (6.17), the aether relations in $(3.37)_1$ are pulled back to the referential configuration using $(3.131)_{1,3}$, or

$$\begin{aligned} \mathbf{d}_{\mathrm{F}0} = J\mathbf{F}^{-1}\mathbf{d}_{\mathrm{F}} &\overset{\text{Aet.}}{=} \varepsilon_0 J\mathbf{F}^{-1}\mathbf{e} + J\mathbf{F}^{-1}\mathbf{p} \\ &= \varepsilon_0 J\mathbf{C}^{-1}\boldsymbol{\mathcal{E}}_0 + \mathbf{p}_0 \\ &= -\rho_0\mathbf{c}_1 - \rho_0\mathbb{c}_2^{\mathrm{T}}\mathbf{E} + \varepsilon_0\big[J\mathbf{C}^{-1}+\rho_0\mathbf{c}_3\big]\boldsymbol{\mathcal{E}}_0 \quad . \end{aligned} \tag{6.35}$$

[12] Note that the magnetic contribution in SCHRÖDER *et al.* [126, Equations 61] is omitted in (6.34). However, their electric and magnetic parts are always uncoupled, as evident from the parameters in [126, Table 3] for piezoelectric and piezomagnetic materials.

[13] For small deformations, it is assumed that the deformation gradient $\mathbf{F}$ does not depart significantly from the identity tensor. Therefore, quadratic terms of the displacement gradient $\mathbf{H}$ are neglected in $\mathbf{C}$ and $\mathbf{E}$, see Equation (2.76).

Here, the gradient relation (6.19) and the referential polarization (6.25) were invoked. In the limit of small deformations Equation (6.35) reduces to

$$\mathbf{d}_{\mathrm{F}0} \overset{\text{Aet.}}{=} -\rho_0 \mathbf{c}_1 - \rho_0 \mathfrak{c}_2^{\mathrm{T}} \boldsymbol{\varepsilon} + \varepsilon_0 \big[\mathbf{I} + \rho_0 \mathbf{c}_3\big] \boldsymbol{\mathcal{E}}_0 \quad . \tag{6.36}$$

A comparison with (6.34) thus yields the parameter conversion

$$\begin{aligned} \rho_0 \mathbf{c}_1 &= \mathbf{0} && && , \\ \rho_0 \mathfrak{c}_2 &= -\mathfrak{e}^{\mathrm{T}} && \text{or} \quad \rho_0 \mathfrak{c}_{2ABC} &= -\mathfrak{e}_{CAB} && , \\ \rho_0 \mathbf{c}_3 &= \boldsymbol{\epsilon}/\varepsilon_0 - \mathbf{I} && \text{or} \quad \rho_0 c_{3AB} &= \epsilon_{AB}/\varepsilon_0 - \delta_{AB} && . \end{aligned} \tag{6.37}$$

Note that $(6.37)_3$ may be intepreted as an anisotropic generalization of the definition for the electric susceptibility $\chi_e = \varepsilon/\varepsilon_0 - 1$, see $(3.39)_{1,2}$.

Transversely Isotropic Model

According to the constitutive model adopted by Schröder *et al.* [126, Equation 59] for transversely isotropic linearly piezoelectric solids, the stiffness tensor $\mathbb{C}$, the piezoelectric parameters $\mathfrak{c}_2$, and the electric susceptibility tensor $\mathbf{c}_3$ are expressed as

$$\begin{aligned} \rho_0 \mathbb{C} &= \lambda \mathbb{I}^{\mathrm{tr}} + 2\mu \mathbb{I}^{\mathrm{sym}} + \omega_1 \boldsymbol{\Xi} + 2\omega_2 \big[\mathbf{M} \otimes \mathbf{M}\big] + \omega_3 \big[\mathbf{I} \otimes \mathbf{M} + \mathbf{M} \otimes \mathbf{I}\big] && , \\ \rho_0 \mathfrak{c}_2 &= \beta_1 \mathbf{I} \otimes \boldsymbol{\alpha} + \beta_2 \mathbf{M} \otimes \boldsymbol{\alpha} + \beta_3 \boldsymbol{\theta}^{\mathrm{T}} && , \\ \varepsilon_0 \rho_0 \mathbf{c}_3 &= -(2\gamma_1 + \varepsilon_0)\mathbf{I} - 2\gamma_2 \mathbf{M} && . \end{aligned} \tag{6.38}$$

Here, Equations $(6.37)_{2,3}$ were employed to convert the notation from $\{\mathfrak{e}, \boldsymbol{\epsilon}\}$ to $\{\mathfrak{c}_2, \mathbf{c}_3\}$, respectively. Recall from $(2.29)_1$ that $\mathbb{I}^{\mathrm{sym}} = \frac{1}{2}(\delta_{ik}\delta_{jl} + \delta_{jk}\delta_{il}) \mathbf{e}_i \otimes \mathbf{e}_j \otimes \mathbf{e}_k \otimes \mathbf{e}_l$ denotes the fourth-order symmetric identity tensor and $\mathbb{I}^{\mathrm{tr}} = \mathbf{I} \otimes \mathbf{I}$ is the trace identity tensor. The vector $\boldsymbol{\alpha}$ represents the preferred crystal direction of the transversely isotropic material.[14] The second-, third-, and fourth-order structural tensors $\mathbf{M}$, $\boldsymbol{\theta}$, and $\boldsymbol{\Xi}$ are defined as

$$\begin{aligned} \mathbf{M} &= \boldsymbol{\alpha} \otimes \boldsymbol{\alpha} && , \\ \boldsymbol{\theta} &= \big[\mathbf{I} \otimes \boldsymbol{\alpha}\big]^{\mathrm{sym}} && , \\ \boldsymbol{\Xi} &= 2\big[\boldsymbol{\alpha} \otimes \mathbf{I} \otimes \boldsymbol{\alpha}\big]^{\mathrm{sym}} = 2\mathbb{I}^{\mathrm{sym}} \big[\boldsymbol{\alpha} \otimes \mathbf{I} \otimes \boldsymbol{\alpha}\big] \mathbb{I}^{\mathrm{sym}} && , \end{aligned} \tag{6.39}$$

where $\mathbb{I}^{\mathrm{sym}}$ is used to enforce the minor symmetries of the fourth-order tensor $\boldsymbol{\Xi}$.[15] The preceding structural tensors are expressed in Cartesian components as

$$\begin{aligned} M_{AB} &= \alpha_A \alpha_B && , \\ \theta_{ABC} &= \tfrac{1}{2}\big(\delta_{AC}\alpha_B + \delta_{AB}\alpha_C\big) && , \\ \Xi_{ABCD} &= \tfrac{1}{2}\big(\alpha_A \delta_{BC} \alpha_D + \alpha_B \delta_{AC} \alpha_D + \alpha_A \delta_{BD} \alpha_C + \alpha_B \delta_{AD} \alpha_C\big) && . \end{aligned} \tag{6.40}$$

[14] The symbols $\boldsymbol{\alpha}$ and $\mathbf{M}$ correspond with $\mathbf{a}$ and $\mathbf{m}$ used by Schröder *et al.* [126]. The notation is modified here to prevent any confusion with the acceleration vector or the magnetic potential $\mathbf{a}$, see (2.115) and (3.12), or with the magnetization $\mathbf{m}$ in (3.28).

[15] The definition of $\boldsymbol{\Xi}$ differs slightly from the one by Schröder *et al.* [126, Equation 60_2]. This is to ensure that not only the major, but also the minor symmetries of $\boldsymbol{\Xi}$ (and thus of $\mathbb{C}$) are enforced.

For transversely isotropic materials of the type in $(6.38)_{1-3}$, the referential form of the polarization in (6.25) evaluates to

$$\mathbf{p}_0 \;=\; -\beta_1\big(\mathrm{tr}\,\mathbf{E}\big)\boldsymbol{\alpha} \,-\, \beta_2\big(\mathbf{M}\cdot\mathbf{E}\big)\boldsymbol{\alpha} \,-\, \beta_3\mathbf{E}\boldsymbol{\alpha} \,+\, \big(2\gamma_1+\varepsilon_0\big)\boldsymbol{\mathcal{E}}_0 \,+\, 2\gamma_2\big(\boldsymbol{\alpha}\cdot\boldsymbol{\mathcal{E}}_0\big)\boldsymbol{\alpha} \quad , \tag{6.41}$$

where use is made of $\boldsymbol{\theta}\mathbf{E}=\mathbf{E}\boldsymbol{\alpha}$ due to the symmetry of $\mathbf{E}$. Likewise, the second PIOLA-KIRCHHOFF stress tensor in (6.26) furnishes

$$\begin{aligned}\mathbf{S} \;=\; &\big\{\lambda\big(\mathrm{tr}\,\mathbf{E}'\big)+\omega_3\big(\mathbf{M}\cdot\mathbf{E}'\big)-\beta_1\big(\boldsymbol{\alpha}\cdot\boldsymbol{\mathcal{E}}_0\big)\big\}\mathbf{I} \,+\, 2\mu\mathbf{E}' \,+\, \omega_1\big[\boldsymbol{\alpha}\otimes\big(\mathbf{E}'\boldsymbol{\alpha}\big)+\big(\mathbf{E}'\boldsymbol{\alpha}\big)\otimes\boldsymbol{\alpha}\big] \\ &+\, \big\{\omega_3\big(\mathrm{tr}\,\mathbf{E}'\big)+2\omega_2\big(\mathbf{M}\cdot\mathbf{E}'\big)-\beta_2\big(\boldsymbol{\alpha}\cdot\boldsymbol{\mathcal{E}}_0\big)\big\}\mathbf{M} \,-\, \tfrac{1}{2}\beta_3\big[\boldsymbol{\alpha}\otimes\boldsymbol{\mathcal{E}}_0+\boldsymbol{\mathcal{E}}_0\otimes\boldsymbol{\alpha}\big] \quad ,\end{aligned} \tag{6.42}$$

where the property $\boldsymbol{\Xi}\mathbf{E}'=\boldsymbol{\alpha}\otimes\big(\mathbf{E}'\boldsymbol{\alpha}\big)+\big(\mathbf{E}'\boldsymbol{\alpha}\big)\otimes\boldsymbol{\alpha}$ was employed. The modified strain tensor $\mathbf{E}'$ in (6.42) accounts for the thermal strain by setting

$$\mathbf{E}' \;=\; \mathbf{E} \,-\, \mathbf{A}\big(\theta-\theta_0\big) \quad . \tag{6.43}$$

The thermomechanical contribution to the stress is thus given by $\mathbb{C}\mathbf{E}'$, see (6.26). Despite the transversely isotropic thermomechanical response, it is assumed that thermal expansion is isotropic. Hence,

$$\mathbf{A} \;\doteq\; \alpha\mathbf{I} \quad , \tag{6.44}$$

where α represents the (scalar) *isotropic coefficient of thermal expansion*.

Free Conduction Current and Heat Flux

COLEMAN and NOLL's method furnishes a reduced CLAUSIUS-DUHEM inequality, restated from $(4.48)_5$ as

$$0 \;\leq\; \mathbf{j}_{\mathrm{F}}\cdot\boldsymbol{\mathcal{E}} \,-\, \hat{\mathbf{q}}\cdot\mathrm{grad}\,\theta/\theta \quad . \tag{6.45}$$

This inequality represents a thermodynamic restriction on the constitutive equations for the dissipative fluxes $\mathbf{j}_{\mathrm{F}}$ and $\hat{\mathbf{q}}$. Furthermore, the requirement of form-invariance implies that the constitutive model exhibits a functional dependence the form $(4.74)_{1,2}$, or

$$\begin{aligned}J\mathbf{F}^{-1}\mathbf{j}_{\mathrm{F}} \;&=\; \bar{\mathbf{j}}_{\mathrm{F}0}(\mathbf{C},\mathbf{F}^{\mathrm{T}}\boldsymbol{\mathcal{E}},\mathbf{F}^{\mathrm{T}}\mathbf{b},\mathbf{F}^{\mathrm{T}}\mathrm{grad}\,\theta,\theta) \quad , \\ J\mathbf{F}^{-1}\hat{\mathbf{q}} \;&=\; \bar{\hat{\mathbf{q}}}_0(\mathbf{C},\mathbf{F}^{\mathrm{T}}\boldsymbol{\mathcal{E}},\mathbf{F}^{\mathrm{T}}\mathbf{b},\mathbf{F}^{\mathrm{T}}\mathrm{grad}\,\theta,\theta) \quad .\end{aligned} \tag{6.46}$$

Note that the dissipative fluxes may well depend on $\mathrm{grad}\,\theta$. This is unlike $\mathbf{p}$, $\boldsymbol{\mathcal{M}}$, and $\mathbf{T}$ in (6.13 - 14), which are derived from the HELMHOLTZ potential. By way of notation, let $\mathbf{g}(\mathbf{x},t)$ and $\mathbf{g}_0(\mathbf{X},t)$ denote the spatial and referential form of the *temperature gradient*, respectively, where

$$\mathbf{g} \;=\; \mathrm{grad}\,\theta \quad \text{and} \quad \mathbf{g}_0 \;=\; \mathbf{F}^{\mathrm{T}}\mathbf{g} \;=\; \mathrm{Grad}\,\theta \quad , \tag{6.47}$$

see the chain rule in (2.82). This is the thermal counterpart to Equation (6.19) for the electric potential.

Recall from Section 4.4.3 that any process in thermodynamic equilibrium (*i.e.*, a process for which both $\boldsymbol{\mathcal{E}} = \mathbf{0}$ and $\operatorname{grad}\theta = \mathbf{0}$) is reversible, because the entropy inequality reduces to an equality. The right-hand side of (6.45) may thus be viewed as a function of $\boldsymbol{\mathcal{E}}$ and $\operatorname{grad}\theta$ which reaches a global minimum in a state of thermodynamic equilibrium. Hence, if the constitutive functions for $\mathbf{j}_{\mathrm{F}}$ and $\hat{\mathbf{q}}$ are differentiable, it can be further shown that a necessary (but not sufficient) condition for an equilibrium state to constitute a minimum is that $\mathbf{j}_{\mathrm{F}} = \mathbf{0}$ and $\hat{\mathbf{q}} = \mathbf{0}$ vanish whenever $\boldsymbol{\mathcal{E}} = \mathbf{0}$ and $\operatorname{grad}\theta = \mathbf{0}$. This corollary of the method of Coleman and Noll is derived without any *a priori* assumptions on the constitutive equations (other than differentiability), see Kovetz [64, Section 57].

A *linear conductor* is characterized by a linear dependence of $\mathbf{j}_{\mathrm{F}}$ and $\hat{\mathbf{q}}$ on the gradients $\boldsymbol{\mathcal{E}}$ and $\mathbf{g}$, while the dependence on any other arguments in (4.74) is assumed to be negligible. These relations must further be homogeneous (*i.e.*, no constant terms) due to the preceding corollary on thermodynamic equilibrium. The constitutive equations are thus given in referential form by

$$\begin{aligned} J\mathbf{F}^{-1}\mathbf{j}_{\mathrm{F}} &= \bar{\mathbf{j}}_{\mathrm{F}0}(\boldsymbol{\mathcal{E}}_0, \mathbf{g}_0) = \boldsymbol{\sigma}\boldsymbol{\mathcal{E}}_0 + \boldsymbol{\beta}\mathbf{g}_0 \quad , \\ J\mathbf{F}^{-1}\hat{\mathbf{q}} &= \bar{\hat{\mathbf{q}}}_0(\boldsymbol{\mathcal{E}}_0, \mathbf{g}_0) = \boldsymbol{\gamma}\boldsymbol{\mathcal{E}}_0 - \boldsymbol{\kappa}\mathbf{g}_0 \quad , \end{aligned} \tag{6.48}$$

where the second-order tensors $\boldsymbol{\sigma}$, $\boldsymbol{\beta}$, $\boldsymbol{\gamma}$, and $\boldsymbol{\kappa}$, represent referential material properties. In view of (6.19) and (6.47), this is readily converted to the current configuration to write

$$\begin{aligned} \mathbf{j}_{\mathrm{F}} &= \check{\mathbf{j}}_{\mathrm{F}}(\boldsymbol{\mathcal{E}}, \mathbf{g}) = \overline{\boldsymbol{\sigma}}\boldsymbol{\mathcal{E}} + \overline{\boldsymbol{\beta}}\mathbf{g} \quad , \\ \hat{\mathbf{q}} &= \check{\hat{\mathbf{q}}}(\boldsymbol{\mathcal{E}}, \mathbf{g}) = \overline{\boldsymbol{\gamma}}\boldsymbol{\mathcal{E}} - \overline{\boldsymbol{\kappa}}\mathbf{g} \quad , \end{aligned} \tag{6.49}$$

where the spatial material parameters $\overline{\boldsymbol{\sigma}}$, $\overline{\boldsymbol{\beta}}$, $\overline{\boldsymbol{\gamma}}$, and $\overline{\boldsymbol{\kappa}}$ are defined as

$$\begin{aligned} \overline{\boldsymbol{\sigma}} &= J^{-1}\mathbf{F}\boldsymbol{\sigma}\mathbf{F}^{\mathrm{T}} \quad , \\ \overline{\boldsymbol{\beta}} &= J^{-1}\mathbf{F}\boldsymbol{\beta}\mathbf{F}^{\mathrm{T}} \quad , \\ \overline{\boldsymbol{\gamma}} &= J^{-1}\mathbf{F}\boldsymbol{\gamma}\mathbf{F}^{\mathrm{T}} \quad , \\ \overline{\boldsymbol{\kappa}} &= J^{-1}\mathbf{F}\boldsymbol{\kappa}\mathbf{F}^{\mathrm{T}} \quad . \end{aligned} \tag{6.50}$$

This is analogous to the conversions for $\mathbf{c}_1$, $\mathfrak{c}_2$, $\mathbf{c}_3$, $\mathbb{C}$, and $\mathbb{C}\mathbf{A}$ in (6.30), except that those parameters are pre-multiplied with the density, $\rho_0\mathbf{c}_1$, *etc.*, so that the inverse Jacobian J^{-1} is absorbed into $\rho\overline{\mathbf{c}}_1$, *etc.* The symmetric and skew-symmetric parts of the material parameters in (6.49) describe various thermoelectric effects.[16]

[16] It is more common to solve the linear system of Equations (6.49) for $\boldsymbol{\mathcal{E}}$ and $\hat{\mathbf{q}}$ rather than $\mathbf{j}_{\mathrm{F}}$ and $\hat{\mathbf{q}}$, see Kovetz [64, Equation 57.6]. The linear thermoelectric effects described by (6.49) are called the Hall, Nernst-Ettingshausen, Righi-Leduc, Thomson, and Peltier effects, see, for example, Goldsmid [34], Landau and Lifshitz [69, Section 25], and Pipkin and Rivlin [119].

Of course, the entropy inequality in (6.45) imposes restrictions on the parameters. For example, it is readily seen that the symmetric parts of the material tensors $\overline{\boldsymbol{\sigma}}$ and $\overline{\boldsymbol{\kappa}}$ must be positive semi-definite, that is,

$$\begin{aligned} \boldsymbol{\mathcal{E}} \cdot \overline{\boldsymbol{\sigma}} \boldsymbol{\mathcal{E}} &\geq 0 \quad \forall\, \boldsymbol{\mathcal{E}} \quad , \\ \hat{\mathbf{q}} \cdot \overline{\boldsymbol{\kappa}} \hat{\mathbf{q}} &\geq 0 \quad \forall\, \hat{\mathbf{q}} \quad , \end{aligned} \tag{6.51}$$

where it was used that the absolute temperature $\theta > 0$ is positive. In the context of this dissertation, any thermoelectric coupling is neglected, hence it is assumed that the tensors $\overline{\boldsymbol{\beta}} \doteq \mathbf{0}$ and $\overline{\boldsymbol{\gamma}} \doteq \mathbf{0}$ vanish. Moreover, transverse electric and thermal effects are neglected, so that $\operatorname{skw}\big[\overline{\boldsymbol{\sigma}}\big] \doteq \mathbf{0}$ and $\operatorname{skw}\big[\overline{\boldsymbol{\kappa}}\big] \doteq \mathbf{0}$. The dissipative fluxes are thus governed by

$$\begin{aligned} \mathbf{j}_{\mathrm{F}} &= \overline{\boldsymbol{\sigma}} \boldsymbol{\mathcal{E}} = -\,\overline{\boldsymbol{\sigma}} \operatorname{grad} \phi \quad , \\ \hat{\mathbf{q}} &= -\overline{\boldsymbol{\kappa}} \mathbf{g} = -\,\overline{\boldsymbol{\kappa}} \operatorname{grad} \theta \quad . \end{aligned} \tag{6.52}$$

Equation $(6.52)_1$ constitutes Ohm*'s law*, where $\overline{\boldsymbol{\sigma}}$ is the (symmetric, spatial) *electric conductivity*. The positive semi-definiteness of $\overline{\boldsymbol{\sigma}}$ in $(6.51)_1$ ensures that the free conduction current $\mathbf{j}_{\mathrm{F}}$ never flows against the direction of the electromotive intensity $\boldsymbol{\mathcal{E}}$. Equation $(6.52)_2$ represents Fourier*'s law*, where $\overline{\boldsymbol{\kappa}}$ denotes the (symmetric, spatial) *thermal conductivity*. Likewise, the condition in $(6.51)_2$ prevents heat from flowing towards increasing temperatures.[17] Despite the name, Ohm's law and Fourier's law should be regarded as constitutive relations rather than laws. In the referential configuration, Equations $(6.52)_{1,2}$ are expressed analogously as

$$\begin{aligned} \mathbf{j}_{\mathrm{F}0} &= J\mathbf{F}^{-1}\mathbf{j}_{\mathrm{F}} = \boldsymbol{\sigma} \boldsymbol{\mathcal{E}}_0 = -\boldsymbol{\sigma} \operatorname{Grad} \phi \quad , \\ \hat{\mathbf{q}}_0 &= J\mathbf{F}^{-1}\hat{\mathbf{q}} = -\boldsymbol{\kappa} \mathbf{g}_0 = -\boldsymbol{\kappa} \operatorname{Grad} \theta \quad , \end{aligned} \tag{6.53}$$

where the referential material parameters $\boldsymbol{\sigma}$ and $\boldsymbol{\kappa}$, too, are symmetric and positive semi-definite. However, recall that the free charge-current distributions $\{q_{\mathrm{F}}, \mathbf{j}_{\mathrm{F}}\}$ are neglected in order to simplify the electromagnetic problem to two scalar Poisson equations, see (6.8). The electric conductivity must therefore vanish,

$$\boldsymbol{\sigma} \doteq \mathbf{0} \quad , \tag{6.54}$$

thus limiting this numerical implementation to perfect dielectrics. The thermal conductivity is assumed to be isotropic,

$$\boldsymbol{\kappa} \doteq \kappa \mathbf{I} \quad , \tag{6.55}$$

where κ represents the (scalar) *isotropic thermal conductivity*.

[17] Actually $\hat{\mathbf{q}}$ represents a generalized heat flux according to definition $(4.39)_2$. This somewhat complicates the physical interpretation of $(6.52)_2$ as Fourier's law. Some authors regard $\hat{\mathbf{q}}$ rather than $\mathbf{q}$ as the heat flux, see for example Kovetz [64, Equation 54.12] and Liu and Müller [77, Section 6]. In the present context, however, this question is moot due to the approximation in $(6.9)_2$.

Summary

According to Equations (6.25 - 26) and $(6.53)_2$, the constitutive equations are expressed in the referential configuration as

$$\begin{aligned} \mathbf{p}_0 &= -\rho_0 \mathbf{c}_1 - \rho_0 \mathfrak{c}_2^{\mathrm{T}} \mathbf{E} + \varepsilon_0 \rho_0 \mathbf{c}_3 \boldsymbol{\mathcal{E}}_0 \quad , \\ \mathbf{S} &= \rho_0 \mathbb{C} \big[\mathbf{E} - \mathbf{A} \big(\theta - \theta_0 \big) \big] + \rho_0 \mathfrak{c}_2 \boldsymbol{\mathcal{E}}_0 \quad , \\ \mathbf{q}_0 &= -\boldsymbol{\kappa} \mathbf{g}_0 \quad , \end{aligned} \tag{6.56}$$

where the approximation in $(6.9)_2$ was used for $\hat{\mathbf{q}}_0$. The referential gradient quantities are derived from the primary variables according to $(2.76)_2$, (6.19), and $(6.47)_2$, that is,

$$\begin{aligned} \mathbf{E} &= \tfrac{1}{2} \big\{ \operatorname{Grad} \mathbf{u} + \operatorname{Grad}^{\mathrm{T}} \mathbf{u} + \operatorname{Grad}^{\mathrm{T}} \mathbf{u} \operatorname{Grad} \mathbf{u} \big\} \quad , \\ \boldsymbol{\mathcal{E}}_0 &= -\operatorname{Grad} \phi \quad , \\ \mathbf{g}_0 &= \operatorname{Grad} \theta \quad . \end{aligned} \tag{6.57}$$

The material tensors in $(6.56)_{1-3}$ for transversely isotropic, linearly piezoelectric solids are given by Equations $(6.37)_1$, (6.38), (6.44), and (6.55) as

$$\begin{aligned} \rho_0 \mathbf{c}_1 &= \mathbf{0} \quad , \\ \rho_0 \mathfrak{c}_2 &= \beta_1 \mathbf{I} \otimes \boldsymbol{\alpha} + \beta_2 \mathbf{M} \otimes \boldsymbol{\alpha} + \beta_3 \boldsymbol{\theta}^{\mathrm{T}} \quad , \\ \varepsilon_0 \rho_0 \mathbf{c}_3 &= -(2\gamma_1 + \varepsilon_0) \mathbf{I} - 2\gamma_2 \mathbf{M} \quad , \\ \rho_0 \mathbb{C} &= \lambda \mathbb{I}^{\mathrm{tr}} + 2\mu \mathbb{I}^{\mathrm{sym}} + \omega_1 \boldsymbol{\Xi} + 2\omega_2 \big[\mathbf{M} \otimes \mathbf{M} \big] + \omega_3 \big[\mathbf{I} \otimes \mathbf{M} + \mathbf{M} \otimes \mathbf{I} \big] \quad , \\ \mathbf{A} &\doteq \alpha \mathbf{I} \quad , \\ \boldsymbol{\kappa} &\doteq \kappa \mathbf{I} \quad . \end{aligned} \tag{6.58}$$

Here, $\mathbf{M}$, $\boldsymbol{\theta}$, and $\boldsymbol{\Xi}$ are second-, third-, and fourth-order structural tensors defined in (6.39) as

$$\begin{aligned} \mathbf{M} &= \boldsymbol{\alpha} \otimes \boldsymbol{\alpha} \quad , \\ \boldsymbol{\theta} &= \big[\mathbf{I} \otimes \boldsymbol{\alpha} \big]^{\mathrm{sym}} \quad , \\ \boldsymbol{\Xi} &= 2 \big[\boldsymbol{\alpha} \otimes \mathbf{I} \otimes \boldsymbol{\alpha} \big]^{\mathrm{sym}} \quad , \end{aligned} \tag{6.59}$$

where $\boldsymbol{\alpha}$ represents the preferred crystal direction of the transversely isotropic continuum. Note that the symmetry operator $[\,\cdot\,]^{\mathrm{sym}}$ refers to the second and third indices of $\boldsymbol{\theta}$ and to all (minor and major) symmetries of $\boldsymbol{\Xi}$. This ensures that the desired symmetries are prevalent in the material tensors in (6.58). The scalar material parameters β_1, β_2, β_3, γ_1, γ_2, λ, μ, ω_1, ω_2, ω_3, α, and κ in (6.58) are assumed to be constant, and shall be defined for a given material based on experimental data, see Section 6.4.1. Note that in practice, as indicated by the left-hand side of (6.58), the density ρ_0 is absorbed into $\mathbf{c}_1$, $\mathfrak{c}_2$, $\mathbf{c}_3$, and $\mathbb{C}$ (or $\mathbb{C}\mathbf{A}$) for simplicity. Moreover, the factor ε_0 is absorbed into $\mathbf{c}_3$.

The fluxes in $(6.56)_{1-3}$ are alternatively expressed in the current configuration according to (6.28 - 29) and $(6.52)_2$, or

$$\begin{aligned} \mathbf{p} &= -\rho\overline{\mathbf{c}}_1 - \rho\overline{\mathbf{c}}_2^{\mathrm{T}}[\mathbf{e}] + \varepsilon_0\rho\overline{\mathbf{c}}_3\boldsymbol{\mathcal{E}} \quad , \\ \mathbf{T} &= \rho\overline{\mathbb{C}}[\mathbf{e}] - \rho\overline{\mathbb{C}\mathbf{A}}\big(\theta-\theta_0\big) + \rho\overline{\mathbf{c}}_2\boldsymbol{\mathcal{E}} \quad , \\ \mathbf{q} &= -\overline{\boldsymbol{\kappa}}\,\mathbf{g} \quad , \end{aligned} \tag{6.60}$$

where $(6.9)_2$ simplifies $\hat{\mathbf{q}}$. The spatial gradient quantities are given by

$$\begin{aligned} [\mathbf{e}] &= \tfrac{1}{2}\big\{\operatorname{grad}\mathbf{u} + \operatorname{grad}^{\mathrm{T}}\mathbf{u} - \operatorname{grad}^{\mathrm{T}}\mathbf{u}\operatorname{grad}\mathbf{u}\big\} \quad , \\ \boldsymbol{\mathcal{E}} &= -\operatorname{grad}\phi \quad , \\ \mathbf{g} &= \operatorname{grad}\theta \quad , \end{aligned} \tag{6.61}$$

see $(2.77)_2$, $(6.12)_1$, and $(6.47)_1$. Meanwhile, the spatial material tensors are obtained from their referential counterparts in (6.58) via the conversion in (6.30) and $(6.50)_4$, that is,

$$\begin{aligned} \rho\overline{\mathbf{c}}_1 &= J^{-1}\mathbf{F}\big(\rho_0\,\mathbf{c}_1\big) \quad , \\ \rho\overline{\mathbb{c}}_{2ijk} &= J^{-1}F_{iA}F_{jB}\big[\rho_0\,\mathbb{c}_{2ABC}\big]F_{kC} \quad , \\ \varepsilon_0\rho\overline{\mathbf{c}}_3 &= J^{-1}\mathbf{F}\big[\varepsilon_0\rho_0\,\mathbf{c}_3\big]\mathbf{F}^{\mathrm{T}} \quad , \\ \rho\overline{\mathbb{C}}_{ijkl} &= J^{-1}F_{iA}F_{jB}\big[\rho_0\,\mathbb{C}_{ABCD}\big]F_{kC}F_{lD} \quad , \\ \rho\overline{\mathbb{C}\mathbf{A}} &= J^{-1}\mathbf{F}\big[\rho_0\mathbb{C}\mathbf{A}\big]\mathbf{F}^{\mathrm{T}} \quad , \\ \overline{\boldsymbol{\kappa}} &= J^{-1}\mathbf{F}\,\boldsymbol{\kappa}\,\mathbf{F}^{\mathrm{T}} \quad . \end{aligned} \tag{6.62}$$

As before in the referential notation, in practice the factors ρ and ε_0 will be absorbed into the spatial material parameter tensors. They are used in (6.62) to emphasize the presence of the JACOBIAN J in this conversion, see (2.137).

6.1.3 Initial and Boundary Conditions

The governing equations of the coupled EMTM problem as well as the relevant constitutive equations were presented in Sections 6.1.1 and 6.1.2, respectively. Lastly, appropriate initial and boundary conditions are needed to complete the IBVP.

Initial conditions are specified within the entire domain $\mathcal{R}_0$ at time t_0 for the displacement, velocity, density, temperature, and the free charge distribution. They simplify substantially due to the fact that (i) the initial configuration is assumed to coincide with the referential configuration, which is stress-free and in thermal equilibrium, (ii) the EMTM problem is entirely (quasi-)static, and (iii) the dielectric

material is assumed to contain no free electric charges.

$$\begin{aligned}
\mathbf{u}(\mathbf{X},0) &= \mathbf{u}_0 = \mathbf{0} \quad , \\
\dot{\mathbf{u}}(\mathbf{X},0) &= \mathbf{v}_0 = \mathbf{0} \quad , \\
\rho(\mathbf{X},0) &= \rho_0 \quad , \\
q_{\mathrm{F}}(\mathbf{X},0) &= q_{\mathrm{F}0} = \mathbf{0} \quad , \\
\theta(\mathbf{X},0) &= \theta_0 \quad , \\
\phi(\mathbf{X},0) &= \phi_0 \quad , \\
\varphi(\mathbf{X},0) &= \varphi_0 \quad .
\end{aligned} \tag{6.63}$$

Initial conditions are typically not needed for static problems as in (6.11) but the density may nevertheless be used to compute the density of the deformed configuration using the relation in $(6.2)_1$.

Each of the primary variables $\mathbf{u}$, θ, ϕ, and φ is subject to boundary conditions. The boundary of the domain in the current configuration is represented by a closed surface Γ. It is subdivided into the so-called DIRICHLET *boundary* where the value of the field itself is specified, and the NEUMANN *boundary* where a condition is instead imposed on the gradient or flux of the field in the outward normal direction of the boundary.

Regions on the DIRICHLET boundary are denoted by $\Gamma_{\mathbf{u}}$, Γ_θ, Γ_ϕ, and Γ_φ, respectively, where the subscript indicates which field is fixed. The value of the respective degree of freedom is fixed at a known value, indicated here with a *bar* accent,

$$\begin{aligned}
\mathbf{u} &= \bar{\mathbf{u}} \quad \text{on} \quad \Gamma_{\mathbf{u}} \quad , \\
\theta &= \bar{\theta} \quad \text{on} \quad \Gamma_\theta \quad , \\
\phi &= \bar{\phi} \quad \text{on} \quad \Gamma_\phi \quad , \\
\varphi &= \bar{\varphi} \quad \text{on} \quad \Gamma_\varphi \quad .
\end{aligned} \tag{6.64}$$

In preparation for the multiscale implementation, the reader is reminded that the microscopic domain corresponds to a representative volume element (RVE) and the DIRICHLET boundary conditions for the RVE are dictated by the macroscopic gradient quantities, see later in Section 7.1.

The domain of the NEUMANN boundary is denoted by $\Gamma_{\mathbf{t}}$, Γ_q, Γ_d, and Γ_b, respectively, where the subscript indicates which flux or gradient is prescribed. The boundary condition is specified relative to the outward normal vector $\mathbf{n}$ according to

$$\begin{aligned}
\mathbf{t}_{(\mathbf{n})} &= \mathbf{T}\,\mathbf{n} = \bar{\mathbf{t}}_{(\mathbf{n})} = \mathbf{0} \quad \text{on} \quad \Gamma_{\mathbf{t}} \quad , \\
q_{(\mathbf{n})} &= \mathbf{q}\cdot\mathbf{n} = \bar{q}_{(\mathbf{n})} = 0 \quad \text{on} \quad \Gamma_q \quad , \\
d_{(\mathbf{n})} &= \mathbf{d}_{\mathrm{F}}\cdot\mathbf{n} = \bar{d}_{(\mathbf{n})} = 0 \quad \text{on} \quad \Gamma_d \quad , \\
b_{(\mathbf{n})} &= \mathbf{b}\cdot\mathbf{n} = \bar{b}_{(\mathbf{n})} = 0 \quad \text{on} \quad \Gamma_b \quad .
\end{aligned} \tag{6.65}$$

In preparation for the multiscale model it is assumed either that the values prescribed at the NEUMANN boundary vanish, or that the entire boundary is composed only of DIRICHLET boundary. Note that a point is considered part of the NEUMANN boundary, if neither the primary quantity nor a (non-zero) flux is imposed.

Of course, any point on the boundary Γ must belong to either the DIRICHLET or the NEUMANN boundary but not both simultaneously. This requirement is formally stated as

$$\begin{aligned}
\overline{\Gamma_{u_i} \cup \Gamma_{t_i}} &= \Gamma \quad \text{and} \quad \Gamma_{u_i} \cap \Gamma_{t_i} = \emptyset \quad , \\
\overline{\Gamma_{\theta} \cup \Gamma_{q}} &= \Gamma \quad \text{and} \quad \Gamma_{\theta} \cap \Gamma_{q} = \emptyset \quad , \\
\overline{\Gamma_{\phi} \cup \Gamma_{d}} &= \Gamma \quad \text{and} \quad \Gamma_{\phi} \cap \Gamma_{d} = \emptyset \quad , \\
\overline{\Gamma_{\varphi} \cup \Gamma_{b}} &= \Gamma \quad \text{and} \quad \Gamma_{\varphi} \cap \Gamma_{b} = \emptyset \quad .
\end{aligned} \tag{6.66}$$

The subscripts Γ_{u_i} and Γ_{t_i} in Equation (6.66) further distinguish independent degrees of freedom of $\mathbf{u}$ and $\mathbf{t}_{(\mathbf{n})}$ for which boundary conditions may be specified individually.

6.1.4 Summary of Simplifying Assumptions

The following list contains a comprehensive summary of the simplifying assumptions introduced during the preparation of the initial/boundary-value problem throughout Section 6.1.

A. Governing equations

(1) The problem is limited to 2 spatial dimensions (plane strain) to reduce the problem size and computational cost in preparation for the multiscale implementation in Chapter 7.

(2) The electromagnetic equations are static, that is, the partial time derivatives in MAXWELL's Equations (3.15) are negligible. This reduces the EM problem to a scalar and (at most) a vectorial POISSON equation for the EM potentials $\{\phi, \mathbf{a}\}$, see $(3.149)_{1,2}$.

(3) The mechanical and thermal equations are static, $\dot{\mathbf{u}} \doteq \mathbf{0}$, $\ddot{\mathbf{u}} \doteq \mathbf{0}$, and $\dot{\boldsymbol{\varepsilon}} \doteq \mathbf{0}$. The convective effect of $\mathbf{v} = \dot{\mathbf{u}}$ is thus negligible. This also implies that (i) the partial, material, and flux derivatives coincide, (ii) the distinction between objective and non-objective quantities collapses, see Section 3.5, (iii) the issue of objectivity of the aether relations in Section 3.4.6 is rendered moot, and (iv) the effect of microscopic velocity fluctuations vanishes in the homogenizations of $\mathbf{T}^{\mathrm{M}}$, $\rho^{\mathrm{M}} \mathbf{f}_{\mathrm{B}}^{\mathrm{M}}$, $\mathbf{q}^{\mathrm{M}}$, and $\rho^{\mathrm{M}} r^{\mathrm{M}}$ in Equations (5.45), (5.46), (5.59), and (5.60).

B. Constitutive relations

(1) The materials are history-independent, hence their response depends only on the current state of the system. This precludes ferroelectricity, for example.

(2) The materials are perfect dielectrics, hence the conductivity $\boldsymbol{\sigma} \doteq \mathbf{0}$ and the free electric current $\mathbf{j}_{\mathrm{F}} \doteq \mathbf{0}$ are negligible.

(3) The materials are non-magnetizable, or $\boldsymbol{\mathcal{M}} \doteq \mathbf{0}$. This also implies in conjunction with (A.3) that $\mathbf{j}_{\mathrm{R}} = \dot{\mathbf{p}} + \operatorname{curl} \boldsymbol{\mathcal{M}} \doteq \mathbf{0}$. Hence the total current $\mathbf{J} \doteq \mathbf{0}$ vanishes and the EM problem reduces to the electrostatic case, governed by a scalar LAPLACE equation for the magnetic potential φ, see (3.144).

(4) Thermoelectric coupling, pyroelectricity, or magnetocaloric effects are neglected.

(5) The coupled electro-mechanical behavior is assumed to be linear (hence Ψ is a quadratic function of $\mathbf{E}$ and $\mathbf{F}^{\mathrm{T}}\boldsymbol{\mathcal{E}}$). A transversely isotropic constitutive model is used.

(6) Thermal expansion and heat conduction are linear. The corresponding thermal expansion coefficient and conductivity are taken to be isotropic.

(7) Material parameters, when expressed in the referential configuration, are taken to be constant (independent of temperature, deformation, *etc.*).

C. External loads, initial conditions, and boundary conditions

(1) Volumetric 'sources' $\mathbf{f}_{\mathrm{B}} \doteq \mathbf{0}$ and $r \doteq 0$ are neglected (as is typical for the microscale RVE in FE2 models).

(2) The initial configuration coincides with the reference configuration. It is assumed to be stress-free, in thermal equilibrium at θ_0, and absent of any EM loads.

(3) The initial free charge density vanishes, $q_{\mathrm{F}0} \doteq 0$. In view of (B.2) the free charge is thus always negligible, $q_{\mathrm{F}} \doteq 0$.

(4) Only DIRICHLET boundary conditions and zero-NEUMANN boundary conditions are prescribed.

6.2 Numerical Solution Strategy

In this section, the essential ingredients for the finite element implementation are put in place. First, the weak form of the IBVP is derived and the residuals of the weak form are deduced. The latter are to be solved using the NEWTON-RAPHSON method. Hence, upon a brief review of the method, the required differentials of the residuals are also derived.

6.2.1 Weak Forms and Residuals

The initial/boundary-value problem outlined in Section 6.1 has the displacements $\mathbf{u}$, temperature θ, electrostatic potential ϕ, and magnetostatic potential φ as unknowns. The so-called *strong form* of the IBVP is stated as follows: Find the primary quantities, with $\mathbf{u}$ subject to the additional requirement in $(6.2)_2$ for the invertibility of the motion, such that that they satisfy the balance laws (6.10) or (6.11) in conjunction with the constitutive relations (6.60) in $\mathcal{R}$ at all times,[18] given the initial conditions (6.63) in $\mathcal{R}$ at time t_0[19] and the boundary conditions (6.64 - 65) on $\partial\mathcal{R}$ at all times. Any external forces, heat sources, or electric charges are neglected as per the simplifications introduced in the preceding section.

Let $\mathbf{u}$, θ, ϕ, and φ be restricted to the space of *admissible solutions*, that is, fields which satisfy the initial conditions (6.63) and the DIRICHLET boundary conditions (6.64). For example, the space $\mathcal{U}_\mathrm{a}$ of admissible displacements is defined as

$$\mathcal{U}_\mathrm{a} = \left\{ \mathbf{u}(\mathbf{x},t) : \mathcal{R}\times\mathbb{R}\to E^3 \;\middle|\; \begin{array}{lll} \det\left[\mathbf{I}+\dfrac{\partial\mathbf{u}}{\partial\mathbf{X}}\right] > 0 & \text{in} & \mathcal{R} \\ u_i(\mathbf{x},t) = \bar{u}_i & \text{on} & \Gamma_{u_i} \\ \mathbf{u}(\mathbf{X},0) = \mathbf{0} \quad , \quad \dot{\mathbf{u}}(\mathbf{X},0) = \mathbf{v}_0 & \text{in} & \mathcal{R}_0 \end{array} \right\} , \tag{6.67}$$

where E^3 denotes the three-dimensional EUCLIDEAN vector space.[20] Likewise, the spaces $\mathcal{T}_\mathrm{a}$, $\mathcal{E}_\mathrm{a}$, and $\mathcal{M}_\mathrm{a}$ of the admissible temperatures, electric potentials, and magnetic potentials are given by

$$\mathcal{T}_\mathrm{a} = \left\{ \theta(\mathbf{x},t) : \mathcal{R}\times\mathbb{R}\to\mathbb{R} \;\middle|\; \begin{array}{lll} \theta(\mathbf{x},t) = \bar{\theta} & \text{on} & \Gamma_\theta \\ \theta(\mathbf{X},0) = \theta_0 & \text{in} & \mathcal{R}_0 \end{array} \right\} , \tag{6.68}$$

$$\mathcal{E}_\mathrm{a} = \left\{ \phi(\mathbf{x},t) : \mathcal{R}\times\mathbb{R}\to\mathbb{R} \;\middle|\; \begin{array}{lll} \phi(\mathbf{x},t) = \bar{\phi} & \text{on} & \Gamma_\phi \\ \phi(\mathbf{X},0) = \phi_0 & \text{in} & \mathcal{R}_0 \end{array} \right\} , \tag{6.69}$$

$$\mathcal{M}_\mathrm{a} = \left\{ \varphi(\mathbf{x},t) : \mathcal{R}\times\mathbb{R}\to\mathbb{R} \;\middle|\; \begin{array}{lll} \varphi(\mathbf{x},t) = \bar{\varphi} & \text{on} & \Gamma_\varphi \\ \varphi(\mathbf{X},0) = \varphi_0 & \text{in} & \mathcal{R}_0 \end{array} \right\} , \tag{6.70}$$

respectively.

Further define the *virtual displacements* $\delta\mathbf{u}$, *virtual temperature* $\delta\theta$, *virtual electrostatic potential* $\delta\phi$, and *virtual magnetostatic potential* $\delta\varphi$. These are restricted to the space of *admissible tangents*, sometimes called *test functions*, which must vanish

[18] Recall that the balance of angular momentum, *i.e.*, the symmetry of $\mathbf{T}$, is 'hard-wired' into the constitutive relation $(6.60)_2$ through the prescribed symmetry of $\rho\overline{\mathbb{C}}$ and $\rho\bar{\mathfrak{C}}$.

[19] As mentioned before, the initial conditions are not necessary for static problems but are nevertheless listed here.

[20] Although the implementation will later be reduced to two-dimensional plane strain problems, the domain is assumed to be three-dimensional for now.

on the DIRICHLET boundary $\Gamma_{\mathbf{u}}$, Γ_θ, Γ_ϕ, or Γ_φ (but not on the NEUMANN boundary). For example, the admissible virtual displacements belong to the space $\delta\mathcal{U}_\mathrm{a}$ defined as

$$\delta\mathcal{U}_\mathrm{a} \;=\; \Big\{\; \delta\mathbf{u}(\mathbf{x},t) \;:\; \mathcal{R}\times\mathbb{R}\to E^3 \;\Big|\; \delta u_i \;=\; 0 \quad \text{on} \quad \Gamma_{u_i} \Big\} \quad . \tag{6.71}$$

The remaining spaces for admissible virtual temperatures $\delta\theta\in\delta\mathcal{T}_\mathrm{a}$, admissible virtual electric potentials $\delta\phi\in\delta\mathcal{E}_\mathrm{a}$, and admissible virtual magnetic potentials $\delta\varphi\in\delta\mathcal{M}_\mathrm{a}$ are defined identically to (6.71).

Weak forms of the governing Equations (6.10) or their simplified forms (6.11) are deduced using the standard GALERKIN approach. Each balance equation is contracted with the respective virtual multiplier and the resulting (scalar-valued) expression is integrated over the domain $\mathcal{R}$ of the RVE (and over time t for the transient case), furnishing

$$\begin{aligned}
-\int_\mathcal{R} \delta\mathbf{u}\cdot\operatorname{div}\mathbf{T}\,\mathrm{d}v + \int_\mathcal{R} \delta\mathbf{u}\cdot\big\{\rho\,\ddot{\mathbf{u}} - \rho\,\mathbf{f}_\mathrm{B} - \mathbf{f}_\mathrm{L}\big\}\,\mathrm{d}v \;&=\; 0 \quad ,\\
\int_\mathcal{R} \delta\theta\operatorname{div}\mathbf{q}\,\mathrm{d}v + \int_\mathcal{R} \delta\theta\big\{\rho\dot{\varepsilon} - \mathbf{T}\cdot\mathbf{L} - \rho r - \mathbf{j}\cdot\boldsymbol{\mathcal{E}}\big\}\,\mathrm{d}v \;&=\; 0 \quad ,\\
-\int_\mathcal{R} \delta\phi\operatorname{div}\big(\operatorname{grad}\phi - \mathbf{p}/\varepsilon_0\big)\,\mathrm{d}v - \int_\mathcal{R} \delta\phi\, q_\mathrm{F}/\varepsilon_0\,\mathrm{d}v \;&=\; 0 \quad ,\\
-\int_\mathcal{R} \delta\varphi\operatorname{div}(\operatorname{grad}\varphi - \mathbf{m})\,\mathrm{d}v \;&=\; 0 \quad .
\end{aligned} \tag{6.72}$$

Here, without loss of generality, the sign of each equation is deliberately chosen such that the tangent matrix resulting from a linearization of $(6.72)_{1-4}$ yields positive entries in the diagonal.

Next, the product rules in $(2.46)_{1,2}$ and the divergence theorem in (2.50) are applied. In particular, it is noted that

$$\begin{aligned}
\delta\mathbf{u}\cdot\operatorname{div}\mathbf{T} \;&=\; -\operatorname{grad}\big(\delta\mathbf{u}\big)\cdot\mathbf{T} + \operatorname{div}\big(\mathbf{T}^\mathrm{T}\delta\mathbf{u}\big) \quad ,\\
\delta\theta\operatorname{div}\mathbf{q} \;&=\; -\operatorname{grad}\big(\delta\theta\big)\cdot\mathbf{q} + \operatorname{div}\big(\delta\theta\,\mathbf{q}\big) \quad ,\\
\delta\phi\operatorname{div}\big(\operatorname{grad}\phi - \mathbf{p}/\varepsilon_0\big) \;&=\; -\operatorname{grad}\big(\delta\phi\big)\cdot\big(\operatorname{grad}\phi - \mathbf{p}/\varepsilon_0\big) + \operatorname{div}\big\{\delta\phi\,\big(\operatorname{grad}\phi - \mathbf{p}/\varepsilon_0\big)\big\} \quad ,\\
\delta\varphi\operatorname{div}\big(\operatorname{grad}\varphi - \mathbf{m}\big) \;&=\; -\operatorname{grad}\big(\delta\varphi\big)\cdot\big(\operatorname{grad}\varphi - \mathbf{m}\big) + \operatorname{div}\big\{\delta\varphi\,\big(\operatorname{grad}\varphi - \mathbf{m}\big)\big\} \quad .
\end{aligned} \tag{6.73}$$

The identities reduce the order of the spatial derivatives in (6.72) in exchange for

derivatives on the test functions and new boundary integrals as

$$\begin{aligned}
r_{\mathbf{u}} &= \int_{\mathcal{R}} \operatorname{grad}\big(\delta\mathbf{u}\big)\cdot\mathbf{T}\,\mathrm{d}v + \int_{\mathcal{R}} \delta\mathbf{u}\cdot\big\{\rho\,\ddot{\mathbf{u}} - \rho\,\mathbf{f}_{\mathrm{B}} - \mathbf{f}_{\mathrm{L}}\big\}\,\mathrm{d}v - \int_{\partial\mathcal{R}} \delta\mathbf{u}\cdot\mathbf{T}\,\mathbf{n}\,\mathrm{d}a \;=\; 0 \quad , \\
r_{\theta} &= -\int_{\mathcal{R}} \operatorname{grad}\big(\delta\theta\big)\cdot\mathbf{q}\,\mathrm{d}v + \int_{\mathcal{R}} \delta\theta\,\big\{\rho\dot{\varepsilon} - \mathbf{T}\cdot\mathbf{L} - \rho r - \mathbf{j}\cdot\boldsymbol{\mathcal{E}}\big\}\,\mathrm{d}v + \int_{\partial\mathcal{R}} \delta\theta\,\mathbf{q}\cdot\mathbf{n}\,\mathrm{d}a \;=\; 0 \quad , \\
r_{\phi} &= \int_{\mathcal{R}} \operatorname{grad}\big(\delta\phi\big)\cdot\big(\operatorname{grad}\phi - \mathbf{p}/\varepsilon_0\big)\,\mathrm{d}v - \int_{\mathcal{R}} \delta\phi\,q_{\mathrm{F}}/\varepsilon_0\,\mathrm{d}v + \frac{1}{\varepsilon_0}\int_{\partial\mathcal{R}} \delta\phi\,\mathbf{d}_{\mathrm{F}}\cdot\mathbf{n}\,\mathrm{d}a \;=\; 0 \quad , \\
r_{\varphi} &= \int_{\mathcal{R}} \operatorname{grad}\big(\delta\varphi\big)\cdot\big(\operatorname{grad}\varphi - \mathbf{m}\big)\,\mathrm{d}v + \frac{1}{\mu_0}\int_{\partial\mathcal{R}} \delta\varphi\,\mathbf{b}\cdot\mathbf{n}\,\mathrm{d}a \;=\; 0 \quad .
\end{aligned} \tag{6.74}$$

For the boundary terms in $(6.74)_{3,4}$ use was made of the relations

$$\begin{aligned}
\mathbf{d}_{\mathrm{F}}/\varepsilon_0 &= \mathbf{p}/\varepsilon_0 - \operatorname{grad}\phi \quad , \\
\mathbf{b}/\mu_0 &= \mathbf{m} - \operatorname{grad}\varphi \quad ,
\end{aligned} \tag{6.75}$$

which are obtained immediately from the aether relations in $(3.37)_{1,2}$ and the gradient quantities $(6.12)_{1,2}$.[21] It can be shown that the weak form (6.74) is equivalent to the aforementioned strong form only if all integrands are continuous functions of $(\mathbf{x}, t)$.

Given the interpretation of $\delta\mathbf{u}$, $\delta\theta$, $\delta\phi$, and $\delta\varphi$ as *variations* of the respective fields, Equation $(6.74)_1$ may be regarded as a statement of virtual work. It states that in aggregate over the whole body (or the RVE) the virtual work done by the internal forces (*i.e.*, the inertial forces and the stresses) is equal to the virtual work expended by the external forces (*i.e.*, the body forces, the LORENTZ forces, and the surface tractions).

The boundary integrals in $(6.74)_{1-4}$ pertain to the entirety of $\Gamma \equiv \partial\mathcal{R}$ which is subdivided into regions of DIRICHLET and NEUMANN boundary conditions according to (6.66). However, since the admissible virtual multipliers are devised to vanish on the DIRICHLET boundary, see (6.71), only the NEUMANN portions of the boundary ($\Gamma_{\mathbf{t}}$, Γ_q, Γ_d, and Γ_b) contribute to the integral. The traction boundary conditions are enforced by substituting the desired quantities $(6.65)_{1-4}$ into the boundary integrals in $(6.74)_{1-4}$.[22]

For the simplified set of governing Equations (6.11), subject to the assumptions

[21] It should be emphasized, however, that Equations $(6.75)_{1,2}$ require the material frame to approximately correspond to the aether frame, and the convective term in $\mathbf{e}$ to be negligible according to (6.6).

[22] Equations $(6.72)_{1-4}$ may be viewed as *weighted residuals*, where the variations $\delta\mathbf{u}$, $\delta\theta$, $\delta\phi$, and $\delta\varphi$ are arbitrary weights which enforce the desired balance equations. Some authors take issue with the fact that the NEUMANN boundary conditions are not explicitly enforced by the aforementioned weighted residuals, see PAPADOPOULOS [115]. Indeed, this would imply that the traction boundary conditions are assumed to be satisfied at the outset, rather than enforced by the weighted residuals.

listed in Section 6.1.4, the weak forms (6.74) reduce to

$$\begin{aligned} r_{\mathbf{u}} &= \int_{\mathcal{R}} \operatorname{grad}\big(\delta\mathbf{u}\big) \cdot \mathbf{T}\, \mathrm{d}v \;=\; 0 \quad , \\ r_{\theta} &= -\int_{\mathcal{R}} \operatorname{grad}\big(\delta\theta\big) \cdot \mathbf{q}\, \mathrm{d}v \;=\; 0 \quad , \\ r_{\phi} &= \int_{\mathcal{R}} \operatorname{grad}\big(\delta\phi\big) \cdot \big(\operatorname{grad}\phi - \mathbf{p}/\varepsilon_0\big)\, \mathrm{d}v \;=\; 0 \quad , \\ r_{\varphi} &= \int_{\mathcal{R}} \operatorname{grad}\big(\delta\varphi\big) \cdot \operatorname{grad}\varphi\, \mathrm{d}v \;=\; 0 \quad . \end{aligned} \tag{6.76}$$

Note that the NEUMANN boundary is subject to the zero-flux assumption in (6.65) so that the boundary integrals vanish entirely.

The scalar quantities $r_{\mathbf{u}}$, r_θ, r_ϕ, and r_φ defined in Equations (6.74) or (6.76) are often termed *residuals*. The weak form problem statement reads: Find the primary quantities (here symbolized collectively as $[\,\cdot\,] = \{\mathbf{u}, \theta, \phi, \varphi\}$) such that the residuals $r_{[\cdot]} = 0$ vanish at all times, given that the fields $[\,\cdot\,]$ and their virtual counterparts $\delta[\,\cdot\,]$ are admissible as defined in (6.67 - 71).

6.2.2 Newton-Raphson Method

Solving the weak form of the problem for $\mathbf{u}$, θ, ϕ, and φ involves finding the roots of the residuals in (6.74) or (6.76), which comprise a set of coupled differential equations. The so-called NEWTON-RAPHSON *Method* and its variants are a standard numerical approach for the solution of equations of the form $\mathbf{r}(\tilde{\mathbf{u}}) = \mathbf{0}$, where $\tilde{\mathbf{u}}$ is the desired solution.[23] The method is based on a first-order Taylor expansion of $\mathbf{r}$ around an initial estimate $\tilde{\mathbf{u}}_0$ of the solution,

$$\mathbf{0} \;=\; \mathbf{r}(\tilde{\mathbf{u}}) \;=\; \mathcal{L}\big[\mathbf{r}; \tilde{\mathbf{u}} - \tilde{\mathbf{u}}_0\big]_{\tilde{\mathbf{u}}_0} + \mathcal{O}(|\tilde{\mathbf{u}} - \tilde{\mathbf{u}}_0|) \quad , \tag{6.77}$$

where $\mathcal{L}\big[\mathbf{r}; \tilde{\mathbf{u}} - \tilde{\mathbf{u}}_0\big]_{\tilde{\mathbf{u}}_0}$ symbolizes the linear part of $\mathbf{r}$ in the direction $\tilde{\mathbf{u}} - \tilde{\mathbf{u}}_0$ at the fixed location $\tilde{\mathbf{u}}_0$, and $\mathcal{O}$ are the higher-order terms of $|\tilde{\mathbf{u}} - \tilde{\mathbf{u}}_0|$. The linear part is expressed in terms of the GÂTEAUX differential $\mathrm{D}\mathbf{r}(\tilde{\mathbf{u}}_0, \tilde{\mathbf{u}} - \tilde{\mathbf{u}}_0)$ of $\mathbf{r}$ at the 'location' $\tilde{\mathbf{u}}_0$ in the 'direction' of $\tilde{\mathbf{u}} - \tilde{\mathbf{u}}_0$ as

$$\mathcal{L}\big[\mathbf{r}; \tilde{\mathbf{u}} - \tilde{\mathbf{u}}_0\big]_{\tilde{\mathbf{u}}_0} \;=\; \mathbf{r}(\tilde{\mathbf{u}}_0) + \mathrm{D}\mathbf{r}(\tilde{\mathbf{u}}_0, \tilde{\mathbf{u}} - \tilde{\mathbf{u}}_0) \quad . \tag{6.78}$$

Recall that the GÂTEAUX differential was introduced in (2.39) and (2.40) for arbitrary functions of a vector-valued or a tensor-valued argument, respectively.

[23] Here, $\tilde{\mathbf{u}}$ and $\mathbf{r}$ are *not* members of the EUCLIDEAN 3-space but rather vectors (in the sense of linear algebra) whose length is determined by the number of residuals and unknowns.

Provided that $\mathbf{r}(\tilde{\mathbf{u}})$ is sufficiently smooth for the so-called FRÉCHET *differential* to exist, the GÂTEAUX differential $\mathrm{D}\mathbf{r}(\tilde{\mathbf{u}}_0, \tilde{\mathbf{u}} - \tilde{\mathbf{u}}_0)$ in (6.78) can alternatively be represented by a matrix-vector product between the FRÉCHET derivative $[\mathbf{J}]$ and the vector $(\tilde{\mathbf{u}} - \tilde{\mathbf{u}}_0)$,

$$\mathrm{D}\mathbf{r}(\tilde{\mathbf{u}}_0, \tilde{\mathbf{u}} - \tilde{\mathbf{u}}_0) \;=\; \big[\mathbf{J}(\tilde{\mathbf{u}}_0)\big]\big(\tilde{\mathbf{u}} - \tilde{\mathbf{u}}_0\big) \quad \text{where} \quad J_{ij}(\tilde{\mathbf{u}}) \;=\; \frac{\partial r_i(\tilde{\mathbf{u}})}{\partial \tilde{u}_j} \quad . \tag{6.79}$$

Note that $[\mathbf{J}]$ represents a JACOBIAN matrix (not tensor) of $\mathbf{r}$ and should not to be confused with the total electric current $\mathbf{J}$ or the JACOBIAN determinant J of the deformation. If the higher-order terms of $|\tilde{\mathbf{u}} - \tilde{\mathbf{u}}_0|$ are neglected, the approximate solution $\mathbf{r} + \mathrm{D}\mathbf{r} \cong \mathbf{0}$ to Equation (6.77) yields the iterative scheme

$$\tilde{\mathbf{u}}^{(\mathrm{k}+1)} \;=\; \tilde{\mathbf{u}}^{(\mathrm{k})} - \Big[\mathbf{J}^{-1}(\tilde{\mathbf{u}}^{(\mathrm{k})})\Big]\Big(\mathbf{r}(\tilde{\mathbf{u}}^{(\mathrm{k})})\Big) \quad . \tag{6.80}$$

At every iteration of this numerical scheme, the residual and the JACOBIAN are computed and an algebraic set of equations is solved.

6.2.3 Differentials of Residuals

In order to apply the NEWTON-RAPHSON method (6.80) to the residuals (6.74) or (6.76), their differentials in the 'direction' of $\{\mathrm{d}\mathbf{u}, \mathrm{d}\theta, \mathrm{d}\phi, \mathrm{d}\varphi\}$ are needed. Within the scope of this implementation only the simplified residuals in (6.76) are linearized. Note that the spatial gradients and the integrals over the current configuration of the RVE themselves depend on the deformation, thereby affecting the differential with respect to the displacements $\mathrm{d}\mathbf{u}$. Therefore, the weak form residuals are first pulled back to the reference configuration. Next, the constitutive relations (6.56) and the gradient quantities (6.57) are linearized. With their aid, the differentials of the residuals are readily expressed in referential form. Lastly, the resulting differentials are transformed back to the current configuration.

The gradients and integral domains in (6.76) are converted to referential form with the aid of (2.79) and (2.82 - 86), furnishing

$$\begin{aligned}
r_{\mathbf{u}} \;&=\; \int_{\mathcal{R}_0} \mathrm{Grad}\big(\delta\mathbf{u}\big) \cdot J\,\mathbf{T}\,\mathbf{F}^{-\mathrm{T}}\,\mathrm{d}V \;=\; 0 \quad , \\
r_{\theta} \;&=\; -\int_{\mathcal{R}_0} \mathrm{Grad}\big(\delta\theta\big) \cdot J\,\mathbf{F}^{-1}\mathbf{q}\,\mathrm{d}V \;=\; 0 \quad , \\
r_{\phi} \;&=\; \int_{\mathcal{R}_0} \mathrm{Grad}\big(\delta\phi\big) \cdot J\big(\mathbf{C}^{-1}\mathrm{Grad}\,\phi - \mathbf{F}^{-1}\mathbf{p}/\varepsilon_0\big)\,\mathrm{d}V \;=\; 0 \quad , \\
r_{\varphi} \;&=\; \int_{\mathcal{R}_0} \mathrm{Grad}\big(\delta\varphi\big) \cdot J\,\mathbf{C}^{-1}\mathrm{Grad}\,\varphi\,\mathrm{d}V \;=\; 0 \quad .
\end{aligned} \tag{6.81}$$

The preceding expressions are linearized according to

$$\begin{aligned}
\mathrm{d}r_{\mathbf{u}} &= \int_{\mathcal{R}_0} \mathrm{Grad}\big(\delta\mathbf{u}\big)\cdot\big[\mathrm{d}\mathbf{F}\,\mathbf{S}+\mathbf{F}\,\mathrm{d}\mathbf{S}\big]\,\mathrm{d}V \quad , \\
\mathrm{d}r_{\theta} &= -\int_{\mathcal{R}_0} \mathrm{Grad}\big(\delta\theta\big)\cdot\mathrm{d}\mathbf{q}_0\,\mathrm{d}V \quad , \\
\mathrm{d}r_{\phi} &= \int_{\mathcal{R}_0} \mathrm{Grad}\big(\delta\phi\big)\cdot\big\{\mathrm{d}\big[J\,\mathbf{C}^{-1}\big]\mathrm{Grad}\phi + J\,\mathbf{C}^{-1}\mathrm{Grad}\big(\mathrm{d}\phi\big) - \mathrm{d}\mathbf{p}_0/\varepsilon_0\big\}\,\mathrm{d}V \quad , \\
\mathrm{d}r_{\varphi} &= \int_{\mathcal{R}_0} \mathrm{Grad}\big(\delta\varphi\big)\cdot\big\{\mathrm{d}\big[J\,\mathbf{C}^{-1}\big]\mathrm{Grad}\varphi + J\,\mathbf{C}^{-1}\mathrm{Grad}\big(\mathrm{d}\varphi\big)\big\}\,\mathrm{d}V \quad ,
\end{aligned} \tag{6.82}$$

where the second PIOLA-KIRCHHOFF stress tensor $\mathbf{S}$, the referential heat flux $\mathbf{q}_0$, and the referential polarization $\mathbf{p}_0$ were employed. It is recalled that these are related to their spatial counterparts $\mathbf{T}$, $\mathbf{q}$, and $\mathbf{p}$ according to Equations (2.149), (2.145), and $(3.131)_3$, respectively.

Preliminaries

The linearization of (6.82) requires knowledge of the differentials of the constitutive relations in the referential notation $(6.56)_{1-3}$ (that is, $\mathrm{d}\mathbf{S}$, $\mathrm{d}\mathbf{q}_0$, and $\mathrm{d}\mathbf{p}_0$). These terms represent the contributions of the material parameters (6.58) to the JACOBIAN in (6.79). For example, the term in $(6.82)_1$ involving $\mathrm{d}\mathbf{S}$ comprises the so-called *material stiffness*. Moreover, Equations (6.82) call for the differentials of the purely kinematic quantities $\mathrm{d}\mathbf{F}$ and $\mathrm{d}[J\,\mathbf{C}^{-1}]$. The former, see $(6.82)_1$, is associated with the so-called *geometric stiffness*, which quantifies the effect of the change in geometry of the spatial configuration (at fixed stress). The latter term, featured in the electromagnetic Equations $(6.82)_{3,4}$, accounts for the distortion of the spatial geometry within which the electrostatic equations are computed. The correct implementation of this term will be verified in Section 6.4.3.

The differentials of the gradients of the primary quantities, $\mathbf{H}$, $\boldsymbol{\mathcal{E}}_0$, and $\mathbf{g}_0$ with respect to the referential configuration are obtained trivially from their definitions in Equations (2.72) and $(6.57)_{1,2}$, respectively. In particular,

$$\begin{aligned}
\mathrm{d}\mathbf{H} &= \mathrm{Grad}\big(\mathrm{d}\mathbf{u}\big) \quad , \\
\mathrm{d}\boldsymbol{\mathcal{E}}_0 &= \mathrm{d}\big[\mathbf{F}^{\mathrm{T}}\boldsymbol{\mathcal{E}}\big] = -\mathrm{Grad}\big(\mathrm{d}\phi\big) \quad , \\
\mathrm{d}\mathbf{g}_0 &= \mathrm{Grad}\big(\mathrm{d}\theta\big) \quad .
\end{aligned} \tag{6.83}$$

The differential of the GREEN-LAGRANGE strain tensor $\mathbf{E}$ is obtained from $(6.83)_1$ using the definitions in $(2.70)_1$, $(2.71)_1$, and (2.74), or

$$\begin{aligned}
\mathrm{d}\mathbf{F} &= \mathrm{d}\Big[\mathbf{1}+\mathbf{H}\Big] = \mathrm{Grad}\big(\mathrm{d}\mathbf{u}\big) \quad , \\
\mathrm{d}\mathbf{E} &= \tfrac{1}{2}\mathrm{d}\mathbf{C} = \tfrac{1}{2}\big[\mathbf{F}^{\mathrm{T}}\mathrm{Grad}\big(\mathrm{d}\mathbf{u}\big) + \mathrm{Grad}^{\mathrm{T}}\big(\mathrm{d}\mathbf{u}\big)\mathbf{F}\big] = \big[\mathbf{F}^{\mathrm{T}}\mathrm{Grad}\big(\mathrm{d}\mathbf{u}\big)\big]^{\mathrm{sym}} \quad .
\end{aligned} \tag{6.84}$$

Of course, the differential of a symmetric tensor must itself be symmetric. Lastly, it remains to express $\mathrm{d}[J\,\mathbf{C}^{-1}]$ in terms of $\mathrm{d}\mathbf{u}$. To this end, it is first noted that

$$\begin{aligned} \mathrm{d}J &= \frac{\partial J}{\partial \mathbf{F}} \cdot \mathrm{d}\mathbf{F} = J\,\mathbf{F}^{-\mathrm{T}} \cdot \mathrm{Grad}\big(\mathrm{d}\mathbf{u}\big) = J\,\mathrm{tr}\big\{\mathrm{Grad}\big(\mathrm{d}\mathbf{u}\big)\,\mathbf{F}^{-1}\big\} \quad , \\ \mathrm{d}\mathbf{F}^{-1} &= \frac{\partial \mathbf{F}^{-1}}{\partial \mathbf{F}} \cdot \mathrm{d}\mathbf{F} = -\mathbf{F}^{-1}\mathrm{Grad}\big(\mathrm{d}\mathbf{u}\big)\,\mathbf{F}^{-1} \quad . \end{aligned} \tag{6.85}$$

The identity in $(6.85)_1$ is derived with the aid of the adjugate of $\mathbf{F}$ defined in (2.81).[24] The relation in $(6.85)_2$ is an adaptation of (A.5) derived in Appendix A.2, which is further employed to deduce that

$$\begin{aligned} \mathrm{d}\mathbf{C}^{-1} &= \mathrm{d}\big[\mathbf{F}^{-1}\mathbf{F}^{-\mathrm{T}}\big] \\ &= -\mathbf{F}^{-1}\big[\mathrm{Grad}\big(\mathrm{d}\mathbf{u}\big)\,\mathbf{F}^{-1} + \mathbf{F}^{-\mathrm{T}}\mathrm{Grad}^{\mathrm{T}}\big(\mathrm{d}\mathbf{u}\big)\big]\,\mathbf{F}^{-\mathrm{T}} \\ &= -2\,\mathbf{F}^{-1}\big[\mathrm{Grad}\big(\mathrm{d}\mathbf{u}\big)\,\mathbf{F}^{-1}\big]^{\mathrm{sym}}\,\mathbf{F}^{-\mathrm{T}} \quad . \end{aligned} \tag{6.86}$$

Of course, the identical result is obtained via the alternate route

$$\mathrm{d}\mathbf{C}^{-1} = \frac{\partial \mathbf{C}^{-1}}{\partial \mathbf{C}} \cdot \mathrm{d}\mathbf{C} = -2\,\mathbf{C}^{-1}\mathrm{d}\mathbf{E}\,\mathbf{C}^{-1} \quad , \tag{6.87}$$

and inserting $(6.84)_2$ into the right-hand side. Equations $(6.85)_1$ and (6.86) are combined to yield the differential

$$\mathrm{d}\big[J\,\mathbf{C}^{-1}\big] = J\,\mathrm{tr}\big\{\mathrm{Grad}\big(\mathrm{d}\mathbf{u}\big)\,\mathbf{F}^{-1}\big\}\,\mathbf{C}^{-1} - 2\,J\,\mathbf{F}^{-1}\big[\mathrm{Grad}\big(\mathrm{d}\mathbf{u}\big)\,\mathbf{F}^{-1}\big]^{\mathrm{sym}}\,\mathbf{F}^{-\mathrm{T}} \quad , \tag{6.88}$$

which is used for the electromagnetic Equations $(6.82)_{3,4}$.

The referential form of the constitutive relations in (6.56) is readily linearized with the aid of $(6.83)_{2,3}$ and $(6.84)_2$,

$$\begin{aligned} \mathrm{d}\mathbf{p}_0 &= -\rho_0\mathfrak{c}_2^{\mathrm{T}}\,\mathrm{d}\mathbf{E} + \varepsilon_0\rho_0\mathbf{c}_3\,\mathrm{d}\boldsymbol{\mathcal{E}}_0 \\ &= -\rho_0\mathfrak{c}_2^{\mathrm{T}}\big[\mathbf{F}^{\mathrm{T}}\mathrm{Grad}\big(\mathrm{d}\mathbf{u}\big)\big]^{\mathrm{sym}} - \varepsilon_0\rho_0\mathbf{c}_3\,\mathrm{Grad}\big(\mathrm{d}\phi\big) \quad , \\ \mathrm{d}\mathbf{S} &= \rho_0\mathbb{C}\,\mathrm{d}\mathbf{E} - \rho_0\mathbb{C}\mathbf{A}\,\mathrm{d}\theta + \rho_0\mathfrak{c}_2\,\mathrm{d}\boldsymbol{\mathcal{E}}_0 \\ &= \rho_0\mathbb{C}\big[\mathbf{F}^{\mathrm{T}}\mathrm{Grad}\big(\mathrm{d}\mathbf{u}\big)\big]^{\mathrm{sym}} - \rho_0\mathbb{C}\mathbf{A}\,\mathrm{d}\theta - \rho_0\mathfrak{c}_2\,\mathrm{Grad}\big(\mathrm{d}\phi\big) \quad , \\ \mathrm{d}\mathbf{q}_0 &= -\boldsymbol{\kappa}\,\mathrm{d}\mathbf{g}_0 \\ &= -\boldsymbol{\kappa}\,\mathrm{Grad}\big(\mathrm{d}\theta\big) \quad . \end{aligned} \tag{6.89}$$

Note that the constant pyroelectric parameter $\mathbf{c}_1$ in $(6.56)_1$ lacks any contribution to the differentials. This justifies dropping the term altogether for a lack of interest, as was done for the constitutive model in $(6.58)_1$.

[24] It was pointed out in (2.81) (without proof) that the adjugate $\mathbf{F}^*$ also represents the tensor derivative $\mathbf{F}^* = \frac{\partial J}{\partial \mathbf{F}}$ of the JACOBIAN determinant J with respect to $\mathbf{F}$.

It was assumed in the derivation of the preceding differentials in $(6.89)_{1-3}$ that the referential material parameters $\mathbf{c}_1$, $\mathfrak{c}_2$, $\mathbf{c}_3$, $\mathbb{C}$, $\mathbb{C}\mathbf{A}$, and $\boldsymbol{\kappa}$ are constant, *i.e.*, unaffected by any changes $\{\mathrm{d}\mathbf{u}, \mathrm{d}\theta, \mathrm{d}\phi, \mathrm{d}\varphi\}$ in the primary variables. This is consistent with the SAINT VENANT-KIRCHHOFF model, where $\mathbb{C}$ is typically constant. For heat conduction, on the other hand, it may be desirable to require that the spatial form of the thermal conductivity tensor $\overline{\boldsymbol{\kappa}}$ be constant rather than the referential parameter $\boldsymbol{\kappa}$, see Equations $(6.60)_3$ and $(6.62)_6$. This of course leads to thermomechanical coupling between $\mathrm{d}\mathbf{q}_0$ and $\mathrm{d}\mathbf{u}$, which is derived with the aid of $(6.85)_{1,2}$ as

$$\begin{aligned} \mathrm{d}\mathbf{q}_0 &= -\mathrm{d}\big[J\,\mathbf{F}^{-1}\overline{\boldsymbol{\kappa}}\,\mathbf{F}^{-\mathrm{T}}\mathrm{Grad}\theta\big] \\ &= \mathrm{tr}\big\{\mathrm{Grad}\big(\mathrm{d}\mathbf{u}\big)\,\mathbf{F}^{-1}\big\}\,\mathbf{q}_0 + 2\,\big[\mathbf{F}^{-1}\mathrm{Grad}\big(\mathrm{d}\mathbf{u}\big)\,\boldsymbol{\kappa}\big]^{\mathrm{sym}}\mathrm{Grad}\theta - \boldsymbol{\kappa}\,\mathrm{Grad}\big(\mathrm{d}\theta\big) \end{aligned} \quad , \tag{6.90}$$

where $\overline{\boldsymbol{\kappa}}$ is assumed to be constant, that is, $\mathrm{d}\overline{\boldsymbol{\kappa}} = \mathbf{0}$. In the upcoming derivation of the single-scale finite element equations, a solution is provided for both variants $(6.89)_3$ and (6.90). However, in the context of the multiscale model of Chapter 7 only the referential form $(6.89)_3$ is implemented.

Mechanical Equation

The preceding results are inserted into the differential $\mathrm{d}r_{\mathbf{u}}$ of the mechanical residual $(6.82)_1$. The referential gradients are converted to spatial ones using Equations (2.82) and (2.84), and spatial integrals are obtained with the aid of (2.79) and (2.137). The differential reads

$$\begin{aligned} \mathrm{d}r_{\mathbf{u}} &= \int_{\mathcal{R}_0} \mathrm{Grad}\big(\delta\mathbf{u}\big)\cdot\big[\mathrm{d}\mathbf{F}\,\mathbf{S} + \mathbf{F}\,\mathrm{d}\mathbf{S}\big]\,\mathrm{d}V \\ &= \int_{\mathcal{R}_0} \frac{\partial\big(\delta\mathbf{u}\big)}{\partial\mathbf{X}}\cdot\left\{\frac{\partial\big(\mathrm{d}\mathbf{u}\big)}{\partial\mathbf{X}}\,\mathbf{S} + \mathbf{F}\left[\rho_0\mathbb{C}\left\{\mathbf{F}^{\mathrm{T}}\frac{\partial\big(\mathrm{d}\mathbf{u}\big)}{\partial\mathbf{X}}\right\}^{\mathrm{sym}} - \rho_0\mathbb{C}\mathbf{A}\,\mathrm{d}\theta - \rho_0\mathfrak{c}_2\frac{\partial\big(\mathrm{d}\phi\big)}{\partial\mathbf{X}}\right]\right\}\mathrm{d}V \\ &= \int_{\mathcal{R}_0} \frac{\partial\big(\delta\mathbf{u}\big)}{\partial\mathbf{x}}\,\mathbf{F}\cdot\frac{\partial\big(\mathrm{d}\mathbf{u}\big)}{\partial\mathbf{x}}\,\mathbf{F}\,\mathbf{S}\,\mathrm{d}V + \int_{\mathcal{R}_0}\frac{\partial\big(\delta\mathbf{u}\big)}{\partial\mathbf{x}}\,\mathbf{F}\cdot\mathbf{F}\left\{\rho_0\mathbb{C}\left[\mathbf{F}^{\mathrm{T}}\frac{\partial\big(\mathrm{d}\mathbf{u}\big)}{\partial\mathbf{x}}\,\mathbf{F}\right]^{\mathrm{sym}}\right\}\mathrm{d}V \\ &\quad - \int_{\mathcal{R}_0}\frac{\partial\big(\delta\mathbf{u}\big)}{\partial\mathbf{x}}\,\mathbf{F}\cdot\mathbf{F}\big[\rho_0\mathbb{C}\mathbf{A}\big]\,\mathrm{d}\theta\,\mathrm{d}V - \int_{\mathcal{R}_0}\frac{\partial\big(\delta\mathbf{u}\big)}{\partial\mathbf{x}}\,\mathbf{F}\cdot\mathbf{F}\left[\rho_0\mathfrak{c}_2\left(\mathbf{F}^{\mathrm{T}}\frac{\partial\big(\mathrm{d}\phi\big)}{\partial\mathbf{x}}\right)\right]\mathrm{d}V \\ &= \int_{\mathcal{R}} \frac{\partial\big(\delta\mathbf{u}\big)}{\partial\mathbf{x}}\cdot\frac{\partial\big(\mathrm{d}\mathbf{u}\big)}{\partial\mathbf{x}}\,\frac{1}{J}\mathbf{F}\mathbf{S}\mathbf{F}^{\mathrm{T}}\,\mathrm{d}v + \int_{\mathcal{R}}\frac{\partial\big(\delta\mathbf{u}\big)}{\partial\mathbf{x}}\cdot\mathbf{F}\left\{\rho\mathbb{C}\left[\mathbf{F}^{\mathrm{T}}\frac{\partial\big(\mathrm{d}\mathbf{u}\big)}{\partial\mathbf{x}}\,\mathbf{F}\right]\right\}\mathbf{F}^{\mathrm{T}}\,\mathrm{d}v \\ &\quad - \int_{\mathcal{R}}\frac{\partial\big(\delta\mathbf{u}\big)}{\partial\mathbf{x}}\cdot\mathbf{F}\big[\rho\mathbb{C}\mathbf{A}\big]\,\mathbf{F}^{\mathrm{T}}\mathrm{d}\theta\,\mathrm{d}v - \int_{\mathcal{R}}\frac{\partial\big(\delta\mathbf{u}\big)}{\partial\mathbf{x}}\cdot\mathbf{F}\left[\rho\mathfrak{c}_2\left(\mathbf{F}^{\mathrm{T}}\frac{\partial\big(\mathrm{d}\phi\big)}{\partial\mathbf{x}}\right)\right]\mathbf{F}^{\mathrm{T}}\,\mathrm{d}v \end{aligned} \tag{6.91}$$

Note that the symmetry operator $[\cdot]^{\mathrm{sym}}$ was dropped on account of the minor symmetry of $\mathbb{C}$ in the third and fourth indices. Finally, the conversion in (6.62) between

the referential and the spatial material tensors simplifies the preceding result to

$$\mathrm{d}r_{\mathbf{u}} = \underbrace{\int_{\mathcal{R}} \frac{\partial(\delta\mathbf{u})}{\partial\mathbf{x}} \cdot \frac{\partial(\mathrm{d}\mathbf{u})}{\partial\mathbf{x}} \mathbf{T}\, \mathrm{d}v}_{\text{geometric stiffness}} + \underbrace{\int_{\mathcal{R}} \frac{\partial(\delta\mathbf{u})}{\partial\mathbf{x}} \cdot \left\{\rho\overline{\mathbb{C}}\left[\frac{\partial(\mathrm{d}\mathbf{u})}{\partial\mathbf{x}}\right]\right\} \mathrm{d}v}_{\text{material stiffness}}$$
$$- \underbrace{\int_{\mathcal{R}} \frac{\partial(\delta\mathbf{u})}{\partial\mathbf{x}} \cdot \left[\rho\overline{\mathbb{C}\mathbf{A}}\,\mathrm{d}\theta\right] \mathrm{d}v}_{\text{thermal expansion}} - \underbrace{\int_{\mathcal{R}} \frac{\partial(\delta\mathbf{u})}{\partial\mathbf{x}} \cdot \left\{\rho\overline{\mathfrak{C}}_2\left(\frac{\partial(\mathrm{d}\phi)}{\partial\mathbf{x}}\right)\right\} \mathrm{d}v}_{\text{piezoelectric effect}} \quad . \tag{6.92}$$

Each term in the linearized tangent (6.92) is clearly attributable to an underlying effect, that is, the change in stiffness due to the geometry, the contribution of the elastic moduli, the thermal expansion, and the piezoelectric strain, respectively. The geometric and material stiffnesses, which relate $\delta\mathbf{u}$ with $\mathrm{d}\mathbf{u}$ and thus lie near the diagonal of the tangent, are symmetric on account of the symmetries of $\mathbf{T}$ and $\overline{\mathbb{C}}$, respectively. However, it will be seen in the upcoming sections that the off-diagonal coupling of the thermal or electric part with the displacements is *not* symmetric.

Thermal Equation

It is first noted that the differential $\mathrm{d}\mathbf{q}_0$ of the referential heat flux obtained in (6.90) can be expressed in terms of the spatial quantities according to

$$J^{-1}\mathbf{F}\,\mathrm{d}\mathbf{q}_0 = \mathrm{div}\big(\mathrm{d}\mathbf{u}\big)\mathbf{q} + 2\left[\mathrm{grad}\big(\mathrm{d}\mathbf{u}\big)\,\overline{\boldsymbol{\kappa}}\right]^{\mathrm{sym}}\mathrm{grad}\theta - \overline{\boldsymbol{\kappa}}\,\mathrm{grad}\big(\mathrm{d}\theta\big) \quad , \tag{6.93}$$

where the definition of the divergence $(2.41)_1$ and the relations in (2.82) and (2.84) were used. The second term in (6.93) made use of the fact that

$$2\left[\mathbf{F}^{-1}\mathrm{Grad}\big(\mathrm{d}\mathbf{u}\big)\,\boldsymbol{\kappa}\right]^{\mathrm{sym}}\mathrm{Grad}\theta = 2\,J\mathbf{F}^{-1}\left[\mathrm{grad}\big(\mathrm{d}\mathbf{u}\big)\,\overline{\boldsymbol{\kappa}}\right]^{\mathrm{sym}}\mathrm{grad}\theta \tag{6.94}$$

The result in (6.93) is inserted into the differential $\mathrm{d}r_\theta$ of the thermal residual, see $(6.82)_2$, furnishing

$$\mathrm{d}r_\theta = -\int_{\mathcal{R}_0} \mathrm{Grad}\big(\delta\theta\big) \cdot \mathrm{d}\mathbf{q}_0\, \mathrm{d}V$$
$$= \underbrace{-\int_{\mathcal{R}} \left(\frac{\partial(\delta\theta)}{\partial\mathbf{x}} \cdot \mathbf{q}\right)\left(\frac{\partial}{\partial\mathbf{x}} \cdot \mathrm{d}\mathbf{u}\right) \mathrm{d}v}_{\text{volume change}} \underbrace{-2\int_{\mathcal{R}} \frac{\partial(\delta\theta)}{\partial\mathbf{x}} \cdot \left(\left[\frac{\partial(\mathrm{d}\mathbf{u})}{\partial\mathbf{x}}\,\overline{\boldsymbol{\kappa}}\right]^{\mathrm{sym}} \frac{\partial\theta}{\partial\mathbf{x}}\right) \mathrm{d}v}_{\text{shape change}}$$
$$+ \underbrace{\int_{\mathcal{R}} \frac{\partial(\delta\theta)}{\partial\mathbf{x}} \cdot \overline{\boldsymbol{\kappa}}\, \frac{\partial(\mathrm{d}\theta)}{\partial\mathbf{x}}\, \mathrm{d}v}_{\text{material 'stiffness'}} \quad , \tag{6.95}$$

where $\frac{\partial}{\partial\mathbf{x}} \cdot \mathrm{d}\mathbf{u}$ denotes the divergence of $\mathrm{d}\mathbf{u}$. The first two terms in (6.95) are associated with changes in the geometry. They are caused by the dependence of the

referential $\boldsymbol{\kappa}$ on the deformation, because it was assumed in (6.90) that the spatial counterpart $\overline{\boldsymbol{\kappa}}$ is constant. On the other hand, if $\boldsymbol{\kappa}$ were kept constant instead, the coupling between $\delta\theta$ and $\mathrm{d}\mathbf{u}$ vanishes according to $\mathrm{d}\mathbf{q}_0$ in $(6.89)_3$. In that case only the third term in (6.95) remains, which accounts purely for the thermal conductivity at a fixed spatial configuration.

The term involving $\mathrm{d}\theta$ is symmetric due to the symmetry of $\overline{\boldsymbol{\kappa}}$. Given that $\overline{\boldsymbol{\kappa}}$ is positive semi-definite, this result confirms the choice for the sign of the thermal residual in $(6.72)_2$, which ensures positive diagonal entries in the tangent matrix. Note that the coupling between $\delta\theta$ and $\mathrm{d}\mathbf{u}$ in the first two terms of (6.95) is different from the reverse coupling between $\delta\mathbf{u}$ and $\mathrm{d}\theta$ in the third term of (6.92). It is thus concluded that the overall tangent will be unsymmetric.

Electric Equation

The results for $\mathrm{d}[J\,\mathbf{C}^{-1}]$ in (6.88) and for $\mathrm{d}\mathbf{p}_0$ in $(6.89)_1$ are inserted into the differential of the electric residual $(6.82)_3$, furnishing

$$
\begin{aligned}
\mathrm{d}r_\phi \;&=\; \int_{\mathcal{R}_0} \mathrm{Grad}\big(\delta\phi\big)\cdot\Big\{\mathrm{d}\big[J\,\mathbf{C}^{-1}\big]\mathrm{Grad}\,\phi + J\,\mathbf{C}^{-1}\mathrm{Grad}\big(\mathrm{d}\phi\big) - \mathrm{d}\mathbf{p}_0/\varepsilon_0\Big\}\,\mathrm{d}V \\
&= \int_{\mathcal{R}_0} \frac{\partial\big(\delta\phi\big)}{\partial\mathbf{X}}\cdot\Big\{J\,\mathrm{tr}\Big(\frac{\partial\big(\mathrm{d}\mathbf{u}\big)}{\partial\mathbf{X}}\,\mathbf{F}^{-1}\Big)\,\mathbf{C}^{-1} - 2\,J\,\mathbf{F}^{-1}\Big[\frac{\partial\big(\mathrm{d}\mathbf{u}\big)}{\partial\mathbf{X}}\,\mathbf{F}^{-1}\Big]^{\mathrm{sym}}\,\mathbf{F}^{-\mathrm{T}}\Big\}\mathrm{Grad}\,\phi\,\mathrm{d}V \\
&\quad + \int_{\mathcal{R}_0} \frac{\partial\big(\delta\phi\big)}{\partial\mathbf{X}}\cdot J\,\mathbf{C}^{-1}\frac{\partial\big(\mathrm{d}\phi\big)}{\partial\mathbf{X}}\,\mathrm{d}V \\
&\quad + \int_{\mathcal{R}_0} \frac{\partial\big(\delta\phi\big)}{\partial\mathbf{X}}\cdot\frac{1}{\varepsilon_0}\Big\{\rho_0\mathfrak{c}_2^{\mathrm{T}}\Big[\mathbf{F}^{\mathrm{T}}\frac{\partial\big(\mathrm{d}\mathbf{u}\big)}{\partial\mathbf{X}}\Big]^{\mathrm{sym}} + \varepsilon_0\rho_0\mathbf{c}_3\frac{\partial\big(\mathrm{d}\phi\big)}{\partial\mathbf{X}}\Big\}\,\mathrm{d}V \\
&= \int_{\mathcal{R}} \frac{\partial\big(\delta\phi\big)}{\partial\mathbf{X}}\cdot\mathbf{F}^{-1}\Big\{\Big(\frac{\partial}{\partial\mathbf{x}}\cdot\mathrm{d}\mathbf{u}\Big)\mathbf{i} - 2\Big[\frac{\partial\big(\mathrm{d}\mathbf{u}\big)}{\partial\mathbf{x}}\Big]^{\mathrm{sym}}\Big\}\mathbf{F}^{-\mathrm{T}}\frac{\partial\phi}{\partial\mathbf{X}}\,\mathrm{d}v \\
&\quad + \int_{\mathcal{R}} \frac{\partial\big(\delta\phi\big)}{\partial\mathbf{X}}\cdot\mathbf{F}^{-1}\mathbf{F}^{-\mathrm{T}}\frac{\partial\big(\mathrm{d}\phi\big)}{\partial\mathbf{X}}\,\mathrm{d}v \\
&\quad + \int_{\mathcal{R}} \frac{\partial\big(\delta\phi\big)}{\partial\mathbf{X}}\cdot\frac{1}{\varepsilon_0}\mathbf{F}^{-1}\Big\{\mathbf{F}\Big(\rho\mathfrak{c}_2^{\mathrm{T}}\Big[\mathbf{F}^{\mathrm{T}}\frac{\partial\big(\mathrm{d}\mathbf{u}\big)}{\partial\mathbf{x}}\mathbf{F}\Big]^{\mathrm{sym}}\Big) + \varepsilon_0\,\rho\,\mathbf{F}\,\mathbf{c}_3\,\mathbf{F}^{\mathrm{T}}\mathbf{F}^{-\mathrm{T}}\frac{\partial\big(\mathrm{d}\phi\big)}{\partial\mathbf{X}}\Big\}\,\mathrm{d}v \\
&= \int_{\mathcal{R}} \frac{\partial\big(\delta\phi\big)}{\partial\mathbf{x}}\cdot\Big\{\Big(\frac{\partial}{\partial\mathbf{x}}\cdot\mathrm{d}\mathbf{u}\Big)\mathbf{i} - 2\Big[\frac{\partial\big(\mathrm{d}\mathbf{u}\big)}{\partial\mathbf{x}}\Big]^{\mathrm{sym}}\Big\}\frac{\partial\phi}{\partial\mathbf{x}}\,\mathrm{d}v + \int_{\mathcal{R}} \frac{\partial\big(\delta\phi\big)}{\partial\mathbf{x}}\cdot\frac{\partial\big(\mathrm{d}\phi\big)}{\partial\mathbf{x}}\,\mathrm{d}v \\
&\quad + \int_{\mathcal{R}} \frac{\partial\big(\delta\phi\big)}{\partial\mathbf{x}}\cdot\frac{1}{\varepsilon_0}\Big\{\mathbf{F}\Big(\rho\mathfrak{c}_2^{\mathrm{T}}\Big[\mathbf{F}^{\mathrm{T}}\frac{\partial\big(\mathrm{d}\mathbf{u}\big)}{\partial\mathbf{x}}\mathbf{F}\Big]^{\mathrm{sym}}\Big) + \varepsilon_0\,\rho\,\mathbf{F}\,\mathbf{c}_3\,\mathbf{F}^{\mathrm{T}}\frac{\partial\big(\mathrm{d}\phi\big)}{\partial\mathbf{x}}\Big\}\,\mathrm{d}v \quad ,
\end{aligned}
\tag{6.96}
$$

where the usual relations $(2.41)_1$, (2.79), (2.82), (2.84), and (2.137) were employed. Lastly, appealing to the definitions of the spatial material parameters $\overline{\mathfrak{c}}_2$ and $\overline{\mathbf{c}}_3$

in $(6.62)_{2,3}$ and exploiting the symmetry $\overline{\mathbb{c}}_{2ijk} = \overline{\mathbb{c}}_{2jik}$ in the first two indices, Equation (6.96) simplifies to

$$\begin{aligned} \mathrm{d}r_\phi \;=\; & \underbrace{\int_{\mathcal{R}} \left(\frac{\partial(\delta\phi)}{\partial \mathbf{x}} \cdot \frac{\partial \phi}{\partial \mathbf{x}}\right)\left(\frac{\partial}{\partial \mathbf{x}} \cdot \mathrm{d}\mathbf{u}\right) \mathrm{d}v}_{\text{volume change}} \; \underbrace{- 2 \int_{\mathcal{R}} \frac{\partial(\delta\phi)}{\partial \mathbf{x}} \cdot \left(\left[\frac{\partial(\mathrm{d}\mathbf{u})}{\partial \mathbf{x}}\right]^{\mathrm{sym}} \frac{\partial \phi}{\partial \mathbf{x}}\right) \mathrm{d}v}_{\text{shape change}} \\ & + \underbrace{\int_{\mathcal{R}} \frac{\partial(\delta\phi)}{\partial \mathbf{x}} \cdot \left(\left[\mathbf{i} + \rho \overline{\mathbf{c}}_3\right] \frac{\partial(\mathrm{d}\phi)}{\partial \mathbf{x}}\right) \mathrm{d}v}_{\text{material 'stiffness'}} + \frac{1}{\varepsilon_0} \underbrace{\int_{\mathcal{R}} \frac{\partial(\delta\phi)}{\partial \mathbf{x}} \cdot \left\{\rho \overline{\mathbf{c}}_2^{\mathrm{T}} \frac{\partial(\mathrm{d}\mathbf{u})}{\partial \mathbf{x}}\right\} \mathrm{d}v}_{\text{piezoelectric effect}} \quad . \end{aligned} \tag{6.97}$$

The first two terms in (6.97) represent the geometric 'stiffness', that is, the change in the electric response exclusively due to a change in the geometry of the current configuration. Note their similarity with the first two terms of the thermal equation (6.95) (except that the second term is additionally modulated by $\overline{\boldsymbol{\kappa}}$). The third term represents the material 'stiffness' due to the (spatial) *relative permittivity tensor* $\boldsymbol{\varepsilon}_r$ or the corresponding *permittivity tensor* $\boldsymbol{\varepsilon}$, which are defined as[25]

$$\begin{aligned} \boldsymbol{\varepsilon}_r \;&=\; \mathbf{i} + \rho \overline{\mathbf{c}}_3 \;=\; \mathbf{i} + \boldsymbol{\chi} \quad , \\ \boldsymbol{\varepsilon} \;&=\; \varepsilon_0 \boldsymbol{\varepsilon}_r \;=\; \varepsilon_0 \mathbf{i} + \varepsilon_0 \rho \overline{\mathbf{c}}_3 \quad , \end{aligned} \tag{6.98}$$

where the (spatial) electric susceptibility tensor $\boldsymbol{\chi}$ was used, see Equation (6.20). Indeed, the relative permittivity tensor $(6.98)_1$ is a tensor-valued (*i.e.*, anisotropic) generalization of the isotropic relative permittivity ε_r. In the isotropic case, that is, for $\boldsymbol{\varepsilon}_r = \varepsilon_r \mathbf{i}$ and $\boldsymbol{\chi} = \chi_e \mathbf{i}$, the relations in $(6.98)_{1,2}$ between $\boldsymbol{\varepsilon}$, $\boldsymbol{\varepsilon}_r$, and $\boldsymbol{\chi}$ reduce to the isotropic relations in $(3.39)_{1,2}$. Lastly, the fourth term in (6.97) accounts for the polarization due to the piezoelectric effect.

As with the mechanical and thermal residuals, it is noted that the term involving $\mathrm{d}\phi$ is symmetric due to the symmetry of $\overline{\mathbf{c}}_3$. However, it is yet again seen that the coupling between $\delta\phi$ and $\mathrm{d}\mathbf{u}$ differs from the reverse coupling between $\delta\mathbf{u}$ and $\mathrm{d}\phi$. It is thus concluded that the electro-mechanical coupling, too, contributes to the asymmetry of the tangent.

Magnetic Equation

Recall that in the context of this implementation the magnetization is neglected from the outset, so that the Poisson Equation $(6.10)_4$ reduces to a Laplace Equation $(6.11)_4$. The corresponding differential $\mathrm{d}r_\varphi$ of the magnetic residual, see $(6.82)_4$,

[25] The reader is cautioned that the material model for the parameters in $\mathbf{c}_3$ in $(6.58)_3$ and thus $\overline{\mathbf{c}}_3$ in $(6.62)_3$ already incorporates the vacuum permittivity ε_0 (as well as the density). Hence, in practice, division by ε_0 may be needed to evaluate the third term in (6.97).

simply reads

$$\mathrm{d}r_\varphi = \underbrace{\int_{\mathcal{R}} \left(\frac{\partial(\delta\varphi)}{\partial \mathbf{x}} \cdot \frac{\partial \varphi}{\partial \mathbf{x}}\right)\left(\frac{\partial}{\partial \mathbf{x}} \cdot \mathrm{d}\mathbf{u}\right) \mathrm{d}v}_{\text{volume change}} - 2 \underbrace{\int_{\mathcal{R}} \frac{\partial(\delta\varphi)}{\partial \mathbf{x}} \cdot \left(\left[\frac{\partial(\mathrm{d}\mathbf{u})}{\partial \mathbf{x}}\right]^{\mathrm{sym}} \frac{\partial \varphi}{\partial \mathbf{x}}\right) \mathrm{d}v}_{\text{shape change}}$$
$$+ \underbrace{\int_{\mathcal{R}} \frac{\partial(\delta\varphi)}{\partial \mathbf{x}} \cdot \frac{\partial(\mathrm{d}\varphi)}{\partial \mathbf{x}} \, \mathrm{d}v}_{\text{vacuum 'stiffness'}} \quad . \tag{6.99}$$

Note that the form of (6.99) is identical to the electric differential in (6.97) for the special case where the susceptibility and the piezoelectricity are neglected, $\overline{\mathbf{c}}_2 = \mathbf{0}$ and $\overline{\mathbf{c}}_3 = \mathbf{0}$. The magnetic variation $\delta\varphi$ is coupled to $\mathrm{d}\mathbf{u}$ only due to the geometric 'stiffness', represented by the first two terms in (6.99). Recall that none of the other variations $\delta\mathbf{u}$, $\delta\theta$, or $\delta\phi$ are coupled with $\mathrm{d}\varphi$, see (6.92), (6.95), and (6.97), hence the magnetic problem can be regarded as a dummy equation.

6.3 Implementation

The goal of this section is to employ the NEWTON-RAPHSON method (6.80) for the solution of the residual Equations $(6.76)_{1-4}$ using the differentials in Equations (6.92), (6.95), (6.97), and (6.99). To achieve this in a numerical setting, the continuous integrals in the aforementioned equations are evaluated by a numerical scheme, that is, GAUSSIAN *quadrature*. Meanwhile, the primary variables, the gradient quantities, and the fluxes, which are comprised of continuous piece-wise smooth functions, are approximated by element-wise *interpolation* (or *shape*) *functions* in conjunction with a finite number of discrete nodal values. In conjunction with the NEWTON-RAPHSON method, this leads to an iterative sequence of linear algebraic equations for the nodal values of the primary variables, which can be solved using standard numerical methods such as GAUSSIAN *elimination* or the *conjugate gradient method*.

This section is organized as follows: First, the so-called VOIGT *notation* is presented, which enables a compact notation for multiplications of tensors up to fourth order. Next, finite element approximations are introduced for the relevant quantities. The preceding results are employed to express the residuals and their differentials in terms of a matrix-vector notation, whose components are given by global integrals of the shape functions, material parameters, and fluxes. Lastly, the preceding global notation is reduced to an element-wise form involving only the element nodal values and integrals over the element domain. The global problem can be recovered by *assembly* of the individual *element residual vectors* and *element stiffness matrices*.

This section does not attempt to present a complete overview of finite element analysis. Enough information is supplied to implement the element residual and stiffness. The GAUSSIAN quadrature of the shape functions, the assembly of the element

stiffnesses into the global form, the incorporation of the DIRICHLET boundary condition using a so-called SCHUR *complement*, and the numerical solution of the ensuing linear system of equations are not discussed here. Furthermore, questions of accuracy, stability, and convergence are not addressed in the context of this dissertation.

6.3.1 Voigt Notation

VOIGT notation allows for a convenient matrix-vector representation of the usual tensor operations (such as tensor multiplication, tensor product, contraction, *etc.*), without having to resort to indicial notation for higher-order tensors. Its basic definitions and identities are introduced here. Note that, in practice, the VOIGT notation can always be deduced from the indicial form of an equation. Nevertheless, a more formal and systematic approach is taken here to express the residuals and their differentials in VOIGT notation.

Vectors and Tensors

Let $\mathbf{u}$, $\mathbf{T}$, $\mathfrak{c}$, and $\mathbb{C}$ represent an arbitrary vector and second-, third-, and fourth-order tensors.[26] In VOIGT notation, the 3×3 independent components T_{ij} of $\mathbf{T}$ are represented by a 9×1 vector. Likewise, the $3\times3\times3\times3=81$ components $\mathbb{C}_{ijkl}$ of $\mathbb{C}$ are expressed as a 9×9 matrix. Third-order tensors $\mathfrak{c}$ are given either by 9×3 or by 3×9 matrices to represent their components $\mathfrak{c}_{ijk}$, depending on how the tensor is intended to operate against other vectors and tensors. For example, the third-order material tensor $\mathfrak{c}_2$ defined in $(6.38)_2$ operates on (symmetric) tensors from the left and vectors from the right, see $(6.56)_{1,2}$, hence its VOIGT notation must be of

[26] For the purposes of this section it is assumed that $\mathbf{u}$, $\mathbf{T}$, $\mathfrak{c}$, and $\mathbb{C}$ are completely arbitrary and unrelated to the displacement, stress or material tensors of the EMTM continuum theory.

dimensions 9×3. Here it is defined that

$$\underset{3\times 1}{\big\langle \mathbf{u} \big\rangle} = \begin{bmatrix} u_1 \\ u_2 \\ u_3 \end{bmatrix} \quad , \quad \underset{9\times 1}{\big\langle \mathbf{T} \big\rangle} = \begin{bmatrix} T_{11} \\ T_{22} \\ T_{33} \\ T_{12} \\ T_{23} \\ T_{31} \\ T_{13} \\ T_{21} \\ T_{32} \end{bmatrix} \quad , \quad \underset{9\times 3}{\big\langle \mathfrak{c} \big\rangle} = \begin{bmatrix} \mathfrak{c}_{111} & \mathfrak{c}_{112} & \mathfrak{c}_{113} \\ \mathfrak{c}_{221} & \mathfrak{c}_{222} & \mathfrak{c}_{223} \\ \mathfrak{c}_{331} & \mathfrak{c}_{332} & \mathfrak{c}_{333} \\ \mathfrak{c}_{121} & \mathfrak{c}_{122} & \mathfrak{c}_{123} \\ \mathfrak{c}_{231} & \mathfrak{c}_{232} & \mathfrak{c}_{233} \\ \mathfrak{c}_{311} & \mathfrak{c}_{312} & \mathfrak{c}_{313} \\ \mathfrak{c}_{131} & \mathfrak{c}_{132} & \mathfrak{c}_{133} \\ \mathfrak{c}_{211} & \mathfrak{c}_{212} & \mathfrak{c}_{213} \\ \mathfrak{c}_{321} & \mathfrak{c}_{322} & \mathfrak{c}_{323} \end{bmatrix} \quad ,$$

$$\underset{9\times 9}{\big\langle \mathbb{C} \big\rangle} = \begin{bmatrix} \mathbb{C}_{1111} & \mathbb{C}_{1122} & \mathbb{C}_{1133} & \mathbb{C}_{1112} & \mathbb{C}_{1123} & \mathbb{C}_{1131} & \mathbb{C}_{1113} & \mathbb{C}_{1121} & \mathbb{C}_{1132} \\ \mathbb{C}_{2211} & \mathbb{C}_{2222} & \mathbb{C}_{2233} & \mathbb{C}_{2212} & \mathbb{C}_{2223} & \mathbb{C}_{2231} & \mathbb{C}_{2213} & \mathbb{C}_{2221} & \mathbb{C}_{2232} \\ \mathbb{C}_{3311} & \mathbb{C}_{3322} & \mathbb{C}_{3333} & \mathbb{C}_{3312} & \mathbb{C}_{3323} & \mathbb{C}_{3331} & \mathbb{C}_{3313} & \mathbb{C}_{3321} & \mathbb{C}_{3332} \\ \mathbb{C}_{1211} & \mathbb{C}_{1222} & \mathbb{C}_{1233} & \mathbb{C}_{1212} & \mathbb{C}_{1223} & \mathbb{C}_{1231} & \mathbb{C}_{1213} & \mathbb{C}_{1221} & \mathbb{C}_{1232} \\ \mathbb{C}_{2311} & \mathbb{C}_{2322} & \mathbb{C}_{2333} & \mathbb{C}_{2312} & \mathbb{C}_{2323} & \mathbb{C}_{2331} & \mathbb{C}_{2313} & \mathbb{C}_{2321} & \mathbb{C}_{2332} \\ \mathbb{C}_{3111} & \mathbb{C}_{3122} & \mathbb{C}_{3133} & \mathbb{C}_{3112} & \mathbb{C}_{3123} & \mathbb{C}_{3131} & \mathbb{C}_{3113} & \mathbb{C}_{3121} & \mathbb{C}_{3132} \\ \mathbb{C}_{1311} & \mathbb{C}_{1322} & \mathbb{C}_{1333} & \mathbb{C}_{1312} & \mathbb{C}_{1323} & \mathbb{C}_{1331} & \mathbb{C}_{1313} & \mathbb{C}_{1321} & \mathbb{C}_{1332} \\ \mathbb{C}_{2111} & \mathbb{C}_{2122} & \mathbb{C}_{2133} & \mathbb{C}_{2112} & \mathbb{C}_{2123} & \mathbb{C}_{2131} & \mathbb{C}_{2113} & \mathbb{C}_{2121} & \mathbb{C}_{2132} \\ \mathbb{C}_{3211} & \mathbb{C}_{3222} & \mathbb{C}_{3233} & \mathbb{C}_{3212} & \mathbb{C}_{3223} & \mathbb{C}_{3231} & \mathbb{C}_{3213} & \mathbb{C}_{3221} & \mathbb{C}_{3232} \end{bmatrix} \quad , \tag{6.100}$$

where $\mathfrak{c}$ is assumed to operate with tensors from the left and vectors from the right.

Greek indices are used occasionally to refer to the components of a tensor in VOIGT notation. For example, the components of $\langle \mathbf{T} \rangle$ are represented by T_α where $\alpha = 1 \dots 9$ correspond with the indices ij according to the ordering defined in $(6.100)_2$. Likewise, the 9×3 components of $\langle \mathfrak{c} \rangle$ are indexed according to $\mathfrak{c}_{\alpha k}$, where $k = 1 \dots 3$, and the 9×9 components of $\langle \mathbb{C} \rangle$ are represented as $\mathbb{C}_{\alpha\beta}$.

Note that slightly different variants of the VOIGT notation exist, where the off-diagonal entries of $\langle \mathbf{T} \rangle$ (*i.e.*, T_α where $\alpha = 4 \dots 9$) are ordered differently. All representations are equivalent as long as they are employed consistently.

Higher-Order Tensor Multiplications

It is easy to verify that matrix-vector operations using the definitions in (6.100) emulate the tensor multiplications of the corresponding tensorial quantities. For example, it is readily seen that

$$\begin{aligned} \underset{9\times 1}{\big\langle \mathfrak{c}\,\mathbf{u} \big\rangle} &= \underset{9\times 3}{\big\langle \mathfrak{c} \big\rangle} \underset{3\times 1}{\big\langle \mathbf{u} \big\rangle} &&= \mathfrak{c}_{\alpha k} u_k \quad &&\leftrightarrow \quad \mathfrak{c}_{ijk} u_k \quad , \\ \underset{3\times 1}{\big\langle \mathfrak{c}^{\mathrm{T}} \mathbf{T} \big\rangle} &= \underset{3\times 9}{\big\langle \mathfrak{c}^{\mathrm{T}} \big\rangle} \underset{9\times 1}{\big\langle \mathbf{T} \big\rangle} &&= \mathfrak{c}_{\alpha k} T_\alpha \quad &&\leftrightarrow \quad \mathfrak{c}_{ijk} T_{ij} \quad , \\ \underset{9\times 1}{\big\langle \mathbb{C}\,\mathbf{T} \big\rangle} &= \underset{9\times 9}{\big\langle \mathbb{C} \big\rangle} \underset{9\times 1}{\big\langle \mathbf{T} \big\rangle} &&= \mathbb{C}_{\alpha\beta} T_\beta \quad &&\leftrightarrow \quad \mathbb{C}_{ijkl} T_{kl} \quad , \end{aligned} \tag{6.101}$$

which is in accordance with the corresponding tensor multiplication.

Second-Order Tensor Multiplication

It is clear from (6.101) that the VOIGT notation conveniently represents tensor multiplications involving higher-order tensors. However, this raises the question of how operations involving vectors and second-order tensors are represented in VOIGT notation. To examine this, let $\mathbf{S}$ and $\mathbf{T}$ be two arbitrary second-order tensors. The components $T_{ik}S_{kj}$ of the tensor multiplication $\mathbf{TS}$ are obtained from a simple matrix multiplication of their 3×3 matrix representation. However, if $\mathbf{S}$ is represented by the 9×1 VOIGT vector $\langle\mathbf{S}\rangle$, then the tensor multiplication must be expressed as

$$\underset{9\times 1}{\langle\mathbf{TS}\rangle} = \begin{bmatrix} T_{1k}S_{k1} \\ T_{2k}S_{k2} \\ T_{3k}S_{k3} \\ T_{1k}S_{k2} \\ T_{2k}S_{k3} \\ T_{3k}S_{k1} \\ T_{1k}S_{k3} \\ T_{2k}S_{k1} \\ T_{3k}S_{k2} \end{bmatrix} = \underbrace{\begin{bmatrix} T_{11} & 0 & 0 & 0 & 0 & T_{13} & 0 & T_{12} & 0 \\ 0 & T_{22} & 0 & T_{21} & 0 & 0 & 0 & 0 & T_{23} \\ 0 & 0 & T_{33} & 0 & T_{32} & 0 & T_{31} & 0 & 0 \\ 0 & T_{12} & 0 & T_{11} & 0 & 0 & 0 & 0 & T_{13} \\ 0 & 0 & T_{23} & 0 & T_{22} & 0 & T_{21} & 0 & 0 \\ T_{31} & 0 & 0 & 0 & 0 & T_{33} & 0 & T_{32} & 0 \\ 0 & 0 & T_{13} & 0 & T_{12} & 0 & T_{11} & 0 & 0 \\ T_{21} & 0 & 0 & 0 & 0 & T_{23} & 0 & T_{22} & 0 \\ 0 & T_{32} & 0 & T_{31} & 0 & 0 & 0 & 0 & T_{33} \end{bmatrix}}_{=\underset{9\times 9}{\langle\mathbf{T}\rangle^{(1)}}} \begin{bmatrix} S_{11} \\ S_{22} \\ S_{33} \\ S_{12} \\ S_{23} \\ S_{31} \\ S_{13} \\ S_{21} \\ S_{32} \end{bmatrix} . \tag{6.102}$$

Similarly, if $\mathbf{T}$ is represented by the 9×1 vector $\langle\mathbf{T}\rangle$, then

$$\underset{9\times 1}{\langle\mathbf{TS}\rangle} = \begin{bmatrix} S_{k1}T_{1k} \\ S_{k2}T_{2k} \\ S_{k3}T_{3k} \\ S_{k2}T_{1k} \\ S_{k3}T_{2k} \\ S_{k1}T_{3k} \\ S_{k3}T_{1k} \\ S_{k1}T_{2k} \\ S_{k2}T_{3k} \end{bmatrix} = \underbrace{\begin{bmatrix} S_{11} & 0 & 0 & S_{21} & 0 & 0 & S_{31} & 0 & 0 \\ 0 & S_{22} & 0 & 0 & S_{32} & 0 & 0 & S_{12} & 0 \\ 0 & 0 & S_{33} & 0 & 0 & S_{13} & 0 & 0 & S_{23} \\ S_{12} & 0 & 0 & S_{22} & 0 & 0 & S_{32} & 0 & 0 \\ 0 & S_{23} & 0 & 0 & S_{33} & 0 & 0 & S_{13} & 0 \\ 0 & 0 & S_{31} & 0 & 0 & S_{11} & 0 & 0 & S_{21} \\ S_{13} & 0 & 0 & S_{23} & 0 & 0 & S_{33} & 0 & 0 \\ 0 & S_{21} & 0 & 0 & S_{31} & 0 & 0 & S_{11} & 0 \\ 0 & 0 & S_{32} & 0 & 0 & S_{12} & 0 & 0 & S_{22} \end{bmatrix}}_{=\underset{9\times 9}{\langle\mathbf{S}\rangle^{(2)}}} \begin{bmatrix} T_{11} \\ T_{22} \\ T_{33} \\ T_{12} \\ T_{23} \\ T_{31} \\ T_{13} \\ T_{21} \\ T_{32} \end{bmatrix} . \tag{6.103}$$

In summary, it is concluded that tensor multiplications between two second-order tensors are alternatively expressed in VOIGT notation as

$$\begin{aligned} \underset{9\times 1}{\langle \mathbf{TS} \rangle} &= \underset{9\times 9}{\langle \mathbf{T} \rangle}^{(1)} \underset{9\times 1}{\langle \mathbf{S} \rangle} \\ &= \underset{9\times 9}{\langle \mathbf{S} \rangle}^{(2)} \underset{9\times 1}{\langle \mathbf{T} \rangle} \quad . \end{aligned} \tag{6.104}$$

where the operators $\langle [\,\cdot\,] \rangle^{(1)}$ and $\langle [\,\cdot\,] \rangle^{(2)}$ convert the components of a second-order tensor into a 9×9 matrix defined by (6.102) or (6.103), respectively.

Note that the preceding result may be viewed as a tensor multiplication between the fourth-order tensors $\mathbb{T}^{(1)}$ or $\mathbb{S}^{(2)}$, represented in VOIGT notation by $\langle \mathbf{T} \rangle^{(1)}$ or $\langle \mathbf{S} \rangle^{(1)}$, and the second-order tensors $\mathbf{S}$ or $\mathbf{T}$, represented in VOIGT notation by $\langle \mathbf{S} \rangle$ or $\langle \mathbf{T} \rangle$, respectively. The components of the aforementioned fourth-order tensors are inferred from

$$\begin{aligned} T_{ik} S_{kj} &= \big[T_{ik} \delta_{jl} \big] S_{kl} \;\leftrightarrow\; \underset{9\times 9}{\langle \mathbf{T} \rangle}^{(1)} = \underset{9\times 9}{\langle \mathbb{T}^{(1)} \rangle} \quad \text{where} \quad \mathbb{T}^{(1)} = T_{ik} \delta_{jl}\, \mathbf{e}_i \otimes \mathbf{e}_j \otimes \mathbf{e}_k \otimes \mathbf{e}_l \\ &= \big[\delta_{ik} S_{lj} \big] T_{kl} \;\leftrightarrow\; \underset{9\times 9}{\langle \mathbf{S} \rangle}^{(2)} = \underset{9\times 9}{\langle \mathbb{S}^{(2)} \rangle} \quad \text{where} \quad \mathbb{S}^{(2)} = \delta_{ik} S_{lj}\, \mathbf{e}_i \otimes \mathbf{e}_j \otimes \mathbf{e}_k \otimes \mathbf{e}_l \quad . \end{aligned} \tag{6.105}$$

According to this result, the second-order tensor multiplication $\mathbf{TS}$, see (2.11), is identical to the fourth-order tensor multiplications $\mathbf{TS} = \mathbb{T}^{(1)}\mathbf{S} = \mathbb{S}^{(2)}\mathbf{T}$, see (2.25), where the components of $\mathbb{T}^{(1)}$ and $\mathbb{S}^{(2)}$ are given by (6.105). This observation is based solely on tensor algebra and is thus independent of VOIGT notation.

It is seen by inspection of the components of $\mathbb{T}^{(1)}$ and $\mathbb{S}^{(2)}$ defined by (6.102 - 103) that for the transpose

$$\begin{aligned} \underset{9\times 9}{\langle \mathbf{T}^{\mathrm{T}} \rangle}^{(1)} &= \Big[\underset{9\times 9}{\langle \mathbf{T} \rangle}^{(1)} \Big]^{\mathrm{T}} \quad , \\ \underset{9\times 9}{\langle \mathbf{T}^{\mathrm{T}} \rangle}^{(2)} &= \Big[\underset{9\times 9}{\langle \mathbf{T} \rangle}^{(2)} \Big]^{\mathrm{T}} \quad . \end{aligned} \tag{6.106}$$

Therefore the symmetry of $\mathbf{T}$ also implies that $\langle \mathbf{T} \rangle^{(1)}$ and $\langle \mathbf{T} \rangle^{(2)}$ are symmetric (and *vice versa*). For the second-order identity tensor $\mathbf{I}$, the result in (6.105) yields

$$\underset{9\times 9}{\langle \mathbf{I} \rangle}^{(1)} = \underset{9\times 9}{\langle \mathbf{I} \rangle}^{(2)} = \underset{9\times 9}{\langle \mathbb{I} \rangle} = \underset{9\times 9}{\mathbf{I}_{(9)}} \quad , \tag{6.107}$$

where $\mathbb{I} = \delta_{ik}\delta_{jl}\, \mathbf{e}_i \otimes \mathbf{e}_j \otimes \mathbf{e}_k \otimes \mathbf{e}_l$ is the fourth-order identity tensor, see (2.29), and $\mathbf{I}_{(9)}$ denotes the 9×9 identity matrix. This result is consistent with $(6.104)_{1,2}$ where the identity $\mathbf{I}$ is substituted into either $\mathbf{T}$ or $\mathbf{S}$.

Vector Mapping

Lastly, consider the linear operation $\mathbf{T}\mathbf{u}$ between the second-order tensor $\mathbf{T}$ and the vector $\mathbf{u}$. This is trivial, of course, if the components of $\mathbf{T}$ are expressed as a 3×3 matrix. However, if $\mathbf{T}$ is instead given in VOIGT notation by the 9×1 vector $\langle\mathbf{T}\rangle$, this operation must be represented as

$$\underset{3\times 1}{\big(\mathbf{T}\mathbf{u}\big)} = \begin{bmatrix} u_k T_{1k} \\ u_k T_{2k} \\ u_k T_{3k} \end{bmatrix} = \underbrace{\begin{bmatrix} u_1 & 0 & 0 & u_2 & 0 & 0 & u_3 & 0 & 0 \\ 0 & u_2 & 0 & 0 & u_3 & 0 & 0 & u_1 & 0 \\ 0 & 0 & u_3 & 0 & 0 & u_1 & 0 & 0 & u_2 \end{bmatrix}}_{= \underset{3\times 9}{\langle \mathbf{u} \rangle^{(3)}}} \begin{bmatrix} T_{11} \\ T_{22} \\ T_{33} \\ T_{12} \\ T_{23} \\ T_{31} \\ T_{13} \\ T_{21} \\ T_{32} \end{bmatrix} \quad . \tag{6.108}$$

Hence, the linear mapping $\mathbf{T}\mathbf{u}$ of the vector $\mathbf{u}$ by the second-order tensor $\mathbf{T}$ is expressed in VOIGT notation as

$$\underset{3\times 1}{\big(\mathbf{T}\mathbf{u}\big)} = \underset{3\times 9}{\langle \mathbf{u} \rangle^{(3)}} \underset{9\times 1}{\langle \mathbf{T} \rangle} \quad . \tag{6.109}$$

A similar identity for the vector $\mathbf{T}\mathbf{u}$ is stated as

$$\underset{3\times 9}{\big\langle \mathbf{T}\mathbf{u} \big\rangle^{(3)}} = \underset{3\times 9}{\langle \mathbf{u} \rangle^{(3)}} \underset{9\times 9}{\langle \mathbf{T} \rangle^{(2)}} \quad , \tag{6.110}$$

which is readily verified by components. Note that, akin to (6.105), $\langle\mathbf{u}\rangle^{(3)}$ may be viewed as the VOIGT notation of a third-order tensor whose components are given by

$$T_{ik}u_k = \big[\delta_{ij}u_k\big]T_{jk} \quad \leftrightarrow \quad \underset{3\times 9}{\langle \mathbf{u} \rangle^{(3)}} = \underset{3\times 9}{\big\langle \mathbf{u}^{(3)} \big\rangle} \quad \text{where} \quad \mathbf{u}^{(3)} = \delta_{ij}u_k\,\mathbf{e}_i \otimes \mathbf{e}_j \otimes \mathbf{e}_k \quad . \tag{6.111}$$

The mapping $\mathbf{T}\mathbf{u}$ defined by (2.8) is identical to the tensor product in $(2.24)_2$ between the third-order tensor $\mathbf{u}^{(3)}$ and the second-order tensor $\mathbf{T}$, *i.e.*, $\mathbf{T}\mathbf{u} = \mathbf{u}^{(3)}\mathbf{T}$.

Similar representations are available for other vector and tensor operations by applying the same principles discussed here. That is, vector or tensor operations are converted to VOIGT notation by deliberately expressing the same result as a multiplication or contraction of higher-order tensors. This has been encountered before in Equation (2.158), where the axial vector of a vector product is equivalently represented by a skew-symmetric second-order tensor.

Tensor Products

The second-order tensor consisting of a tensor product $\mathbf{u}\otimes\mathbf{v}$ between two vectors $\mathbf{u}$ and $\mathbf{v}$ is represented in VOIGT notation as

$$\begin{aligned}\underset{1\times 9}{\left\langle \mathbf{u}\otimes\mathbf{v}\right\rangle}^{\mathrm{T}} &= \begin{bmatrix} u_1v_1 & u_2v_2 & u_3v_3 & u_1v_2 & u_2v_3 & u_3v_1 & u_1v_3 & u_2v_1 & u_3v_2 \end{bmatrix} \\ &= \begin{bmatrix} u_1 & u_2 & u_3 \end{bmatrix} \begin{bmatrix} v_1 & 0 & 0 & v_2 & 0 & 0 & v_3 & 0 & 0 \\ 0 & v_2 & 0 & 0 & v_3 & 0 & 0 & v_1 & 0 \\ 0 & 0 & v_3 & 0 & 0 & v_1 & 0 & 0 & v_2 \end{bmatrix} = \underset{1\times 3}{\left(\mathbf{u}\right)}^{\mathrm{T}} \underset{3\times 9}{\left\langle \mathbf{v}\right\rangle}^{(3)}\end{aligned} \tag{6.112}$$

where the definition in (6.108) was used for $\langle\mathbf{v}\rangle^{(3)}$. Furthermore, it can be shown that

$$\left[\underset{3\times 9}{\left\langle \mathbf{v}\right\rangle}^{(3)}\right]^{\mathrm{T}} \underset{3\times 9}{\left\langle \mathbf{w}\right\rangle}^{(3)} = \left[\underset{9\times 9}{\left\langle \mathbf{v}\otimes\mathbf{w}\right\rangle}^{(2)}\right]^{\mathrm{T}} \quad . \tag{6.113}$$

Meanwhile, the third-order tensor $\mathbf{T}\otimes\mathbf{u}$ resulting from the tensor product between a second-order tensor $\mathbf{T}$ and a vector $\mathbf{u}$ is written as

$$\underset{9\times 3}{\left\langle \mathbf{T}\otimes\mathbf{u}\right\rangle} = \begin{bmatrix} T_{11}u_1 & T_{11}u_2 & T_{11}u_3 \\ T_{22}u_1 & T_{22}u_2 & T_{22}u_3 \\ T_{33}u_1 & T_{33}u_2 & T_{33}u_3 \\ T_{12}u_1 & T_{12}u_2 & T_{12}u_3 \\ T_{23}u_1 & T_{23}u_2 & T_{23}u_3 \\ T_{31}u_1 & T_{31}u_2 & T_{31}u_3 \\ T_{13}u_1 & T_{13}u_2 & T_{13}u_3 \\ T_{21}u_1 & T_{21}u_2 & T_{21}u_3 \\ T_{32}u_1 & T_{32}u_2 & T_{32}u_3 \end{bmatrix} = \begin{bmatrix} T_{11} \\ T_{22} \\ T_{33} \\ T_{12} \\ T_{23} \\ T_{31} \\ T_{13} \\ T_{21} \\ T_{32} \end{bmatrix} \begin{bmatrix} u_1 & u_2 & u_3 \end{bmatrix} = \underset{9\times 1}{\left\langle \mathbf{T}\right\rangle} \underset{1\times 3}{\left(\mathbf{u}\right)}^{\mathrm{T}} \quad . \tag{6.114}$$

However, if the third-order tensor is produced by the opposite tensor product $\mathbf{u}\otimes\mathbf{T}$ while still being considered to operate on tensors from the left (*i.e.*, its VOIGT repre-

sentation is given by a 9×3 matrix), then

$$\begin{aligned}
\underset{9\times 3}{\langle \mathbf{u}\otimes\mathbf{T}\rangle} &= \begin{bmatrix} u_1T_{11} & u_1T_{12} & u_1T_{13} \\ u_2T_{21} & u_2T_{22} & u_2T_{23} \\ u_3T_{31} & u_3T_{32} & u_3T_{33} \\ u_1T_{21} & u_1T_{22} & u_1T_{23} \\ u_2T_{31} & u_2T_{32} & u_2T_{33} \\ u_3T_{11} & u_3T_{12} & u_3T_{13} \\ u_1T_{31} & u_1T_{32} & u_1T_{33} \\ u_2T_{11} & u_2T_{12} & u_2T_{13} \\ u_3T_{21} & u_3T_{22} & u_3T_{23} \end{bmatrix} \\
&= \begin{bmatrix} T_{11} & 0 & 0 & 0 & 0 & T_{13} & 0 & T_{12} & 0 \\ 0 & T_{22} & 0 & T_{21} & 0 & 0 & 0 & 0 & T_{23} \\ 0 & 0 & T_{33} & 0 & T_{32} & 0 & T_{31} & 0 & 0 \\ 0 & T_{12} & 0 & T_{11} & 0 & 0 & 0 & 0 & T_{13} \\ 0 & 0 & T_{23} & 0 & T_{22} & 0 & T_{21} & 0 & 0 \\ T_{31} & 0 & 0 & 0 & 0 & T_{33} & 0 & T_{32} & 0 \\ 0 & 0 & T_{13} & 0 & T_{12} & 0 & T_{11} & 0 & 0 \\ T_{21} & 0 & 0 & 0 & 0 & T_{23} & 0 & T_{22} & 0 \\ 0 & T_{32} & 0 & T_{31} & 0 & 0 & 0 & 0 & T_{33} \end{bmatrix} \begin{bmatrix} u_1 & 0 & 0 \\ 0 & u_2 & 0 \\ 0 & 0 & u_3 \\ u_2 & 0 & 0 \\ 0 & u_3 & 0 \\ 0 & 0 & u_1 \\ u_3 & 0 & 0 \\ 0 & u_1 & 0 \\ 0 & 0 & u_2 \end{bmatrix} \\
&= \underset{9\times 9}{\langle \mathbf{T}\rangle}^{(1)} \left[\underset{3\times 9}{\langle \mathbf{u}\rangle}^{(3)}\right]^{\mathrm{T}} \quad ,
\end{aligned} \tag{6.115}$$

see Equation (6.102). Lastly, a fourth-order tensor defined by the tensor product $\mathbf{S}\otimes\mathbf{T}$ of two second-order tensors is given simply by

$$\underset{9\times 9}{\langle \mathbf{T}\otimes\mathbf{S}\rangle} = \underset{9\times 1}{\langle \mathbf{T}\rangle}\,\underset{1\times 9}{\langle \mathbf{S}\rangle}^{\mathrm{T}} \quad . \tag{6.116}$$

Contraction

Trivially, the contraction between two tensors of equal order, see (2.22) and (2.27), is given in VOIGT notation by the contraction of the respective matrices.

Symmetries and Reduced Voigt Notation

Recall the definition in $(6.100)_4$ of the VOIGT notation for $\langle\mathbb{C}\rangle$ with 9×9 components $\mathbb{C}_{\alpha\beta}$, which represents the fourth-order tensor $\mathbb{C}$ with components $\mathbb{C}_{ijkl}$. It is readily seen that the symmetry of the matrix $\langle\mathbb{C}\rangle$ is equivalent to a *major* symmetry in the corresponding tensor $\mathbb{C}$, since the indices are given by $\mathbb{C}_{ijkl}\leftrightarrow\mathbb{C}_{\alpha\beta}$. However, no such conclusion can be drawn for *minor* symmetries of $\mathbb{C}$. Similarly, symmetries in second-order tensors $\mathbf{T}$ and third-order tensors $\mathfrak{c}$ are not as readily apparent in VOIGT notation.

Recall from (2.29) that the fourth-order identity tensor can be additively decomposed into $\mathbb{I} = \mathbb{I}^{\text{sym}} + \mathbb{I}^{\text{skw}}$, where the mappings $\text{sym}\big[\mathbf{T}\big] = \mathbb{I}^{\text{sym}}\,\mathbf{T}$ and $\text{skw}\big[\mathbf{T}\big] = \mathbb{I}^{\text{skw}}\,\mathbf{T}$ produce the symmetric part and the skew symmetric part of $\mathbf{T}$, respectively. The same decomposition holds in VOIGT notation, where it was already noted in Equation (6.107) that $\mathbb{I}$ produces the 9×9 identity matrix $\mathbf{I}_{(9)}$. Furthermore, let the 9×9 transpose operator $\langle \mathbb{I}^{\text{T}} \rangle$ be given by

$$\underset{9\times 9}{\langle \mathbb{I}^{\text{T}} \rangle} = \begin{bmatrix} 1 & 0 & 0 & 0 & 0 & 0 & 0 & 0 & 0 \\ 0 & 1 & 0 & 0 & 0 & 0 & 0 & 0 & 0 \\ 0 & 0 & 1 & 0 & 0 & 0 & 0 & 0 & 0 \\ 0 & 0 & 0 & 0 & 0 & 0 & 0 & 1 & 0 \\ 0 & 0 & 0 & 0 & 0 & 0 & 0 & 0 & 1 \\ 0 & 0 & 0 & 0 & 0 & 0 & 1 & 0 & 0 \\ 0 & 0 & 0 & 0 & 0 & 1 & 0 & 0 & 0 \\ 0 & 0 & 0 & 1 & 0 & 0 & 0 & 0 & 0 \\ 0 & 0 & 0 & 0 & 1 & 0 & 0 & 0 & 0 \end{bmatrix} \quad . \tag{6.117}$$

Hence, the components of the fourth-order symmetry operator $\mathbb{I}^{\text{sym}}_{ijkl} = \frac{1}{2}(\delta_{ik}\delta_{jl} + \delta_{jk}\delta_{il})$ are expressed in VOIGT notation as

$$\underset{9\times 9}{\langle \mathbb{I}^{\text{sym}} \rangle} = \frac{1}{2}\Big[\underset{9\times 9}{\langle \mathbb{I} \rangle} + \underset{9\times 9}{\langle \mathbb{I}^{\text{T}} \rangle}\Big] = \begin{bmatrix} 1 & 0 & 0 & 0 & 0 & 0 & 0 & 0 & 0 \\ 0 & 1 & 0 & 0 & 0 & 0 & 0 & 0 & 0 \\ 0 & 0 & 1 & 0 & 0 & 0 & 0 & 0 & 0 \\ 0 & 0 & 0 & \frac{1}{2} & 0 & 0 & 0 & \frac{1}{2} & 0 \\ 0 & 0 & 0 & 0 & \frac{1}{2} & 0 & 0 & 0 & \frac{1}{2} \\ 0 & 0 & 0 & 0 & 0 & \frac{1}{2} & \frac{1}{2} & 0 & 0 \\ 0 & 0 & 0 & 0 & 0 & \frac{1}{2} & \frac{1}{2} & 0 & 0 \\ 0 & 0 & 0 & \frac{1}{2} & 0 & 0 & 0 & \frac{1}{2} & 0 \\ 0 & 0 & 0 & 0 & \frac{1}{2} & 0 & 0 & 0 & \frac{1}{2} \end{bmatrix} \quad . \tag{6.118}$$

It is observed that $\langle \mathbb{I}^{\text{sym}} \rangle$ is symmetric, *i.e.*, $\mathbb{I}^{\text{sym}}$ is majorly symmetry,

$$\underset{9\times 9}{\langle \mathbb{I}^{\text{sym}} \rangle} = \underset{9\times 9}{\langle \mathbb{I}^{\text{sym}} \rangle^{\text{T}}} \quad , \tag{6.119}$$

and that the rows and columns 4 through 9 corresponding with the off-diagonals in VOIGT notation exhibit a repeating pattern. It is readily verified that

$$\underset{9\times 9}{\langle \mathbb{I}^{\text{sym}} \rangle}\,\underset{9\times 1}{\langle \mathbf{T} \rangle} = \underset{9\times 1}{\langle \text{sym}\big[\mathbf{T}\big] \rangle} \tag{6.120}$$

indeed produces the components of the symmetric part of $\mathbf{T}$, and that the repeated application

$$\underset{9\times 9}{\langle \mathbb{I}^{\text{sym}} \rangle} = \underset{9\times 9}{\langle \mathbb{I}^{\text{sym}} \rangle}\,\underset{9\times 9}{\langle \mathbb{I}^{\text{sym}} \rangle} \tag{6.121}$$

of the symmetry operator yields the same result.

The symmetric tensor sym[$\mathbf{T}$] contains only six independent components, which is also evidenced in VOIGT notation by the repeating pattern of the entries 4 through 9. Since symmetries are a common occurrence in the EMTM equations, it is economical to introduce a *reduced* VOIGT *notation* for symmetric tensors. To this end, it is observed that

$$\begin{aligned} \underset{9\times9}{\left\langle \mathbb{I}^{\mathrm{sym}} \right\rangle} &= \underset{9\times6}{\left\langle \mathbb{I}^{\mathrm{sym}}_{(1)} \right\rangle^{\mathrm{T}}} \underset{6\times9}{\left\langle \mathbb{I}^{\mathrm{sym}}_{(2)} \right\rangle} \\ &= \underset{9\times6}{\left\langle \mathbb{I}^{\mathrm{sym}}_{(2)} \right\rangle^{\mathrm{T}}} \underset{6\times9}{\left\langle \mathbb{I}^{\mathrm{sym}}_{(1)} \right\rangle} \quad , \end{aligned} \tag{6.122}$$

where reduced symmetry operators were defined as

$$\underset{6\times9}{\left\langle \mathbb{I}^{\mathrm{sym}}_{(1)} \right\rangle} = \begin{bmatrix} 1 & 0 & 0 & 0 & 0 & 0 & 0 & 0 & 0 \\ 0 & 1 & 0 & 0 & 0 & 0 & 0 & 0 & 0 \\ 0 & 0 & 1 & 0 & 0 & 0 & 0 & 0 & 0 \\ 0 & 0 & 0 & \frac{1}{2} & 0 & 0 & 0 & \frac{1}{2} & 0 \\ 0 & 0 & 0 & 0 & \frac{1}{2} & 0 & 0 & 0 & \frac{1}{2} \\ 0 & 0 & 0 & 0 & 0 & \frac{1}{2} & \frac{1}{2} & 0 & 0 \end{bmatrix} \quad , \tag{6.123}$$

and

$$\underset{6\times9}{\left\langle \mathbb{I}^{\mathrm{sym}}_{(2)} \right\rangle} = \begin{bmatrix} 1 & 0 & 0 & 0 & 0 & 0 & 0 & 0 & 0 \\ 0 & 1 & 0 & 0 & 0 & 0 & 0 & 0 & 0 \\ 0 & 0 & 1 & 0 & 0 & 0 & 0 & 0 & 0 \\ 0 & 0 & 0 & 1 & 0 & 0 & 0 & 1 & 0 \\ 0 & 0 & 0 & 0 & 1 & 0 & 0 & 0 & 1 \\ 0 & 0 & 0 & 0 & 0 & 1 & 1 & 0 & 0 \end{bmatrix} \quad . \tag{6.124}$$

The preceding definitions observe the relations

$$\underset{6\times9}{\left\langle \mathbb{I}^{\mathrm{sym}}_{(1)} \right\rangle} \underset{9\times6}{\left\langle \mathbb{I}^{\mathrm{sym}}_{(2)} \right\rangle^{\mathrm{T}}} = \underset{6\times9}{\left\langle \mathbb{I}^{\mathrm{sym}}_{(2)} \right\rangle} \underset{9\times6}{\left\langle \mathbb{I}^{\mathrm{sym}}_{(1)} \right\rangle^{\mathrm{T}}} = \underset{6\times6}{\mathbf{I}_{(6)}} \quad , \tag{6.125}$$

where $\mathbf{I}_{(6)}$ denotes the 6×6 identity matrix. Similar to (6.121), the repeated application of $\langle \mathbb{I}^{\mathrm{sym}} \rangle$ does not alter the reduced symmetry operators,

$$\begin{aligned} \underset{6\times9}{\left\langle \mathbb{I}^{\mathrm{sym}}_{(1)} \right\rangle} &= \underset{6\times9}{\left\langle \mathbb{I}^{\mathrm{sym}}_{(1)} \right\rangle} \underset{9\times9}{\left\langle \mathbb{I}^{\mathrm{sym}} \right\rangle} \quad , \\ \underset{6\times9}{\left\langle \mathbb{I}^{\mathrm{sym}}_{(2)} \right\rangle} &= \underset{6\times9}{\left\langle \mathbb{I}^{\mathrm{sym}}_{(2)} \right\rangle} \underset{9\times9}{\left\langle \mathbb{I}^{\mathrm{sym}} \right\rangle} \quad . \end{aligned} \tag{6.126}$$

The preceding result follows immediately from $(6.122)_{1,2}$ and (6.125).

Note that, when applied to a tensor $\langle \mathbf{T} \rangle$ in VOIGT notation, the operator $\langle \mathbb{I}^{\mathrm{sym}}_{(1)} \rangle$ takes the average of the off-diagonal components of $\mathbf{T}$

$$\underset{6\times 1}{\left\langle \mathbf{T}^{\mathrm{sym}}_{(1)} \right\rangle} = \underset{6\times 9}{\left\langle \mathbb{I}^{\mathrm{sym}}_{(1)} \right\rangle} \underset{9\times 1}{\left\langle \mathbf{T} \right\rangle} = \begin{bmatrix} T_{11} \\ T_{22} \\ T_{33} \\ \frac{1}{2}\left(T_{12}+T_{21}\right) \\ \frac{1}{2}\left(T_{23}+T_{32}\right) \\ \frac{1}{2}\left(T_{31}+T_{13}\right) \end{bmatrix} \quad . \tag{6.127}$$

Conversely, application of $\langle \mathbb{I}^{\mathrm{sym}}_{(2)} \rangle$ to $\langle \mathbf{E} \rangle$ yields the sum of the off-diagonal components of $\mathbf{E}$,

$$\underset{6\times 1}{\left\langle \mathbf{E}^{\mathrm{sym}}_{(2)} \right\rangle} = \underset{6\times 9}{\left\langle \mathbb{I}^{\mathrm{sym}}_{(2)} \right\rangle} \underset{9\times 1}{\left\langle \mathbf{E} \right\rangle} = \begin{bmatrix} E_{11} \\ E_{22} \\ E_{33} \\ E_{12}+E_{21} \\ E_{23}+E_{32} \\ E_{31}+E_{13} \end{bmatrix} \quad , \tag{6.128}$$

thereby introducing a factor of 2 on the entries 4 through 6.

The preceding results are employed to reduce the 9×9 notation of a fourth-order tensor $\mathbb{C}$ to a reduced 6×6 notation by enforcing the minor symmetries in $\mathbb{C}_{ijkl}$. Consider the linear stress-strain relationship $\mathbf{S}=\mathbb{C}\mathbf{E}$, see $(6.56)_2$, where both $\mathbf{S}$ and $\mathbf{E}$ are symmetric second-order tensors (which implies that minor symmetries can be imposed on $\mathbb{C}$ without loss of generality). In VOIGT notation, this implies that $\mathbf{S}$ can be expressed in reduced 6×6 notation $\langle \mathbf{S}^{\mathrm{sym}}_{(1)} \rangle$, see Equation (6.127), according to

$$\begin{aligned} \underset{6\times 1}{\left\langle \mathbf{S}^{\mathrm{sym}}_{(1)} \right\rangle} &= \underset{6\times 9}{\left\langle \mathbb{I}^{\mathrm{sym}}_{(1)} \right\rangle} \underset{9\times 1}{\left\langle \mathbf{S} \right\rangle} \\ &= \underset{6\times 9}{\left\langle \mathbb{I}^{\mathrm{sym}}_{(1)} \right\rangle} \underset{9\times 9}{\left\langle \mathbb{C} \right\rangle} \underset{9\times 1}{\left\langle \mathbf{E} \right\rangle} \\ &= \underset{6\times 9}{\left\langle \mathbb{I}^{\mathrm{sym}}_{(1)} \right\rangle} \underset{9\times 9}{\left\langle \mathbb{C} \right\rangle} \underset{9\times 9}{\left\langle \mathbb{I}^{\mathrm{sym}} \right\rangle} \underset{9\times 1}{\left\langle \mathbf{E} \right\rangle} \\ &= \underbrace{\underset{6\times 9}{\left\langle \mathbb{I}^{\mathrm{sym}}_{(1)} \right\rangle} \underset{9\times 9}{\left\langle \mathbb{C} \right\rangle} \underset{9\times 6}{\left\langle \mathbb{I}^{\mathrm{sym}}_{(1)} \right\rangle^{\mathrm{T}}}}_{\left\langle \mathbb{C}^{\mathrm{sym}}_{(1)} \right\rangle} \underbrace{\underset{6\times 9}{\left\langle \mathbb{I}^{\mathrm{sym}}_{(2)} \right\rangle} \underset{9\times 1}{\left\langle \mathbf{E} \right\rangle}}_{\left\langle \mathbf{E}^{\mathrm{sym}}_{(2)} \right\rangle} = \underset{6\times 6}{\left\langle \mathbb{C}^{\mathrm{sym}}_{(1)} \right\rangle} \underset{6\times 1}{\left\langle \mathbf{E}^{\mathrm{sym}}_{(2)} \right\rangle} \quad , \end{aligned} \tag{6.129}$$

where (6.120) and $(6.122)_1$ were used. The minor symmetries of the fourth-order tensor $\mathbb{C}$ are thus exploited to obtain the reduced 6×6 stiffness matrix

$$\underset{6\times 6}{\left\langle \mathbb{C}^{\mathrm{sym}} \right\rangle} = \underset{6\times 9}{\left\langle \mathbb{I}^{\mathrm{sym}}_{(1)} \right\rangle} \underset{9\times 9}{\left\langle \mathbb{C} \right\rangle} \underset{9\times 6}{\left\langle \mathbb{I}^{\mathrm{sym}}_{(1)} \right\rangle^{\mathrm{T}}} \quad . \tag{6.130}$$

No loss of information is incurred by this reduction if $\mathbb{C}$ is already minorly symmetric, in which case (6.130) is equivalent to setting $\langle \mathbb{C}^{\mathrm{sym}}_{(1)} \rangle$ equal to the first 6×6 entries of the 9×9 matrix $\langle \mathbb{C} \rangle$. The full 9×9 notation of the (still minorly symmetric) tensor $\langle \mathbb{C} \rangle$ is recovered using

$$\underset{9\times 9}{\langle \mathbb{C} \rangle} = \underset{9\times 6}{\langle \mathbb{I}^{\mathrm{sym}}_{(2)} \rangle^{\mathrm{T}}} \underset{6\times 6}{\langle \mathbb{C}^{\mathrm{sym}} \rangle} \underset{6\times 9}{\langle \mathbb{I}^{\mathrm{sym}}_{(2)} \rangle} \quad . \tag{6.131}$$

Note that it is customary to place the factor 2 for the off-diagonal entries (*i.e.*, for indices 4 through 6) on the strain $\langle \mathbf{E}^{\mathrm{sym}}_{(2)} \rangle$ rather than the stress $\langle \mathbf{S}^{\mathrm{sym}}_{(1)} \rangle$, see (6.129). Albeit equally valid, the opposite convention would require $\langle \mathbb{C}^{\mathrm{sym}}_{(2)} \rangle = \langle \mathbb{I}^{\mathrm{sym}}_{(2)} \rangle \langle \mathbb{C} \rangle \langle \mathbb{I}^{\mathrm{sym}}_{(2)} \rangle^{\mathrm{T}}$, which introduces unnecessary factors of 2 and 4 into the reduced 6×6 stiffness. Lastly, it is mentioned that no use was made of the major symmetry of $\mathbb{C}$. Nevertheless, it is observed from (6.130) that the symmetry of $\langle \mathbb{C} \rangle$ is preserved in the reduced notation $\langle \mathbb{C}^{\mathrm{sym}} \rangle$.

In order to derive a reduced 6×3 notation for third-order tensors $\mathfrak{c}$, consider the multiplication of $\mathfrak{c}$ with a symmetric second-order tensor $\mathbf{E}$ from the left, that is, $\mathfrak{c}^{\mathrm{T}}\mathbf{E}$.[27] This is represented in VOIGT notation with the aid of $(6.101)_2$ as

$$\begin{aligned}
\underset{3\times 1}{\langle \mathfrak{c}^{\mathrm{T}}\mathbf{E} \rangle} &= \underset{3\times 9}{\langle \mathfrak{c}^{\mathrm{T}} \rangle} \underset{9\times 1}{\langle \mathbf{E} \rangle} \\
&= \underset{3\times 9}{\langle \mathfrak{c}^{\mathrm{T}} \rangle} \underset{9\times 9}{\langle \mathbb{I}^{\mathrm{sym}} \rangle} \underset{9\times 1}{\langle \mathbf{E} \rangle} \\
&= \underbrace{\underset{3\times 9}{\langle \mathfrak{c}^{\mathrm{T}} \rangle} \underset{9\times 6}{\langle \mathbb{I}^{\mathrm{sym}}_{(1)} \rangle^{\mathrm{T}}}}_{\langle \mathfrak{c}^{\mathrm{sym}} \rangle^{\mathrm{T}}} \underbrace{\underset{6\times 9}{\langle \mathbb{I}^{\mathrm{sym}}_{(2)} \rangle} \underset{9\times 1}{\langle \mathbf{E} \rangle}}_{\langle \mathbf{E}^{\mathrm{sym}}_{(2)} \rangle} \quad .
\end{aligned} \tag{6.132}$$

It is thus concluded, that

$$\underset{6\times 3}{\langle \mathfrak{c}^{\mathrm{sym}} \rangle} = \underset{6\times 9}{\langle \mathbb{I}^{\mathrm{sym}}_{(1)} \rangle} \underset{9\times 3}{\langle \mathfrak{c} \rangle} \quad . \tag{6.133}$$

As before, no information is lost if $\mathfrak{c}$ is already symmetric. The full 9×3 notation of the (albeit still symmetric) tensor $\langle \mathfrak{c} \rangle$ is recovered from

$$\underset{9\times 3}{\langle \mathfrak{c} \rangle} = \underset{9\times 6}{\langle \mathbb{I}^{\mathrm{sym}}_{(2)} \rangle^{\mathrm{T}}} \underset{6\times 3}{\langle \mathfrak{c}^{\mathrm{sym}} \rangle} \quad . \tag{6.134}$$

Note that the definition (6.133) is based on the assumption that $\mathfrak{c}$ operates on the strain, not the stress, where the VOIGT notation of $\langle \mathbf{E}^{\mathrm{sym}}_{(2)} \rangle$ carries a factor of 2 on the shear components.

[27] Recall from the constitutive relation in $(6.56)_1$ that the symmetric strain tensor $\mathbf{E}$ contracts with the piezoelectric tensor $\mathfrak{c}_2$ from the left. This is the motivation for the definition of $\langle \mathfrak{c} \rangle$ as a 9×3 matrix rather than a 3×9 matrix.

Useful Identities

In view of the transpose and the symmetry operators in Equations (6.117) and (6.118), respectively, a pair of convenient identities are available for 3×9 matrices of the form $\langle \mathbf{w}\rangle^{(3)}$ introduced in (6.108). In particular, it is noted that

$$\begin{aligned}
\underset{3\times 9}{\langle \mathbf{w}\rangle^{(3)}}\ \underset{9\times 9}{\langle \mathbb{I}\rangle}\left[\underset{3\times 9}{\langle \mathbf{v}\rangle^{(3)}}\right]^{\mathrm{T}} &= (\mathbf{v}\cdot\mathbf{w})\ \underset{3\times 3}{[\mathbf{I}]} \quad , \\
\underset{3\times 9}{\langle \mathbf{w}\rangle^{(3)}}\ \underset{9\times 9}{\langle \mathbb{I}^{\mathrm{T}}\rangle}\left[\underset{3\times 9}{\langle \mathbf{v}\rangle^{(3)}}\right]^{\mathrm{T}} &= \underset{3\times 3}{[\mathbf{v}\otimes\mathbf{w}]} \quad ,
\end{aligned} \tag{6.135}$$

where $(6.135)_1$ is a special case of the more general statement

$$\underset{3\times 9}{\langle \mathbf{w}\rangle^{(3)}}\ \underset{9\times 9}{\langle \mathbf{T}\rangle^{(2)}}\left[\underset{3\times 9}{\langle \mathbf{v}\rangle^{(3)}}\right]^{\mathrm{T}} = (\mathbf{v}\cdot\mathbf{T}\,\mathbf{w})\ \underset{3\times 3}{[\mathbf{I}]} \quad . \tag{6.136}$$

The preceding results will be used in Section 6.3.4.

Second-Order Transformations

It is instructive to extend the relations in $(6.104)_{1,2}$ to the consecutive tensor multiplication between three second-order tensors $\mathbf{S}$, $\mathbf{T}$, and $\mathbf{U}$. In particular,

$$\underset{9\times 1}{\langle \mathbf{U}\mathbf{T}\mathbf{S}\rangle} = \underset{9\times 9}{\langle \mathbf{U}\rangle^{(1)}}\underset{9\times 9}{\langle \mathbf{S}\rangle^{(2)}}\underset{9\times 1}{\langle \mathbf{T}\rangle} \quad , \tag{6.137}$$

where the properties of $(6.104)_{1,2}$ were deliberately applied to ensure that the tensor $\mathbf{T}$ in the middle of the chain $\mathbf{U}\mathbf{T}\mathbf{S}$ is represented by a 9×1 vector $\langle \mathbf{T}\rangle$. The components of the 9×9 matrix $\langle \mathbf{U}\rangle^{(1)}\langle \mathbf{S}\rangle^{(2)}$ are given by

$$\begin{aligned}
\underset{9\times 9}{\langle \mathbf{U}\rangle^{(1)}}\underset{9\times 9}{\langle \mathbf{S}\rangle^{(2)}} &= \underset{9\times 9}{\langle \mathbb{U}^{(1)}\rangle}\underset{9\times 9}{\langle \mathbb{S}^{(2)}\rangle} = \underset{9\times 9}{\langle \mathbb{U}^{(1)}\mathbb{S}^{(2)}\rangle} \\
&= \begin{bmatrix}
U_{11}S_{11} & U_{12}S_{21} & U_{13}S_{31} & U_{11}S_{21} & U_{12}S_{31} & U_{13}S_{11} & U_{11}S_{31} & U_{11}S_{21} & U_{13}S_{21} \\
U_{21}S_{12} & U_{22}S_{22} & U_{23}S_{32} & U_{21}S_{22} & U_{22}S_{32} & U_{23}S_{12} & U_{21}S_{32} & U_{21}S_{22} & U_{23}S_{22} \\
U_{31}S_{13} & U_{32}S_{23} & U_{33}S_{33} & U_{31}S_{23} & U_{32}S_{33} & U_{33}S_{13} & U_{31}S_{33} & U_{31}S_{23} & U_{33}S_{23} \\
U_{11}S_{12} & U_{12}S_{22} & U_{13}S_{32} & U_{11}S_{22} & U_{12}S_{32} & U_{13}S_{12} & U_{11}S_{32} & U_{11}S_{22} & U_{13}S_{22} \\
U_{21}S_{13} & U_{22}S_{23} & U_{23}S_{33} & U_{21}S_{23} & U_{22}S_{33} & U_{23}S_{13} & U_{21}S_{33} & U_{21}S_{23} & U_{23}S_{23} \\
U_{31}S_{11} & U_{32}S_{21} & U_{33}S_{31} & U_{31}S_{21} & U_{32}S_{31} & U_{33}S_{11} & U_{31}S_{31} & U_{31}S_{21} & U_{33}S_{21} \\
U_{11}S_{13} & U_{12}S_{23} & U_{13}S_{33} & U_{11}S_{23} & U_{12}S_{33} & U_{13}S_{13} & U_{11}S_{33} & U_{11}S_{23} & U_{13}S_{23} \\
U_{21}S_{11} & U_{22}S_{21} & U_{23}S_{31} & U_{21}S_{21} & U_{22}S_{31} & U_{23}S_{11} & U_{21}S_{31} & U_{21}S_{21} & U_{23}S_{21} \\
U_{31}S_{12} & U_{32}S_{22} & U_{33}S_{32} & U_{31}S_{22} & U_{32}S_{32} & U_{33}S_{12} & U_{31}S_{32} & U_{31}S_{22} & U_{33}S_{22}
\end{bmatrix}
\end{aligned} \tag{6.138}$$

and it is readily verified that the fourth-order tensor

$$\begin{aligned}\mathbb{U}^{(1)}\mathbb{S}^{(2)} &= \left[U_{im}\delta_{jn}\,\mathbf{e}_i\otimes\mathbf{e}_j\otimes\mathbf{e}_m\otimes\mathbf{e}_n\right]\left[\delta_{ok}S_{lp}\,\mathbf{e}_o\otimes\mathbf{e}_p\otimes\mathbf{e}_k\otimes\mathbf{e}_l\right]\\ &= U_{ik}S_{lj}\,\mathbf{e}_i\otimes\mathbf{e}_j\otimes\mathbf{e}_k\otimes\mathbf{e}_l\end{aligned}\tag{6.139}$$

satisfies the desired property $\mathbb{U}^{(1)}\mathbb{S}^{(2)}\mathbf{T}=\mathbf{U}\mathbf{T}\mathbf{S}$.

In view of the correspondence $\mathbb{C}_{ijkl}\leftrightarrow\mathbb{C}_{\alpha\beta}$, the transpose of a 9×9 matrix in VOIGT notation is equivalent to switching the pairs of basis vectors $\mathbf{e}_i\otimes\mathbf{e}_j$ and $\mathbf{e}_k\otimes\mathbf{e}_l$, so that

$$\underset{9\times9}{\left\langle U_{ik}S_{lj}\,\mathbf{e}_i\otimes\mathbf{e}_j\otimes\mathbf{e}_k\otimes\mathbf{e}_l\right\rangle^{\mathrm{T}}} = \underset{9\times9}{\left\langle U_{ki}S_{jl}\,\mathbf{e}_i\otimes\mathbf{e}_j\otimes\mathbf{e}_k\otimes\mathbf{e}_l\right\rangle}\quad .\tag{6.140}$$

This implies by comparison of (6.138 - 140) that

$$\left[\underset{9\times9}{\langle\mathbf{U}\rangle^{(1)}}\underset{9\times9}{\langle\mathbf{S}\rangle^{(2)}}\right]^{\mathrm{T}} = \underset{9\times9}{\langle\mathbf{U}^{\mathrm{T}}\rangle^{(1)}}\underset{9\times9}{\langle\mathbf{S}^{\mathrm{T}}\rangle^{(2)}}\quad ,\tag{6.141}$$

which is restated with the aid of $(6.106)_{1,2}$ according to

$$\underset{9\times9}{\langle\mathbf{U}\rangle^{(1)}}\underset{9\times9}{\langle\mathbf{S}\rangle^{(2)}} = \underset{9\times9}{\langle\mathbf{S}\rangle^{(2)}}\underset{9\times9}{\langle\mathbf{U}\rangle^{(1)}}\quad .\tag{6.142}$$

This result states that $\langle\mathbf{U}\rangle^{(1)}$ and $\langle\mathbf{S}\rangle^{(2)}$ are commutative under matrix multiplication.

The results in (6.137 - 142) allow for a convenient VOIGT representation of the contravariant push-forward of second-order tensors, encountered in $(6.30)_3$ for the electric susceptibility parameter $\overline{\mathbf{c}}_3$.[28] It is observed that

$$\underset{9\times1}{\left\langle\mathbf{F}\mathbf{T}\mathbf{F}^{\mathrm{T}}\right\rangle} = \underset{9\times9}{\langle\mathbf{F}\rangle^{(1)}}\underset{9\times9}{\langle\mathbf{F}^{\mathrm{T}}\rangle^{(2)}}\underset{9\times1}{\langle\mathbf{T}\rangle} = \underset{9\times9}{\left\langle\mathbb{F}^{(1)}\mathbb{F}^{(2)\mathrm{T}}\right\rangle}\underset{9\times1}{\langle\mathbf{T}\rangle}\quad ,\tag{6.143}$$

where the property $(6.106)_2$ for the transpose was used. The components of the fourth-order tensor $\mathbb{F}^{(1)}\mathbb{F}^{(2)\mathrm{T}}$ are given by

$$\mathbb{F}^{(1)}\mathbb{F}^{(2)\mathrm{T}} = F_{ik}F_{jl}\,\mathbf{e}_i\otimes\mathbf{e}_j\otimes\mathbf{e}_k\otimes\mathbf{e}_l\quad .\tag{6.144}$$

It is again readily verified that (6.144) operates on $\mathbf{T}$ the same way as a contravariant push-forward, $\mathbb{F}^{(1)}\mathbb{F}^{(2)\mathrm{T}}\mathbf{T}=\mathbf{F}\mathbf{T}\mathbf{F}^{\mathrm{T}}$.

While the CARTESIAN components in (6.144) display neither major nor minor symmetries, it is worth noting that $\mathbb{F}^{(1)}\mathbb{F}^{(2)\mathrm{T}}$ does exhibit a 'mixed' minor symmetry

[28] The contravariant push-forward is chosen for this discussion because it will later be employed for the transformation of the material parameters. Of course, Equations (6.137 - 142) are equally applicable to the covariant push-forward (as well as the contra- or covariant pull-backs), as long as the correct substitutions are made for $\mathbf{U}$ and $\mathbf{S}$.

which requires exchanging the indices $i \leftrightarrow j$ and $k \leftrightarrow l$ simultaneously. As a result, it can be shown that

$$\underset{9\times9}{\big\langle \mathbb{I}^{\mathrm{sym}} \big\rangle}\, \underset{9\times9}{\big\langle \mathbb{F}^{(1)}\mathbb{F}^{(2)\mathrm{T}} \big\rangle} \;=\; \underset{9\times9}{\big\langle \mathbb{F}^{(1)}\mathbb{F}^{(2)\mathrm{T}} \big\rangle}\, \underset{9\times9}{\big\langle \mathbb{I}^{\mathrm{sym}} \big\rangle} \;=\; \underset{9\times9}{\big\langle \mathbb{I}^{\mathrm{sym}} \big\rangle}\, \underset{9\times9}{\big\langle \mathbb{F}^{(1)}\mathbb{F}^{(2)\mathrm{T}} \big\rangle}\, \underset{9\times9}{\big\langle \mathbb{I}^{\mathrm{sym}} \big\rangle} \quad . \tag{6.145}$$

In particular, the preceding property ensures that the push-forward of a symmetric tensor $\mathbf{T}$ (or the minor symmetries of the push-forward of higher-order tensors, see the next section) preserves this symmetry.

Third-Order Transformations

Transformations of higher-order tensors are effected in VOIGT notation using the same tools as described in the preceding section. For example, consider the transformation of a third-order tensor $\mathfrak{c}$ given in components as

$$\overline{\mathfrak{c}}_{ijk} \;=\; S_{iA}T_{jB}\mathfrak{c}_{ABC}U_{kC} \quad . \tag{6.146}$$

It is easy to show from the components in (6.139) that this corresponds to

$$\underset{9\times3}{\big\langle \overline{\mathfrak{c}} \big\rangle} \;=\; \underset{9\times9}{\big\langle \mathbf{S} \big\rangle^{(1)}}\, \underset{9\times9}{\big\langle \mathbf{T}^{\mathrm{T}} \big\rangle^{(2)}}\, \underset{9\times3}{\big\langle \mathfrak{c} \big\rangle}\, \underset{3\times3}{\big[\mathbf{U}^{\mathrm{T}} \big]} \quad . \tag{6.147}$$

In the special case of a contravariant push-forward of $\mathfrak{c}$, as previously encountered in $(6.30)_2$, the preceding result becomes

$$\underset{9\times3}{\big\langle \overline{\mathfrak{c}} \big\rangle} \;=\; \underset{9\times9}{\big\langle \mathbf{F} \big\rangle^{(1)}}\, \underset{9\times9}{\big\langle \mathbf{F}^{\mathrm{T}} \big\rangle^{(2)}}\, \underset{9\times3}{\big\langle \mathfrak{c} \big\rangle}\, \underset{3\times3}{\big[\mathbf{F}^{\mathrm{T}} \big]} \;=\; \underset{9\times9}{\big\langle \mathbf{F}^{(1)}\mathbf{F}^{(2)\mathrm{T}} \big\rangle}\, \underset{9\times3}{\big\langle \mathfrak{c} \big\rangle}\, \underset{3\times3}{\big[\mathbf{F}^{\mathrm{T}} \big]} \quad , \tag{6.148}$$

whose components of the 9×9 transformation matrix were defined in (6.144).

Next, suppose that $\mathfrak{c}_{ABC} = \mathfrak{c}_{BAC}$ is symmetric in the first two indices. This is enforced in VOIGT notation by the condition

$$\underset{9\times3}{\big\langle \mathfrak{c} \big\rangle} \;=\; \underset{9\times9}{\big\langle \mathbb{I}^{\mathrm{sym}} \big\rangle}\, \underset{9\times3}{\big\langle \mathfrak{c} \big\rangle} \quad . \tag{6.149}$$

This is the same assertion as in $(6.132)_2$ (albeit for the transpose, where the symmetry of $\langle \mathbb{I}^{\mathrm{sym}} \rangle$ in (6.119) is used). An immediate consequence of the property in (6.145) for the push-forward (6.148) is that

$$\begin{aligned}
\underset{9\times3}{\big\langle \overline{\mathfrak{c}} \big\rangle} \;&=\; \underset{9\times9}{\big\langle \mathbf{F}^{(1)}\mathbf{F}^{(2)\mathrm{T}} \big\rangle}\, \underset{9\times3}{\big\langle \mathfrak{c} \big\rangle}\, \underset{3\times3}{\big[\mathbf{F}^{\mathrm{T}} \big]} \\
&=\; \underset{9\times9}{\big\langle \mathbf{F}^{(1)}\mathbf{F}^{(2)\mathrm{T}} \big\rangle}\, \underset{9\times9}{\big\langle \mathbb{I}^{\mathrm{sym}} \big\rangle}\, \underset{9\times3}{\big\langle \mathfrak{c} \big\rangle}\, \underset{3\times3}{\big[\mathbf{F}^{\mathrm{T}} \big]} \\
&=\; \underset{9\times9}{\big\langle \mathbb{I}^{\mathrm{sym}} \big\rangle}\, \underset{9\times9}{\big\langle \mathbf{F}^{(1)}\mathbf{F}^{(2)\mathrm{T}} \big\rangle}\, \underset{9\times3}{\big\langle \mathfrak{c} \big\rangle}\, \underset{3\times3}{\big[\mathbf{F}^{\mathrm{T}} \big]} \\
&=\; \underset{9\times9}{\big\langle \mathbb{I}^{\mathrm{sym}} \big\rangle}\, \underset{9\times3}{\big\langle \overline{\mathfrak{c}} \big\rangle} \quad ,
\end{aligned} \tag{6.150}$$

hence the symmetry of $\mathfrak{c}$ is preserved by the push-forward operation. The reduced notation of the transformed quantity, defined in accordance with (6.133), yields

$$\begin{aligned}\underset{6\times3}{\left\langle \overline{\mathfrak{c}}^{\mathrm{sym}} \right\rangle} &= \underset{6\times9}{\left\langle \mathbb{I}^{\mathrm{sym}}_{(1)} \right\rangle} \underset{9\times3}{\left\langle \overline{\mathfrak{c}} \right\rangle} \\ &= \underbrace{\underset{6\times9}{\left\langle \mathbb{I}^{\mathrm{sym}}_{(1)} \right\rangle} \underset{9\times9}{\left\langle \mathbf{F}^{(1)}\mathbf{F}^{(2)\mathrm{T}} \right\rangle} \underset{9\times6}{\left\langle \mathbb{I}^{\mathrm{sym}}_{(2)} \right\rangle^{\mathrm{T}}}}_{(*)} \underbrace{\underset{6\times9}{\left\langle \mathbb{I}^{\mathrm{sym}}_{(1)} \right\rangle} \underset{9\times3}{\left\langle \mathfrak{c} \right\rangle}}_{\left\langle \mathfrak{c}^{\mathrm{sym}} \right\rangle} \underset{3\times3}{\left[\mathbf{F}^{\mathrm{T}} \right]} \quad , \end{aligned} \tag{6.151}$$

where Equations $(6.122)_2$, $(6.126)_1$, (6.133), (6.145), and (6.148) were used. The term $(*)$ in (6.151) represents a 6×6 transformation matrix for the contravariant push-forward of (minorly) symmetric quantities given in reduced notation.

Fourth-Order Transformations

In analogy to the derivations of the preceding section, the transformation of a fourth-order tensor $\mathbb{C}$, whose components are given as

$$\overline{\mathbb{C}}_{ijkl} = S_{iA}T_{jB}\mathbb{C}_{ABCD}U_{kC}V_{lD} \quad , \tag{6.152}$$

is expressed in VOIGT notation according to

$$\begin{aligned}\underset{9\times9}{\left\langle \overline{\mathbb{C}} \right\rangle} &= \underset{9\times9}{\left\langle \mathbf{S} \right\rangle^{(1)}} \underset{9\times9}{\left\langle \mathbf{T}^{\mathrm{T}} \right\rangle^{(2)}} \underset{9\times9}{\left\langle \mathbb{C} \right\rangle} \underset{9\times9}{\left\langle \mathbf{U}^{\mathrm{T}} \right\rangle^{(1)}} \underset{9\times9}{\left\langle \mathbf{V} \right\rangle^{(2)}} \\ &= \underset{9\times9}{\left\langle \mathbf{S} \right\rangle^{(1)}} \underset{9\times9}{\left\langle \mathbf{T}^{\mathrm{T}} \right\rangle^{(2)}} \underset{9\times9}{\left\langle \mathbb{C} \right\rangle} \left[\underset{9\times9}{\left\langle \mathbf{U} \right\rangle^{(1)}} \underset{9\times9}{\left\langle \mathbf{V}^{\mathrm{T}} \right\rangle^{(2)}} \right]^{\mathrm{T}} \quad , \end{aligned} \tag{6.153}$$

where the transpose $(6.106)_{1,2}$ and the commutativity (6.142) were used. In the case of a contravariant push-forward, see $(6.30)_4$, Equation (6.153) becomes

$$\begin{aligned}\underset{9\times9}{\left\langle \overline{\mathbb{C}} \right\rangle} &= \underset{9\times9}{\left\langle \mathbf{F} \right\rangle^{(1)}} \underset{9\times9}{\left\langle \mathbf{F}^{\mathrm{T}} \right\rangle^{(2)}} \underset{9\times9}{\left\langle \mathbb{C} \right\rangle} \left[\underset{9\times9}{\left\langle \mathbf{F} \right\rangle^{(1)}} \underset{9\times9}{\left\langle \mathbf{F}^{\mathrm{T}} \right\rangle^{(2)}} \right]^{\mathrm{T}} \\ &= \underset{9\times9}{\left\langle \mathbf{F}^{(1)}\mathbf{F}^{(2)\mathrm{T}} \right\rangle} \underset{9\times9}{\left\langle \mathbb{C} \right\rangle} \underset{9\times9}{\left\langle \mathbf{F}^{(1)}\mathbf{F}^{(2)\mathrm{T}} \right\rangle^{\mathrm{T}}} \quad , \end{aligned} \tag{6.154}$$

where the same 9×9 transformation matrix is employed as for second- and third-order tensors, see (6.144). It is clear from (6.154) that if the matrix $\langle\mathbb{C}\rangle$ is symmetric (hence the tensor $\mathbb{C}$ is majorly symmetric), then so is $\langle\overline{\mathbb{C}}\rangle$.

Minor symmetries of $\mathbb{C}$ (*i.e.*, the interchangeability of indices $A \leftrightarrow B$ and $C \leftrightarrow D$ in $\mathbb{C}_{ABCD}$) are enforced in VOIGT notation by requiring

$$\underset{9\times9}{\left\langle \mathbb{C} \right\rangle} = \underset{9\times9}{\left\langle \mathbb{I}^{\mathrm{sym}} \right\rangle} \underset{9\times9}{\left\langle \mathbb{C} \right\rangle} \underset{9\times9}{\left\langle \mathbb{I}^{\mathrm{sym}} \right\rangle} \quad . \tag{6.155}$$

It is seen akin to (6.150) that the property in (6.145) preserves the minor symmetries

$$\underset{9\times9}{\left\langle \overline{\mathbb{C}} \right\rangle} = \underset{9\times9}{\left\langle \mathbb{I}^{\mathrm{sym}} \right\rangle} \underset{9\times9}{\left\langle \overline{\mathbb{C}} \right\rangle} \underset{9\times9}{\left\langle \mathbb{I}^{\mathrm{sym}} \right\rangle} \quad . \tag{6.156}$$

Lastly, it can be shown that the reduced 6×6 notation defined by (6.130) is transformed according to

$$\begin{aligned} \underset{6\times6}{\left\langle \overline{\mathbb{C}}^{\mathrm{sym}} \right\rangle} &= \underset{6\times9}{\left\langle \mathbb{I}^{\mathrm{sym}}_{(1)} \right\rangle} \underset{9\times9}{\left\langle \overline{\mathbb{C}} \right\rangle} \underset{9\times6}{\left\langle \mathbb{I}^{\mathrm{sym}}_{(1)} \right\rangle^{\mathrm{T}}} \\ &= \underbrace{\underset{6\times9}{\left\langle \mathbb{I}^{\mathrm{sym}}_{(1)} \right\rangle} \underset{9\times9}{\left\langle \mathbb{F}^{(1)}\mathbb{F}^{(2)\mathrm{T}} \right\rangle} \underset{9\times6}{\left\langle \mathbb{I}^{\mathrm{sym}}_{(2)} \right\rangle^{\mathrm{T}}}}_{(*)} \underbrace{\underset{6\times9}{\left\langle \mathbb{I}^{\mathrm{sym}}_{(1)} \right\rangle} \underset{9\times9}{\left\langle \mathbb{C} \right\rangle} \underset{9\times6}{\left\langle \mathbb{I}^{\mathrm{sym}}_{(1)} \right\rangle^{\mathrm{T}}}}_{\left\langle \mathbb{C}^{\mathrm{sym}} \right\rangle} \underbrace{\underset{9\times6}{\left\langle \mathbb{I}^{\mathrm{sym}}_{(2)} \right\rangle} \underset{9\times9}{\left\langle \mathbb{F}^{(1)}\mathbb{F}^{(2)\mathrm{T}} \right\rangle^{\mathrm{T}}} \underset{6\times9}{\left\langle \mathbb{I}^{\mathrm{sym}}_{(1)} \right\rangle^{\mathrm{T}}}}_{(*)^{\mathrm{T}}} \end{aligned} , \tag{6.157}$$

where the term $(*)$ represents the same 6×6 transformation matrix as in (6.151). If minor symmetries are available, as is the case for the EMTM material tensors (6.58), Equation (6.157) constitutes a memory-efficient alternative to the full 9×9 push-forward operation in (6.154).

6.3.2 Finite Element Discretization

It was established in Section 6.2.1 that the weak form is equivalent to the strong form of the IBVP, provided that the integrands are continuous. The weak form Equations (6.74) or (6.76) must be satisfied by the solution $\{\mathbf{u}, \theta, \phi, \varphi\}$ under the arbitrary admissible variations $\{\delta\mathbf{u}, \delta\theta, \delta\phi, \delta\varphi\}$. In order to turn the search for the primary variables into a discrete set of algebraic equations amenable for a numerical implementation, the primary variables and their variations are approximated using a finite element discretization.

Nodal Vector and Shape Functions

At any given time, the primary variables $\{\mathbf{u}, \theta, \phi, \varphi\}$, typically continuous functions of $\mathbf{x}$, are approximated by a linear combination of n predefined shape functions $N_i(\mathbf{x})$ weighted by n discrete nodal values $\{\hat{\mathbf{u}}_i, \hat{\theta}_i, \hat{\phi}_i, \hat{\varphi}_i\}$, $i = 1 \dots n$.[29] Likewise, the corresponding continuous variations $\{\delta\mathbf{u}, \delta\theta, \delta\phi, \delta\varphi\}$ are represented by a linear combination of the same shape functions $N_i(\mathbf{x})$ multiplied with the nodal val-

[29] It is emphasized that $N_i(\mathbf{x})$ represent the global (as opposed to the element) shape functions, hence they are defined on the entirety of the problem domain (rather than on the domain of a single element). Accordingly, n denotes the total number of nodes in the global finite element mesh.

ues $\{\delta\hat{\mathbf{u}}_i, \delta\hat{\theta}_i, \delta\hat{\phi}_i, \delta\hat{\varphi}_i\}$,

$$
\begin{aligned}
\mathbf{u}(\mathbf{x}) &\doteq \sum_{i=1}^{n} N_i(\mathbf{x})\,\hat{\mathbf{u}}_i \quad , \quad \delta\mathbf{u}(\mathbf{x}) \doteq \sum_{i=1}^{n} N_i(\mathbf{x})\,\delta\hat{\mathbf{u}}_i \quad , \\
\theta(\mathbf{x}) &\doteq \sum_{i=1}^{n} N_i(\mathbf{x})\,\hat{\theta}_i \quad , \quad \delta\theta(\mathbf{x}) \doteq \sum_{i=1}^{n} N_i(\mathbf{x})\,\delta\hat{\theta}_i \quad , \\
\phi(\mathbf{x}) &\doteq \sum_{i=1}^{n} N_i(\mathbf{x})\,\hat{\phi}_i \quad , \quad \delta\phi(\mathbf{x}) \doteq \sum_{i=1}^{n} N_i(\mathbf{x})\,\delta\hat{\phi}_i \quad , \\
\varphi(\mathbf{x}) &\doteq \sum_{i=1}^{n} N_i(\mathbf{x})\,\hat{\varphi}_i \quad , \quad \delta\varphi(\mathbf{x}) \doteq \sum_{i=1}^{n} N_i(\mathbf{x})\,\delta\hat{\varphi}_i \quad .
\end{aligned}
\tag{6.158}
$$

The nodal values of the primary variables $\{\hat{\mathbf{u}}_i, \hat{\theta}_i, \hat{\phi}_i, \hat{\varphi}_i\}$ are yet to be determined, whereas the corresponding variations $\{\delta\hat{\mathbf{u}}_i, \delta\hat{\theta}_i, \delta\hat{\phi}_i, \delta\hat{\varphi}_i\}$ are assumed to be arbitrary.[30]

Recall the expressions for the residuals $\{r_{\mathbf{u}}, r_\theta, r_\phi, r_\varphi\}$ in Equations $(6.76)_{1-4}$ and their differentials $\{\mathrm{d}r_{\mathbf{u}}, \mathrm{d}r_\theta, \mathrm{d}r_\phi, \mathrm{d}r_\varphi\}$ in (6.92), (6.95), (6.97), and (6.99). Each equation contains an integral over $\mathcal{R}$ which, given the approximations (6.158), amounts to a linear combination of integrals over $\mathcal{R}$ for each shape function. The aforementioned residuals and differentials give rise to the global finite element residual and the global stiffness matrix, respectively. For illustration purposes, the shape functions $N_i(\mathbf{x})$ are regarded as global functions defined in the whole domain $\mathcal{R}$, where $i = 1 \ldots n$ refers to any of a total of n nodes in the entire finite element model.[31] Note that the shape functions $N_i(\mathbf{x})$ are assumed to depend on the *spatial* position, hence its derivatives represent spatial gradients. This is in accordance with the notation chosen for the residuals and their differentials, which are expressed in terms of spatial derivatives and spatial integrals.

The approximations introduced in (6.158) are more conveniently expressed in

[30] Recall that admissible test functions were assumed to vanish on the DIRICHLET boundary, see (6.71). This implies that the nodal values $\{\delta\hat{\mathbf{u}}_i, \delta\hat{\theta}_i, \delta\hat{\phi}_i, \delta\hat{\varphi}_i\}$ of the test functions vanish on $\{\Gamma_{\mathbf{u}}, \Gamma_\theta, \Gamma_\phi, \Gamma_\varphi\}$, whereas the nodal values of the primary variables $\{\hat{\mathbf{u}}_i, \hat{\theta}_i, \hat{\phi}_i, \hat{\varphi}_i\}$ are given by the value of $\{\bar{\mathbf{u}}, \bar{\theta}, \bar{\phi}, \bar{\varphi}\}$ at the respective boundary location, see (6.64). For the sake of simplicity, it is assumed here that *all* nodal variations $\{\delta\hat{\mathbf{u}}_i, \delta\hat{\theta}_i, \delta\hat{\phi}_i, \delta\hat{\varphi}_i\}$ are arbitrary. Thereafter, the enforcement of the DIRICHLET boundary condition amounts to the evaluation of a SCHUR *complement*.

[31] Of course, in a typical finite element setting, the shape functions are non-zero only in the vicinity of the corresponding node. The only non-zero contributions to the global integral involving a given shape function $N_i(\mathbf{x})$ originate from elements adjacent to the node i. Hence, in practice, the global integral is subdivided into integrals over the element domains $\Omega^e \subset \mathcal{R}$ which furnish the *element residual* and *element stiffness matrix*. They can be *assembled* into the global residual and stiffness matrix if needed.

matrix form according to

$$\begin{aligned}
\underset{3\times1}{\mathbf{u}(\mathbf{x})} &\doteq \underset{3\times3n}{\left[\mathbf{N}^{(3)}(\mathbf{x})\right]}\,\underset{3n\times1}{\left[\,\hat{\mathbf{u}}\,\right]} \quad , \quad \underset{3\times1}{\delta\mathbf{u}(\mathbf{x})} \doteq \underset{3\times3n}{\left[\mathbf{N}^{(3)}(\mathbf{x})\right]}\,\underset{3n\times1}{\left[\,\delta\hat{\mathbf{u}}\,\right]} \quad , \\
\underset{1\times1}{\theta(\mathbf{x})} &\doteq \underset{1\times n}{\left[\mathbf{N}^{(1)}(\mathbf{x})\right]}\,\underset{n\times1}{\left[\,\hat{\theta}\,\right]} \quad , \quad \underset{1\times1}{\delta\theta(\mathbf{x})} \doteq \underset{1\times n}{\left[\mathbf{N}^{(1)}(\mathbf{x})\right]}\,\underset{n\times1}{\left[\,\delta\hat{\theta}\,\right]} \quad , \\
\underset{1\times1}{\phi(\mathbf{x})} &\doteq \underset{1\times n}{\left[\mathbf{N}^{(1)}(\mathbf{x})\right]}\,\underset{n\times1}{\left[\,\hat{\phi}\,\right]} \quad , \quad \underset{1\times1}{\delta\phi(\mathbf{x})} \doteq \underset{1\times n}{\left[\mathbf{N}^{(1)}(\mathbf{x})\right]}\,\underset{n\times1}{\left[\,\delta\hat{\phi}\,\right]} \quad , \\
\underset{1\times1}{\varphi(\mathbf{x})} &\doteq \underset{1\times n}{\left[\mathbf{N}^{(1)}(\mathbf{x})\right]}\,\underset{n\times1}{\left[\,\hat{\varphi}\,\right]} \quad , \quad \underset{1\times1}{\delta\varphi(\mathbf{x})} \doteq \underset{1\times n}{\left[\mathbf{N}^{(1)}(\mathbf{x})\right]}\,\underset{n\times1}{\left[\,\delta\hat{\varphi}\,\right]} \quad .
\end{aligned} \tag{6.159}$$

Here, the matrices $[\mathbf{N}^{(3)}(\mathbf{x})]$ and $[\mathbf{N}^{(1)}(\mathbf{x})]$ for the shape functions are defined as

$$\underset{3\times3n}{\left[\mathbf{N}^{(3)}\right]} = \left[N_1(\mathbf{x})\,\underset{3\times3}{\left[\mathbf{I}_{(3)}\right]} \quad N_2(\mathbf{x})\,\underset{3\times3}{\left[\mathbf{I}_{(3)}\right]} \quad \cdots \quad N_{n-1}(\mathbf{x})\,\underset{3\times3}{\left[\mathbf{I}_{(3)}\right]} \quad N_n(\mathbf{x})\,\underset{3\times3}{\left[\mathbf{I}_{(3)}\right]}\right] \quad , \tag{6.160}$$

and

$$\underset{1\times n}{\left[\mathbf{N}^{(1)}\right]} = \left[N_1(\mathbf{x}) \quad N_2(\mathbf{x}) \quad \cdots \quad N_{n-1}(\mathbf{x}) \quad N_n(\mathbf{x})\right] \quad , \tag{6.161}$$

where $\mathbf{I}_{(3)}$ denotes the 3×3 identity matrix. Meanwhile, the nodal values are compiled into the vectors

$$\begin{aligned}
\underset{3n\times1}{\left[\,\hat{\mathbf{u}}\,\right]} &= \begin{bmatrix} \hat{\mathbf{u}}_1 \\ \hat{\mathbf{u}}_2 \\ \vdots \\ \hat{\mathbf{u}}_{n-1} \\ \hat{\mathbf{u}}_n \end{bmatrix} \quad , \quad \underset{n\times1}{\left[\,\hat{\theta}\,\right]} = \begin{bmatrix} \hat{\theta}_1 \\ \hat{\theta}_2 \\ \vdots \\ \hat{\theta}_{n-1} \\ \hat{\theta}_n \end{bmatrix} \quad , \quad \underset{n\times1}{\left[\,\hat{\phi}\,\right]} = \begin{bmatrix} \hat{\phi}_1 \\ \hat{\phi}_2 \\ \vdots \\ \hat{\phi}_{n-1} \\ \hat{\phi}_n \end{bmatrix} \quad , \quad \underset{n\times1}{\left[\,\hat{\varphi}\,\right]} = \begin{bmatrix} \hat{\varphi}_1 \\ \hat{\varphi}_2 \\ \vdots \\ \hat{\varphi}_{n-1} \\ \hat{\varphi}_n \end{bmatrix} \quad , \\
\underset{3n\times1}{\left[\,\delta\hat{\mathbf{u}}\,\right]} &= \begin{bmatrix} \delta\hat{\mathbf{u}}_1 \\ \delta\hat{\mathbf{u}}_2 \\ \vdots \\ \delta\hat{\mathbf{u}}_{n-1} \\ \delta\hat{\mathbf{u}}_n \end{bmatrix} \quad , \quad \underset{n\times1}{\left[\,\delta\hat{\theta}\,\right]} = \begin{bmatrix} \delta\hat{\theta}_1 \\ \delta\hat{\theta}_2 \\ \vdots \\ \delta\hat{\theta}_{n-1} \\ \delta\hat{\theta}_n \end{bmatrix} \quad , \quad \underset{n\times1}{\left[\,\delta\hat{\phi}\,\right]} = \begin{bmatrix} \delta\hat{\phi}_1 \\ \delta\hat{\phi}_2 \\ \vdots \\ \delta\hat{\phi}_{n-1} \\ \delta\hat{\phi}_n \end{bmatrix} \quad , \quad \underset{n\times1}{\left[\,\delta\hat{\varphi}\,\right]} = \begin{bmatrix} \delta\hat{\varphi}_1 \\ \delta\hat{\varphi}_2 \\ \vdots \\ \delta\hat{\varphi}_{n-1} \\ \delta\hat{\varphi}_n \end{bmatrix} \quad .
\end{aligned} \tag{6.162}$$

Derivatives of Discretized Functions

Gradients of the finite element approximations for the vector- and real-valued fields in Equations (6.158) are determined from the spatial derivatives of the shape func-

tions $N_i(\mathbf{x})$. Using the matrix form in (6.159), this yields

$$\begin{aligned}
\underset{9\times1}{\left\langle \frac{\partial \mathbf{u}}{\partial \mathbf{x}} \right\rangle} &\doteq \underset{9\times3n}{\left[\mathbf{B}^{(3)}(\mathbf{x})\right]} \underset{3n\times1}{\left[\hat{\mathbf{u}}\right]} \quad , \quad \underset{9\times1}{\left\langle \frac{\partial \delta\mathbf{u}}{\partial \mathbf{x}} \right\rangle} \doteq \underset{9\times3n}{\left[\mathbf{B}^{(3)}(\mathbf{x})\right]} \underset{3n\times1}{\left[\delta\hat{\mathbf{u}}\right]} \quad , \\
\underset{3\times1}{\left(\frac{\partial \theta}{\partial \mathbf{x}}\right)} &\doteq \underset{3\times n}{\left[\mathbf{B}^{(1)}(\mathbf{x})\right]} \underset{n\times1}{\left[\hat{\theta}\right]} \quad , \quad \underset{3\times1}{\left(\frac{\partial \delta\theta}{\partial \mathbf{x}}\right)} \doteq \underset{3\times n}{\left[\mathbf{B}^{(1)}(\mathbf{x})\right]} \underset{n\times1}{\left[\delta\hat{\theta}\right]} \quad , \\
\underset{3\times1}{\left(\frac{\partial \phi}{\partial \mathbf{x}}\right)} &\doteq \underset{3\times n}{\left[\mathbf{B}^{(1)}(\mathbf{x})\right]} \underset{n\times1}{\left[\hat{\phi}\right]} \quad , \quad \underset{3\times1}{\left(\frac{\partial \delta\phi}{\partial \mathbf{x}}\right)} \doteq \underset{3\times n}{\left[\mathbf{B}^{(1)}(\mathbf{x})\right]} \underset{n\times1}{\left[\delta\hat{\phi}\right]} \quad , \\
\underset{3\times1}{\left(\frac{\partial \varphi}{\partial \mathbf{x}}\right)} &\doteq \underset{3\times n}{\left[\mathbf{B}^{(1)}(\mathbf{x})\right]} \underset{n\times1}{\left[\hat{\varphi}\right]} \quad , \quad \underset{3\times1}{\left(\frac{\partial \delta\varphi}{\partial \mathbf{x}}\right)} \doteq \underset{3\times n}{\left[\mathbf{B}^{(1)}(\mathbf{x})\right]} \underset{n\times1}{\left[\delta\hat{\varphi}\right]} \quad .
\end{aligned} \tag{6.163}$$

Here, the gradient matrix $[\mathbf{B}^{(3)}]$ of the shape functions in $[\mathbf{N}^{(3)}]$ is defined as

$$\underset{9\times3n}{\left[\mathbf{B}^{(3)}\right]} = \left[\underset{9\times3}{\left[\mathbf{B}_1^{(3)}\right]} \quad \underset{9\times3}{\left[\mathbf{B}_2^{(3)}\right]} \quad \cdots \quad \underset{9\times3}{\left[\mathbf{B}_{n-1}^{(3)}\right]} \quad \underset{9\times3}{\left[\mathbf{B}_n^{(3)}\right]} \right] \quad , \tag{6.164}$$

where each 9×3 sub-matrix $\left[\mathbf{B}_i^{(3)}\right]$ consists of the derivatives

$$\underset{9\times3}{\left[\mathbf{B}_i^{(3)}\right]} = \begin{bmatrix} N_{i,1} & 0 & 0 \\ 0 & N_{i,2} & 0 \\ 0 & 0 & N_{i,3} \\ N_{i,2} & 0 & 0 \\ 0 & N_{i,3} & 0 \\ 0 & 0 & N_{i,1} \\ N_{i,3} & 0 & 0 \\ 0 & N_{i,1} & 0 \\ 0 & 0 & N_{i,2} \end{bmatrix} \quad . \tag{6.165}$$

Similarly, the gradient matrix $[\mathbf{B}^{(1)}]$ of the shape functions in $[\mathbf{N}^{(1)}]$ is defined as

$$\underset{3\times n}{\left[\mathbf{B}^{(1)}\right]} = \left[\underset{3\times1}{\left(\mathbf{B}_1^{(1)}\right)} \quad \underset{3\times1}{\left(\mathbf{B}_2^{(1)}\right)} \quad \cdots \quad \underset{3\times1}{\left(\mathbf{B}_{n-1}^{(1)}\right)} \quad \underset{3\times1}{\left(\mathbf{B}_n^{(1)}\right)} \right] \quad , \tag{6.166}$$

where each 3×1 sub-vector $\left[\mathbf{B}_i^{(1)}\right]$ contains the derivatives

$$\underset{3\times1}{\left(\mathbf{B}_i^{(1)}\right)} = \begin{bmatrix} N_{i,1} \\ N_{i,2} \\ N_{i,3} \end{bmatrix} \quad . \tag{6.167}$$

Equations (6.165) and (6.167) are related via

$$\underset{9\times3}{\left[\mathbf{B}_i^{(3)}\right]} = \left[\underset{3\times1}{\left\langle \left(\mathbf{B}_i^{(1)}\right) \right\rangle^{(3)}} \right]^{\mathrm{T}} \quad , \tag{6.168}$$

where the definition of the 3×9 matrix $\langle \mathbf{u} \rangle^{(3)}$ in (6.108) was used.

Equations $(6.163)_{1,2}$ make use of VOIGT notation to represent the second-order tensors ensuing from the gradient of vector-valued quantities. The symmetric part of the displacement gradient is defined in reduced VOIGT notation in accordance with (6.128), or

$$\underset{6\times 1}{\left\langle \left[\frac{\partial \mathbf{u}}{\partial \mathbf{x}}\right]^{\mathrm{sym}} \right\rangle} = \underset{6\times 9}{\left\langle \mathbb{I}^{\mathrm{sym}}_{(2)} \right\rangle} \underset{9\times 1}{\left\langle \frac{\partial \mathbf{u}}{\partial \mathbf{x}} \right\rangle} = \begin{bmatrix} u_{1,1} \\ u_{2,2} \\ u_{3,3} \\ u_{1,2}+u_{2,1} \\ u_{2,3}+u_{3,2} \\ u_{3,1}+u_{1,3} \end{bmatrix} \quad . \tag{6.169}$$

This implies a reduced gradient matrix $[\mathbf{B}^{(3)}]^{\mathrm{sym}}$ given by

$$\underset{6\times 3n}{\left[\mathbf{B}^{(3)}\right]^{\mathrm{sym}}} = \left[\underset{6\times 3}{\left[\mathbf{B}^{(3)}_1\right]^{\mathrm{sym}}} \quad \underset{6\times 3}{\left[\mathbf{B}^{(3)}_2\right]^{\mathrm{sym}}} \quad \cdots \quad \underset{6\times 3}{\left[\mathbf{B}^{(3)}_{n-1}\right]^{\mathrm{sym}}} \quad \underset{6\times 3}{\left[\mathbf{B}^{(3)}_n\right]^{\mathrm{sym}}} \right] \quad , \tag{6.170}$$

where each 6×3 sub-matrix $\left[\mathbf{B}^{(3)}_i\right]^{\mathrm{sym}}$ consists of the derivatives

$$\underset{6\times 3}{\left[\mathbf{B}^{(3)}_i\right]^{\mathrm{sym}}} = \underset{6\times 9}{\left\langle \mathbb{I}^{\mathrm{sym}}_{(2)} \right\rangle} \underset{9\times 3}{\left[\mathbf{B}^{(3)}_i\right]} = \begin{bmatrix} N_{i,1} & 0 & 0 \\ 0 & N_{i,2} & 0 \\ 0 & 0 & N_{i,3} \\ N_{i,2} & N_{i,1} & 0 \\ 0 & N_{i,3} & N_{i,2} \\ N_{i,3} & 0 & N_{i,1} \end{bmatrix} \quad . \tag{6.171}$$

Note that the definition in (6.169) places a factor of 2 on the off-diagonal entries of the displacement gradient (*i.e.*, for indices 4 through 6). This is consistent with the remarks following Equation (6.134).

The product between the displacement gradient (in VOIGT notation) and a vector $\mathbf{w}$ is obtained with the aid of Equations (6.108 - 109),

$$\underset{3\times 1}{\left(\frac{\partial \mathbf{u}}{\partial \mathbf{x}}\,\mathbf{w}\right)} = \underset{3\times 9}{\left\langle \mathbf{w} \right\rangle^{(3)}} \underset{9\times 1}{\left\langle \frac{\partial \mathbf{u}}{\partial \mathbf{x}} \right\rangle} \doteq \underbrace{\underset{3\times 9}{\left\langle \mathbf{w} \right\rangle^{(3)}} \underset{9\times 3n}{\left[\mathbf{B}^{(3)}(\mathbf{x})\right]}}_{(*)} \underset{3n\times 1}{\left[\,\hat{\mathbf{u}}\,\right]} \quad . \tag{6.172}$$

It is readily verified that the $3\times 3n$ components of $(*)$ can be written as

$$\underset{3\times 9}{\left\langle \mathbf{w} \right\rangle^{(3)}} \underset{9\times 3n}{\left[\mathbf{B}^{(3)}(\mathbf{x})\right]} = \left[w_1 \frac{\partial}{\partial x_1} \underset{3\times 3n}{\left[\mathbf{N}^{(3)}\right]} + w_2 \frac{\partial}{\partial x_2} \underset{3\times 3n}{\left[\mathbf{N}^{(3)}\right]} + w_3 \frac{\partial}{\partial x_3} \underset{3\times 3n}{\left[\mathbf{N}^{(3)}\right]} \right] \quad , \tag{6.173}$$

where (6.160) was used.

Lastly, the divergence of the displacement vector is approximated by the finite element discretization according to

$$\begin{aligned} \operatorname{div}\mathbf{u} &= \operatorname{tr}\big[\operatorname{grad}\mathbf{u}\big] \\ &\doteq \underbrace{\underset{1\times 9}{\big\langle \mathbf{I} \big\rangle}^{\mathrm{T}} \underset{9\times 3n}{\big[\mathbf{B}^{(3)}\big]}}_{\big[\mathbf{B}^{(2)}\big]} \underset{3n\times 1}{\big[\,\hat{\mathbf{u}}\,\big]} \quad , \end{aligned} \tag{6.174}$$

where $\langle \mathbf{I} \rangle$ is the second-order identity tensor in VOIGT notation. The components of the $1 \times 3n$ array $[\mathbf{B}^{(2)}]$ are obtained as

$$\begin{aligned} \underset{1\times 3n}{\big[\mathbf{B}^{(2)}\big]} &= \underset{1\times 9}{\big\langle \mathbf{I} \big\rangle}^{\mathrm{T}} \underset{9\times 3n}{\big[\mathbf{B}^{(3)}\big]} \\ &= \Big[\big[N_{1,1} \quad N_{1,2} \quad N_{1,3}\big] \quad \big[N_{2,1} \quad N_{2,2} \quad N_{2,3}\big] \quad \cdots \quad \big[N_{n,1} \quad N_{n,2} \quad N_{n,3}\big] \Big] \quad . \end{aligned} \tag{6.175}$$

6.3.3 Global Residual and Stiffness Matrix

Recall from Section 6.2.2 that the NEWTON-RAPHSON method provides a framework for solving the weak form problem using the residuals and their differentials. Owing to the finite element discretization introduced in Section 6.3.2, the problem can be converted into a system of linear algebraic equations, which will be derived in this section with the aid of the VOIGT notation discussed in Section 6.3.1.

Residuals

The residuals $\{r_{\mathbf{u}}, r_\theta, r_\phi, r_\varphi\}$ are given in Equations $(6.76)_{1-4}$. The mechanical residual is discretized with the aid of the virtual multiplier in $(6.163)_2$ according to

$$\begin{aligned} r_{\mathbf{u}} &= \int_{\mathcal{R}} \frac{\partial(\delta\mathbf{u})}{\partial\mathbf{x}} \cdot \mathbf{T}\, \mathrm{d}v \\ &\doteq \int_{\mathcal{R}} \Big[\underset{9\times 3n}{\big[\mathbf{B}^{(3)}\big]} \underset{3n\times 1}{\big[\,\delta\hat{\mathbf{u}}\,\big]} \Big]^{\mathrm{T}} \underset{9\times 1}{\big\langle \mathbf{T} \big\rangle}\, \mathrm{d}v \\ &= \underset{1\times 3n}{\big[\,\delta\hat{\mathbf{u}}\,\big]}^{\mathrm{T}} \int_{\mathcal{R}} \underset{3n\times 9}{\big[\mathbf{B}^{(3)}\big]}^{\mathrm{T}} \underset{9\times 1}{\big\langle \mathbf{T} \big\rangle}\, \mathrm{d}v \\ &= \underset{1\times 3n}{\big[\,\delta\hat{\mathbf{u}}\,\big]}^{\mathrm{T}} \int_{\mathcal{R}} \Big[\underset{6\times 3n}{\big[\mathbf{B}^{(3)}\big]}^{\mathrm{sym}} \Big]^{\mathrm{T}} \underset{6\times 1}{\big\langle \mathbf{T}^{\mathrm{sym}}_{(1)} \big\rangle}\, \mathrm{d}v \quad , \end{aligned} \tag{6.176}$$

where the symmetry of $\mathbf{T}$ is exploited using Equations (6.120), $(6.122)_2$, (6.127), and (6.170). Note that the above integral is computed numerically using GAUSSIAN quadrature, hence the current stress $\mathbf{T}$ is evaluated from the constitutive relations

using the primary variables and the gradient quantities at the GAUSSIAN integration points.

Meanwhile, the thermal residual $(6.76)_2$ is expressed using the discretization of $\delta\theta$ in $(6.163)_4$ as

$$\begin{aligned} r_\theta &= -\int_{\mathcal{R}} \frac{\partial(\delta\theta)}{\partial \mathbf{x}} \cdot \mathbf{q}\, \mathrm{d}v \\ &\doteq -\int_{\mathcal{R}} \underset{3\times n}{\left[\mathbf{B}^{(1)}\right]}^{\mathrm{T}} \underset{n\times 1}{\left[\delta\hat{\theta}\right]}^{\mathrm{T}} \underset{3\times 1}{\left(\mathbf{q}\right)}\, \mathrm{d}v \\ &= -\underset{1\times n}{\left[\delta\hat{\theta}\right]}^{\mathrm{T}} \int_{\mathcal{R}} \underset{n\times 3}{\left[\mathbf{B}^{(1)}\right]}^{\mathrm{T}} \underset{3\times 1}{\left(\mathbf{q}\right)}\, \mathrm{d}v \quad . \end{aligned} \tag{6.177}$$

Again, the constitutive equation for the heat flux $\mathbf{q}$ is evaluated at the integration points in order to effect the GAUSSIAN quadrature.

The electric residual $(6.76)_3$ is given with the aid of the finite element approximation for $\delta\phi$ in $(6.163)_6$ as

$$\begin{aligned} r_\phi &= \int_{\mathcal{R}} \frac{\partial(\delta\phi)}{\partial \mathbf{x}} \cdot \left(\frac{\partial\phi}{\partial \mathbf{x}} - \frac{\mathbf{p}}{\varepsilon_0}\right) \mathrm{d}v \\ &\doteq \int_{\mathcal{R}} \underset{3\times n}{\left[\mathbf{B}^{(1)}\right]}^{\mathrm{T}} \underset{n\times 1}{\left[\delta\hat{\phi}\right]}^{\mathrm{T}} \underset{3\times 1}{\left(\frac{\partial\phi}{\partial \mathbf{x}} - \frac{\mathbf{p}}{\varepsilon_0}\right)}\, \mathrm{d}v \\ &= \underset{1\times n}{\left[\delta\hat{\phi}\right]}^{\mathrm{T}} \int_{\mathcal{R}} \underset{n\times 3}{\left[\mathbf{B}^{(1)}\right]}^{\mathrm{T}} \underset{3\times 1}{\left(\frac{\partial\phi}{\partial \mathbf{x}} - \frac{\mathbf{p}}{\varepsilon_0}\right)}\, \mathrm{d}v \quad , \end{aligned} \tag{6.178}$$

where $\mathrm{grad}\phi$ and $\mathbf{p}$ are evaluated at the GAUSS points.

Lastly, the magnetic residual is restated from $(6.76)_3$ with the aid of the finite element discretization in $(6.163)_8$ according to

$$\begin{aligned} r_\varphi &= \int_{\mathcal{R}} \frac{\partial(\delta\varphi)}{\partial \mathbf{x}} \cdot \frac{\partial\varphi}{\partial \mathbf{x}}\, \mathrm{d}v \\ &\doteq \int_{\mathcal{R}} \underset{3\times n}{\left[\mathbf{B}^{(1)}\right]}^{\mathrm{T}} \underset{n\times 1}{\left[\delta\hat{\varphi}\right]}^{\mathrm{T}} \underset{3\times 1}{\left(\frac{\partial\varphi}{\partial \mathbf{x}}\right)}\, \mathrm{d}v \\ &= \underset{1\times n}{\left[\delta\hat{\varphi}\right]}^{\mathrm{T}} \int_{\mathcal{R}} \underset{n\times 3}{\left[\mathbf{B}^{(1)}\right]}^{\mathrm{T}} \underset{3\times 1}{\left(\frac{\partial\varphi}{\partial \mathbf{x}}\right)}\, \mathrm{d}v \quad , \end{aligned} \tag{6.179}$$

where only the gradient quantity $\mathrm{grad}\phi$, but no constitutive equation, is computed for the GAUSSIAN quadrature.

Differentials

The differential $\mathrm{d}r_{\mathbf{u}}$ of the mechanical residual was derived in Equation (6.92). It is restated using the finite element discretization for $\mathrm{d}\mathbf{u}$, $\delta\mathbf{u}$, $\mathrm{d}\theta$, $\delta\phi$, and their derivatives, see (6.159) and (6.163), as

$$
\begin{aligned}
\mathrm{d}r_{\mathbf{u}} \;=\; & \int_{\mathcal{R}} \frac{\partial(\delta\mathbf{u})}{\partial\mathbf{x}} \cdot \frac{\partial(\mathrm{d}\mathbf{u})}{\partial\mathbf{x}}\,\mathbf{T}\,\mathrm{d}v + \int_{\mathcal{R}} \frac{\partial(\delta\mathbf{u})}{\partial\mathbf{x}} \cdot \left\{\rho\overline{\mathbb{C}}\left[\frac{\partial(\mathrm{d}\mathbf{u})}{\partial\mathbf{x}}\right]\right\}\mathrm{d}v \\
& - \int_{\mathcal{R}} \frac{\partial(\delta\mathbf{u})}{\partial\mathbf{x}} \cdot \left[\rho\overline{\mathbb{C}\mathbf{A}}\,\mathrm{d}\theta\right]\mathrm{d}v - \int_{\mathcal{R}} \frac{\partial(\delta\mathbf{u})}{\partial\mathbf{x}} \cdot \left\{\rho\overline{\mathfrak{c}}_2\left(\frac{\partial(\mathrm{d}\phi)}{\partial\mathbf{x}}\right)\right\}\mathrm{d}v \\
\doteq\; & \int_{\mathcal{R}} \underset{9\times 3n}{\left[\mathbf{B}^{(3)}\right]}^{\mathrm{T}} \underset{3n\times 1}{\left[\delta\hat{\mathbf{u}}\right]}^{\mathrm{T}} \underset{9\times 9}{\left\langle\mathbf{T}\right\rangle^{(2)}} \underset{9\times 3n}{\left[\mathbf{B}^{(3)}\right]} \underset{3n\times 1}{\left[\mathrm{d}\hat{\mathbf{u}}\right]}\,\mathrm{d}v \\
& + \int_{\mathcal{R}} \underset{9\times 3n}{\left[\mathbf{B}^{(3)}\right]}^{\mathrm{T}} \underset{3n\times 1}{\left[\delta\hat{\mathbf{u}}\right]}^{\mathrm{T}} \left\{\underset{9\times 9}{\left\langle\rho\overline{\mathbb{C}}\right\rangle} \underset{9\times 3n}{\left[\mathbf{B}^{(3)}\right]} \underset{3n\times 1}{\left[\mathrm{d}\hat{\mathbf{u}}\right]}\right\}\mathrm{d}v \\
& - \int_{\mathcal{R}} \underset{9\times 3n}{\left[\mathbf{B}^{(3)}\right]}^{\mathrm{T}} \underset{3n\times 1}{\left[\delta\hat{\mathbf{u}}\right]}^{\mathrm{T}} \underset{9\times 1}{\left\langle\rho\overline{\mathbb{C}\mathbf{A}}\right\rangle} \underset{1\times n}{\left[\mathbf{N}^{(1)}\right]} \underset{n\times 1}{\left[\mathrm{d}\hat{\theta}\right]}\,\mathrm{d}v \\
& - \int_{\mathcal{R}} \underset{9\times 3n}{\left[\mathbf{B}^{(3)}\right]}^{\mathrm{T}} \underset{3n\times 1}{\left[\delta\hat{\mathbf{u}}\right]}^{\mathrm{T}} \left\{\underset{9\times 3}{\left\langle\rho\overline{\mathfrak{c}}_2\right\rangle} \underset{3\times n}{\left[\mathbf{B}^{(1)}\right]} \underset{n\times 1}{\left[\mathrm{d}\hat{\phi}\right]}\right\}\mathrm{d}v \\
= \; & \underset{1\times 3n}{\left[\delta\hat{\mathbf{u}}\right]}^{\mathrm{T}} \int_{\mathcal{R}} \underset{3n\times 9}{\left[\mathbf{B}^{(3)}\right]}^{\mathrm{T}} \underset{9\times 9}{\left\langle\mathbf{T}\right\rangle^{(2)}} \underset{9\times 3n}{\left[\mathbf{B}^{(3)}\right]}\,\mathrm{d}v\, \underset{3n\times 1}{\left[\mathrm{d}\hat{\mathbf{u}}\right]} \\
& + \underset{1\times 3n}{\left[\delta\hat{\mathbf{u}}\right]}^{\mathrm{T}} \int_{\mathcal{R}} \underset{6\times 3n}{\left[\mathbf{B}^{(3)}\right]^{\mathrm{sym}}}^{\mathrm{T}} \underset{6\times 6}{\left\langle\rho\overline{\mathbb{C}}^{\mathrm{sym}}\right\rangle} \underset{6\times 3n}{\left[\mathbf{B}^{(3)}\right]^{\mathrm{sym}}}\,\mathrm{d}v\, \underset{3n\times 1}{\left[\mathrm{d}\hat{\mathbf{u}}\right]} \\
& - \underset{1\times 3n}{\left[\delta\hat{\mathbf{u}}\right]}^{\mathrm{T}} \int_{\mathcal{R}} \underset{6\times 3n}{\left[\mathbf{B}^{(3)}\right]^{\mathrm{sym}}}^{\mathrm{T}} \underset{6\times 1}{\left\langle\rho\overline{\mathbb{C}\mathbf{A}}^{\mathrm{sym}}\right\rangle} \underset{1\times n}{\left[\mathbf{N}^{(1)}\right]}\,\mathrm{d}v\, \underset{n\times 1}{\left[\mathrm{d}\hat{\theta}\right]} \\
& - \underset{1\times 3n}{\left[\delta\hat{\mathbf{u}}\right]}^{\mathrm{T}} \int_{\mathcal{R}} \underset{6\times 3n}{\left[\mathbf{B}^{(3)}\right]^{\mathrm{sym}}}^{\mathrm{T}} \underset{6\times 3}{\left\langle\rho\overline{\mathfrak{c}}_2^{\mathrm{sym}}\right\rangle} \underset{3\times n}{\left[\mathbf{B}^{(1)}\right]}\,\mathrm{d}v\, \underset{n\times 1}{\left[\mathrm{d}\hat{\phi}\right]} \quad .
\end{aligned}
\tag{6.180}
$$

Here, the minor symmetries of $\overline{\mathbb{C}\mathbf{A}}$, $\overline{\mathbb{C}}$, and $\overline{\mathfrak{c}}_2$ were exploited to use the reduced 6×6 notation introduced in (6.127), (6.130), and (6.133), in conjunction with the reduced gradient operator defined by (6.170). However, no reduction is possible for the term involving $\left\langle\mathbf{T}\right\rangle^{(2)}$, see $(6.104)_2$, because it lacks the necessary minor symmetries, that is,

$$
\begin{aligned}
\underset{9\times 9}{\left\langle\mathbb{C}\right\rangle} \;&\neq\; \underset{9\times 9}{\left\langle\mathbb{I}^{\mathrm{sym}}\right\rangle} \underset{9\times 9}{\left\langle\mathbf{T}\right\rangle^{(2)}} \\
&\neq\; \underset{9\times 9}{\left\langle\mathbf{T}\right\rangle^{(2)}} \underset{9\times 9}{\left\langle\mathbb{I}^{\mathrm{sym}}\right\rangle} \quad ,
\end{aligned}
\tag{6.181}
$$

as immediately evident by inspection of its components in (6.103).

The differential for the thermal residual $\mathrm{d}r_\theta$ in Equation (6.95) is similarly discretized using $\mathrm{d}\mathbf{u}$, $\delta\theta$, and $\mathrm{d}\theta$ from Equations (6.159) and their derivatives in (6.163),

to write

$$
\begin{aligned}
\mathrm{d}r_\theta \;=\; & -\int_{\mathcal{R}} \Big(\frac{\partial(\delta\theta)}{\partial\mathbf{x}}\cdot\mathbf{q}\Big)\Big(\frac{\partial}{\partial\mathbf{x}}\cdot\mathrm{d}\mathbf{u}\Big)\,\mathrm{d}v \;-\; 2\int_{\mathcal{R}} \frac{\partial(\delta\theta)}{\partial\mathbf{x}}\cdot\Big(\Big[\frac{\partial(\mathrm{d}\mathbf{u})}{\partial\mathbf{x}}\,\overline{\boldsymbol{\kappa}}\Big]^{\mathrm{sym}}\frac{\partial\theta}{\partial\mathbf{x}}\Big)\,\mathrm{d}v \\
& + \int_{\mathcal{R}} \frac{\partial(\delta\theta)}{\partial\mathbf{x}}\cdot\overline{\boldsymbol{\kappa}}\,\frac{\partial(\mathrm{d}\theta)}{\partial\mathbf{x}}\,\mathrm{d}v \\
\doteq\; & -\int_{\mathcal{R}} \Big(\Big[\underset{3\times n}{[\mathbf{B}^{(1)}]}\;\underset{n\times 1}{[\delta\hat{\theta}]}\Big]^{\mathrm{T}}\underset{3\times 1}{(\mathbf{q})}\Big)\Big(\underset{1\times 3n}{[\mathbf{B}^{(2)}]}\;\underset{3n\times 1}{[\mathrm{d}\hat{\mathbf{u}}]}\Big)\,\mathrm{d}v \\
& - \int_{\mathcal{R}} \Big[\underset{3\times n}{[\mathbf{B}^{(1)}]}\;\underset{n\times 1}{[\delta\hat{\theta}]}\Big]^{\mathrm{T}}\underset{3\times 9}{\Big\langle 2\frac{\partial\theta}{\partial\mathbf{x}}\Big\rangle^{(3)}}\underset{9\times 9}{\big\langle\mathbb{I}^{\mathrm{sym}}\big\rangle}\underset{9\times 9}{\big\langle\overline{\boldsymbol{\kappa}}\big\rangle^{(2)}}\underset{9\times 3n}{[\mathbf{B}^{(3)}]}\;\underset{3n\times 1}{[\mathrm{d}\hat{\mathbf{u}}]}\,\mathrm{d}v \\
& + \int_{\mathcal{R}} \Big[\underset{3\times n}{[\mathbf{B}^{(1)}]}\;\underset{n\times 1}{[\delta\hat{\theta}]}\Big]^{\mathrm{T}}\underset{3\times 3}{[\overline{\boldsymbol{\kappa}}]}\;\underset{3\times n}{[\mathbf{B}^{(1)}]}\;\underset{n\times 1}{[\mathrm{d}\hat{\theta}]}\,\mathrm{d}v \\
=\; & -\underset{1\times n}{[\delta\hat{\theta}]}^{\mathrm{T}}\int_{\mathcal{R}}\underset{n\times 3}{[\mathbf{B}^{(1)}]}^{\mathrm{T}}\underset{3\times 1}{(\mathbf{q})}\;\underset{1\times 3n}{[\mathbf{B}^{(2)}]}\,\mathrm{d}v\;\underset{3n\times 1}{[\mathrm{d}\hat{\mathbf{u}}]} \\
& - \underset{1\times n}{[\delta\hat{\theta}]}^{\mathrm{T}}\int_{\mathcal{R}}\underset{n\times 3}{[\mathbf{B}^{(1)}]}^{\mathrm{T}}\underset{3\times 9}{\Big\langle 2\frac{\partial\theta}{\partial\mathbf{x}}\Big\rangle^{(3)}}\underset{9\times 9}{\big\langle\mathbb{I}^{\mathrm{sym}}\big\rangle}\underset{9\times 9}{\big\langle\overline{\boldsymbol{\kappa}}\big\rangle^{(2)}}\underset{9\times 3n}{[\mathbf{B}^{(3)}]}\,\mathrm{d}v\;\underset{3n\times 1}{[\mathrm{d}\hat{\mathbf{u}}]} \\
& + \underset{1\times n}{[\delta\hat{\theta}]}^{\mathrm{T}}\int_{\mathcal{R}}\underset{n\times 3}{[\mathbf{B}^{(1)}]}^{\mathrm{T}}\underset{3\times 3}{[\overline{\boldsymbol{\kappa}}]}\;\underset{3\times n}{[\mathbf{B}^{(1)}]}\,\mathrm{d}v\;\underset{n\times 1}{[\mathrm{d}\hat{\theta}]} \quad . \qquad (6.182)
\end{aligned}
$$

Here, the VOIGT notation for multiplications in $(6.104)_2$ and (6.108), the symmetry operator in (6.120), and the divergence in (6.174 - 175) were used. Recall that the first two terms in the differential (6.95), and thus the first two terms in (6.182), are due to the assumption in (6.90) that the thermal conductivity tensor is constant in the current configuration. If instead a referential form of FOURIER's law is adopted according to $(6.89)_3$, then the first two terms in the preceding result (*i.e.*, the coupling between $\delta\hat{\theta}$ and $\mathrm{d}\hat{\mathbf{u}}$) vanish and only the third term remains.

The differential of the electric residual, presented in (6.97), is discretized along

the same lines as the preceding differentials to obtain

$$
\begin{aligned}
\mathrm{d}r_\phi \;=\; & \int_{\mathcal{R}} \Big(\frac{\partial(\delta\phi)}{\partial\mathbf{x}}\cdot\frac{\partial\phi}{\partial\mathbf{x}}\Big)\Big(\frac{\partial}{\partial\mathbf{x}}\cdot\mathrm{d}\mathbf{u}\Big)\,\mathrm{d}v \;-\; 2\int_{\mathcal{R}} \frac{\partial(\delta\phi)}{\partial\mathbf{x}}\cdot\Big(\Big[\frac{\partial(\mathrm{d}\mathbf{u})}{\partial\mathbf{x}}\Big]^{\mathrm{sym}}\frac{\partial\phi}{\partial\mathbf{x}}\Big)\,\mathrm{d}v \\
& + \int_{\mathcal{R}} \frac{\partial(\delta\phi)}{\partial\mathbf{x}}\cdot\Big(\Big[\mathbf{i}+\rho\,\overline{\mathbf{c}}_3\Big]\frac{\partial(\mathrm{d}\phi)}{\partial\mathbf{x}}\Big)\,\mathrm{d}v \;+\; \frac{1}{\varepsilon_0}\int_{\mathcal{R}} \frac{\partial(\delta\phi)}{\partial\mathbf{x}}\cdot\Big(\rho\,\overline{\mathbf{c}}_2^{\mathrm{T}}\frac{\partial(\mathrm{d}\mathbf{u})}{\partial\mathbf{x}}\Big)\,\mathrm{d}v \\
\doteq\; & \int_{\mathcal{R}} \underset{3\times n}{\big[\mathbf{B}^{(1)}\big]}\,\underset{n\times 1}{\big[\delta\hat{\phi}\big]}^{\mathrm{T}}\,\underset{3\times 1}{\Big(\frac{\partial\phi}{\partial\mathbf{x}}\Big)}\,\underset{1\times 3n\;\;3n\times 1}{\big[\mathbf{B}^{(2)}\big]\big[\,\mathrm{d}\hat{\mathbf{u}}\,\big]}\,\mathrm{d}v \\
& - \int_{\mathcal{R}} \underset{3\times n}{\big[\mathbf{B}^{(1)}\big]}\,\underset{n\times 1}{\big[\delta\hat{\phi}\big]}^{\mathrm{T}}\,\underset{3\times 9}{\Big\langle 2\frac{\partial\phi}{\partial\mathbf{x}}\Big\rangle^{(3)}}\,\underset{9\times 9}{\big\langle\mathbb{I}^{\mathrm{sym}}\big\rangle}\,\underset{9\times 3n}{\big[\mathbf{B}^{(3)}\big]}\,\underset{3n\times 1}{\big[\,\mathrm{d}\hat{\mathbf{u}}\,\big]}\,\mathrm{d}v \\
& + \int_{\mathcal{R}} \underset{3\times n}{\big[\mathbf{B}^{(1)}\big]}\,\underset{n\times 1}{\big[\delta\hat{\phi}\big]}^{\mathrm{T}}\,\underset{3\times 3}{\big[\,\mathbf{i}+\rho\,\overline{\mathbf{c}}_3\,\big]}\,\underset{3\times n}{\big[\mathbf{B}^{(1)}\big]}\,\underset{n\times 1}{\big[\,\mathrm{d}\hat{\phi}\,\big]}\,\mathrm{d}v \\
& + \int_{\mathcal{R}} \underset{3\times n}{\big[\mathbf{B}^{(1)}\big]}\,\underset{n\times 1}{\big[\delta\hat{\phi}\big]}^{\mathrm{T}}\,\underset{3\times 9}{\big\langle\tfrac{\rho}{\varepsilon_0}\,\overline{\mathbf{c}}_2\big\rangle^{\mathrm{T}}}\,\underset{9\times 3n}{\big[\mathbf{B}^{(3)}\big]}\,\underset{3n\times 1}{\big[\,\mathrm{d}\hat{\mathbf{u}}\,\big]}\,\mathrm{d}v \\
= \; & \underset{1\times n}{\big[\,\delta\hat{\phi}\,\big]}^{\mathrm{T}}\int_{\mathcal{R}} \underset{n\times 3}{\big[\mathbf{B}^{(1)}\big]}^{\mathrm{T}}\,\underset{3\times 1}{\Big(\frac{\partial\phi}{\partial\mathbf{x}}\Big)}\,\underset{1\times 3n}{\big[\mathbf{B}^{(2)}\big]}\,\mathrm{d}v\;\underset{3n\times 1}{\big[\,\mathrm{d}\hat{\mathbf{u}}\,\big]} \\
& + \underset{1\times n}{\big[\,\delta\hat{\phi}\,\big]}^{\mathrm{T}}\int_{\mathcal{R}} \underset{n\times 3}{\big[\mathbf{B}^{(1)}\big]}^{\mathrm{T}}\,\underset{3\times 6}{\Big[\big\langle\tfrac{\rho}{\varepsilon_0}\,\overline{\mathbf{c}}_2^{\mathrm{sym}}\big\rangle^{\mathrm{T}} - \Big\langle 2\frac{\partial\phi}{\partial\mathbf{x}}^{\mathrm{sym}}\Big\rangle^{(3)}\Big]}\,\underset{6\times 3n}{\big[\mathbf{B}^{(3)}\big]^{\mathrm{sym}}}\,\mathrm{d}v\;\underset{3n\times 1}{\big[\,\mathrm{d}\hat{\mathbf{u}}\,\big]} \\
& + \underset{1\times n}{\big[\,\delta\hat{\phi}\,\big]}^{\mathrm{T}}\int_{\mathcal{R}} \underset{n\times 3}{\big[\mathbf{B}^{(1)}\big]}^{\mathrm{T}}\underset{3\times 3}{\big[\,\mathbf{i}+\rho\,\overline{\mathbf{c}}_3\,\big]}\,\underset{3\times n}{\big[\mathbf{B}^{(1)}\big]}\,\mathrm{d}v\;\underset{n\times 1}{\big[\,\mathrm{d}\hat{\phi}\,\big]} \quad . \qquad (6.183)
\end{aligned}
$$

As before, the symmetry for third-order tensors, see (6.133) and (6.170), was exploited for the reduced notation.

Lastly, the magnetic differential $\mathrm{d}r_\varphi$ in Equation (6.99) is discretized. Due to its similarity with the electric differential (6.183), only the result is stated here as

$$
\begin{aligned}
\mathrm{d}r_\varphi \;\doteq\; & \underset{1\times n}{\big[\,\delta\hat{\varphi}\,\big]}^{\mathrm{T}}\int_{\mathcal{R}} \underset{n\times 3}{\big[\mathbf{B}^{(1)}\big]}^{\mathrm{T}}\,\underset{3\times 1}{\Big(\frac{\partial\varphi}{\partial\mathbf{x}}\Big)}\,\underset{1\times 3n}{\big[\mathbf{B}^{(2)}\big]}\,\mathrm{d}v\;\underset{3n\times 1}{\big[\,\mathrm{d}\hat{\mathbf{u}}\,\big]} \\
& - \underset{1\times n}{\big[\,\delta\hat{\varphi}\,\big]}^{\mathrm{T}}\int_{\mathcal{R}} \underset{n\times 3}{\big[\mathbf{B}^{(1)}\big]}^{\mathrm{T}}\,\underset{3\times 6}{\Big\langle 2\frac{\partial\varphi}{\partial\mathbf{x}}^{\mathrm{sym}}\Big\rangle^{(3)}}\,\underset{6\times 3n}{\big[\mathbf{B}^{(3)}\big]^{\mathrm{sym}}}\,\mathrm{d}v\;\underset{3n\times 1}{\big[\,\mathrm{d}\hat{\mathbf{u}}\,\big]} \\
& + \underset{1\times n}{\big[\,\delta\hat{\varphi}\,\big]}^{\mathrm{T}}\int_{\mathcal{R}} \underset{n\times 3}{\big[\mathbf{B}^{(1)}\big]}^{\mathrm{T}}\underset{3\times n}{\big[\mathbf{B}^{(1)}\big]}\,\mathrm{d}v\;\underset{n\times 1}{\big[\,\mathrm{d}\hat{\varphi}\,\big]} \quad . \qquad (6.184)
\end{aligned}
$$

Summary

The residuals and their differentials derived in the preceding discussion are summarized in the form of the global residual and stiffness matrix. To this end, recall that

the NEWTON-RAPHSON method (6.77) is of the form

$$r + \mathrm{d}r = 0 \quad \text{where} \quad \begin{aligned} r &= r_{\mathbf{u}} + r_\theta + r_\phi + r_\varphi \quad , \\ \mathrm{d}r &= \mathrm{d}r_{\mathbf{u}} + \mathrm{d}r_\theta + \mathrm{d}r_\phi + \mathrm{d}r_\varphi \quad . \end{aligned} \tag{6.185}$$

It is clear from the residuals in Equations (6.176 - 179) that the vectors of arbitrary nodal variations $[\delta\hat{\mathbf{u}}]$, $[\delta\hat{\theta}]$, $[\delta\hat{\phi}]$, and $[\delta\hat{\varphi}]$ can be factored out of each expression. The same is true for the corresponding differentials in (6.180 - 184) where, in addition, the differentials $[\mathrm{d}\hat{\mathbf{u}}]$, $[\mathrm{d}\hat{\theta}]$, $[\mathrm{d}\hat{\phi}]$, and $[\mathrm{d}\hat{\varphi}]$ of the discrete nodal vectors can be factored out. For convenience, all nodal variations and all nodal differentials are combined into one vector each, defined as

$$\underset{6n\times 1}{\big[\,\delta\hat{\mathbf{U}}\,\big]} = \begin{bmatrix} \underset{3n\times 1}{\big[\,\delta\hat{\mathbf{u}}\,\big]} \\ \underset{n\times 1}{\big[\,\delta\hat{\theta}\,\big]} \\ \underset{n\times 1}{\big[\,\delta\hat{\phi}\,\big]} \\ \underset{n\times 1}{\big[\,\delta\hat{\varphi}\,\big]} \end{bmatrix} \quad \text{and} \quad \underset{6n\times 1}{\big[\,\mathrm{d}\hat{\mathbf{U}}\,\big]} = \begin{bmatrix} \underset{3n\times 1}{\big[\,\mathrm{d}\hat{\mathbf{u}}\,\big]} \\ \underset{n\times 1}{\big[\,\mathrm{d}\hat{\theta}\,\big]} \\ \underset{n\times 1}{\big[\,\mathrm{d}\hat{\phi}\,\big]} \\ \underset{n\times 1}{\big[\,\mathrm{d}\hat{\varphi}\,\big]} \end{bmatrix} \quad . \tag{6.186}$$

Equation (6.185) can thus be restated as

$$\underset{1\times 6n}{\big[\,\delta\hat{\mathbf{U}}\,\big]^{\mathrm{T}}} \Big\{ -\underset{6n\times 1}{\big[\,\mathbf{R}\,\big]} + \underset{6n\times 6n}{\big[\,\mathbf{K}\,\big]}\, \underset{6n\times 1}{\big[\,\mathrm{d}\hat{\mathbf{U}}\,\big]} \Big\} = 0 \quad , \tag{6.187}$$

where it was defined that

$$\begin{aligned} r &= -\underset{1\times 6n}{\big[\,\delta\hat{\mathbf{U}}\,\big]^{\mathrm{T}}}\, \underset{6n\times 1}{\big[\,\mathbf{R}\,\big]} \quad , \\ \mathrm{d}r &= \underset{1\times 6n}{\big[\,\delta\hat{\mathbf{U}}\,\big]^{\mathrm{T}}}\, \underset{6n\times 6n}{\big[\,\mathbf{K}\,\big]}\, \underset{6n\times 1}{\big[\,\mathrm{d}\hat{\mathbf{U}}\,\big]} \quad . \end{aligned} \tag{6.188}$$

Due to the arbitrariness of the nodal variations $[\delta\hat{\mathbf{U}}]$ (except at the DIRICHLET boundary, where admissible test functions must vanish), Equation (6.187) implies that

$$\underset{6n\times 6n}{\big[\,\mathbf{K}\,\big]}\, \underset{6n\times 1}{\big[\,\mathrm{d}\hat{\mathbf{U}}\,\big]} = \underset{6n\times 1}{\big[\,\mathbf{R}\,\big]} \quad , \tag{6.189}$$

which represents a system of algebraic equations for the nodal differentials $[\mathrm{d}\hat{\mathbf{U}}]$. Here, it is assumed that the DIRICHLET boundary conditions are enforced after the fact, by eliminating the corresponding degrees of freedom from (6.189) using a SCHUR complement.

The entries in the so-called *residual vector* $[\mathbf{R}]$ and the *stiffness matrix* $[\mathbf{K}]$ are inferred from Equations (6.176 - 179) and (6.180 - 184). For convenience, the algebraic system (6.189) is expanded back to

$$\underbrace{\begin{bmatrix} \underset{3n\times 3n}{[\mathbf{K}_{\mathbf{uu}}]} & \underset{3n\times n}{[\mathbf{K}_{\mathbf{u}\theta}]} & \underset{3n\times n}{[\mathbf{K}_{\mathbf{u}\phi}]} & \underset{3n\times n}{[\mathbf{K}_{\mathbf{u}\varphi}]} \\ \underset{n\times 3n}{[\mathbf{K}_{\theta\mathbf{u}}]} & \underset{n\times n}{[\mathbf{K}_{\theta\theta}]} & \underset{n\times n}{[\mathbf{K}_{\theta\phi}]} & \underset{n\times n}{[\mathbf{K}_{\theta\varphi}]} \\ \underset{n\times 3n}{[\mathbf{K}_{\phi\mathbf{u}}]} & \underset{n\times n}{[\mathbf{K}_{\phi\theta}]} & \underset{n\times n}{[\mathbf{K}_{\phi\phi}]} & \underset{n\times n}{[\mathbf{K}_{\phi\varphi}]} \\ \underset{n\times 3n}{[\mathbf{K}_{\varphi\mathbf{u}}]} & \underset{n\times n}{[\mathbf{K}_{\varphi\theta}]} & \underset{n\times n}{[\mathbf{K}_{\varphi\phi}]} & \underset{n\times n}{[\mathbf{K}_{\varphi\varphi}]} \end{bmatrix}}_{\underset{6n\times 6n}{[\mathbf{K}]}} \underbrace{\begin{bmatrix} \underset{3n\times 1}{[\mathrm{d}\hat{\mathbf{u}}]} \\ \underset{n\times 1}{[\mathrm{d}\hat{\theta}]} \\ \underset{n\times 1}{[\mathrm{d}\hat{\phi}]} \\ \underset{n\times 1}{[\mathrm{d}\hat{\varphi}]} \end{bmatrix}}_{\underset{6n\times 1}{[\mathrm{d}\hat{\mathbf{U}}]}} = \underbrace{\begin{bmatrix} \underset{3n\times 1}{[\mathbf{R}_{\mathbf{u}}]} \\ \underset{n\times 1}{[\mathbf{R}_{\theta}]} \\ \underset{n\times 1}{[\mathbf{R}_{\phi}]} \\ \underset{n\times 1}{[\mathbf{R}_{\varphi}]} \end{bmatrix}}_{\underset{6n\times 1}{[\mathbf{R}]}} \quad . \tag{6.190}$$

The entries in the residual vector are obtained from (6.176 - 179) as

$$\begin{aligned} \underset{3n\times 1}{[\mathbf{R}_{\mathbf{u}}]} &= -\int_{\mathcal{R}} \underset{6\times 3n}{\left[[\mathbf{B}^{(3)}]^{\mathrm{sym}}\right]^{\mathrm{T}}} \underset{6\times 1}{\langle \mathbf{T}^{\mathrm{sym}}_{(1)} \rangle} \,\mathrm{d}v \quad , \\ \underset{n\times 1}{[\mathbf{R}_{\theta}]} &= \int_{\mathcal{R}} \underset{n\times 3}{[\mathbf{B}^{(1)}]^{\mathrm{T}}} \underset{3\times 1}{(\mathbf{q})} \,\mathrm{d}v \quad , \\ \underset{n\times 1}{[\mathbf{R}_{\phi}]} &= -\int_{\mathcal{R}} \underset{n\times 3}{[\mathbf{B}^{(1)}]^{\mathrm{T}}} \underset{3\times 1}{\left(\frac{\partial \phi}{\partial \mathbf{x}} - \frac{\mathbf{p}}{\varepsilon_0}\right)} \mathrm{d}v \quad , \\ \underset{n\times 1}{[\mathbf{R}_{\varphi}]} &= -\int_{\mathcal{R}} \underset{n\times 3}{[\mathbf{B}^{(1)}]^{\mathrm{T}}} \underset{3\times 1}{\left(\frac{\partial \varphi}{\partial \mathbf{x}}\right)} \mathrm{d}v \quad . \end{aligned} \tag{6.191}$$

The first row of $[\mathbf{K}]$ is inferred from Equation (6.180) according to

$$\begin{aligned} \underset{3n\times 3n}{[\mathbf{K}_{\mathbf{uu}}]} &= \int_{\mathcal{R}} \underset{3n\times 9}{[\mathbf{B}^{(3)}]^{\mathrm{T}}} \underset{9\times 9}{\langle \mathbf{T} \rangle^{(2)}} \underset{9\times 3n}{[\mathbf{B}^{(3)}]} \,\mathrm{d}v + \int_{\mathcal{R}} \underset{6\times 3n}{\left[[\mathbf{B}^{(3)}]^{\mathrm{sym}}\right]^{\mathrm{T}}} \underset{6\times 6}{\langle \rho \overline{\mathbb{C}}^{\mathrm{sym}} \rangle} \underset{6\times 3n}{[\mathbf{B}^{(3)}]^{\mathrm{sym}}} \,\mathrm{d}v \quad , \\ \underset{3n\times n}{[\mathbf{K}_{\mathbf{u}\theta}]} &= -\int_{\mathcal{R}} \underset{6\times 3n}{\left[[\mathbf{B}^{(3)}]^{\mathrm{sym}}\right]^{\mathrm{T}}} \underset{6\times 1}{\langle \rho \overline{\mathbb{C}\mathbf{A}}^{\mathrm{sym}} \rangle} \underset{1\times n}{[\mathbf{N}^{(1)}]} \,\mathrm{d}v \quad , \\ \underset{3n\times n}{[\mathbf{K}_{\mathbf{u}\phi}]} &= -\int_{\mathcal{R}} \underset{6\times 3n}{\left[[\mathbf{B}^{(3)}]^{\mathrm{sym}}\right]^{\mathrm{T}}} \underset{6\times 3}{\langle \rho \overline{\mathbf{c}}^{\mathrm{sym}}_{2} \rangle} \underset{3\times n}{[\mathbf{B}^{(1)}]} \,\mathrm{d}v \quad , \\ \underset{3n\times n}{[\mathbf{K}_{\mathbf{u}\varphi}]} &= \mathbf{0} \quad . \end{aligned} \tag{6.192}$$

The second row of $[\mathbf{K}]$ is given by the thermal differential (6.182) as

$$\begin{aligned}
\underset{n\times 3n}{\big[\mathbf{K}_{\theta\mathbf{u}}\big]} &= -\int_{\mathcal{R}} \underset{n\times 3}{\big[\mathbf{B}^{(1)}\big]^{\mathrm{T}}} \underset{3\times 1}{\big(\mathbf{q}\big)} \underset{1\times 3n}{\big[\mathbf{B}^{(2)}\big]}\,\mathrm{d}v - \int_{\mathcal{R}} \underset{n\times 3}{\big[\mathbf{B}^{(1)}\big]^{\mathrm{T}}} \underset{3\times 9}{\Big\langle 2\frac{\partial\theta}{\partial\mathbf{x}}\Big\rangle^{(3)}} \underset{9\times 9}{\big\langle \mathbb{I}^{\mathrm{sym}}\big\rangle} \underset{9\times 9}{\big\langle \overline{\boldsymbol{\kappa}}\big\rangle^{(2)}} \underset{9\times 3n}{\big[\mathbf{B}^{(3)}\big]}\,\mathrm{d}v \quad , \\
\underset{n\times n}{\big[\mathbf{K}_{\theta\theta}\big]} &= \int_{\mathcal{R}} \underset{n\times 3}{\big[\mathbf{B}^{(1)}\big]^{\mathrm{T}}} \underset{3\times 3}{\big[\overline{\boldsymbol{\kappa}}\big]} \underset{3\times n}{\big[\mathbf{B}^{(1)}\big]}\,\mathrm{d}v \quad , \\
\underset{n\times n}{\big[\mathbf{K}_{\theta\phi}\big]} &= \mathbf{0} \quad , \\
\underset{n\times n}{\big[\mathbf{K}_{\theta\varphi}\big]} &= \mathbf{0} \quad .
\end{aligned} \tag{6.193}$$

The expression for $[\mathbf{K}_{\theta\mathbf{u}}]$ in $(6.193)_1$ vanishes if a referential form of FOURIER's law is adopted, implying that the thermal equation is uncoupled from the deformation. Indeed, it is readily seen that $[\mathbf{K}_{\theta\mathbf{u}}]$ arises from the additional terms in the linearization of FOURIER's law in (6.90) as opposed to the referential form in $(6.89)_3$. The electric differential (6.183) gives rise to the third row of $[\mathbf{K}]$, given by

$$\begin{aligned}
\underset{n\times 3n}{\big[\mathbf{K}_{\phi\mathbf{u}}\big]} &= \int_{\mathcal{R}} \underset{n\times 3}{\big[\mathbf{B}^{(1)}\big]^{\mathrm{T}}} \underset{3\times 1}{\Big(\frac{\partial\phi}{\partial\mathbf{x}}\Big)} \underset{1\times 3n}{\big[\mathbf{B}^{(2)}\big]}\,\mathrm{d}v \\
&\qquad + \int_{\mathcal{R}} \underset{n\times 3}{\big[\mathbf{B}^{(1)}\big]^{\mathrm{T}}} \Big[\underset{3\times 6}{\Big\langle \tfrac{\rho}{\varepsilon_0}\overline{\mathfrak{C}}_2^{\mathrm{sym}}\Big\rangle^{\mathrm{T}}} - \underset{3\times 6}{\Big\langle 2\frac{\partial\phi}{\partial\mathbf{x}}^{\mathrm{sym}}\Big\rangle^{(3)}} \Big] \underset{6\times 3n}{\big[\mathbf{B}^{(3)}\big]^{\mathrm{sym}}}\,\mathrm{d}v \quad , \\
\underset{n\times n}{\big[\mathbf{K}_{\phi\theta}\big]} &= \mathbf{0} \quad , \\
\underset{n\times n}{\big[\mathbf{K}_{\phi\phi}\big]} &= \int_{\mathcal{R}} \underset{n\times 3}{\big[\mathbf{B}^{(1)}\big]^{\mathrm{T}}} \underset{3\times 3}{\big[\,\mathbf{i} + \rho\overline{\mathbf{c}}_3\,\big]} \underset{3\times n}{\big[\mathbf{B}^{(1)}\big]}\,\mathrm{d}v \quad , \\
\underset{n\times n}{\big[\mathbf{K}_{\phi\varphi}\big]} &= \mathbf{0} \quad .
\end{aligned} \tag{6.194}$$

Lastly, the differential of the magnetic residual in (6.184) is employed to write the fourth row of $[\mathbf{K}]$ as

$$\begin{aligned}
\underset{n\times 3n}{\big[\mathbf{K}_{\varphi\mathbf{u}}\big]} &= \int_{\mathcal{R}} \underset{n\times 3}{\big[\mathbf{B}^{(1)}\big]^{\mathrm{T}}} \underset{3\times 1}{\Big(\frac{\partial\varphi}{\partial\mathbf{x}}\Big)} \underset{1\times 3n}{\big[\mathbf{B}^{(2)}\big]}\,\mathrm{d}v - \int_{\mathcal{R}} \underset{n\times 3}{\big[\mathbf{B}^{(1)}\big]^{\mathrm{T}}} \underset{3\times 6}{\Big\langle 2\frac{\partial\varphi}{\partial\mathbf{x}}^{\mathrm{sym}}\Big\rangle^{(3)}} \underset{6\times 3n}{\big[\mathbf{B}^{(3)}\big]^{\mathrm{sym}}}\,\mathrm{d}v \quad , \\
\underset{n\times n}{\big[\mathbf{K}_{\varphi\theta}\big]} &= \mathbf{0} \quad , \\
\underset{n\times n}{\big[\mathbf{K}_{\varphi\phi}\big]} &= \mathbf{0} \quad , \\
\underset{n\times n}{\big[\mathbf{K}_{\varphi\varphi}\big]} &= \int_{\mathcal{R}} \underset{n\times 3}{\big[\mathbf{B}^{(1)}\big]^{\mathrm{T}}} \underset{3\times n}{\big[\mathbf{B}^{(1)}\big]}\,\mathrm{d}v \quad .
\end{aligned} \tag{6.195}$$

6.3.4 Nodal Residual and Stiffness Matrix

Recall that the number of $6n$ equations in (6.190) (before accounting for DIRICHLET nodes) is determined by the number of degrees of freedom (DoF) per node times the total number of nodes n of the finite element problem. Every row in the $6n \times 6n$ global stiffness matrix $[\mathbf{K}]$ is associated with the variation of a given node and DoF from the vector $[\delta\hat{\mathbf{U}}]$. Likewise, every column of $[\mathbf{K}]$ accounts for the contribution of the differential of a given node and DoF within the vector $[\mathrm{d}\hat{\mathbf{U}}]$.

The global expressions for $[\mathbf{R}]$ and $[\mathbf{K}]$ derived in the preceding section involve large matrices of the shape functions and their derivatives, such as the $9 \times 3n$ matrix $[\mathbf{B}^{(3)}]$, which are not amenable to numerical implementation. In this section, the residual and the stiffness matrix are expressed only for the degrees of freedom of a single variational node i and a single differential node j. The resulting subsets $[\mathbf{R}^i]$ and $[\mathbf{K}^{ij}]$ of size 6×6 can be conveniently assembled into the element (and global) residual and stiffness matrix.

The global system of algebraic Equations (6.190) is rewritten for each differential node j as

$$\sum_{j=1}^{n} \underbrace{\begin{bmatrix} \underset{3\times3}{[\mathbf{K}^{ij}_{\mathbf{uu}}]} & \underset{3\times1}{[\mathbf{K}^{ij}_{\mathbf{u}\theta}]} & \underset{3\times1}{[\mathbf{K}^{ij}_{\mathbf{u}\phi}]} & \underset{3\times1}{[\mathbf{0}]} \\ \underset{1\times3}{[\mathbf{K}^{ij}_{\theta\mathbf{u}}]} & \underset{1\times1}{[\mathbf{K}^{ij}_{\theta\theta}]} & \underset{1\times1}{[0]} & \underset{1\times1}{[0]} \\ \underset{1\times3}{[\mathbf{K}^{ij}_{\phi\mathbf{u}}]} & \underset{1\times1}{[0]} & \underset{1\times1}{[\mathbf{K}^{ij}_{\phi\phi}]} & \underset{1\times1}{[0]} \\ \underset{1\times3}{[\mathbf{K}^{ij}_{\varphi\mathbf{u}}]} & \underset{1\times1}{[0]} & \underset{1\times1}{[0]} & \underset{1\times1}{[\mathbf{K}^{ij}_{\varphi\varphi}]} \end{bmatrix}}_{\underset{6\times6}{[\mathbf{K}^{ij}]}} \underbrace{\begin{bmatrix} \underset{3\times1}{[\mathrm{d}\hat{\mathbf{u}}^j]} \\ \underset{1\times1}{[\mathrm{d}\hat{\theta}^j]} \\ \underset{1\times1}{[\mathrm{d}\hat{\phi}^j]} \\ \underset{1\times1}{[\mathrm{d}\hat{\varphi}^j]} \end{bmatrix}}_{\underset{6\times1}{[\mathrm{d}\hat{\mathbf{U}}^j]}} = \underbrace{\begin{bmatrix} \underset{3\times1}{[\mathbf{R}^i_{\mathbf{u}}]} \\ \underset{1\times1}{[\mathbf{R}^i_{\theta}]} \\ \underset{1\times1}{[\mathbf{R}^i_{\phi}]} \\ \underset{1\times1}{[\mathbf{R}^i_{\varphi}]} \end{bmatrix}}_{\underset{6\times1}{[\mathbf{R}^i]}} . \tag{6.196}$$

The residuals in (6.191) are stated for the i-th variational node by reducing $\left[\mathbf{B}^{(3)}\right]$ and $\left[\mathbf{B}^{(1)}\right]$ to their constituent submatrices $\left[\mathbf{B}^{(3)}_i\right]$ and $\left[\mathbf{B}^{(1)}_i\right]$ according to the definitions

in (6.164) and (6.166). In particular,

$$
\begin{aligned}
\underset{3\times1}{\big[\,\mathbf{R}^i_{\mathbf{u}}\,\big]} &= -\int_{\mathcal{R}} \underset{3\times9}{\big[\mathbf{B}^{(3)}_i\big]^{\mathrm{T}}}\,\underset{9\times1}{\big\langle\mathbf{T}\big\rangle}\,\mathrm{d}v \\
&= -\int_{\mathcal{R}} \underset{3\times3}{\big[\mathbf{T}\big]}\,\underset{3\times1}{\big(\mathbf{B}^{(1)}_i\big)}\,\mathrm{d}v \qquad , \\
\underset{1\times1}{\big[\,\mathbf{R}^i_{\theta}\,\big]} &= \int_{\mathcal{R}} \underset{1\times3}{\big[\mathbf{B}^{(1)}_i\big]^{\mathrm{T}}}\,\underset{3\times1}{\big(\mathbf{q}\big)}\,\mathrm{d}v \qquad , \\
\underset{1\times1}{\big[\,\mathbf{R}^i_{\phi}\,\big]} &= -\int_{\mathcal{R}} \underset{1\times3}{\big[\mathbf{B}^{(1)}_i\big]^{\mathrm{T}}}\,\underset{3\times1}{\left(\frac{\partial\phi}{\partial\mathbf{x}}-\frac{\mathbf{p}}{\varepsilon_0}\right)}\,\mathrm{d}v \qquad , \\
\underset{1\times1}{\big[\,\mathbf{R}^i_{\varphi}\,\big]} &= -\int_{\mathcal{R}} \underset{1\times3}{\big[\mathbf{B}^{(1)}_i\big]^{\mathrm{T}}}\,\underset{3\times1}{\left(\frac{\partial\varphi}{\partial\mathbf{x}}\right)}\,\mathrm{d}v \qquad .
\end{aligned}
\tag{6.197}
$$

Note that $(\mathbf{B}^{(1)}_i)$ represents a 3×1 vector which is related to $[\mathbf{B}^{(3)}_i]$ via Equation (6.168). Therefore, (6.109) can be employed to simplify operations of the form $[\mathbf{B}^{(3)}_i]^{\mathrm{T}}\langle\mathbf{T}\rangle$ into simple 3×3 matrix-vector products of the form $[\mathbf{T}](\mathbf{B}^{(1)}_i)$, see $(6.197)_1$. The preceding result is stated in components as

$$
\underset{3\times1}{\big[\,\mathbf{R}^i\,\big]} = \int_{\mathcal{R}} \begin{bmatrix} -T_{11} & -T_{12} & -T_{31} \\ -T_{12} & -T_{22} & -T_{23} \\ -T_{31} & -T_{23} & -T_{33} \\ q_1 & q_2 & q_3 \\ -(\phi_{,1}-\frac{1}{\varepsilon}p_1) & -(\phi_{,2}-\frac{1}{\varepsilon}p_2) & -(\phi_{,3}-\frac{1}{\varepsilon}p_3) \\ -\varphi_{,1} & -\varphi_{,2} & -\varphi_{,3} \end{bmatrix} \begin{bmatrix} N_{i,1} \\ N_{i,2} \\ N_{i,3} \end{bmatrix} \mathrm{d}v \quad . \tag{6.198}
$$

The non-zero entries of $[\mathbf{K}^{ij}]$ are similarly deduced from (6.192 - 195), in particular with the aid of the identities in $(6.135)_{1,2}$ and (6.136). It is readily seen that the entries of the nodal-based stiffness matrix are given by

$$
\begin{aligned}
\underset{3\times3}{\big[\,\mathbf{K}^{ij}_{\mathbf{uu}}\,\big]} &= \int_{\mathcal{R}} \underbrace{\underset{3\times9}{\big[\mathbf{B}^{(3)}_i\big]^{\mathrm{T}}}\,\underset{9\times9}{\big\langle\mathbf{T}\big\rangle^{(2)}}\,\underset{9\times3}{\big[\mathbf{B}^{(3)}_j\big]}}_{\left(\underset{1\times3}{\big[\mathbf{B}^{(1)}_j\big]^{\mathrm{T}}}\,\underset{3\times3}{\big[\mathbf{T}\big]}\,\underset{3\times1}{\big[\mathbf{B}^{(1)}_i\big]}\right)\,\underset{3\times3}{\big[\mathbf{I}\big]}}\,\mathrm{d}v + \int_{\mathcal{R}} \underset{6\times3}{\Big[\big[\mathbf{B}^{(3)}_i\big]^{\mathrm{sym}}\Big]^{\mathrm{T}}}\,\underset{6\times6}{\big\langle\rho\overline{\mathbb{C}}^{\mathrm{sym}}\big\rangle}\,\underset{6\times3}{\big[\mathbf{B}^{(3)}_j\big]^{\mathrm{sym}}}\,\mathrm{d}v \\
&= \int_{\mathcal{R}} \left(\begin{bmatrix} N_{j,1} & N_{j,2} & N_{j,3} \end{bmatrix} \begin{bmatrix} T_{11} & T_{12} & T_{31} \\ T_{12} & T_{22} & T_{23} \\ T_{31} & T_{23} & T_{33} \end{bmatrix} \begin{bmatrix} N_{i,1} \\ N_{i,2} \\ N_{i,3} \end{bmatrix} \right) \mathrm{d}v \begin{bmatrix} 1 & 0 & 0 \\ 0 & 1 & 0 \\ 0 & 0 & 1 \end{bmatrix}
\end{aligned}
$$

$$+\int_{\mathcal{R}}\begin{bmatrix}N_{i,1} & 0 & 0 & N_{i,2}N_{i,1} & 0\\ 0 & N_{i,2} & 0 & 0 & N_{i,3}N_{i,2}\\ 0 & 0 & N_{i,3}N_{i,3} & 0 & N_{i,1}\end{bmatrix}\rho\begin{bmatrix}\overline{\mathbb{C}}_{1111} & \overline{\mathbb{C}}_{1122} & \overline{\mathbb{C}}_{1133} & \overline{\mathbb{C}}_{1112} & \overline{\mathbb{C}}_{1123} & \overline{\mathbb{C}}_{1131}\\ \overline{\mathbb{C}}_{2211} & \overline{\mathbb{C}}_{2222} & \overline{\mathbb{C}}_{2233} & \overline{\mathbb{C}}_{2212} & \overline{\mathbb{C}}_{2223} & \overline{\mathbb{C}}_{2231}\\ \overline{\mathbb{C}}_{3311} & \overline{\mathbb{C}}_{3322} & \overline{\mathbb{C}}_{3333} & \overline{\mathbb{C}}_{3312} & \overline{\mathbb{C}}_{3323} & \overline{\mathbb{C}}_{3331}\\ \overline{\mathbb{C}}_{1211} & \overline{\mathbb{C}}_{1222} & \overline{\mathbb{C}}_{1233} & \overline{\mathbb{C}}_{1212} & \overline{\mathbb{C}}_{1223} & \overline{\mathbb{C}}_{1231}\\ \overline{\mathbb{C}}_{2311} & \overline{\mathbb{C}}_{2322} & \overline{\mathbb{C}}_{2333} & \overline{\mathbb{C}}_{2312} & \overline{\mathbb{C}}_{2323} & \overline{\mathbb{C}}_{2331}\\ \overline{\mathbb{C}}_{3111} & \overline{\mathbb{C}}_{3122} & \overline{\mathbb{C}}_{3133} & \overline{\mathbb{C}}_{3112} & \overline{\mathbb{C}}_{3123} & \overline{\mathbb{C}}_{3131}\end{bmatrix}\begin{bmatrix}N_{j,1} & 0 & 0\\ 0 & N_{j,2} & 0\\ 0 & 0 & N_{j,3}\\ N_{j,2}N_{j,1} & 0 & 0\\ 0 & N_{j,3}N_{j,2} & 0\\ N_{j,3} & 0 & N_{j,1}\end{bmatrix}\mathrm{d}v \quad , \tag{6.199}$$

$$\begin{aligned}\underset{3\times1}{\left[\mathbf{K}^{ij}_{\mathbf{u}\theta}\right]} &= -\int_{\mathcal{R}}\underset{3\times9}{\left[\mathbf{B}^{(3)}_i\right]^{\mathrm{T}}}\underset{9\times1}{\left\langle\rho\overline{\mathbb{C}\mathbf{A}}\right\rangle}\underset{1\times1}{N_j}\,\mathrm{d}v\\ &= -\int_{\mathcal{R}}\underset{3\times3}{\left[\rho\overline{\mathbb{C}\mathbf{A}}\right]}\underset{3\times1}{\left(\mathbf{B}^{(1)}_i\right)}\underset{1\times1}{N_j}\,\mathrm{d}v\\ &= -\int_{\mathcal{R}}\rho\begin{bmatrix}\overline{\mathbb{C}}_{11kl}\overline{A}_{kl} & \overline{\mathbb{C}}_{12kl}\overline{A}_{kl} & \overline{\mathbb{C}}_{31kl}\overline{A}_{kl}\\ \overline{\mathbb{C}}_{12kl}\overline{A}_{kl} & \overline{\mathbb{C}}_{22kl}\overline{A}_{kl} & \overline{\mathbb{C}}_{23kl}\overline{A}_{kl}\\ \overline{\mathbb{C}}_{31kl}\overline{A}_{kl} & \overline{\mathbb{C}}_{23kl}\overline{A}_{kl} & \overline{\mathbb{C}}_{33kl}\overline{A}_{kl}\end{bmatrix}\begin{bmatrix}N_{i,1}\\ N_{i,2}\\ N_{i,3}\end{bmatrix}N_j\,\mathrm{d}v \quad ,\end{aligned} \tag{6.200}$$

$$\begin{aligned}\underset{3\times1}{\left[\mathbf{K}^{ij}_{\mathbf{u}\phi}\right]} &= -\int_{\mathcal{R}}\underset{6\times3}{\left[\left[\mathbf{B}^{(3)}_i\right]^{\mathrm{sym}}\right]^{\mathrm{T}}}\underset{6\times3}{\left\langle\rho\overline{\mathbb{C}}^{\mathrm{sym}}_2\right\rangle}\underset{3\times1}{\left[\mathbf{B}^{(1)}_j\right]}\mathrm{d}v\\ &= -\int_{\mathcal{R}}\begin{bmatrix}N_{i,1} & 0 & 0 & N_{i,2}N_{i,1} & 0\\ 0 & N_{i,2} & 0 & 0 & N_{i,3}N_{i,2}\\ 0 & 0 & N_{i,3}N_{i,3} & 0 & N_{i,1}\end{bmatrix}\rho\begin{bmatrix}\overline{\mathbb{C}}_{111} & \overline{\mathbb{C}}_{112} & \overline{\mathbb{C}}_{113}\\ \overline{\mathbb{C}}_{221} & \overline{\mathbb{C}}_{222} & \overline{\mathbb{C}}_{223}\\ \overline{\mathbb{C}}_{331} & \overline{\mathbb{C}}_{332} & \overline{\mathbb{C}}_{333}\\ \overline{\mathbb{C}}_{121} & \overline{\mathbb{C}}_{122} & \overline{\mathbb{C}}_{123}\\ \overline{\mathbb{C}}_{231} & \overline{\mathbb{C}}_{232} & \overline{\mathbb{C}}_{233}\\ \overline{\mathbb{C}}_{311} & \overline{\mathbb{C}}_{312} & \overline{\mathbb{C}}_{313}\end{bmatrix}\begin{bmatrix}N_{j,1}\\ N_{j,2}\\ N_{j,3}\end{bmatrix}\mathrm{d}v \quad ,\end{aligned} \tag{6.201}$$

$$\begin{aligned}\underset{1\times3}{\left[\mathbf{K}^{ij}_{\theta\mathbf{u}}\right]} &= -\int_{\mathcal{R}}\underset{1\times3}{\left[\mathbf{B}^{(1)}_i\right]^{\mathrm{T}}}\underset{3\times1}{\left(\mathbf{q}\right)}\underset{1\times3}{\left[\mathbf{B}^{(2)}_j\right]}\mathrm{d}v - \int_{\mathcal{R}}\underset{1\times3}{\left[\mathbf{B}^{(1)}_i\right]^{\mathrm{T}}}\underset{3\times9}{\left\langle 2\frac{\partial\theta}{\partial\mathbf{x}}\right\rangle^{(3)}}\underset{9\times9}{\left\langle\mathbb{I}^{\mathrm{sym}}\right\rangle}\underset{9\times9}{\left\langle\overline{\boldsymbol{\kappa}}\right\rangle^{(2)}}\underset{9\times3}{\left[\mathbf{B}^{(3)}_j\right]}\mathrm{d}v\\ &= -\int_{\mathcal{R}}\left(\begin{bmatrix}N_{i,1} & N_{i,2} & N_{i,3}\end{bmatrix}\begin{bmatrix}q_1\\ q_2\\ q_3\end{bmatrix}\right)\begin{bmatrix}N_{j,1} & N_{j,2} & N_{j,3}\end{bmatrix}\mathrm{d}v\\ &\quad -\int_{\mathcal{R}}\left(\begin{bmatrix}N_{j,1} & N_{j,2} & N_{j,3}\end{bmatrix}\begin{bmatrix}\overline{\kappa}_{11} & \overline{\kappa}_{12} & \overline{\kappa}_{31}\\ \overline{\kappa}_{12} & \overline{\kappa}_{22} & \overline{\kappa}_{23}\\ \overline{\kappa}_{31} & \overline{\kappa}_{23} & \overline{\kappa}_{33}\end{bmatrix}\begin{bmatrix}\theta_{,1}\\ \theta_{,2}\\ \theta_{,3}\end{bmatrix}\right)\begin{bmatrix}N_{i,1} & N_{i,2} & N_{i,3}\end{bmatrix}\mathrm{d}v\\ &\quad -\int_{\mathcal{R}}\left(\begin{bmatrix}N_{j,1} & N_{j,2} & N_{j,3}\end{bmatrix}\begin{bmatrix}\overline{\kappa}_{11} & \overline{\kappa}_{12} & \overline{\kappa}_{31}\\ \overline{\kappa}_{12} & \overline{\kappa}_{22} & \overline{\kappa}_{23}\\ \overline{\kappa}_{31} & \overline{\kappa}_{23} & \overline{\kappa}_{33}\end{bmatrix}\begin{bmatrix}N_{i,1}\\ N_{i,2}\\ N_{i,3}\end{bmatrix}\right)\begin{bmatrix}\theta_{,1} & \theta_{,2} & \theta_{,3}\end{bmatrix}\mathrm{d}v \quad ,\end{aligned} \tag{6.202}$$

$$\underset{1\times1}{\left[\mathbf{K}^{ij}_{\theta\theta}\right]} = \int_{\mathcal{R}}\underset{1\times3}{\left[\mathbf{B}^{(1)}_i\right]^{\mathrm{T}}}\underset{3\times3}{\left[\overline{\boldsymbol{\kappa}}\right]}\underset{3\times1}{\left[\mathbf{B}^{(1)}_j\right]}\mathrm{d}v$$

$$= \int_{\mathcal{R}} \left(\begin{bmatrix} N_{i,1} & N_{i,2} & N_{i,3} \end{bmatrix} \begin{bmatrix} \overline{\kappa}_{11} & \overline{\kappa}_{12} & \overline{\kappa}_{31} \\ \overline{\kappa}_{12} & \overline{\kappa}_{22} & \overline{\kappa}_{23} \\ \overline{\kappa}_{31} & \overline{\kappa}_{23} & \overline{\kappa}_{33} \end{bmatrix} \begin{bmatrix} N_{j,1} \\ N_{j,2} \\ N_{j,3} \end{bmatrix} \right) \mathrm{d}v \quad , \tag{6.203}$$

$$\underset{1\times 3}{\left[\mathbf{K}^{ij}_{\phi\mathbf{u}}\right]} = \int_{\mathcal{R}} \underset{1\times 3}{\left[\mathbf{B}^{(1)}_i\right]^{\mathrm{T}}} \underset{3\times 1}{\left(\frac{\partial \phi}{\partial \mathbf{x}}\right)} \underset{1\times 3}{\left[\mathbf{B}^{(2)}_j\right]} \mathrm{d}v + \int_{\mathcal{R}} \underset{1\times 3}{\left[\mathbf{B}^{(1)}_i\right]^{\mathrm{T}}} \underset{3\times 6}{\left\langle \tfrac{\rho}{\varepsilon_0} \overline{\mathbf{c}}^{\,\mathrm{sym}}_2 \right\rangle^{\mathrm{T}}} \underset{6\times 3}{\left[\mathbf{B}^{(3)}_j\right]^{\mathrm{sym}}} \mathrm{d}v$$

$$- \int_{\mathcal{R}} \underbrace{\underset{1\times 3}{\left[\mathbf{B}^{(1)}_i\right]^{\mathrm{T}}} \underset{3\times 6}{\left\langle 2\frac{\partial \phi}{\partial \mathbf{x}}^{\mathrm{sym}} \right\rangle^{(3)}} \underset{6\times 3}{\left[\mathbf{B}^{(3)}_j\right]^{\mathrm{sym}}}}_{\left(\underset{1\times 3}{\left[\mathbf{B}^{(1)}_j\right]^{\mathrm{T}}} \underset{3\times 1}{\left[\frac{\partial \phi}{\partial \mathbf{x}}\right]}\right) \underset{1\times 3}{\left[\mathbf{B}^{(1)}_i\right]^{\mathrm{T}}} + \left(\underset{1\times 3}{\left[\mathbf{B}^{(1)}_j\right]^{\mathrm{T}}} \underset{3\times 1}{\left[\mathbf{B}^{(1)}_i\right]}\right) \underset{1\times 3}{\left[\frac{\partial \phi}{\partial \mathbf{x}}\right]^{\mathrm{T}}}} \mathrm{d}v$$

$$= \int_{\mathcal{R}} \left(\begin{bmatrix} N_{i,1} & N_{i,2} & N_{i,3} \end{bmatrix} \begin{bmatrix} \phi_{,1} \\ \phi_{,2} \\ \phi_{,3} \end{bmatrix} \right) \begin{bmatrix} N_{j,1} & N_{j,2} & N_{j,3} \end{bmatrix} \mathrm{d}v$$

$$+ \int_{\mathcal{R}} \left(\begin{bmatrix} N_{j,1} & 0 & 0 & N_{j,2}N_{j,1} & 0 \\ 0 & N_{j,2} & 0 & 0 & N_{j,3}N_{j,2} \\ 0 & 0 & N_{j,3}N_{j,3} & 0 & N_{j,1} \end{bmatrix} \frac{\rho}{\varepsilon_0} \begin{bmatrix} \overline{\mathbb{C}}_{111} \overline{\mathbb{C}}_{112} \overline{\mathbb{C}}_{113} \\ \overline{\mathbb{C}}_{221} \overline{\mathbb{C}}_{222} \overline{\mathbb{C}}_{223} \\ \overline{\mathbb{C}}_{331} \overline{\mathbb{C}}_{332} \overline{\mathbb{C}}_{333} \\ \overline{\mathbb{C}}_{121} \overline{\mathbb{C}}_{122} \overline{\mathbb{C}}_{123} \\ \overline{\mathbb{C}}_{231} \overline{\mathbb{C}}_{232} \overline{\mathbb{C}}_{233} \\ \overline{\mathbb{C}}_{311} \overline{\mathbb{C}}_{312} \overline{\mathbb{C}}_{313} \end{bmatrix} \begin{bmatrix} N_{i,1} \\ N_{i,2} \\ N_{i,3} \end{bmatrix} \right)^{\mathrm{T}} \mathrm{d}v$$

$$- \int_{\mathcal{R}} \left(\begin{bmatrix} N_{j,1} & N_{j,2} & N_{j,3} \end{bmatrix} \begin{bmatrix} \phi_{,1} \\ \phi_{,2} \\ \phi_{,3} \end{bmatrix} \right) \begin{bmatrix} N_{i,1} & N_{i,2} & N_{i,3} \end{bmatrix} \mathrm{d}v$$

$$- \int_{\mathcal{R}} \left(\begin{bmatrix} N_{i,1} & N_{i,2} & N_{i,3} \end{bmatrix} \begin{bmatrix} N_{j,1} \\ N_{j,2} \\ N_{j,3} \end{bmatrix} \right) \begin{bmatrix} \phi_{,1} & \phi_{,2} & \phi_{,3} \end{bmatrix} \mathrm{d}v \quad , \tag{6.204}$$

$$\underset{1\times 1}{\left[\mathbf{K}^{ij}_{\phi\phi}\right]} = \int_{\mathcal{R}} \underset{1\times 3}{\left[\mathbf{B}^{(1)}_i\right]^{\mathrm{T}}} \underset{3\times 3}{\left[\,\mathbf{i} + \rho \overline{\mathbf{c}}_3\,\right]} \underset{3\times 1}{\left[\mathbf{B}^{(1)}_j\right]} \mathrm{d}v$$

$$= \int_{\mathcal{R}} \left(\begin{bmatrix} N_{i,1} & N_{i,2} & N_{i,3} \end{bmatrix} \begin{bmatrix} \rho\overline{\mathbf{c}}_{11}+1 & \rho\overline{\mathbf{c}}_{12} & \rho\overline{\mathbf{c}}_{31} \\ \rho\overline{\mathbf{c}}_{12} & \rho\overline{\mathbf{c}}_{22}+1 & \rho\overline{\mathbf{c}}_{23} \\ \rho\overline{\mathbf{c}}_{31} & \rho\overline{\mathbf{c}}_{23} & \rho\overline{\mathbf{c}}_{33}+1 \end{bmatrix} \begin{bmatrix} N_{j,1} \\ N_{j,2} \\ N_{j,3} \end{bmatrix} \right) \mathrm{d}v \quad , \tag{6.205}$$

$$\underset{1\times 3}{\left[\mathbf{K}^{ij}_{\varphi\mathbf{u}}\right]} = \int_{\mathcal{R}} \underset{1\times 3}{\left[\mathbf{B}^{(1)}_i\right]^{\mathrm{T}}} \underset{3\times 1}{\left(\frac{\partial \varphi}{\partial \mathbf{x}}\right)} \underset{1\times 3}{\left[\mathbf{B}^{(2)}_j\right]} \mathrm{d}v - \int_{\mathcal{R}} \underbrace{\underset{1\times 3}{\left[\mathbf{B}^{(1)}_i\right]^{\mathrm{T}}} \underset{3\times 6}{\left\langle 2\frac{\partial \varphi}{\partial \mathbf{x}}^{\mathrm{sym}} \right\rangle^{(3)}} \underset{6\times 3}{\left[\mathbf{B}^{(3)}_j\right]^{\mathrm{sym}}}}_{\left(\underset{1\times 3}{\left[\mathbf{B}^{(1)}_j\right]^{\mathrm{T}}} \underset{3\times 1}{\left[\frac{\partial \varphi}{\partial \mathbf{x}}\right]}\right) \underset{1\times 3}{\left[\mathbf{B}^{(1)}_i\right]^{\mathrm{T}}} + \left(\underset{1\times 3}{\left[\mathbf{B}^{(1)}_j\right]^{\mathrm{T}}} \underset{3\times 1}{\left[\mathbf{B}^{(1)}_i\right]}\right) \underset{1\times 3}{\left[\frac{\partial \varphi}{\partial \mathbf{x}}\right]^{\mathrm{T}}}} \mathrm{d}v$$

$$
\begin{aligned}
&= \int_{\mathcal{R}} \left(\begin{bmatrix} N_{i,1} & N_{i,2} & N_{i,3} \end{bmatrix} \begin{bmatrix} \varphi_{,1} \\ \varphi_{,2} \\ \varphi_{,3} \end{bmatrix} \right) \begin{bmatrix} N_{j,1} & N_{j,2} & N_{j,3} \end{bmatrix} \mathrm{d}v \\
&- \int_{\mathcal{R}} \left(\begin{bmatrix} N_{j,1} & N_{j,2} & N_{j,3} \end{bmatrix} \begin{bmatrix} \varphi_{,1} \\ \varphi_{,2} \\ \varphi_{,3} \end{bmatrix} \right) \begin{bmatrix} N_{i,1} & N_{i,2} & N_{i,3} \end{bmatrix} \mathrm{d}v \\
&- \int_{\mathcal{R}} \left(\begin{bmatrix} N_{i,1} & N_{i,2} & N_{i,3} \end{bmatrix} \begin{bmatrix} N_{j,1} \\ N_{j,2} \\ N_{j,3} \end{bmatrix} \right) \begin{bmatrix} \varphi_{,1} & \varphi_{,2} & \varphi_{,3} \end{bmatrix} \mathrm{d}v \quad , \qquad (6.206)
\end{aligned}
$$

$$
\begin{aligned}
\underset{1\times1}{\left[\mathbf{K}^{ij}_{\varphi\varphi} \right]} &= \int_{\mathcal{R}} \underset{1\times3}{\left[\mathbf{B}^{(1)}_i \right]^{\mathrm{T}}} \underset{3\times1}{\left[\mathbf{B}^{(1)}_j \right]} \mathrm{d}v \\
&= \int_{\mathcal{R}} \left(\begin{bmatrix} N_{i,1} & N_{i,2} & N_{i,3} \end{bmatrix} \begin{bmatrix} N_{j,1} \\ N_{j,2} \\ N_{j,3} \end{bmatrix} \right) \mathrm{d}v \quad . \qquad (6.207)
\end{aligned}
$$

As discussed in the context of $(6.193)_1$, the terms for $[\mathbf{K}^{ij}_{\theta\mathbf{u}}]$ in (6.202) vanish if a referential form of FOURIER's law is adopted, because this implies that the linearization in $(6.89)_3$ holds rather than the deformation-dependent result in (6.90). For 2-dimensional plane strain problems, the nodal residual and stiffness matrix are reduced to 5 degrees of freedom by eliminating the superfluous parts from the preceding results, that is, any terms involving derivatives in the out-of plane direction, $N_{i,3} \doteq 0$.

6.4 Verification of Implementation

In this section, the residuals and differentials of the static[32] problem derived in Section 6.3 are implemented in FEAP [142], a Fortran-based finite element analysis program. The ensuing single-scale finite element model is subjected to a range of simple tests. The algorithm is limited to 2-dimensional plane-strain problems so as to minimize the computational cost of the multiscale implementation in Chapter 7, which itself is built upon the single-scale code. The coupled electro-magneto-thermo-mechanical (EMTM) constitutive model is of the type summarized in Equations (6.56 - 62), that is, a linearly coupled transversely isotropic piezoelectric material with a preferred crystal orientation.

This section is organized as follows: First, the material parameters for the aforementioned constitutive model are listed. Next, a purely thermomechanical test problem is compared to an existing implementation of a SAINT VENANT-KIRCHHOFF hyperelastic thermomechanical material. This is followed by an electrostatic test

[32] Recall that the problem is assumed to be mechanically, thermally, and electrically static. See the list in Section 6.1.4 for a comprehensive summary of the simplifying assumptions.

problem for a non-piezoelectric material with deformed and undeformed problem domains, designed to verify the implementation of the POISSON solver associated with the purely electrostatic problem. Next, the convergence of the residual for successive iterations of the NEWTON-RAPHSON scheme is examined and, lastly, the numerical values of the element stiffness matrix are verified by comparison with a numerical approximation using complex arithmetic.

6.4.1 Material Properties

Both the single- and multi-scale finite element implementations are tested using the material properties of *barium titanate* (or $BaTiO_3$). Recall that the expressions in $(6.58)_{2-4}$ for $\mathfrak{c}_2$, $\mathbf{c}_3$, and $\mathbb{C}$ are derived from the work by SCHRÖDER *et al.* [126], hence the corresponding linearly elastic and piezoelectric material parameters of $BaTiO_3$ are obtained from the same source.[33] In particular, this includes the isotropic LAMÉ coefficients λ and μ, the transversely isotropic elasticity parameters ω_{1-3}, the piezoelectric coefficients β_{1-3}, as well as the parameters γ_{1-2} related to the permittivity of the dielectric. Note that SCHRÖDER *et al.* limit their model to small strains. However, it is assumed here that the model can be extended to large deformations using the same parameters according to the SAINT VENANT-KIRCHHOFF hyperelastic constitutive model.

Although the authors provide the properties in terms of the components of the material tensors in (6.34), SCHRÖDER *et al.* [126, Equations 82] include conversion formulae for the aforementioned coordinate-independent material parameters. They are given by

$$\begin{aligned}
\lambda &= \mathbb{C}_{12} &&, \quad \mu = \tfrac{1}{2}\big(\mathbb{C}_{11}-\mathbb{C}_{12}\big) &&, \\
\omega_1 &= 2\mathbb{C}_{44}+\mathbb{C}_{12}-\mathbb{C}_{11} &&, \quad \omega_2 = \tfrac{1}{2}\big(\mathbb{C}_{11}+\mathbb{C}_{33}\big)-2\mathbb{C}_{44}-\mathbb{C}_{13} &&, \quad \omega_3 = \mathbb{C}_{13}-\mathbb{C}_{12} \quad , \\
\beta_1 &= -\mathbb{e}_{31} &&, \quad \beta_2 = \mathbb{e}_{31}-\mathbb{e}_{33}+2\mathbb{e}_{\mathbb{e}_{15}} &&, \quad \beta_3 = -2\mathbb{e}_{15} \quad , \\
\gamma_1 &= -\tfrac{1}{2}\epsilon_{11} &&, \quad \gamma_2 = \tfrac{1}{2}\big(\epsilon_{11}-\epsilon_{33}\big) &&,
\end{aligned} \tag{6.208}$$

where VOIGT notation is used for the components of $\mathbb{C}$ and $\mathbb{e}$. The numerical values adopted for the parameters in (6.208) for $BaTiO_3$ are listed in Table 6.1. The isotropic portion of the elastic moduli are alternatively expressed in terms of the YOUNG's modulus and POISSON's ratio using the usual conversion

$$E = \frac{\mu(3\lambda+2\mu)}{\lambda+\mu} \quad \text{and} \quad \nu = \frac{\lambda}{2(\lambda+\mu)} \quad . \tag{6.209}$$

Note that the electromagnetic properties of the vacuum in the aether relations (3.35) must be specified in units consistent with the material parameters defined. For ex-

[33] It is mentioned that SCHRÖDER *et al.* [126] themselves obtained the parameters for their model from the works of BECHMANN [4] and LEE *et al.* [73].

Electro-Mechanical Parameters of $BaTiO_3$						Units
λ	76.6×10^3	μ	44.7×10^3			N/mm^2
ω_1	-3.6×10^3	ω_2	0.7×10^3	ω_3	0.9×10^3	N/mm^2
β_1	4.4	β_2	0.2	β_3	-23.2	C/m^2
γ_1	-5.6×10^{-3}	γ_2	-0.7×10^{-3}			$mC/(kV\,m)$

Table 6.1: Coordinate-independent material parameters of Barium Titanate ($BaTiO_3$) obtained from Schröder *et al.* [126] using Equations (6.208).

Thermal Properties of $BaTiO_3$					
Conductivity			Expansion Coefficient		
κ	2.7	$W/(m\,K)$	α	6.1×10^{-6}	$1/K$

Table 6.2: Thermal properties of Barium Titanate ($BaTiO_3$) obtained from He [43] for (isotropic) polycrystalline $BaTiO_3$.

ample, the permittivity ε_0 is alternatively given by $\varepsilon_0 = 8.854\,188 \times 10^{-6}\,mC/(kV\,m)$, which is consistent with the units of γ_1 and γ_2 in Table 6.1.

In addition to the aforementioned parameters, the anisotropic response of the material depends strongly on the preferred crystal orientation $\boldsymbol{\alpha}$. This unit vector gives rise to the second-, third- and fourth-order structural tensors in (6.59). Given that the upcoming finite element implementation is limited to two dimensions, it is reasonable to assume that the crystal orientation $\boldsymbol{\alpha}$ lies within the plane of the 2-dimensional domain of the problem. It is thus assumed that the out-of-plane component $\alpha_3 \doteq 0$ vanishes.[34]

Lastly, the thermal properties for $BaTiO_3$ are sourced from He [43, Table 1], who provides experimental results for test samples of two different suppliers. In particular, approximate values for the thermal conductivity and the coefficient of thermal expansion are given at room temperature in Table 6.2. Note that the experiments in [43] were conducted on samples of polycrystalline $BaTiO_3$, hence the measured thermal properties are isotropic. This suffices for the scope of this implementation where the thermal behavior is not of main concern. However, as He points out, the thermal expansion of monocrystalline $BaTiO_3$ is indeed expected to be anisotropic.

6.4.2 Purely Thermomechanical Case

Before the coupled EMTM behavior of the single-scale FEAP implementation is tested, it is first verified that the purely thermomechanical part is in agreement with

[34] Note that the only alternative choice for $\boldsymbol{\alpha}$ compatible with the plane-strain assumption is $\alpha_1 = \alpha_2 \doteq 0$, thus $\alpha_3 \doteq 1$. However, this renders the in-plane behavior isotropic, thereby precluding the observation of any orientation-dependent effects. This would substantially limit the scope of this implementation. Indeed, the testing and validation of the multiscale implementation of Chapter 7 relies in part on variations of $\boldsymbol{\alpha}$ within the microstructure of the RVE.

an existing implementation of a SAINT VENANT-KIRCHHOFF hyperelastic material model. This material is invoked in FEAP using the command `ELAStic STVK E nu` for isotropic behavior or by `ELAStic ORTHotropic e1 e2 e3 nu12 nu23 nu31 g12 g23 g31` for orthotropic materials. This material is capable of representing finite deformations[35] for materials consistent with the thermomechanical part of the constitutive model introduced in Section 6.1.2. The existing implementation of the SAINT VENANT-KIRCHHOFF model is based on the referential form of FOURIER's law for the heat flux, that is, Equation $(6.89)_3$ rather than (6.90). Therefore, to accurately compare the two implementations under large deformations, the terms for $[\mathbf{K}^{ij}_{\theta\mathbf{u}}]$ in (6.202) must be neglected.

Contour plots of the resulting fluxes, such as the components of the CAUCHY stress tensor or the heat flux vector, are constructed in FEAP using a local least-squares method to project the values from the integration points to the nodes, see GOVINDJEE *et al.* [35] and ZIENKIEWICZ and TAYLOR [159]. Note that the built-in models `ELAStic STVK` and `ELAStic ORTHotropic` generate plots for the *referential* heat flux vector $\mathbf{q}_0$ (*i.e.*, the PIOLA transform of $\mathbf{q}$) rather than the spatial flux. This is somewhat inconsistent, given that stress contour plots are based on the components of the spatial (CAUCHY) stress. To ensure that the implementation of the EMTM material is consistent with the built-in thermomechanical models in FEAP, the heat flux is thus first pulled back to the reference configuration according to Equation (2.145) before the least-squares projection algorithm is applied.

It is observed that both the built-in model and the EMTM implementation produce identical results for the displacement, temperature, stress, and heat flux. For example, Figure 6.1 shows the displacement and temperature distributions for a rectangular region of an arbitrary thermoelastic material subjected to external shear forces and a linear (referential) temperature gradient. The finite element mesh is comprised of quadrilateral elements with bi-linear shape functions. The EMTM model produces identical contour plots as the built-in STVK material, provided that the referential form of FOURIER's law is used and the heat flux is pulled back to the reference configuration. Furthermore, it is observed that the number of iterations needed for the EMTM model to converge is identical to the STVK model. This suggests that the thermomechanical part of the EMTM tangent matrix in (6.196) is implemented correctly, thereby preserving the convergence properties of the NEWTON-RAPHSON scheme.

6.4.3 Purely Electrostatic Case

Recall that the electrostatic problem consists of the POISSON Equation $(6.10)_3$. Due to the spatial nature of the corresponding LAPLACE operator, this results in a ge-

[35] It is mentioned that `ELAStic ORTHotropic` must be followed by the command `FINIte` in order to enable finite deformations, see FEAP user manual [142, Section 7.3.2]. This keyword is optional for the isotropic model `ELAStic STVK`.

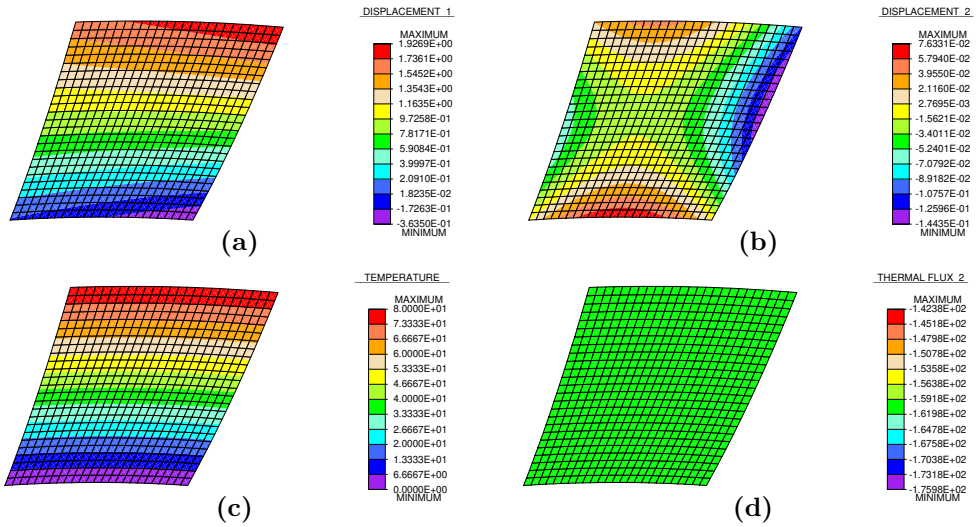

Figure 6.1: Rectangular thermomechanical material subjected to uniform shear and linear temperature gradient. The EMTM implementation and the pre-existing STVK model produce identical results, shown here for (a) X-displacement, (b) Y-displacement, (c) temperature, and (d) heat flux in Y-direction. Deformations are shown to scale.

ometric stiffness represented by the first two integrals in the electric residual Equation (6.97). Consequently, the coupling terms $\mathbf{K}^{ij}_{\phi\mathbf{u}}$ in the stiffness matrix in (6.204) do not vanish even for non-piezoelectric materials, $\mathfrak{C} = \mathbf{0}$. This becomes particularly important under large deformations, where the spatial domain for the POISSON equation may differ significantly from the undeformed configuration.

To verify that the geometric tangent of the electromagnetic equation is implemented correctly, the following set of numerical experiments is devised: In the first experiment, a rectangular material region is subjected to large deformation under uniaxial normal stress or simple shear, resulting in a distorted rectangle or parallelogram, respectively. The material is assumed to be non-piezoelectric, so that the deformation does not affect the polarization and *vice versa*. A non-uniform electric potential is prescribed at the boundary, whose solution is governed by the aforementioned POISSON equation. In the second experiment, the (undeformed) initial configuration of the problem domain is chosen to coincide with the deformed shape of experiment 1. When subjected to the same electric potential distribution at the boundary, the solution for the electric potential is identical in the two experiments. This indicates that the effect of the geometric nonlinearity due to the spatial LAPLACE operator is implemented correctly.

6.4.4 Convergence

The convergence properties of the fully coupled two-dimensional implementation are examined using a simple rectangular problem domain subjected to a range of mixed

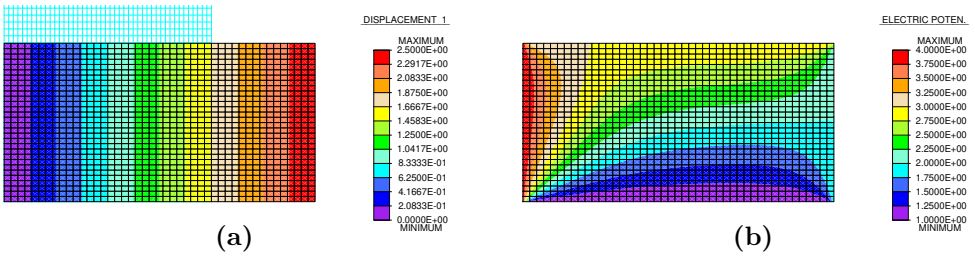

Figure 6.2: Electrostatic equation for a non-piezoelectric material: The solution is independent of whether or not the spatial geometry includes any deformation. (a) Square region under uniaxial stretch of 50% (see undeformed mesh in background). (b) The solution of the electrostatic equation, obtained with either a deformed or undeformed model.

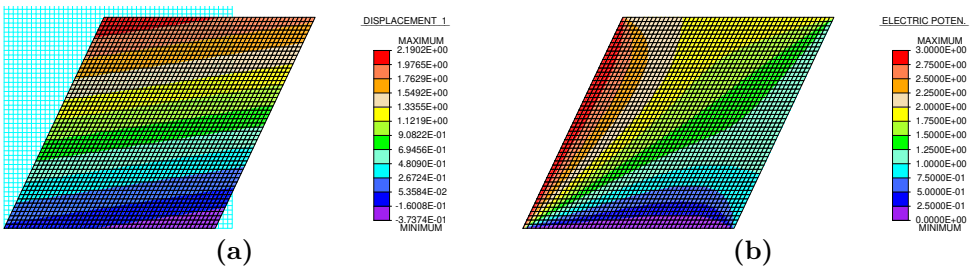

Figure 6.3: Similar to Figure 6.2: (a) Parallelogrammatic region obtained from a square domain under simple shear. (b) The solution of the electrostatic equation is identical for a deformed or undeformed model.

EMTM boundary loads. The uniform material is described by the parameters for barium titanate provided in Section 6.4.1, with a crystal orientation of $\boldsymbol{\alpha} = \frac{1}{\sqrt{5}}\mathbf{e}_1 + \frac{2}{\sqrt{5}}\mathbf{e}_2$ according to the constitutive equations outlined in (6.58 - 59). The external loads consist of tensile and shear forces, a thermal gradient, as well as an electric potential gradient. They are chosen to be large enough that the resulting strains are finite, thus leading to nonlinear geometric effects in the residuals. The mechanical, thermal, and electric loads are adjusted relative to each other such that each field leads to deformations comparable in magnitude.

It is expected that, if correctly implemented, the Newton-Raphson method furnishes an asymptotically quadratic rate of convergence.[36] As shown in Figure 6.4, the homogeneous single-scale problem converges in only 5 iterations despite the finite deformations imposed.[37] It is further seen that the mechanical, thermal, and electric equations converge at different rates over the course of the solution iterations. The thermal residual reaches close to zero in a single iteration, whereas the residual of the

[36] For a formal discussion of the convergence properties of the Newton-Raphson method, see, for example, the monographs by Kantorovich and Akilov [59] as well as Ortega and Rheinboldt [111].

[37] The problem is considered to have converged when the relative energy norm of the residual reaches below 1×10^{-16} compared to the initial value.

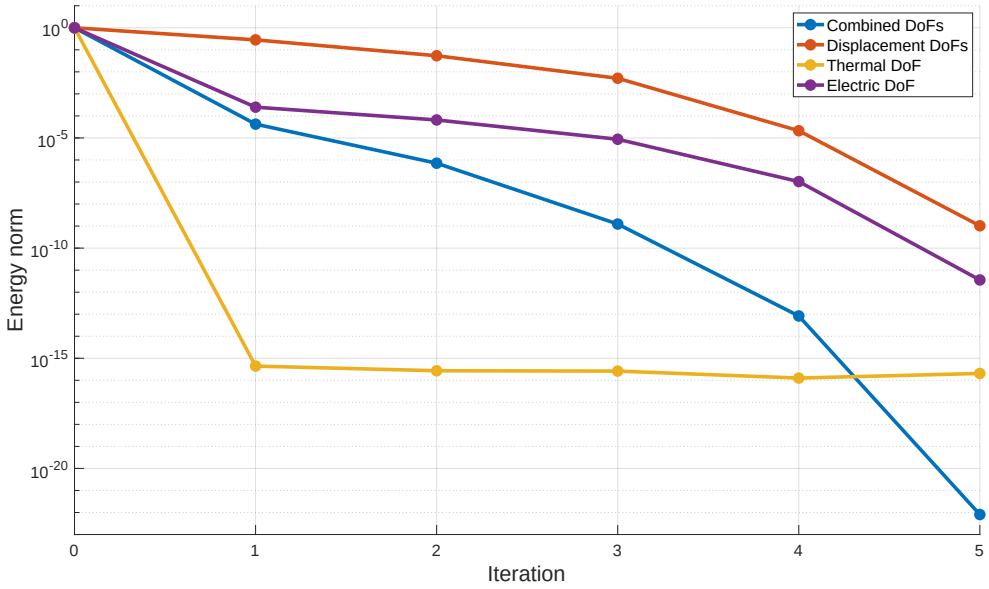

Figure 6.4: Residual for each successive iteration of the NEWTON-RAPHSON scheme, measured in terms of the energy norm relative to the initial value. The rate of convergence is at least quadratic overall, although the different degrees of freedom (displacement, temperature, and electric potential) converge at different rates.

displacement degrees of freedom initially reduces at the slowest rate. This is in part because the initial (absolute) value of the energy norm of the displacement degree of freedom is smaller than the energy norm of the thermal and electric residuals, see Table 6.3.

6.4.5 Numerical Tangent using Complex Arithmetic

In Section 6.2, the governing equations of EMTM were converted into the weak form and written in terms of the residuals. Furthermore, explicit expressions for the differentials of the residuals were derived in preparation for the NEWTON-RAPHSON

Residual - Energy Norm				
	total	displacement	thermal	electric
initial value	5.6301672e+11	2.0753010e+00	7.5000000e+01	7.4736963e+03
iteration 1	2.3847904e+07	4.5788630e-01	3.3083459e-14	1.8650586e+00
iteration 2	4.0206298e+05	8.3212803e-02	2.0365399e-14	4.8986347e-01
iteration 3	6.9734247e+02	7.8877107e-03	1.9644869e-14	6.5246365e-02
iteration 4	4.6808039e-02	3.2827591e-05	9.4719931e-15	7.8253889e-04
iteration 5	4.5539096e-11	1.5897537e-09	1.5350916e-14	2.6822840e-08

Table 6.3: Energy norm for successive iterations of the NEWTON-RAPHSON scheme, for the total problem and separately for the different types of degrees of freedom.

method. In Section 6.3, a finite element discretization was introduced to convert the residuals and their differentials into a finite-dimensional set of algebraic equations. In the present section, an alternative method is introduced for the numerical approximation of the differentials using complex-valued arithmetic. This approximation is used to verify the aforementioned exact expression for the differentials by comparing the numeric values of the element stiffness matrix obtained with the exact and with the approximate methods.

For simplicity, consider a scalar-valued function $f(x)$ of a scalar argument x. The numerical differentiation of f at some location x_0 is often performed using a first-order *finite difference* (FD) scheme of the form

$$\left.\frac{\partial f}{\partial x}\right|_{x=x_0} \doteq \frac{f(x_0+h)-f(x_0)}{h} \quad , \tag{6.210}$$

where h represents a small perturbation from x_0. Of course, the approximation in (6.210) converges to the exact derivative in the limit of $h \to 0$, provided that $f(x)$ is differentiable at x_0. In a numerical setting, however, this method can introduce substantial round-off errors if the numerator on the right-hand side of (6.210) is small compared to the absolute value of $f(x_0)$. This numerical error is further exacerbated if the perturbation h is decreased. The choice of h thus represents a tradeoff between the truncation error of the first-order approximation in (6.210) and the round-off error of the numerical scheme.

To avoid the computation of differences between two similar values, an alternative numerical differentiation scheme using complex arithmetic was proposed by Lyness and Moler [78, 79]. According to this method, the function $f(x)$ is extended to the complex plane by allowing x to assume complex values. At any given (real-valued) location x_0 a perturbation h is introduced along the imaginary axis. The resulting perturbation in $f(x)$ is limited (in a first-order approximation) to the imaginary axis as well, thereby avoiding the round-off error observed in the FD scheme (6.210). To see this, consider the Taylor series expansion of $f(x)$ around x_0 given by

$$f(x_0+ih) \;=\; f(x_0) + ih\,f'(x_0) - \tfrac{1}{2!}h^2 f''(x_0) - \tfrac{1}{3!}ih^3 f'''(x_0) + \ldots \quad , \tag{6.211}$$

where i represents the imaginary unit number, $i^2 = -1$, and $n!$ denotes a factorial of n. Here, it is assumed that x_0 and thus $f(x_0)$ are real-valued, whereas the (real-valued) perturbation h is applied solely along the imaginary axis. The real and imaginary parts of the series in (6.211) are thus given by

$$\Re\big\{f(x_0+ih)\big\} \;=\; f(x_0) + \mathcal{O}(h^2) \quad , \tag{6.212}$$

and

$$\Im\big\{f(x_0+ih)\big\} \;=\; h\,f'(x_0) + \mathcal{O}(h^3) \quad , \tag{6.213}$$

respectively. The derivative f' at x_0 is thus readily obtained by dividing the imaginary part in (6.213) with the perturbation h, that is,

$$f'(x_0) \doteq \frac{\Im\{f(x_0+ih)\}}{h} \quad . \tag{6.214}$$

Note that, since a reduction of h does not introduce any round-off errors to the numerical differentiation scheme (6.214), the approximate derivative is obtained to within the numerical precision declared in the implementation.

The preceding numerical differentiation scheme is readily generalized to higher-order functions of higher-order arguments. For example, recall the definition in (2.39) of the gradient of a function $\mathcal{F}(\mathbf{x})$ by means of the GÂTEAUX differential $\mathrm{D}\mathcal{F}(\mathbf{x},\mathbf{h})$, that is, the directional derivative of $\mathcal{F}(\mathbf{x})$ in direction $\mathbf{h}$. It can be shown that

$$\mathrm{D}\mathcal{F}(\mathbf{x},\mathbf{h}) = \frac{\mathrm{d}}{\mathrm{d}\alpha}\Big[\mathcal{F}(\mathbf{x}+\alpha\mathbf{h})\Big]_{\alpha=0} = \lim_{\alpha\to 0}\frac{\mathcal{F}(\mathbf{x}+\alpha\mathbf{h})-\mathcal{F}(\mathbf{x})}{\alpha} \quad . \tag{6.215}$$

Equation $(6.215)_2$ immediately leads to the FD scheme

$$\mathrm{D}\mathcal{F}(\mathbf{x},\mathbf{h}) \doteq \frac{\mathcal{F}(\mathbf{x}+\alpha\mathbf{h})-\mathcal{F}(\mathbf{x})}{\alpha} \quad , \tag{6.216}$$

which suffers the same numerical shortcomings as the scalar version in (6.210) when the perturbation α is chosen to be too small. On the other hand, a TAYLOR expansion of $\mathcal{F}$ around $\mathbf{x}$ with respect to a small perturbation $i\alpha\mathbf{h}$ in direction $\mathbf{h}$ leads to the complex-valued scheme

$$\mathrm{D}\mathcal{F}(\mathbf{x},\mathbf{h}) \doteq \frac{\Im\{\mathcal{F}(\mathbf{x}+i\alpha\mathbf{h})\}}{\alpha} \quad . \tag{6.217}$$

As before, this scheme does not introduce a round-off error because the perturbation is applied along the imaginary axis rather than the real axis. Therefore, the resulting approximation for the differential $\mathrm{D}\mathcal{F}(\mathbf{x},\mathbf{h})$ is expected to be to within machine precision as long as a sufficiently small α is selected, since the truncation error of the first-order approximation in (6.217) scales with $\mathcal{O}(\alpha^3)$.

Note that, in view of $(2.4)_2$ and (2.39), the differentiation scheme in (6.217) must be separately applied to all directions of the orthonormal basis $\mathbf{h}=\{\mathbf{e}_1,\mathbf{e}_2,\mathbf{e}_3\}$ in order to numerically approximate all CARTESIAN components of the gradient, that is,

$$\mathrm{D}\mathcal{F}(\mathbf{x},\mathbf{e}_i) = \frac{\partial\mathcal{F}}{\partial\mathbf{x}}\cdot\mathbf{e}_i = \frac{\partial\mathcal{F}}{\partial x_i} \quad \forall \quad i \quad . \tag{6.218}$$

Therefore, the numerical approximation of the components of a gradient involves a total of 3 independent complex-step computations. Likewise, the method is readily adapted to the GÂTEAUX differential $\mathrm{D}\mathcal{F}(\mathbf{T},\mathbf{H})$ of functions of tensor-valued arguments, see Equation (2.40). Thus, the approximation of the components of a tensor

derivative involves 9 independent applications of the complex-valued differentiation scheme, once for each direction of the orthonormal basis $\mathbf{H} = \mathbf{e}_i \otimes \mathbf{e}_j$.[38]

Recall from Section 6.2.2 that the NEWTON-RAPHSON method, which is employed to solve a nonlinear problem $\mathbf{r}(\tilde{\mathbf{u}}) = \mathbf{0}$ for $\tilde{\mathbf{u}}$, relies on the GÂTEAUX differential $\mathrm{D}\mathbf{r}(\tilde{\mathbf{u}}_0, \tilde{\mathbf{u}} - \tilde{\mathbf{u}}_0)$ around the initial estimate $\tilde{\mathbf{u}}_0$ in the direction of $\tilde{\mathbf{u}} - \tilde{\mathbf{u}}_0$. This method applies to vectors of arbitrary length (in the conventional sense used in linear algebra). For example, if both the residual $\mathbf{r}$ and the desired solution $\tilde{\mathbf{u}}$ are vectors of length n, then the FRÉCHET derivative $\mathbf{J}$ in (6.79) furnishes an $n \times n$ matrix to be employed in the iterative scheme (6.80). Accordingly, in view of the definitions in $(6.188)_{1,2}$, the finite element stiffness matrix $\mathbf{K}$ in (6.189) may be computed by means of numerical differentiation of the residual vector $\mathbf{R}$ using n repetitions of the complex-step algorithm.[39] Thereby, a complex-valued perturbation is introduced to the i-th entry of the solution vector $\hat{\mathbf{U}}$. This leads to complex-valued gradient quantities, from which complex-valued fluxes are obtained via the constitutive equations. The imaginary part (divided by α) of the resulting residual $\mathbf{R}(\hat{\mathbf{U}})$ then furnishes the i-th column of $\mathbf{K}$. Lastly, in the interest of computational efficiency, the residual itself may be extracted from the real part of $\mathbf{R}(\hat{\mathbf{U}})$ during any of the n iterations. Its value is accurate to within machine precision provided that α is sufficiently small, since the truncation error in the real part is of order $\mathcal{O}(\alpha^2)$, see (6.212).

In the context of this dissertation, the complex-step algorithm is implemented as an alternative to the exact expressions for the computation of the finite element stiffness matrix derived in Section 6.3. The complex numerical approximation is thereafter compared with the exact solution under a variety of coupled EMTM loading conditions. For example, consider a simple rectangular domain of 4 elements per dimension, see Figure 6.5. Tensile and shear forces of $f_x = 1\,\mathrm{kN}$, $f_y = 5\,\mathrm{kN}$, and $f_\tau = 2\,\mathrm{kN}$ are applied (per millimeter of thickness in the out-of-plane direction), respectivly. A linear temperature gradient is prescribed in the y-direction with $T_1 = 0\,^\circ\mathrm{C}$ and $T_2 = 16 \times 10^3\,^\circ\mathrm{C}$, where the reference temperature for thermal expansion is set at $0\,^\circ\mathrm{C}$. Lastly, an electric potential gradient is applied with $\phi_1 = 10\,\mathrm{kV}$ and $\phi_2 = 0\,\mathrm{V}$. The aforementioned loading is not intended to be realistic, of course, but is instead designed to elicit large deformations due to a combination of mechanical, thermal, and electrostatic loads.

Table 6.4 lists the ensuing residual $\mathbf{R}^i$ and the 5×5 entries[40] of the element stiffness matrix $\mathbf{K}^{ij}$ of an interior element for the degrees of freedom associated with the variational node $i = 1$ and the differential node $j = 3$, see Section 6.3.4, where i

[38] This method was applied, for example, by TANAKA *et al.* [141] to the computation of tangent moduli from the stress-strain relationships of hyperelastic material models.

[39] See KIM *et al.* [61] for an application of the complex-step algorithm to the approximation of element tangent matrices.

[40] The size of $\mathbf{K}^{ij}$ is 5×5, rather than 6×6, because the problem is 2-dimensional, thereby removing one degree of freedom per node. Furthermore, it is noted that the stiffness matrix is not symmetric, see Table 6.4.

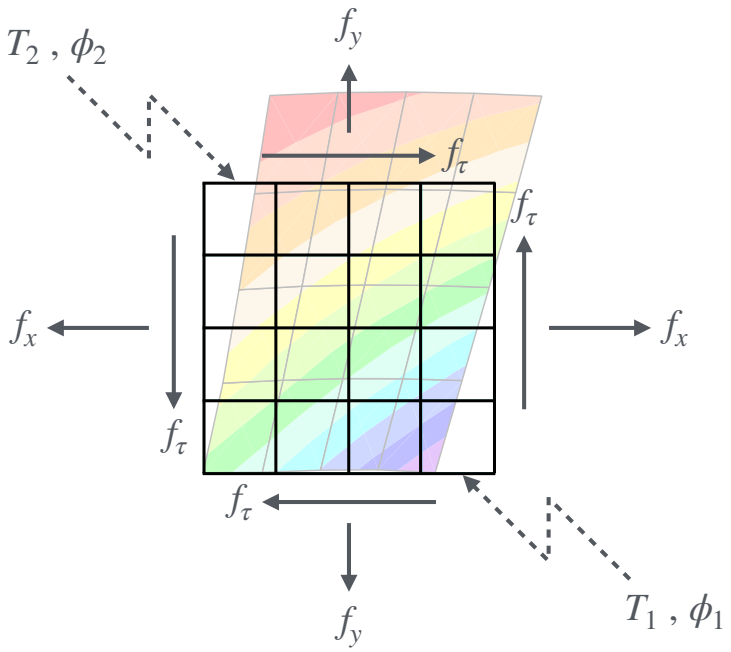

Figure 6.5: Geometry and boundary conditions of a test problem used to compare the exact implementation of the element residual and tangent with a numerical approximation using complex arithmetic. The contour plot in the background represents the x-displacement in the deformed configuration.

and j were arbitrarily chosen. As shown in Table 6.5, the relative error between the complex approximation and the exact result remains on the order of 10^{-15}, indicating that the two implementations agree to within double-precision accuracy, which is consistent with the variable declaration employed for the arrays $\mathbf{R}$ and $\mathbf{K}$. It is therefore concluded that the derivation and implementation of the exact EMTM tangents in Equations (6.198 - 207) are indeed correct.

Residual and Stiffness of the Exact Implementation						
	residual $\mathbf{R}^i$	element stiffness $\mathbf{K}^{ij}$				
		u_1	u_2	θ	ϕ	φ
u_1	2.3050E+03	-4.9767E+04	-4.8231E+04	4.0350E+01	-5.2155E+00	-0.0000E+00
u_2	4.6586E+03	-4.8395E+04	-5.7182E+04	4.2063E+01	-6.7668E+00	-0.0000E+00
θ	1.2500E+02	-0.0000E+00	-0.0000E+00	-3.3333E+00	-0.0000E+00	-0.0000E+00
ϕ	-2.4617E+06	5.8103E+05	7.6489E+05	-0.0000E+00	-4.7955E+02	-0.0000E+00
φ	0.0000E+00	-0.0000E+00	-0.0000E+00	-0.0000E+00	-0.0000E+00	-2.6078E-01

Table 6.4: Example of numerical values for the element residual $\mathbf{R}^i$ and stiffness matrix $\mathbf{K}^{ij}$ associated with variational node $i=1$ and differential node $j=3$ of an interior element of the finite element model depicted in Figure 6.5.

Relative Error between Exact *vs.* Complex Implementation						
	residual $\mathbf{R}^i$	element stiffness $\mathbf{K}^{ij}$				
		u_1	u_2	θ	ϕ	φ
u_1	3.9458E-15	8.7721E-16	7.5429E-16	1.7610E-16	8.5147E-16	NaN
u_2	1.3666E-15	4.5104E-16	6.3621E-16	0.0000E+00	6.5628E-16	NaN
θ	4.5475E-16	NaN	NaN	6.6613E-16	NaN	NaN
ϕ	1.8916E-16	8.0145E-16	7.6100E-16	NaN	5.9267E-16	NaN
φ	NaN	NaN	NaN	NaN	NaN	8.5147E-16

Table 6.5: Relative error between the exact implementation and the complex approximation of $\mathbf{R}^i$ and $\mathbf{K}^{ij}$ listed in Table 6.4. Note that the relative error is undefined for vanishing entries of $\mathbf{R}^i$ and $\mathbf{K}^{ij}$. For all non-zero entries, the error is in the order of machine precision.

Chapter 7

Numerical Implementation of EMTM on Two Scales

The preceding chapter offers a detailed account of the single-scale implementation, including the governing equations and their weak forms, the constitutive model, the boundary conditions, the linearization of the residuals, and the algebraic system of equations resulting from a finite element discretization. Many aspects of the single-scale implementation, such as the residuals and their linearizations, apply identically to the multiscale problem discussed in the present chapter.

The multiscale problem differs from the single-scale model in the following ways: First, the boundary conditions of the microscopic scale (*i.e.*, the RVE) are dictated by the macroscopic gradient quantities. In particular, a DIRICHLET boundary condition is imposed such that the volumetric average of the microscale gradient coincides with the macroscopic gradient. Second, the macroscopic fluxes and material tangents are obtained not from a constitutive model, but from homogenization of the response of the RVE to the aforementioned boundary conditions. Likewise, any volumetric sources on the macroscopic scale are obtained from homogenization of the microscopic counterparts.

Hence, for each iteration of the macroscopic NEWTON-RAPHSON scheme and at each GAUSSIAN quadrature point of the macroscopic problem, a nonlinear RVE model is discretized and solved. The macroscopic gradients are passed to the RVE and applied as boundary conditions. Once the microscopic problem has converged, the homogenized fluxes, volumetric source terms (if applicable), and material tensors are computed at the RVE and returned to the macroscopic problem. This is used to compute the contribution of the given GAUSS point to the macroscopic residual and stiffness matrix according to the expressions derived in Section 6.3.4. After collecting this information from the RVEs at all GAUSS points, the macroscopic system of equations is solved and the NEWTON-RAPHSON scheme proceeds to the next iteration.

This chapter is organized as follows: First, the RVE boundary conditions, which prescribe the primary variables at the DIRICHLET boundary in terms of the macro-

scopic gradient quantities, are introduced. Next, the macroscopic fluxes are expressed by integrals of the microscopic quantities over the RVE volume. This is followed by the linearization of the macroscopic fluxes, from which the material moduli are inferred. Lastly, a range of simple test problems are presented to demonstrate the validity of the numerical implementation of the multiscale model.

7.1 RVE Boundary Conditions

Recall from Section 5.1 that macroscopic and microscopic quantities are denoted by upper- and lowercase superscripts $[\cdot]^{\mathrm{M}}(\mathbf{y},t)$ and $[\cdot]^{\mathrm{m}}(\mathbf{x},t)$, respectively, and depend functionally on the spatial coordinates $\mathbf{y}$ and $\mathbf{x}$. Alternatively, a referential description may be employed using the undeformed macroscopic and microscopic coordinates $\mathbf{Y}$ and $\mathbf{X}$, respectively. The kinematic, thermal, electrostatic, and the magnetostatic Dirichlet boundary conditions of the microscale RVE are determined from the macroscopic variables according to

$$\begin{aligned}
\mathbf{x} &= \mathbf{y} + \mathbf{F}^{\mathrm{M}}\big(\mathbf{X}-\mathbf{X}^{\mathrm{c}}\big) && \text{on} \quad \Gamma_{\mathbf{u}} \quad , \\
\theta^{\mathrm{m}} &= \theta^{\mathrm{M}} + \mathrm{Grad}_{\mathbf{Y}}\,\theta^{\mathrm{M}}\cdot\big(\mathbf{X}-\mathbf{X}^{\mathrm{c}}\big) && \text{on} \quad \Gamma_{\theta} \quad , \\
\phi^{\mathrm{m}} &= \phi^{\mathrm{M}} + \mathrm{Grad}_{\mathbf{Y}}\,\phi^{\mathrm{M}}\cdot\big(\mathbf{X}-\mathbf{X}^{\mathrm{c}}\big) && \text{on} \quad \Gamma_{\phi} \quad , \\
\varphi^{\mathrm{m}} &= \varphi^{\mathrm{M}} + \mathrm{Grad}_{\mathbf{Y}}\,\varphi^{\mathrm{M}}\cdot\big(\mathbf{X}-\mathbf{X}^{\mathrm{c}}\big) && \text{on} \quad \Gamma_{\varphi} \quad ,
\end{aligned} \tag{7.1}$$

respectively, where $\mathbf{X}^{\mathrm{c}}$ represents the location of the centroid of the RVE in the reference configuration. This corresponds to a linear extrapolation of the average (*i.e.*, the macroscopic) field to the boundary. Since $\mathbf{F}^{\mathrm{M}} = \big[\mathbf{I} + \mathrm{Grad}_{\mathbf{Y}}\,\mathbf{u}^{\mathrm{M}}\big]$, Equation $(7.1)_1$ may restated in terms of the displacements $\mathbf{u}^{\mathrm{m}} = \mathbf{x} - \mathbf{X}$ and $\mathbf{u}^{\mathrm{M}} = \mathbf{y} - \mathbf{Y}$ as

$$\mathbf{u}^{\mathrm{m}} = \mathbf{u}^{\mathrm{M}} + \big[\mathrm{Grad}_{\mathbf{Y}}\,\mathbf{u}^{\mathrm{M}}\big]\big(\mathbf{X}-\mathbf{X}^{\mathrm{c}}\big) \quad \text{on} \quad \Gamma_{\mathbf{u}} \quad , \tag{7.2}$$

provided that the RVE center coincides with the macroscopic location, $\mathbf{X}^{\mathrm{c}} = \mathbf{Y}$. The notation in (7.2) is more closely aligned with $(7.1)_{2-4}$.

Equations (7.1) may be regarded as a generalization of the boundary conditions proposed by Kouznetsova *et al.* [63, Equation 8] for the purely mechanical case, which were augmented with a similar thermal condition by Sengupta *et al.* [127, Equation 13]. The conditions in (7.1) ensure that the volume average of the gradient

within the RVE is equal to the macroscopic value, that is,[1]

$$\begin{aligned}
\mathbf{F}^{\mathrm{M}} &= \frac{1}{V_0}\int_{\mathcal{R}_0} \mathbf{F}^{\mathrm{m}}\,\mathrm{d}V^{\mathrm{m}} \quad , \\
\mathrm{Grad}_{\mathbf{Y}}\,\theta^{\mathrm{M}} &= \frac{1}{V_0}\int_{\mathcal{R}_0} \mathrm{Grad}_{\mathbf{X}}\,\theta^{\mathrm{m}}\,\mathrm{d}V^{\mathrm{m}} \quad , \\
\mathrm{Grad}_{\mathbf{Y}}\,\phi^{\mathrm{M}} &= \frac{1}{V_0}\int_{\mathcal{R}_0} \mathrm{Grad}_{\mathbf{X}}\,\phi^{\mathrm{m}}\,\mathrm{d}V^{\mathrm{m}} \quad , \\
\mathrm{Grad}_{\mathbf{Y}}\,\varphi^{\mathrm{M}} &= \frac{1}{V_0}\int_{\mathcal{R}_0} \mathrm{Grad}_{\mathbf{X}}\,\varphi^{\mathrm{m}}\,\mathrm{d}V^{\mathrm{m}} \quad ,
\end{aligned} \tag{7.3}$$

where $V_0 = \int_{\mathcal{R}_0} \mathrm{d}V^{\mathrm{m}}$ denotes the volume of the RVE in the reference configuration. Again, Equation $(7.3)_1$ is equivalently stated in terms of the displacements as

$$\mathrm{Grad}_{\mathbf{Y}}\,\mathbf{u}^{\mathrm{M}} = \frac{1}{V_0}\int_{\mathcal{R}_0} \mathrm{Grad}_{\mathbf{X}}\,\mathbf{u}^{\mathrm{m}}\,\mathrm{d}V^{\mathrm{m}} \quad , \tag{7.4}$$

where $\mathbf{F}^{\mathrm{m}} = \left[\mathbf{I} + \mathrm{Grad}_{\mathbf{X}}\,\mathbf{u}^{\mathrm{m}}\right]$ was used.

The space of admissible solutions, see Equations (6.67 - 70), can be restated for the microscopic problem to explicitly reflect the conditions imposed by (7.1 - 2) on the DIRICHLET boundary of the RVE. For example, the space $\mathcal{U}_{\mathrm{a}}$ of admissible microscopic displacements reads

$$\mathcal{U}_{\mathrm{a}}^{\mathrm{m}} = \left\{ \mathbf{u}^{\mathrm{m}}(\mathbf{x},t) \;:\; \mathcal{R}\times\mathbb{R}\to E^3 \;\middle|\; \begin{array}{lll} \det\left[\mathbf{I}+\dfrac{\partial \mathbf{u}^{\mathrm{m}}}{\partial \mathbf{X}}\right] > 0 & \text{in} & \mathcal{R} \\ u_i^{\mathrm{m}}(\mathbf{x},t) = u_i^{\mathrm{M}} + \dfrac{\partial u_i^{\mathrm{M}}}{\partial Y_A}\left(X_A - Y_A\right) & \text{on} & \Gamma_{u_i} \\ \mathbf{u}^{\mathrm{m}}(\mathbf{X},0) = \mathbf{0} \quad , \quad \dot{\mathbf{u}}^{\mathrm{m}}(\mathbf{X},0) = \mathbf{v}_0^{\mathrm{m}} & \text{in} & \mathcal{R}_0 \end{array} \right\} \quad . \tag{7.5}$$

The spaces $\mathcal{T}_{\mathrm{a}}$, $\mathcal{E}_{\mathrm{a}}$, and $\mathcal{M}_{\mathrm{a}}$ of admissible temperatures, electric potentials, and magnetic potentials are defined analogously. Meanwhile, the definitions for the spaces of admissible virtual displacements $\delta\mathcal{U}_{\mathrm{a}}$, temperatures $\delta\mathcal{T}_{\mathrm{a}}$, electric potentials $\delta\mathcal{E}_{\mathrm{a}}$, and magnetic potentials $\delta\mathcal{M}_{\mathrm{a}}$ remain unchanged. For example, admissible virtual displacements vanish on the DIRICHLET boundary,

$$\delta\mathcal{U}_{\mathrm{a}}^{\mathrm{m}} = \left\{ \delta\mathbf{u}^{\mathrm{m}}(\mathbf{x},t) \;:\; \mathcal{R}\times\mathbb{R}\to E^3 \;\middle|\; \delta u_i^{\mathrm{m}} = 0 \quad \text{on} \quad \Gamma_{u_i} \right\} \quad , \tag{7.6}$$

in accordance with Equation (6.71).

In the context of this implementation, it is assumed that the entire RVE boundary is comprised only of the DIRICHLET type described in (7.1). This forces the primary

[1] This scale transition is discussed in ÖZDEMIR *et al.* [162, Equations 4-8] for the purely thermal problem. Equation $(7.1)_2$ represents the special case where the constraint in [162, Equation 8] is strictly enforced everywhere on the boundary.

quantities to adopt an entirely linear distribution around the RVE boundary which, as observed by MERCER *et al.* [89] for the purely mechanical case, leads to a slight overestimation of the homogenized stiffness of the RVE. Alternatively, LAGRANGE multipliers may be employed to enforce the constraints in $(7.3)_{1-4}$. In conjunction with zero-NEUMANN boundary conditions for the RVE akin to (6.65), the LAGRANGE multipliers effectively impose a traction on the NEUMANN boundary required to satisfy the constraints, see [89, Equation 28].

7.2 Homogenized RVE Response

To solve the IBVP of the macroscopic scale, the homogenized response of the microscale must be quantified at each macroscopic integration point. This requires the RVE to provide two types of quantities to the macroscale: First, the homogenized fluxes (and the volumetric sources, if applicable) are computed by averaging the microscopic quantities over the RVE domain according to the relations derived in Chapter 5. These averaged quantities are subsequently returned to the macroscopic problem, in particular the fluxes $\left\{\mathbf{T}^{\mathrm{M}}, \mathbf{q}^{\mathrm{M}}, \mathbf{p}^{\mathrm{M}}\right\}$.

Second, homogenized material moduli are used in lieu of the constitutive equations. They quantify the response $\left\{\mathrm{d}\mathbf{T}^{\mathrm{M}}, \mathrm{d}\mathbf{q}^{\mathrm{M}}, \mathrm{d}\mathbf{p}^{\mathrm{M}}\right\}$ of the RVE to any changes $\left\{\mathrm{d}\mathbf{u}^{\mathrm{M}}, \mathrm{d}\theta^{\mathrm{M}}, \mathrm{d}\phi^{\mathrm{M}}\right\}$ in the primary variables, akin to the linearized constitutive equations in (6.89). This homogenized response of the RVE is derived in two steps: First, the homogenization formulae for the macroscopic fluxes $\left\{\mathbf{T}^{\mathrm{M}}, \mathbf{q}^{\mathrm{M}}, \mathbf{p}^{\mathrm{M}}\right\}$ are linearized with respect to the microscopic primary variables $\left\{\mathrm{d}\mathbf{u}^{\mathrm{m}}, \mathrm{d}\theta^{\mathrm{m}}, \mathrm{d}\phi^{\mathrm{m}}\right\}$. Upon introducing a finite element discretization, the differentials of the macroscopic fluxes are given in terms of the differentials of the degrees of freedom of the RVE (including the internal and the boundary nodes). Second, the DIRICHLET boundary conditions $(7.1)_{1-4}$ are incorporated into the system of equations, thereby expressing the primary quantities at the boundary nodes in terms of the macroscopic gradient quantities. In conjunction with the RVE system of algebraic equations in (6.190), a linear relationship between $\left\{\mathrm{d}\mathbf{T}^{\mathrm{M}}, \mathrm{d}\mathbf{q}^{\mathrm{M}}, \mathrm{d}\mathbf{p}^{\mathrm{M}}\right\}$ and $\left\{\mathrm{d}\mathbf{u}^{\mathrm{M}}, \mathrm{d}\theta^{\mathrm{M}}, \mathrm{d}\phi^{\mathrm{M}}\right\}$ is derived from a SCHUR complement of the combined system of equations.

This section begins with the homogenization of the RVE fluxes. This is followed by a linearization thereof, which furnishes expressions for $\left\{\mathrm{d}\mathbf{T}^{\mathrm{M}}, \mathrm{d}\mathbf{q}^{\mathrm{M}}, \mathrm{d}\mathbf{p}^{\mathrm{M}}\right\}$ in terms of the microscopic differentials $\left\{\mathrm{d}\mathbf{u}^{\mathrm{m}}, \mathrm{d}\theta^{\mathrm{m}}, \mathrm{d}\phi^{\mathrm{m}}\right\}$. Next, the microscopic differentials are replaced by the nodal degrees of freedom $\left\{\mathrm{d}\hat{\mathbf{u}}^{\mathrm{m}}, \mathrm{d}\hat{\theta}^{\mathrm{m}}, \mathrm{d}\hat{\phi}^{\mathrm{m}}\right\}$ of the finite element approximation. Lastly, the RVE boundary conditions are applied and, in conjunction with the algebraic system of equations of the RVE, the desired relation between $\left\{\mathrm{d}\mathbf{T}^{\mathrm{M}}, \mathrm{d}\mathbf{q}^{\mathrm{M}}, \mathrm{d}\mathbf{p}^{\mathrm{M}}\right\}$ and $\left\{\mathrm{d}\mathbf{u}^{\mathrm{M}}, \mathrm{d}\theta^{\mathrm{M}}, \mathrm{d}\phi^{\mathrm{M}}\right\}$ is obtained.

7.2.1 Homogenization of the Fluxes

Recall that the fluxes $\mathbf{T}^{\mathrm{M}}$, $\mathbf{q}^{\mathrm{M}}$, $\mathbf{p}^{\mathrm{M}}$, and $\mathbf{m}^{\mathrm{M}}$ are homogenized according to Equations (5.45), (5.59), (5.76), and (5.78), respectively. Likewise, the volumetric source terms $\rho^{\mathrm{M}}\mathbf{f}_{\mathrm{B}}^{\mathrm{M}}+\mathbf{f}_{\mathrm{L}}^{\mathrm{M}}$ and $\rho^{\mathrm{M}}r^{\mathrm{M}}+\mathbf{j}^{\mathrm{M}}\cdot\boldsymbol{\mathcal{E}}^{\mathrm{M}}$ are obtained in the macroscopic scale from the homogenizations in (5.46) and (5.60). However, in the context of this implementation it is assumed that volumetric sources are negligible and that both the electric and thermomechanical problems are static. This implies the absence of free charges, currents, or magnetization, and that any velocity fluctuations $\mathbf{v}^{\mathrm{m}}-\mathbf{v}^{\mathrm{M}}$ are negligible. The homogenizations of the fluxes $\mathbf{T}^{\mathrm{M}}$, $\mathbf{q}^{\mathrm{M}}$, and $\mathbf{p}^{\mathrm{M}}$ thus reduce to simple weighted volume averages

$$\begin{aligned}\mathbf{T}^{\mathrm{M}} &= \int_{\mathcal{R}} \mathbf{T}^{\mathrm{m}}\, g(\mathbf{y},\mathbf{x})\,\mathrm{d}v^{\mathrm{m}} \quad ,\\ \mathbf{q}^{\mathrm{M}} &= \int_{\mathcal{R}} \mathbf{q}^{\mathrm{m}}\, g(\mathbf{y},\mathbf{x})\,\mathrm{d}v^{\mathrm{m}} \quad ,\\ \mathbf{p}^{\mathrm{M}} &= \int_{\mathcal{R}} \mathbf{p}^{\mathrm{m}}\, g(\mathbf{y},\mathbf{x})\,\mathrm{d}v^{\mathrm{m}} \quad ,\end{aligned} \tag{7.7}$$

see Equations (5.45), (5.59), and (5.76). The simplest choice for the weighting function is characterized by a uniform step function of the form

$$g(\mathbf{y},\mathbf{x}) = \begin{cases} 1/V & \text{if} \quad \mathbf{x}\in\mathcal{R}_{\mathrm{RVE}} \\ 0 & \text{otherwise} \end{cases} \quad , \tag{7.8}$$

where $\mathcal{R}_{\mathrm{RVE}}\subset\mathcal{R}$ denotes the subregion of $\mathcal{R}$ occupied by the RVE associated with the macroscopic point $\mathbf{y}$, and where V represents the volume of the RVE in the current configuration. In this case, the homogenizations in (7.7) further simplify to

$$\begin{aligned}\mathbf{T}^{\mathrm{M}} &= \frac{1}{V}\int_{\mathcal{R}_{\mathrm{RVE}}} \mathbf{T}^{\mathrm{m}}\,\mathrm{d}v^{\mathrm{m}} \quad ,\\ \mathbf{q}^{\mathrm{M}} &= \frac{1}{V}\int_{\mathcal{R}_{\mathrm{RVE}}} \mathbf{q}^{\mathrm{m}}\,\mathrm{d}v^{\mathrm{m}} \quad ,\\ \mathbf{p}^{\mathrm{M}} &= \frac{1}{V}\int_{\mathcal{R}_{\mathrm{RVE}}} \mathbf{p}^{\mathrm{m}}\,\mathrm{d}v^{\mathrm{m}} \quad .\end{aligned} \tag{7.9}$$

After a given RVE model has solved, the homogenized fluxes in (7.9) are readily computed from a Gaussian quadrature within each element followed by an accumulation over all elements of the RVE mesh divided by the RVE volume.[2] Once returned to the macroscopic scale, this information is used to compute the contribution of the Gauss point associated with the current RVE to the macroscopic residual.

[2]It is mentioned that this summation of element contributions, especially for RVE models comprising a very large number of elements, can lead to an accumulation of round-off errors. A variety of algorithms can be found in the literature to mitigate a potential loss of precision, such as the Kahan summation algorithm, see Higham [48]. Due to the limited number of RVE elements in this dissertation, such strategies are not further pursued here.

7.2.2 Linearization of Homogenization Formulae

In this section, the homogenization formulae for the macroscopic fluxes $\{\mathbf{T}^{\mathrm{M}}, \mathbf{q}^{\mathrm{M}}, \mathbf{p}^{\mathrm{M}}\}$ in Equations $(7.9)_{1-3}$ are linearized with respect to the microscopic primary variables, furnishing a relation between $\{\mathrm{d}\mathbf{T}^{\mathrm{M}}, \mathrm{d}\mathbf{q}^{\mathrm{M}}, \mathrm{d}\mathbf{p}^{\mathrm{M}}\}$ and $\{\mathrm{d}\mathbf{u}^{\mathrm{m}}, \mathrm{d}\theta^{\mathrm{m}}, \mathrm{d}\phi^{\mathrm{m}}\}$.

Stress

The macroscopic CAUCHY stress $(7.9)_1$ is linearized with respect to the microscopic primary quantities $\{\mathbf{u}^{\mathrm{m}}, \theta^{\mathrm{m}}, \phi^{\mathrm{m}}\}$ according to

$$\begin{aligned}
\mathrm{d}\mathbf{T}^{\mathrm{M}} &= \mathrm{d}\Big[\frac{1}{V}\int_{\mathcal{R}_{\mathrm{RVE}}} \mathbf{T}^{\mathrm{m}}\,\mathrm{d}v^{\mathrm{m}}\Big] \\
&= -\frac{\mathrm{d}V}{V^2}\int_{\mathcal{R}_{\mathrm{RVE}}} \mathbf{T}^{\mathrm{m}}\,\mathrm{d}v^{\mathrm{m}} + \frac{1}{V}\,\mathrm{d}\Big[\int_{\mathcal{R}_{\mathrm{RVE}}} \mathbf{T}^{\mathrm{m}}\,\mathrm{d}v^{\mathrm{m}}\Big] \\
&= -\frac{\mathrm{d}V}{V}\,\mathbf{T}^{\mathrm{M}} + \frac{1}{V}\int_{\mathcal{R}_{\mathrm{RVE}0}} \mathrm{d}\big[J^{\mathrm{m}}\mathbf{T}^{\mathrm{m}}\big]\,\mathrm{d}V^{\mathrm{m}} \quad .
\end{aligned} \tag{7.10}$$

The first term on the right side of (7.10) involves the linearization of the RVE volume with respect to the microscopic displacements, and is given by

$$\begin{aligned}
\mathrm{d}V &= \mathrm{d}\Big[\int_{\mathcal{R}_{\mathrm{RVE}}} \mathrm{d}v^{\mathrm{m}}\Big] \\
&= \int_{\mathcal{R}_{\mathrm{RVE}0}} \mathrm{d}J^{\mathrm{m}}\,\mathrm{d}V^{\mathrm{m}} \\
&= \int_{\mathcal{R}_{\mathrm{RVE}}} \mathrm{div}_{\mathbf{x}}\big(\mathrm{d}\mathbf{u}^{\mathrm{m}}\big)\,\mathrm{d}v^{\mathrm{m}} \quad ,
\end{aligned} \tag{7.11}$$

where (2.41), (2.84), and $(6.85)_1$ were used to obtain the identity $\mathrm{d}J = J\mathrm{div}\,\mathrm{d}\mathbf{u}$. The second term on the right side of (7.10) calls for the linearization of the so-called KIRCHHOFF *stress tensor*[3] according to

$$\begin{aligned}
\mathrm{d}\big[J^{\mathrm{m}}\mathbf{T}^{\mathrm{m}}\big] &= \mathrm{d}\big[\mathbf{F}^{\mathrm{m}}\mathbf{S}^{\mathrm{m}}\mathbf{F}^{\mathrm{m}\mathrm{T}}\big] \\
&= \big[\mathrm{Grad}_{\mathbf{X}}\,\mathrm{d}\mathbf{u}^{\mathrm{m}}\big]\mathbf{S}^{\mathrm{m}}\mathbf{F}^{\mathrm{m}\mathrm{T}} + \mathbf{F}^{\mathrm{m}}\mathbf{S}^{\mathrm{m}}\big[\mathrm{Grad}_{\mathbf{X}}\,\mathrm{d}\mathbf{u}^{\mathrm{m}}\big]^{\mathrm{T}} \\
&\quad + \mathbf{F}^{\mathrm{m}}\rho_0^{\mathrm{m}}\mathbb{C}^{\mathrm{m}}\big[\mathbf{F}^{\mathrm{m}\mathrm{T}}\mathrm{Grad}_{\mathbf{X}}\big(\mathrm{d}\mathbf{u}^{\mathrm{m}}\big)\big]^{\mathrm{sym}}\mathbf{F}^{\mathrm{m}\mathrm{T}} \\
&\quad - \mathbf{F}^{\mathrm{m}}\rho_0^{\mathrm{m}}\big[\mathbb{C}\mathbf{A}\big]^{\mathrm{m}}\mathbf{F}^{\mathrm{m}\mathrm{T}}\mathrm{d}\theta^{\mathrm{m}} - \mathbf{F}^{\mathrm{m}}\big[\rho_0^{\mathrm{m}}\mathbf{c}_2^{\mathrm{m}}\mathrm{Grad}_{\mathbf{X}}\big(\mathrm{d}\phi^{\mathrm{m}}\big)\big]\mathbf{F}^{\mathrm{m}\mathrm{T}} \quad ,
\end{aligned} \tag{7.12}$$

[3]The KIRCHHOFF stress tensor is often represented by $\boldsymbol{\tau} = J\mathbf{T}$ in the literature. However, this notation is avoided here because of the same symbol was used in the context of the method of COLEMAN and NOLL, see (4.39) and $(4.48)_1$. The relation between the KIRCHHOFF stress tensor and the second PIOLA-KIRCHHOFF stress tensor $\mathbf{S}$ is readily obtained from (2.149).

where the differentials $\mathrm{d}\mathbf{F}^{\mathrm{m}}$ and $\mathrm{d}\mathbf{S}^{\mathrm{m}}$ are given by Equations $(6.84)_1$ and $(6.89)_2$, respectively. Equation (7.12) is readily converted into spatial form as

$$\begin{aligned}\frac{1}{J^{\mathrm{m}}}\mathrm{d}\big[J^{\mathrm{m}}\mathbf{T}^{\mathrm{m}}\big] \;=\; &\big[\mathrm{grad}_{\mathbf{x}}\,\mathrm{d}\mathbf{u}^{\mathrm{m}}\big]\mathbf{T}^{\mathrm{m}} + \mathbf{T}^{\mathrm{m}}\big[\mathrm{grad}_{\mathbf{x}}\,\mathrm{d}\mathbf{u}^{\mathrm{m}}\big]^{\mathrm{T}} \\ &+ \rho^{\mathrm{m}}\overline{\mathbb{C}}^{\mathrm{m}}\big[\mathrm{grad}_{\mathbf{x}}\big(\mathrm{d}\mathbf{u}^{\mathrm{m}}\big)\big]^{\mathrm{sym}} - \rho^{\mathrm{m}}\overline{\mathbb{C}\mathbf{A}}^{\mathrm{m}}\mathrm{d}\theta^{\mathrm{m}} - \rho^{\mathrm{m}}\overline{\mathfrak{c}}_2^{\mathrm{m}}\,\mathrm{grad}_{\mathbf{x}}\big(\mathrm{d}\phi^{\mathrm{m}}\big) \quad ,\end{aligned} \tag{7.13}$$

where (2.84), (2.137), (2.149), and $(6.62)_{2,4,5}$ were used. The differential of the macroscopic CAUCHY stress (7.10) is therefore expressed as

$$\begin{aligned}\mathrm{d}\mathbf{T}^{\mathrm{M}} \;=\; &-\mathbf{T}^{\mathrm{M}}\frac{1}{V}\int_{\mathcal{R}_{\mathrm{RVE}}}\Big(\frac{\partial}{\partial\mathbf{x}^{\mathrm{m}}}\cdot\mathrm{d}\mathbf{u}^{\mathrm{m}}\Big)\,\mathrm{d}v^{\mathrm{m}} + \frac{1}{V}\int_{\mathcal{R}_{\mathrm{RVE}}}\Big[\frac{\partial\big(\mathrm{d}\mathbf{u}^{\mathrm{m}}\big)}{\partial\mathbf{x}}\Big]\mathbf{T}^{\mathrm{m}}\,\mathrm{d}v^{\mathrm{m}} \\ &+ \frac{1}{V}\int_{\mathcal{R}_{\mathrm{RVE}}}\mathbf{T}^{\mathrm{m}}\Big[\frac{\partial\big(\mathrm{d}\mathbf{u}^{\mathrm{m}}\big)}{\partial\mathbf{x}}\Big]^{\mathrm{T}}\mathrm{d}v^{\mathrm{m}} + \frac{1}{V}\int_{\mathcal{R}_{\mathrm{RVE}}}\rho^{\mathrm{m}}\overline{\mathbb{C}}^{\mathrm{m}}\Big[\frac{\partial\big(\mathrm{d}\mathbf{u}^{\mathrm{m}}\big)}{\partial\mathbf{x}}\Big]\mathrm{d}v^{\mathrm{m}} \\ &- \frac{1}{V}\int_{\mathcal{R}_{\mathrm{RVE}}}\rho^{\mathrm{m}}\overline{\mathbb{C}\mathbf{A}}^{\mathrm{m}}\mathrm{d}\theta^{\mathrm{m}}\,\mathrm{d}v^{\mathrm{m}} - \frac{1}{V}\int_{\mathcal{R}_{\mathrm{RVE}}}\rho^{\mathrm{m}}\overline{\mathfrak{c}}_2^{\mathrm{m}}\Big(\frac{\partial\big(\mathrm{d}\phi^{\mathrm{m}}\big)}{\partial\mathbf{x}}\Big)\mathrm{d}v^{\mathrm{m}} \quad ,\end{aligned} \tag{7.14}$$

where the symmetry operator from Equation (7.13) was dropped on account of the minor symmetry in the third and fourth indices of $\overline{\mathbb{C}}^{\mathrm{m}}$.

Heat Flux

Repeating the procedure in (7.10) for the macroscopic heat flux $(7.9)_2$, its differential is expressed as

$$\mathrm{d}\mathbf{q}^{\mathrm{M}} \;=\; -\frac{\mathrm{d}V}{V}\,\mathbf{q}^{\mathrm{M}} + \frac{1}{V}\int_{\mathcal{R}_{\mathrm{RVE}}}\frac{1}{J^{\mathrm{m}}}\mathrm{d}\big[J^{\mathrm{m}}\mathbf{q}^{\mathrm{m}}\big]\,\mathrm{d}v^{\mathrm{m}} \quad . \tag{7.15}$$

The first term on the right side of (7.15), *i.e.*, the differential of the RVE volume, is again given by (7.11). The second term is obtained using the differentials for $\mathrm{d}\mathbf{F}^{\mathrm{m}}$ and $\mathrm{d}\mathbf{q}_0^{\mathrm{m}}$ in Equations $(6.84)_1$ and $(6.89)_3$,

$$\begin{aligned}\frac{1}{J^{\mathrm{m}}}\,\mathrm{d}\big(J^{\mathrm{m}}\mathbf{q}^{\mathrm{m}}\big) \;&=\; \frac{1}{J^{\mathrm{m}}}\,\mathrm{d}\big(\mathbf{F}^{\mathrm{m}}\mathbf{q}_0^{\mathrm{m}}\big) \\ &=\; \frac{1}{J^{\mathrm{m}}}\big[\mathrm{Grad}_{\mathbf{X}}\,\mathrm{d}\mathbf{u}^{\mathrm{m}}\big]\mathbf{q}_0^{\mathrm{m}} + \frac{1}{J^{\mathrm{m}}}\,\mathbf{F}^{\mathrm{m}}\boldsymbol{\kappa}^{\mathrm{m}}\,\mathrm{Grad}_{\mathbf{X}}\big(\mathrm{d}\theta^{\mathrm{m}}\big) \\ &=\; \big[\mathrm{grad}_{\mathbf{x}}\,\mathrm{d}\mathbf{u}^{\mathrm{m}}\big]\mathbf{q}^{\mathrm{m}} + \overline{\boldsymbol{\kappa}}^{\mathrm{m}}\,\mathrm{grad}_{\mathbf{x}}\big(\mathrm{d}\theta^{\mathrm{m}}\big) \quad ,\end{aligned} \tag{7.16}$$

where Equations (2.84), (2.137), (2.145), and $(6.62)_6$ are employed for the final step in (7.16). Note that, for simplicity, the referential form of FOURIER's law in $(6.56)_3$ is adopted.[4] In view of the preceding results, Equation (7.15) is written in terms of

[4] This implies that the linearization of FOURIER's law is given by Equation $(6.89)_3$ rather than (6.90), hence the thermal differential is uncoupled from the deformation $\mathrm{d}\mathbf{u}$. The choice of FOURIER's law must be consistent with the linearization of the residuals at both scales. Therefore, the corresponding terms in $\mathrm{d}r_\theta$ in Equations (6.95) and (6.182), and consequently the entries $[\mathbf{K}_{\theta\mathbf{u}}]$ and $[\mathbf{K}^{ij}_{\theta\mathbf{u}}]$ of the stiffness matrix $(6.193)_1$ and (6.202), are assumed to vanish.

the differentials of the microscopic primary variables according to

$$\begin{aligned} \mathrm{d}\mathbf{q}^{\mathrm{M}} \;=\; & -\mathbf{q}^{\mathrm{M}}\frac{1}{V}\int_{\mathcal{R}_{\mathrm{RVE}}}\Big(\frac{\partial}{\partial\mathbf{x}^{\mathrm{m}}}\cdot\mathrm{d}\mathbf{u}^{\mathrm{m}}\Big)\,\mathrm{d}v^{\mathrm{m}} + \frac{1}{V}\int_{\mathcal{R}_{\mathrm{RVE}}}\Big[\frac{\partial(\mathrm{d}\mathbf{u}^{\mathrm{m}})}{\partial\mathbf{x}}\Big]\mathbf{q}^{\mathrm{m}}\,\mathrm{d}v^{\mathrm{m}} \\ & - \frac{1}{V}\int_{\mathcal{R}_{\mathrm{RVE}}}\overline{\boldsymbol{\kappa}}^{\mathrm{m}}\Big(\frac{\partial(\mathrm{d}\theta^{\mathrm{m}})}{\partial\mathbf{x}}\Big)\,\mathrm{d}v^{\mathrm{m}} \quad . \end{aligned} \tag{7.17}$$

Polarization

The differential of the macroscopic polarization $\mathbf{p}^{\mathrm{M}}$ is derived using the same approach as in the preceding section for the heat flux $\mathbf{q}^{\mathrm{M}}$. In particular, Equations (2.84), (2.137), $(3.131)_3$, (6.25), $(6.62)_{2,3}$, and (7.11) furnish

$$\begin{aligned} \mathrm{d}\mathbf{p}^{\mathrm{M}} \;=\; & -\frac{\mathrm{d}V}{V}\,\mathbf{p}^{\mathrm{M}} + \frac{1}{V}\int_{\mathcal{R}_{\mathrm{RVE}}}\frac{1}{J^{\mathrm{m}}}\mathrm{d}\big[J^{\mathrm{m}}\mathbf{p}^{\mathrm{m}}\big]\,\mathrm{d}v^{\mathrm{m}} \\ \;=\; & -\mathbf{p}^{\mathrm{M}}\frac{1}{V}\int_{\mathcal{R}_{\mathrm{RVE}}}\Big(\frac{\partial}{\partial\mathbf{x}^{\mathrm{m}}}\cdot\mathrm{d}\mathbf{u}^{\mathrm{m}}\Big)\,\mathrm{d}v^{\mathrm{m}} + \frac{1}{V}\int_{\mathcal{R}_{\mathrm{RVE}}}\Big[\frac{\partial(\mathrm{d}\mathbf{u}^{\mathrm{m}})}{\partial\mathbf{x}}\Big]\mathbf{p}^{\mathrm{m}}\,\mathrm{d}v^{\mathrm{m}} \\ & - \frac{1}{V}\int_{\mathcal{R}_{\mathrm{RVE}}}\big[\rho^{\mathrm{m}}\overline{\mathfrak{c}}_2^{\mathrm{m}}\big]^{\mathrm{T}}\Big[\frac{\partial(\mathrm{d}\mathbf{u}^{\mathrm{m}})}{\partial\mathbf{x}}\Big]\,\mathrm{d}v^{\mathrm{m}} - \frac{1}{V}\int_{\mathcal{R}_{\mathrm{RVE}}}\varepsilon_0\rho^{\mathrm{m}}\overline{\mathbf{c}}_3^{\mathrm{m}}\Big(\frac{\partial(\mathrm{d}\phi^{\mathrm{m}})}{\partial\mathbf{x}}\Big)\,\mathrm{d}v^{\mathrm{m}} \quad , \end{aligned} \tag{7.18}$$

where the symmetry in the first two indices of $\overline{\mathfrak{c}}_2^{\mathrm{m}}$ was used to omit the symmetry operator in $[\mathrm{grad}_{\mathbf{x}}\,\mathrm{d}\mathbf{u}^{\mathrm{m}}]^{\mathrm{sym}}$.

7.2.3 Finite Element Approximation

Equations (7.14), (7.17), and $(7.18)_2$ express $\big\{\mathrm{d}\mathbf{T}^{\mathrm{M}}, \mathrm{d}\mathbf{q}^{\mathrm{M}}, \mathrm{d}\mathbf{p}^{\mathrm{M}}\big\}$ in terms of the differentials of the microscopic primary variables $\big\{\mathrm{d}\mathbf{u}^{\mathrm{m}}, \mathrm{d}\theta^{\mathrm{m}}, \mathrm{d}\phi^{\mathrm{m}}\big\}$. In this section, the finite element discretization of Section 6.3.2 is employed to rewrite the components of $\big\{\mathrm{d}\mathbf{T}^{\mathrm{M}}, \mathrm{d}\mathbf{q}^{\mathrm{M}}, \mathrm{d}\mathbf{p}^{\mathrm{M}}\big\}$, in VOIGT notation, as a set of algebraic equations of the $6n\times 1$ vector[5] of the nodal degrees of freedom of the RVE mesh, $[\mathrm{d}\hat{\mathbf{U}}]$, defined in $(6.186)_2$.

Stress

The differential of the macroscopic CAUCHY stress in Equation (7.14) is discretized by expressing the microscopic primary variables $\big\{\mathrm{d}\mathbf{u}^{\mathrm{m}}, \mathrm{d}\theta^{\mathrm{m}}, \mathrm{d}\phi^{\mathrm{m}}\big\}$ in terms of their finite element approximations in (6.158). In view of the finite element discretization of the

[5] Recall from Section 6.3.2 that n represents the total number of nodes in the global finite element mesh, *i.e.*, the number of nodes of the RVE model. Therefore, the (static) EMTM problem exhibits $6n$ nodal degrees of freedom. This number decreases to $5n$, for example, in the two-dimensional plane-strain case, or to $4n$ in a three-dimensional thermomechanical model. Note that, for the purposes of this derivation, the number n includes internal and boundary nodes alike, because it is assumed that boundary conditions have not yet been enforced.

divergence operator, see Equations (6.174 - 175), the differential of the RVE volume in (7.11) is approximated by the nodal displacement vector of the RVE problem according to

$$\mathrm{d}V \doteq \left[\int_{\mathcal{R}_{\mathrm{RVE}}} \underset{1\times 3n}{\left[\mathbf{B}^{(2)}\right]}\,\mathrm{d}v^{\mathrm{m}}\right] \underset{3n\times 1}{\left[\mathrm{d}\hat{\mathbf{u}}^{\mathrm{m}}\right]} \quad . \tag{7.19}$$

Therefore, Equation (7.14) is expressed as a linear combination of the nodal values according to

$$\begin{aligned}\underset{9\times 1}{\left\langle \mathrm{d}\mathbf{T}^{\mathrm{M}}\right\rangle} \doteq & -\frac{1}{V}\underset{9\times 1}{\left\langle \mathbf{T}^{\mathrm{M}}\right\rangle}\int_{\mathcal{R}_{\mathrm{RVE}}} \underset{1\times 3n}{\left[\mathbf{B}^{(2)}\right]}\,\mathrm{d}v^{\mathrm{m}}\,\underset{3n\times 1}{\left[\mathrm{d}\hat{\mathbf{u}}^{\mathrm{m}}\right]} \\ & + \frac{1}{V}\int_{\mathcal{R}_{\mathrm{RVE}}} 2\underset{9\times 9}{\left\langle \mathbb{I}^{\mathrm{sym}}\right\rangle}\underset{9\times 9}{\left\langle \mathbf{T}\right\rangle^{(2)}}\underset{9\times 3n}{\left[\mathbf{B}^{(3)}\right]}\,\mathrm{d}v^{\mathrm{m}}\,\underset{3n\times 1}{\left[\mathrm{d}\hat{\mathbf{u}}\right]} \\ & + \frac{1}{V}\int_{\mathcal{R}_{\mathrm{RVE}}} \underset{9\times 9}{\left\langle \rho\overline{\mathbb{C}}\right\rangle}\underset{9\times 3n}{\left[\mathbf{B}^{(3)}\right]}\,\mathrm{d}v^{\mathrm{m}}\,\underset{3n\times 1}{\left[\mathrm{d}\hat{\mathbf{u}}\right]} \\ & + \frac{1}{V}\int_{\mathcal{R}_{\mathrm{RVE}}} \underset{9\times 1}{\left\langle \rho\overline{\mathbb{C}\mathbf{A}}\right\rangle}\underset{1\times n}{\left[\mathbf{N}^{(1)}\right]}\,\mathrm{d}v^{\mathrm{m}}\,\underset{n\times 1}{\left[\mathrm{d}\hat{\theta}\right]} \\ & + \frac{1}{V}\int_{\mathcal{R}_{\mathrm{RVE}}} \underset{9\times 3}{\left\langle \rho\overline{\mathfrak{C}}_2\right\rangle}\underset{3\times n}{\left[\mathbf{B}^{(1)}\right]}\,\mathrm{d}v^{\mathrm{m}}\,\underset{n\times 1}{\left[\mathrm{d}\hat{\phi}\right]} \quad . \end{aligned} \tag{7.20}$$

The symmetry of the macroscopic CAUCHY stress $\mathbf{T}^{\mathrm{M}}$, hence also its differential $\mathrm{d}\mathbf{T}^{\mathrm{M}}$ in (7.20), is invoked to employ the reduced VOIGT notation,

$$\underset{6\times 1}{\left\langle \mathrm{d}\mathbf{T}^{\mathrm{M}\,\mathrm{sym}}\right\rangle} = \underset{6\times 9}{\left\langle \mathbb{I}^{\mathrm{sym}}_{(1)}\right\rangle}\underset{9\times 1}{\left\langle \mathrm{d}\mathbf{T}^{\mathrm{M}}\right\rangle} \quad , \tag{7.21}$$

where use was made of the reduced symmetry operator $\left\langle \mathbb{I}^{\mathrm{sym}}_{(1)}\right\rangle$, see (6.123), in accordance with the convention for the representation of shear stresses and strains in (6.127 - 128). It follows that Equation (7.20) reduces to

$$\begin{aligned}\underset{6\times 1}{\left\langle \mathrm{d}\mathbf{T}^{\mathrm{M}\,\mathrm{sym}}\right\rangle} \doteq & -\frac{1}{V}\underset{6\times 1}{\left\langle \mathbf{T}^{\mathrm{M}\,\mathrm{sym}}\right\rangle}\int_{\mathcal{R}_{\mathrm{RVE}}} \underset{1\times 3n}{\left[\mathbf{B}^{(2)}\right]}\,\mathrm{d}v^{\mathrm{m}}\,\underset{3n\times 1}{\left[\mathrm{d}\hat{\mathbf{u}}^{\mathrm{m}}\right]} \\ & + \frac{1}{V}\int_{\mathcal{R}_{\mathrm{RVE}}} 2\underset{6\times 9}{\left\langle \mathbb{I}^{\mathrm{sym}}_{(1)}\right\rangle}\underset{9\times 9}{\left\langle \mathbf{T}\right\rangle^{(2)}}\underset{9\times 3n}{\left[\mathbf{B}^{(3)}\right]}\,\mathrm{d}v^{\mathrm{m}}\,\underset{3n\times 1}{\left[\mathrm{d}\hat{\mathbf{u}}\right]} \\ & + \frac{1}{V}\int_{\mathcal{R}_{\mathrm{RVE}}} \underset{6\times 6}{\left\langle \rho\overline{\mathbb{C}}^{\mathrm{sym}}\right\rangle}\underset{6\times 3n}{\left[\mathbf{B}^{(3)}\right]^{\mathrm{sym}}}\,\mathrm{d}v^{\mathrm{m}}\,\underset{3n\times 1}{\left[\mathrm{d}\hat{\mathbf{u}}\right]} \\ & + \frac{1}{V}\int_{\mathcal{R}_{\mathrm{RVE}}} \underset{6\times 1}{\left\langle \rho\overline{\mathbb{C}\mathbf{A}}^{\mathrm{sym}}\right\rangle}\underset{1\times n}{\left[\mathbf{N}^{(1)}\right]}\,\mathrm{d}v^{\mathrm{m}}\,\underset{n\times 1}{\left[\mathrm{d}\hat{\theta}\right]} \\ & + \frac{1}{V}\int_{\mathcal{R}_{\mathrm{RVE}}} \underset{6\times 3}{\left\langle \rho\overline{\mathfrak{C}}^{\mathrm{sym}}_2\right\rangle}\underset{3\times n}{\left[\mathbf{B}^{(1)}\right]}\,\mathrm{d}v^{\mathrm{m}}\,\underset{n\times 1}{\left[\mathrm{d}\hat{\phi}\right]} \quad , \end{aligned} \tag{7.22}$$

where the properties in (6.122), (6.130), and (6.133) were used.

Heat Flux

The preceding derivation is repeated for the discretization of the differential of the macroscopic heat flux in Equation (7.17). In view of the finite element approximations in (6.158) and (7.19), $\mathrm{d}\mathbf{q}^{\mathrm{M}}$ can be expressed as

$$\begin{aligned}\underset{3\times1}{\left(\mathrm{d}\mathbf{q}^{\mathrm{M}}\right)} \doteq & -\frac{1}{V}\underset{3\times1}{\left(\mathbf{q}^{\mathrm{M}}\right)}\int_{\mathcal{R}_{\mathrm{RVE}}}\underset{1\times3n}{\left[\mathbf{B}^{(2)}\right]}\,\mathrm{d}v^{\mathrm{m}}\,\underset{3n\times1}{\left[\mathrm{d}\hat{\mathbf{u}}^{\mathrm{m}}\right]}\\ & + \frac{1}{V}\int_{\mathcal{R}_{\mathrm{RVE}}}\underset{3\times9}{\left\langle\,\mathbf{q}\,\right\rangle^{(3)}}\underset{9\times3n}{\left[\mathbf{B}^{(3)}\right]}\,\mathrm{d}v^{\mathrm{m}}\,\underset{3n\times1}{\left[\mathrm{d}\hat{\mathbf{u}}\right]}\\ & - \frac{1}{V}\int_{\mathcal{R}_{\mathrm{RVE}}}\underset{3\times3}{\left[\overline{\boldsymbol{\kappa}}\right]}\underset{3\times n}{\left[\mathbf{B}^{(1)}\right]}\,\mathrm{d}v^{\mathrm{m}}\,\underset{n\times1}{\left[\mathrm{d}\hat{\theta}\right]}\quad,\end{aligned}\tag{7.23}$$

where the notation in (6.109) was used.

Polarization

Following the same method, the discretization of the differential of the macroscopic polarization in Equation (7.18) is approximated by a finite element discretization according to

$$\begin{aligned}\underset{3\times1}{\left(\mathrm{d}\mathbf{p}^{\mathrm{M}}\right)} \doteq & -\frac{1}{V}\underset{3\times1}{\left(\mathbf{p}^{\mathrm{M}}\right)}\int_{\mathcal{R}_{\mathrm{RVE}}}\underset{1\times3n}{\left[\mathbf{B}^{(2)}\right]}\,\mathrm{d}v^{\mathrm{m}}\,\underset{3n\times1}{\left[\mathrm{d}\hat{\mathbf{u}}^{\mathrm{m}}\right]}\\ & + \frac{1}{V}\int_{\mathcal{R}_{\mathrm{RVE}}}\underset{3\times9}{\left\langle\,\mathbf{p}\,\right\rangle^{(3)}}\underset{9\times3n}{\left[\mathbf{B}^{(3)}\right]}\,\mathrm{d}v^{\mathrm{m}}\,\underset{3n\times1}{\left[\mathrm{d}\hat{\mathbf{u}}\right]}\\ & - \frac{1}{V}\int_{\mathcal{R}_{\mathrm{RVE}}}\underset{3\times9}{\left\langle\rho\overline{\mathbf{c}}_2\right\rangle^{\mathrm{T}}}\underset{9\times3n}{\left[\mathbf{B}^{(3)}\right]}\,\mathrm{d}v^{\mathrm{m}}\,\underset{3n\times1}{\left[\mathrm{d}\hat{\mathbf{u}}\right]}\\ & - \frac{1}{V}\int_{\mathcal{R}_{\mathrm{RVE}}}\underset{3\times3}{\left[\varepsilon_0\rho\overline{\mathbf{c}}_3\right]}\underset{3\times n}{\left[\mathbf{B}^{(1)}\right]}\,\mathrm{d}v^{\mathrm{m}}\,\underset{n\times1}{\left[\mathrm{d}\hat{\phi}\right]}\quad.\end{aligned}\tag{7.24}$$

The symmetry of $\overline{\mathbf{c}}_2$ in the first two indices can be exploited to write the third term on the right-hand-side of (7.24) in reduced VOIGT notation.

Global Homogenization Matrix

The preceding results form a system of algebraic equations, where the differentials of the macroscopic fluxes are given by a linear combination of the differentials of the primary variables of the microscale RVE. This algebraic system is conveniently

expressed according to

$$\underbrace{\begin{bmatrix} \underset{6\times 3n}{\left[\mathbf{H}_{\mathbf{T}\mathbf{u}}\right]} & \underset{6\times n}{\left[\mathbf{H}_{\mathbf{T}\theta}\right]} & \underset{6\times n}{\left[\mathbf{H}_{\mathbf{T}\phi}\right]} & \underset{6\times n}{\left[\mathbf{H}_{\mathbf{T}\varphi}\right]} \\ \underset{3\times 3n}{\left[\mathbf{H}_{\mathbf{q}\mathbf{u}}\right]} & \underset{3\times n}{\left[\mathbf{H}_{\mathbf{q}\theta}\right]} & \underset{3\times n}{\left[\mathbf{H}_{\mathbf{q}\phi}\right]} & \underset{3\times n}{\left[\mathbf{H}_{\mathbf{q}\varphi}\right]} \\ \underset{3\times 3n}{\left[\mathbf{H}_{\mathbf{p}\mathbf{u}}\right]} & \underset{3\times n}{\left[\mathbf{H}_{\mathbf{p}\theta}\right]} & \underset{3\times n}{\left[\mathbf{H}_{\mathbf{p}\phi}\right]} & \underset{3\times n}{\left[\mathbf{H}_{\mathbf{p}\varphi}\right]} \\ \underset{3\times 3n}{\left[\mathbf{H}_{\boldsymbol{\mathcal{M}}\mathbf{u}}\right]} & \underset{3\times n}{\left[\mathbf{H}_{\boldsymbol{\mathcal{M}}\theta}\right]} & \underset{3\times n}{\left[\mathbf{H}_{\boldsymbol{\mathcal{M}}\phi}\right]} & \underset{3\times n}{\left[\mathbf{H}_{\boldsymbol{\mathcal{M}}\varphi}\right]} \end{bmatrix}}_{\underset{15\times 6n}{\left[\mathbf{H}\right]}} \underbrace{\begin{bmatrix} \underset{3n\times 1}{\left[\mathrm{d}\hat{\mathbf{u}}\right]} \\ \underset{n\times 1}{\left[\mathrm{d}\hat{\theta}\right]} \\ \underset{n\times 1}{\left[\mathrm{d}\hat{\phi}\right]} \\ \underset{n\times 1}{\left[\mathrm{d}\hat{\varphi}\right]} \end{bmatrix}}_{\underset{6n\times 1}{\left[\mathrm{d}\hat{\mathbf{U}}\right]}} = \underbrace{\begin{bmatrix} \underset{6\times 1}{\left[\mathrm{d}\mathbf{T}^{\mathrm{M}}\right]} \\ \underset{3\times 1}{\left[\mathrm{d}\mathbf{q}^{\mathrm{M}}\right]} \\ \underset{3\times 1}{\left[\mathrm{d}\mathbf{p}^{\mathrm{M}}\right]} \\ \underset{3\times 1}{\left[\mathrm{d}\boldsymbol{\mathcal{M}}^{\mathrm{M}}\right]} \end{bmatrix}}_{\underset{15\times 1}{\left[\mathrm{d}\hat{\mathbf{T}}^{\mathrm{M}}\right]}} \quad . \tag{7.25}$$

Note the similarity of (7.25) with the global finite element equations in (6.190), where the stiffness matrix $[\mathbf{K}]$ operates on the $6n$ nodal degrees of freedom of the RVE problem, represented by $\mathrm{d}\hat{\mathbf{U}}$. The matrix $[\mathbf{H}]$ will be subsequently referred to as the (global) *homogenization matrix*, and its $15\times 6n$ entries are deduced from Equations (7.22 - 24). In particular, it is readily seen that the first row of $[\mathbf{H}]$ is given by

$$\begin{aligned}
\underset{6\times 3n}{\left[\mathbf{H}_{\mathbf{T}\mathbf{u}}\right]} &= -\frac{1}{V}\underset{6\times 1}{\left\langle \mathbf{T}^{\mathrm{M}\,\mathrm{sym}}\right\rangle}\int_{\mathcal{R}_{\mathrm{RVE}}}\underset{1\times 3n}{\left[\mathbf{B}^{(2)}\right]}\,\mathrm{d}v^{\mathrm{m}} + \frac{1}{V}\int_{\mathcal{R}_{\mathrm{RVE}}} 2\underset{6\times 9}{\left\langle \mathbb{I}_{(1)}^{\mathrm{sym}}\right\rangle}\underset{9\times 9}{\left\langle \mathbf{T}\right\rangle^{(2)}}\underset{9\times 3n}{\left[\mathbf{B}^{(3)}\right]}\,\mathrm{d}v^{\mathrm{m}} \\
&\quad + \frac{1}{V}\int_{\mathcal{R}_{\mathrm{RVE}}}\underset{6\times 6}{\left\langle \rho\overline{\mathbb{C}}^{\mathrm{sym}}\right\rangle}\underset{6\times 3n}{\left[\mathbf{B}^{(3)}\right]^{\mathrm{sym}}}\,\mathrm{d}v^{\mathrm{m}} \quad , \\
\underset{6\times n}{\left[\mathbf{H}_{\mathbf{T}\theta}\right]} &= \frac{1}{V}\int_{\mathcal{R}_{\mathrm{RVE}}}\underset{6\times 1}{\left\langle \rho\overline{\mathbb{C}\mathbf{A}}^{\mathrm{sym}}\right\rangle}\underset{1\times n}{\left[\mathbf{N}^{(1)}\right]}\,\mathrm{d}v^{\mathrm{m}} \quad , \\
\underset{6\times n}{\left[\mathbf{H}_{\mathbf{T}\phi}\right]} &= \frac{1}{V}\int_{\mathcal{R}_{\mathrm{RVE}}}\underset{6\times 3}{\left\langle \rho\overline{\mathbf{c}}_2^{\mathrm{sym}}\right\rangle}\underset{3\times n}{\left[\mathbf{B}^{(1)}\right]}\,\mathrm{d}v^{\mathrm{m}} \quad , \\
\underset{6\times n}{\left[\mathbf{H}_{\mathbf{T}\varphi}\right]} &= \mathbf{0} \quad .
\end{aligned} \tag{7.26}$$

Likewise, the second row of $[\mathbf{H}]$ is obtained from (7.23) as

$$\begin{aligned}
\underset{3\times 3n}{\left[\mathbf{H}_{\mathbf{q}\mathbf{u}}\right]} &= -\frac{1}{V}\underset{3\times 1}{\left(\mathbf{q}^{\mathrm{M}}\right)}\int_{\mathcal{R}_{\mathrm{RVE}}}\underset{1\times 3n}{\left[\mathbf{B}^{(2)}\right]}\,\mathrm{d}v^{\mathrm{m}} + \frac{1}{V}\int_{\mathcal{R}_{\mathrm{RVE}}}\underset{3\times 9}{\left\langle \mathbf{q}\right\rangle^{(3)}}\underset{9\times 3n}{\left[\mathbf{B}^{(3)}\right]}\,\mathrm{d}v^{\mathrm{m}} \quad , \\
\underset{3\times n}{\left[\mathbf{H}_{\mathbf{q}\theta}\right]} &= -\frac{1}{V}\int_{\mathcal{R}_{\mathrm{RVE}}}\underset{3\times 3}{\left[\overline{\boldsymbol{\kappa}}\right]}\underset{3\times n}{\left[\mathbf{B}^{(1)}\right]}\,\mathrm{d}v^{\mathrm{m}} \quad , \\
\underset{3\times n}{\left[\mathbf{H}_{\mathbf{q}\phi}\right]} &= \mathbf{0} \quad , \\
\underset{3\times n}{\left[\mathbf{H}_{\mathbf{q}\varphi}\right]} &= \mathbf{0} \quad ,
\end{aligned} \tag{7.27}$$

and the third row of $[\mathbf{H}]$ is determined by (7.24) as

$$\begin{aligned}
\underset{3\times 3n}{\big[\mathbf{H}_{\mathbf{pu}}\big]} &= -\frac{1}{V}\underset{3\times 1}{\big(\mathbf{p}^{\mathrm{M}}\big)}\int_{\mathcal{R}_{\mathrm{RVE}}}\underset{1\times 3n}{\big[\mathbf{B}^{(2)}\big]}\,\mathrm{d}v^{\mathrm{m}} + \frac{1}{V}\int_{\mathcal{R}_{\mathrm{RVE}}}\underset{3\times 9}{\big\langle\,\mathbf{p}\,\big\rangle^{(3)}}\underset{9\times 3n}{\big[\mathbf{B}^{(3)}\big]}\,\mathrm{d}v^{\mathrm{m}} \\
&\quad - \frac{1}{V}\int_{\mathcal{R}_{\mathrm{RVE}}}\underset{3\times 9}{\big\langle\rho\overline{\mathbf{c}}_2\big\rangle^{\mathrm{T}}}\underset{9\times 3n}{\big[\mathbf{B}^{(3)}\big]}\,\mathrm{d}v^{\mathrm{m}} \qquad , \\
\underset{3\times n}{\big[\mathbf{H}_{\mathbf{p}\theta}\big]} &= \mathbf{0} \qquad , \\
\underset{3\times n}{\big[\mathbf{H}_{\mathbf{p}\phi}\big]} &= -\frac{1}{V}\int_{\mathcal{R}_{\mathrm{RVE}}}\underset{3\times 3}{\big[\varepsilon_0\rho\overline{\mathbf{c}}_3\big]}\underset{3\times n}{\big[\mathbf{B}^{(1)}\big]}\,\mathrm{d}v^{\mathrm{m}} \qquad , \\
\underset{3\times n}{\big[\mathbf{H}_{\mathbf{p}\varphi}\big]} &= \mathbf{0} \qquad .
\end{aligned} \tag{7.28}$$

Lastly, the fourth row of $[\mathbf{H}]$ is zero, given that the material is assumed to be non-magnetizable.

Nodal Homogenization Matrix

Similarly to the nodal residual and stiffness matrix derived in Section 6.3.4, the algebraic system of equations in (7.25) may be expressed by a sum of the contributions of each node,

$$\sum_{j=1}^{n}\underbrace{\begin{bmatrix}
\underset{6\times 3}{\big[\mathbf{H}^j_{\mathbf{Tu}}\big]} & \underset{6\times 1}{\big[\mathbf{H}^j_{\mathbf{T}\theta}\big]} & \underset{6\times 1}{\big[\mathbf{H}^j_{\mathbf{T}\phi}\big]} & \underset{6\times 1}{\big[\mathbf{0}\big]} \\
\underset{3\times 3}{\big[\mathbf{H}^j_{\mathbf{qu}}\big]} & \underset{3\times 1}{\big[\mathbf{H}^j_{\mathbf{q}\theta}\big]} & \underset{3\times 1}{\big[\mathbf{0}\big]} & \underset{3\times 1}{\big[\mathbf{0}\big]} \\
\underset{3\times 3}{\big[\mathbf{H}^j_{\mathbf{pu}}\big]} & \underset{3\times 1}{\big[\mathbf{0}\big]} & \underset{3\times 1}{\big[\mathbf{H}^j_{\mathbf{p}\phi}\big]} & \underset{3\times 1}{\big[\mathbf{0}\big]} \\
\underset{3\times 3}{\big[\mathbf{0}\big]} & \underset{3\times 1}{\big[\mathbf{0}\big]} & \underset{3\times 1}{\big[\mathbf{0}\big]} & \underset{3\times 1}{\big[\mathbf{0}\big]}
\end{bmatrix}}_{\underset{15\times 6}{\big[\mathbf{H}^j\big]}}\underbrace{\begin{bmatrix}
\underset{3\times 1}{\big[\mathrm{d}\hat{\mathbf{u}}^j\big]} \\
\underset{1\times 1}{\big[\mathrm{d}\hat{\theta}^j\big]} \\
\underset{1\times 1}{\big[\mathrm{d}\hat{\phi}^j\big]} \\
\underset{1\times 1}{\big[\mathrm{d}\hat{\varphi}^j\big]}
\end{bmatrix}}_{\underset{6\times 1}{\big[\mathrm{d}\hat{\mathbf{U}}^j\big]}} = \underbrace{\begin{bmatrix}
\underset{6\times 1}{\big[\mathrm{d}\mathbf{T}^{\mathrm{M}}\big]} \\
\underset{3\times 1}{\big[\mathrm{d}\mathbf{q}^{\mathrm{M}}\big]} \\
\underset{3\times 1}{\big[\mathrm{d}\mathbf{p}^{\mathrm{M}}\big]} \\
\underset{3\times 1}{\big[\mathrm{d}\boldsymbol{\mathcal{M}}^{\mathrm{M}}\big]}
\end{bmatrix}}_{\underset{15\times 1}{\big[\mathrm{d}\hat{\mathbf{T}}^{\mathrm{M}}\big]}} . \tag{7.29}$$

The element-wise entries in the 15×6 matrix $[\mathbf{H}^j]$ are given as

$$\begin{aligned}
\underset{6\times 3}{\big[\mathbf{H}^j_{\mathbf{Tu}}\big]} &= -\frac{1}{V}\underset{6\times 1}{\big\langle\mathbf{T}^{\mathrm{M}\mathrm{sym}}\big\rangle}\int_{\mathcal{R}_{\mathrm{RVE}}}\underset{1\times 3}{\big[\mathbf{B}^{(2)}_j\big]}\,\mathrm{d}v^{\mathrm{m}} + \frac{1}{V}\int_{\mathcal{R}_{\mathrm{RVE}}}2\underset{6\times 9}{\big\langle\mathbb{I}^{\mathrm{sym}}_{(1)}\big\rangle}\underset{9\times 9}{\big\langle\mathbf{T}\big\rangle^{(2)}}\underset{9\times 3}{\big[\mathbf{B}^{(3)}_j\big]}\,\mathrm{d}v^{\mathrm{m}} \\
&\quad + \frac{1}{V}\int_{\mathcal{R}_{\mathrm{RVE}}}\underset{6\times 6}{\big\langle\rho\overline{\mathbb{C}}^{\mathrm{sym}}\big\rangle}\underset{6\times 3}{\big[\mathbf{B}^{(3)}_j\big]^{\mathrm{sym}}}\,\mathrm{d}v^{\mathrm{m}}
\end{aligned}$$

$$
\begin{aligned}
&= -\frac{1}{V}\begin{bmatrix} T^{\mathrm{M}}_{11} \\ T^{\mathrm{M}}_{22} \\ T^{\mathrm{M}}_{33} \\ \frac{1}{2}\left(T^{\mathrm{M}}_{12}+T^{\mathrm{M}}_{21}\right) \\ \frac{1}{2}\left(T^{\mathrm{M}}_{23}+T^{\mathrm{M}}_{32}\right) \\ \frac{1}{2}\left(T^{\mathrm{M}}_{31}+T^{\mathrm{M}}_{13}\right) \end{bmatrix} \int_{\mathcal{R}_{\mathrm{RVE}}} \begin{bmatrix} N_{j,1} & N_{j,2} & N_{j,3} \end{bmatrix} \mathrm{d}v^{\mathrm{m}} \\
&\quad + \frac{1}{V}\int_{\mathcal{R}_{\mathrm{RVE}}} \begin{bmatrix} 2T_{i1}N_{j,i} & 0 & 0 \\ 0 & 2T_{i2}N_{j,i} & 0 \\ 0 & 0 & 2T_{i3}N_{j,i} \\ T_{i2}N_{j,i} & T_{i1}N_{j,i} & 0 \\ 0 & T_{i3}N_{j,i} & T_{i2}N_{j,i} \\ T_{i3}N_{j,i} & 0 & T_{i1}N_{j,i} \end{bmatrix} \mathrm{d}v^{\mathrm{m}} \\
&\quad + \frac{1}{V}\int_{\mathcal{R}_{\mathrm{RVE}}} \rho \begin{bmatrix} \overline{\mathbb{C}}_{1111} & \overline{\mathbb{C}}_{1122} & \overline{\mathbb{C}}_{1133} & \overline{\mathbb{C}}_{1112} & \overline{\mathbb{C}}_{1123} & \overline{\mathbb{C}}_{1131} \\ \overline{\mathbb{C}}_{2211} & \overline{\mathbb{C}}_{2222} & \overline{\mathbb{C}}_{2233} & \overline{\mathbb{C}}_{2212} & \overline{\mathbb{C}}_{2223} & \overline{\mathbb{C}}_{2231} \\ \overline{\mathbb{C}}_{3311} & \overline{\mathbb{C}}_{3322} & \overline{\mathbb{C}}_{3333} & \overline{\mathbb{C}}_{3312} & \overline{\mathbb{C}}_{3323} & \overline{\mathbb{C}}_{3331} \\ \overline{\mathbb{C}}_{1211} & \overline{\mathbb{C}}_{1222} & \overline{\mathbb{C}}_{1233} & \overline{\mathbb{C}}_{1212} & \overline{\mathbb{C}}_{1223} & \overline{\mathbb{C}}_{1231} \\ \overline{\mathbb{C}}_{2311} & \overline{\mathbb{C}}_{2322} & \overline{\mathbb{C}}_{2333} & \overline{\mathbb{C}}_{2312} & \overline{\mathbb{C}}_{2323} & \overline{\mathbb{C}}_{2331} \\ \overline{\mathbb{C}}_{3111} & \overline{\mathbb{C}}_{3122} & \overline{\mathbb{C}}_{3133} & \overline{\mathbb{C}}_{3112} & \overline{\mathbb{C}}_{3123} & \overline{\mathbb{C}}_{3131} \end{bmatrix} \begin{bmatrix} N_{j,1} & 0 & 0 \\ 0 & N_{j,2} & 0 \\ 0 & 0 & N_{j,3} \\ N_{j,2} & N_{j,1} & 0 \\ 0 & N_{j,3} & N_{j,2} \\ N_{j,3} & 0 & N_{j,1} \end{bmatrix} \mathrm{d}v^{\mathrm{m}} \quad , \qquad (7.30)
\end{aligned}
$$

$$
\underset{6\times 1}{\left[\mathbf{H}^{j}_{\mathbf{T}\theta}\right]} = \frac{1}{V}\int_{\mathcal{R}_{\mathrm{RVE}}} \underset{6\times 1}{\left\langle \rho \overline{\mathbb{C}\mathbf{A}}^{\mathrm{sym}} \right\rangle} \underset{1\times 1}{N_j}\, \mathrm{d}v^{\mathrm{m}} \quad , \qquad (7.31)
$$

$$
\begin{aligned}
\underset{6\times 1}{\left[\mathbf{H}^{j}_{\mathbf{T}\phi}\right]} &= \frac{1}{V}\int_{\mathcal{R}_{\mathrm{RVE}}} \underset{6\times 3}{\left\langle \rho \overline{\mathbb{C}}^{\mathrm{sym}}_{2} \right\rangle} \underset{3\times 1}{\left[\mathbf{B}^{(1)}_{j}\right]} \mathrm{d}v^{\mathrm{m}} \\
&= \frac{1}{V}\int_{\mathcal{R}_{\mathrm{RVE}}} \rho \begin{bmatrix} \overline{\mathbb{C}}_{111} & \overline{\mathbb{C}}_{112} & \overline{\mathbb{C}}_{113} \\ \overline{\mathbb{C}}_{221} & \overline{\mathbb{C}}_{222} & \overline{\mathbb{C}}_{223} \\ \overline{\mathbb{C}}_{331} & \overline{\mathbb{C}}_{332} & \overline{\mathbb{C}}_{333} \\ \overline{\mathbb{C}}_{121} & \overline{\mathbb{C}}_{122} & \overline{\mathbb{C}}_{123} \\ \overline{\mathbb{C}}_{231} & \overline{\mathbb{C}}_{232} & \overline{\mathbb{C}}_{233} \\ \overline{\mathbb{C}}_{311} & \overline{\mathbb{C}}_{312} & \overline{\mathbb{C}}_{313} \end{bmatrix} \begin{bmatrix} N_{j,1} \\ N_{j,2} \\ N_{j,3} \end{bmatrix} \mathrm{d}v^{\mathrm{m}} \quad , \qquad (7.32)
\end{aligned}
$$

$$
\begin{aligned}
\underset{3\times 3}{\left[\mathbf{H}^{j}_{\mathbf{qu}}\right]} &= -\frac{1}{V}\underset{3\times 1}{\left(\mathbf{q}^{\mathrm{M}}\right)} \int_{\mathcal{R}_{\mathrm{RVE}}} \underset{1\times 3}{\left[\mathbf{B}^{(2)}_{j}\right]} \mathrm{d}v^{\mathrm{m}} + \frac{1}{V}\int_{\mathcal{R}_{\mathrm{RVE}}} \underset{3\times 9}{\left\langle \mathbf{q} \right\rangle^{(3)}} \underset{9\times 3}{\left[\mathbf{B}^{(3)}_{j}\right]} \mathrm{d}v^{\mathrm{m}} \\
&= -\frac{1}{V}\begin{bmatrix} q^{\mathrm{M}}_{1} \\ q^{\mathrm{M}}_{2} \\ q^{\mathrm{M}}_{3} \end{bmatrix} \int_{\mathcal{R}_{\mathrm{RVE}}} \begin{bmatrix} N_{j,1} & N_{j,2} & N_{j,3} \end{bmatrix} \mathrm{d}v^{\mathrm{m}} \\
&\quad + \frac{1}{V}\int_{\mathcal{R}_{\mathrm{RVE}}} \left(\begin{bmatrix} q_1 & q_2 & q_3 \end{bmatrix} \begin{bmatrix} N_{j,1} \\ N_{j,2} \\ N_{j,3} \end{bmatrix} \right) \mathrm{d}v^{\mathrm{m}} \underset{3\times 3}{\left[\mathbf{I}\right]} \quad , \qquad (7.33)
\end{aligned}
$$

$$\begin{aligned}
\underset{3\times1}{\left[\,\mathbf{H}^{j}_{\mathbf{q}\theta}\,\right]} &= -\frac{1}{V}\int_{\mathcal{R}_{\mathrm{RVE}}} \underset{3\times3}{\left[\,\overline{\boldsymbol{\kappa}}\,\right]}\,\underset{3\times1}{\left[\,\mathbf{B}^{(1)}_{j}\,\right]}\,\mathrm{d}v^{\mathrm{m}} \\
&= -\frac{1}{V}\int_{\mathcal{R}_{\mathrm{RVE}}} \begin{bmatrix} \overline{\kappa}_{11} & \overline{\kappa}_{12} & \overline{\kappa}_{31} \\ \overline{\kappa}_{12} & \overline{\kappa}_{22} & \overline{\kappa}_{23} \\ \overline{\kappa}_{31} & \overline{\kappa}_{23} & \overline{\kappa}_{33} \end{bmatrix} \begin{bmatrix} N_{j,1} \\ N_{j,2} \\ N_{j,3} \end{bmatrix} \mathrm{d}v^{\mathrm{m}} \quad , \qquad (7.34)
\end{aligned}$$

$$\begin{aligned}
\underset{3\times3}{\left[\,\mathbf{H}^{j}_{\mathbf{pu}}\,\right]} &= -\frac{1}{V}\underset{3\times1}{\left(\mathbf{p}^{\mathrm{M}}\right)}\int_{\mathcal{R}_{\mathrm{RVE}}} \underset{1\times3}{\left[\,\mathbf{B}^{(2)}_{j}\,\right]}\,\mathrm{d}v^{\mathrm{m}} + \frac{1}{V}\int_{\mathcal{R}_{\mathrm{RVE}}} \underset{3\times9}{\left\langle\,\mathbf{p}\,\right\rangle^{(3)}}\underset{9\times3}{\left[\,\mathbf{B}^{(3)}_{j}\,\right]}\,\mathrm{d}v^{\mathrm{m}} \\
&\quad - \frac{1}{V}\int_{\mathcal{R}_{\mathrm{RVE}}} \underset{3\times6}{\left\langle\,\rho\overline{\mathfrak{C}}^{\mathrm{sym}}_{2}\,\right\rangle^{\mathrm{T}}}\underset{6\times3}{\left[\,\mathbf{B}^{(3)}_{j}\,\right]^{\mathrm{sym}}}\,\mathrm{d}v^{\mathrm{m}} \\
&= -\frac{1}{V}\begin{bmatrix} p^{\mathrm{M}}_{1} \\ p^{\mathrm{M}}_{2} \\ p^{\mathrm{M}}_{3} \end{bmatrix}\int_{\mathcal{R}_{\mathrm{RVE}}} \begin{bmatrix} N_{j,1} & N_{j,2} & N_{j,3} \end{bmatrix}\mathrm{d}v^{\mathrm{m}} \\
&\quad + \frac{1}{V}\int_{\mathcal{R}_{\mathrm{RVE}}} \left(\begin{bmatrix} p_1 & p_2 & p_3 \end{bmatrix} \begin{bmatrix} N_{j,1} \\ N_{j,2} \\ N_{j,3} \end{bmatrix} \right) \mathrm{d}v^{\mathrm{m}}\,\underset{3\times3}{\left[\,\mathbf{I}\,\right]} \\
&\quad - \frac{1}{V}\int_{\mathcal{R}_{\mathrm{RVE}}} \rho \begin{bmatrix} \overline{\mathfrak{C}}_{111} & \overline{\mathfrak{C}}_{221} & \overline{\mathfrak{C}}_{331} & \overline{\mathfrak{C}}_{121} & \overline{\mathfrak{C}}_{231} & \overline{\mathfrak{C}}_{311} \\ \overline{\mathfrak{C}}_{112} & \overline{\mathfrak{C}}_{222} & \overline{\mathfrak{C}}_{332} & \overline{\mathfrak{C}}_{122} & \overline{\mathfrak{C}}_{232} & \overline{\mathfrak{C}}_{312} \\ \overline{\mathfrak{C}}_{113} & \overline{\mathfrak{C}}_{223} & \overline{\mathfrak{C}}_{333} & \overline{\mathfrak{C}}_{123} & \overline{\mathfrak{C}}_{233} & \overline{\mathfrak{C}}_{313} \end{bmatrix} \begin{bmatrix} N_{j,1} & 0 & 0 \\ 0 & N_{j,2} & 0 \\ 0 & 0 & N_{j,3} \\ N_{j,2} & N_{j,1} & 0 \\ 0 & N_{j,3} & N_{j,2} \\ N_{j,3} & 0 & N_{j,1} \end{bmatrix} \mathrm{d}v^{\mathrm{m}} \quad , \qquad (7.35)
\end{aligned}$$

$$\begin{aligned}
\underset{3\times1}{\left[\,\mathbf{H}^{j}_{\mathbf{p}\phi}\,\right]} &= -\frac{1}{V}\int_{\mathcal{R}_{\mathrm{RVE}}} \underset{3\times3}{\left[\,\varepsilon_0\rho\overline{\mathbf{c}}_{3}\,\right]}\,\underset{3\times1}{\left[\,\mathbf{B}^{(1)}_{j}\,\right]}\,\mathrm{d}v^{\mathrm{m}} \\
&= -\frac{1}{V}\int_{\mathcal{R}_{\mathrm{RVE}}} \varepsilon_0\rho \begin{bmatrix} \overline{\mathbf{c}}_{11} & \overline{\mathbf{c}}_{12} & \overline{\mathbf{c}}_{31} \\ \overline{\mathbf{c}}_{12} & \overline{\mathbf{c}}_{22} & \overline{\mathbf{c}}_{23} \\ \overline{\mathbf{c}}_{31} & \overline{\mathbf{c}}_{23} & \overline{\mathbf{c}}_{33} \end{bmatrix} \begin{bmatrix} N_{j,1} \\ N_{j,2} \\ N_{j,3} \end{bmatrix} \mathrm{d}v^{\mathrm{m}} \quad . \qquad (7.36)
\end{aligned}$$

The remaining entries in the element homogenization matrix $[\,\mathbf{H}^{j}\,]$ are zero, as indicated in Equation (7.29).

7.2.4 Homogenized Material Moduli

Recall that the homogenized response of the RVE serves as constitutive model for the macroscopic material, whose behavior is governed by its microstructure. The RVE not only furnishes the homogenized fluxes $\mathbf{T}^{\mathrm{M}}$, $\mathbf{q}^{\mathrm{M}}$, $\mathbf{p}^{\mathrm{M}}$, and $\boldsymbol{\mathcal{M}}^{\mathrm{M}}$, but also the material moduli[6] such as $\overline{\mathfrak{c}}_2$, $\overline{\mathbf{c}}_3$, $\overline{\mathbf{C}}$, and $\overline{\mathbf{CA}}$.

[6]The reader is reminded that the overline accent, such as in $\overline{\mathfrak{c}}_2$, signifies that the material moduli are expressed in spatial form. They are related to their referential counterparts, for example $\mathfrak{c}_2$, via

In the preceding section, the differentials $\mathrm{d}\mathbf{T}^{\mathrm{M}}$, $\mathrm{d}\mathbf{q}^{\mathrm{M}}$, $\mathrm{d}\mathbf{p}^{\mathrm{M}}$, and $\mathrm{d}\boldsymbol{\mathcal{M}}^{\mathrm{M}}$ of the macroscopic fluxes were expressed in terms of the $6n \times 1$ vector $[\mathrm{d}\hat{\mathbf{U}}]$ of the nodal degrees of freedom of the RVE mesh, see $(6.186)_2$. The corresponding algebraic system of Equations (7.25) is governed by the $15 \times 6n$ global homogenization matrix $[\mathbf{H}]$. In order to extract homogenized tangent moduli from the RVE, a direct relationship must be established between the aforementioned differentials of the macroscopic fluxes and the differentials of the macroscopic primary variables, $\mathrm{d}\mathbf{u}^{\mathrm{M}}$, $\mathrm{d}\theta^{\mathrm{M}}$, $\mathrm{d}\phi^{\mathrm{M}}$, and $\mathrm{d}\varphi^{\mathrm{M}}$.

This is achieved as follows: First, the DIRICHLET boundary conditions in (7.1) are converted into differential form. This furnishes a relation between $\mathrm{d}\mathbf{u}^{\mathrm{m}}$, $\mathrm{d}\theta^{\mathrm{m}}$, $\mathrm{d}\phi^{\mathrm{m}}$, and $\mathrm{d}\varphi^{\mathrm{m}}$ on the RVE boundary and their macroscopic counterparts. Next, these boundary conditions are applied to the global finite element equations in (6.190) as well as the global algebraic system for the homogenization of the RVE in (7.25). This separates the internal degrees of freedom of the RVE equations from the DIRICHLET boundary nodes. Lastly, the desired relation between the fluxes $\mathrm{d}\mathbf{T}^{\mathrm{M}}$, $\mathrm{d}\mathbf{q}^{\mathrm{M}}$, $\mathrm{d}\mathbf{p}^{\mathrm{M}}$, and $\mathrm{d}\boldsymbol{\mathcal{M}}^{\mathrm{M}}$ and the primary variables $\mathrm{d}\mathbf{u}^{\mathrm{M}}$, $\mathrm{d}\theta^{\mathrm{M}}$, $\mathrm{d}\phi^{\mathrm{M}}$, and $\mathrm{d}\varphi^{\mathrm{M}}$ is extracted from the ensuing system of equations by means of a SCHUR complement.

Differential Form of the Boundary Conditions

The DIRICHLET boundary conditions for the RVE in Equations (7.1) are restated in differential form as

$$\begin{aligned}
\mathrm{d}\mathbf{u}^{\mathrm{m}} &= \mathrm{d}\mathbf{F}^{\mathrm{M}} \cdot \mathbf{X} && \text{on} \quad \Gamma_{\mathbf{u}} \quad , \\
\mathrm{d}\theta^{\mathrm{m}} &= \mathrm{d}\theta^{\mathrm{M}} + \mathrm{Grad}_{\mathbf{Y}}\, \mathrm{d}\theta^{\mathrm{M}} \cdot \mathbf{X} && \text{on} \quad \Gamma_{\theta} \quad , \\
\mathrm{d}\phi^{\mathrm{m}} &= \mathrm{Grad}_{\mathbf{Y}}\, \mathrm{d}\phi^{\mathrm{M}} \cdot \mathbf{X} && \text{on} \quad \Gamma_{\phi} \quad , \\
\mathrm{d}\varphi^{\mathrm{m}} &= \mathrm{Grad}_{\mathbf{Y}}\, \mathrm{d}\varphi^{\mathrm{M}} \cdot \mathbf{X} && \text{on} \quad \Gamma_{\varphi} \quad .
\end{aligned} \tag{7.37}$$

Here, the centroid of the undeformed RVE is assumed to be located at the origin. Furthermore, the absolute values of the displacement, electric potential, and magnetic potential are neglected because, according to the constitutive model outlined in Section 6.1.2, they do not affect the resulting fluxes. Only their gradients are needed to determine the corresponding material response. The temperature, however, *does* affect the fluxes via thermal expansion (and, possibly, via a temperature dependence of the material parameters). For this reason, the term $\mathrm{d}\theta^{\mathrm{M}}$ is retained in Equation $(7.37)_2$.

Distinction Between Interior and Boundary Nodes

Any incremental change $\mathrm{d}\mathbf{u}^{\mathrm{M}}$, $\mathrm{d}\theta^{\mathrm{M}}$, $\mathrm{d}\phi^{\mathrm{M}}$, and $\mathrm{d}\varphi^{\mathrm{M}}$ in the macroscopic primary variables is imparted on the RVE via the boundary nodes according to Equations (7.37). These boundary conditions are not yet explicitly accounted for in the global finite

a contravariant push-forward operation according to Equations (6.30).

element equations of the RVE in (6.190) as well as the homogenization in (7.25). To do so, the $6n \times 1$ vector of nodal degrees of freedom $[\mathrm{d}\hat{\mathbf{U}}]$ is split into the interior nodes $[\mathrm{d}\hat{\mathbf{U}}^{\mathrm{int}}]$ and boundary nodes $[\mathrm{d}\hat{\mathbf{U}}^{\mathrm{ext}}]$. The linear algebraic system of equations for the global finite element problem reduces to $6n^{\mathrm{int}}$ equations for the degrees of freedom of the interior nodes of the RVE, given by

$$\underbrace{\begin{bmatrix} \underset{3n^{\mathrm{int}}\times 3n^{\mathrm{int}}}{[\mathbf{K}^{\mathrm{int}}_{\mathbf{uu}}]} & \underset{3n^{\mathrm{int}}\times n^{\mathrm{int}}}{[\mathbf{K}^{\mathrm{int}}_{\mathbf{u}\theta}]} & \underset{3n^{\mathrm{int}}\times n^{\mathrm{int}}}{[\mathbf{K}^{\mathrm{int}}_{\mathbf{u}\phi}]} & \underset{3n^{\mathrm{int}}\times n^{\mathrm{int}}}{[\mathbf{K}^{\mathrm{int}}_{\mathbf{u}\varphi}]} \\ \underset{n^{\mathrm{int}}\times 3n^{\mathrm{int}}}{[\mathbf{K}^{\mathrm{int}}_{\theta\mathbf{u}}]} & \underset{n^{\mathrm{int}}\times n^{\mathrm{int}}}{[\mathbf{K}^{\mathrm{int}}_{\theta\theta}]} & \underset{n^{\mathrm{int}}\times n^{\mathrm{int}}}{[\mathbf{K}^{\mathrm{int}}_{\theta\phi}]} & \underset{n^{\mathrm{int}}\times n^{\mathrm{int}}}{[\mathbf{K}^{\mathrm{int}}_{\theta\varphi}]} \\ \underset{n^{\mathrm{int}}\times 3n^{\mathrm{int}}}{[\mathbf{K}^{\mathrm{int}}_{\phi\mathbf{u}}]} & \underset{n^{\mathrm{int}}\times n^{\mathrm{int}}}{[\mathbf{K}^{\mathrm{int}}_{\phi\theta}]} & \underset{n^{\mathrm{int}}\times n^{\mathrm{int}}}{[\mathbf{K}^{\mathrm{int}}_{\phi\phi}]} & \underset{n^{\mathrm{int}}\times n^{\mathrm{int}}}{[\mathbf{K}^{\mathrm{int}}_{\phi\varphi}]} \\ \underset{n^{\mathrm{int}}\times 3n^{\mathrm{int}}}{[\mathbf{K}^{\mathrm{int}}_{\varphi\mathbf{u}}]} & \underset{n^{\mathrm{int}}\times n^{\mathrm{int}}}{[\mathbf{K}^{\mathrm{int}}_{\varphi\theta}]} & \underset{n^{\mathrm{int}}\times n^{\mathrm{int}}}{[\mathbf{K}^{\mathrm{int}}_{\varphi\phi}]} & \underset{n^{\mathrm{int}}\times n^{\mathrm{int}}}{[\mathbf{K}^{\mathrm{int}}_{\varphi\varphi}]} \end{bmatrix}}_{\underset{6n^{\mathrm{int}}\times 6n^{\mathrm{int}}}{[\mathbf{K}^{\mathrm{int}}]}} \underbrace{\begin{bmatrix} \underset{3n^{\mathrm{int}}\times 1}{[\mathrm{d}\hat{\mathbf{u}}^{\mathrm{int}}]} \\ \underset{n^{\mathrm{int}}\times 1}{[\mathrm{d}\hat{\theta}^{\mathrm{int}}]} \\ \underset{n^{\mathrm{int}}\times 1}{[\mathrm{d}\hat{\phi}^{\mathrm{int}}]} \\ \underset{n^{\mathrm{int}}\times 1}{[\mathrm{d}\hat{\varphi}^{\mathrm{int}}]} \end{bmatrix}}_{\underset{6n^{\mathrm{int}}\times 1}{[\mathrm{d}\hat{\mathbf{U}}^{\mathrm{int}}]}}$$

$$+ \underbrace{\begin{bmatrix} \underset{3n^{\mathrm{int}}\times 3n^{\mathrm{ext}}}{[\mathbf{K}^{\mathrm{ext}}_{\mathbf{uu}}]} & \underset{3n^{\mathrm{int}}\times n^{\mathrm{ext}}}{[\mathbf{K}^{\mathrm{ext}}_{\mathbf{u}\theta}]} & \underset{3n^{\mathrm{int}}\times n^{\mathrm{ext}}}{[\mathbf{K}^{\mathrm{ext}}_{\mathbf{u}\phi}]} & \underset{3n^{\mathrm{int}}\times n^{\mathrm{ext}}}{[\mathbf{K}^{\mathrm{ext}}_{\mathbf{u}\varphi}]} \\ \underset{n^{\mathrm{int}}\times 3n^{\mathrm{ext}}}{[\mathbf{K}^{\mathrm{ext}}_{\theta\mathbf{u}}]} & \underset{n^{\mathrm{int}}\times n^{\mathrm{ext}}}{[\mathbf{K}^{\mathrm{ext}}_{\theta\theta}]} & \underset{n^{\mathrm{int}}\times n^{\mathrm{ext}}}{[\mathbf{K}^{\mathrm{ext}}_{\theta\phi}]} & \underset{n^{\mathrm{int}}\times n^{\mathrm{ext}}}{[\mathbf{K}^{\mathrm{ext}}_{\theta\varphi}]} \\ \underset{n^{\mathrm{int}}\times 3n^{\mathrm{ext}}}{[\mathbf{K}^{\mathrm{ext}}_{\phi\mathbf{u}}]} & \underset{n^{\mathrm{int}}\times n^{\mathrm{ext}}}{[\mathbf{K}^{\mathrm{ext}}_{\phi\theta}]} & \underset{n^{\mathrm{int}}\times n^{\mathrm{ext}}}{[\mathbf{K}^{\mathrm{ext}}_{\phi\phi}]} & \underset{n^{\mathrm{int}}\times n^{\mathrm{ext}}}{[\mathbf{K}^{\mathrm{ext}}_{\phi\varphi}]} \\ \underset{n^{\mathrm{int}}\times 3n^{\mathrm{ext}}}{[\mathbf{K}^{\mathrm{ext}}_{\varphi\mathbf{u}}]} & \underset{n^{\mathrm{int}}\times n^{\mathrm{ext}}}{[\mathbf{K}^{\mathrm{ext}}_{\varphi\theta}]} & \underset{n^{\mathrm{int}}\times n^{\mathrm{ext}}}{[\mathbf{K}^{\mathrm{ext}}_{\varphi\phi}]} & \underset{n^{\mathrm{int}}\times n^{\mathrm{ext}}}{[\mathbf{K}^{\mathrm{ext}}_{\varphi\varphi}]} \end{bmatrix}}_{\underset{6n^{\mathrm{int}}\times 6n^{\mathrm{ext}}}{[\mathbf{K}^{\mathrm{ext}}]}} \underbrace{\begin{bmatrix} \underset{3n^{\mathrm{ext}}\times 1}{[\mathrm{d}\hat{\mathbf{u}}^{\mathrm{ext}}]} \\ \underset{n^{\mathrm{ext}}\times 1}{[\mathrm{d}\hat{\theta}^{\mathrm{ext}}]} \\ \underset{n^{\mathrm{ext}}\times 1}{[\mathrm{d}\hat{\phi}^{\mathrm{ext}}]} \\ \underset{n^{\mathrm{ext}}\times 1}{[\mathrm{d}\hat{\varphi}^{\mathrm{ext}}]} \end{bmatrix}}_{\underset{6n^{\mathrm{ext}}\times 1}{[\mathrm{d}\hat{\mathbf{U}}^{\mathrm{ext}}]}} = \underbrace{\begin{bmatrix} \underset{3n^{\mathrm{int}}\times 1}{[\mathbf{R}^{\mathrm{int}}_{\mathbf{u}}]} \\ \underset{n^{\mathrm{int}}\times 1}{[\mathbf{R}^{\mathrm{int}}_{\theta}]} \\ \underset{n^{\mathrm{int}}\times 1}{[\mathbf{R}^{\mathrm{int}}_{\phi}]} \\ \underset{n^{\mathrm{int}}\times 1}{[\mathbf{R}^{\mathrm{int}}_{\varphi}]} \end{bmatrix}}_{\underset{6n^{\mathrm{int}}\times 1}{[\mathbf{R}^{\mathrm{int}}]}} . \tag{7.38}$$

The remaining $6n^{\mathrm{ext}}$ equations of the extended finite element system in (6.190), typically used to compute nodal reaction forces associated with the DIRICHLET boundary via a SCHUR complement, are not needed in the context of this derivation and are thus discarded. Note that the extended $6n \times 6n$ stiffness matrix $[\mathbf{K}]$ is typically singular. Only after enforcing appropriate DIRICHLET boundary conditions akin to (7.38) does the linear algebraic system yield a unique solution. This implies that the reduced matrix $[\mathbf{K}^{\mathrm{int}}]$ is invertible. It is further noted that, during each iteration of the macroscopic problem, the RVE model is first solved using the boundary displacements (7.1) at the current macroscopic values of $\mathbf{u}^{\mathrm{M}}$, θ^{M}, ϕ^{M}, and φ^{M} before homogenization is performed. Hence, by the time homogenization is performed, the residual vector $[\mathbf{R}^{\mathrm{int}}]$ vanishes since the NEWTON-RAPHSON scheme of the RVE problem has converged. The global system of Equations (7.38) thus reads

$$\underset{6n^{\mathrm{int}}\times 6n^{\mathrm{int}}}{[\mathbf{K}^{\mathrm{int}}]} \; \underset{6n^{\mathrm{int}}\times 1}{[\mathrm{d}\hat{\mathbf{U}}^{\mathrm{int}}]} + \underset{6n^{\mathrm{int}}\times 6n^{\mathrm{ext}}}{[\mathbf{K}^{\mathrm{ext}}]} \; \underset{6n^{\mathrm{ext}}\times 1}{[\mathrm{d}\hat{\mathbf{U}}^{\mathrm{ext}}]} = \underset{6n^{\mathrm{int}}\times 1}{[\mathbf{0}]} \quad . \tag{7.39}$$

Meanwhile, the linear algebraic system of Equations (7.25) associated with the linearization of the homogenization formulae for the macroscopic fluxes is restated as

$$\underbrace{\begin{bmatrix} \underset{6\times 3n^{\text{int}}}{\left[\mathbf{H}^{\text{int}}_{\mathbf{Tu}}\right]} & \underset{6\times n^{\text{int}}}{\left[\mathbf{H}^{\text{int}}_{\mathbf{T}\theta}\right]} & \underset{6\times n^{\text{int}}}{\left[\mathbf{H}^{\text{int}}_{\mathbf{T}\phi}\right]} & \underset{6\times n^{\text{int}}}{\left[\mathbf{H}^{\text{int}}_{\mathbf{T}\varphi}\right]} \\ \underset{3\times 3n^{\text{int}}}{\left[\mathbf{H}^{\text{int}}_{\mathbf{qu}}\right]} & \underset{3\times n^{\text{int}}}{\left[\mathbf{H}^{\text{int}}_{\mathbf{q}\theta}\right]} & \underset{3\times n^{\text{int}}}{\left[\mathbf{H}^{\text{int}}_{\mathbf{q}\phi}\right]} & \underset{3\times n^{\text{int}}}{\left[\mathbf{H}^{\text{int}}_{\mathbf{q}\varphi}\right]} \\ \underset{3\times 3n^{\text{int}}}{\left[\mathbf{H}^{\text{int}}_{\mathbf{pu}}\right]} & \underset{3\times n^{\text{int}}}{\left[\mathbf{H}^{\text{int}}_{\mathbf{p}\theta}\right]} & \underset{3\times n^{\text{int}}}{\left[\mathbf{H}^{\text{int}}_{\mathbf{p}\phi}\right]} & \underset{3\times n^{\text{int}}}{\left[\mathbf{H}^{\text{int}}_{\mathbf{p}\varphi}\right]} \\ \underset{3\times 3n^{\text{int}}}{\left[\mathbf{H}^{\text{int}}_{\boldsymbol{\mathcal{M}}\mathbf{u}}\right]} & \underset{3\times n^{\text{int}}}{\left[\mathbf{H}^{\text{int}}_{\boldsymbol{\mathcal{M}}\theta}\right]} & \underset{3\times n^{\text{int}}}{\left[\mathbf{H}^{\text{int}}_{\boldsymbol{\mathcal{M}}\phi}\right]} & \underset{3\times n^{\text{int}}}{\left[\mathbf{H}^{\text{int}}_{\boldsymbol{\mathcal{M}}\varphi}\right]} \end{bmatrix}}_{\underset{15\times 6n^{\text{int}}}{\left[\mathbf{H}^{\text{int}}\right]}} \underbrace{\begin{bmatrix} \underset{3n^{\text{int}}\times 1}{\left[\mathrm{d}\hat{\mathbf{u}}^{\text{int}}\right]} \\ \underset{n^{\text{int}}\times 1}{\left[\mathrm{d}\hat{\theta}^{\text{int}}\right]} \\ \underset{n^{\text{int}}\times 1}{\left[\mathrm{d}\hat{\phi}^{\text{int}}\right]} \\ \underset{n^{\text{int}}\times 1}{\left[\mathrm{d}\hat{\varphi}^{\text{int}}\right]} \end{bmatrix}}_{\underset{6n^{\text{int}}\times 1}{\left[\mathrm{d}\hat{\mathbf{U}}^{\text{int}}\right]}}$$

$$+ \underbrace{\begin{bmatrix} \underset{6\times 3n^{\text{ext}}}{\left[\mathbf{H}^{\text{ext}}_{\mathbf{Tu}}\right]} & \underset{6\times n^{\text{ext}}}{\left[\mathbf{H}^{\text{ext}}_{\mathbf{T}\theta}\right]} & \underset{6\times n^{\text{ext}}}{\left[\mathbf{H}^{\text{ext}}_{\mathbf{T}\phi}\right]} & \underset{6\times n^{\text{ext}}}{\left[\mathbf{H}^{\text{ext}}_{\mathbf{T}\varphi}\right]} \\ \underset{3\times 3n^{\text{ext}}}{\left[\mathbf{H}^{\text{ext}}_{\mathbf{qu}}\right]} & \underset{3\times n^{\text{ext}}}{\left[\mathbf{H}^{\text{ext}}_{\mathbf{q}\theta}\right]} & \underset{3\times n^{\text{ext}}}{\left[\mathbf{H}^{\text{ext}}_{\mathbf{q}\phi}\right]} & \underset{3\times n^{\text{ext}}}{\left[\mathbf{H}^{\text{ext}}_{\mathbf{q}\varphi}\right]} \\ \underset{3\times 3n^{\text{ext}}}{\left[\mathbf{H}^{\text{ext}}_{\mathbf{pu}}\right]} & \underset{3\times n^{\text{ext}}}{\left[\mathbf{H}^{\text{ext}}_{\mathbf{p}\theta}\right]} & \underset{3\times n^{\text{ext}}}{\left[\mathbf{H}^{\text{ext}}_{\mathbf{p}\phi}\right]} & \underset{3\times n^{\text{ext}}}{\left[\mathbf{H}^{\text{ext}}_{\mathbf{p}\varphi}\right]} \\ \underset{3\times 3n^{\text{ext}}}{\left[\mathbf{H}^{\text{ext}}_{\boldsymbol{\mathcal{M}}\mathbf{u}}\right]} & \underset{3\times n^{\text{ext}}}{\left[\mathbf{H}^{\text{ext}}_{\boldsymbol{\mathcal{M}}\theta}\right]} & \underset{3\times n^{\text{ext}}}{\left[\mathbf{H}^{\text{ext}}_{\boldsymbol{\mathcal{M}}\phi}\right]} & \underset{3\times n^{\text{ext}}}{\left[\mathbf{H}^{\text{ext}}_{\boldsymbol{\mathcal{M}}\varphi}\right]} \end{bmatrix}}_{\underset{15\times 6n^{\text{ext}}}{\left[\mathbf{H}^{\text{ext}}\right]}} \underbrace{\begin{bmatrix} \underset{3n^{\text{ext}}\times 1}{\left[\mathrm{d}\hat{\mathbf{u}}^{\text{ext}}\right]} \\ \underset{n^{\text{ext}}\times 1}{\left[\mathrm{d}\hat{\theta}^{\text{ext}}\right]} \\ \underset{n^{\text{ext}}\times 1}{\left[\mathrm{d}\hat{\phi}^{\text{ext}}\right]} \\ \underset{n^{\text{ext}}\times 1}{\left[\mathrm{d}\hat{\varphi}^{\text{ext}}\right]} \end{bmatrix}}_{\underset{6n^{\text{ext}}\times 1}{\left[\mathrm{d}\hat{\mathbf{U}}^{\text{ext}}\right]}} = \underbrace{\begin{bmatrix} \underset{6\times 1}{\left[\mathrm{d}\mathbf{T}^{\text{M}}\right]} \\ \underset{3\times 1}{\left[\mathrm{d}\mathbf{q}^{\text{M}}\right]} \\ \underset{3\times 1}{\left[\mathrm{d}\mathbf{p}^{\text{M}}\right]} \\ \underset{3\times 1}{\left[\mathrm{d}\boldsymbol{\mathcal{M}}^{\text{M}}\right]} \end{bmatrix}}_{\underset{15\times 1}{\left[\mathrm{d}\hat{\mathbf{T}}^{\text{M}}\right]}} . \tag{7.40}$$

Unlike (7.39), which represents a reduced form of the linear algebraic system of Equations (6.189), the expression in (7.40) is entirely analogous to the 15 equations given by (7.25). Equations (7.39 - 40) are restated more compactly as

$$\begin{bmatrix} \underset{6n^{\text{int}}\times 6n^{\text{int}}}{\left[\mathbf{K}^{\text{int}}\right]} & \underset{6n^{\text{int}}\times 6n^{\text{ext}}}{\left[\mathbf{K}^{\text{ext}}\right]} \\ \underset{15\times 6n^{\text{int}}}{\left[\mathbf{H}^{\text{int}}\right]} & \underset{15\times 6n^{\text{ext}}}{\left[\mathbf{H}^{\text{ext}}\right]} \end{bmatrix} \begin{bmatrix} \underset{6n^{\text{int}}\times 1}{\left[\mathrm{d}\hat{\mathbf{U}}^{\text{int}}\right]} \\ \underset{6n^{\text{ext}}\times 1}{\left[\mathrm{d}\hat{\mathbf{U}}^{\text{ext}}\right]} \end{bmatrix} = \begin{bmatrix} \underset{6n^{\text{int}}\times 1}{\left[\mathbf{0}\right]} \\ \underset{15\times 1}{\left[\mathrm{d}\hat{\mathbf{T}}^{\text{M}}\right]} \end{bmatrix} , \tag{7.41}$$

since both equations involve the $6n \times 1$ vector of nodal degrees of freedom $[\mathrm{d}\hat{\mathbf{U}}]$ comprised of the internal and the boundary nodes.

Enforcement of the Boundary Conditions

According to the boundary conditions for the RVE, given in differential form by (7.37), the degrees of freedom $[\mathrm{d}\hat{\mathbf{U}}^{\text{ext}}]$ of the boundary nodes are determined from their referential position $\mathbf{X}$ in conjunction with the gradients of the macroscopic primary variables $\mathrm{d}\mathbf{F}^{\text{M}}$, $\mathrm{Grad}_{\mathbf{Y}}\,\mathrm{d}\theta^{\text{M}}$, $\mathrm{Grad}_{\mathbf{Y}}\,\mathrm{d}\phi^{\text{M}}$, and $\mathrm{Grad}_{\mathbf{Y}}\,\mathrm{d}\varphi^{\text{M}}$, as well as the macroscopic temperature $\mathrm{d}\theta^{\text{M}}$. The matrix-vector products associated with $[\mathbf{K}^{\text{ext}}]$ and $[\mathbf{H}^{\text{ext}}]$ in (7.41)

can thus be reformulated in terms of the macroscopic primary variables. The system of equations in (7.41) is rewritten as

$$\begin{bmatrix} \underset{6n^{\mathrm{int}}\times 6n^{\mathrm{int}}}{\left[\hat{\mathbf{K}}\right]} & \underset{6n^{\mathrm{int}}\times 19}{\left[\hat{\mathbf{G}}_1\right]} \\ \underset{15\times 6n^{\mathrm{int}}}{\left[\hat{\mathbf{G}}_2\right]} & \underset{15\times 19}{\left[\hat{\mathbf{H}}\right]} \end{bmatrix} \begin{bmatrix} \underset{6n^{\mathrm{int}}\times 1}{\left[\mathrm{d}\hat{\mathbf{U}}^{\mathrm{int}}\right]} \\ \underset{19\times 1}{\left[\mathrm{d}\hat{\mathbf{F}}^{\mathrm{M}}\right]} \end{bmatrix} = \begin{bmatrix} \underset{6n^{\mathrm{int}}\times 1}{\left[\mathbf{0}\right]} \\ \underset{15\times 1}{\left[\mathrm{d}\hat{\mathbf{T}}^{\mathrm{M}}\right]} \end{bmatrix} \quad , \tag{7.42}$$

where, for convenience, the sub-matrices in the first column on the left-hand side of (7.41) were renamed in (7.42), that is,

$$\begin{aligned} \left[\hat{\mathbf{K}}\right] &= \left[\mathbf{K}^{\mathrm{int}}\right] \quad , \\ \left[\hat{\mathbf{G}}_2\right] &= \left[\mathbf{H}^{\mathrm{int}}\right] \quad . \end{aligned} \tag{7.43}$$

Meanwhile, a 19×1 vector $[\mathrm{d}\hat{\mathbf{F}}^{\mathrm{M}}]$ was defined for the macroscopic primary (gradient) quantities according to

$$\underset{19\times 1}{\left[\mathrm{d}\hat{\mathbf{F}}^{\mathrm{M}}\right]} = \begin{bmatrix} \underset{9\times 1}{\left[\mathrm{d}\mathbf{F}^{\mathrm{M}}\right]} \\ \underset{1\times 1}{\left[\mathrm{d}\theta^{\mathrm{M}}\right]} \\ \underset{3\times 1}{\left[\mathrm{Grad}_{\mathbf{Y}}\,\mathrm{d}\theta^{\mathrm{M}}\right]} \\ \underset{3\times 1}{\left[\mathrm{Grad}_{\mathbf{Y}}\,\mathrm{d}\phi^{\mathrm{M}}\right]} \\ \underset{3\times 1}{\left[\mathrm{Grad}_{\mathbf{Y}}\,\mathrm{d}\varphi^{\mathrm{M}}\right]} \end{bmatrix} \quad . \tag{7.44}$$

The entries in the matrices $[\hat{\mathbf{G}}_1]$ and $[\hat{\mathbf{H}}]$ of the second column on the left-hand side of (7.42) are obtained from a comparison between Equations (7.42 - 41). In particular, $[\hat{\mathbf{G}}_1]$ is deduced from the relation

$$\underset{6n^{\mathrm{int}}\times 6n^{\mathrm{ext}}}{\left[\mathbf{K}^{\mathrm{ext}}\right]} \underset{6n^{\mathrm{ext}}\times 1}{\left[\mathrm{d}\hat{\mathbf{U}}^{\mathrm{ext}}\right]} = \underset{6n^{\mathrm{int}}\times 19}{\left[\hat{\mathbf{G}}_1\right]} \underset{19\times 1}{\left[\mathrm{d}\hat{\mathbf{F}}^{\mathrm{M}}\right]} \quad , \tag{7.45}$$

and $[\hat{\mathbf{H}}]$ is given by

$$\underset{15\times 6n^{\mathrm{ext}}}{\left[\mathbf{H}^{\mathrm{ext}}\right]} \underset{6n^{\mathrm{ext}}\times 1}{\left[\mathrm{d}\hat{\mathbf{U}}^{\mathrm{ext}}\right]} = \underset{15\times 19}{\left[\hat{\mathbf{H}}\right]} \underset{19\times 1}{\left[\mathrm{d}\hat{\mathbf{F}}^{\mathrm{M}}\right]} \quad , \tag{7.46}$$

where the nodal values $[\mathrm{d}\hat{\mathbf{U}}^{\mathrm{ext}}]$ at the RVE boundary are related to the macroscopic gradients $[\mathrm{d}\hat{\mathbf{F}}^{\mathrm{M}}]$ at the macroscopic integration point corresponding to the present RVE via the boundary conditions in (7.37).

Upon expanding the system of equations into the displacement, thermal, electric, and magnetic degrees of freedom, the condition in (7.45) for the finite element equations reads

$$
\underbrace{\begin{bmatrix}
\underset{3n^{\mathrm{int}}\times 3n^{\mathrm{ext}}}{\left[\mathbf{K}^{\mathrm{ext}}_{\mathbf{uu}}\right]} & \underset{3n^{\mathrm{int}}\times n^{\mathrm{ext}}}{\left[\mathbf{K}^{\mathrm{ext}}_{\mathbf{u}\theta}\right]} & \underset{3n^{\mathrm{int}}\times n^{\mathrm{ext}}}{\left[\mathbf{K}^{\mathrm{ext}}_{\mathbf{u}\phi}\right]} & \underset{3n^{\mathrm{int}}\times n^{\mathrm{ext}}}{\left[\mathbf{K}^{\mathrm{ext}}_{\mathbf{u}\varphi}\right]} \\
\underset{n^{\mathrm{int}}\times 3n^{\mathrm{ext}}}{\left[\mathbf{K}^{\mathrm{ext}}_{\theta\mathbf{u}}\right]} & \underset{n^{\mathrm{int}}\times n^{\mathrm{ext}}}{\left[\mathbf{K}^{\mathrm{ext}}_{\theta\theta}\right]} & \underset{n^{\mathrm{int}}\times n^{\mathrm{ext}}}{\left[\mathbf{K}^{\mathrm{ext}}_{\theta\phi}\right]} & \underset{n^{\mathrm{int}}\times n^{\mathrm{ext}}}{\left[\mathbf{K}^{\mathrm{ext}}_{\theta\varphi}\right]} \\
\underset{n^{\mathrm{int}}\times 3n^{\mathrm{ext}}}{\left[\mathbf{K}^{\mathrm{ext}}_{\phi\mathbf{u}}\right]} & \underset{n^{\mathrm{int}}\times n^{\mathrm{ext}}}{\left[\mathbf{K}^{\mathrm{ext}}_{\phi\theta}\right]} & \underset{n^{\mathrm{int}}\times n^{\mathrm{ext}}}{\left[\mathbf{K}^{\mathrm{ext}}_{\phi\phi}\right]} & \underset{n^{\mathrm{int}}\times n^{\mathrm{ext}}}{\left[\mathbf{K}^{\mathrm{ext}}_{\phi\varphi}\right]} \\
\underset{n^{\mathrm{int}}\times 3n^{\mathrm{ext}}}{\left[\mathbf{K}^{\mathrm{ext}}_{\varphi\mathbf{u}}\right]} & \underset{n^{\mathrm{int}}\times n^{\mathrm{ext}}}{\left[\mathbf{K}^{\mathrm{ext}}_{\varphi\theta}\right]} & \underset{n^{\mathrm{int}}\times n^{\mathrm{ext}}}{\left[\mathbf{K}^{\mathrm{ext}}_{\varphi\phi}\right]} & \underset{n^{\mathrm{int}}\times n^{\mathrm{ext}}}{\left[\mathbf{K}^{\mathrm{ext}}_{\varphi\varphi}\right]}
\end{bmatrix}}_{\underset{6n^{\mathrm{int}}\times 6n^{\mathrm{ext}}}{\left[\mathbf{K}^{\mathrm{ext}}\right]}}
\underbrace{\begin{bmatrix}
\underset{3n^{\mathrm{ext}}\times 1}{\left[\mathrm{d}\hat{\mathbf{u}}^{\mathrm{ext}}\right]} \\
\underset{n^{\mathrm{ext}}\times 1}{\left[\mathrm{d}\hat{\theta}^{\mathrm{ext}}\right]} \\
\underset{n^{\mathrm{ext}}\times 1}{\left[\mathrm{d}\hat{\phi}^{\mathrm{ext}}\right]} \\
\underset{n^{\mathrm{ext}}\times 1}{\left[\mathrm{d}\hat{\varphi}^{\mathrm{ext}}\right]}
\end{bmatrix}}_{\underset{6n^{\mathrm{ext}}\times 1}{\left[\mathrm{d}\hat{\mathbf{U}}^{\mathrm{ext}}\right]}}
$$

$$
= \underbrace{\begin{bmatrix}
\underset{3n^{\mathrm{int}}\times 9}{\left[\mathbf{G}^{(1)}_{\mathbf{uF}}\right]} & \underset{3n^{\mathrm{int}}\times 1}{\left[\mathbf{G}^{(1)}_{\mathbf{u}\theta}\right]} & \underset{3n^{\mathrm{int}}\times 3}{\left[\mathbf{G}^{(1)}_{\mathbf{u}\nabla\theta}\right]} & \underset{3n^{\mathrm{int}}\times 3}{\left[\mathbf{G}^{(1)}_{\mathbf{u}\nabla\phi}\right]} & \underset{3n^{\mathrm{int}}\times 3}{\left[\mathbf{G}^{(1)}_{\mathbf{u}\nabla\varphi}\right]} \\
\underset{n^{\mathrm{int}}\times 9}{\left[\mathbf{G}^{(1)}_{\theta\mathbf{F}}\right]} & \underset{n^{\mathrm{int}}\times 1}{\left[\mathbf{G}^{(1)}_{\theta\theta}\right]} & \underset{n^{\mathrm{int}}\times 3}{\left[\mathbf{G}^{(1)}_{\theta\nabla\theta}\right]} & \underset{n^{\mathrm{int}}\times 3}{\left[\mathbf{G}^{(1)}_{\theta\nabla\phi}\right]} & \underset{n^{\mathrm{int}}\times 3}{\left[\mathbf{G}^{(1)}_{\theta\nabla\varphi}\right]} \\
\underset{n^{\mathrm{int}}\times 9}{\left[\mathbf{G}^{(1)}_{\phi\mathbf{F}}\right]} & \underset{n^{\mathrm{int}}\times 1}{\left[\mathbf{G}^{(1)}_{\phi\theta}\right]} & \underset{n^{\mathrm{int}}\times 3}{\left[\mathbf{G}^{(1)}_{\phi\nabla\theta}\right]} & \underset{n^{\mathrm{int}}\times 3}{\left[\mathbf{G}^{(1)}_{\phi\nabla\phi}\right]} & \underset{n^{\mathrm{int}}\times 3}{\left[\mathbf{G}^{(1)}_{\phi\nabla\varphi}\right]} \\
\underset{n^{\mathrm{int}}\times 9}{\left[\mathbf{G}^{(1)}_{\varphi\mathbf{F}}\right]} & \underset{n^{\mathrm{int}}\times 1}{\left[\mathbf{G}^{(1)}_{\varphi\theta}\right]} & \underset{n^{\mathrm{int}}\times 3}{\left[\mathbf{G}^{(1)}_{\varphi\nabla\theta}\right]} & \underset{n^{\mathrm{int}}\times 3}{\left[\mathbf{G}^{(1)}_{\varphi\nabla\phi}\right]} & \underset{n^{\mathrm{int}}\times 3}{\left[\mathbf{G}^{(1)}_{\varphi\nabla\varphi}\right]}
\end{bmatrix}}_{\underset{6n^{\mathrm{int}}\times 19}{\left[\hat{\mathbf{G}}_1\right]}}
\underbrace{\begin{bmatrix}
\underset{9\times 1}{\left[\mathrm{d}\mathbf{F}^{\mathrm{M}}\right]} \\
\underset{1\times 1}{\left[\mathrm{d}\theta^{\mathrm{M}}\right]} \\
\underset{3\times 1}{\left[\mathrm{Grad}_{\mathbf{Y}}\,\mathrm{d}\theta^{\mathrm{M}}\right]} \\
\underset{3\times 1}{\left[\mathrm{Grad}_{\mathbf{Y}}\,\mathrm{d}\phi^{\mathrm{M}}\right]} \\
\underset{3\times 1}{\left[\mathrm{Grad}_{\mathbf{Y}}\,\mathrm{d}\varphi^{\mathrm{M}}\right]}
\end{bmatrix}}_{\underset{19\times 1}{\left[\mathrm{d}\hat{\mathbf{F}}^{\mathrm{M}}\right]}} .
\tag{7.47}
$$

For example, in view of the boundary condition in $(7.37)_1$, Equation (7.47) implies that the first column of entries in $[\hat{\mathbf{G}}_1]$ is obtained from the requirement that

$$
\begin{aligned}
\underset{3n^{\mathrm{int}}\times 3n^{\mathrm{ext}}}{\left[\mathbf{K}^{\mathrm{ext}}_{\mathbf{uu}}\right]}\ \underset{3n^{\mathrm{ext}}\times 1}{\left[\mathrm{d}\hat{\mathbf{u}}^{\mathrm{ext}}\right]} &= \underset{3n^{\mathrm{int}}\times 9}{\left[\mathbf{G}^{(1)}_{\mathbf{uF}}\right]}\ \underset{9\times 1}{\left[\mathrm{d}\mathbf{F}^{\mathrm{M}}\right]} \quad , \\
\underset{n^{\mathrm{int}}\times 3n^{\mathrm{ext}}}{\left[\mathbf{K}^{\mathrm{ext}}_{\theta\mathbf{u}}\right]}\ \underset{3n^{\mathrm{ext}}\times 1}{\left[\mathrm{d}\hat{\mathbf{u}}^{\mathrm{ext}}\right]} &= \underset{n^{\mathrm{int}}\times 9}{\left[\mathbf{G}^{(1)}_{\theta\mathbf{F}}\right]}\ \underset{9\times 1}{\left[\mathrm{d}\mathbf{F}^{\mathrm{M}}\right]} \quad , \\
\underset{n^{\mathrm{int}}\times 3n^{\mathrm{ext}}}{\left[\mathbf{K}^{\mathrm{ext}}_{\phi\mathbf{u}}\right]}\ \underset{3n^{\mathrm{ext}}\times 1}{\left[\mathrm{d}\hat{\mathbf{u}}^{\mathrm{ext}}\right]} &= \underset{n^{\mathrm{int}}\times 9}{\left[\mathbf{G}^{(1)}_{\phi\mathbf{F}}\right]}\ \underset{9\times 1}{\left[\mathrm{d}\mathbf{F}^{\mathrm{M}}\right]} \quad , \\
\underset{n^{\mathrm{int}}\times 3n^{\mathrm{ext}}}{\left[\mathbf{K}^{\mathrm{ext}}_{\varphi\mathbf{u}}\right]}\ \underset{3n^{\mathrm{ext}}\times 1}{\left[\mathrm{d}\hat{\mathbf{u}}^{\mathrm{ext}}\right]} &= \underset{n^{\mathrm{int}}\times 9}{\left[\mathbf{G}^{(1)}_{\varphi\mathbf{F}}\right]}\ \underset{9\times 1}{\left[\mathrm{d}\mathbf{F}^{\mathrm{M}}\right]} \quad .
\end{aligned}
\tag{7.48}
$$

Likewise, on account of the thermal boundary condition $(7.37)_2$, the second and third

columns of entries in $[\hat{\mathbf{G}}_1]$ are extracted from Equation (7.47) according to

$$\begin{aligned}
\underbrace{\left[\mathbf{K}^{\mathrm{ext}}_{\mathbf{u}\theta}\right]}_{3n^{\mathrm{int}}\times n^{\mathrm{ext}}}\underbrace{\left[\mathrm{d}\hat{\theta}^{\mathrm{ext}}\right]}_{n^{\mathrm{ext}}\times 1} &= \underbrace{\left[\mathbf{G}^{(1)}_{\mathbf{u}\theta}\right]}_{3n^{\mathrm{int}}\times 1}\underbrace{\left[\mathrm{d}\theta^{\mathrm{M}}\right]}_{1\times 1} + \underbrace{\left[\mathbf{G}^{(1)}_{\mathbf{u}\nabla\theta}\right]}_{3n^{\mathrm{int}}\times 3}\underbrace{\left[\mathrm{Grad}_{\mathbf{Y}}\,\mathrm{d}\theta^{\mathrm{M}}\right]}_{3\times 1} \quad , \\
\underbrace{\left[\mathbf{K}^{\mathrm{ext}}_{\theta\theta}\right]}_{n^{\mathrm{int}}\times n^{\mathrm{ext}}}\underbrace{\left[\mathrm{d}\hat{\theta}^{\mathrm{ext}}\right]}_{n^{\mathrm{ext}}\times 1} &= \underbrace{\left[\mathbf{G}^{(1)}_{\theta\theta}\right]}_{n^{\mathrm{int}}\times 1}\underbrace{\left[\mathrm{d}\theta^{\mathrm{M}}\right]}_{1\times 1} + \underbrace{\left[\mathbf{G}^{(1)}_{\theta\nabla\theta}\right]}_{n^{\mathrm{int}}\times 3}\underbrace{\left[\mathrm{Grad}_{\mathbf{Y}}\,\mathrm{d}\theta^{\mathrm{M}}\right]}_{3\times 1} \quad , \\
\underbrace{\left[\mathbf{K}^{\mathrm{ext}}_{\phi\theta}\right]}_{n^{\mathrm{int}}\times n^{\mathrm{ext}}}\underbrace{\left[\mathrm{d}\hat{\theta}^{\mathrm{ext}}\right]}_{n^{\mathrm{ext}}\times 1} &= \underbrace{\left[\mathbf{G}^{(1)}_{\phi\theta}\right]}_{n^{\mathrm{int}}\times 1}\underbrace{\left[\mathrm{d}\theta^{\mathrm{M}}\right]}_{1\times 1} + \underbrace{\left[\mathbf{G}^{(1)}_{\phi\nabla\theta}\right]}_{n^{\mathrm{int}}\times 3}\underbrace{\left[\mathrm{Grad}_{\mathbf{Y}}\,\mathrm{d}\theta^{\mathrm{M}}\right]}_{3\times 1} \quad , \\
\underbrace{\left[\mathbf{K}^{\mathrm{ext}}_{\varphi\theta}\right]}_{n^{\mathrm{int}}\times n^{\mathrm{ext}}}\underbrace{\left[\mathrm{d}\hat{\theta}^{\mathrm{ext}}\right]}_{n^{\mathrm{ext}}\times 1} &= \underbrace{\left[\mathbf{G}^{(1)}_{\varphi\theta}\right]}_{n^{\mathrm{int}}\times 1}\underbrace{\left[\mathrm{d}\theta^{\mathrm{M}}\right]}_{1\times 1} + \underbrace{\left[\mathbf{G}^{(1)}_{\varphi\nabla\theta}\right]}_{n^{\mathrm{int}}\times 3}\underbrace{\left[\mathrm{Grad}_{\mathbf{Y}}\,\mathrm{d}\theta^{\mathrm{M}}\right]}_{3\times 1} \quad .
\end{aligned} \tag{7.49}$$

Lastly, the fourth column of $[\hat{\mathbf{G}}_1]$ in Equation (7.47) is determined from

$$\begin{aligned}
\underbrace{\left[\mathbf{K}^{\mathrm{ext}}_{\mathbf{u}\phi}\right]}_{3n^{\mathrm{int}}\times n^{\mathrm{ext}}}\underbrace{\left[\mathrm{d}\hat{\phi}^{\mathrm{ext}}\right]}_{n^{\mathrm{ext}}\times 1} &= \underbrace{\left[\mathbf{G}^{(1)}_{\mathbf{u}\nabla\phi}\right]}_{3n^{\mathrm{int}}\times 3}\underbrace{\left[\mathrm{Grad}_{\mathbf{Y}}\,\mathrm{d}\phi^{\mathrm{M}}\right]}_{3\times 1} \quad , \\
\underbrace{\left[\mathbf{K}^{\mathrm{ext}}_{\theta\phi}\right]}_{n^{\mathrm{int}}\times n^{\mathrm{ext}}}\underbrace{\left[\mathrm{d}\hat{\phi}^{\mathrm{ext}}\right]}_{n^{\mathrm{ext}}\times 1} &= \underbrace{\left[\mathbf{G}^{(1)}_{\theta\nabla\phi}\right]}_{n^{\mathrm{int}}\times 3}\underbrace{\left[\mathrm{Grad}_{\mathbf{Y}}\,\mathrm{d}\phi^{\mathrm{M}}\right]}_{3\times 1} \quad , \\
\underbrace{\left[\mathbf{K}^{\mathrm{ext}}_{\phi\phi}\right]}_{n^{\mathrm{int}}\times n^{\mathrm{ext}}}\underbrace{\left[\mathrm{d}\hat{\phi}^{\mathrm{ext}}\right]}_{n^{\mathrm{ext}}\times 1} &= \underbrace{\left[\mathbf{G}^{(1)}_{\phi\nabla\phi}\right]}_{n^{\mathrm{int}}\times 3}\underbrace{\left[\mathrm{Grad}_{\mathbf{Y}}\,\mathrm{d}\phi^{\mathrm{M}}\right]}_{3\times 1} \quad , \\
\underbrace{\left[\mathbf{K}^{\mathrm{ext}}_{\varphi\phi}\right]}_{n^{\mathrm{int}}\times n^{\mathrm{ext}}}\underbrace{\left[\mathrm{d}\hat{\phi}^{\mathrm{ext}}\right]}_{n^{\mathrm{ext}}\times 1} &= \underbrace{\left[\mathbf{G}^{(1)}_{\varphi\nabla\phi}\right]}_{n^{\mathrm{int}}\times 3}\underbrace{\left[\mathrm{Grad}_{\mathbf{Y}}\,\mathrm{d}\phi^{\mathrm{M}}\right]}_{3\times 1} \quad ,
\end{aligned} \tag{7.50}$$

and the fifth column is obtained analogously.

The condition in (7.46), which originates from the reformulation of the homogenization Equations (7.40) in terms of the macroscopic gradient quantities, is expanded

akin to (7.47) into

$$\underbrace{\begin{bmatrix} \underset{6\times 3n^{\mathrm{ext}}}{\left[\mathbf{H}^{\mathrm{ext}}_{\mathbf{Tu}}\right]} & \underset{6\times n^{\mathrm{ext}}}{\left[\mathbf{H}^{\mathrm{ext}}_{\mathbf{T}\theta}\right]} & \underset{6\times n^{\mathrm{ext}}}{\left[\mathbf{H}^{\mathrm{ext}}_{\mathbf{T}\phi}\right]} & \underset{6\times n^{\mathrm{ext}}}{\left[\mathbf{H}^{\mathrm{ext}}_{\mathbf{T}\varphi}\right]} \\ \underset{3\times 3n^{\mathrm{ext}}}{\left[\mathbf{H}^{\mathrm{ext}}_{\mathbf{qu}}\right]} & \underset{3\times n^{\mathrm{ext}}}{\left[\mathbf{H}^{\mathrm{ext}}_{\mathbf{q}\theta}\right]} & \underset{3\times n^{\mathrm{ext}}}{\left[\mathbf{H}^{\mathrm{ext}}_{\mathbf{q}\phi}\right]} & \underset{3\times n^{\mathrm{ext}}}{\left[\mathbf{H}^{\mathrm{ext}}_{\mathbf{q}\varphi}\right]} \\ \underset{3\times 3n^{\mathrm{ext}}}{\left[\mathbf{H}^{\mathrm{ext}}_{\mathbf{pu}}\right]} & \underset{3\times n^{\mathrm{ext}}}{\left[\mathbf{H}^{\mathrm{ext}}_{\mathbf{p}\theta}\right]} & \underset{3\times n^{\mathrm{ext}}}{\left[\mathbf{H}^{\mathrm{ext}}_{\mathbf{p}\phi}\right]} & \underset{3\times n^{\mathrm{ext}}}{\left[\mathbf{H}^{\mathrm{ext}}_{\mathbf{p}\varphi}\right]} \\ \underset{3\times 3n^{\mathrm{ext}}}{\left[\mathbf{H}^{\mathrm{ext}}_{\boldsymbol{\mathcal{M}}\mathbf{u}}\right]} & \underset{3\times n^{\mathrm{ext}}}{\left[\mathbf{H}^{\mathrm{ext}}_{\boldsymbol{\mathcal{M}}\theta}\right]} & \underset{3\times n^{\mathrm{ext}}}{\left[\mathbf{H}^{\mathrm{ext}}_{\boldsymbol{\mathcal{M}}\phi}\right]} & \underset{3\times n^{\mathrm{ext}}}{\left[\mathbf{H}^{\mathrm{ext}}_{\boldsymbol{\mathcal{M}}\varphi}\right]} \end{bmatrix}}_{\underset{15\times 6n^{\mathrm{ext}}}{\left[\mathbf{H}^{\mathrm{ext}}\right]}} \underbrace{\begin{bmatrix} \underset{3n^{\mathrm{ext}}\times 1}{\left[\mathrm{d}\hat{\mathbf{u}}^{\mathrm{ext}}\right]} \\ \underset{n^{\mathrm{ext}}\times 1}{\left[\mathrm{d}\hat{\theta}^{\mathrm{ext}}\right]} \\ \underset{n^{\mathrm{ext}}\times 1}{\left[\mathrm{d}\hat{\phi}^{\mathrm{ext}}\right]} \\ \underset{n^{\mathrm{ext}}\times 1}{\left[\mathrm{d}\hat{\varphi}^{\mathrm{ext}}\right]} \end{bmatrix}}_{\underset{6n^{\mathrm{ext}}\times 1}{\left[\mathrm{d}\hat{\mathbf{U}}^{\mathrm{ext}}\right]}}$$

$$= \underbrace{\begin{bmatrix} \underset{6\times 9}{\left[\mathbf{H}^{\mathrm{M}}_{\mathbf{TF}}\right]} & \underset{6\times 1}{\left[\mathbf{H}^{\mathrm{M}}_{\mathbf{T}\theta}\right]} & \underset{6\times 3}{\left[\mathbf{H}^{\mathrm{M}}_{\mathbf{T}\nabla\theta}\right]} & \underset{6\times 3}{\left[\mathbf{H}^{\mathrm{M}}_{\mathbf{T}\nabla\phi}\right]} & \underset{6\times 3}{\left[\mathbf{H}^{\mathrm{M}}_{\mathbf{T}\nabla\varphi}\right]} \\ \underset{3\times 9}{\left[\mathbf{H}^{\mathrm{M}}_{\mathbf{qF}}\right]} & \underset{3\times 1}{\left[\mathbf{H}^{\mathrm{M}}_{\mathbf{q}\theta}\right]} & \underset{3\times 3}{\left[\mathbf{H}^{\mathrm{M}}_{\mathbf{q}\nabla\theta}\right]} & \underset{3\times 3}{\left[\mathbf{H}^{\mathrm{M}}_{\mathbf{q}\nabla\phi}\right]} & \underset{3\times 3}{\left[\mathbf{H}^{\mathrm{M}}_{\mathbf{q}\nabla\varphi}\right]} \\ \underset{3\times 9}{\left[\mathbf{H}^{\mathrm{M}}_{\mathbf{pF}}\right]} & \underset{3\times 1}{\left[\mathbf{H}^{\mathrm{M}}_{\mathbf{p}\theta}\right]} & \underset{3\times 3}{\left[\mathbf{H}^{\mathrm{M}}_{\mathbf{p}\nabla\theta}\right]} & \underset{3\times 3}{\left[\mathbf{H}^{\mathrm{M}}_{\mathbf{p}\nabla\phi}\right]} & \underset{3\times 3}{\left[\mathbf{H}^{\mathrm{M}}_{\mathbf{p}\nabla\varphi}\right]} \\ \underset{3\times 9}{\left[\mathbf{H}^{\mathrm{M}}_{\boldsymbol{\mathcal{M}}\mathbf{F}}\right]} & \underset{3\times 1}{\left[\mathbf{H}^{\mathrm{M}}_{\boldsymbol{\mathcal{M}}\theta}\right]} & \underset{3\times 3}{\left[\mathbf{H}^{\mathrm{M}}_{\boldsymbol{\mathcal{M}}\nabla\theta}\right]} & \underset{3\times 3}{\left[\mathbf{H}^{\mathrm{M}}_{\boldsymbol{\mathcal{M}}\nabla\phi}\right]} & \underset{3\times 3}{\left[\mathbf{H}^{\mathrm{M}}_{\boldsymbol{\mathcal{M}}\nabla\varphi}\right]} \end{bmatrix}}_{\underset{15\times 19}{\left[\hat{\mathbf{H}}\right]}} \underbrace{\begin{bmatrix} \underset{9\times 1}{\left[\mathrm{d}\mathbf{F}^{\mathrm{M}}\right]} \\ \underset{1\times 1}{\left[\mathrm{d}\theta^{\mathrm{M}}\right]} \\ \underset{3\times 1}{\left[\mathrm{Grad}_{\mathbf{Y}}\,\mathrm{d}\theta^{\mathrm{M}}\right]} \\ \underset{3\times 1}{\left[\mathrm{Grad}_{\mathbf{Y}}\,\mathrm{d}\phi^{\mathrm{M}}\right]} \\ \underset{3\times 1}{\left[\mathrm{Grad}_{\mathbf{Y}}\,\mathrm{d}\varphi^{\mathrm{M}}\right]} \end{bmatrix}}_{\underset{19\times 1}{\left[\mathrm{d}\hat{\mathbf{F}}^{\mathrm{M}}\right]}} . \tag{7.51}$$

The implications of (7.51) for the individual entries in the 15×19 matrix $[\hat{\mathbf{H}}]$ are entirely analogous to the expressions in (7.48 - 50), and are not repeated here.

Detailed Derivation of Entries in $[\hat{\mathbf{G}}_1]$

To simplify the preceding results, consider the 6×6 nodal stiffness matrix $[\mathbf{K}^{\alpha\beta}]$ associated with a variational node α and a differential node β, whose components are given according to (6.196) by

$$\underset{6\times 6}{\left[\mathbf{K}^{\alpha\beta}\right]} = \begin{bmatrix} \underset{3\times 3}{\left[\mathbf{K}^{\alpha\beta}_{\mathbf{uu}}\right]} & \underset{3\times 1}{\left[\mathbf{K}^{\alpha\beta}_{\mathbf{u}\theta}\right]} & \underset{3\times 1}{\left[\mathbf{K}^{\alpha\beta}_{\mathbf{u}\phi}\right]} & \underset{3\times 1}{\left[\mathbf{0}\right]} \\ \underset{1\times 3}{\left[\mathbf{K}^{\alpha\beta}_{\theta\mathbf{u}}\right]} & \underset{1\times 1}{\left[\mathbf{K}^{\alpha\beta}_{\theta\theta}\right]} & \underset{1\times 1}{\left[0\right]} & \underset{1\times 1}{\left[0\right]} \\ \underset{1\times 3}{\left[\mathbf{K}^{\alpha\beta}_{\phi\mathbf{u}}\right]} & \underset{1\times 1}{\left[0\right]} & \underset{1\times 1}{\left[\mathbf{K}^{\alpha\beta}_{\phi\phi}\right]} & \underset{1\times 1}{\left[0\right]} \\ \underset{1\times 3}{\left[\mathbf{K}^{\alpha\beta}_{\varphi\mathbf{u}}\right]} & \underset{1\times 1}{\left[0\right]} & \underset{1\times 1}{\left[0\right]} & \underset{1\times 1}{\left[\mathbf{K}^{\alpha\beta}_{\varphi\varphi}\right]} \end{bmatrix} . \tag{7.52}$$

It is assumed that the index α is associated only with internal nodes, whereas β denotes only boundary nodes. Hence $[\mathbf{K}^{\alpha\beta}]$ represents a portion of the $6n^{\text{int}} \times 6n^{\text{ext}}$ matrix $[\mathbf{K}^{\text{ext}}]$ associated with the boundary terms in the reduced finite element system of Equations (7.38).

It is readily seen that, for the $3n^{\text{int}}$ displacement degrees of freedom of the internal nodes $\alpha = 1 \dots n^{\text{int}}$, the left-hand side of Equation $(7.48)_1$ furnishes

$$\sum_{\beta=1}^{n^{\text{ext}}} \underset{3\times3}{\big[\,\mathbf{K}^{\alpha\beta}_{\mathbf{uu}}\,\big]}\, \underset{3\times1}{\big[\,\mathrm{d}\hat{\mathbf{u}}^{\beta}\,\big]} = \sum_{\beta=1}^{n^{\text{ext}}} \underset{3\times3}{\big[\,\mathbf{K}^{\alpha\beta}_{\mathbf{uu}}\,\big]}\, \underset{3\times3}{\big[\,\mathrm{d}\mathbf{F}^{\mathrm{M}}\,\big]}\, \underset{3\times1}{\big[\,\hat{\mathbf{X}}^{\beta}\,\big]} \quad , \tag{7.53}$$

where the boundary condition $(7.37)_1$ was used. To arrive at the desired expression for $[\mathbf{G}^{(1)}_{\mathbf{uF}}]$, the macroscopic deformation gradient on the right-hand side of (7.53) must be converted to 9×1 VOIGT notation. To facilitate this conversion, the preceding result is first restated using index notation as

$$\sum_{\beta=1}^{n^{\text{ext}}} \big[\,\mathbf{K}^{\alpha\beta}_{\mathbf{uu}}\,\big]_{ij}\, \big[\,\mathrm{d}\hat{\mathbf{u}}^{\beta}\,\big]_{j} = \underbrace{\sum_{\beta=1}^{n^{\text{ext}}} \big[\mathbf{K}^{\alpha\beta}_{\mathbf{uu}}\big]_{ij}\, \big[\hat{\mathbf{X}}^{\beta}\big]_{A}}_{\big[\,\mathbf{G}^{(1)}_{\mathbf{uF}}\,\big]^{\alpha}_{ijA}}\, \big[\mathrm{d}\mathbf{F}^{\mathrm{M}}\big]_{jA} \quad , \tag{7.54}$$

where the indices i and α correspond with the $3n^{\text{int}}$ rows of $[\mathbf{G}^{(1)}_{\mathbf{uF}}]$ and the indices j and A produce its 9 columns. It can be shown with the aid of (6.106), (6.115), and (6.117), that a tensor multiplication of the form $\mathbf{TSu} = T_{ij}u_kS_{jk}\mathbf{e}_i$ can be represented using the VOIGT notation according to

$$\begin{aligned}
\underset{3\times3}{\big[\,\mathbf{T}\,\big]}\, \underset{3\times3}{\big[\,\mathbf{S}\,\big]}\, \underset{3\times1}{\big(\,\mathbf{u}\,\big)} &= \underset{3\times9}{\big\langle \mathbf{u}\otimes\mathbf{T}^{\mathrm{T}}\big\rangle^{\mathrm{T}}}\, \underset{9\times1}{\big\langle \mathbf{S}^{\mathrm{T}}\big\rangle} \\
&= \left[\underset{9\times9}{\big\langle \mathbf{T}^{\mathrm{T}}\big\rangle^{(1)}}\, \left[\underset{3\times9}{\big\langle \mathbf{u}\big\rangle^{(3)}}\right]^{\mathrm{T}}\right]^{\mathrm{T}}\, \underset{9\times9}{\big\langle \mathbb{I}^{\mathrm{T}}\big\rangle}\, \underset{9\times1}{\big\langle \mathbf{S}\big\rangle} \\
&= \underset{3\times9}{\big\langle \mathbf{u}\big\rangle^{(3)}}\, \underset{9\times9}{\big\langle \mathbf{T}\big\rangle^{(1)}}\, \underset{9\times9}{\big\langle \mathbb{I}^{\mathrm{T}}\big\rangle}\, \underset{9\times1}{\big\langle \mathbf{S}\big\rangle} \quad ,
\end{aligned} \tag{7.55}$$

where $\langle \mathbb{I}^{\mathrm{T}} \rangle$ denotes the transpose operator for second-order tensors in VOIGT notation. This identity is used to reformulate Equation (7.53) using VOIGT notation consistent with $(7.48)_1$ as

$$\sum_{\beta=1}^{n^{\text{ext}}} \underset{3\times3}{\big[\,\mathbf{K}^{\alpha\beta}_{\mathbf{uu}}\,\big]}\, \underset{3\times1}{\big[\,\mathrm{d}\hat{\mathbf{u}}^{\beta}\,\big]} = \underbrace{\sum_{\beta=1}^{n^{\text{ext}}} \underset{3\times9}{\big\langle \hat{\mathbf{X}}^{\beta}\big\rangle^{(3)}}\, \underset{9\times9}{\big\langle \mathbf{K}^{\alpha\beta}_{\mathbf{uu}}\big\rangle^{(1)}}\, \underset{9\times9}{\big\langle \mathbb{I}^{\mathrm{T}}\big\rangle}}_{\underset{3\times9}{\big[\,\mathbf{G}^{(1)}_{\mathbf{uF}}\,\big]^{\alpha}}}\, \underset{9\times1}{\big\langle \mathrm{d}\mathbf{F}^{\mathrm{M}}\big\rangle} \quad , \tag{7.56}$$

where the $3n^{\text{int}} \times 9$ matrix $[\mathbf{G}^{(1)}_{\mathbf{uF}}]$ is assembled from the 3×9 sub-matrices $[\mathbf{G}^{(1)}_{\mathbf{uF}}]^{\alpha}$ associated with each internal node α. This 3×9 matrix may be loosely interpreted as containing the components of a third-order tensor obtained from a tensor product between a second-order tensor and a vector, $\mathbf{K}^{\alpha\beta}_{\mathbf{uu}} \otimes \hat{\mathbf{X}}^{\beta}$.

Using the same procedure as before, the remaining entries in the first column of $[\hat{\mathbf{G}}_1]$ are readily deduced from the conditions in $(7.48)_{2-4}$. For example, the left-hand side of $(7.48)_2$ is restated with the aid of the displacement boundary condition $(7.37)_1$ as

$$\sum_{\beta=1}^{n^{\text{ext}}} \underset{1\times3}{\big[\,\mathbf{K}^{\alpha\beta}_{\theta\mathbf{u}}\,\big]}\, \underset{3\times1}{\big[\,\mathrm{d}\hat{\mathbf{u}}^{\beta}\,\big]} = \sum_{\beta=1}^{n^{\text{ext}}} \underset{1\times3}{\big[\,\mathbf{K}^{\alpha\beta}_{\theta\mathbf{u}}\,\big]}\, \underset{3\times3}{\big[\,\mathrm{d}\mathbf{F}^{\mathrm{M}}\,\big]}\, \underset{3\times1}{\big[\,\hat{\mathbf{X}}^{\beta}\,\big]} = \underbrace{\sum_{\beta=1}^{n^{\text{ext}}} \underset{1\times3}{\big[\,\mathbf{K}^{\alpha\beta}_{\theta\mathbf{u}}\,\big]}\, \underset{3\times9}{\big\langle\,\hat{\mathbf{X}}^{\beta}\,\big\rangle^{(3)}}}_{\underset{1\times9}{\big[\,\mathbf{G}^{(1)}_{\theta\mathbf{F}}\,\big]^{\alpha}}}\, \underset{9\times1}{\big\langle\,\mathrm{d}\mathbf{F}^{\mathrm{M}}\,\big\rangle} \quad , \tag{7.57}$$

where use was made of Equation (6.112) for the VOIGT notation of a tensor product between two vectors. Analogous results are obtained for the 1×9 sub-matrices $[\mathbf{G}^{(1)}_{\phi\mathbf{F}}]^{\alpha}$ and $[\mathbf{G}^{(1)}_{\varphi\mathbf{F}}]^{\alpha}$.

In summary, it is concluded that the first 9 columns in the $6n^{\text{int}} \times 19$ matrix $[\hat{\mathbf{G}}_1]$ are given by

$$\begin{aligned}
\underset{3\times9}{\big[\,\mathbf{G}^{(1)}_{\mathbf{uF}}\,\big]^{\alpha}} &= \sum_{\beta=1}^{n^{\text{ext}}} \underset{3\times9}{\big\langle\,\hat{\mathbf{X}}^{\beta}\,\big\rangle^{(3)}}\, \underset{9\times9}{\big\langle\,\mathbf{K}^{\alpha\beta}_{\mathbf{uu}}\,\big\rangle^{(1)}}\, \underset{9\times9}{\big\langle\,\mathbb{I}^{\mathrm{T}}\,\big\rangle} \quad , \\
\underset{1\times9}{\big[\,\mathbf{G}^{(1)}_{\theta\mathbf{F}}\,\big]^{\alpha}} &= \sum_{\beta=1}^{n^{\text{ext}}} \underset{1\times3}{\big[\,\mathbf{K}^{\alpha\beta}_{\theta\mathbf{u}}\,\big]}\, \underset{3\times9}{\big\langle\,\hat{\mathbf{X}}^{\beta}\,\big\rangle^{(3)}} \quad , \\
\underset{1\times9}{\big[\,\mathbf{G}^{(1)}_{\phi\mathbf{F}}\,\big]^{\alpha}} &= \sum_{\beta=1}^{n^{\text{ext}}} \underset{1\times3}{\big[\,\mathbf{K}^{\alpha\beta}_{\phi\mathbf{u}}\,\big]}\, \underset{3\times9}{\big\langle\,\hat{\mathbf{X}}^{\beta}\,\big\rangle^{(3)}} \quad , \\
\underset{1\times9}{\big[\,\mathbf{G}^{(1)}_{\varphi\mathbf{F}}\,\big]^{\alpha}} &= \sum_{\beta=1}^{n^{\text{ext}}} \underset{1\times3}{\big[\,\mathbf{K}^{\alpha\beta}_{\varphi\mathbf{u}}\,\big]}\, \underset{3\times9}{\big\langle\,\hat{\mathbf{X}}^{\beta}\,\big\rangle^{(3)}} \quad ,
\end{aligned} \tag{7.58}$$

where $\alpha = 1 \ldots n^{\text{int}}$ indicates the sub-matrix associated with each internal nodes of the RVE mesh. The components in (7.58) represent the first column block of entries in $[\hat{\mathbf{G}}_1]$ on the right-hand side of (7.47).

Next, consider the second and third blocks of entries in $[\hat{\mathbf{G}}_1]$, which are associated with the thermal boundary of the RVE. They are deduced from Equations $(7.49)_{1-4}$ by appealing to the DIRICHLET boundary condition in $(7.37)_2$. To simplify this, the 6×6 nodal stiffness matrix $[\mathbf{K}^{\alpha\beta}]$ is employed where, as before, α denotes an interior variational node whereas β represents a differential node on the boundary of

the RVE. For example, the left-hand side of $(7.49)_1$ is restated as

$$\sum_{\beta=1}^{n^{\mathrm{ext}}} \underset{3\times1}{\big[\,\mathbf{K}_{\mathbf{u}\theta}^{\alpha\beta}\,\big]}\,\underset{1\times1}{\big[\,\mathrm{d}\hat{\theta}^{\beta}\,\big]} = \underbrace{\sum_{\beta=1}^{n^{\mathrm{ext}}} \underset{3\times1}{\big[\,\mathbf{K}_{\mathbf{u}\theta}^{\alpha\beta}\,\big]}}_{\underset{3\times1}{\big[\,\mathbf{G}_{\mathbf{u}\theta}^{(1)}\,\big]^{\alpha}}}\,\underset{1\times1}{\big[\,\mathrm{d}\theta^{\mathrm{M}}\,\big]} + \underbrace{\sum_{\beta=1}^{n^{\mathrm{ext}}} \underset{3\times1}{\big[\,\mathbf{K}_{\mathbf{u}\theta}^{\alpha\beta}\,\big]}\,\underset{1\times3}{\big[\,\hat{\mathbf{X}}^{\beta}\,\big]^{\mathrm{T}}}}_{\underset{3\times3}{\big[\,\mathbf{G}_{\mathbf{u}\nabla\theta}^{(1)}\,\big]^{\alpha}}}\,\underset{3\times1}{\big[\,\mathrm{Grad}_{\mathbf{Y}}\,\mathrm{d}\theta^{\mathrm{M}}\big]} \quad . \tag{7.59}$$

Likewise, the condition in $(7.49)_2$ furnishes

$$\sum_{\beta=1}^{n^{\mathrm{ext}}} \underset{1\times1}{\big[\,\mathbf{K}_{\theta\theta}^{\alpha\beta}\,\big]}\,\underset{1\times1}{\big[\,\mathrm{d}\hat{\theta}^{\beta}\,\big]} = \underbrace{\sum_{\beta=1}^{n^{\mathrm{ext}}} \underset{1\times1}{\big[\,\mathbf{K}_{\theta\theta}^{\alpha\beta}\,\big]}}_{\underset{1\times1}{\big[\,\mathbf{G}_{\theta\theta}^{(1)}\,\big]^{\alpha}}}\,\underset{1\times1}{\big[\,\mathrm{d}\theta^{\mathrm{M}}\,\big]} + \underbrace{\sum_{\beta=1}^{n^{\mathrm{ext}}} \underset{1\times1}{\big[\,\mathbf{K}_{\theta\theta}^{\alpha\beta}\,\big]}\,\underset{1\times3}{\big[\,\hat{\mathbf{X}}^{\beta}\,\big]^{\mathrm{T}}}}_{\underset{1\times3}{\big[\,\mathbf{G}_{\theta\nabla\theta}^{(1)}\,\big]^{\alpha}}}\,\underset{3\times1}{\big[\,\mathrm{Grad}_{\mathbf{Y}}\,\mathrm{d}\theta^{\mathrm{M}}\big]} \quad , \tag{7.60}$$

and Equations $(7.49)_{3,4}$ lead to analogous results. The corresponding columns of the $6n^{\mathrm{int}}\times19$ matrix $[\,\hat{\mathbf{G}}_1]$ thus read

$$\begin{aligned}
\underset{3\times1}{\big[\,\mathbf{G}_{\mathbf{u}\theta}^{(1)}\,\big]^{\alpha}} &= \sum_{\beta=1}^{n^{\mathrm{ext}}} \underset{3\times1}{\big[\,\mathbf{K}_{\mathbf{u}\theta}^{\alpha\beta}\,\big]} \quad , \quad \underset{3\times3}{\big[\,\mathbf{G}_{\mathbf{u}\nabla\theta}^{(1)}\big]^{\alpha}} = \sum_{\beta=1}^{n^{\mathrm{ext}}} \underset{3\times1}{\big[\,\mathbf{K}_{\mathbf{u}\theta}^{\alpha\beta}\,\big]}\,\underset{1\times3}{\big[\,\hat{\mathbf{X}}^{\beta}\,\big]^{\mathrm{T}}} \quad , \\
\underset{1\times1}{\big[\,\mathbf{G}_{\theta\theta}^{(1)}\,\big]^{\alpha}} &= \sum_{\beta=1}^{n^{\mathrm{ext}}} \underset{1\times1}{\big[\,\mathbf{K}_{\theta\theta}^{\alpha\beta}\,\big]} \quad , \quad \underset{1\times3}{\big[\,\mathbf{G}_{\theta\nabla\theta}^{(1)}\big]^{\alpha}} = \sum_{\beta=1}^{n^{\mathrm{ext}}} \underset{1\times1}{\big[\,\mathbf{K}_{\theta\theta}^{\alpha\beta}\,\big]}\,\underset{1\times3}{\big[\,\hat{\mathbf{X}}^{\beta}\,\big]^{\mathrm{T}}} \quad , \\
\underset{1\times1}{\big[\,\mathbf{G}_{\phi\theta}^{(1)}\,\big]^{\alpha}} &= \sum_{\beta=1}^{n^{\mathrm{ext}}} \underset{1\times1}{\big[\,\mathbf{K}_{\phi\theta}^{\alpha\beta}\,\big]} \quad , \quad \underset{1\times3}{\big[\,\mathbf{G}_{\phi\nabla\theta}^{(1)}\big]^{\alpha}} = \sum_{\beta=1}^{n^{\mathrm{ext}}} \underset{1\times1}{\big[\,\mathbf{K}_{\phi\theta}^{\alpha\beta}\,\big]}\,\underset{1\times3}{\big[\,\hat{\mathbf{X}}^{\beta}\,\big]^{\mathrm{T}}} \quad , \\
\underset{1\times1}{\big[\,\mathbf{G}_{\varphi\theta}^{(1)}\,\big]^{\alpha}} &= \sum_{\beta=1}^{n^{\mathrm{ext}}} \underset{1\times1}{\big[\,\mathbf{K}_{\varphi\theta}^{\alpha\beta}\,\big]} \quad , \quad \underset{1\times3}{\big[\,\mathbf{G}_{\varphi\nabla\theta}^{(1)}\big]^{\alpha}} = \sum_{\beta=1}^{n^{\mathrm{ext}}} \underset{1\times1}{\big[\,\mathbf{K}_{\varphi\theta}^{\alpha\beta}\,\big]}\,\underset{1\times3}{\big[\,\hat{\mathbf{X}}^{\beta}\,\big]^{\mathrm{T}}} \quad .
\end{aligned} \tag{7.61}$$

The components in (7.61), assembled for all $\alpha=1\ldots n^{\mathrm{int}}$, comprise the second and third blocks of columns in $[\,\hat{\mathbf{G}}_1]$ as defined in (7.47).

Following the same procedure, it is readily seen that the last two blocks of entries

in $[\hat{\mathbf{G}}_1]$ are given by

$$\begin{aligned}
\underset{3\times3}{\left[\mathbf{G}^{(1)}_{\mathbf{u}\nabla\phi}\right]^{\alpha}} &= \sum_{\beta=1}^{n^{\text{ext}}} \underset{3\times1}{\left[\mathbf{K}^{\alpha\beta}_{\mathbf{u}\phi}\right]} \underset{1\times3}{\left[\hat{\mathbf{X}}^{\beta}\right]^{\text{T}}} \quad , \\
\underset{1\times3}{\left[\mathbf{G}^{(1)}_{\theta\nabla\phi}\right]^{\alpha}} &= \sum_{\beta=1}^{n^{\text{ext}}} \underset{1\times1}{\left[\mathbf{K}^{\alpha\beta}_{\theta\phi}\right]} \underset{1\times3}{\left[\hat{\mathbf{X}}^{\beta}\right]^{\text{T}}} \quad , \\
\underset{1\times3}{\left[\mathbf{G}^{(1)}_{\phi\nabla\phi}\right]^{\alpha}} &= \sum_{\beta=1}^{n^{\text{ext}}} \underset{1\times1}{\left[\mathbf{K}^{\alpha\beta}_{\phi\phi}\right]} \underset{1\times3}{\left[\hat{\mathbf{X}}^{\beta}\right]^{\text{T}}} \quad , \\
\underset{1\times3}{\left[\mathbf{G}^{(1)}_{\varphi\nabla\phi}\right]^{\alpha}} &= \sum_{\beta=1}^{n^{\text{ext}}} \underset{1\times1}{\left[\mathbf{K}^{\alpha\beta}_{\varphi\phi}\right]} \underset{1\times3}{\left[\hat{\mathbf{X}}^{\beta}\right]^{\text{T}}} \quad ,
\end{aligned} \tag{7.62}$$

and

$$\begin{aligned}
\underset{3\times3}{\left[\mathbf{G}^{(1)}_{\mathbf{u}\nabla\varphi}\right]^{\alpha}} &= \sum_{\beta=1}^{n^{\text{ext}}} \underset{3\times1}{\left[\mathbf{K}^{\alpha\beta}_{\mathbf{u}\varphi}\right]} \underset{1\times3}{\left[\hat{\mathbf{X}}^{\beta}\right]^{\text{T}}} \quad , \\
\underset{1\times3}{\left[\mathbf{G}^{(1)}_{\theta\nabla\varphi}\right]^{\alpha}} &= \sum_{\beta=1}^{n^{\text{ext}}} \underset{1\times1}{\left[\mathbf{K}^{\alpha\beta}_{\theta\varphi}\right]} \underset{1\times3}{\left[\hat{\mathbf{X}}^{\beta}\right]^{\text{T}}} \quad , \\
\underset{1\times3}{\left[\mathbf{G}^{(1)}_{\phi\nabla\varphi}\right]^{\alpha}} &= \sum_{\beta=1}^{n^{\text{ext}}} \underset{1\times1}{\left[\mathbf{K}^{\alpha\beta}_{\phi\varphi}\right]} \underset{1\times3}{\left[\hat{\mathbf{X}}^{\beta}\right]^{\text{T}}} \quad , \\
\underset{1\times3}{\left[\mathbf{G}^{(1)}_{\varphi\nabla\varphi}\right]^{\alpha}} &= \sum_{\beta=1}^{n^{\text{ext}}} \underset{1\times1}{\left[\mathbf{K}^{\alpha\beta}_{\varphi\varphi}\right]} \underset{1\times3}{\left[\hat{\mathbf{X}}^{\beta}\right]^{\text{T}}} \quad .
\end{aligned} \tag{7.63}$$

The components of $[\hat{\mathbf{G}}_1]$ are thus given by Equations (7.58) and (7.61 - 63).

Lastly, it is noted that the 15×19 entries of $[\hat{\mathbf{H}}]$, see on the right-hand side of Equation (7.51), depend on the $15\times6n^{\text{ext}}$ matrix $[\mathbf{H}^{\text{ext}}]$ in the exact same way as the $6n^{\text{int}}\times19$ components of $[\hat{\mathbf{G}}_1]$ are obtained from the $6n^{\text{int}}\times6n^{\text{ext}}$ matrix $[\mathbf{K}^{\text{ext}}]$. Hence, a detailed derivation of the entries in $[\hat{\mathbf{H}}]$ is not presented here.

Homogenized Macroscopic Moduli

Recall the system of Equations (7.42), reproduced here as

$$\begin{bmatrix} \underset{6n^{\text{int}}\times6n^{\text{int}}}{\left[\hat{\mathbf{K}}\right]} & \underset{6n^{\text{int}}\times19}{\left[\hat{\mathbf{G}}_1\right]} \\ \underset{15\times6n^{\text{int}}}{\left[\hat{\mathbf{G}}_2\right]} & \underset{15\times19}{\left[\hat{\mathbf{H}}\right]} \end{bmatrix} \begin{bmatrix} \underset{6n^{\text{int}}\times1}{\left[\mathrm{d}\hat{\mathbf{U}}^{\text{int}}\right]} \\ \underset{19\times1}{\left[\mathrm{d}\hat{\mathbf{F}}^{\text{M}}\right]} \end{bmatrix} = \begin{bmatrix} \underset{6n^{\text{int}}\times1}{\left[\mathbf{0}\right]} \\ \underset{15\times1}{\left[\mathrm{d}\hat{\mathbf{T}}^{\text{M}}\right]} \end{bmatrix} \quad . \tag{7.64}$$

The components of $[\hat{\mathbf{K}}]$ and $[\hat{\mathbf{G}}_2]$ are obtained immediately from the $6n\times6n$ global stiffness matrix $[\mathbf{K}]$ and the $15\times6n$ homogenization matrix $[\mathbf{H}]$, respectively, by ex-

tracting the entries associated with the internal nodes of the RVE. The components of $[\hat{\mathbf{G}}_1]$ and $[\hat{\mathbf{H}}]$, on the other hand, are extracted from the sub-matrices of the boundary nodes in $[\mathbf{K}]$ and $[\mathbf{H}]$ according to the preceding derivation. The first line of (7.64) yields the nodal differential vector $[\mathrm{d}\hat{\mathbf{U}}^{\mathrm{int}}]$ for the finite element equations of the RVE,

$$\underset{6n^{\mathrm{int}}\times 1}{\left[\mathrm{d}\hat{\mathbf{U}}^{\mathrm{int}}\right]} = -\underset{6n^{\mathrm{int}}\times 6n^{\mathrm{int}}}{\left[\hat{\mathbf{K}}\right]^{-1}} \underset{6n^{\mathrm{int}}\times 19}{\left[\hat{\mathbf{G}}_1\right]} \underset{19\times 1}{\left[\mathrm{d}\hat{\mathbf{F}}^{\mathrm{M}}\right]} \quad . \tag{7.65}$$

Note that the inverse of $[\hat{\mathbf{K}}]$ indeed exists, because it is obtained from the (singular) extended stiffness matrix $[\mathbf{K}]$ by applying appropriate DIRICHLET boundary conditions. Next, Equation (7.65) is inserted into the second line of (7.64) to eliminate $[\mathrm{d}\hat{\mathbf{U}}^{\mathrm{int}}]$. This yields the desired relation between $[\mathrm{d}\hat{\mathbf{F}}^{\mathrm{M}}]$ and $[\mathrm{d}\hat{\mathbf{T}}^{\mathrm{M}}]$,

$$\underset{15\times 1}{\left[\mathrm{d}\hat{\mathbf{T}}^{\mathrm{M}}\right]} = \left\{\underset{15\times 19}{\left[\hat{\mathbf{H}}\right]} - \underset{15\times 6n^{\mathrm{int}}}{\left[\hat{\mathbf{G}}_2\right]} \underset{6n^{\mathrm{int}}\times 6n^{\mathrm{int}}}{\left[\hat{\mathbf{K}}\right]^{-1}} \underset{6n^{\mathrm{int}}\times 19}{\left[\hat{\mathbf{G}}_1\right]}\right\} \underset{19\times 1}{\left[\mathrm{d}\hat{\mathbf{F}}^{\mathrm{M}}\right]} \quad . \tag{7.66}$$

The expression in braces in (7.66) comprises the SCHUR complement of the matrix in (7.64). This 15×19 matrix quantifies the change in macroscopic fluxes in response to a change in the macroscopic primary variables and gradient quantities. Hence, Equation (7.66) may be regarded as a constitutive model for the homogenized behavior of the RVE.

7.2.5 Summary

At each integration point of the macroscale mesh (and during each iteration of the macroscopic NEWTON-RAPHSON scheme) a microscale RVE model is created and solved. The RVE takes as input the macroscopic temperature θ^{M}, as well as the referential gradient quantities[7] $\mathbf{F}^{\mathrm{M}}$, $\mathrm{Grad}_{\mathbf{Y}}\theta^{\mathrm{M}}$, $\mathrm{Grad}_{\mathbf{Y}}\phi^{\mathrm{M}}$, and $\mathrm{Grad}_{\mathbf{Y}}\varphi^{\mathrm{M}}$ at the corresponding integration point of the macroscopic finite element problem. These macroscopic primary variables and gradient quantities determine the RVE DIRICHLET boundary loads according to (7.1).[8]

Given the aforementioned boundary conditions, each RVE problem is solved using the NEWTON-RAPHSON method, which involves a succession of linear algebraic

[7] Recall definition (2.66) for the deformation gradient $\mathbf{F}$. In general, gradients with respect to the referential coordinates are denoted by a capital $\mathrm{Grad}[\cdot]=\frac{\partial[\cdot]}{\partial\mathbf{X}}$ as opposed to spatial gradients $\mathrm{grad}[\cdot]=\frac{\partial[\cdot]}{\partial\mathbf{x}}$. In the context of multiscale modeling, an additional subscript $\mathrm{Grad}_{\mathbf{Y}}[\cdot]^{\mathrm{M}}$ or $\mathrm{Grad}_{\mathbf{X}}[\cdot]^{\mathrm{m}}$ serves as a reminder that the gradient operates on the macro- or microscopic referential coordinates $\mathbf{Y}$ or $\mathbf{X}$, respectively.

[8] The reader is reminded that, according to the constitutive model in Section 6.1.2, the material response (*i.e.*, the fluxes) is independent of the absolute values of the macroscopic displacements $\mathbf{u}^{\mathrm{M}}=\mathbf{y}-\mathbf{Y}$, electrostatic potential ϕ^{M}, and magnetostatic potential φ^{M}. Hence, in the context of this implementation, the values of $\mathbf{u}^{\mathrm{M}}$, ϕ^{M}, and φ^{M} do not necessarily need to be communicated to the RVE. This fact was taken into account in (7.37).

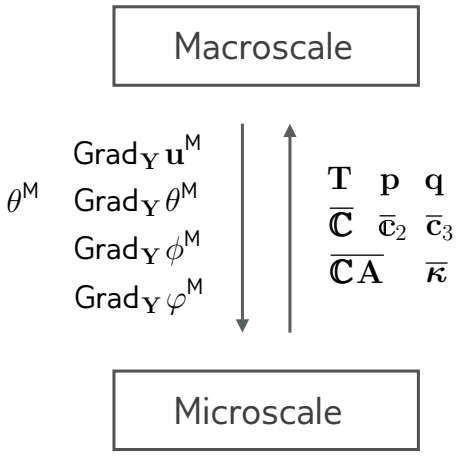

Figure 7.1: Exchange of information between the two scales: The macroscopic scale provides the average temperature and gradient quantities at a given integration point. Using this information to apply boundary conditions to the RVE, the microscopic scale solves the RVE problem and returns the homogenized fluxes and material moduli.

systems of equations of the form (6.189). Once converged, the method furnishes the primary quantities $\mathbf{u}^{\mathrm{m}} = \mathbf{x} - \mathbf{X}$, θ^{m}, ϕ^{m}, and φ^{m} (in form of the nodal solution vector $[\hat{\mathbf{U}}]$), the corresponding fluxes $\mathbf{T}^{\mathrm{m}}$, $\mathbf{q}^{\mathrm{m}}$, $\mathbf{p}^{\mathrm{m}}$, and $\boldsymbol{\mathcal{M}}^{\mathrm{m}}$ computed from the constitutive response of the microstructure (evaluated at the GAUSSIAN integration points), as well as the $6n \times 6n$ extended global finite element stiffness matrix $[\mathbf{K}]$.

Next, the homogenized macroscopic fluxes are obtained from a volumetric average of their microscopic counterparts, see (7.9). In the context of a finite element implementation, this involves an element-wise GAUSSIAN quadrature followed by a summation over each element. Similarly, the $15 \times 6n$ homogenization matrix $[\mathbf{H}]$ is computed according to Equations (7.25 - 28) using element-wise GAUSSIAN quadrature and subsequent accumulation.

Lastly, the system of Equations (7.42) is derived by subdividing $[\mathbf{K}]$ and $[\mathbf{H}]$ into entries associated with the internal and boundary nodes, respectively. The internal nodes give rise to the reduced stiffness and homogenization matrices $[\hat{\mathbf{K}}]$ and $[\hat{\mathbf{G}}_2]$. The parts associated with the boundary nodes, in conjunction with the boundary conditions of the form (7.37), give rise to $[\hat{\mathbf{G}}_1]$ and $[\hat{\mathbf{H}}]$. Their components are given by Equations (7.58) and (7.61 - 63). Thereafter, the SCHUR complement in (7.66) furnishes the homogenized material moduli, which are returned to the macroscopic scale along with the homogenized fluxes. A schematic depiction of the flow of information between the two scales is provided in Figure 7.1.

7.3 Verification and Examples

The multiscale algorithm outlined in Section 7.2 is implemented in the finite element software FEAP [142] for two-dimensional plane strain quasi-static EMTM problems. The constitutive model employed in the microscopic scale is identical to the single-scale model, hence it is limited to the transversely isotropic piezoelectric behavior described by Equations (6.56 - 62). Likewise, the computation of the residual and stiffness matrix are identical to the single-scale problem, see Section 6.3.4.

This section begins with a broad outline of the algorithmic structure of the multiscale model using parallel processing. Thereafter, the implementation is tested using a range of simple RVE models and load cases. In particular, these include a problem comprised of a fully homogeneous microstructure, a random mixture between two different materials, as well as a transversely isotropic material with a random distribution of crystal orientation.

7.3.1 Outline of the Program Structure

The Fortran-based multiscale algorithm makes use of Open MPI [36], or *Open Message Passing Interface*, which is an open-source implementation of the MPI standard for parallel processing. One processor (subsequently referred to as `rank=0`) is reserved solely for solving the macroscopic problem. The remaining processors (`rank>0`) are tasked with successively solving RVE problems as requested by `rank=0`. The basic structure of the code is outlined in this section. In particular, the distribution of workload and the communication between the `rank=0` and `rank>0` processes is discussed.

Input Files

To run a multiscale simulation using the present FEAP implementation, at least three input files are required. Examples for these input files are provided in Figures 7.2 - 7.4. The first file describes the macroscopic problem, including the mesh, material assignments, load distributions, boundary conditions, solution commands, and any post-processing instructions. During the material assignments, the multiscale EMTM material is identified by the name `emtm_2d`.[9] Furthermore, among the material parameters for `emtm_2d`, an RVE input file name must be specified using the `MRVE` input command. This second input file contains the commands necessary to build the finite element model of the RVE. However, the RVE input file only specifies information about the RVE mesh, the microscopic material parameters, and the Dirichlet

[9] The material name `emtm_2d` invokes the user element `elmt02.f`. Note that the same subroutine is used to handle both the macroscopic and microscopic scales. Some tasks (such as the computation of the constitutive response) differ between the two scales. In that case, the user element subroutine performs the appropriate tasks based on the process `rank` from which the routine was called.

boundary identifiers. It does *not* specify any loads or invoke any solution commands. Unlike the macroscopic scale, whose constitutive model is based on the RVE response, the RVE employs the same transversely isotropic piezoelectric constitutive model used for the single-scale model. Even though the same user-defined element `emtm_2d` is used on both scales, the commands associated with the material parameter definitions differ significantly between the macroscopic and microscopic input files.

A third input file, called `solve_mpi`, is used to specify the solution commands for the RVE problem.[10] The structure of this input file is dominated by the `FE2` command, which prompts the program to call the subroutine `pfe2solv.f`. In particular, the command `FE2 STARt <switch>`[11] is invoked to allocate arrays and prepare for MPI communications. Thereafter, `solve_mpi` enters an infinite loop, during which the command `FE2 GET` prompts the RVE to await an MPI message with instructions from `rank=0`. Upon performing the requested task, the RVE returns the results to the macroscopic scale via `FE2 SEND`.

Macroscopic Problem

The `rank=0` process is responsible for the macroscopic finite element problem. This includes (i) the pre-processing of the macroscopic mesh, material properties, boundary conditions, and external loads, (ii) the solution of the ensuing nonlinear problem using the NEWTON-RAPHSON method, and (iii) the post-processing of results such as least-squares projection and plotting.

Each NEWTON-RAPHSON iteration involves the following tasks: (a) communicating the primary and gradient quantities at each macroscopic integration point to the RVE processors via MPI messages, (b) collecting the resulting homogenized fluxes and material moduli that characterize the RVE response, (c) constructing the element residual vector and stiffness matrix, (d) assembling the global finite element arrays, and (e) solving the ensuing linear algebraic system of equations. With the exception of the constitutive model, the basic structure of the macroscopic algorithm is similar to the single-scale implementation.

During the solution process, any MPI communications of `rank=0` with the `rank>0` processes is handled by `rvesr.f`. This subroutine uses the variable `frvel(*,nrecv)` to store the macroscopic gradients and `srvel(*,nrecv)` to store the resulting RVE response returned by `rank>0`, that is, the homogenized fluxes and material moduli.

[10] This file name of `solve_mpi` is currently hard-wired into the FEAP code structure. Multiscale problems are initialized by FEAP in `mpi_start_feap.f`, where a temporary input file is automatically generated for each `rank>0` process using `pfe2outf.f`. This temporary input file later invokes `solve_mpi` via the `INCLude` command.

[11] It is mentioned that `FE2 STARt <switch>` creates a parameter whose name is specified by `<switch>`. Upon receipt of an MPI message during `FE2 GET`, this parameter is assigned the current value of `isw`, which is a variable used internally in FEAP to encode different tasks. This allows the input commands in `solve_mpi` to explicitly depend on the value of `isw` using an `IF - ELSEif - ENDIf` structure.

```
feap  *  *  <TITLE>
  0 0 0 2 5 4               ! no need to specify the control record

global
  norm node 1 1 2 3 4       ! set groups for convergence data output

MATErial 1                  ! electro-magneto-thermo-mechanical fe2 model
  emtm_2d                   ! elmt02.f
    ACTIve equations 5      ! limit the #DoF if desired (default ndf = 5)
    QUADrature order 2      ! for pstyp
    FOURier REFErential     ! referential / spatial Fourier's law
    MRVE <rve_inputfile>
    TYPE KIRK

block
  cart <n> <n>
   material 1               ! generate mesh
    ...

CBOUndary codes             ! identify Dirichlet boundary nodes and edges
  ...
EBOUndary codes
  ...

CSURface                    ! apply boundary loads
  NORMal
  ...
CSURface
  TRACtion 1
  ...
CSURface
  DISPlacement 3
  ...

end                         ! finish problem setup

batch
  rve                       ! activate FE2 solution
  set opar o1 o2            ! random RVE assignment
 dt,,1.0
  time
  loop,,30
    utang,,1                ! Newton-Raphson iteration
 next
  STREss ALL                ! project the stresses onto the nodes
  plot ...                  ! plots 1-10 for fluxes, 11-20 for grads.
end

inter                       ! interactive mode

stop
```

Figure 7.2: Outline of a typical input file describing the macroscopic boundary-value problem.

```
feap  *  *  <TITLE>
  <numnp> <numel> <numma> 2 5 4               ! specify control record for RVE

! note:
!   numnp = ( n+1)*( n+1) (for QUADrature order 2)
!   numnp = (2n+1)*(2n+1) (for QUADrature order 3)
!   numel = n^2

MATErial 1                                    ! multiscale EMTM model
  emtm_2d                                     ! elmt02.f
    ACTIve equations 5                        ! limit the #DoF (default ndf = 5)
    QUADrature order 2                        ! for pstyp
    FOURier REFErential                       ! referential / spatial Fourier's law
    ELAStic ISOTropic 117627.7 0.315746       ! Young's modulus E, Poisson's nu
    ELAStic TRANsverse -3600 700 900          ! transversely isotropic omega w(3)
    FOURier ISOTropic 2.7                     ! kappa
    ELAStic ALPHa 6.1d-6  0.0                 ! thermal expansion alpha, reference T0
    VACUum properties 8.8541878d-6 1.25663706 ! eps0 and mu0
    ORIEntation vector 1 2 0                  ! preferred crystal orientation a(3)
    PYROelectric polarization 0.0 0.0 0.0     ! pyroelectric polarization C1(3)
    PIEZoelectric TRANsverse 4.4 0.2 -23.2    ! piezoelectric parameters beta b(3)
    POLArization TRANsverse -0.0056 -0.0007   ! polarization properties gamma g(2)
    MAGNetization TRANsverse -0.63 0          ! magnetization properties xi(2)

MATErial 2
  emtm_2d                                     ! elmt02.f
    ...

block                                         ! generate mesh (RVE centered around origin)
  cart <n> <n>
   material 1
    ...

EBOUndary codes                               ! Dirichlet boundary only
     1  -d   1   1   1   1   1
     1   d   1   1   1   1   1
     2  -d   1   1   1   1   1
     2   d   1   1   1   1   1
! xdim loc  u1  u2   T Phi phi

end
```

Figure 7.3: Outline of a typical input file for setting up the RVE model (without solution commands).

```
batch
  fe2  start sw 0            ! initiate RVE and switch parameter
  fe2  plot  pl <n1> 1       ! request plot of <n1>-th integration point handled by rank 1
  fe2  plot  pl <n2> 2       ! request plot of <n2>-th integration point handled by rank 2
  loop,infinite              ! enter infinite solution loop
    fe2  get                 ! MPI_Recv instructions and gradients from macroscale
    if sw-12                 ! time step (isw = 12)
      noprint                ! (do nothing statement needed)
    else sw-3                ! solution step (3 <= isw < 12)
      loop,,30               ! iterate local solution
        utan, ,1
      next                   ! solution converged
    endif
    if pl                    ! add plot commands here
      plot ...
    endif
    fe2  send                ! MPI_Send return RVE response back to macroscale
  next                       ! go to next macroscale Gauss point
end
```

Figure 7.4: Solution commands in `solve_mpi` to be executed by each RVE processor.

The constitutive model, implemented in the subroutine `emtm02.f`, is superseded in the macroscopic scale by the RVE response. Hence, for the `rank=0` process, the subroutine `u_frvemat.f` is tasked with retrieving the material response from the data in `srvel(*,nrecv)` previously collected by `rvesr.f`.[12]

Microscopic Problem

In an attempt to evenly distribute the computational workload, each `rank>0` processor is assigned an approximately[13] equal number of macroscopic integration points (each corresponding to an individual RVE problem to be solved). During the preprocessing phase, each `rank>0` processor is prompted by the `FE2FEAP` input command to call the function `fe2prob.f`. Here, the `rank>0` processor awaits an MPI message[14] from `rank=0` with the necessary information to build the RVE mesh it was assigned. As soon as this message is received, the `rank>0` process executes the RVE input file commands and thereafter enters an infinite loop in `solve_mpi` to await further instructions from `rank=0`. The RVE will continue to perform tasks as requested until it receives a termination command (encoded by an MPI message with `ni=-999`).

Aside from the macroscopic primary variables and the components of their gradients, a typical MPI request from `rank=0` can include information about the current integration point number `ni`, time step, time increment, iteration count, and a variety of flags. Most importantly the MPI message contains the `isw` number, which specifies the type of task to be performed by the RVE. In particular, `isw=3` is a request to compute the RVE response for the given set of DIRICHLET boundary loads, whereas `isw=6` and `isw=12` signify RVE initialization and time step update tasks.

[12] The subroutine `rvesr.f` is called via the path `formfe.f` → `pform.f` → `rvesr.f`, upon which the variables `frvel` and `srvel` are stored within the dynamically allocated common block variable `hr(*)` using the pointers `np(260)` and `np(261)`. The subroutine `formfe.f` is responsible for forming the finite element arrays. This invokes the user element `formfe.f` → `pform.f` → `pforma.f` → `elmt02.f` to compute the element residual and stiffness. The fluxes and material moduli are obtained by `elmt02.f` → `stif02.f` → `emtm02.f`, where, for `rank=0`, the constitutive model is replaced with the RVE response using `u_frvemat.f`.

[13] The macroscopic problem setup may specify multiple RVE models. However, at least one processor is needed per each RVE model. For example, a macroscopic problem consisting of two different multiscale materials requires a minimum of 3 processors: One for the macroscale (`rank=0`) and one for each RVE model (`rank=1` and `rank=2`). The number of processors assigned to each material `ma` is stored in the variable `unproc(ma)`. If multiple processors are available for one RVE model, the corresponding macroscale integration points are evenly distributed across the available processors. The corresponding task allocation table is stored in `rvesd(ncol,nrow)` within the dynamically allocated integer common block `mr(*)` at pointer `np(270)`.

[14] Note that the `FE2FEAP` command is issued by the same temporary RVE input file which later issues the `INCLude solve_mpi` command. The aforementioned MPI message originates from the `rank=0` subroutine `pfe2rve.f`, which is invoked by the macroscopic solution command `RVE`. The MPI message contains a filename `matfile(ma)` specifying the input commands for the pre-processing of the RVE mesh associated with the macroscopic material `ma`, as well as the parameters `prtyp(1:3,ma)` to specify the basic RVE type (*e.g.*, an IRVING-KIRKWOOD type for finite deformations).

A typical RVE computation adheres to the following basic sequence: In executing the command `FE2 GET`, the `rank>0` processor receives an MPI message from `rank=0`. For example, let the switch value `isw=3` indicate that an RVE response is requested.

First, RVE data associated with the current macroscale integration point are retrieved from storage using `pfe2setio.f`. Next, the macroscopic primary variables and gradients are extracted from the MPI message by `pfe2setrv.f`, and subsequently applied as DIRICHLET boundary conditions to the RVE in `ufe2setd.f`. This concludes the command `FE2 GET`. Based on the value of `isw=3`, the input file `solve_mpi` executes solution commands to solve the RVE problem. This typically comprises the sequence of commands `LOOP`, `UTANgent`, and `NEXT`.

After the solution has converged the command `FE2 SEND` is issued, which prompts `pfe2setio.f` to return the RVE data back to storage. The subroutine `iksets.f` is tasked with computing the homogenized RVE response. This routine performs one more sweep of `formfe.f`, where `mrve02.f` integrates the fluxes in `u_flux(*)` as well as the element-wise components of the homogenization matrix $[\mathbf{H}]$, see (7.25), in `u_multi(*,ndf,nel)`. Thereafter, `ikprojuu.f` computes the matrices $[\hat{\mathbf{G}}_1]$ and $[\hat{\mathbf{H}}]$ from the values of `u_multi`, as well as the volume-averaged fluxes `u_ints(*)` from `u_flux(*)`. This is followed by `formhh.f`, which evaluates the SCHUR complement in Equation (7.66). This results in the homogenized material moduli `u_tang(*,*)`,[15] which are sent back to `rank=0` via MPI message along with the homogenized fluxes. The infinite loop in `solve_mpi` brings the `rank>0` process back to `FE2 GET` to await further instructions.

Random RVE Mesh

In the context of this dissertation, two types of RVE models are implemented, namely (i) an RVE with two different sets of material properties randomly assigned to the elements of the mesh and (ii) an RVE consisting of a single material but where the crystal orientation of the orthotropic material is assigned randomly for each element. In both cases, a random number generator with uniform probability distribution is employed. The two options are controlled by the solution command `SET OPAR <o1> <o2>` issued in the input file of the macroscopic problem.

The parameter `o1` is stored in the FEAP variable `itype`. The option `o1=1` signifies the random material assignment, where `0<=o2<=1` specifies the approximate fraction of elements assigned to material 2. For example, the command `SET OPAR 1 0.25` will generate an RVE mesh where approximately 75% of elements consist of material `ma=1` and the remaining 25% are assigned to `ma=2`.

On the other hand, the option `o1=2` signifies an RVE mesh with element-wise random crystal orientation. In this case, the second parameter `o2` (`0<=o2<=1`) indicates

[15] The arrays for `u_flux(*)`, `u_multi(*,ndf,nel)`, `u_ints(*)`, and `u_tang(*,*)` are declared such that the dimension `*` corresponds to 13 components in two-dimensional problems or 18 in three dimensions.

the range (relative to the orientation vector specified by the material parameters in the RVE input file) across which the orientation vector is allowed to vary. For example, `SET OPAR 2 0.25` signifies that each element of the RVE is randomly oriented between $\pm 45^\circ$ around the preferred crystal orientation.

Note that, even for problems consisting only of a single RVE material, each integration point is associated with its own individual random RVE. Hence, the macroscopic problem consists of a collection of randomly generated RVEs, all of which are characterized by the approximate distributions of elements set by the `o2` parameter.[16]

7.3.2 Homogeneous RVE

The numerical implementation of the multiscale EMTM model is first tested using an entirely homogeneous RVE. It is expected that the multiscale model, if implemented correctly, yields results that are identical to the single-scale implementation discussed in Section 6.4.

Homogenized Material Moduli

The homogenization procedure for the material moduli, implemented in the FEAP subroutines `ikprojuu.f` and `formhh.f`, is tested using a multiscale problem with homogeneous RVE. The geometry and mesh of the macroscopic problem may be chosen arbitrarily. Here, for example, a square block of 4×4 quadrilateral elements with bi-linear shape functions is defined. No external loads are applied, except for the zero-DIRICHLET boundary conditions necessary for the stiffness matrix to become invertible. The RVE model is comprised of a rectangular mesh with 10×10 elements. Its dimensions are much smaller than the macroscopic problem (by a factor of 10^6) and its centroid is located at the coordinate origin. The homogeneous RVE material is assumed to consist of monocrystalline Barium Titanate, a transversely isotropic piezoelectric material characterized by the parameters listed in Section 6.4.1. Given the absence of any loading or deformation, the finite element problem is entirely linear. As a result, the referential material moduli in (6.58) coincide with their spatial counterparts in (6.62).

As expected, the homogenized material moduli of the RVE, extracted from the 13×13 array `u_tang(*,*)`, are found to be in agreement with the the single-scale implementation of the constitutive model using (6.62) with the material parameters

[16] The `SET OPAR` command calls the subroutine `pfe2solv.f` → `ufe2opar.f`, where a set of random numbers is seeded, computed, and stored as variable `randn` under the dynamically allocated array `hr(*)` associated with the pointer `np(384)`. The random material assignment for `o1=1` is performed by `ufe2opar.f`, whereas the random crystal orientation for `o1=2` is implemented in `emtm02.f`. Since each `rank>0` processor is responsible for multiple RVEs (*i.e.*, macroscopic integration points), the random numbers of each RVE must be retained for future iterations of the macroscopic NEWTON-RAPHSON scheme. This is accomplished by writing and reading the pertinent information to and from a data file using the subroutine `pfe2setio.f`.

of $BaTiO_3$. In particular, the numerical values[17] of $\overline{\mathfrak{c}}_2$, $\overline{\mathfrak{c}}_3$, $\overline{\mathbb{C}}$, $\overline{\mathbb{C}\mathbf{A}}$, and $\overline{\kappa}$ are equal to the single-scale constitutive model to within about 10 significant digits. For example, the two-dimensional form of the elastic moduli $\overline{\mathbb{C}}$ is obtained in VOIGT notation as

$$\overline{\mathbb{C}} = \begin{bmatrix} 0.165E+06 & 0.777E+05 & 0.000E+00 & -.968E+03 \\ 0.777E+05 & 0.163E+06 & 0.000E+00 & -.632E+03 \\ 0.000E+00 & 0.000E+00 & 0.000E+00 & 0.000E+00 \\ -.968E+03 & -.632E+03 & 0.000E+00 & 0.431E+05 \end{bmatrix} , \tag{7.67}$$

and the piezo-electric tensor $\overline{\mathfrak{c}}_2$ evaluates to

$$\overline{\mathfrak{c}}_2 = \begin{bmatrix} -.839E+01 & 0.204E+01 & 0.000E+00 & -.103E+02 \\ 0.397E+01 & -.167E+02 & 0.000E+00 & -.512E+01 \end{bmatrix} . \tag{7.68}$$

These results are in agreement with the components of $(6.58)_{2,4}$, or alternatively with $(6.62)_{2,4}$. Furthermore, it is observed that `u_tang(*,*)` is approximately symmetric and that the homogenized fluxes obtained from `u_ints(*)` are indeed zero as expected in the absence of any loading.

Comparison with Single Scale under Loading

In the preceding section, it was confirmed that the multiscale model successfully extracts the material moduli of the underlying homogeneous RVE in the absence of loading or deformation. Next, the same homogeneous multiscale EMTM model is subjected to a mixture of mechanical, thermal, and electrostatic boundary loads. The resulting deformations and fluxes are compared with the single-scale implementation discussed in Section 6.4.

In particular, consider the single-scale EMTM problem illustrated in Figure 6.5, which was designed to compare the exact implementation of the element stiffness matrix with a numerical approximation using the complex-step method. As before, tensile forces of $f_x = 1\,\mathrm{kN}$ and $f_y = 5\,\mathrm{kN}$ are applied, along with shear tractions amounting to $f_\tau = 2\,\mathrm{kN}$ (per millimeter of thickness). Linear distributions are prescribed along the thermal and electric DIRICHLET boundaries, where $T_1 = 0\,^\circ\mathrm{C}$ and $T_2 = 16 \times 10^3\,^\circ\mathrm{C}$ (relative to a reference temperature of $T_1 = 0\,^\circ\mathrm{C}$) as well as $\phi_1 = 10\,\mathrm{kV}$ and $\phi_2 = 0\,\mathrm{V}$. The same rectangular domain with 4 elements per dimension is used for the macroscopic model, whereas the RVE mesh consists of 10×10 elements, as in the preceding example.

It is observed that the distributions of the primary variables (*i.e.*, the displacement, temperature, and electric potential) and the fluxes (*i.e.*, the stress, heat flux, and polarization) are virtually identical in the multiscale implementation and in the single-scale EMTM model. For example, the contour plots for the X-displacement and

[17] Recall that, in the context of the numerical implementation, the factors ρ_0 (or ρ) and ε_0 were absorbed into the referential (or spatial) material parameters for simplicity.

the X-polarization of the multiscale model, shown in Figure 7.5, are indiscernible from the single-scale results. Furthermore, it is seen that the components of the element residual $\mathbf{R}^i$ and stiffness matrix $\mathbf{K}^{ij}$ for the macroscopic problem is consistent with the residual and stiffness observed in the single-scale implementation. In particular, the components of $\mathbf{R}^i$ and $\mathbf{K}^{ij}$ associated with variational node $i=1$ and differential node $j=3$, tabulated in Table 6.4 for the same element in the single-scale model, are indeed identical to within 10 significant digits.

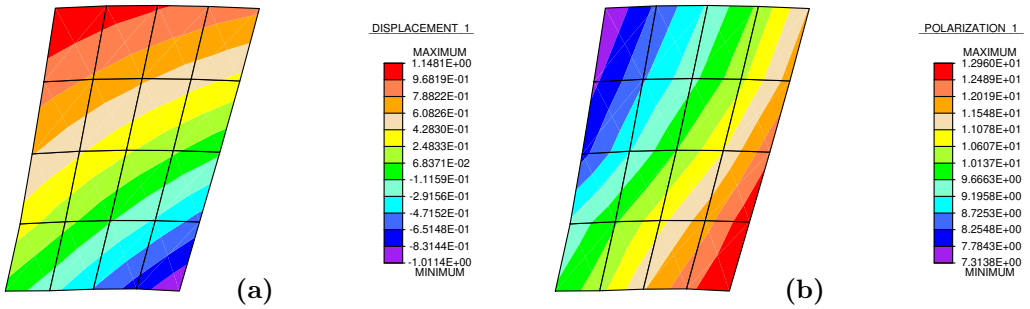

Figure 7.5: The EMTM problem illustrated in Figure 6.5, is run as a multiscale model with homogeneous RVE. As expected, the resulting deformation and fluxes are identical to the single-scale solution. Here, contour plots are shown for (a) the X-component of displacement and (b) the X-component of polarization.

Lastly, it is noted that the multiscale implementation converges within the same number of iterations as the single-scale model. This serves as further indication that the RVE material response, and thus the residual and stiffness matrix, are computed correctly. However, note that the multiscale model demands significantly more CPU time overall. The increase is primarily due to the additional computational workload required to process the RVE models, as well as the time spent communicating among the processors.

For example, Table 7.1 shows an excerpt of the FEAP log file produced by the single-scale implementation. Each time step is solved within 4 iterations, requiring a total CPU time of about 60 ms. On the other hand, the log file of the multiscale model with a 10×10 RVE mesh is shown in Table 7.3. The macroscopic problem still solves within 4 iterations but takes almost three times longer to compute, at a total CPU time of about 170 ms. The simulation associated with the log file in Table 7.2 represents an intermediate case, where the multiscale user element `emtm_2d` is employed to solve a single-scale problem by executing the fe2-version of FEAP serially.[18] In this case, the problem initialization takes about 50 ms longer than the serial version of

[18]Let `$FEAPHOME` denote the parent directory of the FEAP program structure. The single-scale, serial version of FEAP is executed using the command `$FEAPHOME/main/feap`. On the other hand, the parallel version of FEAP is invoked by `mpirun` from the `./fe2` folder. For example, a command of the form `$PETSC_DIR/$PETSC_ARCH/bin/mpirun -np 6 $FEAPHOME/fe2/feap` enlists a total of 6 parallel processors to solve the multiscale problem. The `./fe2` version of FEAP can alternatively be run serially by executing `$FEAPHOME/fe2/feap` without the use of `mpirun`.

FEAP in Table 7.1, but the iterative solution itself completes approximately within the same CPU time.

Note that a slight difference in the final energy norm is observed for the multiscale model, see the penultimate column of Table 7.3, compared with the single-scale simulations in Tables 7.1 and 7.2. This is caused by minute differences in the homogenized material moduli, which have a small but cumulative effect on the iterative solution process. However, this does not adversely affect the accuracy of the final result. Indeed, in 4 iterations the energy norm went down by more than a factor of 10^{-18} from the initial value, which is well within the default tolerance of 10^{-16}. Moreover, any additional iteration would further bring down the energy norm by several orders of magnitude.

Load Step	Total Tang+Form		Solution Time	Time Incr.	Residual Norm Initial	Residual Norm Final	Energy Norm Initial	Energy Norm Final	CPU Time (Seconds)	Cn
1	4	0	1.000E-01	1.00E-01	2.08E+04	1.67E-05	6.13E+03	5.22E-15	0.03	EQ
2	4	0	2.000E-01	1.00E-01	2.16E+04	1.43E-05	6.05E+03	3.71E-15	0.04	EQ
3	4	0	3.000E-01	1.00E-01	2.24E+04	1.33E-05	5.99E+03	3.08E-15	0.06	EQ

Table 7.1: Excerpt from the log file for an EMTM test problem using the single-scale implementation from Section 6.4.

Load Step	Total Tang+Form		Solution Time	Time Incr.	Residual Norm Initial	Residual Norm Final	Energy Norm Initial	Energy Norm Final	CPU Time (Seconds)	Cn
0	0	0	0.000E+00	1.00E-01	0.00E+00	0.00E+00	0.00E+00		0.08	UN
1	4	0	1.000E-01	1.00E-01	2.08E+04	1.67E-05	6.13E+03	5.22E-15	0.08	EQ
2	4	0	2.000E-01	1.00E-01	2.16E+04	1.43E-05	6.05E+03	3.71E-15	0.09	EQ
3	4	0	3.000E-01	1.00E-01	2.24E+04	1.33E-05	5.99E+03	3.08E-15	0.11	EQ

Table 7.2: Excerpt from the log file for an EMTM test problem using the multiscale element, but employed as a single-scale model by running FEAP serially.

Load Step	Total Tang+Form		Solution Time	Time Incr.	Residual Norm Initial	Residual Norm Final	Energy Norm Initial	Energy Norm Final	CPU Time (Seconds)	Cn
0	0	0	0.000E+00	1.00E-01	0.00E+00	0.00E+00	0.00E+00		0.07	UN
1	4	0	1.000E-01	1.00E-01	2.08E+04	1.67E-05	6.13E+03	5.22E-15	0.11	EQ
2	4	0	2.000E-01	1.00E-01	2.16E+04	1.43E-05	6.05E+03	3.71E-15	0.13	EQ
3	4	0	3.000E-01	1.00E-01	2.24E+04	1.33E-05	5.99E+03	3.09E-15	0.17	EQ

Table 7.3: Excerpt from the log file for an EMTM test problem using the multiscale element using a homogeneous RVE with parallel computing using `mpirun`.

Dependence of Macroscopic Convergence on RVE Dimensions

In the preceding examples, the size of the RVE was deliberately chosen to measure about five orders of magnitude less than the dimensions of the macroscopic domain.

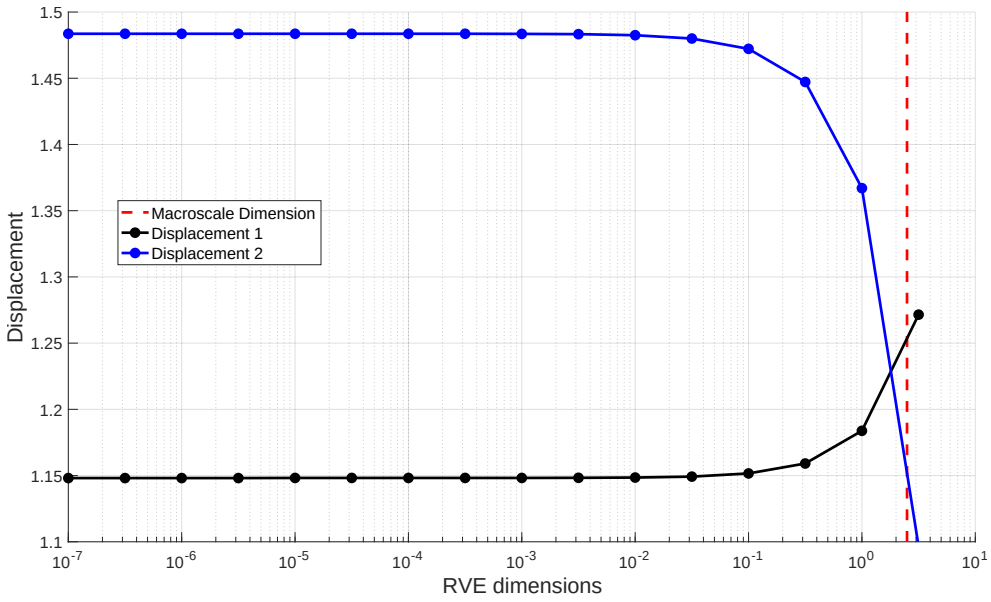

Figure 7.6: The X- and Y-displacements of the top right corner of the macroscopic mesh, plotted as a function of the RVE size. The size of the macroscale problem is indicated by the vertical dashed line. As the dimensions of the RVE model approach the macroscopic size scale, the displacements begin to diverge. Further increasing the size of the RVE leads to a complete loss of convergence of the macroscopic problem.

The actual size of the RVE does not significantly affect its behavior or the macroscopic result, as long as it several orders of magnitude smaller than the macroscopic model. For example, the preceding results are readily reproduced using an RVE which is, say, eight orders of magnitude smaller than the macroscale problem.

Note, however, that the results of the macroscopic EMTM model begin to diverge as the RVE size approaches an order of magnitude similar to the macroscopic model dimensions. This is demonstrated in Figure 7.6 by tracking the X- and Y- displacements of the upper-right corner node of the macroscopic mesh as a function of the RVE size. Each dot on the graph corresponds to a separate multiscale simulation with a different RVE geometry size. It is seen that the macroscopic displacement is independent of the RVE dimension as long as it remains well below the macroscopic size (say, by at least two orders of magnitude). As the RVE size increases further, the displacements begin to deviate as the macroscopic problem struggles to converge until, finally, the numerical scheme diverges.

This loss of convergence is further illustrated in Figure 7.7, which shows the energy norm for successive Newton-Raphson iterations. As long as the RVE is small, the macroscopic problem converges in four iterations. As the RVE size increases, the number of iterations needed to satisfy the convergence criterion begins to increase, until eventually the energy norm diverges entirely.

It is emphasized that the aforementioned dependence on RVE size is observed only

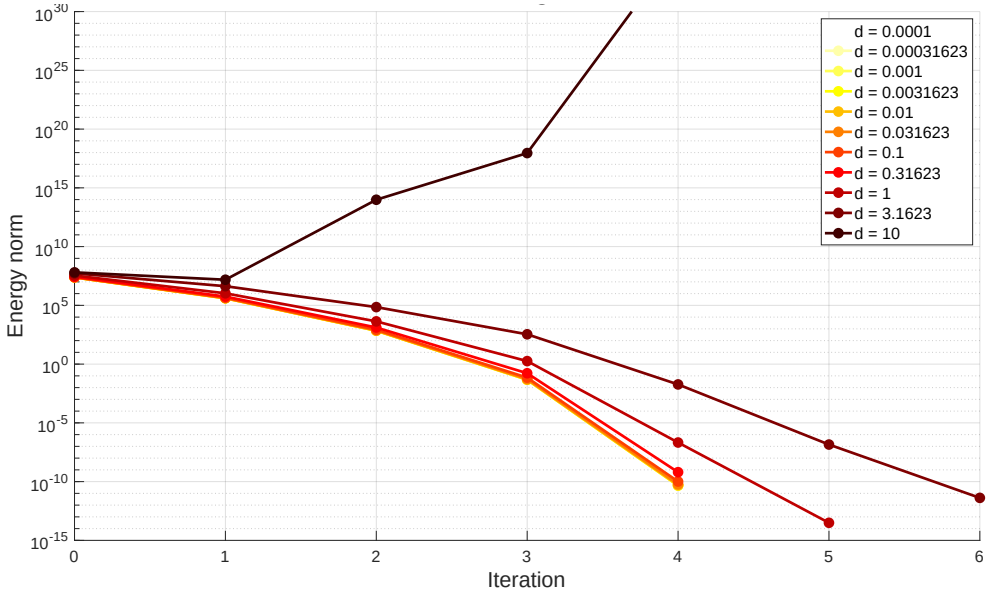

Figure 7.7: Dependence of macroscopic convergence on the size of the RVE. Each curve shows the residual energy norm for successive iterations of the NEWTON-RAPHSON scheme. As the RVE size is increased beyond $d = 1$, convergence becomes slower and eventually ceases entirely.

in EMTM problems exhibiting thermal expansion in the presence of a temperature gradient. If either the macroscopic temperature is uniform, or if the coefficient of thermal expansion of the RVE material vanishes, the diverging behavior in Figures 7.6 and 7.7 disappears. It is therefore concluded that this loss of convergence is directly related to thermal expansion.

Indeed, thermal expansion is distinct from the other constitutive behaviors in the sense that the resulting deformation depends on the *absolute* value of a primary quantity (*i.e.*, the temperature) rather than its gradient. In view of the thermal DIRICHLET boundary condition in Equation $(7.1)_2$, an increase in the RVE size leads to a similar increase in the absolute temperature at the RVE boundary, since its value is proportional to the distance from the centroid as well as to the macroscopic temperature gradient (which is considered to be constant). As the RVE experiences extreme temperatures at the boundaries, the corresponding thermal strains impede the convergence of the RVE equations.

7.3.3 Random Material Mixture

In Section 7.3.2, the multiscale model was examined using a purely homogeneous RVE material. In the present section, an element-wise random material assignment is introduced to the RVE mesh. For this purpose, two different material parameter sets are defined in the RVE input file. Thereafter, the multiscale algorithm employs a set of random numbers to assign either material `ma=1` or `ma=2` to each element

Parameters of Non-Piezoelectric Version of $BaTiO_3$						Units
λ	76.6×10^3	μ	44.7×10^3			N/mm^2
ω_1	-3.6×10^3	ω_2	0.7×10^3	ω_3	0.9×10^3	N/mm^2
β_1	0.0	β_2	0.0	β_3	0.0	C/m^2
γ_1	$8.854\,188 \times 10^{-6}$	γ_2	0.0			$mC/(kV\,m)$

Table 7.4: Coordinate-independent material parameters of a fictitious, non-piezoelectric and non-polarizable adaptation of Barium Titanate ($BaTiO_3$), see Table 6.1.

of the RVE mesh. As elaborated in Section 7.3.1, the random material assignment is controlled by the macroscopic solution command `SET OPAR 1 <o2>`, where the parameter `o2` (with `0<=o2<=1`) specifies the approximate fraction of elements that are assigned to `ma=2`.

The preceding numerical examples were based on Barium Titanate, whose transversely isotropic piezoelectric properties are listed in Section 6.4.1. For the purpose of demonstrating the random RVE material assignment, a second set of material properties is introduced. This fictitious material exhibits the same thermomechanical properties as $BaTiO_3$, but is assumed to be non-piezoelectric and non-polarizable. This implies that the parameters β_{1-3} and γ_2 in Equations $(6.58)_{2,3}$ are zero, whereas $\gamma_1 = \varepsilon_0$ is equal to the electric permittivity of vacuum, see Section 3.3. The material parameters of this electrically inert material are summarized in Table 7.4.

Effect of Inhomogeneous Microstructure on RVE Solution

To illustrate the random nature of the material assignment within the RVE (and across different macroscopic integration points), consider a domain composed of an inhomogeneous RVE microstructure and subjected to mixed EMTM loads. Let the macroscale be given by a 4×4 rectangular mesh comprised of quadrilateral elements with bi-linear shape functions, whereas the RVE model consists of 30×30 elements. Using the command `SET OPAR 1 0.5`, about half of the RVE elements are randomly attributed to material `ma=1` and the remaining half to `ma=2`. The mixed EMTM boundary conditions previously employed in Section 7.3.2 are applied to the macroscale problem.

A linear distribution of electric potential is applied to the boundary of the macroscopic model along the Y-direction. This results in an approximately[19] linear distribution of ϕ throughout the body, which corresponds to a uniform Y-component of the electric field. This is illustrated in Figure 7.8, which shows contour plots of the macroscopic primary variables of displacement, temperature, and electric potential. The macroscopic electric potential gradient is transferred to the RVE boundary as part of the DIRICHLET boundary condition in Equation $(7.1)_3$. The resulting distribu-

[19] Since each integration point is associated with a different random RVE, small variations in the macroscopic constitutive properties persist. This can be seen in the electric potential in Figure 7.8.

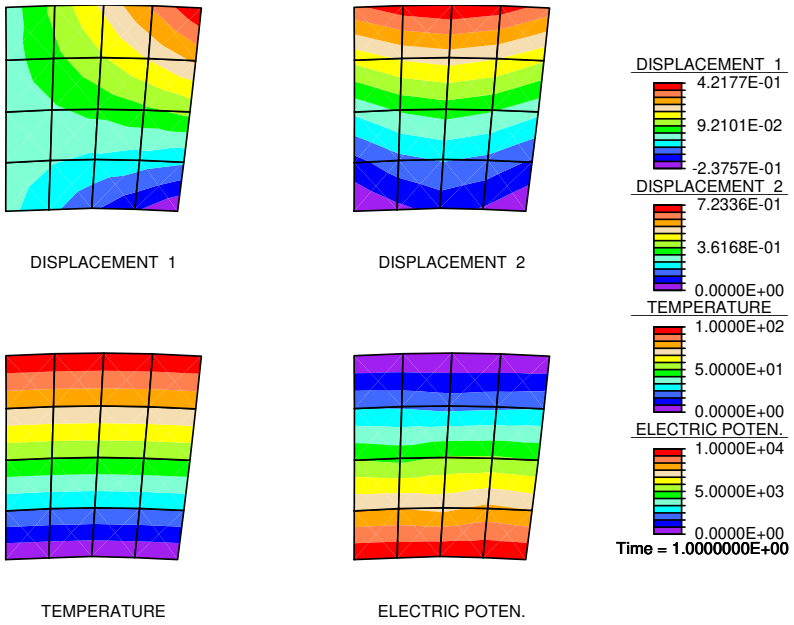

Figure 7.8: Contour plots of the macroscopic primary variables, *i.e.*, the displacements, temperature, and the electric potential. A mixture of mechanical, thermal, and electrostatic loads are applied to the boundary of the 4×4 macroscopic mesh. The electric properties of the 30×30 RVE elements is randomly assigned, see Figures 7.9 and 7.10, causing the macroscopic electric potential to deviate slightly from a perfectly linear distribution.

tion of electric potential on the microscopic scale is illustrated in Figure 7.9 for four arbitrarily chosen RVEs, each corresponding to a different macroscopic integration point.[20]

Figure 7.9 shows that, despite the linear prescription of ϕ at the boundary, the electric potential in the interior of the RVE departs significantly from the linear distribution otherwise expected of a homogeneous RVE. This illustrates that the effect of an inhomogeneous RVE microstructure on the distribution of the primary variables can be substantial. Moreover, the internal distribution of ϕ varies considerably across the different RVEs. As a consequence, the randomness on the RVE level is appreciable even on the macroscopic scale, where each integration point exhibits slightly different homogenized material moduli.

Figure 7.10 depicts the Y-component of dielectric polarization for the same RVEs used in Figure 7.9. Approximately half of the elements comprising the RVE mesh are non-polarizable, and hence colored in uniform blue color in the contour plots of

[20]More specifically, plots are provided for (a) `np=10`, `rank=2`, (b) `np=13`, `rank=2`, (c) `np=13`, `rank=3`, and (d) `np=13`, `rank=4`, where `np` and `rank` signify the `np`-th integration point handled by processor `rank`. The macroscopic node associated with this integration point can be retrieved from the task allocation table `rvesd(rank,np)`. Because of how tasks are distributed to the RVEs (in the subroutine `psetrvsd.f`), the node number is given by `(np-1)*(ntasks-1)+rank`, where `ntasks` is the total number of processors. The present simulation was run with `mpirun -np 6`, *i.e.*, `ntasks=6`.

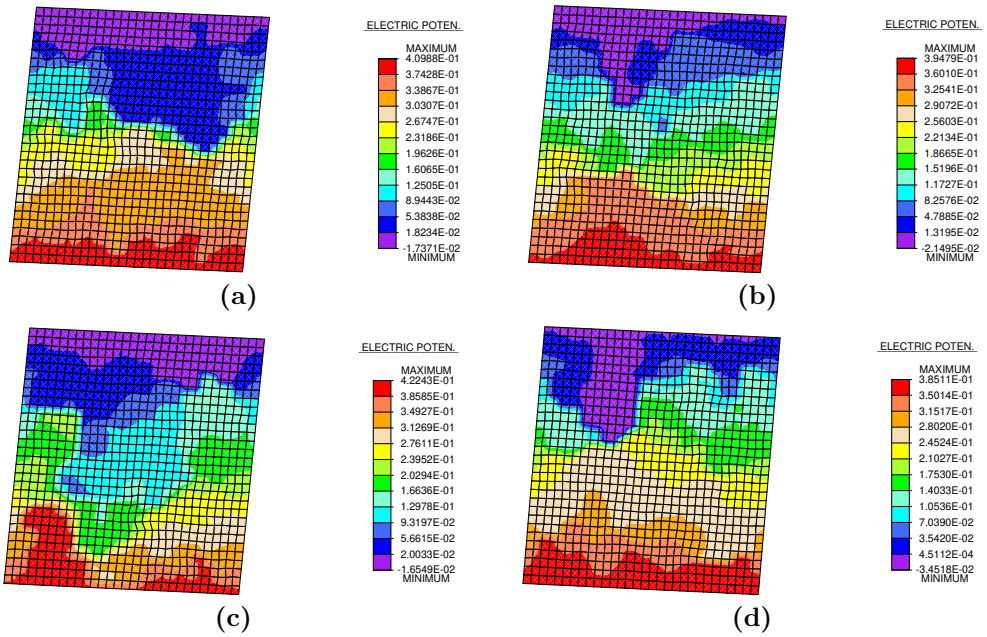

Figure 7.9: Examples of RVE contour plots of the electric potential, associated with different integration points in the macroscopic model shown in Figure 7.8. Plots are provided for (a) `np=10` and `rank=2`, (b) `np=13` and `rank=2`, (c) `np=13` and `rank=3`, and (d) `np=13` and `rank=4`, which denotes the `np`-th macroscopic integration point computed by the RVE processor `rank`.

Figure 7.10. As expected from the element-wise prescription of material parameters, the polarization is observed to be highly discontinuous across element boundaries.

Effect of Volume Fraction on Piezoelectric Behavior

Next, the multiscale model with random RVE material assignment is used to examine the effect of the volume fraction (*i.e.*, the value of the parameter `o2`) on the resulting piezoelectric behavior. To this end, consider yet again a macroscopic domain comprised of 4×4 quadrilateral elements. Unlike before, however, its boundary is subjected only to an electric potential without any mechanical or thermal loads applied. The electric potential at the boundary is varied linearly in the Y-direction such that the macroscale Y-component of the electric field amounts to $1\,\mathrm{kV/m}$ on average. The body is simply supported using the corners on the lower edge.

Meanwhile, the elements of the 10×10 RVE mesh are randomly assigned to the same set of materials used in the preceding example, that is, Barium Titanate and its fictitious, electrically inert counterpart, see the parameters in Tables 6.1 and 7.4. The crystal orientation vector of these transversely isotropic materials is set to $\boldsymbol{\alpha} = \frac{1}{\sqrt{5}}\mathbf{e}_1 + \frac{2}{\sqrt{5}}\mathbf{e}_2$ according to the constitutive relations in (6.58 - 59). The volume fraction of the RVE material mixture is prescribed using the command `SET OPAR 1 <o2>`. The parameter is varied from `o2=0.0` (*i.e.*, a homogeneous RVE consisting only of

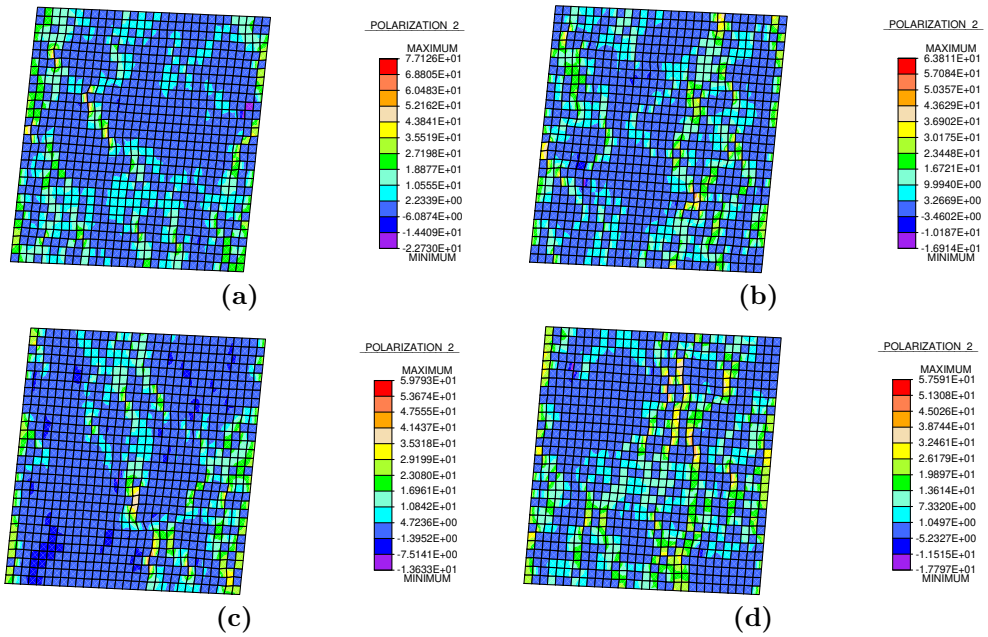

Figure 7.10: Contour plots of the dielectric polarization throughout the RVE. The same macroscopic integration points as in Figure 7.9 are selected for plotting, namely (a) `np=10` and `rank=2`, (b) `np=13` and `rank=2`, (c) `np=13` and `rank=3`, and (d) `np=13` and `rank=4`.

material `ma=1`) to `o2=1.0` (only `ma=2`) in increments of 5 %.

Figure 7.11 depicts the X- and Y-displacements of the top-right corner of the macroscopic domain as a function of the volume fraction of the RVE attributed to material `ma=2`. For the homogeneous RVE of monocrystalline $BaTiO_3$, or `o2=0.0`, the external electric field induces a piezo electric deformation. Due to the simply supported domain and the diagonal orientation of the crystal direction $\boldsymbol{\alpha}$, the upper-right corner displaces in both the X- and the Y-directions. On the other hand, the displacements vanish as expected for `o2=1.0` where the RVE consists entirely of the non-piezoelectric material `ma=2`. In between the two homogeneous extremes, there is a nonlinear relation between the volume fraction and the resulting piezoelectric deformation. The rule of mixtures, *i.e.*, the volume-weighted average of the piezoelectric constants in $\mathfrak{C}_2$ for the two materials, furnishes an upper bound for the effective piezoelectric moduli. This is confirmed by the result in Figure 7.11, because the deformation is proportional to the homogenized piezoelectric constants. Note that the graph appears to be slightly erratic due to the relatively small number of RVE elements available for random material assignment.

The sequence of contour plots in Figure 7.12 illustrates the effect of volume fraction on the piezoelectric deformation of the RVE. For the pure Barium Titanate the piezoelectric deformation leads to a trapezoidal shape. With increasing volume fraction of `ma=2` the piezoelectric deformation gradually reduces to zero. The distribution of the electric potential is perfectly linear only in the homogeneous cases `o2=0.0` and

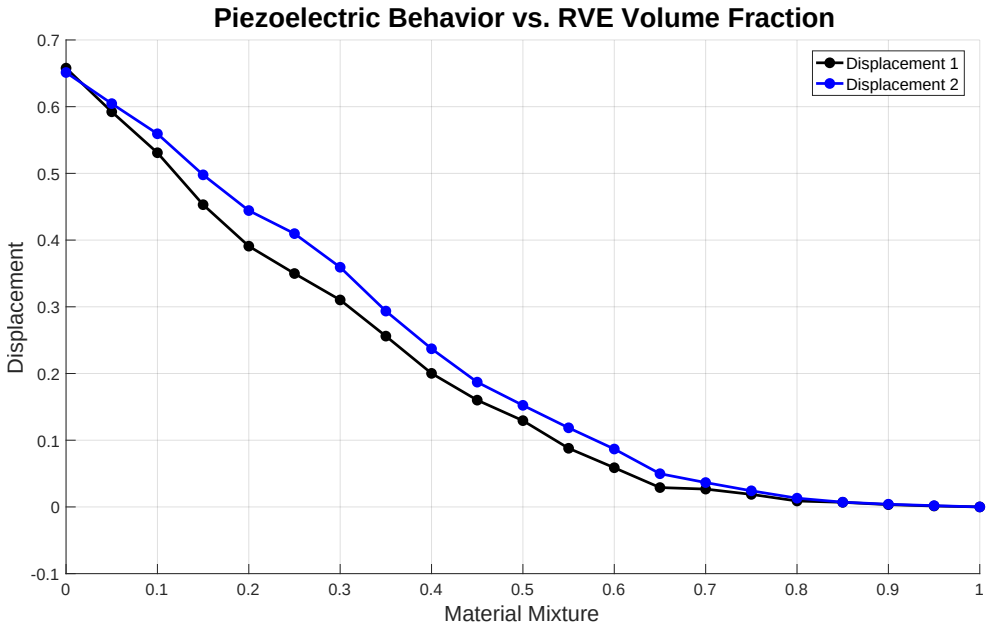

Figure 7.11: Piezoelectric deformation as a function of the RVE volume fraction between Barium Titanate and its non-piezoelectric counterpart. A nonlinear dependence is observed between the homogeneous monocrystalline $BaTiO_3$ (for `o2=0.0`) and the electrically inert material (for `o2=1.0`). The piezoelectric deformation is quantified in terms of the deflection of the top-right node of a simply supported domain subjected to an electric gradient in the Y-direction.

`o2=1.0`. Meanwhile, it is evident from the contour plots of the polarization depicted in Figure 7.13 which elements of the RVE were randomly assigned to the non-polarizable material.

7.3.4 Random Crystal Orientation

The preceding discussion in Section 7.3.3 was based on a multiscale model, where two different kinds of materials are randomly assigned to each element of the RVE mesh at a prescribed target volume fraction. In the present section, the RVE consists of only one material (Barium Titanate). Instead, each element is assigned a random crystal orientation vector $\boldsymbol{\alpha}$ using a random number generator with a uniform probability distribution.

This option is invoked by the macroscopic solution command `SET OPAR 2 <o2>`, where the parameter `0<=o2<=1` specifies the extent to which $\boldsymbol{\alpha}$ is allowed to vary. For example, `SET OPAR 2 0.0` corresponds to a homogeneous RVE comprised of monocrystalline $BaTiO_3$ oriented in the direction of $\boldsymbol{\alpha}_0$ specified by the RVE material parameter input. On the other hand, `SET OPAR 2 1.0` causes the orientation $\boldsymbol{\alpha}$ of the transversely isotropic material to vary randomly in any direction within the two-dimensional plane of the problem. For any intermediate value of `<o2>`, the angle of $\boldsymbol{\alpha}$ varies within a range of $\pm\pi$ `<o2>` around the target direction $\boldsymbol{\alpha}_0$.

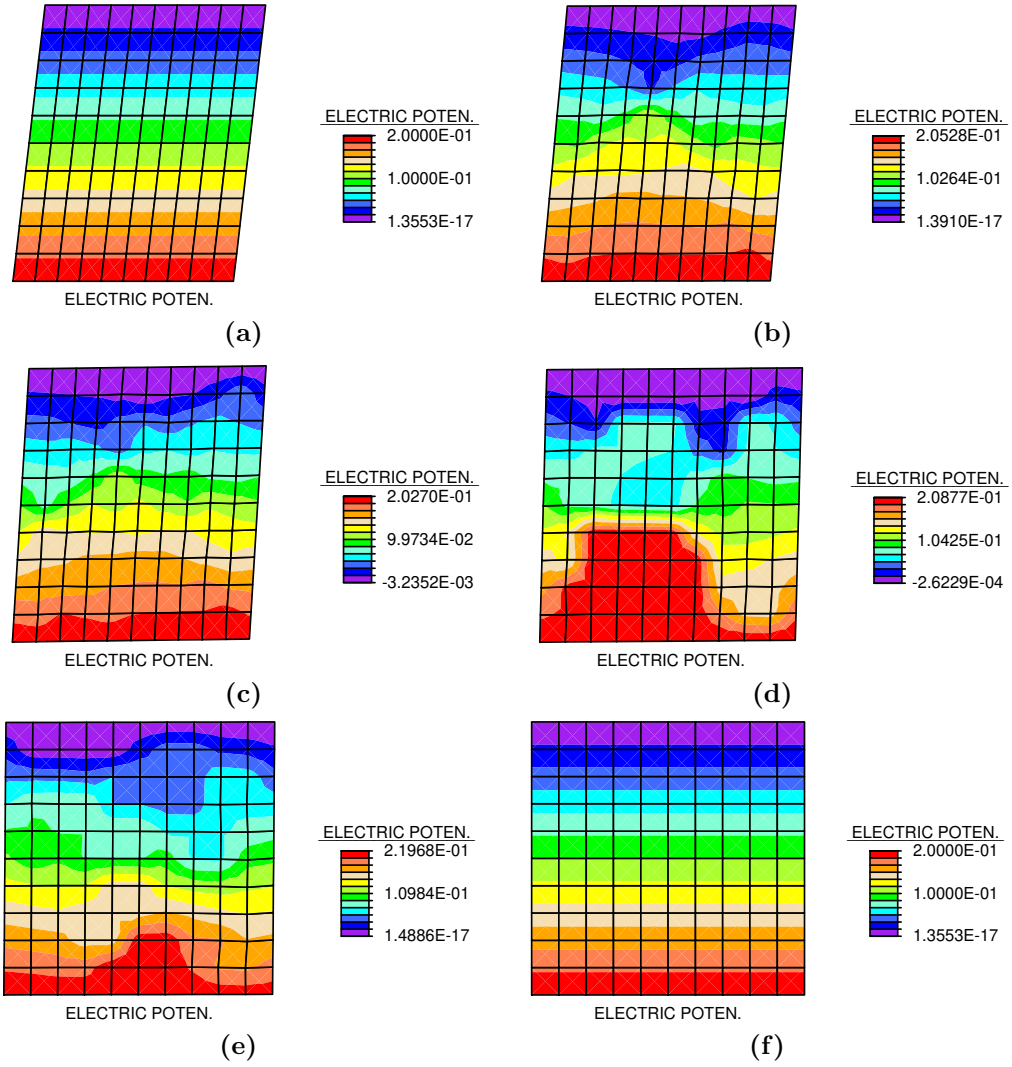

Figure 7.12: Contour plot of the electric potential within a typical RVE, depending on the volume fractions of the randomly assigned RVE materials `ma=1` and `ma=2`. Volume fraction of (a) `o2=0.0` (monocrystalline $BaTiO_3$), (b) `o2=0.1`, (c) `o2=0.25`, (d) `o2=0.45`, (e) `o2=0.7`, (f) `o2=1.0` (homogeneous non-piezoelectric material).

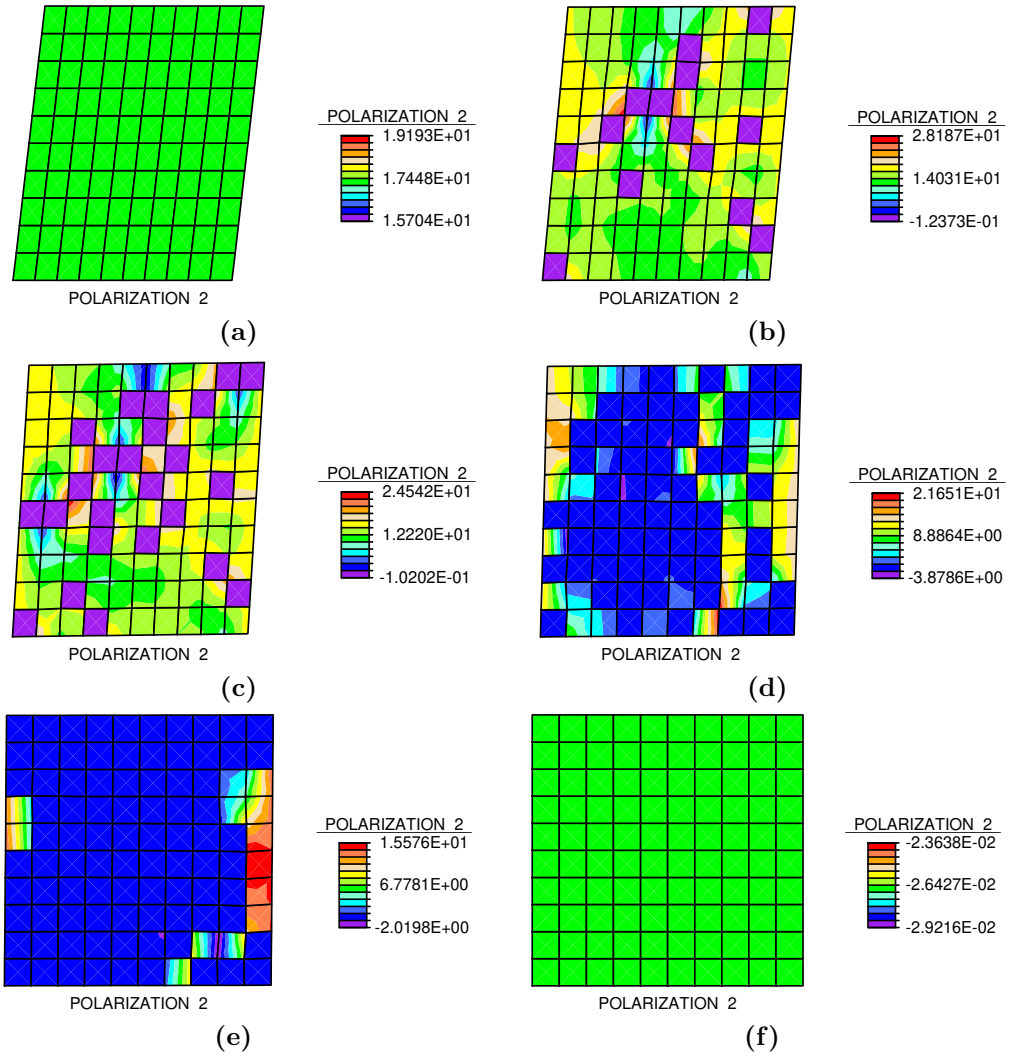

Figure 7.13: Contour plots of the polarization along the Y-direction for different volume fractions of $BaTiO_3$ and its non-polarizable counterpart. See Figure 7.12 for a list of the parameter `o2` employed in Figures (a)-(f).

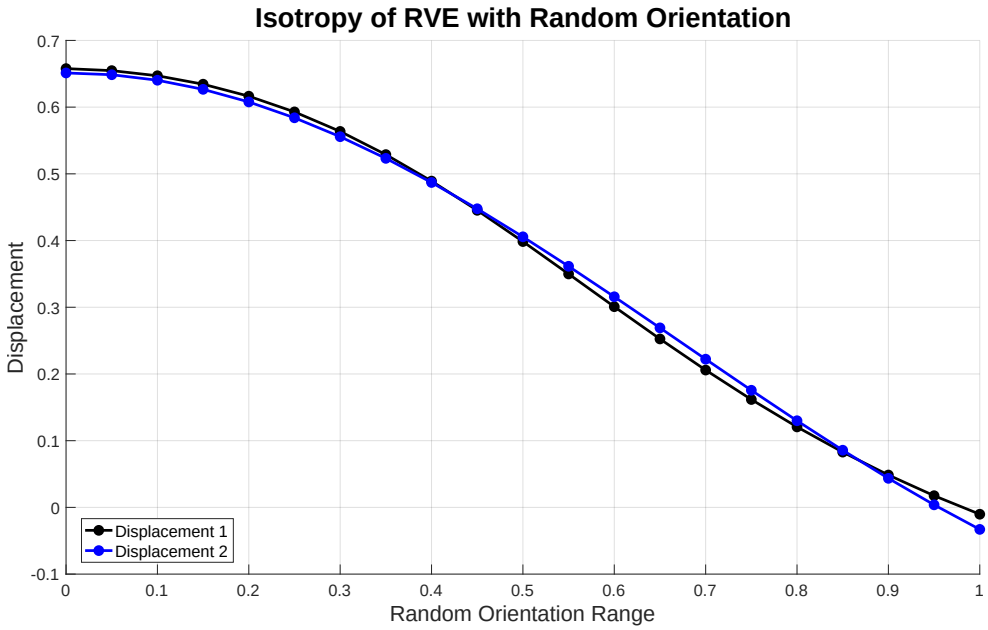

Figure 7.14: X- and Y-displacements of the top-right corner of the macroscopic mesh as a function of the level of randomness attributed to the crystal orientation of individual RVE elements. The simply supported macroscopic domain is subjected to a linearly varying electric potential at the boundary. The macroscopic piezoelectric deformation gradually reduces to zero with increasing randomness of the RVE, until its homogenized behavior is approximately isotropic.

To test the capability of this feature, consider once again a macroscopic domain of 4×4 elements, which is simply supported at the bottom and subjected to an electric potential gradient in the Y-direction. To assess the piezoelectric behavior of the homogenized material, the X- and Y-displacements on the upper-right corner are tracked. Provided that the RVE comprises a sufficiently large number of elements, it is expected that the macroscopic behavior is approximately isotropic when the microscopic crystal orientations are completely random (`o2=1.0`).

Figure 7.14 depicts the X- and Y-displacements of the top-right node as a function of the parameter `<o2>`. Note that, since a value of `o2=0.0` corresponds to monocrystalline Barium Titanate, the graphs in Figures 7.11 and 7.14 exhibit the same Y-intercepts. With increasing randomness of the RVE, the macroscopic displacement reduces to approximately zero. This is expected from an isotropic material comprised of a microscale of randomly oriented crystal grains, because the piezoelectric deformation of the RVE is on average isochoric (in the absence of additional mechanical or thermal loads). Note that the data in Figure 7.14 appears smoother than the previous graph in Figure 7.11 in part because the RVE is comprised of a larger number of elements.

Figure 7.15 illustrates the distribution of the Y-deformation within the RVE for varying degrees of randomness `<o2>`. It is apparent from the overall shape of the

RVE (drawn here to scale) that the overall piezoelectric deformation of the multiscale material diminishes with increasing randomness and isotropy. The trapezoidal shape characteristic of the piezoelectric deformation of monocrystalline $BaTiO_3$ gradually gives way to a virtually undeformed macroscale. Nevertheless, the RVE is subject to significant micro-stresses due to the competing piezoelectric deformation of adjacent crystal grains. This is evident, for example, from the significant distortion observed in the RVE mesh of Figure 7.15(f).

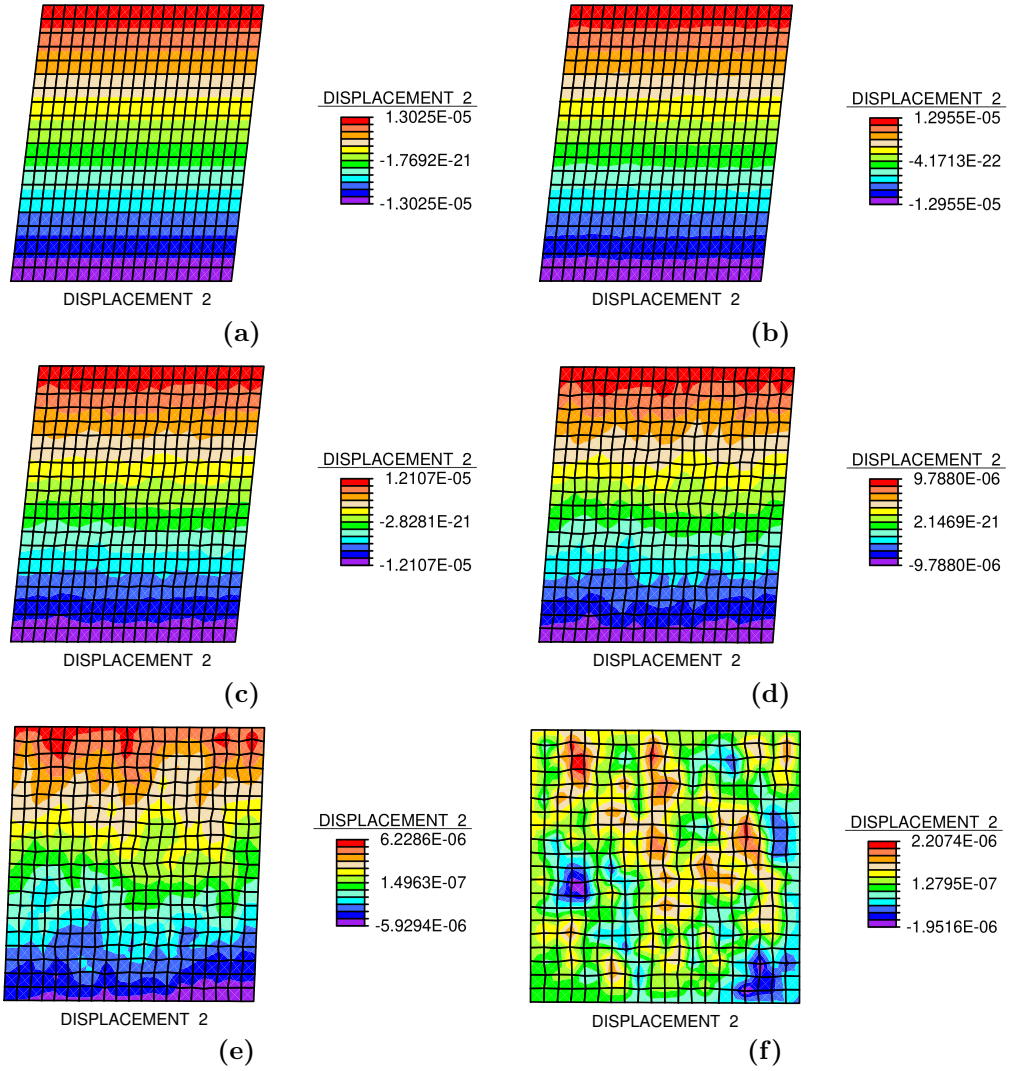

Figure 7.15: Contour plots of the Y-displacement for RVEs with varying levels of random crystal orientation. The degree of randomness is given by (a) `o2=0.0` (monocrystalline $BaTiO_3$), (b) `o2=0.1`, (c) `o2=0.25`, (d) `o2=0.45`, (e) `o2=0.7`, (f) `o2=1.0` (completely random crystal orientation).

Lastly, it is observed that the rate of convergence for the macroscopic problem depends on `<o2>`, *i.e.*, the range of random orientation defined for the RVE. As

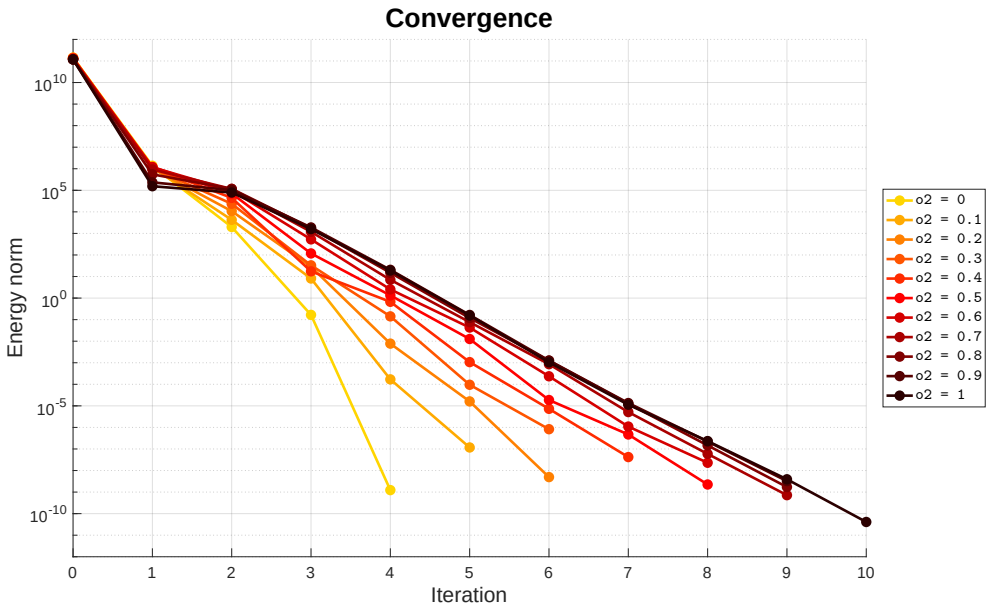

Figure 7.16: Convergence behavior of the macroscopic NEWTON-RAPHSON scheme for different values of `<o2>`. This parameter controls the range of the random orientation angles assigned to the elements of the RVE mesh. Each line depicts the energy norm of the residual until the convergence criterion is satisfied. It is observed that the computational workload increases for RVE models with greater levels of randomness.

before, the macroscopic problem is considered to have converged when the energy norm of the global residual has decreased by at least a factor of 10^{-16} relative to its initial value. Recall that it was found in Section 7.3.2 that the homogeneous model (`o2=0.0`) converges in only four iterations, see Figure 7.7. On the other hand, a multiscale model with completely random RVE orientations (`o2=1.0`) requires a total of ten macroscopic iterations to solve. Figure 7.16 shows the energy norm of the residual for successive iterations of the NEWTON-RAPHSON scheme. Each curve represents a separate simulation with a different value of the parameter `<o2>`. The general tendency of more iterations necessary for increasing values `<o2>` is apparent from Figure 7.16.

Chapter 8

Concluding Remarks

The multiscale modeling of coupled electro-magneto-thermo-mechanical media is an important subject with a wide range of applications, from the constitutive description of the coupled behavior of engineering and biological materials with complex microstructures, to the design of metamaterials with tailored electromechanical or magnetomechanical properties. In this dissertation, the following three overarching goals were accomplished: First, an in-depth review of Maxwell's equations and the balances of momenta and energy for coupled EMTM materials was conducted from the perspective of conventional continuum mechanics. Special attention was paid to the transformation properties of the relevant fields under superposed rigid-body motion. This highlighted the need for a pre-metric treatment of electrodynamics consistent with Galilean invariance. This implies that the aether relations are *not* invoked from the outset, and that the electromagnetic momentum and energy are *not* integrated into the overall momentum and energy of the underlying body, as would otherwise be customary in the context of the Maxwell–Minkowski formulation. Moreover, the Green-Naghdi-Rivlin theorem was called upon to highlight that the balances of mass and momenta are derivable from the energy balance. This serves as important confirmation that the choice of linear and angular momentum balances is consistent with the energy equation.

Next, a consistent multiscale homogenization scheme was introduced for the coupled EMTM behavior. The upscaling behavior of the relevant quantities was deduced from the postulated weighted volumetric averaging of certain extensive quantities in accordance with the Irving-Kirkwood theory. In particular, the mass, linear momentum, thermomechanical energy, and electric charge were prescribed with the aforementioned averaging scheme. This represents the minimal set of assumptions needed to upscale all relevant quantities. Due to the extensivity of these quantities, their macroscopic densities (per unit volume) are naturally given by volume averages of their microscopic counterparts. This homogenization scheme eliminates the need for an energy-based micro-macro criterion such as the Hill-Mandel condition. In addition, it offers greater versatility in the range of RVE boundary conditions

permitted, as well as allowing the study of micro-inertial effects.

Lastly, a numerical implementation of the multiscale model was devised using a first-order FE2 strategy. Each macroscopic integration point is associated with an individual RVE, whose boundary value problem is solved during each iteration of the macroscopic NEWTON-RAPHSON solution scheme. The macroscale provides the gradients necessary to apply the RVE boundary conditions, and the RVE reports back the homogenized fluxes and material moduli. The homogenized fluxes are computed from volumetric averages of the relevant quantities over the RVE mesh, whereas the homogenized material moduli are obtained by means of a linearization of the averaged fluxes followed by a SCHUR complement of the ensuing system of linear algebraic equations.

The multiscale finite element algorithm was validated using a variety of quasi-static two-dimensional test problems, employing both homogeneous and inhomogeneous RVE models. It was shown that, as expected, an FE2 model with homogeneous RVE furnishes identical results as a single-scale model comprised of the same material. However, for problems involving a non-zero thermal gradient in conjunction with a non-zero coefficient of thermal expansion, it was observed that the convergence of the macroscopic NEWTON-RAPHSON scheme depends on the RVE dimension. In particular, the RVE dimensions must be at least two orders of magnitude smaller than the macroscopic problem size in order to ensure an accurate result. Inhomogeneous RVE models were simulated, where each element of the finite element mesh is randomly assigned one of two different materials, or where the crystal orientation of the material is randomly selected. It was shown that RVE models whose elements are randomly oriented exhibit isotropic behavior on the macroscale, as expected of polycrystalline materials with random texture.

The present multiscale theory and finite element implementation are subject to several limitations. First, the EM fields were assumed to be continuously differentiable when the local forms of MAXWELL's equations (as well as the weak forms of the finite element problem) were derived. However, discontinuities are of central importance for electric conductors, where free electric charges tend to accumulate at surfaces and boundaries. Such surface charges typically entail discontinuous EM fields which must be accounted for using jump conditions. In a multiscale framework, discontinuities within the RVE must be taken into consideration during homogenization. Second, the numerical implementation was limited to the electrostatic case. It was therefore assumed that the material is dielectric, *i.e.*, electric currents and associated JOULE heating were neglected. It was further postulated that there are no free charges distributed across the body. These conditions imply the absence of any EM volumetric source terms in the momentum and energy balances, since neither JOULE heating nor LORENTZ forces occur. This removes an important mechanism for EMTM coupling via the balance equations. Any interactions between the EM fields and the underlying body are thus confined to the coupling prescribed by the constitutive equations. A quasi-static finite element model for electrical conductors requires

the solution of the magnetostatic equations. These involve a curl operator, whose numerical implementation was beyond the scope of this dissertation. Lastly, it is acknowledged that the lack of objectivity of the aether relations under non-relativistic SRBM remains unaddressed. Instead, this matter was circumvented altogether by the assumption that any convective terms are negligible. A proper treatment of objectivity within the framework of Galilean electrodynamics requires the use of nonlinear aether relations. These depend on which Galilean limit of Maxwell's equations is under consideration (*i.e.*, the electric limit or the magnetic limit). Alternatively, a consistent theory may be constructed from a fully relativistic treatment of both electromagnetism and thermodynamics. All the above topics represent fertile ground for further research.

Bibliography

[1] R. Abraham, J. E. Marsden, and T. Ratiu. *Manifolds, Tensor Analysis, and Applications*, volume 75 of *Applied Mathematical Sciences*. Springer New York, New York, NY, 1988.

[2] R. Aris. *Vectors, tensors, and the basic equations of fluid mechanics*. Dover books on engineering. Dover Publications, New York, dover edition, 1989.

[3] J. M. Ball. Convexity conditions and existence theorems in nonlinear elasticity. *Archive for Rational Mechanics and Analysis*, 63(4):337–403, December 1976.

[4] R. Bechmann. Elastic, Piezoelectric, and Dielectric Constants of Polarized Barium Titanate Ceramics and Some Applications of the Piezoelectric Equations. *The Journal of the Acoustical Society of America*, 28(3):347–350, 1956.

[5] R. Beig and B. G. Schmidt. Relativistic elasticity. *Classical and Quantum Gravity*, 20(5):889–904, March 2003.

[6] H. Bhatia, G. Norgard, V. Pascucci, and P-T. Bremer. The Helmholtz-Hodge Decomposition—A Survey. *IEEE Transactions on Visualization and Computer Graphics*, 19(8):1386–1404, 2013.

[7] M. I. Bichurin, V. M. Petrov, S. V. Averkin, and E. Liverts. Present status of theoretical modeling the magnetoelectric effect in magnetostrictive-piezoelectric nanostructures. Part II: Magnetic and magnetoacoustic resonance ranges. *Journal of Applied Physics*, 107(5):053905, March 2010.

[8] M. I. Bichurin, V. M. Petrov, and G. Srinivasan. Theory of low-frequency magnetoelectric coupling in magnetostrictive-piezoelectric bilayers. *Physical Review B*, 68(5):054402, August 2003.

[9] P. Boyraz, G. Runge, and A. Raatz. An Overview of Novel Actuators for Soft Robotics. *Actuators*, 7(3):48, August 2018.

[10] E. Brusa, A. Carrera, and C. Delprete. A Review of Piezoelectric Energy Harvesting: Materials, Design, and Readout Circuits. *Actuators*, 12(12):457, December 2023.

[11] C. Böhm, B. Hudobivnik, M. Marino, and P. Wriggers. Electro-magneto-mechanically response of polycrystalline materials: Computational homogenization via the Virtual Element Method. *Computer Methods in Applied Mechanics and Engineering*, 380:113775, 2021.

[12] B. Carter and H. Quintana. Foundations of general relativistic high-pressure elasticity theory. *Proceedings of the Royal Society of London. A. Mathematical and Physical Sciences*, 331(1584):57–83, November 1972.

[13] P. Chadwick. *Continuum mechanics: concise theory and problems*. Wiley, New York, 1976.

[14] Y-C. Chen and L. Wheeler. Derivatives of the stretch and rotation tensors. *Journal of Elasticity*, 32(3):175–182, 1993.

[15] P. Ciarlet, H. Wu, and J. Zou. Edge Element Methods for Maxwell's Equations with Strong Convergence for Gauss' Laws. *SIAM Journal on Numerical Analysis*, 52(2):779–807, 2014.

[16] P. G. Ciarlet. *Mathematical elasticity*. Number v. 20, 27, 29 in Studies in mathematics and its applications. North-Holland ; Sole distributors for the U.S.A. and Canada, Elsevier Science Pub. Co, Amsterdam ; New York : New York, N.Y., U.S.A, 1988.

[17] B. D. Coleman and W. Noll. The thermodynamics of elastic materials with heat conduction and viscosity. *Archive for Rational Mechanics and Analysis*, 13(1):167–178, 1963.

[18] A. Curnier. *Computational Methods in Solid Mechanics*, volume 29 of *Solid Mechanics and Its Applications*. Springer, Dordrecht Netherlands, 1994.

[19] M. De Montigny and G. Rousseaux. On the electrodynamics of moving bodies at low velocities. 2005.

[20] L. Demkowicz. *Computing with hp-Adaptive Finite Elements: One and Two Dimensional Elliptic and Maxwell Problems, volume 1*. Chapman and Hall/CRC, Boca Raton, 2006.

[21] L. Dorfmann and R. W. Ogden. *Nonlinear theory of electroelastic and magnetoelastic interactions*. Springer, New York, 2014.

[22] J. L. Ericksen. On Formulating and Assessing Continuum Theories of Electromagnetic Fields in Elastic Materials. *Journal of Elasticity*, 87(2):95–108, 2007.

[23] J. L. Ericksen. Magnetizable and Polarizable Elastic Materials. *Mathematics and Mechanics of Solids*, 13(1):38–54, 2008.

[24] A. C. Eringen and G. A. Maugin. *Electrodynamics of Continua I*. Springer New York, New York, NY, 1990.

[25] A. Erturk and D. J. Inman. *Piezoelectric energy harvesting*. Wiley, Chichester, West Sussex, U.K Hoboken, N.J, 2011.

[26] R. P. Feynman, R. B. Leighton, and M. L. Sands. *The Feynman lectures on physics. Volume II, Mainly electromagnetism and matter*. Basic Books, New York, new millennium edition, 2010.

[27] R. P. Feynman, R. B. Leighton, and M. L. Sands. *The Feynman lectures on physics. Volume III, Quantum mechanics*. Basic Books, New York, new millennium edition, 2011.

[28] J. Fish and R. Fan. Mathematical homogenization of nonperiodic heterogeneous media subjected to large deformation transient loading. *International Journal for Numerical Methods in Engineering*, 76(7):1044–1064, 2008.

[29] R. Fosdick and H. Tang. Electrodynamics and Thermomechanics of Material Bodies. *Journal of Elasticity*, 88(3):255–297, 2007.

[30] V. I. Fushchich, V. M. Shtelen, and N. I. Serov. *Symmetry Analysis and Exact Solutions of Equations of Nonlinear Mathematical Physics*. Number 246 in Mathematics and Its Applications. Springer, Dordrecht, 1993.

[31] M. G. D. Geers, V. Kouznetsova, K. Matouš, and J. Yvonnet. Homogenization Methods and Multiscale Modeling: Nonlinear Problems. In E. Stein, R. Borst, and T. J. R. Hughes, editors, *Encyclopedia of Computational Mechanics Second Edition*, pages 1–34. Wiley, 1 edition, December 2017.

[32] M.G.D. Geers, V.G. Kouznetsova, and W.A.M. Brekelmans. Multi-scale computational homogenization: Trends and challenges. *Journal of Computational and Applied Mathematics*, 234(7):2175–2182, August 2010.

[33] G. A. Goldin and V. M. Shtelen. On Galilean invariance and nonlinearity in electrodynamics and quantum mechanics. *Physics Letters A*, 279(5):321–326, 2001.

[34] H. J. Goldsmid. *Introduction to thermoelectricity*. Number 121 in Springer series in materials science. Springer, Heidelberg ; New York, 2010.

[35] S. Govindjee, J. Strain, T. J. Mitchell, and R. L. Taylor. Convergence of an efficient local least-squares fitting method for bases with compact support. *Computer Methods in Applied Mechanics and Engineering*, 213-216:84–92, 2012.

[36] R. L. Graham, J. Squyres, G. Bosilca, B. Barrett, and others. Open MPI: Open Source High Performance Computing.

[37] A. E. Green and R. S. Rivlin. On cauchy's equations of motion. *Zeitschrift für angewandte Mathematik und Physik ZAMP*, 15(3):290–292, 1964.

[38] D. J. Griffiths. *Introduction to electrodynamics*. Prentice Hall, Upper Saddle River, N.J, 3rd ed edition, 1999.

[39] J. M. Guedes and N. Kikuchi. Preprocessing and postprocessing for materials based on the homogenization method with adaptive finite element methods. *Computer Methods in Applied Mechanics and Engineering*, 83(2):143–198, October 1990.

[40] M. E. Gurtin. *An introduction to continuum mechanics*, volume 158 of *Mathematics in science and engineering*. Academic Press, New York, 1981.

[41] N. Hanappier, E. Charkaluk, and N. Triantafyllidis. A coupled electromagnetic–thermomechanical approach for the modeling of electric motors. *Journal of the Mechanics and Physics of Solids*, 149:104315, 2021.

[42] G. Harshe, J.P. Dougherty, and R.E. Newnham. Theoretical modelling of multilayer magnetoelectric composites. *International journal of applied electromagnetics in materials*, 4(2):145 – 159, 1993. Type: Article.

[43] Y. He. Heat capacity, thermal conductivity, and thermal expansion of barium titanate-based ceramics. *Thermochimica Acta*, 419(1):135–141, 2004.

[44] F. W. Hehl, Y. Itin, and Y. N. Obukhov. Recent developments in premetric classical electrodynamics. 2006.

[45] F. W. Hehl and Y. N. Obukhov. A gentle introduction to the foundations of classical electrodynamics: The meaning of the excitations (D,H) and the field strengths (E, B), September 2000. arXiv:physics/0005084.

[46] F. W. Hehl and Y. N. Obukhov. *Foundations of classical electrodynamics: charge, flux, and metric*. Number v. 33 in Progress in mathematical physics. Birkhäuser, Boston, 2003.

[47] J. A. Heras. The Galilean limits of Maxwell's equations. *American Journal of Physics*, 78(10):1048–1055, October 2010.

[48] N. J. Higham. *Accuracy and stability of numerical algorithms*. Society for Industrial and Applied Mathematics, Philadelphia, 2nd ed edition, 2002.

[49] R. Hill. Elastic properties of reinforced solids: Some theoretical principles. *Journal of the Mechanics and Physics of Solids*, 11(5):357–372, 1963.

[50] R. Hill. On constitutive macro-variables for heterogeneous solids at finite strain. *Proceedings of the Royal Society of London. A. Mathematical and Physical Sciences*, 326(1565):131–147, 1972.

[51] R. Hiptmair, F. Kramer, and J. Ostrowski. A Robust Maxwell Formulation for All Frequencies. *IEEE Transactions on Magnetics*, 44(6):682–685, 2008.

[52] G. A. Holzapfel. *Nonlinear solid mechanics: a continuum approach for engineering*. Wiley, Chichester Weinheim, 2010.

[53] J. H. Huang and W-S. Kuo. The analysis of piezoelectric/piezomagnetic composite materials containing ellipsoidal inclusions. *Journal of Applied Physics*, 81(3):1378–1386, February 1997.

[54] T. J. R. Hughes, editor. *The finite element method: linear static and dynamic finite element analysis*. Dover Publications, Mineola, NY, 2000.

[55] K. Hutter. On thermodynamics and thermostatics of viscous thermoelastic solids in the electromagnetic fields. A lagrangian formulation. *Archive for Rational Mechanics and Analysis*, 58(4):339–368, 1975.

[56] K. Hutter, A. A. F. Van de Ven, and A. Ursescu. *Electromagnetic field matter interactions in thermoelastic solids and viscous fluids*. Number 710 in Lecture notes in physics. Springer, Berlin ; New York, 2006.

[57] J. H. Irving and J. G. Kirkwood. The Statistical Mechanical Theory of Transport Processes. IV. The Equations of Hydrodynamics. *The Journal of Chemical Physics*, 18(6):817–829, 1950.

[58] K. P. Jayachandran, J. M. Guedes, and H. C. Rodrigues. A generic homogenization model for magnetoelectric multiferroics. *Journal of Intelligent Material Systems and Structures*, 25(10):1243–1255, July 2014.

[59] L. V. Kantorovich and G. P. Akilov. *Functional analysis*. Pergamon Press, Oxford ; New York, 2d ed edition, 1982.

[60] E. S. Keneth, R. Lieberman, A. Pahima, V. B. Varma, Vinay Sharma, Chao Yuan, Qi Ge, R. V. Ramanujan, and Shlomo Magdassi. Untethered magnetothermal flexible actuators for soft robotics. *Sensors and Actuators A: Physical*, 363:114683, 2023.

[61] S. Kim, J. Ryu, and M. Cho. Numerically generated tangent stiffness matrices using the complex variable derivative method for nonlinear structural analysis. *Computer Methods in Applied Mechanics and Engineering*, 200(1):403–413, 2011.

[62] V. Kouznetsova. Computational homogenization for the multi-scale analysis of multi-phase materials, 2002.

[63] V. Kouznetsova, W. A. M. Brekelmans, and F. P. T. Baaijens. An approach to micro-macro modeling of heterogeneous materials. *Computational Mechanics*, 27(1):37–48, January 2001.

[64] A. Kovetz. *Electromagnetic theory*. Oxford science publications. Oxford University Press, Oxford; New York, 2000.

[65] H-Y. Kuo and Y-L. Wang. Optimization of magnetoelectricity in multiferroic fibrous composites. *Mechanics of Materials*, 50:88–99, July 2012.

[66] W. Känzig. Ferroelectrics and Antiferroeletrics. In F. Seitz and D. Turnbull, editors, *Solid State Physics*, volume 4, pages 1–197. Academic Press, 1957.

[67] M. Labusch. *A two-scale homogenization scheme for the prediction of magnetoelectric product properties*. Number Nr. 20 in Bericht / Universität Duisburg-Essen, Ingenieurwissenschaften, Abt. Bauwissenschaften, Institut für Mechanik. Institut für Mechanik, Fakultät für Ingenieurwissenschaften, Abteilung Bauwissenschaften, Universität Duisburg-Essen, Essen, 2021.

[68] L. D. Landau and E. M. Lifšic. *Fluid mechanics*. Number v. 6 in Course of theoretical physics. Pergamon Press, Oxford, England New York, 2nd ed., 2nd english ed., rev edition, 1987.

[69] L. D. Landau and E. M. Lifšic. *The classical theory of fields*, volume 2 of *Course of theoretical physics*. Elsevier Butterworth Heinemann, Amsterdam Heidelberg, 4. rev. engl. ed., repr edition, 2010.

[70] M. Lax and D. F. Nelson. Maxwell equations in material form. *Physical Review B*, 13(4):1777–1784, 1976.

[71] M. Le Bellac and J. M. Lévy-Leblond. Galilean electromagnetism. *Il Nuovo Cimento B (1971-1996)*, 14(2):217–234, 1973.

[72] E. Lee. An L2-finite element approximation of the solution to div/curl-systems with nonempty null space. *Applied Numerical Mathematics*, 192:70–83, 2023.

[73] J. Lee, J. G. Boyd, and D. Lagoudas. Effective properties of three-phase electro-magneto-elastic composites. *International Journal of Engineering Science*, 43(10):790–825, 2005.

[74] X. Li, X. Li, and H. Yang. Multiscale Finite Element Method for Coupling Analysis of Heterogeneous Magneto-Electro-Elastic Structures in Thermal Environment. *Journal of Applied Mathematics and Physics*, 12(09):3099–3113, 2024.

[75] E. M. Lifšic, L. P. Pitaevskij, and L. D. Landau. *Electrodynamics of continuous media*, volume 8 of *Course of theoretical physics / by L. D. Landau and E. M. Lifshitz*. Pergamon Press, Oxford, 2. ed., rev. and enl., 1. reprinted (with corr.) edition, 1993.

[76] H. Liu, J. Zhong, C. Lee, S-W. Lee, and L. Lin. A comprehensive review on piezoelectric energy harvesting technology: Materials, mechanisms, and applications. *Applied Physics Reviews*, 5(4):041306, December 2018.

[77] I-S. Liu and I. Müller. On the thermodynamics and thermostatics of fluids in electromagnetic fields. *Archive for Rational Mechanics and Analysis*, 46(2):149–176, 1972.

[78] J. N. Lyness. Differentiation formulas for analytic functions. *Mathematics of Computation*, 22(102):352–362, 1968.

[79] J. N. Lyness and C. B. Moler. Numerical Differentiation of Analytic Functions. *SIAM Journal on Numerical Analysis*, 4(2):202–210, 1967. Publisher: Society for Industrial and Applied Mathematics.

[80] A. Malyarenko. *Random Fields of Piezoelectricity and Piezomagnetism: Correlation Structures*. SpringerBriefs in Applied Sciences and Technology Ser. Springer International Publishing AG, Cham, 2020.

[81] K. K. Mandadapu, B. E. Abali, and P. Papadopoulos. On the polar nature and invariance properties of a thermomechanical theory for continuum-on-continuum homogenization. *Mathematics and Mechanics of Solids*, 26(11):1581–1598, 2021.

[82] K. K. Mandadapu, A. Sengupta, and P. Papadopoulos. A homogenization method for thermomechanical continua using extensive physical quantities. *Proceedings of the Royal Society A: Mathematical, Physical and Engineering Sciences*, 468(2142):1696–1715, 2012.

[83] J. Mandel. *Plasticité classique et viscoplasticité: course held at the Department of mechanics of solids, September-October 1971*. Number 97 in CISM courses and lectures. Springer, Wien New York, 1972.

[84] J. E. Marsden and T. J. R. Hughes. *Mathematical Foundations of Elasticity*. Dover Civil and Mechanical Engineering. Dover Publications, Newburyport, 1994.

[85] J. E. Marsden and A. Tromba. *Vector calculus*. W.H. Freeman, New York, 6th international edition, 2012.

[86] C. Maruccio, L. De Lorenzis, L. Persano, and D. Pisignano. Computational homogenization of fibrous piezoelectric materials. *Computational Mechanics*, 55(5):983–998, May 2015.

[87] L. Mañosa, A. Planes, and M. Acet. Advanced materials for solid-state refrigeration. *Journal of Materials Chemistry A*, 1(16):4925, 2013.

[88] Q. Meng, J. Dong, P. Nie, L. Xu, J. Wang, S. Jiang, H. Zuo, J. Zhang, X. Li, Z. Zhu, L. Balents, and K. Behnia. Magnetostriction, piezomagnetism and domain nucleation in a Kagome antiferromagnet. *Nature Communications*, 15(1):6921, August 2024.

[89] B. S. Mercer, K. K. Mandadapu, and P. Papadopoulos. Novel formulations of microscopic boundary-value problems in continuous multiscale finite element methods. *Computer Methods in Applied Mechanics and Engineering*, 286:268–292, 2015.

[90] B. S. Mercer, K. K. Mandadapu, and P. Papadopoulos. Homogenization of high-frequency wave propagation in linearly elastic layered media using a continuum Irving-Kirkwood theory. *International Journal of Solids and Structures*, 96:162–172, 2016.

[91] A. A. Michelson. The relative motion of the Earth and of the luminiferous ether. *American Journal of Science*, 22(128):120–129, 1881.

[92] A. A. Michelson and E. W. Morley. Influence of motion of the medium on the velocity of light. *American Journal of Science*, 31(185):377–385, 1886.

[93] A. A. Michelson and E. W. Morley. On the relative motion of the Earth and the luminiferous ether. *American Journal of Science*, 34(203):333–345, 1887.

[94] C. Miehe, D. Rosato, and B. Kiefer. Variational principles in dissipative electro-magneto-mechanics: A framework for the macro-modeling of functional materials. *International Journal for Numerical Methods in Engineering*, 86(10):1225–1276, June 2011.

[95] C. Miehe, J. Schotte, and M. Lambrecht. Homogenization of inelastic solid materials at finite strains based on incremental minimization principles. Application to the texture analysis of polycrystals. *Journal of the Mechanics and Physics of Solids*, 50(10):2123–2167, 2002.

[96] C. Miehe, J. Schotte, and J. Schröder. Computational micro–macro transitions and overall moduli in the analysis of polycrystals at large strains. *Computational Materials Science*, 16(1-4):372–382, December 1999.

[97] P. Monk. *Finite Element Methods for Maxwell's Equations*. Oxford University Press, 2003.

[98] S. M. Montgomery, S. Wu, X. Kuang, C. D. Armstrong, C. Zemelka, Q. Ze, R. Zhang, R. Zhao, and H. J. Qi. Magneto-Mechanical Metamaterials with Widely Tunable Mechanical Properties and Acoustic Bandgaps. *Advanced Functional Materials*, 31(3):2005319, January 2021.

[99] T. Mori and K. Tanaka. Average stress in matrix and average elastic energy of materials with misfitting inclusions. *Acta Metallurgica*, 21(5):571–574, May 1973.

[100] S. J. Murray, M. Marioni, S. M. Allen, R. C. O'Handley, and T. A. Lograsso. 6% magnetic-field-induced strain by twin-boundary motion in ferromagnetic Ni–Mn–Ga. *Applied Physics Letters*, 77(6):886–888, August 2000.

[101] I. Müller. On the entropy inequality. *Archive for Rational Mechanics and Analysis*, 26(2):118–141, 1967.

[102] I. Müller. *Thermodynamics*. Interaction of mechanics and mathematics series. Pitman, Boston, 1985.

[103] W. H. Müller, E. N. Vilchevskaya, and V. A. Eremeyev. Electrodynamics from the viewpoint of modern continuum theory—A review. *ZAMM - Zeitschrift für Angewandte Mathematik und Mechanik*, 103(4), 2023.

[104] C-W. Nan, G. Liu, Y. Lin, and H. Chen. Magnetic-Field-Induced Electric Polarization in Multiferroic Nanostructures. *Physical Review Letters*, 94(19):197203, May 2005.

[105] S. Nicaise. Edge Elements on Anisotropic Meshes and Approximation of the Maxwell Equations. *SIAM Journal on Numerical Analysis*, 39(3):784–816, 2001.

[106] I. Niyonzima, Y. Jiao, and J. Fish. Modeling and simulation of nonlinear electro-thermo-mechanical continua with application to shape memory polymeric medical devices. *Computer Methods in Applied Mechanics and Engineering*, 350:511–534, 2019.

[107] E. Noether. Invariante Variationsprobleme. *Nachrichten von der Gesellschaft der Wissenschaften zu Göttingen, Mathematisch-Physikalische Klasse*, pages 235–257, 1918.

[108] W. Noll. The Foundations of Classical Mechanics in the Light of Recent Advances in Continuum Mechanics. In *Studies in Logic and the Foundations of Mathematics*, volume 27, pages 266–281. Elsevier, 1959.

[109] J. C. Nédélec. Mixed finite elements in R3. *Numerische Mathematik*, 35(3):315–341, 1980.

[110] J. C. Nédélec. A new family of mixed finite elements in R3. *Numerische Mathematik*, 50(1):57–81, 1986.

[111] J. M. Ortega and W. C. Rheinboldt. *Iterative solution of nonlinear equations in several variables*. Computer science and applied mathematics. Academic Press, New York, 1970.

[112] F. Otero, S. Oller, and X. Martinez. Multiscale Computational Homogenization: Review and Proposal of a New Enhanced-First-Order Method. *Archives of Computational Methods in Engineering*, 25(2):479–505, April 2018.

[113] N. S. Ottosen and H. Petersson. *Introduction to the finite element method*. Prentice Hall, New York, 1992.

[114] L. Page. *Introduction to Theoretical Physics*. Van Nostrand, 2nd edition, 1935.

[115] P. Papadopoulos. *Lecture notes for ME280B: Finite Element Methods for Nonlinear Continua*. Berkeley, CA, 2022.

[116] V. K. Pecharsky and K. A. Gschneidner Jr. Magnetocaloric effect and magnetic refrigeration. *Journal of Magnetism and Magnetic Materials*, 200(1):44–56, 1999.

[117] Physical Measurement Laboratory of NIST. The NIST Reference on Constants, Units, and Uncertainty, https://physics.nist.gov/cuu/Constants/index.html, 2024.

[118] A. C. Pipkin and R. S. Rivlin. The formulation of constitutive equations in continuum physics. I. *Archive for Rational Mechanics and Analysis*, 4(1):129–144, 1959.

[119] A. C. Pipkin and R. S. Rivlin. Galvanomagnetic and Thermomagnetic Effects in Isotropic Materials. *Journal of Mathematical Physics*, 1(6):542–546, 1960.

[120] G. Preti, F. De Felice, and L. Masiero. On the Galilean non-invariance of classical electromagnetism. *European Journal of Physics*, 30(2):381–391, March 2009.

[121] Y. Qin, B. Qin, D. Wang, C. Chang, and L.-D. Zhao. Solid-state cooling: thermoelectrics. *Energy & Environmental Science*, 15(11):4527–4541, 2022.

[122] A. Raoult. Non-polyconvexity of the stored energy function of a Saint Venant-Kirchhoff material. *Aplikace matematiky*, 31(6):417–419, 1986. Publisher: Institute of Mathematics, Academy of Sciences of the Czech Republic.

[123] Germain Rousseaux. Forty years of Galilean Electromagnetism (1973–2013). *The European Physical Journal Plus*, 128(8):81, August 2013.

[124] J. Schröder. A numerical two-scale homogenization scheme: the FE2-method. In F. Pfeiffer, F. G. Rammerstorfer, E. Guazzelli, B. Schrefler, P. Serafini, J. Schröder, and K. Hackl, editors, *Plasticity and Beyond*, volume 550, pages 1–64. Springer Vienna, Vienna, 2014. Series Title: CISM International Centre for Mechanical Sciences.

[125] J. Schröder and M-A. Keip. Two-scale homogenization of electromechanically coupled boundary value problems. *Computational Mechanics*, 50(2):229–244, August 2012.

[126] J. Schröder, M. Labusch, and M-A. Keip. Algorithmic two-scale transition for magneto-electro-mechanically coupled problems: FE2-scheme: Localization and homogenization. *Computer Methods in Applied Mechanics and Engineering*, 302:253–280, 2016.

[127] A. Sengupta, P. Papadopoulos, and R. L. Taylor. A multiscale finite element method for modeling fully coupled thermomechanical problems in solids. *International Journal for Numerical Methods in Engineering*, 91(13):1386–1405, 2012.

[128] M. Seong, K. Sun, S. Kim, H. Kwon, S-W. Lee, S. C. Veerla, D.K. Kang, J. Kim, S. Kondaveeti, S. M. Tawfik, H.W. Park, and H.E. Jeong. Multifunctional Magnetic Muscles for Soft Robotics. *Nature Communications*, 15(1):7929, September 2024.

[129] J. Serrin. Mathematical Principles of Classical Fluid Mechanics. In C. Truesdell, editor, *Fluid Dynamics I / Strömungsmechanik I*, pages 125–263. Springer Berlin Heidelberg, Berlin, Heidelberg, 1959.

[130] J. Sim and R. R. Zhao. Magneto-Mechanical Metamaterials: A Perspective. *Journal of Applied Mechanics*, 91(3):031004, March 2024.

[131] G. F. Smith. On isotropic integrity bases. *Archive for Rational Mechanics and Analysis*, 18(4):282–292, 1965.

[132] I. S. Sokolnikoff. *Tensor Analysis: Theory and Applications*. Applied mathematics series. Wiley, 1951.

[133] Y. Song. A Note On Galilean Invariants In Semi-Relativistic Electromagnetism, 2013. Version Number: 1.

[134] A. Sozinov, A. A. Likhachev, N. Lanska, and K. Ullakko. Giant magnetic-field-induced strain in NiMnGa seven-layered martensitic phase. *Applied Physics Letters*, 80(10):1746–1748, March 2002.

[135] A. J. M. Spencer and R. S. Rivlin. Isotropic integrity bases for vectors and second-order tensors: Part I. *Archive for Rational Mechanics and Analysis*, 9(1):45–63, 1962.

[136] S. Srinivas, J. Y. Li, Y. C. Zhou, and A. K. Soh. The effective magnetoelectroelastic moduli of matrix-based multiferroic composites. *Journal of Applied Physics*, 99(4):043905, February 2006.

[137] D. J. Steigmann. On the Formulation of Balance Laws for Electromagnetic Continua. *Mathematics and Mechanics of Solids*, 14(4):390–402, 2009.

[138] J. Stewart. *Calculus: early transcendentals*. Brooks/Cole, Belmont, CA, 7th edition, 2012.

[139] J. A. Stratton. *Electromagnetic theory*. IEEE Press series on electromagnetic wave theory. IEEE Press, Piscataway, NJ, 2007.

[140] J. L. Synge and A. Schild. *Tensor calculus*. Dover Publications, New York, 1978.

[141] M. Tanaka, M. Fujikawa, D. Balzani, and J. Schröder. Robust numerical calculation of tangent moduli at finite strains based on complex-step derivative approximation and its application to localization analysis. *Computer Methods in Applied Mechanics and Engineering*, 269:454–470, 2014.

[142] R. L. Taylor and S. Govindjee. FEAP – A Finite Element Analysis Program, Version 8.6, User Manual, 2021.

[143] Y. Tong, S. Lombeyda, A. N. Hirani, and M. Desbrun. Discrete multiscale vector field decomposition. *ACM Transactions on Graphics*, 22(3):445–452, 2003.

[144] R. A. Toupin. The Elastic Dielectric. *Journal of Rational Mechanics and Analysis*, 5(6):849–915, 1956.

[145] R. A. Toupin. A dynamical theory of elastic dielectrics. *International Journal of Engineering Science*, 1(1):101–126, 1963.

[146] C. Truesdell and W. Noll. *The Non-Linear Field Theories of Mechanics*. Springer, Berlin; Heidelberg, 2004.

[147] C. Truesdell and R. A. Toupin. The Classical Field Theories. In S. Flügge, editor, *Principles of Classical Mechanics and Field Theory / Prinzipien der Klassischen Mechanik und Feldtheorie*, pages 226–858. Springer, Berlin; Heidelberg, 1960.

[148] K. Ullakko, J. K. Huang, C. Kantner, R. C. O'Handley, and V. V. Kokorin. Large magnetic-field-induced strains in Ni2MnGa single crystals. *Applied Physics Letters*, 69(13):1966–1968, September 1996.

[149] A. A. F. Van de Ven. Interaction of electromagnetic and elastic fields in solids, 1975.

[150] A. N. Vasil'ev, V. D. Buchel'nikov, T. Takagi, V. V. Khovailo, and E. I. Estrin. Shape memory ferromagnets. 2003.

[151] Y. Wang and Z. Jing. Multiscale modelling and numerical homogenization of the coupled multiphysical behaviors of high-field high temperature superconducting magnets. *Composite Structures*, 313:116863, 2023.

[152] H. Weyl. *The Classical Groups: Their Invariants and Representations*. Princeton University Press, 1966.

[153] L. Wheeler. On the derivatives of the stretch and rotation with respect to the deformation gradient. *Journal of Elasticity*, 24(1-3):129–133, 1990.

[154] E. T. Whittaker. *A History of the Theories of Aether and Electricity*. Dublin University Press, 1910.

[155] J. Yang. *An Introduction to the Theory of Piezoelectricity*. Number 9 in Advances in Mechanics and Mathematics. Springer International Publishing, Cham, 2nd ed. 2018 edition, 2018.

[156] A. Yavari and J. E. Marsden. Covariant balance laws in continua with microstructure. *Reports on Mathematical Physics*, 63(1):1–42, 2009.

[157] C. Yu and G. Kang. A multiscale magneto-thermo-mechanically coupled model for ultra-low-field induced magneto-elastocaloric effect in magnetostrictive-shape memory alloy composite system. *International Journal of Engineering Science*, 168:103539, November 2021.

[158] Q.-S. Zheng. Theory of Representations for Tensor Functions—A Unified Invariant Approach to Constitutive Equations. *Applied Mechanics Reviews*, 47(11):545–587, 1994.

[159] O. C. Zienkiewicz and R. L. Taylor. *The finite element method*. Butterworth-Heinemann, Oxford, 5th ed edition, 2000.

[160] O. C. Zienkiewicz, R. L. Taylor, and D. Fox. *The finite element method for solid and structural mechanics*. Elsevier/Butterworth-Heinemann, Amsterdam; Boston, 7th ed edition, 2014.

[161] B. Zou, Z. Liang, D. Zhong, Z. Cui, K. Xiao, S. Shao, and J. Ju. Magneto-Thermomechanically Reprogrammable Mechanical Metamaterials. *Advanced Materials*, 35(8):2207349, February 2023.

[162] I. Özdemir, W. A. M. Brekelmans, and M. G. D. Geers. Computational homogenization for heat conduction in heterogeneous solids. *International Journal for Numerical Methods in Engineering*, 73(2):185–204, 2008.

[163] I. Özdemir, W.A.M. Brekelmans, and M.G.D. Geers. FE2 computational homogenization for the thermo-mechanical analysis of heterogeneous solids. *Computer Methods in Applied Mechanics and Engineering*, 198(3-4):602–613, December 2008.

Appendix A

Ancillary Derivations

The contents of this appendix are referenced throughout Chapters 2 - 4. In particular, Sections A.1 - A.3 provide detailed derivations for some of the more tedious results of vector calculus employed in Chapter 2. An alternative derivation for the invariance properties of the electromagnetic fields obtained in Chapter 3 are presented in Appendix A.4, followed by a brief discussion of the wave equations in Appendix A.5. Lastly, Appendix A.6 presents an alternative form of the balances of momenta and energy, where the concept of momentum and energy is generalized to include electromagnetic effects.

A.1 Corollaries of the Divergence Theorem

Equation (2.51) is deduced from the classical form (2.50) of the divergence theorem as follows: The vector field $\mathbf{w}(\mathbf{x})$ is substituted with $\mathbf{w}(\mathbf{x})\times\mathbf{c}$, where $\mathbf{c}$ is an *arbitrary constant* vector. Identity $(2.46)_6$ simplifies to $\operatorname{div}(\mathbf{w}\times\mathbf{c})=\mathbf{c}\cdot(\operatorname{curl}\mathbf{w})$ and consequently

$$\begin{aligned} 0 \;&=\; \int_{\mathcal{P}} \operatorname{div}\big(\mathbf{w}\times\mathbf{c}\big)\,\mathrm{d}v \;-\; \int_{\partial\mathcal{P}} \big(\mathbf{w}\times\mathbf{c}\big)\cdot\mathbf{n}\,\mathrm{d}a \\ &=\; \mathbf{c}\cdot\left(\int_{\mathcal{P}} \operatorname{curl}\mathbf{w}\,\mathrm{d}v - \int_{\partial\mathcal{P}} \big(\mathbf{n}\times\mathbf{w}\big)\,\mathrm{d}a\right) \quad \forall \text{ constant } \mathbf{c} \quad . \end{aligned} \tag{A.1}$$

Since $\mathbf{c}$ is an arbitrary constant vector it is concluded that the term in parentheses must vanish, giving rise to the desired result (2.51).

Corollary (2.52) of the divergence theorem is obtained following a similar approach. The vector field $\mathbf{w}(\mathbf{x})$ is instead replaced by $[\mathbf{T}(\mathbf{x})]^{\mathrm{T}}\mathbf{c}$, where $\mathbf{c}$ is again arbitrary and constant. Identity $(2.46)_3$ simplifies to $\operatorname{div}(\mathbf{T}^{\mathrm{T}}\mathbf{c})=\mathbf{c}\cdot(\operatorname{div}\mathbf{T})$ and Equa-

tion (2.50) becomes

$$\begin{aligned} 0 \;&=\; \int_{\mathcal{P}} \operatorname{div}\bigl(\mathbf{T}^{\mathrm{T}}\mathbf{c}\bigr)\,\mathrm{d}v \;-\; \int_{\partial\mathcal{P}} \bigl(\mathbf{T}^{\mathrm{T}}\mathbf{c}\bigr)\cdot\mathbf{n}\,\mathrm{d}a \\ &=\; \mathbf{c}\cdot\left(\int_{\mathcal{P}} \operatorname{div}\mathbf{T}\,\mathrm{d}v \;-\; \int_{\partial\mathcal{P}} \mathbf{T}\mathbf{n}\,\mathrm{d}a\right) \quad \forall \text{ constant } \mathbf{c} \quad , \end{aligned} \tag{A.2}$$

which immediately leads to Equation (2.52). Note that despite (A.1) and (A.2) being scalar expressions, the extracted equations are vector-valued owing to the arbitrariness of vector $\mathbf{c}$.

A.2 Material Time Derivative of $\mathbf{T}^{-1}$

Expression $(2.102)_2$ for $\overset{\cdot}{\mathbf{T}^{-1}}$ may be derived as follows (assuming that the inverse $\mathbf{T}^{-1}$ exists). Let $\mathbf{A}(\mathbf{T})$ and $\mathbf{B}(\mathbf{T})$ be two differentiable tensor-valued functions of a tensor argument $\mathbf{T}$. The product rule for the GÂTEAUX differential (2.40) reads

$$\begin{aligned} \frac{\partial}{\partial\mathbf{T}}\Bigl(\mathbf{A}(\mathbf{T})\mathbf{B}(\mathbf{T})\Bigr)\cdot\mathbf{H} \;&=\; \frac{\partial}{\partial T_{lm}}\Bigl(A_{ik}(\mathbf{T})\,B_{kj}(\mathbf{T})\mathbf{e}_i\otimes\mathbf{e}_j\Bigr)H_{lm} \\ &=\; \left(\left[\frac{\partial A_{ik}}{\partial T_{lm}}\,B_{kj} \;+\; A_{ik}\,\frac{\partial B_{kj}}{\partial T_{lm}}\right]\mathbf{e}_i\otimes\mathbf{e}_j\right)H_{lm} \\ &=\; \left[\frac{\partial\mathbf{A}}{\partial\mathbf{T}}\cdot\mathbf{H}\right]\mathbf{B} \;+\; \mathbf{A}\left[\frac{\partial\mathbf{B}}{\partial\mathbf{T}}\cdot\mathbf{H}\right] \quad . \end{aligned} \tag{A.3}$$

This product rule is applied to the identity tensor $\mathbf{i}=\mathbf{T}^{-1}\mathbf{T}$,

$$\mathbf{0} \;=\; \frac{\partial}{\partial\mathbf{T}}\bigl(\mathbf{T}^{-1}\mathbf{T}\bigr)\cdot\mathbf{H} \;=\; \left[\frac{\partial\mathbf{T}^{-1}}{\partial\mathbf{T}}\cdot\mathbf{H}\right]\mathbf{T} \;+\; \mathbf{T}^{-1}\Bigl[\mathbb{I}\cdot\mathbf{H}\Bigr] \quad , \tag{A.4}$$

where $\mathbb{I}=\delta_{ik}\delta_{jl}\,\mathbf{e}_i\otimes\mathbf{e}_j\otimes\mathbf{e}_k\otimes\mathbf{e}_l$ is the *fourth-order identity tensor*, which maps any second-order tensor onto itself. Equation (A.4) thus furnishes

$$\frac{\partial\mathbf{T}^{-1}}{\partial\mathbf{T}}\cdot\mathbf{H} \;=\; -\mathbf{T}^{-1}\mathbf{H}\mathbf{T}^{-1} \quad , \tag{A.5}$$

which in the special case $\mathbf{H}\equiv\dot{\mathbf{T}}$ immediately leads to the desired result $(2.102)_2$. Note that, although the preceding notation suggests that $\mathbf{T}$ is a spatial tensor, the derivation applies identically to referential tensors.

A.3 SRBM Transformation of Flux Derivative

The definition of the flux derivative in $(2.106)_3$ is applied to the vector field $\bar{\mathbf{w}}^+(\mathbf{x}^+,t)$ in the transformed system according to

$$\begin{aligned}\big(\bar{\mathbf{w}}^+\big)^\star &= \frac{\partial\bar{\mathbf{w}}^+}{\partial t} + \big(\mathrm{div}^+\mathbf{w}^+\big)\mathbf{v}^+ - \mathrm{curl}^+\big(\mathbf{v}^+\times\mathbf{w}^+\big)\\ &= \frac{\partial\tilde{\mathbf{w}}^+}{\partial t} - \big[\mathrm{grad}\,\mathbf{w}^+\big]\boldsymbol{\beta} + \mathrm{div}\big(\mathbf{Q}^{\mathrm{T}}\mathbf{w}^+\big)\mathbf{Q}\big(\mathbf{v}+\boldsymbol{\beta}\big)\\ &\qquad - \mathbf{Q}\,\mathrm{curl}\big\{\big(\mathbf{v}+\boldsymbol{\beta}\big)\times\big(\mathbf{Q}^{\mathrm{T}}\mathbf{w}^+\big)\big\}\quad ,\end{aligned} \tag{A.6}$$

where $(2.38)_2$, $(2.155)_3$, (2.165), (2.168), and $(2.181)_2$ were used. As indicated by the accents, the first partial time derivative is taken at fixed $\mathbf{x}^+$ whereas the second derivative is at fixed $\mathbf{x}$. By product rule, the time derivative is expanded into

$$\frac{\partial\tilde{\mathbf{w}}^+}{\partial t} = \mathbf{Q}\frac{\partial}{\partial t}\Big(\mathbf{Q}^{\mathrm{T}}\tilde{\mathbf{w}}^+\Big) + \mathbf{Q}\boldsymbol{\Omega}\mathbf{Q}^{\mathrm{T}}\tilde{\mathbf{w}}^+\quad , \tag{A.7}$$

where the properties of $\boldsymbol{\Omega}$ in $(2.156)_1$ and (2.157) were employed. Appealing to the uniformity of $\mathbf{Q}$, the identities in $(2.46)_5$ and $(2.47)_2$, and the properties of $\boldsymbol{\beta}$ in $(2.159)_{1,2}$, it is readily seen that

$$\begin{aligned}\big[\mathrm{grad}\,\mathbf{w}^+\big]\boldsymbol{\beta} &= \mathbf{Q}\big[\mathrm{grad}\big(\mathbf{Q}^{\mathrm{T}}\mathbf{w}^+\big)\big]\boldsymbol{\beta} = \mathbf{Q}\,\mathrm{div}\big[\big(\mathbf{Q}^{\mathrm{T}}\mathbf{w}^+\big)\otimes\boldsymbol{\beta}\big]\quad ,\\ \mathrm{div}\big(\mathbf{Q}^{\mathrm{T}}\mathbf{w}^+\big)\mathbf{Q}\boldsymbol{\beta} &= \mathbf{Q}\big\{\mathrm{div}\big[\boldsymbol{\beta}\otimes\big(\mathbf{Q}^{\mathrm{T}}\mathbf{w}^+\big)\big] - \boldsymbol{\Omega}\mathbf{Q}^{\mathrm{T}}\mathbf{w}^+\big\}\quad ,\\ \mathbf{Q}\,\mathrm{curl}\big\{\boldsymbol{\beta}\times\big(\mathbf{Q}^{\mathrm{T}}\mathbf{w}^+\big)\big\} &= \mathbf{Q}\big\{\mathrm{div}\big[\boldsymbol{\beta}\otimes\big(\mathbf{Q}^{\mathrm{T}}\mathbf{w}^+\big)\big] - \mathrm{div}\big[\big(\mathbf{Q}^{\mathrm{T}}\mathbf{w}^+\big)\otimes\boldsymbol{\beta}\big]\big\}\quad .\end{aligned} \tag{A.8}$$

Therefore, Equation (A.6) simplifies to

$$\begin{aligned}\big(\bar{\mathbf{w}}^+\big)^\star &= \mathbf{Q}\Big\{\frac{\partial}{\partial t}\Big(\mathbf{Q}^{\mathrm{T}}\tilde{\mathbf{w}}^+\Big) + \mathrm{div}\big(\mathbf{Q}^{\mathrm{T}}\mathbf{w}^+\big)\mathbf{v} - \mathrm{curl}\big\{\mathbf{v}\times\big(\mathbf{Q}^{\mathrm{T}}\mathbf{w}^+\big)\big\}\Big\}\\ &\qquad \underbrace{-\mathbf{Q}\dot{\mathbf{Q}}^{\mathrm{T}}\mathbf{w}^+ - \big[\mathrm{grad}\,\mathbf{w}^+\big]\boldsymbol{\beta} + \mathrm{div}\big(\mathbf{Q}^{\mathrm{T}}\mathbf{w}^+\big)\mathbf{Q}\boldsymbol{\beta} - \mathbf{Q}\,\mathrm{curl}\big\{\boldsymbol{\beta}\times\big(\mathbf{Q}^{\mathrm{T}}\mathbf{w}^+\big)\big\}}_{\text{(i)}}\\ &= \mathbf{Q}\big(\mathbf{Q}^{\mathrm{T}}\tilde{\mathbf{w}}^+\big)^\star\quad ,\end{aligned} \tag{A.9}$$

where Equations (A.7) and $(A.8)_{1-3}$ imply that the term (i) vanishes. This is the desired result in (2.183).

A.4 Invariance Properties of Electromagnetic Fields using Local Equations

The postulated form-invariance of an integral statement automatically implies the form-invariance of the corresponding local statement as well. Provided that the fields

are sufficiently differentiable, the two postulates hold equal predictive power and the same inferences can be drawn from either the global or local form. To demonstrate this, the transformation formulae of the electromagnetic quantities in Section 3.4 are re-derived from the local equations.

A.4.1 Current

Suppose that $\mathbf{j}^+$ is derived from invariance of the local principle of charge conservation (3.5) rather than its global counterpart (3.1),

$$\frac{\partial \bar{q}^+}{\partial t} + \operatorname{div}^+\left(\mathbf{j}^+ + q^+\mathbf{v}^+\right) = \frac{\partial \tilde{q}}{\partial t} + \operatorname{div}\left(\mathbf{j} + q\mathbf{v}\right) \quad . \tag{A.10}$$

The functional form of $q^+ = \bar{q}^+(\mathbf{x}^+, t)$ and $q = \tilde{q}(\mathbf{x}, t)$ must be taken into account for the partial time derivative according to $(2.181)_1$. Upon application of transformation rules (2.165), (3.43), and (2.155), Equation (A.10) simplifies to

$$\operatorname{div}\left(\mathbf{Q}^{\mathrm{T}}\mathbf{j}^+ - \mathbf{j} + q\boldsymbol{\beta}\right) - (\operatorname{grad} q)\cdot\boldsymbol{\beta} = 0 \quad . \tag{A.11}$$

The contribution of $\boldsymbol{\beta}$ vanishes in view of the product rule $(2.46)_1$ and the property $(2.159)_2$, furnishing

$$\operatorname{div}\left(\mathbf{Q}^{\mathrm{T}}\mathbf{j}^+ - \mathbf{j}\right) = 0 \quad . \tag{A.12}$$

Hence, the conduction current transforms to within a divergence-free term according to Equation (3.48).

A.4.2 Charge and Current Potentials

Form-invariance of Gauss' law $(3.15)_1$ and the objectivity of q in (3.43) immediately lead to

$$\operatorname{div}\left(\mathbf{Q}^{\mathrm{T}}\mathbf{d}^+ - \mathbf{d}\right) = 0 \quad , \tag{A.13}$$

giving rise to (3.52) for the transformation of the charge potential. Form-invariance of Ampère's circuital law $(3.15)_2$ implies that

$$\mathbf{Q}^{\mathrm{T}}\mathbf{J}^+ - \mathbf{J} = \mathbf{Q}^{\mathrm{T}}\left(\operatorname{curl}^+\mathbf{h}^+ - \frac{\partial \bar{\mathbf{d}}^+}{\partial t}\right) - \left(\operatorname{curl}\mathbf{h} - \frac{\partial \tilde{\mathbf{d}}}{\partial t}\right) \quad . \tag{A.14}$$

Application of transformation rules (3.49), (2.168), (3.52), and $(2.181)_2$ leads to

$$q\boldsymbol{\beta} = \operatorname{curl}\left(\mathbf{Q}^{\mathrm{T}}\mathbf{h}^+ - \mathbf{h}\right) - \mathbf{Q}^{\mathrm{T}}\dot{\mathbf{Q}}\left(\mathbf{d} + \operatorname{curl}\mathbf{y}\right) - \frac{\partial}{\partial t}\left[\operatorname{curl}\mathbf{y}\right] + \left[\operatorname{grad}(\mathbf{d} + \operatorname{curl}\mathbf{y})\right]\boldsymbol{\beta} \quad . \tag{A.15}$$

This is further simplified using identities $(2.46)_5$, $(2.47)_2$, $(2.159)_{1,2}$, and $(3.15)_1$, as well as the commutativity of the curl with the partial time derivative, furnishing

$$\operatorname{curl}\left(\mathbf{Q}^{\mathrm{T}}\mathbf{h}^+ - \mathbf{h} - \frac{\partial \mathbf{y}}{\partial t} - \boldsymbol{\beta}\times\left(\mathbf{d} + \operatorname{curl}\mathbf{y}\right)\right) = \mathbf{0} \quad . \tag{A.16}$$

Integration of this result leads to (3.58).

A.4.3 Electric and Magnetic Fields

It follows immediately from (2.165) and the form-invariance of GAUSS' law for magnetism in $(3.15)_3$ that

$$\operatorname{div}\big(\mathbf{Q}^{\mathrm{T}}\mathbf{b}^{+}-\mathbf{b}\big) \;=\; 0 \quad . \tag{A.17}$$

Hence the magnetic flux density is objective, see (3.63), if the ensuing divergence-free 'integration constant' is precluded on physical grounds. The form-invariance of FARADAY's law of induction $(3.15)_4$ furnishes

$$\operatorname{curl}\Big\{\mathbf{Q}^{\mathrm{T}}\mathbf{e}^{+}-\mathbf{e}+\boldsymbol{\beta}\times\mathbf{b}\Big\} \;=\; 0 \quad , \tag{A.18}$$

which leads to the transformation of the electric field in (3.67). The derivation employs Equations $(2.46)_5$, $(2.47)_2$, $(2.159)_1$, (2.168), $(2.181)_2$, and (3.63). Since it follows closely along the lines of derivation (A.14 - 16), it is not repeated here. An irrotational (curl-free) term was dismissed on physical grounds.

A.5 Electromagnetic Wave Equations

The electric permittivity ε_0 and magnetic permeability μ_0 in the aether relations (3.35) determine the speed of light c in empty space, which is obtained from a wave solution of the MAXWELL equations with vanishing charge-currents $\{q,\mathbf{j}\}$. AMPÈRE's circuital law $(3.15)_2$ and FARADAY's law of induction $(3.15)_4$ read

$$\operatorname{curl}\mathbf{b} \;=\; \mu_0\varepsilon_0\frac{\partial\mathbf{e}}{\partial t} \quad , \quad \operatorname{curl}\mathbf{e} \;=\; -\frac{\partial\mathbf{b}}{\partial t} \quad , \tag{A.19}$$

and GAUSS' laws $(3.15)_{1,3}$ imply that $\mathbf{e}$ and $\mathbf{b}$ are divergence-free. An additional application of the curl operator to both sides of (A.19) yields

$$\operatorname{curl}\big(\operatorname{curl}\mathbf{b}\big) \;=\; \mu_0\varepsilon_0\frac{\partial}{\partial t}\Big(\operatorname{curl}\mathbf{e}\Big) \quad , \quad \operatorname{curl}\big(\operatorname{curl}\mathbf{e}\big) \;=\; -\frac{\partial}{\partial t}\Big(\operatorname{curl}\mathbf{b}\Big) \quad , \tag{A.20}$$

where the fields are assumed to be sufficiently smooth for the spatial and temporal derivatives to commute.

Equations $(A.19)_{1,2}$ are inserted into the right-hand sides of $(A.20)_{1,2}$ in order to separate the variables. Meanwhile, the left-hand sides simplify on account of the identity in $(2.49)_3$, furnishing

$$\Delta\mathbf{b} \;=\; \mu_0\varepsilon_0\frac{\partial^2\mathbf{b}}{\partial t^2} \quad , \quad \Delta\mathbf{e} \;=\; \mu_0\varepsilon_0\frac{\partial^2\mathbf{e}}{\partial t^2} \quad , \tag{A.21}$$

where the LAPLACE operator $\Delta[\cdot]=\operatorname{div}(\operatorname{grad}[\cdot])$ is used. These are the well-known *electromagnetic wave equations*. Their solution using a wave ansatz leads to continuous EM waves whose phase velocity in vacuum is given by the expression in (3.36).

To obtain the uncoupled wave equations in (A.21), the curl operator was applied to Equations (A.19). Note that the same result may be attained following a similar procedure, but instead taking the partial time derivative of (A.19).

A.6 Alternative Representations of the Balance Equations

Recall from Sections 4.1.4 and 4.2.3 that the LORENTZ force $\mathbf{f}_{\mathrm{L}}$ and the EM power density $\mathbf{J}\cdot\mathbf{e}$ may be expressed in terms of the EM fields using MAXWELL's Equations $(3.15)_{1-4}$. This furnishes the expressions in (4.9) and (4.20), which look like balance equations of linear momentum and energy, respectively, for the EM fields. They are subsequently substituted into the balance equations of momentum and energy, where the material time derivative of the conserved TM quantity is (somewhat haphazardly) combined with its EM counterpart. This furnishes expressions which may be loosely interpreted as a combined EMTM momentum or energy, respectively.

It is, however, once again stressed that the interpretation of the aforementioned relations as EM momentum and energy balances is rather controversial. In this text, they are instead regarded as mere identities derived from MAXWELL's equations. Furthermore, the justification for the interpretation of $\mathbf{T}_{\mathrm{M}}$ in (4.11) as the MAXWELL stress tensor and u in (4.21) as the stored EM energy density is predicated on the applicability of the aether relations (3.35). Outside of the aether frame the analogy with momentum and energy breaks down.

Note that the resulting balance laws are entirely in agreement with those presented in Sections 4.1 and 4.2. Since they rely only on the EM (and TM) fields, they may be of advantage if it is preferable not to make explicit use of the charge-currents $\{q, \mathbf{J}\}$. However, in the context of this dissertation, any potential benefits are outweighed by the increase in the number of terms and the lack of a clear physical interpretation for the quantities involved.

Such alternative formulations of the balance equations are used in different variations by many authors, most notably by KOVETZ [64].[1] Other authors who incorporate the electromagnetic 'momentum' and 'energy' into the balance equations include FOSDICK and TANG [29, Section 3.1], HANAPPIER *et al.* [41], HUTTER *et al.* [56, Chapter 3.4], MÜLLER [102, Chapter 9.5], and VAN DE VEN [149, Chapter II].

A.6.1 Linear Momentum Balance

Equation (4.9) for the LORENTZ force $\mathbf{f}_{\mathrm{L}}$ is substituted into the linear momentum balance (4.5) of the EMTM model, leading to

$$\frac{\mathrm{d}}{\mathrm{d}t}\int_{\mathcal{P}}\rho\mathbf{v}\,\mathrm{d}v+\int_{\mathcal{P}}\frac{\partial}{\partial t}\big(\mathbf{d}\times\mathbf{b}\big)\,\mathrm{d}v\;=\int_{\partial\mathcal{P}}\mathbf{T}\mathbf{n}\,\mathrm{d}a+\int_{\mathcal{P}}\rho\mathbf{f}_{\mathrm{B}}\,\mathrm{d}v+\int_{\mathcal{P}}\mathbf{t}_{\mathrm{M}}\,\mathrm{d}v\quad. \tag{A.22}$$

[1] According to STEIGMANN [137] (despite some questions raised by ERICKSEN [22]), KOVETZ' work is entirely compatible with the results from other authors, including the derivations in Chapter 4 of this dissertation.

The local form of the linear momentum balance (4.6) becomes

$$\rho\mathbf{a} + \frac{\partial}{\partial t}\big(\mathbf{d}\times\mathbf{b}\big) \;=\; \operatorname{div}\mathbf{T} + \rho\mathbf{f}_{\mathrm{B}} + \mathbf{t}_{\mathrm{M}} \quad , \tag{A.23}$$

where MAXWELL's 'traction vector' $\mathbf{t}_{\mathrm{M}}$ is defined in (4.10) independent of the frame of reference.

By employing the objective expression for $\mathbf{f}_{\mathrm{L}}$ in (4.12) rather than (4.9), an objective[2] form of (A.23) is obtained, according to which

$$\rho\mathbf{a} + \big(\overset{\star}{\mathbf{d}}\times\mathbf{b} + \mathbf{d}\times\overset{\star}{\mathbf{b}}\big) \;=\; \operatorname{div}\mathbf{T} + \rho\mathbf{f}_{\mathrm{B}} + \boldsymbol{\tau}_{\mathrm{M}} \quad . \tag{A.24}$$

Here, $\boldsymbol{\tau}_{\mathrm{M}}$ represents the objective counterpart to $\mathbf{t}_{\mathrm{M}}$, defined as

$$\boldsymbol{\tau}_{\mathrm{M}} \;=\; \operatorname{div}\big[\boldsymbol{\mathcal{E}}\otimes\mathbf{d} + \boldsymbol{\mathcal{H}}\otimes\mathbf{b}\big] - \Big(\big[\operatorname{grad}\boldsymbol{\mathcal{E}}\big]^{\mathrm{T}}\mathbf{d} + \big[\operatorname{grad}\boldsymbol{\mathcal{H}}\big]^{\mathrm{T}}\mathbf{b}\Big) \quad . \tag{A.25}$$

It is mentioned that, similar to the MAXWELL stress $\mathbf{T}_{\mathrm{M}}$ in (4.11), $\boldsymbol{\tau}_{\mathrm{M}}$ can be written in terms of the divergence of a tensor $\boldsymbol{\mathcal{T}}_{\mathrm{M}}$. However, this works only for the alternative[3] aether relations in (3.90) rather than the standard form (3.35). In that case the objective version $\boldsymbol{\mathcal{T}}_{\mathrm{M}}$ of the MAXWELL stress is given by

$$\boldsymbol{\tau}_{\mathrm{M}} \overset{\text{Aet.*}}{=} \operatorname{div}\boldsymbol{\mathcal{T}}_{\mathrm{M}} \quad \text{where} \quad \boldsymbol{\mathcal{T}}_{\mathrm{M}} \;=\; \big[\boldsymbol{\mathcal{E}}\otimes\mathbf{d} + \boldsymbol{\mathcal{H}}\otimes\mathbf{b}\big] - \tfrac{1}{2}\big(\boldsymbol{\mathcal{E}}\cdot\mathbf{d} + \boldsymbol{\mathcal{H}}\cdot\mathbf{b}\big)\mathbf{i} \quad , \tag{A.26}$$

where the superscript $\overset{\text{Aet.*}}{=}$ indicates that the expression is predicated on the alternative aether Equations (3.90). Equations with $\overset{\text{Aet.}}{=}$ and $\overset{\text{Aet.*}}{=}$ are mutually incompatible, as they are valid under different aether relations. Although enticing, the alternative aether relations are not pursued any further in this dissertation.

Motivated by the interpretation of $\mathbf{d}\times\mathbf{b}$ as a momentum density of the EM fields, it is combined with the mechanical momentum $\rho\mathbf{v}$ using REYNOLDS' transport theorem (2.104) to write

$$\frac{\mathrm{d}}{\mathrm{d}t}\int_{\mathcal{P}}\big\{\rho\mathbf{v} + \mathbf{d}\times\mathbf{b}\big\}\,\mathrm{d}v \;=\; \int_{\partial\mathcal{P}}\big(\mathbf{d}\times\mathbf{b}\big)(\mathbf{v}\cdot\mathbf{n})\,\mathrm{d}a + \int_{\partial\mathcal{P}}\mathbf{T}\mathbf{n}\,\mathrm{d}a + \int_{\mathcal{P}}\rho\mathbf{f}_{\mathrm{B}}\,\mathrm{d}v + \int_{\mathcal{P}}\mathbf{t}_{\mathrm{M}}\,\mathrm{d}v \quad . \tag{A.27}$$

In local form, Equation (A.27) amounts to

$$\rho\big[\mathbf{v} + \mathbf{d}\times\mathbf{b}/\rho\big]^{\bullet} \;=\; \operatorname{div}\big[\big(\mathbf{d}\times\mathbf{b}\big)\otimes\mathbf{v}\big] + \operatorname{div}\mathbf{T} + \rho\mathbf{f}_{\mathrm{B}} + \mathbf{t}_{\mathrm{M}} \quad , \tag{A.28}$$

or, equivalently,

$$\rho\mathbf{a} + \big[\mathbf{d}\times\mathbf{b}\big]^{\bullet} \;=\; \big[\operatorname{grad}\big(\mathbf{d}\times\mathbf{b}\big)\big]\,\mathbf{v} + \operatorname{div}\mathbf{T} + \rho\mathbf{f}_{\mathrm{B}} + \mathbf{t}_{\mathrm{M}} \quad . \tag{A.29}$$

[2] Although $\mathbf{a}$ and $\mathbf{f}_{\mathrm{B}}$ are not individually objective, their difference $(\mathbf{f}_{\mathrm{B}} - \mathbf{a})$ is, see (2.177). All other terms in (A.24) are objective.

[3] Recall that these relations were introduced in an attempt to resolve the lack of form-invariance of the standard aether relations, see HUTTER *et al.* [56, Chapter 3.4].

Equation (A.29) readily follows from (A.28) using the identities in $(2.46)_5$ and (2.111), or from (A.23) using $(2.96)_2$.

Let the generalized velocity $\mathbf{v}_\mathrm{K}$ be defined such that the combined EMTM momentum corresponds to $\rho\mathbf{v}_\mathrm{K}$. Furthermore, use the aether frame to write $\mathbf{t}_\mathrm{M}$ in terms of the Maxwell stress tensor (4.11) and combine all divergence terms in (A.28) into a generalized stress $\mathbf{T}_\mathrm{K}$,

$$\mathbf{v}_\mathrm{K} \;=\; \mathbf{v} + \mathbf{d}\times\mathbf{b}/\rho \quad \text{and} \quad \mathbf{T}_\mathrm{K} \;=\; \mathbf{T} + \mathbf{T}_\mathrm{M} + \big(\mathbf{d}\times\mathbf{b}\big)\otimes\mathbf{v} \quad . \tag{A.30}$$

Equation (A.28) immediately simplifies to

$$\rho\dot{\mathbf{v}}_\mathrm{K} \overset{\text{Aet.}}{=} \operatorname{div}\mathbf{T}_\mathrm{K} + \rho\mathbf{f}_\mathrm{B} \quad , \tag{A.31}$$

which looks much like the thermomechanical balance of linear momentum (2.115).

Although this balance equation looks simple, it can be at times confusing due to the dissociation of $\mathbf{v}_\mathrm{K}$ and $\mathbf{T}_\mathrm{K}$ from straightforward physical quantities. It is nevertheless in complete agreement with the theory presented in Section 4. Note that this approach is (tacitly[4]) taken by Kovetz [64, Equation 54.9], who uses (A.31) as a primitive statement of momentum balance throughout his monograph. Fosdick and Tang [29, Equation 3.1.10a] adopt an intermediate stance, whereby the stress tensor is given by the transpose of $(A.30)_2$ but the generalized momentum in $(A.30)_1$ is not used.

A.6.2 Angular Momentum Balance

With the aid of the definitions in $(A.30)_{1,2}$ for the generalized $\mathbf{v}_\mathrm{K}$ and $\mathbf{T}_\mathrm{K}$, the balance of angular momentum (4.7) is alternatively stated by

$$\frac{\mathrm{d}}{\mathrm{d}t}\int_\mathcal{P} \mathbf{x}\times\rho\mathbf{v}_\mathrm{K}\,\mathrm{d}v \overset{\text{Aet.}}{=} \int_{\partial\mathcal{P}} \mathbf{x}\times\mathbf{T}_\mathrm{K}\mathbf{n}\,\mathrm{d}a + \int_\mathcal{P} \mathbf{x}\times\rho\mathbf{f}_\mathrm{B}\,\mathrm{d}v \quad , \tag{A.32}$$

which again closely resembles the purely thermomechanical balance (2.116). The local form is derived following the standard procedure outlined in Section 2.3.3. However, since $\mathbf{v}$ and $\mathbf{v}_\mathrm{K}$ are generally not collinear, an additional term arises on the left-hand side,

$$\int_\mathcal{P} \big\{\mathbf{v}\times\rho\mathbf{v}_\mathrm{K} + \mathbf{x}\times\rho\dot{\mathbf{v}}_\mathrm{K}\big\}\,\mathrm{d}v \overset{\text{Aet.}}{=} \int_\mathcal{P} \big\{T^\mathrm{K}_{ij}\mathbf{e}_j\times\mathbf{e}_i + \mathbf{x}\times\operatorname{div}\mathbf{T}_\mathrm{K}\big\}\,\mathrm{d}v + \int_\mathcal{P} \mathbf{x}\times\rho\mathbf{f}_\mathrm{B}\,\mathrm{d}v \quad . \tag{A.33}$$

[4] In Kovetz' notation the generalized velocity $\mathbf{v}_\mathrm{K}$ is represented by a vector $\mathbf{g}$ whereas $\mathbf{T}_\mathrm{K}$ is represented by $\mathbf{T}$, see [64, Equation 54.1]. Although Kovetz does not derive the conversion in $(A.30)_1$ universally, Steigmann [137, Equation $31_{(1)}$] points out that "*For the examples that he considers, pertaining to viscous and inviscid fluids and elastic solids,* $\mathbf{g}$ *is always found to reduce to* $[(A.30)_1]$."

Here, Equation (2.112) was used for the time derivative and (2.118) for $\mathbf{T}_\mathrm{K}$. Upon application of linear momentum balance (A.31) and the localization theorem,

$$\rho\mathbf{v}\times\mathbf{v}_\mathrm{K} \overset{\text{Aet.}}{=} T^\mathrm{K}_{ij}\mathbf{e}_j\times\mathbf{e}_i \quad . \tag{A.34}$$

With $\mathbf{e}_i\times\mathbf{e}_j=\epsilon_{ijk}\mathbf{e}_k$, see (2.6), the statement is more conveniently written as

$$\epsilon_{ijk}\big(\rho v_i v^\mathrm{K}_j + T^\mathrm{K}_{ij}\big)\mathbf{e}_k \overset{\text{Aet.}}{=} 0 \quad , \tag{A.35}$$

which implies that $\rho\mathbf{v}\otimes\mathbf{v}_\mathrm{K}+\mathbf{T}_\mathrm{K}$ is symmetric. The same statement of angular momentum balance is attained by Kovetz [64, Equation 54.10]. It is readily verified using the definitions in $(\text{A.30})_{1,2}$ that (A.35) is in agreement with the earlier results that $\mathbf{T}$ and $\mathbf{T}_\mathrm{M}$ are symmetric (but not $\mathbf{T}_\mathrm{K}$). Fosdick and Tang [29, Equation 3.1.11b] arrive at an equivalent conclusion, namely that $\mathbf{T}^\mathrm{T}_\mathrm{K}-\mathbf{v}\otimes(\mathbf{d}\times\mathbf{b})$ is symmetric.

A.6.3 Energy Balance

Similar to the substitution of $\mathbf{f}_\mathrm{L}$ in the linear momentum balance, Poynting's theorem (4.20) is employed to replace $\mathbf{J}\cdot\mathbf{e}$ in the energy balance (4.17), furnishing

$$\begin{aligned}\frac{\mathrm{d}}{\mathrm{d}t}\int_\mathcal{P}\rho\left(\frac{1}{2}\mathbf{v}\cdot\mathbf{v}+\varepsilon\right)\mathrm{d}v + \int_\mathcal{P}\left(\mathbf{e}\cdot\frac{\partial\mathbf{d}}{\partial t}+\mathbf{h}\cdot\frac{\partial\mathbf{b}}{\partial t}\right)\mathrm{d}v \;&=\; \int_\mathcal{P}\rho\mathbf{f}_\mathrm{B}\cdot\mathbf{v}\,\mathrm{d}v \\ &+\int_{\partial\mathcal{P}}\mathbf{T}\mathbf{n}\cdot\mathbf{v}\,\mathrm{d}a+\int_\mathcal{P}\rho r\,\mathrm{d}v-\int_{\partial\mathcal{P}}\mathbf{q}\cdot\mathbf{n}\,\mathrm{d}a-\int_{\partial\mathcal{P}}\big(\mathbf{e}\times\mathbf{h}\big)\cdot\mathbf{n}\,\mathrm{d}a \quad .\end{aligned} \tag{A.36}$$

The corresponding local form (4.18) becomes

$$\begin{aligned}\rho\big[\tfrac{1}{2}\mathbf{v}\cdot\mathbf{v}+\varepsilon\big]^\bullet+\left(\mathbf{e}\cdot\frac{\partial\mathbf{d}}{\partial t}+\mathbf{h}\cdot\frac{\partial\mathbf{b}}{\partial t}\right) \;&=\; \rho\mathbf{f}_\mathrm{B}\cdot\mathbf{v}+\operatorname{div}\big(\mathbf{T}^\mathrm{T}\mathbf{v}\big) \\ &+\rho r-\operatorname{div}\mathbf{q}-\operatorname{div}\big(\mathbf{e}\times\mathbf{h}\big) \quad ,\end{aligned} \tag{A.37}$$

or alternatively using (4.16) and (4.23)

$$\begin{aligned}\rho\big[\tfrac{1}{2}\mathbf{v}\cdot\mathbf{v}+\varepsilon\big]^\bullet+\big[\boldsymbol{\mathcal{E}}\cdot\overset{\star}{\mathbf{d}}+\boldsymbol{\mathcal{H}}\cdot\overset{\star}{\mathbf{b}}\big] \;&=\; \rho\mathbf{f}_\mathrm{B}\cdot\mathbf{v}+\operatorname{div}\big(\mathbf{T}^\mathrm{T}\mathbf{v}\big) \\ &+\rho r-\operatorname{div}\mathbf{q}-\operatorname{div}\big(\boldsymbol{\mathcal{E}}\times\boldsymbol{\mathcal{H}}\big)+\mathbf{f}_\mathrm{L}\cdot\mathbf{v} \quad .\end{aligned} \tag{A.38}$$

In the aether frame, the partial time derivatives in (A.37) can be isolated according to Equation (4.21), allowing for Poynting's theorem to be interpreted as an energy balance. This electromagnetic energy may then be combined with the kinetic and internal energies, $\rho\frac{1}{2}\mathbf{v}\cdot\mathbf{v}$ and $\rho\varepsilon$, respectively. The partial and total time derivatives of the EM energy u may be related using $(2.46)_1$, $(2.96)_1$, and (2.111) by

$$\frac{\partial u}{\partial t} \;=\; \rho\big[u/\rho\big]^\bullet-\operatorname{div}\big(u\mathbf{v}\big) \quad . \tag{A.39}$$

The energy balance (A.37), in the aether frame, may thus be restated as

$$\rho\big[\tfrac{1}{2}\mathbf{v}\cdot\mathbf{v}+\varepsilon+u/\rho\big]^{\bullet}\overset{\text{Aet.}}{=}\rho\mathbf{f}_{\mathrm{B}}\cdot\mathbf{v}+\operatorname{div}\big(\big[\mathbf{T}+u\mathbf{i}\big]^{\mathrm{T}}\mathbf{v}\big)+\rho r-\operatorname{div}\mathbf{q}-\operatorname{div}\big(\mathbf{e}\times\mathbf{h}\big)\quad,\tag{A.40}$$

or by invoking (4.24) for the objective POYNTING vector and definition $(A.30)_2$ for $\mathbf{T}_{\mathrm{K}}$,

$$\rho\big[\tfrac{1}{2}\mathbf{v}\cdot\mathbf{v}+\varepsilon+u/\rho\big]^{\bullet}\overset{\text{Aet.}}{=}\rho\mathbf{f}_{\mathrm{B}}\cdot\mathbf{v}+\operatorname{div}\big(\mathbf{T}_{\mathrm{K}}^{\mathrm{T}}\mathbf{v}\big)+\rho r-\operatorname{div}\mathbf{q}-\operatorname{div}\big(\boldsymbol{\mathcal{E}}\times\boldsymbol{\mathcal{H}}\big)\quad.\tag{A.41}$$

Note that Equation (A.41) is in agreement with KOVETZ [64, Equation 54.11].

By defining a generalized internal energy ε_{K} and heat flux $\mathbf{q}_{\mathrm{K}}$,

$$\varepsilon_{\mathrm{K}}=\varepsilon+u/\rho\quad\text{and}\quad\mathbf{q}_{\mathrm{K}}=\mathbf{q}+\boldsymbol{\mathcal{E}}\times\boldsymbol{\mathcal{H}}\quad,\tag{A.42}$$

the energy balance simplifies in the aether frame to

$$\rho\big[\tfrac{1}{2}\mathbf{v}\cdot\mathbf{v}+\varepsilon_{\mathrm{K}}\big]^{\bullet}\overset{\text{Aet.}}{=}\rho\mathbf{f}_{\mathrm{B}}\cdot\mathbf{v}+\operatorname{div}\big(\mathbf{T}_{\mathrm{K}}^{\mathrm{T}}\mathbf{v}\big)+\rho r-\operatorname{div}\mathbf{q}_{\mathrm{K}}\quad,\tag{A.43}$$

which resembles the thermomechanical case (2.124).

As expected the generalized quantities $\mathbf{v}_{\mathrm{K}}$, $\mathbf{T}_{\mathrm{K}}$, ε_{K}, and $\mathbf{q}_{\mathrm{K}}$ reduce to their thermomechanical counterparts $\mathbf{v}$, $\mathbf{T}$, ε, and $\mathbf{q}$ when the EM fields are negligible. However, this analogy is somewhat misleading for several reasons. Despite ε and $\mathbf{T}$ being objective according to $(2.174)_2$ and $(2.175)_1$, their generalized versions ε_{K} and $\mathbf{T}_{\mathrm{K}}$ are *not*, because u (4.25) and $\mathbf{T}_{\mathrm{M}}$ themselves are not objective. Furthermore, $\mathbf{T}_{\mathrm{K}}$ as defined by $(A.30)_2$ is *not* symmetric unlike $\mathbf{T}$ and $\mathbf{T}_{\mathrm{M}}$. Lastly, the generalized velocity $\mathbf{v}_{\mathrm{K}}$ does *not* fully replace $\mathbf{v}$ in the angular momentum and energy balances (A.34) and (A.43) respectively. Instead, $\mathbf{v}_{\mathrm{K}}$ is regarded by KOVETZ as a new quantity which is yet to be constitutively determined via the method of COLEMAN and NOLL. Of course, starting with the same CLAUSIUS-DUHEM inequality in (4.40) for the entropy of EMTM materials, KOVETZ arrives at constitutive expressions for $\mathbf{v}_{\mathrm{K}}$ identical to $(A.30)_1$.

The balance of thermal energy (4.19) may be re-derived by subtracting the balance of mechanical energy, *i.e.*, Equation (A.31) dotted with velocity $\mathbf{v}$, from the total energy balance (A.43), furnishing

$$\rho\dot{\varepsilon}_{\mathrm{K}}=\rho\big[\mathbf{d}\times\mathbf{b}/\rho\big]^{\bullet}\cdot\mathbf{v}+\mathbf{T}_{\mathrm{K}}\cdot\mathbf{L}+\rho r-\operatorname{div}\mathbf{q}_{\mathrm{K}}\quad.\tag{A.44}$$

Outside of the aether frame, the partial time derivatives do not combine into an EM energy u and the EM traction $\mathbf{t}_{\mathrm{M}}$ cannot be written in terms of the divergence of the MAXWELL stress tensor. The corresponding balance of thermal energy is thus less compact, reading

$$\rho\dot{\varepsilon}+\left(\mathbf{e}\cdot\frac{\partial\mathbf{d}}{\partial t}+\mathbf{h}\cdot\frac{\partial\mathbf{b}}{\partial t}\right)=\frac{\partial}{\partial t}(\mathbf{d}\times\mathbf{b})\cdot\mathbf{v}+\mathbf{T}\cdot\mathbf{L}-\mathbf{t}_{\mathrm{M}}\cdot\mathbf{v}+\rho r-\operatorname{div}\big(\mathbf{q}+\mathbf{e}\times\mathbf{h}\big)\quad.\tag{A.45}$$